Understanding the Role of Dormancy in Glioblastoma Radio-resistance

Rhyla Mae Santiago

University College London

Cancer Institute

A thesis submitted for the degree of

Doctor of Philosophy

University College London

September 2024

Declaration

I, Rhyla Mae Santiago, confirm that the work presented in this thesis is my own. Where information has been derived from other sources, I confirm that this has been indicated in the thesis.

Abstract

Glioblastoma is the most common and aggressive type of brain cancer in adults. Although it is treated with combined surgery and chemoradiotherapy, patients inevitably experience tumour recurrence. The efficacy of this treatment is limited partly by the increased radio-resistance of this disease. One source of this radio-resistance may in fact be tumour cell dormancy, a state of reversible cell cycle arrest. Indeed, radiotherapy is thought to preferentially target proliferating tumour cells, which may progress rapidly through the cell cycle with attenuated capacity for DNA repair. The extended presence of radiation-induced DNA damage in these proliferating tumour cells eventually triggers cell death. Thus, dormant cells are thought to survive radiotherapy, yet the mechanisms underpinning this radio-resistance remain unclear. Another layer of complexity arises from the potential heterogeneity of the dormant population in glioblastoma. This tumour is distributed into the cell states resembling that of normal neurodevelopment, it follows that the dormant population may also consist of multiple cell states with potentially heterogenous mechanisms of radio-resistance. Given this context, we sought to first characterise the dormant population in an immunocompetent mouse model of glioblastoma and assess its radiation-response. In fact, we identified a dormant astrocyte-like population that was radioresistant, and interestingly, driven by tumour-derived BMP signalling. We modelled this population *in vitro* through BMP4/FGF treatment to determine the mechanisms underlying their radio-resistance. To this end, we demonstrated the significance of MMEJ in the DNA Damage repair of this dormant population *in vitro*. Certainly, we demonstrated that MMEJ inhibition significantly improved the survival benefit of chemoradiotherapy *in vivo*. Collectively, this work advances our understanding of the radio-

resistance mechanisms of the dormant tumour cells in glioblastoma and highlights the potential in utilising MMEJ inhibition to target this radio-resistant dormant population.

Impact Statement

Glioblastoma is the most common and aggressive type of brain cancer in adults (Hanif et al., 2017; Louis et al., 2021). Despite standard treatment involving surgery, radiotherapy, and chemotherapy (Stupp et al., 2005), patients will inevitably experience tumour recurrence (Hanif et al., 2017). As a result, the five-year survival rate for glioblastoma remains at approximately 7%, underscoring the urgent need to develop more effective therapeutic strategies (Hanif et al., 2017; Ostrom et al., 2021).

Although a range of novel interventions have been explored in recent decades, none have led to significant improvements in patient outcomes (Miller et al., 2021). Indeed, radiotherapy, which was introduced to glioblastoma treatment in the 1940s, remains one of the most effective and widely applied modalities for this disease (Gzell et al., 2017). Given this context, enhancing the efficacy of radiotherapy is essential to improving glioblastoma patient outcomes.

Radiotherapy targets actively proliferating tumour cells, as their rapid cell cycle progression and dysfunctional cell cycle checkpoints impair their capacity to repair radiation-induced DNA damage, such as double strand breaks (DSBs) (Abuetabh et al., 2022; Y. Zhou et al., 2021). The persistent DNA damage ultimately triggers cell death (Abuetabh et al., 2022; Y. Zhou et al., 2021). However, not all tumour cells are actively dividing; some enter a reversible state of cell cycle arrest, known as tumour cell dormancy (Aguirre-Ghiso, 2007; Hadfield, 1954). These dormant tumour cells are thought to survive radiotherapy, yet the mechanisms underlying their radio-resistance remain elusive.

To add to the complexity of dormant tumour cell radio-resistance, glioblastoma is known to be comprised of tumour cell that resemble the cell states of normal neurodevelopment (Couturier et al., 2020; Neftel et al., 2019). It is possible that the dormant population is also comprised of different cell states with potentially different mechanisms of radio-resistance.

Indeed, we identified an astrocyte-like population of dormant tumour cells in an immunocompetent glioblastoma mouse model (Garcia-Diaz et al., 2023), that was radio-resistant. Leveraging an *in vitro* model of this dormant population, we characterised their radiation response *in vitro*. Interestingly, we found that the MMEJ DSB repair pathway contributed to the DNA damage repair of these dormant tumour cells. Importantly, we showed that a novel inhibitor of MMEJ repair increased the radiosensitivity of these dormant tumour cells *in vitro*. We further explored its impact on the survival of glioblastoma-bearing mice, remarkably, MMEJ inhibition in combination with chemoradiotherapy extended the survival in these mice compared to chemoradiotherapy alone. Given that MMEJ is thought to be upregulated in cancers, this finding suggests that therapeutically targeting MMEJ could improve the efficacy of standard treatment without harming normal cells (Ceccaldi et al., 2015; Higgins et al., 2010).

Overall, the research presented in this thesis contributes to the growing understanding of the molecular mechanisms underlying radio-resistance in glioblastoma and suggests a potential avenue for improving therapeutic efficacy.

Acknowledgements

Firstly, I would like to express my gratitude to Prof. Simona Parrinello and Dr Simon Boulton for offering me the opportunity to pursue this PhD. I am especially grateful to Simona for hosting me in her lab and for all the advice and support she has given me. My PhD has also benefited greatly from the guidance of Lucy Brooks. I am incredibly grateful for the time she devoted to nurturing me as a scientist. I would also like to extend a thank you to Dr Mark Robinson and Dr Martin Barr, my first supervisors who inspired me to pursue my PhD.

To all the members of the Parrinello lab, both past and present, thank you for your support and collaboration in these past four years. A special thanks is in order for Mel, Holly, Meghan and Valeria, for the time they devoted to teaching me. I would like to extend my sincere gratitude to Zan, Jenda and Rachel for their moral support. I am deeply thankful to Anni Poysti for her support, both moral and scientific.

To all my friends in the Cancer Institute, although I cannot name you all, I will always remember your kind words of encouragement, and the heartwarming memories we shared together.

Thank you all for celebrating me when I would succeed, picking me up when I was down, and exploring new avenues of research with me. Thank you for the belief you held in me which carried me through the difficult parts of this journey. I am incredibly grateful that you have been part of my life for the last four years.

I am profoundly grateful to my parents, Larry and Elenita Santiago, my brother, Rohn Allen Santiago and to my partner, Aidan Lee. Whenever I stumbled on this journey, your unwavering support and love helped to keep me going.

Finally, I would like to extend a special thanks to Ycofel Joy Dotimas Mauyao. *Maraming salamat Ate,* for the gift of your smile and the memory of your laughter. The persevering love you held for your family reminds me every day why cancer research is meaningful. I like to dream that you would have enjoyed reading this.

Table of Contents

Table of figures

List of tables

Abbreviations

53BP1	p53 Binding Protein 1
5-ALA	5-Aminolevulinic Acid
ATM	Ataxia-telangiectasia-mutated
ATR	ataxia telangiectasia and Rad3-related
ATRIP	ATR interacting proteins
BMP	Bone Morpheogenetic Protein
BRCA1	Breast Cancer gene 1
Bulk RNAseq	Bulk RNA Sequencing
CAR	Chimeric Antigen Receptor
Cdc25	Cell division cycle 25
CDK	Cyclin-dependent kinases
CDKN	Cyclin Dependent Kinase
CNS	Central Nervous System
CT	Computer Tomography
CTLA4	cytotoxic T-lymphocyte-associated antigen 4
DDR	DNA Damage Response
DNA	Deoxyribonucleic Acid
DNA-PK	DNA-dependent protein kinase catalytic subunit
DSB	Double Strand Break
EAAT1	excitatory amino acid transporter 1
EGF	Epidermal Growth Factor
EGFR	Epidermal Growth Factor Receptor
EMT	Epithelial Mesenchymal Transition
Exo1	Exonuclease
FEN1	Flap Endonuclease 1
FGF	fibroblast growth factor
GABRA1	Gamma-aminobutyric acid receptor subunit alpha-1
GFAP	Glial fibrillary acidic protein
GM-CSF	granulocyte-macrophage colony-stimulating factor
GO	Gene Ontology
GSEA	Gene Set Enrichment Analysis

H2O2	Hydrogen Peroxide
H3	Histone 3
HR	Homologous Repair
IDH	Isocitrate Dehydrogenase
IFN	Interferon
IL	Interleukin
MAPK	Mitogen-Activated Protein Kinase
MDC1	Mediator of DNA damage checkpoint protein 1
MDM2	Murine Double Minute 2
MGMT	O6-methylguanine–DNA methyltransferase
MMEJ	Microhomology mediated end joining
MRI	Magnetic Resonance Imaging
MRN	Mre11-Rad50-Nsb1
MYC	myelocytomatosis
NEFL	Neurofilament light polypeptide
NES	Normalised Enrichment Score
NF1	Neurofibromatosis type 1
NFkB	nuclear factor kappa-light-chain-enhancer of activated B cells
NHEJ	Non-Homologous end joining
O2-	superoxide anion
OH-	hydroxyl radical
OS	Overall Survival
PARP1	Poly (ADP-ribose) polymerase 1
PD1	Programmed cell death protein 1
PDGFR	Platelet-derived Growth Factor Receptor Alpha
PFA	Paraformaldehyde
PI3K	Phospho-Inositol 3 Kinase
POLθ	Polymerase θ
PTEN	Phosphatase and Tensin homolog deleted on chromosome 10
RB1	Retinoblastoma 1
ROS	Reactive Oxygen Species
RPA	Replication Protein A
scRNAseq	single cell RNA sequencing

Ser	Serine
SFK	src family kinases
SLC4A4	Solute Carrier Family 4 Member 4
SSB	Single Strand Break
ssDNA	single stranded DNA
TERT	Telomerase Reverse Transcriptase
TGFβ	Tumour Growth Factor β
Thr	Threonine
TNF	Tumour Necrosis Factor
TOPB1	DNA topoisomerase 2-binding protein 1
VEGF	Vascular endothelial growth factor
WHO	World Health Organisation
WRN	Werner Syndrome
XRCC4	X-ray repair cross-complementing protein 4
γH2AX	Gamma H2A histone family member X

Chapter 1. Introduction

1.1 Glioblastoma is a complex disease with unmet clinical need

1.1.1 A rare but incurable disease

Glioblastoma is the most aggressive type of brain tumour in adults, classified as a grade 4 central nervous system (CNS) tumour by the WHO (Louis et al., 2021). These tumours are characterised by necrosis, microvascular proliferation, and infiltration (Hanif et al., 2017). Glioblastoma is also the most common malignant CNS tumour in adults, accounting for 49.1% of all CNS tumours and 57.7% of gliomas (Ostrom et al., 2021). However, it remains a rare tumour in the general population, with an incidence rate of approximately 3 in 100'000 people (Ostrom et al., 2021). The incidence of glioblastoma increases with age, rising to 19 per 100'000 people aged 75-84 (Louis et al., 2021). Importantly, recent changes to the glioblastoma classification criteria may impact these statistics (Louis et al., 2021). Isocitrate dehydrogenase (IDH)-mutant tumours were previously classified as glioblastoma; however, the current standards limit glioblastoma to IDH-wildtype tumours (Louis et al., 2021).

The only confirmed risk factors for glioblastoma are age, prior exposure to radiation and rare genetic syndromes including Li Fraumeni syndrome, Lynch syndrome and Neurofibromatosis type 1 (Nf1) syndrome (Bowers et al., 2013; Rice et al., 2016). Previous studies have investigated risk factors such as alcohol consumption, diabetes mellitus, body mass index, or familial aggregation, but no clear link with glioblastoma was established (Yoshikawa et al., 2023). Glioblastoma patients commonly present with seizures, cognitive disorders, increased intracranial pressure, headaches, and personality changes (McKinnon et

al., 2021). Once glioblastoma is suspected, patients will undergo a magnetic resonance imaging (MRI) or computer tomography (CT) scan to confirm the presence of a tumour lesion, followed by a biopsy. A diagnosis of glioblastoma is confirmed when the tumour is IDH-wildtype, histone 3 (H3)-wildtype and presents with one or more of the following histological or genetic features: microvascular proliferation, necrosis, TERT mutation, EGFR amplification and gain of chromosome 7 or loss of chromosome 10 (Louis et al., 2021).

Standard treatment for glioblastoma currently includes de-bulking surgery followed by concomitant radiotherapy and chemotherapy (Stupp et al., 2005, 2009). However, for elderly patients the treatment regimen may vary from palliative treatment to aggressive surgery followed by chemoradiotherapy (Chahal et al., 2022). Temozolomide, a monofunctional alkylating agent, is the standard chemotherapy used for glioblastoma. Patients receive 75 mg/m^2 of temozolomide for 42 days starting on the same day as radiotherapy, followed by adjuvant temozolomide at 150-200 mg/m^2 for an additional six cycles (Stupp et al., 2005). The radiotherapy treatment regimen has undergone several iterations since being introduced to glioblastoma treatment in the 1940s but at present, patients will receive a fractionated dose of 60 Gy for six weeks (Baskar et al., 2012; Gzell et al., 2017; Stupp et al., 2005). Despite this multimodal treatment, the prognosis for glioblastoma is dismal, with elderly patients exhibiting the worst outcomes following treatment compared to other age groups (Ostrom et al., 2021). Glioblastoma patients inevitably experience tumour recurrence as early as seven months (Hanif et al., 2017). Moreover, the median survival time is 12-15 months, and the five-year survival rate is at approximately 7% (Hanif et al., 2017; Ostrom et al., 2021). Although glioblastoma is a rare disease in the general population, it is virtually incurable despite aggressive therapy.

1.1.2 Glioblastoma heterogeneity poses a challenge to treatment

Glioblastoma is a highly complex tumour that exhibits both inter- and intra- tumoural heterogeneity (Cancer Genome Atlas Research Network, 2008; Neftel et al., 2019; Sottoriva et al., 2013; Verhaak et al., 2010; Q. Wang et al., 2017). This complexity poses a challenge to treatment of this disease; thus, it follows that significant efforts have been made to elucidate this heterogeneity in order to advance therapeutic strategies.

Our current understanding of molecular features of glioblastoma can be attributed to the substantial efforts by the Cancer Genome Atlas Research Network which analysed whole exome, whole genome and RNA sequencing data from 206 glioblastoma patients (Cancer Genome Atlas Research Network, 2008). This work identified common genetic alterations in *PTEN, TP53, EGFR, NF1, RB1* AND *PDGFRA* (Cancer Genome Atlas Research Network, 2008). Analysing the multitude of altered genes in the patient samples revealed that three major signalling pathways were altered in 74% of all patient samples: the P53 pathway, the RTK pathway and the retinoblastoma (Rb) tumour suppressor pathway (Cancer Genome Atlas Research Network, 2008). Later, Verhaak *et al.* leveraged the TCGA dataset to identify four molecular subtypes in glioblastoma described as the classical, proneural, mesenchymal and neural subtypes (Verhaak et al., 2010).

These subtypes were associated with specific features: the classical subtype was associated with EGFR amplification and CDKN2A loss, the proneural subtype was associated with PDGFRA mutations, P53 mutations and increased oligodendrocyte-associated genes, the mesenchymal subtype was associated with NF1 and PTEN loss and finally the neural subtype

was associated with expression of neural markers such as GABRA1 and NEFL (Verhaak et al., 2010). It is important to note that the TCGA dataset included both IDH-wildtype and the IDH-mutant tumours which are no longer considered glioblastoma (Louis et al., 2021). However, it was later demonstrated that the proneural, classical and mesenchymal signatures were conserved even if the TCGA dataset is limited to IDH-wildtype tumour samples (Q. Wang et al., 2017). On the other hand, this analysis determined the neural subtype was in fact contaminant from normal brain tissue (Wang et al., 2017).

Despite the effort taken to classify glioblastoma into clinically relevant subtypes, this classification has had little impact on treatment decisions for this disease. Although initial studies linked the mesenchymal subtype with poorer patient outcomes, this observation was not conserved when glioblastoma was limited to IDH-wildtype tumours (Phillips et al., 2006; Verhaak et al., 2010; Q. Wang et al., 2017). A study assessing only IDH-wildtype glioblastoma, identified a trend towards poorer survival for patients with mesenchymal glioblastoma, however, this analysis did not reach significance (Q. Wang et al., 2017). In addition, the identification of common molecular alterations in glioblastoma has promoted investigation into targeted therapies, yet these therapies remain unsuccessful. For example, inhibition of EGFR, which is altered in at least 40% of glioblastoma patients, remains ineffective as a treatment (Cancer Genome Atlas Research Network, 2008; Darmanis et al., 2017; Pan & Magge, 2020).

The failure of therapies targeted against common molecular alterations is partly due to the high degree of intra-tumoural heterogeneity within glioblastoma. In fact, it has been shown that there is cellular heterogeneity within tumours classified as the same subtype, as will be discussed in subsequent paragraphs (Neftel et al., 2019). Studies have shown how this

heterogeneity persists not only across different regions of the tumour but also within a single region (Darmanis et al., 2017; Sottoriva et al., 2013). Sottoriva *et al.* demonstrated the transcriptional heterogeneity of samples acquired from different regions of a patient's tumour, while further work from Darmanis *et al.* revealed the potential transcriptional heterogeneity within one tumour region (Darmanis et al., 2017; Sottoriva et al., 2013).

Further single cell RNA sequencing (scRNAseq) studies have shown that this transcriptional heterogeneity is in large part driven by the expression of neurodevelopmental lineage programs (Couturier et al., 2020; Neftel et al., 2019; Patel et al., 2014; Yuan et al., 2018). Normal neurodevelopment involves the differentiation of neural stem cells towards lineage-committed progenitor cells that eventually give rise to terminally differentiated astrocytes, oligodendrocytes and neurons (Anthony et al., 2004; Kriegstein & Alvarez-Buylla, 2009; Ojalvo-Sanz & López-Mascaraque, 2021). Indeed, Neftel *et al.* identified such cellular states in glioblastoma through the scRNAseq analysis of 28 patient samples (Neftel et al., 2019). This work described four main states: a mesenchymal-like (MES) state, an astrocyte-like (AC) state, an oligodendrocyte progenitor-like (OPC) state, and a neural progenitor cell-like (NPC) state (Neftel et al., 2019). Although the MES-like state is not found within normal neurodevelopment, this state is thought to resemble reactive astrocytes (Niklasson et al., 2019; Richards et al., 2021). Reactive astrocytes are astrocytes that have undergone transcriptional and morphological changes in response to brain injury and disease (Sofroniew, 2020). Further work by Couturier *et al.* also identified these four states in glioblastoma patients, and thus the nomenclature used by Neftel *et al.* is the most commonly used to describe the different cell states within glioblastoma.

Consistent with an earlier scRNAseq glioblastoma study, Neftel *et al.* noted that some cells could not be discretely identified as a single state, instead these 'hybrid' cells pointed towards the potential for cell-state plasticity (Neftel et al., 2019; Patel et al., 2014). This plasticity was supported by the finding that cells of one cellular state gave rise to xenografts with cells distributed amongst all four cellular states (Neftel et al., 2019). The plasticity of glioblastoma is further complicated by treatment, for there is much evidence to suggest that radiotherapy can promote a shift towards the mesenchymal cell fate (Bhat et al., 2013; Halliday et al., 2014). Indeed, this cell state plasticity within glioblastoma likely serves as a hindrance to therapies targeting specific cell types.

The studies discussed above highlight that glioblastoma is a disease with multiple driver mutations and a high degree of inter- and intra-tumoural heterogeneity. The development of treatment strategies for glioblastoma must take this heterogeneity into consideration, as it is unlikely that a single approach will suffice to eradicate this disease.

1.1.3 Despite therapeutic advancements, patient outcomes have not improved

Almost two decades ago, surgery and radiotherapy were the only pillars of glioblastoma treatment. This changed when the critical Phase III clinical trial by Stupp *et al.* demonstrated that combining temozolomide with radiotherapy improved median survival from 12.1 months to 14.6 months, compared to radiotherapy alone (Stupp et al., 2005). Since the Stupp trial in 2005, there have been efforts to improve the efficacy of surgery, chemotherapy and radiotherapy in glioblastoma.

To improve the efficacy of surgery, multiple strategies have been introduced to achieve maximal safe resection, as it is well known that improving the extent of resection can improve patient survival while sparing healthy brain tissue (Lacroix et al., 2001; Oppenlander et al., 2014). For example, the use of 5-ALA, a natural precursor of haemoglobin which is metabolised by glioblastoma cells to the fluorescent metabolite protoporphyrin IX, has become an essential surgical aid (McCracken et al., 2022). 5-ALA improved the extent of tumour resection in patients and progression free survival (PFS) measured at six months (Stummer et al., 2006). However, tumour recurrence remains inevitable as surgery is unable to fully eradicate this highly invasive tumour.

The efficacy of temozolomide is currently limited by its short half-life of approximately two to three hours (Amarandi et al., 2022). Unfortunately, increasing the dose of temozolomide will lead to intolerable side-effects including nausea, fatigue and seizures. Hence, multiple strategies are being developed to improve the delivery of temozolomide into the brain. To this end, several temozolomide-liposomal formulations have been approved for phase I and II clinical trials (Amarandi et al., 2022). Despite these efforts, the impact of temozolomide remains impeded in patients with altered O6-methylguanine–DNA methyltransferase (MGMT) promoter methylation (Szylberg et al., 2022). MGMT repairs the DNA damage induced by temozolomide (Szylberg et al., 2022). Hence, temozolomide is more effective in patients where the MGMT promoter is methylated and consequently silenced (Szylberg et al., 2022). However, MGMT methylation occurs in approximately 43% of patients, thus, temozolomide remains ineffective for the majority of glioblastoma patients (Szylberg et al., 2022).

Multiple technical advancements have greatly enhanced the delivery of radiotherapy. The technological improvements to computers, software and delivery systems have allowed

for more accurate delivery of radiation to the tumour tissue whilst sparing normal tissues (Baskar et al., 2012; Hau et al., 2016). Improvements to imaging techniques such as MRI have also greatly contributed to the improvement of radiotherapy efficacy (Briere et al., 2017; Shaffer et al., 2010). For example, the use of image guided radiotherapy has been shown to significantly reduce toxic side effects in patients (Gill et al., 2011). In addition, switching from 2D whole brain radiotherapy to 3D conformal radiotherapy and eventually to intensity-modulated radiotherapy and volumetric arc radiotherapy have made significant improvements to the sparing of normal tissues (Briere et al., 2017; Shaffer et al., 2010). Although these technological advancements have improved the efficacy of radiotherapy delivery, glioblastoma patient outcomes remain dismal (Hanif et al., 2017; Ostrom et al., 2021). There are multiple reasons for the poor outcomes associated with radiotherapy which include the higher levels of hypoxia and increased invasiveness of glioblastoma (Hanif et al., 2017).

In addition to improving the current standard of treatment, novel strategies have been investigated in the last two decades including immunotherapy and targeted therapies (Carlsson et al., 2014; Preusser et al., 2011; Sulman et al., 2017). One targeted therapy that showed initial promise is Bevacizumab. It is a recombinant humanized monoclonal antibody targeting vascular endothelial growth factor (VEGF) which plays a significant role in tumour angiogenesis and is known to be upregulated in glioblastoma (Field et al., 2015; M. M. Kim et al., 2018). Initial phase II clinical trials with Bevacizumab reported increased progression free survival (PFS) in previously treated glioblastoma (Moen, 2010; Vredenburgh et al., 2007). The success of these trials resulted in the accelerated approval of bevacizumab for use in recurrent glioblastoma by the FDA in 2009. However, these results have not been reproducible in subsequent phase II clinical trials (Field et al., 2017; Taal et al., 2014). One possible

explanation for these contradictory results is the use of contrast-enhanced MRI to assess PFS. Bevacizumab's inhibition of VEGFA-mediated angiogenesis which resulted in decreased vascular permeability may have mimicked tumour shrinkage as observed by MRI scans (Kim et al., 2018). Furthermore, recent phase III clinical trials showed that Bevacizumab does not significantly extend PFS or overall survival (OS) as a first-line glioblastoma treatment (Chinot et al., 2014; Gilbert et al., 2013). Together these results demonstrate that the use of Bevacizumab is unlikely to improve glioblastoma patient outcomes.

Immunotherapy has garnered significant interest in glioblastoma with multiple checkpoint inhibitors and chimeric antigen receptor (CAR) T-cells advancing to clinical trials (Fu et al., 2023; Luksik et al., 2023). Unfortunately, current data suggests that immune checkpoint inhibitors against CTLA-4 and PD1 provide no improvement to OS or PFS (Arrieta et al., 2023; Brown et al., 2023; Omuro et al., 2023). Similarly, CAR T-cell therapies have yet to demonstrate a significant increase in survival for glioblastoma patients (Durgin et al., 2021; Goff et al., 2019; Luksik et al., 2023; O'Rourke et al., 2017). Notably, there have been CAR T-cells engineered to target common mutations in glioblastoma, such as EGFRvIII. However, these CAR-T cells have not shown a survival benefit thus far despite the frequent occurrence of EGFRvIII mutations in glioblastoma, where 25-64% of tumours have shown EGFRvIII mutations (Durgin et al., 2021; Feldkamp et al., 1999; Goff et al., 2019; Luksik et al., 2023; O'Rourke et al., 2017; Saikali et al., 2007). This is partly attributed to the high degree of heterogeneity in glioblastoma, which complicates the identification of a single target for CAR T-cell therapy (Darmanis et al., 2017; Neftel et al., 2019; Sottoriva et al., 2013; Q. Wang et al., 2017).

Despite these efforts to address the clinical challenges of glioblastoma, patient survival has seen little improvement over the past two decades. While the five-year survival rate for all malignant brain tumours increased from 23% to 36% between 1995-1997 and 2009-2015, glioblastoma only experienced a marginal increase in its five-year survival rate from 4% to 7% (Miller et al., 2021). This underscores the fact that advancements in glioblastoma outcomes lags significantly behind that of other CNS tumours. Although developing novel therapeutic strategies is crucial for improving glioblastoma treatment, this process is time-consuming. Therefore, it remains essential to optimize currently used therapies by addressing the mechanisms of treatment resistance in glioblastoma.

1.2 Glioblastoma Radiation Resistance

1.2.1 Radiotherapy in glioblastoma

Radiotherapy is the most effective treatment for glioblastoma to date, yet it is not curative. In fact, it is well established that glioblastoma is highly resistant to radiotherapy. Multiple clinical trials have reported that the 12-month PFS is approximately 9% in glioblastoma patients treated with radiotherapy alone (Stupp et al., 2005; Yin et al., 2013). Hence, it is vital that we improve our understanding of radio-resistance mechanisms in glioblastoma.

Radiotherapy acts by inducing DNA damage which eventually leads to cell death. Specifically, radiation induces multiple DNA lesions from DNA cross-linking, DNA base damage, single strand breaks (SSBs) and double strand breaks (DSBs). As the name suggests, DSBs affect both complementary strands, which poses a challenge to repairing the DNA with high fidelity (Sax, 1938). This challenge associated with repairing DSBs inevitably leads to mutations or deletions in the genome. Hence, DSBs are considered the most cytotoxic type of DNA damage (Cantoni et al., 1994; Dahm-Daphi et al., 2000). Radiation induces this DNA damage directly or indirectly. The direct transfer of energy from an ionizing radiation particle to biological tissue results in direct DNA damage (Yokoya et al., 2008). Otherwise, radiotherapy can induce DNA damage indirectly through the generation of reactive oxygen species (ROS) which are largely derived from H_2O (Yamaguchi et al., 2005). ROS are a group of highly reactive molecules and free radicals that include one oxygen atom (Bardaweel et al., 2018; Sies et al., 2022; J. Zhang et al., 2016). This group includes the free radical superoxide (O2•-) and the hydroxyl radical (OH•), and the nonradical hydrogen peroxide (H2O2). ROS have been shown to interact with the hydrogen atoms in the deoxyribose of DNA, which drives the production of

DSBs (Balasubramanian et al., 1998; Dahm-Daphi et al., 2000; Schraufstätter et al., 1988). Radiation-induced DNA damage, if left unrepaired, ultimately leads to cell death through multiple known molecular mechanisms which include apoptosis, necrosis, mitotic catastrophe, ferroptosis or pyroptosis (Boustani et al., 2019; Steel et al., 1989). In addition to these fates, radiation may result in senescence (Boustani et al., 2019; Steel et al., 1989). However, cancer cells may escape these fates through mechanisms including alterations to their DNA damage response (DDR) and DNA repair, or by becoming dormant, these factors will be discussed in greater detail in the next sections.

1.2.2 DNA Damage Response and DNA repair play a role in radiosensitivity

The DDR exists primarily to preserve genome integrity. It involves a network of protein kinases that detect DNA lesions and mediate cell cycle arrest, DNA repair, and cell death (Jackson & Bartek, 2009; Jurkovicova et al., 2022; Majd et al., 2021). Within this protein network are three master regulators of DDR; Ataxia-telangiectasia-mutated (ATM), ataxia telangiectasia and Rad3-related (ATR) and DNA-dependent protein kinase catalytic subunit (DNA-PKcs) (Blackford & Jackson, 2017). ATM and DNA-PKcs are both activated in response to DSBs, whereas ATR is activated in response to single strand DNA (ssDNA) (Blackford & Jackson, 2017).

As mentioned above, ATM is activated in the presence of DSBs through autophosphorylation at Ser1981 (Shibata & Jeggo, 2021). ATM is known to play key roles in DNA repair via mediating homologous repair (HR) and cell cycle arrest. Upon phosphorylation, ATM is recruited to the DSB site by the Mre11-Rad50-Nsb1 (MRN) complex, where ATM

subsequently phosphorylates histone H2AX at Ser139 (Burma et al., 2001). Phosphorylated H2AX (γH2AX), allows for the recruitment of mediator of DNA damage checkpoint 1 (MDC1) which is in turn phosphorylated by ATM at multiple sites (Reinhardt & Yaffe, 2009). MDC1 is a scaffold protein and its phosphorylation eventually results in the recruitment of BRCA1 to the DSB site which promotes DNA repair via Homologous repair (HR) which will be described further in the next section (Bothmer et al., 2010; Bouwman et al., 2010; Bunting et al., 2010). In addition to promoting HR, ATM exerts control over cell cycle progression through phosphorylation of Chk2 at Thr68 and through direct phosphorylation of P53 (Banin et al., 1998; Matsuoka et al., 2000).

Unlike ATM, ATR is activated by the presence of single stranded DNA (ssDNA), which can be generated during radiation and also during replication fork collapse (Thada & Cortez, 2021). ATR is constitutively bound to ATR interacting proteins (ATRIP) (Zou & Elledge, 2003). Replication protein A (RPA) coated ssDNA directly interacts with ATRIP, thus allowing for the recruitment of ATR to the ssDNA site (Zou & Elledge, 2003). Once recruited to the ssDNA site, ATR activation is completed by binding to either TOPB1 or EAAT1 (Thada & Cortez, 2021). The activated ATR then mediates cell cycle arrest in response to this DNA damage. This is primarily through ATR activation of Chk1 via phosphorylation of Ser317 and Ser345, and by the activation of P53 (H. Zhao & Piwnica-Worms, 2001).

DNA-PKcs is also activated in response to DSBs, where it may undergo autophosphorylation or phosphorylation by ATM and ATR on Thr2609 and Ser2056 (B. P. C. Chen et al., 2007; Dobbs et al., 2010). DNA-PKcs is recruited to the DSB site by interaction with Ku70 and Ku80 where it then plays a role in the initiation of non-homologous end joining (NHEJ) as will be discussed in the next section (Singleton et al., 1999). In addition to its role in

promoting NHEJ, DNA-PKcs has been shown to also mediate cell cycle arrest to some degree; Chk1 and Chk2 which have traditionally been considered targets of ATR and ATM respectively, have also been shown to be substrates of DNA-PKcs (Buisson et al., 2015; Shang et al., 2014).

As discussed above, ATM, ATR and DNA-PKcs converge on the activation of Chk1 and Chk2 to regulate cell cycle progression. Both the activated Chk1 and Chk2 then phosphorylate and consequently inhibit the Cdc25 family of phosphatases (Reinhardt & Yaffe, 2009). This phosphatase family includes Cdc25a, Cdc25b and Cdc25c which have overlapping functions to regulate cell cycle progression through the inhibition of cyclin-dependent kinases (CDKs) (Liu et al., 2020; T. Shen & Huang, 2012). In addition to the Cdc25 phosphatase family, Chk1 and Chk2 also play a role in the stabilisation of P53 which is a key regulator of cell cycle arrest and apoptosis (X.-P. Zhang et al., 2011).

It is well known that P53 activation is a key component of the DDR (Abuetabh et al., 2022). There is continuous turnover of P53 in the cell at baseline, hence, upon the presence of DNA lesions, the DDR kinases upstream of P53 aim to activate it mainly through disrupting its interaction with murine double minute 2 (MDM2) (Sherr & Weber, 2000). MDM2 negatively regulates P53 by blocking its transactivation of target genes and by promoting its degradation (Sherr & Weber, 2000). Activated P53 can translocate to the nucleus to mediate cell cycle arrest through the upregulation of CDK inhibitor p21 (Abuetabh et al., 2022). However, in the extended presence of DNA damage, P53 is phosphorylated on Ser46 which allows it to promote apoptosis through upregulation of proapoptotic genes including *PUMA* and *BAX* (Abuetabh et al., 2022; X.-P. Zhang et al., 2011).

As previously mentioned, the DDR mediates the activation of different DNA repair pathways in response to radiation. There are three DSB repair pathways that may be activated: HR, NHEJ and microhomology mediated end joining (MMEJ).

1.2.2.1 Homologous Recombination Repair

HR is a DSB repair pathway that uses a complementary sister chromatid as a template for repair (Ciccia & Elledge, 2010; Fugger & West, 2016). The use of a template during HR is considered advantageous as it may allow for repair with higher fidelity (Ciccia & Elledge, 2010; Fugger & West, 2016). The essential need for a DNA template limits HR activity to the S and G2 phases of the cell cycle where a sister chromatid would be available (Mao et al., 2008; Rothkamm et al., 2003). BRCA1 plays a role in HR initiation by interfering with the binding or activity of P53-binding protein 1 (53BP1) to the DSB site (Bothmer et al., 2010; Bouwman et al., 2010; Bunting et al., 2010). Briefly, 53BP1 is rapidly recruited to DSB ends which prevents end resection, a process where the 5' ends of broken DNA are degraded to create 3' overhangs necessary to initiate HR (Bothmer et al., 2010; Bouwman et al., 2010; Bunting et al., 2010). Indeed, BRCA1 interferes with 53BP1 activity and contributes to the recruitment of the MRN complex to initiate HR (Bothmer et al., 2010; Bouwman et al., 2010; Bunting et al., 2010). Specifically, the initial 5’ to 3’ end resection is mediated by Mre11 endonuclease activity, which is then continued by Exo1 or WRN (Cejka & Symington, 2021; Garcia et al., 2011; Gnügge & Symington, 2021). The exposed ssDNA is coated and thus stabilised by RPA (Cejka & Symington, 2021; Gnügge & Symington, 2021). Eventually, the RPA is replaced by Rad51. This ssDNA-Rad51 nucleoprotein filament will perform the single strand invasion of the

homologous template and identify the homologous sequence to form a branched nucleic acid structure called a Holliday junction (Ciccia & Elledge, 2010; Smith et al., 2010; Cejka & Symington, 2021; Gnügge & Symington, 2021). HR is then completed with subsequent DNA synthesis, ligation and resolution of the Holliday junction (Ciccia & Elledge, 2010; Mao et al., 2008; Smith et al., 2010).

1.2.2.2 Non-Homologous End Joining (NHEJ)

NHEJ is considered a rapid template-free mechanism of DSB repair (Gauss & Lieber, 1996; Karanam et al., 2012). Whilst NHEJ is considered the fastest type of DNA repair, its template-free repair mechanism may allow for loss of DNA pairs following a DSB (Gauss & Lieber, 1996; Karanam et al., 2012). NHEJ is active throughout interphase, however, it is commonly superseded by HR in the S and G2 phases of the cell cycle (Karanam et al., 2012; Mao et al., 2008; Rothkamm et al., 2003). As discussed above, this choice in DSB repair pathway is mediated through BRCA1 displacement of 53BP1 (Bothmer et al., 2010; Bouwman et al., 2010; Bunting et al., 2010). NHEJ is initiated with the rapid binding of Ku70 and Ku80 to the two ends of the DSB, effectively stabilising the ends to prevent resection (Mari et al., 2006). The Ku proteins then recruit DNA-PKcs and Artemis to the DSB site (Gottlieb & Jackson, 1993). Once at the DSB site, DNA-PKcs is activated through autophosphorylation or phosphorylation by ATM and ATR as mentioned above (B. P. C. Chen et al., 2007; Dobbs et al., 2010). The activated DNA-PKcs will then activate the endo/exonuclease activity of Artemis which may remove any DNA overhangs to prepare two blunt ends for joining (Goodarzi et al., 2006; Soubeyrand et al., 2006). Once two blunt ends have been generated, the XRCC4 and DNA ligase IV complex then

mediates joining of the blunt ends of the DNA duplex (Groelly et al., 2023; Lord & Ashworth, 2012).

1.2.2.3 Microhomology-mediated end joining (MMEJ)

MMEJ, a type of alternative end joining, is mechanism of DNA repair that utilises microhomologies to repair DSBs. PARP1 plays a role in promoting MMEJ by competing with Ku70 and Ku80 to bind to DSB ends (Cheng et al., 2011; M. Wang et al., 2006). It is proposed that MMEJ involves five main steps: resection at the DSB ends, annealing of the microhomologous region, removal of heterologous flaps, DNA synthesis and ligation (Sfeir & Symington, 2015; H. Wang & Xu, 2017). It is proposed that the MRN complex, initiates the end resection in MMEJ, as it does in HR (Cejka & Symington, 2021; Garcia et al., 2011; Gnügge & Symington, 2021). However, in MMEJ the end resection is limited to less than 20 base pairs (Cejka & Symington, 2021; Garcia et al., 2011; Gnügge & Symington, 2021). The next step is annealing of the microhomology regions, which is not fully understood. The annealing step generates non-homologous flaps which must be subsequently removed. The XPF-ERCC1 complex was initially presumed to mediate the flap removal step, however, more recent evidence suggests that FEN1 is more relevant to this step of MMEJ (Ma et al., 2003; Sharma et al., 2015). Once the flaps have been removed, the gaps in the DNA strands are filled in by the DNA polymerase theta (POLθ), also known as POLQ (Ceccaldi et al., 2015; Mateos-Gomez et al., 2015). Interestingly, POLθ is also thought to promote MMEJ by interfering with Rad51 binding of ssDNA (Ceccaldi et al., 2015). In addition, POLθ is known to be a polymerase with low fidelity, thus MMEJ is considered more mutagenic than HR or NHEJ (Ceccaldi et al., 2015;

Mateos-Gomez et al., 2015). Finally, MMEJ is completed with ligation by DNA Ligase I or III (Sfeir & Symington, 2015; H. Wang & Xu, 2017).

1.2.3 DNA Damage Repair is altered in cancer – a risk and an opportunity

Given that the DDR and DNA repair exist to maintain genome integrity, it follows that aberrations to these mechanisms may be associated with cancer incidence and radiotherapy resistance. It is well-known that mutations in two key players in HR, BRCA1 and BRCA2 are linked to the development of breast cancer and ovarian cancer (Arun et al., 2024). The prevalence of BRCA mutations in patients with breast cancer and ovarian cancer are approximately 4% and 14%, respectively (Alsop et al., 2012; Armstrong et al., 2019). However, the presence of a BRCA mutation increases the risk of developing breast or ovarian cancer up to approximately 70% and 40%, respectively (Kuchenbaecker et al., 2017). In addition to breast and ovarian cancer, mutations in BRCA genes have also been identified in glioblastoma, lung adenocarcinoma and colorectal cancer (M.-N. Lee et al., 2007; Meimand et al., 2022; Narod & Salmena, 2011; Sopik et al., 2015). Furthermore, multiple studies have reported increased cancer incidence in association with mutations in ATM and ATR, which are both central players of the DDR (M. Choi et al., 2016; Lecona & Fernandez-Capetillo, 2018; Weber & Ryan, 2015). In addition to these central DDR protein kinases, several studies have identified aberrations in the NHEJ and HR DSB repair pathways in multiple solid tumours. One study showed that mutations in XRCC5 and XRCC6, which encode the essential NHEJ proteins Ku70 and Ku80, are associated with increased risk of brain cancer (Willems et al., 2008). In addition,

XRCC5 was also found to be silenced in approximately 32% of squamous cell carcinomas (M.-N. Lee et al., 2007). The more recently characterized MMEJ pathway for DSB repair is thought to have increased activity in cancers; multiple studies report increased expression of POLθ, an essential polymerase in MMEJ, in cancers compared to normal tissue (Ceccaldi et al., 2015; Mateos-Gomez et al., 2015). There is further evidence that MMEJ activity is upregulated in HR deficient tumours (H. Wang & Xu, 2017; Zatreanu et al., 2021). These studies collectively highlight the multitude of aberrations that may occur in the DDR in association with cancer.

Building on this point, there are also multiple studies highlighting DDR and DNA repair aberrations specifically in glioblastoma. For example, the P53 pathway is disrupted in at least 70% of glioblastomas, given the role of P53 in mediating radiation-response, alterations to this pathway may contribute to the radio-resistance of this cancer (Cancer Genome Atlas Research Network, 2008). However, it is important to note that genomic assays are not the best indicator for alterations in DDR activity given that post-translational phosphorylation events play a key role in the activation of DDR. Additionally, glioma stem cells may have increased activity of DDR and DNA repair, work by Bao *et al.* showed that CD133+ glioma stem cells exhibit faster DNA repair compared to their CD133- counterparts (Bao *et al.*, 2006). Indeed, there is evidence that glioma stem cells exhibit increased activation of ATM, Chk1 and Chk2 following radiation (Bao et al., 2006; W. Zhou et al., 2013). This finding highlights the role of increased DDR and DNA repair activity in the radio-resistance of the glioma stem cell population. In addition, there is some evidence to suggest that NHEJ activity may be upregulated in glioblastoma (T. Lan et al., 2016; Y. Wang et al., 2018). Lan *et al.* showed that DNA-PK activation is increased in glioblastoma compared to both lower grade gliomas and normal tissue in human patient samples (T. Lan et al., 2016). Whilst one may speculate this was due to higher levels of DNA

damage in glioblastoma, this study found no significant differences in the levels of γH2AX between glioblastoma and the lower grade gliomas (T. Lan et al., 2016). Additionally, increased levels of DNA-PK are associated with poor survival outcomes in glioblastoma which points towards its role in treatment resistance (Migliozzi et al., 2023). Together these studies highlight the potential for alterations in DDR and DNA repair to impact glioblastoma treatment. However, glioblastoma exhibits high intra- and inter-tumoural heterogeneity (See Chapter 1.1.2). It is therefore important to understand differences in DDR and DNA repair alterations within the multiple cellular and proliferative states of glioblastoma.

While alterations to the DDR and DNA repair can attenuate the impact of cancer treatment, these alterations may also serve as vulnerabilities that can be targeted to enhance therapy response. To this end, several inhibitors of the DDR have been developed and provided benefit to cancer patients. The most clinically advanced inhibitors of DDR are PARP inhibitors. Olaparib was the first PARP inhibitor approved for clinical use in 2014 resulting in improved PFS in BRCA-mutated ovarian cancer (Ledermann, 2016; Morganti et al., 2024). Several PARP inhibitors have been approved since then including talazoparib, rucaparib and niraparaib. Additionally, the efficacy of PARP inhibitors for glioblastoma patients have been recently assessed through the PARADIGM trial (Derby et al., 2024). The results of this phase I clinical trial highlight that Olaparib when combined with radiotherapy was tolerable in glioblastoma patients (Derby et al., 2024). Although ATM inhibitors are not as clinically advanced as PARP inhibitors, there are currently two ATM inhibitors in phase I/II clinical trials: AZD0156 (NCT02588105) and AZD1390 (NCT03423628). Interestingly, AZD1390 was specifically designed to have high penetrance of the blood brain barrier (BBB) and is currently in phase I clinical trial for newly diagnosed and recurrent glioblastoma (NCT03423628). Currently, the

results show AZD13390 was well-tolerated in glioblastoma patients (NCT03423628). Similar to ATM inhibitors, ATR inhibitors are currently in development with several inhibitors in clinical trials including berzosertib, ceralasertib, gartisertib (Burris et al., 2024; Javed et al., 2024; S. T. Kim et al., 2021). The phase I clinical trial for berzosertib was recently concluded, showing that the drug is tolerable when given with combined chemoradiation in oesophageal cancer (Javed et al., 2024). Additionally, several DNA-PK inhibitors are currently in phase I/II clinical trials including AZD7648 (NCT03907969). Multiple inhibitors are in development to target MMEJ through inhibition of POLθ; novobiocin (NCT05687110) and ART-558 (Rodriguez-Berriguete et al., 2023; J. Zhou et al., 2021). ART-558 has shown promise of successfully inhibiting POLθ in HCT116, H460 and T24 cells (Rodriguez-Berriguete et al., 2023; J. Zhou et al., 2021). Together the increasing number of DDR inhibitors in development and the clinical success of PARP inhibition in HR deficient cancers highlight the potential of targeting the DDR and DNA repair in improving radiotherapy efficacy.

1.3 Tumour Cell Dormancy: a source of radiotherapy resistance

1.3.1 Defining the slowly dividing population of cells in glioblastoma

The concept of tumour cell dormancy was initially developed to explain the long periods of tumour remission observed before eventual recurrence (Hadfield, 1954). These periods of remission lasted years and in some cases decades, suggesting that any surviving or disseminated tumour cells were in a state of deep cell cycle arrest (Hadfield, 1954; Sosa et al., 2014; Yeh & Ramaswamy, 2015). In 1954, based on the long periods of remission he observed in solid tumours such as breast cancer, Hadfield defined dormant tumour cells as a state of reversible cell cycle exit into a G0 or extended G1 cell cycle phase (Hadfield, 1954). Since dormancy was first defined, multiple terms have emerged that describe populations overlapping with dormant tumour cells. In fact, they are often used interchangeably which adds confusion to what we define as dormant cells. These additional terms include tumour mass dormancy, senescence, quiescence and cancer stem cells. To precisely define dormancy, it is important to understand dormant tumour cells in the context of these similar yet distinct terms.

Importantly, tumour cell dormancy is distinct from tumour mass dormancy, where the tumour mass remains stable through the balance of tumour cell proliferation and cell death (Aguirre-Ghiso, 2007). Dormancy is also distinct from senescence. Traditionally, senescence referred to the irreversible cell cycle arrest associated with phenotypical changes known as the senescence associated phenotype. However, current views on senescence in cancer now suggest that it is not strictly irreversible, which may impact our definition of dormancy in future

(Reimann et al., 2024). Additionally, quiescence, like dormancy, is a term that describes a reversible exit into the G0 or extended G1 phase of the cell cycle. Whilst this definition is consistent with dormancy, quiescence is more often used in the context of normal physiology as opposed to cancer. Unfortunately, both quiescence and dormancy are not clearly defined in literature and are often used interchangeably.

In addition, the concepts of dormancy and cancer stem cells (CSCs) are often conflated in cancer biology research. CSCs are a population of tumour cells with stem-like properties such as treatment resistance, the expression of stemness markers, the capacity to self-renew and the ability to initiate new tumours (Aguirre-Ghiso, 2007; Dick, 2005; Singh et al., 2004; Sosa et al., 2014). CSCs were first described in acute myeloid leukaemia by Dick *et al.* where they reported that CSCs marked as CD34+CD38- were more capable than non-CSCs of initiating new tumours when injected into immunodeficient mice compared to that of non-CSCs (Bonnet & Dick, 1997; Dick, 2005). The CSC would later be described in glioblastoma by Singh *et al.* who identified glioma stem cells (GSCs) from glioblastoma using the marker CD133 (Singh et al., 2004). CSCs and dormant tumour cells both describe populations of cells that are likely treatment resistant, which is likely why they are often conflated in literature. However, while they may describe overlapping populations, dormant tumour cells are distinct from CSCs.

There are multiple studies in glioblastoma that describe a dormant stem-like population, however, the dormant and stem-like populations in glioblastoma are not always identical. Early label retention studies using glioblastoma patient-derived lines identified dormant populations that were enriched for stem associated markers such as SOX2 (Deleyrolle et al., 2011; Richichi et al., 2013). Additionally, Deleyrolle *et al.* showed functionally through *in vivo*

limiting dilution assays that the dormant or slow-cycling population of glioblastoma had increased tumorigenic potential compared to their faster cycling counterparts (Deleyrolle et al., 2011). This suggests that the dormant or slow-cycling population identified in this study was stem-like (Deleyrolle et al., 2011). However, subsequent label retention studies using patient-derived glioblastoma cell lines identified dormant populations that were not enriched for stem-like markers (Campos et al., 2014; Tejero et al., 2019). Yang *et al*. found that some but not all slow-cycling glioblastoma cells, identified using a label retention dye, expressed stemness markers such as CD133, CD44 or SOX2 as demonstrated by flow cytometry (C. Yang et al., 2022). Together these studies suggest that the dormant population in glioblastoma consists of both stem-like and non-stem-like cells.

As discussed above, there are multiple terms that overlap with dormancy. This confusion about what constitutes dormancy may stem from the fact that there is no strict empirical definition for dormancy in literature. Indeed, a variety of methods are used to describe dormant tumour cells. Multiple markers have been used to identify dormant tumour cells at a fixed timepoint. One key marker is the absence of Ki67, which is often used to define cells that have exited the cell cycle, and are thus considered dormant cells (Uxa et al., 2021). Interestingly, in glioblastoma only 15-20% of patient tumour cells have been reported as Ki67+, yet despite this, the absence of Ki67 is still considered a marker of dormant cells in glioblastoma (Louis et al., 2016). Reporter systems have also been used, for example the Parada group developed a mouse model to identify stem-like cells using *Nestin*, a well-established stemness marker (J. Chen et al., 2012; Xie et al., 2022). This mouse model labelled *Nestin* positive tumour cells with GFP (J. Chen et al., 2012; Xie et al., 2022). Parada *et al*. found this GFP+ stem-like population rarely stained for Ki67 and they suggest this stem-like

population was dormant (J. Chen et al., 2012; Xie et al., 2022). Additionally, dormant cells have been identified based on gene expression data (X. Lan et al., 2017). Whilst these methods are commonly used, they do not describe the length of time the tumour cells have been arrested. In this regard, label retention methods such as the inducible GFP tagged histone 2B (H2B-GFP) system may provide more information. Garcia-Diaz *et al.* utilised a doxycycline-induced H2B-GFP system in mouse models of glioblastoma to identify a slow-cycling population of tumour cells *in vivo* (Garcia-Diaz et al., 2023). Here administration of doxycycline induced expression of H2B-GFP, which was incorporated into chromatin. Once doxycycline was removed, the faster-cycling cells diluted out their H2B-GFP whereas the slower-cycling dormant cells retained H2B-GFP (Garcia-Diaz et al., 2023). This study allowed two weeks for the H2B-GFP to be diluted out by actively proliferating tumour cells *in vivo* (Garcia-Diaz et al., 2023). In effect, the population with high levels of H2B-GFP was likely enriched for dormant tumour cells. However, this H2B-GFP high population may have also contained tumour cells that are comparatively more slowly dividing than their more proliferative H2B-GFP counterparts. Should the dilution period be extended, these slowly dividing tumour cells would be excluded from the identified H2B-GFP high dormant population. Indeed, the time for label dilution remains in the researcher's discretion. This is to say that across literature there is no strict definition for what constitutes tumour cell dormancy. It is unknown exactly how long the dormant population within a tumour remains in cell cycle arrest or what controls the shift between proliferation and dormancy. Taking this into consideration, it is understandable why dormancy is a term used broadly and likely describes a heterogenous population. Indeed, the dormant cells identified by the studies discussed above cannot be distinguished from non-proliferating tumour cells. Nevertheless, studies based on the methods described above

suggest only a small proportion of glioblastoma cells are dormant (Garcia-Diaz et al., 2023; Tejero et al., 2019; Xie et al., 2022).

1.3.2 Tumour cell dormancy is promoted by multiple signalling pathways

Current literature suggests that there are multiple pathways which may regulate dormancy in glioblastoma. These pathways include BMP signalling, TGFβ signalling, IFNγ signalling and hypoxia (Carén et al., 2015; Du et al., 2017; Garcia-Diaz et al., 2023; Hofstetter et al., 2012; Sachdeva et al., 2019; Tejero et al., 2019).

1.3.2.1 Bmp signalling

Bone morphogenetic proteins (BMPs) are members of the transforming growth factor-β (TGFβ) superfamily of proteins. A total of 15 different BMPs have been identified. BMPs are so called for their role in bone formation (Heubel & Nohe, 2021). However, BMPs have been shown to play diverse roles in different organ systems, including vascular remodelling, tissue repair and dormancy regulation (Gomez-Puerto et al., 2019; R. N. Wang et al., 2014). Specifically in the brain, BMPs have dynamic effects throughout the development of the CNS, they are also thought to play a role in maintaining neural stem cell niches, and in plasticity following brain disease or injury (Bond et al., 2012; Cole et al., 2016; Jensen et al., 2021).

BMPs can signal through both canonical and non-canonical pathways. In the canonical signalling pathway, BMPs are known to interact with dimeric receptor complexes, usually type I and type II serine/threonine kinases. The four type I receptors known to bind BMPs include

type 1A BMP receptor (BMPR-1A or ALK3), type 1B BMP receptor (BMPR-1B or ALK6), activin receptor like kinase 1 (ACVRL1 or Alk1) and type 1A activin receptor (ActR-1A or ALK2) (Al-Sammarraie & Ray, 2021; Gomez-Puerto et al., 2019). There are three type II receptors that bind BMPs: type 2 BMP receptor (BMPR-2), type 2 activin receptor (ActR-2A), and type 2B activin receptor (ActR-2B) (Al-Sammarraie & Ray, 2021; Gomez-Puerto et al., 2019). BMP interaction with its type I and II serine/threonine receptors induces phosphorylation and thus activation of SMAD1/5/8 (Al-Sammarraie & Ray, 2021; Gomez-Puerto et al., 2019). The phosphorylated SMAD1/5/8 will form a complex with SMAD4 and co-translate to the nucleus to induce transcription of BMP target genes (Gomez-Puerto et al., 2019; R. N. Wang et al., 2014). Several SMAD independent, non-canonical BMP signalling pathways have been identified; there is evidence that BMP signalling can result in the activation of the MAPK, PI3K/Akt, and Rho-GTPase pathways (Gomez-Puerto et al., 2019).

There is evidence to suggest that BMP signalling may play a role in inducing dormancy in glioblastoma. It has been shown in normal neural stem cells that inhibition of BMP signalling *in vivo* leads to a two-fold increase in the percentage of neural stem cells in S-phase (Mira et al., 2010). Additionally, 72 hrs of BMP4/FGF treatment is an established method for inducing cell cycle arrest in normal neural stem cells and patient derived glioblastoma lines (Blomfield et al., 2019; Sachdeva et al., 2019). However, the role of BMP4 signalling in inducing dormancy has yet to be assessed *in vivo* in glioblastoma. BMP4/FGF-treatment for 72 hrs has previously been shown to maintain stemness in neural stem cells (Y. Sun et al., 2011). In addition to the role of BMP4 in maintaining stemness, BMP4 signalling is also associated with astrocyte differentiation of both neural stem cells and GSCs (Carén et al., 2015; Cole et al., 2016; Han, Cai, et al., 2022; Pollard et al., 2009a). Although these studies treated cells with BMP4 without

FGF for up to two weeks which may account for the conflicting reports from Sun *et al.* (Y. Sun et al., 2011).

1.3.2.2 TGFβ signalling

TGFβ, like BMPs, is part of the TGFβ superfamily of proteins. In normal physiology, TGFβ is known to play a role in cell proliferation, differentiation, wound healing and even immune responses (Morikawa et al., 2016). Multiple functions have been described for TGFβ in the brain including synaptic plasticity and ischemia-related injury response (Caraci et al., 2015; Dobolyi et al., 2012).

There are three isoforms of TGFβ; TGFβ1, TGFβ2 and TGFβ3. Usually, each TGFβ forms a homodimer, however, there is evidence that TGFβ heterodimers may form (Derynck et al., 2021). TGFβ will bind and activate a combination of type I and II serine/threonine receptor kinases, specifically TβRI and TβRII. This results in the phosphorylation and thus activation of SMAD2 and SMAD3. The activated SMADs will translocate to the nucleus with SMAD4 to induce the transcription of TGFβ target genes. Similarly to BMP signalling, TGFβ can also activate SMAD-independent pathways such as PI3k-Akt, MAPK and Rho-GTPase signalling pathways (Derynck et al., 2021). The overlapping signalling pathways of TGFβ and BMP4 suggests there may be redundancy between these two pathways.

TGFβ signalling has also been implicated in regulating dormancy. Tejero *et al.* used a TGFβ inhibitor to decrease the fraction of dormant glioblastoma cells *in vitro*, suggesting it plays a role in tumour cell dormancy (Tejero et al., 2019). However, Sachdeva *et al.* showed that TGFβ1 treatment results in an almost two-fold increase in proliferation of GSCs (Sachdeva

et al., 2019). The precise contribution of this pathway to dormancy in glioblastoma requires further investigation.

1.3.2.3 IFN signalling

The interferons (IFN) are a family of pro-inflammatory cytokines that can be divided into two classes; type I (IFN-α, IFN-β and IFN-ω) and type II (IFNγ) (Jorgovanovic et al., 2020; Platanias, 2005). The type I interferons bind to the type I IFN receptor, whereas IFNγ, the sole type II interferon, binds the type II interferon receptor (Platanias, 2005). Binding of IFN to their respective receptors leads to activation of the JAK/STAT signalling pathway (Platanias, 2005). This leads to an increase in the transcription of IFN stimulated genes. IFNs may also lead to the activation of the MAPK and PI3K signalling pathways (Platanias, 2005).

There is much evidence to suggest that IFN signalling plays a role in regulating dormancy. In normal neural stem cells, IFNβ treatment is sufficient to decrease proliferation (Carvajal Ibañez et al., 2023). Whilst in glioblastoma, the effect of IFN treatment on proliferation has been demonstrated in multiple *in vitro* studies (Du et al., 2017; Garcia-Diaz et al., 2023; Garrison et al., 1996; Han, Jin, et al., 2022; Happold et al., 2014; Kominsky et al., 1998). For example, Han *et al.* showed that treating patient-derived tumour cells with IFNβ resulted in the downregulation of genes associated with cell cycle progression such as cyclin A2, cyclin B1 and cyclin B2 (Han et al., 2022). In addition, Du *et al.* showed that IFNα treatment *in* vitro impacts spherogenicity of the patient-derived tumour cells (Du et al., 2017). Furthermore, Garcia-Diaz *et al.* identified a slow-cycling population with increased IFN signalling, which they described as injured NPC like dormant cells (Garcia-Diaz et al., 2023). Importantly, T-cells are known to be an important source of IFN; Garcia-Diaz *et al.* showed

significant co-localisation of the T-cells with GFP-high dormant tumour cells (Garcia-Diaz et al., 2023). Additionally, they showed that co-culture of freshly isolated tumour cells with freshly isolated T-cells, activated with CD28 reduced proliferation of the tumour cells (Garcia-Diaz et al., 2023).

1.3.2.4 Hypoxia

Hypoxia occurs when oxygen levels are lower than normal tissue levels. The effects of hypoxia are mediated through transcription factors called hypoxia inducible factors (HIFs). There are two classes of HIFs: HIFα which is normally targeted for degradation but is stabilised with hypoxic conditions, and HIFβ which is constitutively expressed and localised to the nucleus (Butturini et al., 2019). In hypoxic conditions the stabilised HIFα will translocate into the nucleus to dimerize with HIFβ (Butturini et al., 2019). This complex will promote the transcription of genes associated with invasion, metabolism, angiogenesis and cell growth (Butturini et al., 2019).

Hypoxia is another potential factor involved in tumour dormancy in glioblastoma. Tejero *et al*. used a H2B-GFP label retention system to identify slow-cycling cells in their patient derived tumour organoids; using this system they showed through gene set enrichment analysis (GSEA) of the proliferating versus slow-cycling cells that hypoxia is significantly upregulated in slow-cycling cells (Tejero et al., 2019). They validated this by showing the colocalization of HIF1α with the slow-cycling H2B-GFP high tumour cells. Additionally, they demonstrated a role for hypoxia in inducing tumour cell dormancy through culturing organoids in hypoxic (3% O2) conditions for one week which resulted in an increase in the fraction of the

dormant H2B-GFP high cells (Tejero et al., 2019). Furthermore, Hofstetter *et al.* demonstrated that culturing of patient-derived glioblastoma tumour cells in hypoxic conditions, 1% O2, leads to an increase in cyclin G2 expression and reduced proliferation as measured by BrdU incorporation (Hofstetter et al., 2012).

Although there is evidence that BMP, TGFβ and IFN signalling promote dormancy, this conflicts with the idea that these signalling pathways activate the PI3K and MAPK pathways which are often associated with the promotion of cell growth and proliferation (Braicu et al., 2019; Shaw & Cantley, 2006). However, as evident through the highly diverse functions of the BMP BMP, TGFβ and IFN signalling throughout normal physiology, the outcome of the activation of these pathways is highly regulated by a balance of different signalling cascades. For example, BMP4 has also been shown to promote differentiation in rat neural stem cells and in glioblastoma cells, however, when these cells are cultured with BMP4 and FGF, their differentiation is inhibited (Pollard et al., 2009a; Y. Sun et al., 2011). This highlights that the impact of these pathways on cell physiology is under tight regulation. Additionally, it suggests that multiple signals may be required to induce dormancy.

Furthermore, the multiple potential signals involved in inducing dormancy suggest that there are likely multiple dormant states. This idea is explored by Coller *et al.* in normal fibroblasts where different methods of inducing quiescence, contact inhibition, growth factor removal or loss of adhesion, confirmed with a reduction to <1% of BrdU incorporation, resulted in unique transcriptional changes associated with the different methods of inducing quiescence (Coller et al., 2006). These included unique alterations in genes that were associated with similar processes including lipid metabolism or RNA metabolism. In addition, multiple scRNAseq studies suggest that the dormant population in glioblastoma is comprised

of cells in different states (Garcia-Diaz et al., 2023; Neftel et al., 2019). Further work is necessary to define the multiple dormant states in glioblastoma and how they could exhibit unique responses to treatment.

1.3.3 Dormant tumour cells are linked to radio-resistance

In addition to alterations in the DDR and DNA repair discussed in chapter 1.2.2, tumour cell dormancy is yet another source of radiotherapy resistance. Traditionally, radiotherapy is thought to preferentially target tumour cells due to their rapid and uncontrolled proliferation. Specifically, the combination of rapid cell cycle progression and dysfunctional cell cycle checkpoints in proliferating tumour cells leaves little time for efficient and high-fidelity DNA repair. Consequently, the extended presence of unrepaired DNA damage may activate multiple cell death mechanisms (Abuetabh et al., 2022; Y. Zhou et al., 2021). Furthermore, should these actively proliferating tumour cells pre-maturely enter mitosis with unrepaired DNA, they may experience failure or aberrations of mitosis that result in mitotic catastrophe, and eventual cell death of the non-clonogenic progeny (Chan et al., 1999; Vakifahmetoglu et al., 2008). Given this context, it is commonly thought that dormant tumour cells, which have reversibly exited the cell cycle, would survive radiotherapy (Aguirre-Ghiso, 2007; Hadfield, 1954; Sosa et al., 2014).

It is thus surprising that only a handful of studies have directly demonstrated the radio-resistance of the dormant population in glioblastoma *in vitro* (Sachdeva et al., 2019; Tejero et al., 2019). It has been shown that dormant patient-derived tumour cells, identified based on label retention methods, were radio-resistant *in vitro* (Tejero et al., 2019). In addition,

BMP4/FGF-treatment, which induced dormancy in patient-derived tumour cells, was shown to be protective against combined treatment with temozolomide (25 μM) and 5 days of 2 Gy radiation (Sachdeva et al., 2019). Sachdeva *et al*. highlight that tumour cells treated with BMP4 and FGF are resistant to both temozolomide and radiotherapy, however, it is known that temozolomide-induced cell death is dependent on cell division. Thus, it would be interesting to specifically assess the radioresistance of tumour cells treated with BMP4 and FGF. Furthermore, there is also evidence that BMP4 and FGF play a role in promoting stemness in both non-tumour and tumour cells (Mira et al., 2010; Pollard et al., 2009b; Y. Sun et al., 2011). Thus, it is possible that the treatment resistance exhibited by tumour cells may be due to increased levels of stemness as well as their dormant state. Indeed, there is much evidence to suggest that stem-like tumour cells are resistant to chemotherapy and radiotherapy (Bao et al., 2006; J. Chen et al., 2012; Xie et al., 2022). These studies collectively highlight the radio-resistance of the dormant population within glioblastoma, however, the mechanisms of dormant cell survival following radiotherapy have yet to be elucidated.

In contrast to dormant cell radio-resistance, the chemoresistance of the dormant population in glioblastoma is well studied *in vitro* and *in vivo*. A series of *in vitro* studies have shown that dormant patient-derived tumour cells, identified using label retention methods, are resistant to temozolomide (Campos et al., 2014; Garcia-Diaz et al., 2023; Hoang-Minh et al., 2018; Tejero et al., 2019). These findings are also supported by multiple *in vivo* mouse studies (J. Chen et al., 2012; Hoang-Minh et al., 2018; Xie et al., 2022).

Another potential challenge dormant tumour cells pose to glioblastoma treatment is that they may be capable of invading the surrounding tissue. One study has shown that dormant patient-derived tumour cells, identified using label retention methods, have

increased expression of tenascin C and fibronectin-1, both of which are associated with invasiveness (Tejero et al., 2019). Additionally, Hoang-*Minh et al.* also showed that patient-derived dormant cells have increased motility *in vitro* and that upon re-injection orthotopically, these dormant cells are more capable of infiltrating the surrounding tissue than faster-cycling cells (Hoang-Minh et al., 2018). However, the dormant population may be heterogenous as discussed above, and thus different cell states may yet exhibit different levels of invasiveness. Indeed, Garcia *et al.* described how dormant tumour cells, whose cell cycle arrest was mediated by IFNγ, exhibited decreased migration *in vitro* (Garcia-Diaz et al., 2023). Nonetheless, the possibility that dormant tumour cells may infiltrate the surrounding tissue means they are unlikely to be removed by debulking surgery. Given the treatment resistance of the dormant population, they are thus likely to persist following standard treatment.

Not only is the dormant population linked to treatment resistance, but it is also thought to contribute to tumour recurrence in glioblastoma (Campos et al., 2014; J. Chen et al., 2012; Xie et al., 2022). The Parada group have demonstrated in *de novo* mouse models of glioblastoma and patient-derived xenografts that stem-like dormant cells are capable of re-activating following temozolomide treatment (J. Chen et al., 2012; Xie et al., 2022). Interestingly, work from Campos *et al.* using patient-derived cells suggests that the re-activation of dormant cells can be regulated by interactions with faster-cycling cells *in vitro* (Campos et al., 2014). Campos *et al.* demonstrated that dormant patient-derived cells, identified using label retention methods, proliferated when cultured in isolation but this was inhibited when they were co-cultured with faster-cycling cells (Campos et al., 2014). This implies that if the proliferating population were eliminated, the dormant cells may re-activate and thus

contribute to tumour recurrence. Together, these studies emphasize that the dormant tumour population poses a significant challenge to glioblastoma therapy.

1.3.4 Current strategies to target dormant tumour cells

There is strong evidence to suggest that tumour cell dormancy poses a challenge to cancer treatment; dormant tumour cells likely play a role in tumour recurrence and are resistant to current anti-proliferative therapies. Hence, targeting this tumour population could yield significant improvement to patient outcomes. Following this, multiple strategies to target dormant tumour cells are currently being developed.

One strategy is to re-activate the dormant tumour cells in the hopes of making them more sensitive to anti-proliferative therapy such as radiotherapy (Essers & Trumpp, 2010). In the context of haematological malignancies, cytokines such cytokines such as IFNα and granulocyte-colony stimulating factor as well as arsenic trioxide have been shown to induce the proliferation of dormant tumour cells, leading to an improvement in chemotherapy efficacy (Essers & Trumpp, 2010). Additionally, inhibition of TGFβ signalling may be a potential method of inducing cell-cycle re-entry. In breast cancer, treatment with the TGFβ agonist Coco, lead to the re-activation of dormant tumour cells (Gao et al., 2012). However, re-activating the dormant tumour cells may provide more risk than benefit to patients as anti-proliferative therapies such as chemotherapy and radiotherapy are unlikely to fully eradicate all proliferating tumour cells.

On the other hand, another potential strategy to tackle tumour cell dormancy is in fact to maintain dormancy indefinitely. Touny *et al.* showed that the inhibition of src family kinase

(SFK) signalling and MAPK signalling in a dormant breast cancer cell line prevents their re-activation (Touny et al., 2014). Importantly, inhibition of SFK signalling and MAPK signalling alone was insufficient to kill the breast cancer cells, whereas dual inhibition of SFK and MAPK signalling resulted in increased apoptosis of the breast cancer cells (Touny et al., 2014). However, this strategy to maintain tumour cell dormancy is not ideal as continuous life-long intervention is necessary to prevent tumour recurrence.

It would be preferable to eliminate dormant tumour cells while they remain dormant or slow cycling. Given their role in the treatment resistance of glioblastoma as discussed previously, targeting dormant tumour cells could greatly impact glioblastoma patient outcomes. However, the dormant population in glioblastoma may be heterogenous and therefore, it may be difficult to identify and directly target this population. One potential strategy could be to improve the sensitivity of the dormant population to radiotherapy given that all tumour cells regardless of proliferative status will experience DNA damage induced by radiation.

1.4 Aims

Glioblastoma is a highly aggressive disease with a five-year survival rate of merely 6.8% (Ostrom et al., 2021). Given that the median survival of glioblastoma is 12-15 months, it is generally considered an incurable disease (Hanif et al., 2017). Nevertheless, almost all patients receive radiotherapy as part of standard care (Stupp et al., 2005). Thus, understanding the radio-resistance mechanisms of glioblastoma are vital in improving radiotherapy efficacy.

One potential source of radiotherapy resistance in glioblastoma is the dormant tumour population, comprised of cells which have reversibly exited the cell cycle (Aguirre-Ghiso, 2007; Hadfield, 1954; Sosa et al., 2014). Radiotherapy is thought to preferentially target tumour cells that are actively proliferating; these tumour cells are likely to progress through the cell cycle with unrepaired DNA damage, which may inevitably trigger cell death mechanisms (Boustani et al., 2019; Steel et al., 1989). Hence, dormant tumour cells are generally thought to survive radiotherapy induced DNA damage. However, the mechanisms underlying dormant tumour cell survival remain unclear.

The DDR and DNA repair, which play a major role in mediating tumour cell response to radiation, have yet to be characterised in the dormant population in glioblastoma (Boustani et al., 2019). Furthermore, there is evidence that the dormant population consists of cells in different cellular states (Garcia-Diaz et al., 2023; Neftel et al., 2019). The potential heterogeneity of the dormant population may impact the radiation response, with different cellular states potentially conferring different levels of radiosensitivity (Bao et al., 2006; Bhat et al., 2013).

Hence, this thesis sought to explore the mechanisms underlying the radio-resistance of the dormant population in glioblastoma. Given the potential heterogeneity of this population, we approached this task by first characterising the dormant populations within a *Nf1*$^{-/-}$*/Pten*$^{-/-}$*/P53*$^{-/-}$ mouse model of glioblastoma. We then assessed the radio-resistance of this potentially heterogenous population *in vivo*, before investigating potential mechanisms of radio-resistance *in vitro*. To this end, we modelled a potentially radio-resistant dormant population *in vitro* and sought to characterise this model's response to radiation. Specifically, we focused on identifying potential DDR and DNA repair mechanisms underpinning the radio-resistance of this population. Using this dual *in vitro* and *in vivo* approach, we endeavoured to identify specific mechanisms of radio-resistance that could potentially be targeted in order to kill the dormant tumour population.

Chapter 2. A radio-resistant astrocyte-like population is driven by BMP signalling

Tumour cell dormancy is a likely source of radio-resistance in glioblastoma (See chapter 1.3.3). Indeed, radiotherapy is thought to preferentially target proliferating tumour cells given that their rapid cell cycle progression restricts their capacity for effective DNA repair. Eventually, the extended presence of this radiation-induced DNA damage may trigger cell death (Abuetabh et al., 2022; Chan et al., 1999; Vakifahmetoglu et al., 2008; Y. Zhou et al., 2021). Whilst there are some *in vitro* studies that have demonstrated the radio-resistance of dormant glioblastoma cells, the mechanisms underpinning this radio-resistance remain elusive (Sachdeva et al., 2019; Tejero et al., 2019).

Furthermore, to fully understand the radio-resistance of the dormant population within glioblastoma, it is essential to consider the potential heterogeneity of this population. It is well-established that glioblastoma is comprised of tumour cells that resemble the cellular states found in normal neurodevelopment, including the AC-like, MES-like, OPC-like and NPC-like cellular states (Couturier et al., 2020; Neftel et al., 2019). Neftel *et al.* found both proliferating and non-proliferating cells within each of these cellular states which supports the idea of a heterogenous dormant population (Neftel et al., 2019). Building on this point, Garcia-Diaz *et al.* utilised an inducible H2B-GFP label retention system (See Chapter 1.3.1) to identify a dormant population in an immunocompetent mouse model of glioblastoma; through scRNAseq analysis, they identified that the majority but not all of that dormant population was in an

injured NPC-like state which points towards the potential heterogeneity of this population (Garcia-Diaz et al., 2023). Taking these studies into consideration, we hypothesized that the dormant population within the *Nf1*$^{-/-}$/*Pten*$^{-/-}$/*P53*$^{-/-}$ mouse model of glioblastoma may be comprised of cells in different cellular states, with potentially different mechanisms of radio-resistance.

Hence, we first sought to identify the dormant populations within glioblastoma and subsequently assess their radio-resistance. Once radio-resistant populations were identified, we further investigated the signalling pathways that may regulate these cells. For this work, we utilised the *Nf1*$^{-/-}$/*Pten*$^{-/-}$/*P53*$^{-/-}$ glioblastoma mouse model previously characterised and published by Garcia-Diaz *et al*. (Garcia-Diaz et al., 2023). Not only are these mutations commonly altered in glioblastoma patients but p53 loss, in particular, is associated with increased radio-resistance (Abuetabh et al., 2022; Cancer Genome Atlas Research Network, 2008). Additionally, this model is immunocompetent which is thought to play a role in tumour response to radiotherapy (Boustani et al., 2019). One consideration for this model, however, is its variable latency. In this author's experience the latency of this mouse model is within 15-18 weeks, thus it is important to confirm the presence of a tumour before proceeding with experiments through *in vivo* luciferase assays. For these reasons, elucidating the radio-resistance mechanisms in this tumour model would be valuable to current efforts to enhance radiotherapy efficacy.

2.1 The *Nf1*$^{-/-}$/*Pten*$^{-/-}$/*P53*$^{-/-}$ glioblastoma mouse model contains a radio-resistant Astrocyte-like dormant population

In order to assess the radio-resistance of a potentially heterogenous dormant population, we first sought to characterise this population (Darmanis et al., 2017; Garcia-Diaz et al., 2023; Neftel et al., 2019). To this end, we performed scRNAseq on the previously published *Nf1*$^{-/-}$/*Pten*$^{-/-}$/*P53*$^{-/-}$ glioblastoma mouse model where all transformed tumour cells expressed TdTomato (Tdtom) (Garcia-Diaz et al., 2023). The sample collection was performed by Dr Ciaran Hill and Zan Florjanic Baronik (See Methods Chapter 7.2). Eight *Nf1*$^{-/-}$/*Pten*$^{-/-}$/*P53*$^{-/-}$ mouse brains were processed for 10x scRNAseq and the subsequent scRNAseq analysis was completed by Dr Wenhao Tang (See Methods Chapter 7.2). The dataset derived from these samples consists of 66'080 tumour and non-tumour cells, and a total of 17957 genes (See Methods Chapter 7.2). For this thesis, the dataset was limited to tumour cells based on the number of TdTomato reads within each cell; a threshold of ≥ 5 TdTomato reads was used to denote a tumour cell (See Methods Chapter 7.2). This tumour-only dataset was comprised of 59520 cells, from which Dr Wenhao Tang generated the graphical user interface (Shinyapp). This graphical user interface was utilised by this author to explore this scRNAseq dataset and to generate the UMAPs, bar charts, violin plots and heatmaps presented in this thesis.

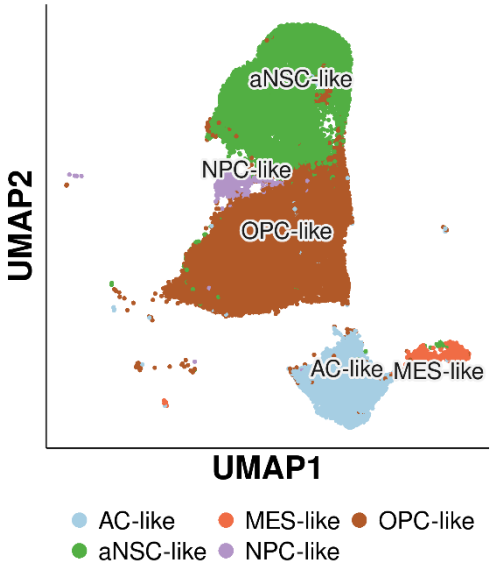

***Figure 2.1* Tumour populations of the Nf1$^{-/-}$/Pten$^{-/-}$/P53$^{-/-}$ glioblastoma mouse model**

scRNAseq of the Nf1$^{-/-}$/Pten$^{-/-}$/P53$^{-/-}$ glioblastoma mouse model was performed by Dr Ciaran Hill and Zan Florjanic-Baronik (See Methods Chapter 7.2). The scRNAseq analysis was completed Dr Wenhao Tang, who generated a user graphical interface (Shinyapp) for this dataset, from which we generated the plots shown above (See Methods Chapter 7.2). UMAP showing the clusters identified in the Nf1$^{-/-}$/Pten$^{-/-}$/P53$^{-/-}$ glioblastoma mouse model. AC = astrocyte, MES = Mesenchymal, NPC = Neural progenitor cell, aNSC = actively proliferating Neural Stem Cell, OPC = Oligodendrocyte Progenitor Cell.

A total of five tumour clusters were identified in the scRNAseq dataset of the *Nf1$^{-/-}$/Pten$^{-/-}$/P53$^{-/-}$* glioblastoma mouse model (Fig 2.1A). Amongst the identified tumour cell clusters were those that resembled the AC-like, MES-like, OPC-like and NPC-like cellular states previously identified by Neftel *et al.* in glioblastoma patient samples (Neftel et al., 2019). The tumour cell populations identified included the AC-like, the actively proliferating neural stem cell (aNSC)-like, the OPC-like, the NPC-like, and the MES-like populations (Fig 2.1). These findings are largely consistent with previously published data of the *Nf1$^{-/-}$/Pten$^{-/-}$/P53$^{-/-}$* glioblastoma mouse

model (Garcia-Diaz et al., 2023). Previously, Garcia-Diaz *et al.* also identified an AC-like, OPC-like and an actively proliferating NSC-like population (Garcia-Diaz et al., 2023). In this study, they described an injured NPC-like population which mostly resembled the Neftel MES-like population (Garcia-Diaz et al., 2023).

Next, we assessed the proliferative state of tumour populations identified in this *Nf1*$^{-/-}$*/Pten*$^{-/-}$*/P53*$^{-/-}$ mouse model of glioblastoma to distinguish potentially dormant populations. To this end, we examined the expression of previously published quiescence or dormancy signatures within these populations.

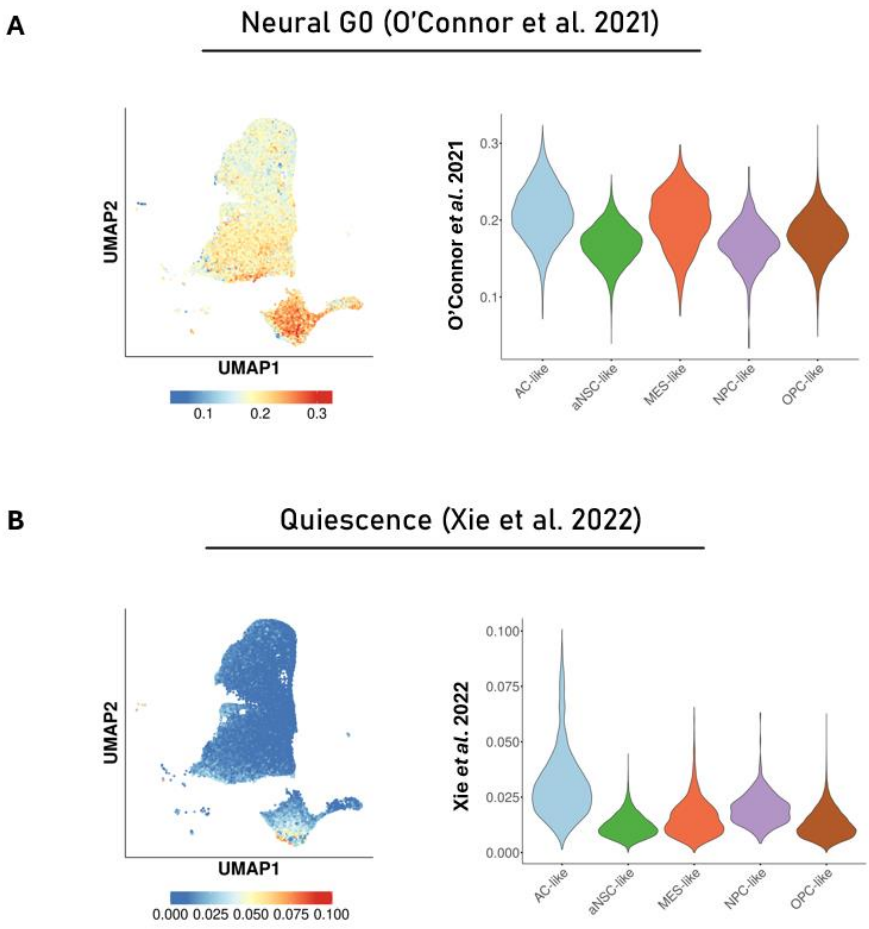

Figure 2.2 There is an astrocyte-like dormant population in glioblastoma

scRNAseq of the Nf1$^{-/-}$/Pten$^{-/-}$/P53$^{-/-}$ glioblastoma mouse model was performed by Dr Ciaran Hill and Zan Florjanic-Baronik (See Methods Chapter 7.2). The data analysis was completed Dr Wenhao Tang, who generated a user graphical interface (Shinyapp) for this dataset, from which we generated the plots shown above (See Methods Chapter 7.2). (A) Expression of the Quiescence transcriptional signature acquired from O'Connor et al. 2021 shown as a UMAP (left) and as a violin plot (right). (B) Expression of the Quiescence transcriptional signature acquired from Xie et al. 2022 shown as a UMAP (left) and a violin plot (right). In regard to the violin plots, the y-axis represents the expression level of the selected gene signature. Statistical analysis was not performed, this analysis was exploratory. AC = astrocyte, MES = Mesenchymal, NPC = Neural progenitor cell, aNSC = actively proliferating Neural Stem Cell, OPC = Oligodendrocyte Progenitor Cell.

We first utilised the 'Neural G0' quiescence signature derived from scRNAseq of human neural stem cells cultured *in vitro* (O'Connor et al., 2021). Interestingly, this quiescence signature was most highly expressed in the AC-like and MES-like tumour populations (Fig 2.2A). In addition to the 'Neural G0' signature, we utilised a quiescence signature derived from an *Nf1*$^{-/-}$/*Pten*$^{-/-}$/*P53*$^{-/-}$ mouse model of glioblastoma (Xie et al., 2022). In this mouse model used by Xie *et al*. tumour cells expressing *Nestin,* a marker for stemness, were labelled with GFP; these GFP+ tumour cells were shown to be Ki67- and thus likely dormant (J. Chen et al., 2012; Xie et al., 2022). The quiescence signature was generated from these dormant GFP *Nestin*+ tumour cells (Xie et al., 2022). Interestingly, we found this signature was most highly expressed by the AC-like population compared to all other tumour populations (Fig 2.2B).

Collectively, this analysis highlights that both the AC-like and MES-like populations may contain dormant cells. Indeed, this observation indicates that the dormant population in the *Nf1*$^{-/-}$/*Pten*$^{-/-}$/*P53*$^{-/-}$ mouse model of glioblastoma may be distributed into different cellular states. Taking this into consideration, we next examined the radiosensitivity of these different dormant states *in vivo*.

In order to achieve this aim, we employed a Cytometry by Time-of-Flight (CyTOF) approach to evaluate shifts in cellular state proportions after radiotherapy to identify radioresistant populations. CyTOF is a recently developed method which combines flow cytometry with traditional mass spectrometry to assess a large panel of markers on individual cells (Iyer et al., 2022). In collaboration with Dr Anni Poysti and Dr Lucy Brooks, we irradiated mice bearing *Nf1*$^{-/-}$/*Pten*$^{-/-}$/*P53*$^{-/-}$ tumours with 2 Gy for 5 days (See Methods Chapter 7.1.3). One week following the end of treatment, the mice were collected and processed for CyTOF analysis by Dr Lucy Brooks, utilising the panel she developed for this mouse model (See

Methods Chapter 7.2). This panel included SPARCL1, BLBP, GFAP and SLC4A4 (astrocyte-like markers). In addition, SOX10 (Oligodendrocyte-like marker), Bst2 (Mesenchymal-like marker), DCX (NPC-like marker) and RFP (tumour cell marker) were used to distinguish the different cellular populations within the tumour mice. The full list of markers is described in methods section 7.3.

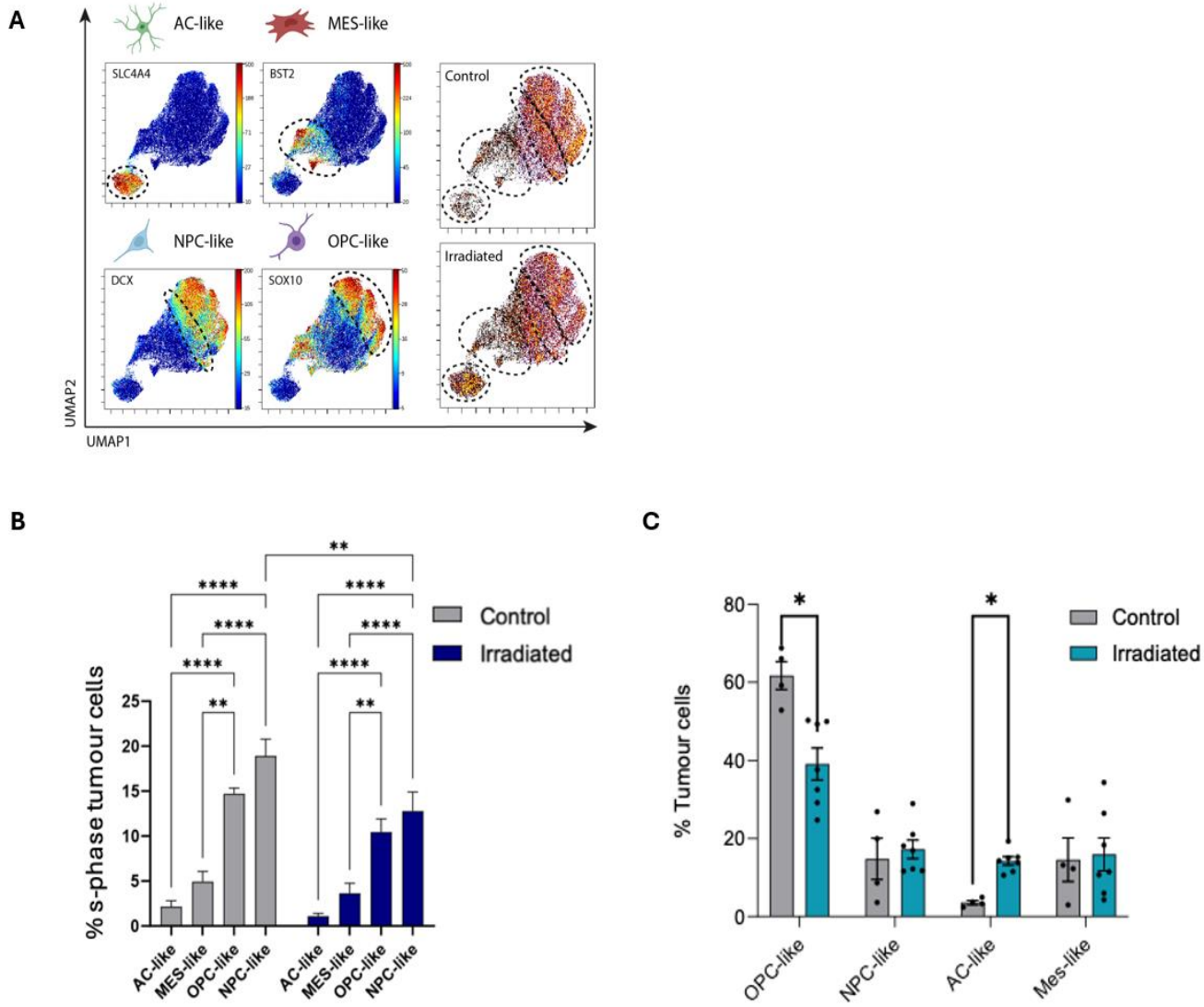

Figure 2.3 Dormant AC-like tumour cells are enriched after radiation

The Nf1$^{-/-}$/Pten$^{-/-}$/P53$^{-/-}$ glioblastoma mice were treated with fractionated radiotherapy (2 Gy x 5 days) and collected one week later in collaboration with Dr Lucy Brooks and Dr Anni Poysti. CyTOF analysis of the Nf1$^{-/-}$/Pten$^{-/-}$/P53$^{-/-}$ glioblastoma mouse model was then performed by Dr Lucy Brooks. CyTOF

*analysis and in vivo collection is described in detail in chapter 7.1.6. (A) Plots illustrating the gating strategy to identify the AC-like, MES-like, OPC-like, and NPC-like cell populations based on a panel of markers (B) Bar chart representing the percentage of tumour cells in S-phase. Mean±SEM, Tukey's multiple comparison test (C) Bar chart representing each population as a percentage of total tumour cells. Multiple unpaired t-tests with two-stage step-up method of Benjamini, Krieger and Yakutieli to control the FDR. (*p<0.05, **p<0.01, ****p<0.0001). For both (B) and (C) n=4 control mice, n=7 irradiated mice.*

The CyTOF analysis identified an AC-like, MES-like, OPC-like and NPC-like cell state within the *Nf1*$^{-/-}$*/Pten*$^{-/-}$*/P53*$^{-/-}$ mouse model of glioblastoma (Fig 2.3A). This analysis demonstrated that the AC-like population was the least proliferative population in this mouse model, which was in line with their increased expression of quiescent signatures (Fig 2.3B). The MES-like population, which also highly expressed the 'Neural G0' signature, exhibited higher levels of proliferation than the AC-like population, but it was less proliferative than both the OPC-like and NPC-like populations (Fig 2.3B). Interestingly, the NPC-like population exhibited the highest levels of proliferation which was significantly reduced following radiation (Fig 2.3B). On the other hand, radiation did not significantly impact the proliferation of the AC-like, MES-like and OPC-like populations (Fig 2.3B). Although radiation reduced the levels of proliferation in the NPC-like population, the proportion of NPC-like tumour cells were not impacted by radiation (Fig 2.3C). Similarly, the proportion of MES-like tumour cells were not significantly impacted by radiation (Fig 2.3C). On the other hand, we observed a significant reduction in the percentage of OPC-like tumour cells accompanied with a significant increase in the percentage of AC-like tumour cells (Fig 2.3C).

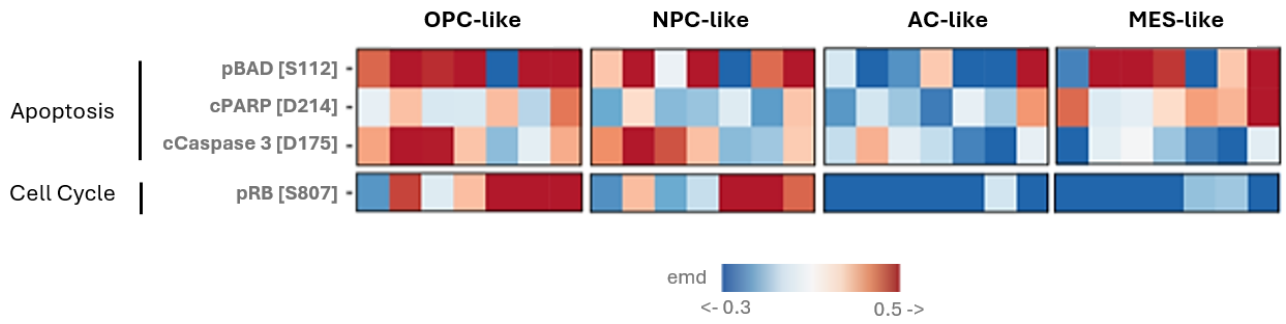

Figure 2.4 Apoptosis and cell cycle marker expression in the cell populations of irradiated tumours

The Nf1$^{-/-}$/Pten$^{-/-}$/P53$^{-/-}$ glioblastoma mice were treated with fractionated radiotherapy (2 Gy x 5 days) and collected 1 week later in collaboration with Dr Lucy Brooks and Dr Anni Poysti. CyTOF analysis of the Nf1$^{-/-}$/Pten$^{-/-}$/P53$^{-/-}$ glioblastoma mouse model was then performed by Dr Lucy Brooks. CyTOF analysis and in vivo collection is described in detail in chapter 7.1.6. Heatmap shows the expression of DNA damage, Apoptosis and Cell Cycle markers in the four tumour cell populations (OPC-like, NPC-like, AC-like and MES-like) in the irradiated mouse samples. n=7 irradiated tumour bearing mice.

In addition to assessing changes in the proportions of different cell states, through CyTOF analysis, we further compared the expression of markers associated with apoptosis after radiation in the OPC-like, NPC-like, AC-like and MES-like populations. This analysis showed that the OPC-like tumour cells had increased expression of the markers for apoptosis, pBAD and cCaspase 3 (Fig 2.4). Indeed, this finding suggests that the observed decrease in the percentage of OPC-like tumour cells may be attributed to higher levels of cell death (Fig 2.4). Although the proportion of NPC-like tumour cells were not altered by radiotherapy, the NPC-like population also showed increased expression of pBAD and cCaspase 3 (Fig 2.4). Similarly, the MES-like population showed increased expression of pBAD and cPARP despite the fact that radiation did not impact the proportion of MES-like tumour cells (Fig 2.4). Finally, the AC-like

population, which was enriched following radiotherapy expressed comparatively less pBAD, cPARP and cCaspase 3 than the other tumour populations (Fig 2.4).

Collectively the CyTOF data indicates that the AC-like dormant population is likely radioresistant. However, based on this data alone it is not confirmed whether this enrichment may be attributed to expansion of the AC-like population or radiation-induced changes in other tumour populations. Based on the proliferation levels of the AC-like population one week after radiation, we may speculate that changes in other tumour populations might be a more likely explanation. Indeed, we observed a decrease in the percentage of OPC-like tumour cells that was likely due to increased cell death. On the other hand, it remains unknown whether tumour cells shifted from one cell state to another following radiation. Additionally, it is interesting that the percentage of the NPC-like tumour cells was not altered following radiation despite their observed decrease in proliferation and increase in cell death. It is unknown whether the NPC-like cells would succumb to radiation-induced cell death at a later time point, or if they undergo cell cycle arrest as a means to escape radiation-induced cell death.

Nevertheless, this data suggests that one week following radiation the AC-like state is likely radio-resistant whilst the OPC-like state exhibits higher radiosensitivity. It is important to note, however, that this data alone does not confirm whether the MES-like and NPC-like populations were comparatively less radioresistant since the proportion of these populations were unchanged following radiation.

2.2 BMP signalling plays a role in regulating the AC-like dormant population

Since, we have established that the AC-like dormant population is likely radioresistant, we next explored what signalling pathway may be driving this dormant population. It is thought that multiple signalling pathways may regulate tumour cell dormancy in glioblastoma (See Chapter 1.3.2). However, BMP signalling in particular has been demonstrated to also promote astrocytic differentiation in patient-derived glioblastoma lines (Carén et al., 2015; Han, Cai, et al., 2022; Pollard et al., 2009a). Based on these studies, we investigated the potential role for BMP signalling in driving the AC-like dormant population.

We leveraged the scRNAseq data to probe whether BMP signalling was active in the AC-like population. Specifically, we assessed the expression of the GO 'Response to BMP signalling' pathway in the different tumour populations in the *Nf1*$^{-/-}$/*Pten*$^{-/-}$/*P53*$^{-/-}$ mouse model. The scRNAseq data analysis was completed by Dr Wenhao Tang as described above (See Methods Chapter 7.2).

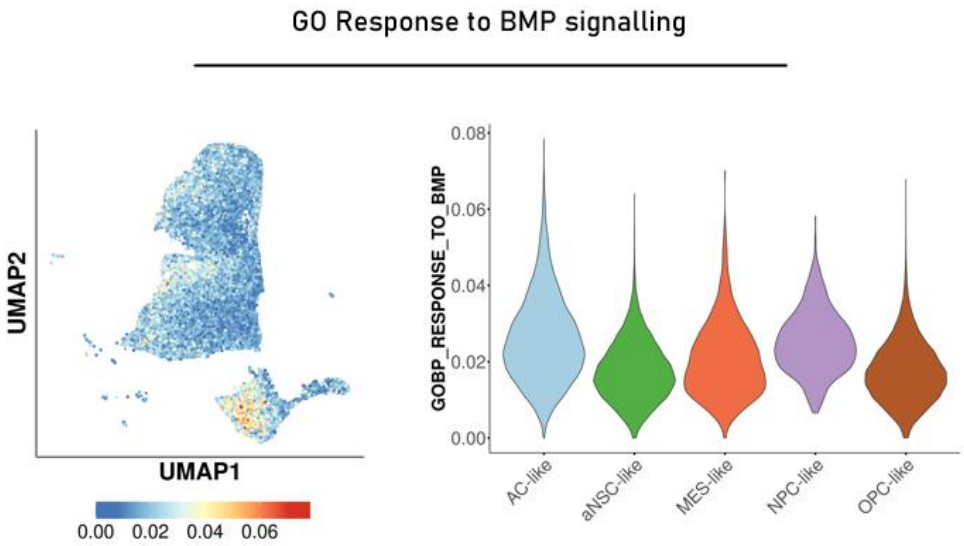

Figure 2.5 scRNAseq analysis shows the AC-like cels have upregulated response to BMP signalling

scRNAseq of the Nf1$^{-/-}$/Pten$^{-/-}$/P53$^{-/-}$ glioblastoma mouse model was performed by Dr Ciaran Hill and Zan Florjanic-Baronik (See Methods Chapter 7.2). The data analysis was completed Dr Wenhao Tang, who generated a user graphical interface (Shinyapp) for this dataset, from which we generated the plots shown above (See Methods Chapter 7.2). AC = astrocyte, MES = Mesenchymal, NPC = Neural progenitor cell, aNSC = actively proliferating Neural Stem Cell, OPC = Oligodendrocyte Progenitor Cell. Expression of the GO response to BMP signalling is shown as a UMAP (left) and a violin plot (right).

This analysis showed that amongst the tumour cell populations, the BMP signalling pathway was indeed highly expressed in the AC-like dormant tumour cells (Fig 2.4). Notably, the BMP signalling pathway was also highly expressed in the MES-like and NPC-like populations (Fig 2.4). This suggests that BMP signalling may be upregulated in the AC-like dormant cells. Thus, we sought to validate this finding in *Nf1$^{-/-}$/Pten$^{-/-}$/P53$^{-/-}$* tumour tissue. To achieve this objective, we assessed the expression of Id3, a BMP target gene, in the AC-like

dormant cells through RNAscope of *Nf1*$^{-/-}$/*Pten*$^{-/-}$/*P53*$^{-/-}$ tumours from three mice (See Methods Chapter 7.4) (Jensen et al., 2021). Tumour cells were identified through staining for TdTomato expression (See Methods Chapter 7.4).

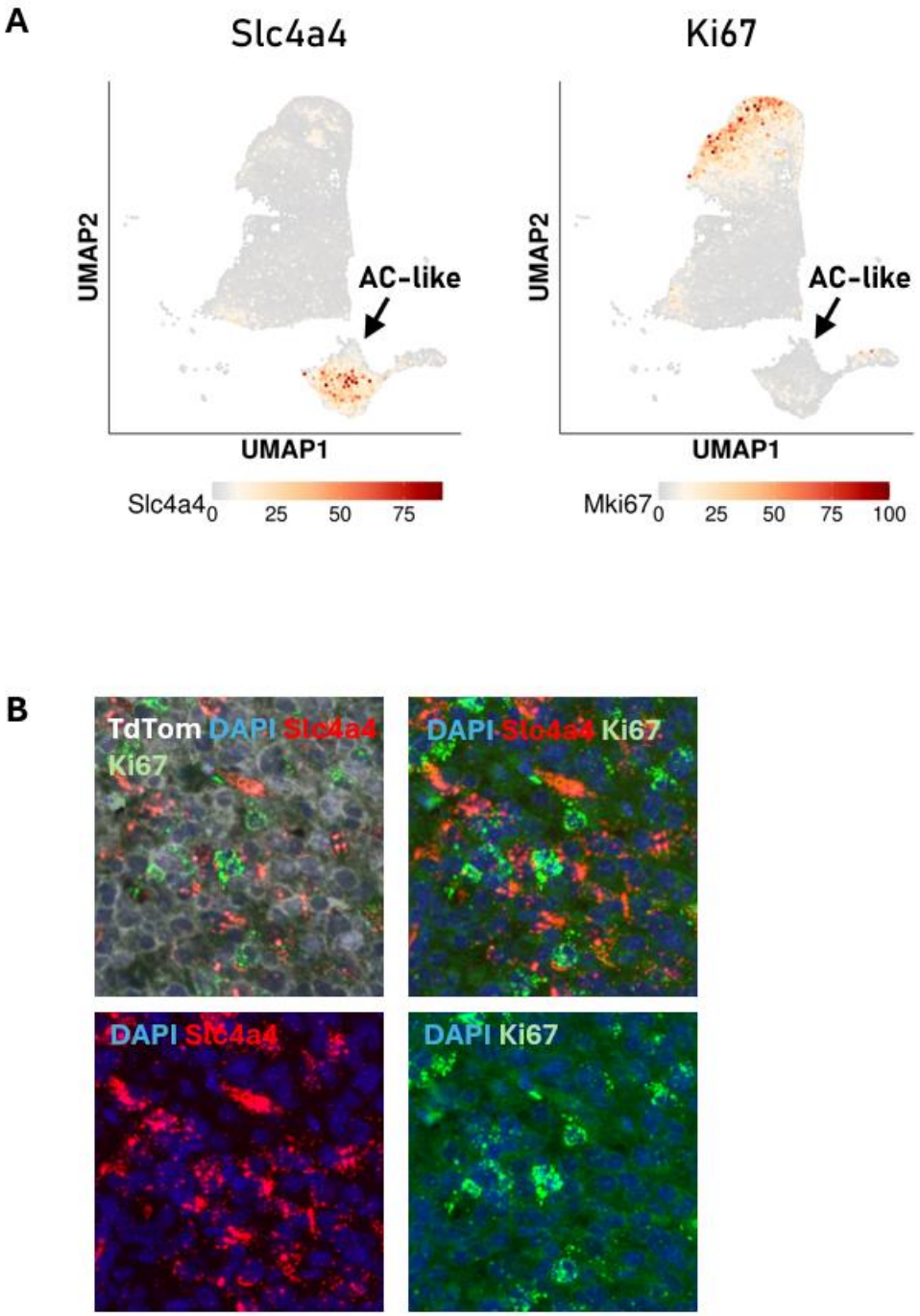

Figure 2.6 RNAscope demonstrates the presence of a Ki67- Slc4a4+ population in vivo

RNAScope was performed as described in Chapter 7.8 on tissue from the Nf1$^{-/-}$/Pten$^{-/-}$/P53$^{-/-}$ glioblastoma mouse model. (A) UMAP showing the expression of Slc4a4 and Ki67. Quantification was performed in collaboration with Simon Castillo. (B) Representative images of RNAScope showing TdTomato immunofluorescence staining (White) and the signal from the Slc4a4 (Red) and Ki67 (Green) probes. Tissue was counterstained with Dapi (Blue).

Firstly, to identify the AC-like population we assessed the potential of Slc4a4 as a suitable marker for this population. Slc4a4 was amongst the top upregulated markers within the AC-like dormant population (Fig 2.5A). We found that the TdTom+Slc4a4+ cells were distributed throughout the tumour, within the denser tumour bulk areas, the leading edge of the tumour and within the surrounding tissue. To assess the proliferative status of these TdTom+Slc4a4+ cells, we used Ki67, a commonly used marker of the cell cycle (Uxa et al., 2021). Evidently, the scRNAseq analysis shows that the AC-like cluster did not highly express Ki67 (Fig 2.5A). RNAscope validation in the tumour tissue revealed consistent anti-correlation between Slc4a4 and Ki67 as illustrated in figure 2.6. This highlights that the population of tumour cells identified by the Slc4a4 marker are largely Ki67-, suggesting that these cells may be dormant.

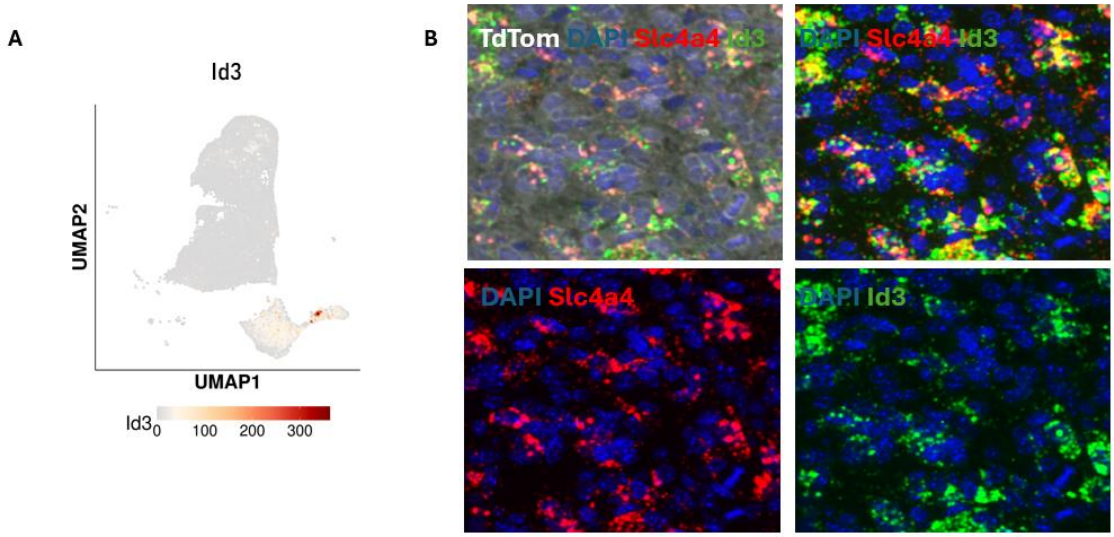

Figure 2.7 RNAscope demonstrates Slc4a4+ tumour cells are Id3+

RNAScope was performed as described in Chapter 7.8 on tissue from the Nf1$^{-/-}$/Pten$^{-/-}$/P53$^{-/-}$ glioblastoma mouse model. (A) Representative images of RNAScope showing TdTomato immunofluorescence staining (White) and the signal from the Slc4a4 (Red) and Id3 (Green) probes. Tissue was counterstained with Dapi (Blue). (C) Quantification of the Slc4a4+Id3+Tdtomato+ tumour cells.

Given that Slc4a4 likely represents a dormant AC-like tumour cell population, we next assessed whether Id3 was expressed in these tumour cells. Id3 is a downstream gene upregulated by BMP signalling (Jensen et al., 2021). Indeed, the scRNAseq data suggests that the AC-like cluster expresses Id3 (Fig 2.7). Additionally, RNAscope validation in the tissue showed consistent expression of Id3 by the TdTom+Slc4a4+ as illustrated in figure 2.6B.

Collectively, these results suggest that BMP signalling is likely upregulated in the AC-like dormant population. Whilst this finding supports the hypothesis that BMP signalling may drive the AC-like dormant population, further work is needed to functionally validate whether BMP signalling is sufficient to drive tumour cells towards a dormant AC-like cell fate. In

addition, based on this data alone we cannot exclude the possibility that other signalling pathways may also regulate this population. Thus, further work is also necessary to determine the role of other signalling pathways in the dormant AC-like population.

2.3 Tumour cells are the source of this BMP signalling

In the previous section, we confirmed that BMP signalling likely plays a role in maintaining the AC-like dormant population. This finding then prompted us to investigate the actual source of this BMP signalling. The canonical BMP signalling pathway is mediated by interaction between a total of 15 identified BMPs and dimeric receptor complexes (Cole et al., 2016; Han, Cai, et al., 2022; Heubel & Nohe, 2021). Amongst the BMPs that have been previously identified, there is much evidence to suggest that BMP2 and BMP4 regulate quiescence and astrocyte differentiation in normal neural stem cells (Blomfield et al., 2019; Gomes et al., 2003; Mabie et al., 1997; Mira et al., 2010; Nakashima et al., 1999, 2001; Y. Sun et al., 2011; Yao et al., 2014). Additionally, one study has shown the role for BMP2 and BMP7 in regulating cell cycle arrest in gliomas (Huchedé et al., 2024). There is also evidence that BMP7 may increase the expression of GFAP, an astrocyte marker, in glioblastoma (Savary et al., 2013). Furthermore, there is considerable evidence demonstrating the role of BMP4 in mediating dormancy and astrocyte differentiation in glioblastoma (Carén et al., 2015; Han, Cai, et al., 2022; Niklasson et al., 2024; Pollard et al., 2009a; Sachdeva et al., 2019).Thus, in order to probe for the potential source of the BMP signalling driving the AC-like population, we first assessed the expression of these three BMPs along with the type I and type II BMP receptors in the scRNAseq data. scRNAseq analysis was performed as described above in chapter 2.1.

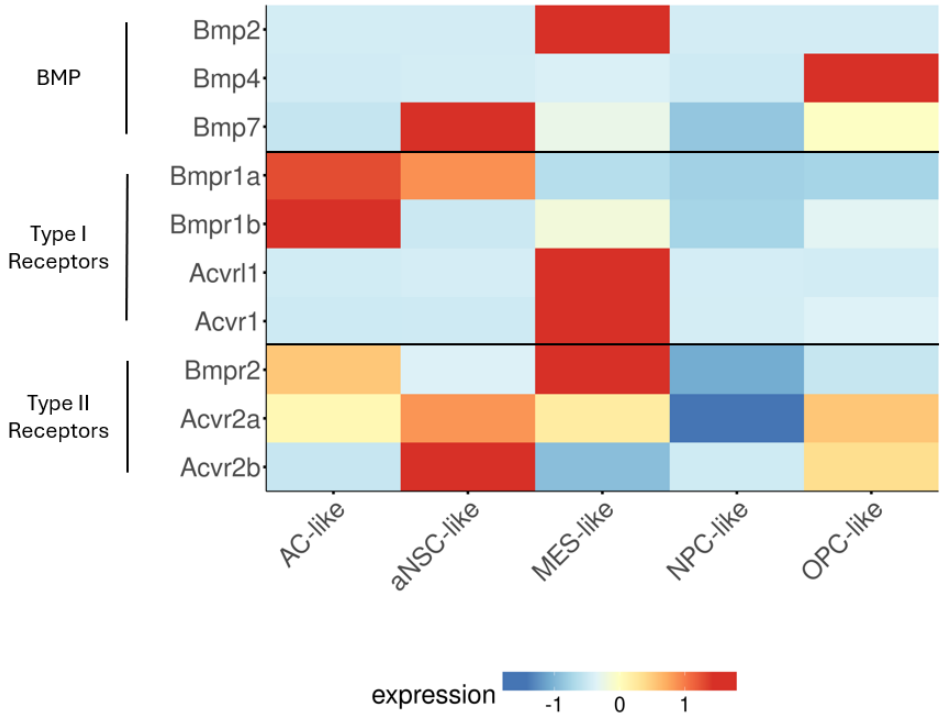

Figure 2.8 BMP and BMP receptor expression in the tumour and non-tumour populations

scRNAseq of the Nf1$^{-/-}$/Pten$^{-/-}$/P53$^{-/-}$ glioblastoma mouse model was performed by Dr Ciaran Hill and Zan Florjanic-Baronik (See Methods Chapter 7.2). The data analysis was completed Dr Wenhao Tang, who generated a user graphical interface (Shinyapp) for this dataset, from which we generated the plots shown above (See Methods Chapter 7.2). AC = astrocyte, MES = Mesenchymal, NPC = Neural progenitor cell, aNSC = actively proliferating Neural Stem Cell, OPC = Oligodendrocyte Progenitor Cell. Heatmap showing the expression of the BMPS (BMP2, BMP4 and BMP7) and the BMP type I receptor (Bmpr1a, Bmpr1b, Acvrl1 and Acvr1) and BMP type II receptor (Bmpr2, Acvr2a, Acvr2b) expression.

In the scRNAseq data we observed that *Bmp2*, *Bmp4* and *Bmp7* were most highly expressed in the MES-like, OPC-like and aNSC-like populations respectively (Fig 2.8). We next investigated the expression of type I and type II BMP receptors in the tumour. Interestingly, out of all the type I receptors, we observed increased expression of *Bmpr1a* and *Bmpr1b* in the AC-

like population (Fig 2.8). In fact, *Bmpr1a* and *Bmpr1b* are expressed most highly by the AC-like population compared to the other tumour populations (Fig 2.8). Additionally, all of the type II BMP receptors appeared to be expressed by the AC-like population, with *Bmpr2* being the most highly expressed (Fig 2.8).

While the type II receptors are thought to have broad binding affinity to the different BMPs, it is thought that the type I receptors have more specific affinity for particular BMPs (Gomez-Puerto et al., 2019; Heinecke et al., 2009; Khodr et al., 2020). It is thought that both BMPR1a and BMPR1b have increased affinity for BMP2 and BMP4 (Gomez-Puerto et al., 2019; Heinecke et al., 2009; Khodr et al., 2020). Given the upregulation of these receptors on the AC-like tumour cells, it is reasonable to speculate that BMP signalling in this population is potentially mediated mainly through either BMP2 or BMP4 signalling. Since it is thought that BMP2 and BMP4 behave similarly (Mira et al., 2010), we elected to focus on investigating *Bmp4* expression further, especially given the evidence suggesting a role for BMP4 in promoting dormancy and astrocyte differentiation in glioblastoma (Carén et al., 2015; Han, Cai, et al., 2022; Niklasson et al., 2024; Pollard et al., 2009a; Sachdeva et al., 2019).

Whilst *Bmp4* was most highly expressed by the OPC-like population compared to all other populations identified in the *Nf1*$^{-/-}$*/Pten*$^{-/-}$*/P53*$^{-/-}$ glioblastoma mouse (Fig 2.8), *Bmp4* was not expressed by all of the OPC-like population (Fig 2.9). Thus, we assessed the correlation between the expression of *Bmp4* and other known markers of the OPC-like state.

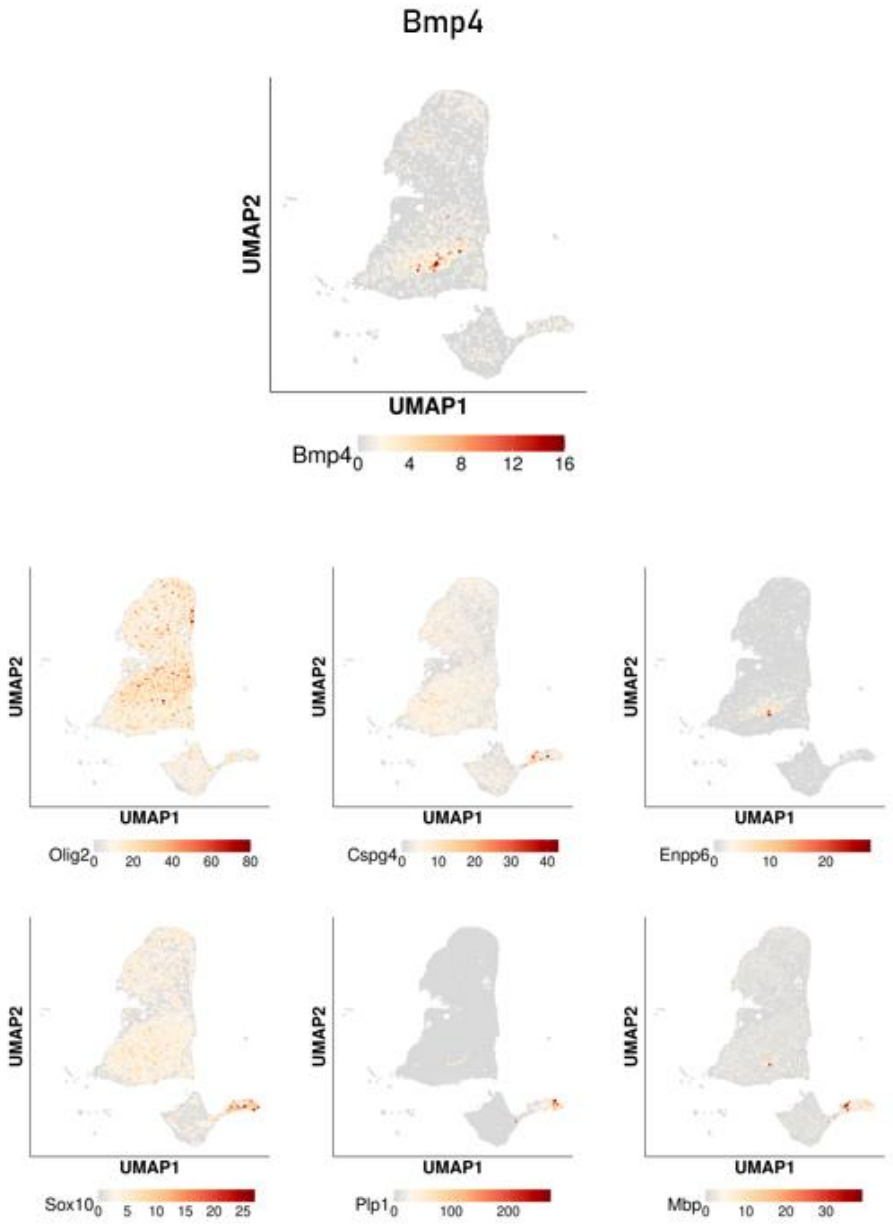

Figure 2.9 Expression of Bmp4 and Oligodendrocyte markers in the scRNAseq data

scRNAseq of the Nf1$^{-/-}$/Pten$^{-/-}$/P53$^{-/-}$ glioblastoma mouse model was performed by Dr Ciaran Hill and Zan Florjanic-Baronik (See Methods Chapter 7.2). The data analysis was completed Dr Wenhao Tang, who generated a user graphical interface (Shinyapp) for this dataset, from which we generated the plots shown above (See Methods Chapter 7.2). AC = astrocyte, MES = Mesenchymal, NPC = Neural progenitor cell, aNSC = actively proliferating Neural Stem Cell, OPC = Oligodendrocyte Progenitor

Cell. UMAPs showing the expression of Bmp4 and different Oligodendrocyte lineage markers: Olig2, Cspg4, Enpp6, Sox10, Plp1 and Bmp.

This analysis revealed that *Bmp4* expression was largely remarkably limited to *Enpp6* positive tumour cells, a marker for developing oligodendrocytes (Fig 2.9) (Morita et al., 2016). Since the scRNAseq data suggested that the subset of *Enpp6*+ OPC-like tumour cells were the source of BMP4, we sought to validate this finding through RNAScope of *Nf1*$^{-/-}$*/Pten*$^{-/-}$*/P53*$^{-/-}$ tumour tissue as described above (See Methods Chapter 7.4). In this analysis we assessed for the expression of both *Enpp6* and *Bmp4*. Analysis of the *Enpp6* and *Bmp4* gene expression, and TdTomato protein expression was completed in collaboration with Dr Simon Castillo, a bioinformatician from Dr Yinyin Yuan's Machine learning and digital pathology group at the MD Anderson Cancer Centre.

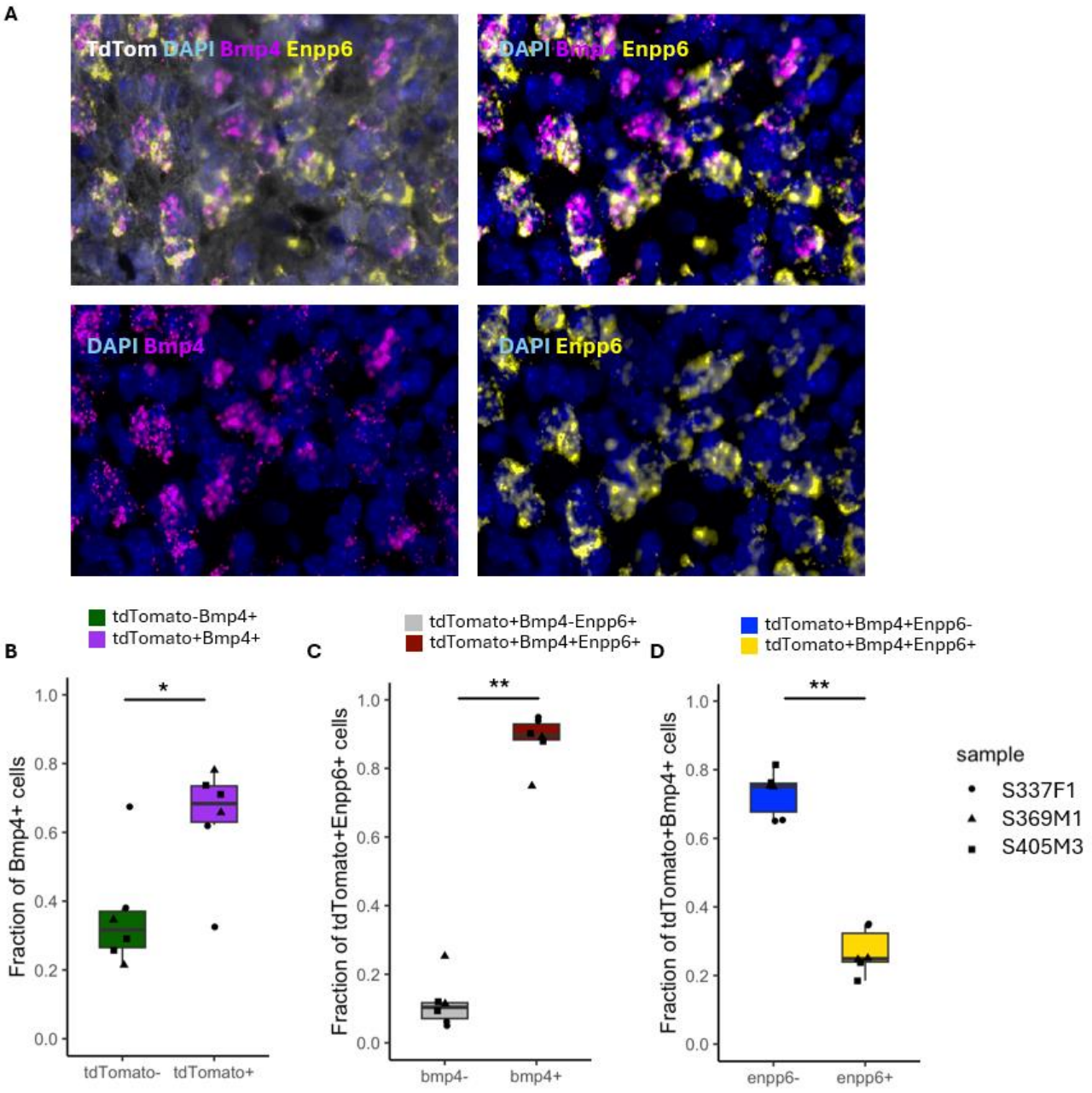

Figure 2.10 Enpp6+ OPC-like tumour cells are a source of BMP4

RNAScope was performed as described in Chapter 7.4 on tissue from the Nf1$^{-/-}$/Pten$^{-/-}$/P53$^{-/-}$ glioblastoma mouse model. (A) Representative images of RNAScope showing TdTomato (TdTom) immunofluorescence staining (White) and the signal from the Bmp4 (Purple) and Enpp6 (Yellow) probes. Tissue was counterstained with Dapi (Blue). (B) Bar chart showing the fraction of Tdtom+ and Tdtom- cells that are Bmp4+. (C) Graph showing the Bmp expression levels in the TdTom+ and TdTom- cells (D) Bar chart showing the fraction of TdTom+Bmp4+ cells that are Enpp6+ or Enpp6-. (E) Graph

*showing the Bmp expression levels in the Enpp6- and Enpp6+ tumour cells.(B,D) each point represents a coronal tissue section, boxplots contain the median (thick horizontal line), interquartile range (box boundaries), and data range without outliers (whiskers). *p<0.05, **p<0.01 for generalized mixed model. (C, E) boxplots contain the median (thick horizontal line), interquartile range (box boundaries), and data range without outliers (whiskers). Adjacent density plots show the distribution of the points (cells) across all sections and individuals. ***p<0.001 for Wilcoxon test.*

We observed a correlation between the *Enpp6*+ cells and the *Bmp4*+ cells as illustrated in figure 2.9A. Further quantification identified the tumour cells (TdTom+) based on TdTomato expression. Additionally, the tumour cells were defined as *Bmp4* expressing tumour cells (*Bmp4*+) or as *Enpp6* expressing tumour cells based on the presence of one *Bmp4* or *Enpp6* foci respectively (See Methods chapter 7.4).

This analysis revealed that approximately 70% of the *Bmp4*+ cells were indeed TdTom+ (Fig 2.9B). Furthermore, the TdTom+ tumour cells had significantly higher levels of *Bmp4* expression than TdTom- non-tumour cells, suggesting that the majority of BMP4 is indeed tumour derived (Fig 2.9C). However, only approximately 30% of these *Bmp4*+*TdTom*+ cells were also *Enpp6*+ (Fig 2.9D). Yet, further analysis found higher levels of *bmp4* expression in the *Enpp6*+*TdTom*+ cells than the *Enpp6*-*TdTom*+ cells (Fig 2.9E). Collectively, these observations suggest that although the *Enpp6*+ tumour cells did not account for the majority of *Bmp4* expressing tumour cells, they are likely an abundant source of *Bmp4*.

2.4 Discussion

In this chapter, we identified multiple tumour populations within the *Nf1*$^{-/-}$/*Pten*$^{-/-}$/*P53*$^{-/-}$ glioblastoma mouse model that were enriched for quiescence signatures. Of these potentially

dormant populations, only the AC-like population was enriched one week after radiation *in vivo*. Our results suggest that this radio-resistant population had increased BMP signalling activity, and that tumour-derived BMP4 may be driving this signalling.

While we demonstrated that the dormant AC-like cells may be radio-resistant, these cells may resemble a chemo-resistant population previously described by Xie *et al.* (Xie et al., 2022). Indeed, the quiescence signature from Xie *et al.* was most highly expressed by the AC-like population (Xie et al., 2022). As mentioned above, this quiescence signature was originally generated from *Nestin*+ dormant tumour cells identified in an *Nf1*$^{-/-}$/*Pten*$^{-/-}$/*P53*$^{-/-}$ mouse model (Xie et al., 2022). In this study, that quiescence signature was leveraged to identify a cell surface marker, F3, to isolate dormant tumour cells from patient samples from which patient-derived xenografts were generated in mice (Xie et al., 2022). Following temozolomide treatment, they found these F3+ dormant cells were enriched, which pointed towards their chemo-resistance (Xie et al., 2022). Hence, we may speculate that the radio-resistant AC-like population may also be chemo-resistant.

Xie *et al.* also linked their dormant F3+ population with tumour recurrence based on scRNAseq analysis of the PDX tumours which identified a proliferative F3+ population after temozolomide treatment (Xie et al., 2022). This finding suggests that the dormant AC-like population we identified in this chapter may also re-activate following treatment. Whilst the observed enrichment of the AC-like population may support this hypothesis, assessment of both the proliferation levels and the proportion of AC-like tumour cells at later time points post-radiation is necessary to determine the role of this population in tumour recurrence.

It was surprising that the mesenchymal population was not enriched in this tumour model following *in vivo* radiotherapy. This finding is in contrast to previous studies that have

demonstrated a mesenchymal shift following radiation (Bhat et al., 2013; Halliday et al., 2014). One potential explanation for this unexpected finding may be the time point used to assess the proportion of different cell populations. Previous studies generally assessed for the mesenchymal signature upon tumour recurrence, which is far beyond the time point used in this chapter (Neftel et al., 2019; Phillips et al., 2006; Q. Wang et al., 2017). However, there is evidence that the mesenchymal shift can occur within 6 hrs following a single dose of radiation *in vivo* (Halliday et al., 2014). In this study, Halliday *et al.* noted that P53 and its target genes may be important drivers of this mesenchymal shift (Halliday et al., 2014). Given that the P53 loss in the *Nf1*$^{-/-}$*/Pten*$^{-/-}$*/P53*$^{-/-}$ glioblastoma mouse model, this may explain why we did not observe a mesenchymal shift within one week after radiation.

The CyTOF analysis also revealed the potential radiosensitivity of the OPC-like population. It is well known that non-malignant oligodendrocytes and their progenitors are sensitive to oxidative stress (Husain & Juurlink, 1995; Mitrovic et al., 1994; Thorburne & Juurlink, 1996). Non-malignant OPCs, in particular, are known to be more sensitive to oxidative stress than other glial cells (Barbarese & Barry, 1989; R. X. Lee & Tang, 2022). Given that radiation generates ROS, the proposed sensitivity of normal OPC and oligodendrocyte cells to oxidative stress may explain the observed decrease in the proportion of OPC-like tumour cells after *in vivo* radiation.

In addition, the potential loss of the OPC-like tumour cells after radiation may have consequences on the AC-like tumour population. Considering that the OPC-like population was a source of BMP4, one may speculate that the AC-like tumour cells may be allowed to expand. However, one week following radiation we observed no increase in proliferation of the AC-like population. It is possible that the AC-like population may need more time to re-enter

the cell cycle. On the other hand, other sources of BMP4 or perhaps other BMP molecules may compensate for the potential reduction in BMP4 producing tumour cells.

With this in mind, it is important to consider that other signalling pathways may be involved in regulating the AC-like dormant population. Indeed, the scRNAseq analysis and tissue validation through RNAscope collectively suggest that the AC-like dormant population responds to BMP signalling. We explored this signalling pathway first given the multitude of studies that have demonstrated a role for BMP signalling in regulating both dormancy and astrocyte differentiation (Blomfield et al., 2019; Carén et al., 2015, 2015; Pollard et al., 2009a; Y. Sun et al., 2011). However, this data does not exclude the possibility that other signalling pathways may contribute to regulating the AC-like population. There is evidence that activation of the JAK/STAT signalling pathways may play a role in AC-like differentiation with multiple studies demonstrating the role for STAT3 in astrogliogenesis (Cao et al., 2010; Fukuda et al., 2007). Additionally, Nakashima *et al.* demonstrated that the Notch target gene *Hes5* played a role in mediating astrocyte differentiation (Nakashima et al., 2001). Taking this into consideration, the potential loss of BMP4 may be compensated for through these signalling pathways.

Building on this point, while we focused on BMP4 as a driver of the AC-like population, it is not the only BMP that may regulate this population. The role for BMP2 in regulating quiescence and astrocyte differentiation in normal neural stem cells is well described (Mabie et al., 1997; Mira et al., 2010; Nakashima et al., 1999, 2001; Yao et al., 2014). Whilst there is additional evidence to suggest it may also mediate these processes in glioblastoma (Huchedé et al., 2024). Furthermore, BMP7 may be another candidate driver of the AC-like population, as it has been shown to reduce proliferation in gliomas and increase upregulation of the astrocytic

marker GFAP in glioblastoma (Huchedé et al., 2024; Savary et al., 2013). Indeed, the scRNAseq analysis suggested that both BMP2 and BMP7 were expressed by the tumour cells. It is therefore plausible to speculate that a combination of BMPs may act to regulate the AC-like population.

It is worth noting that the BMP signalling was tumour derived. To this author's knowledge, glioblastoma as a source of BMP signalling has not been previously described in literature. This finding suggests that the tumour itself produces this signal to maintain a treatment resistant population. Whilst we identified that the OPC-like cells may produce BMP4, there are no previous studies to suggest that normal OPCs or mature oligodendrocytes produce BMP4. Further research is needed to assess whether this tumour-derived BMP is exhibited by tumour models with different mutations.

Chapter 3. Modelling the radiotherapy resistant AC-like dormant population *in vitro*

In the previous chapter, we established that there was an AC-like dormant population in the *Nf1*$^{-/-}$/*Pten*$^{-/-}$/*P53*$^{-/-}$ glioblastoma mouse model. Importantly, we demonstrated that the AC-like dormant population was enriched following fractionated radiotherapy *in vivo*. In this chapter, we sought to establish an *in vitro* model of the AC-like dormant population to eventually characterize the mechanisms underlying their radio-resistance.

We observed in chapter 2.2 that BMP signalling likely plays a role in maintaining the AC-like dormant population. As previously discussed, BMP4/FGF-treatment for three days has been demonstrated to induce quiescence whilst maintaining stemness in normal neural stem cells *in vitro* (Blomfield et al., 2019; Y. Sun et al., 2011). BMP4/FGF-treatment has also been shown to induce cell-cycle arrest in glioblastoma patient-derived lines *in vitro* (Sachdeva et al., 2019). It is also known that BMP4 plays a role in astrocytic differentiation (Cole et al., 2016). There is indeed evidence that BMP4 treatment induces astrocytic differentiation in glioblastoma patient-derived lines. Carén *et al.* observed astrocytic differentiation in glioblastoma patient-derived lines cultured with BMP4 for two weeks (Carén et al., 2015). Furthermore, Han *et al.* showed that human glioma stem cells treated with BMP4 significantly upregulated the astrocytic marker GFAP (Han, Cai, et al., 2022).

We hypothesized that BMP4/FGF-treatment for three days may induce cell cycle arrest and astrocytic differentiation in *Nf1*$^{-/-}$/*Pten*$^{-/-}$/*P53*$^{-/-}$ tumour cells *in vitro*. To test whether BMP4/FGF-treatment successfully modelled the AC-like dormant population observed *in vivo,* we assessed the effect of BMP4/FGF-treatment on transcription, cell cycle arrest, and radiosensitivity of the *Nf1*$^{-/-}$/*Pten*$^{-/-}$/*P53*$^{-/-}$ tumour cells *in vitro*. The *Nf1*$^{-/-}$/*Pten*$^{-/-}$/*P53*$^{-/-}$ tumour cells used in this thesis were isolated from mice with full-blown *Nf1*$^{-/-}$/*Pten*$^{-/-}$/*P53*$^{-/-}$ tumours (See Methods Chapter 7.6).

3.1 Bulk RNAseq suggests that *in vitro* BMP4/FGF-treatment transcriptionally recapitulates the astrocyte-like dormant state

To assess whether BMP4/FGF-treatment induces transcriptional changes that resemble the AC-like dormant state, we used a bulk RNA sequencing (bulk RNAseq) approach *in vitro*. Specifically, we performed bulk RNAseq on *Nf1*$^{-/-}$/*Pten*$^{-/-}$/*P53*$^{-/-}$ tumour cells cultured in media with either BMP4/FGF or EGF/FGF for three days. EGF/FGF was selected as a control as these growth factors are commonly used to maintain primary glioblastoma cell lines *in vitro* (Garcia-Diaz et al., 2023; Pollard et al., 2009a). Notably, the culture of tumour cells with EGF/FGF promotes a more stem-like phenotype (Pollard et al., 2009a). This approach allowed us to determine whether BMP4/FGF-treated tumour cells accurately model the AC-like dormant population *in vitro*.

Three days of BMP4/FGF-treatment was chosen as it is consistent with the treatment time previously used to induce robust cell cycle arrest in patient-derived lines or neural stem cells (Blomfield et al., 2019; Sachdeva et al., 2019). The RNA was extracted and BulkRNAseq performed as described in methods chapter 7.8. QC and sequence alignment were performed by Dr Wenhao Tang. Subsequently, we performed differential expression analysis using the DESeq2 package in R. The complete list of genes significantly altered by BMP4/FGF-treatment are listed in appendix chapter 8.1.

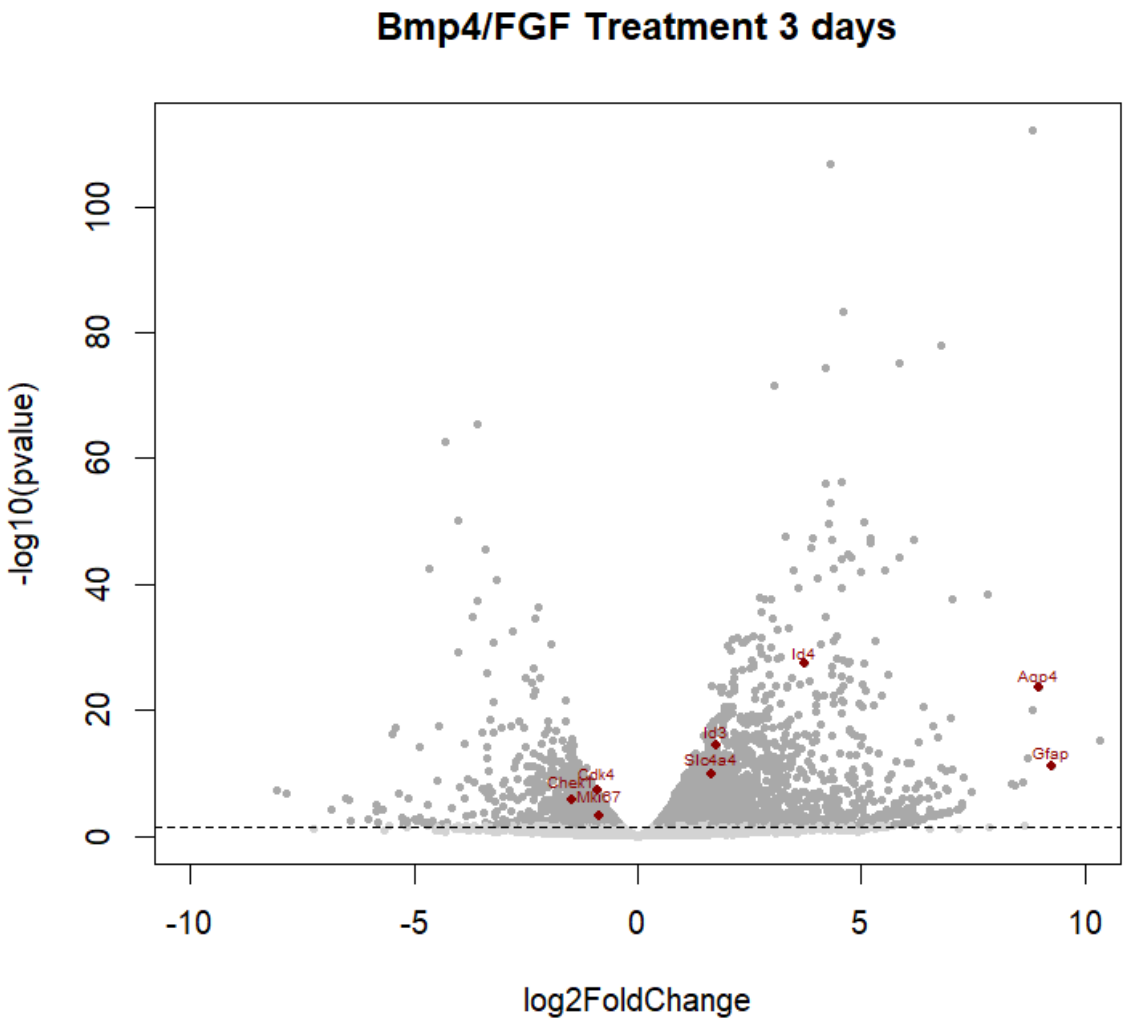

Figure 3.1 Differentially expressed genes in BMP4/FGF-treated tumour cells

Volcano plot illustrating the differentially expressed genes of Nf1$^{-/-}$/Pten$^{-/-}$/P53$^{-/-}$ tumour cells cultured in BMP4/FGF for three days compared to tumour cells treated with EGF/FGF for three days. Bulk RNAseq was performed as described in chapter 7.8. Differential gene expression analysis was performed using the DESeq2 package in R.

BMP4/FGF-treatment for three days induced a plethora of transcriptional changes in the *Nf1$^{-/-}$/Pten$^{-/-}$/P53$^{-/-}$* tumour cells as illustrated by the volcano plot in figure 3.1. There were 3017 upregulated genes, and 20'441 downregulated genes in the BMP4/FGF-treated tumour cells with a padj value <0.05 (Fig 3.1). Firstly, we observed significant upregulation of genes downstream of BMP signalling such as *Id1*, *Id2*, *Id3* and *Id4* (Gomez-Puerto et al., 2019; R. N. Wang et al., 2014) (Fig 3.1). There was also significant upregulation of the inhibitory *Smad* genes, *Smad6* and *Smad7* (Gomez-Puerto et al., 2019; R. N. Wang et al., 2014) (Fig 3.1). The tumour cells may have upregulated the inhibitory *Smad* genes as part of a negative feedback loop. Together this collection of differentially expressed genes suggest that the tumour cells are indeed responding to BMP4.

In addition, we observed significant downregulation of genes associated with cell cycle progression including *Ki67*, *Cdk4*, *Ccn1* and *Ccnb1* (Ding et al., 2020; Uxa et al., 2021) (Fig. 3.1). In addition, several astrocyte markers were significantly upregulated in the BMP4/FGF-treated tumour cells including *Gfap*, *Slc4a4* and *Aqp4* (Khakipoor et al., 2017; Szu & Binder, 2016; Z. Yang & Wang, 2015) (Fig 3.1). Notably, these markers are also upregulated in the AC-like dormant population (See Chapter 2.2). This data suggests that BMP4/FGF-treatment may have induced a downregulation in cell cycle accompanied with increased astrocyte-differentiation.

Given the large number of genes that were differentially expressed in the BMP4/FGF-treated tumour cells compared to the proliferating tumour cells, we performed GSEA to understand what pathways were significantly altered. For this analysis we assessed alterations in pathways described by the Hallmarks gene set. GSEA was performed using the fgsea package in R. The normalised enrichment score (NES), padj values and leading genes of all significantly altered pathways are listed in Appendix chapter 8.2.

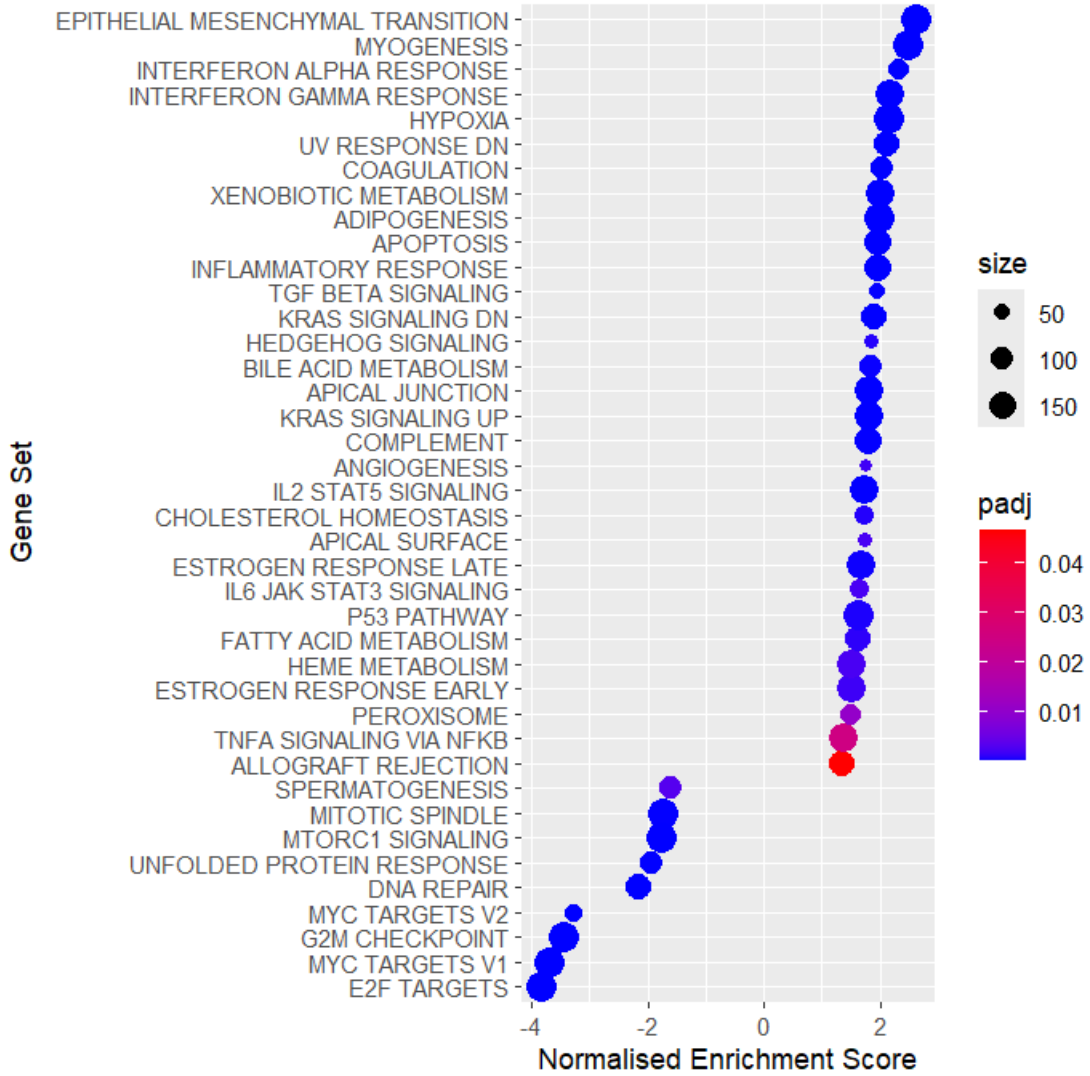

Figure 3.2 Significantly enriched pathways in the BMP4/FGF-treated tumour cells

Bulk RNAseq (See Methods Chapter 7.8) was performed on tumour cells cultured in BMP4/FGF or EGF/FGF for three days. Bubble plot showing the significantly (p<0.05) enriched pathways induced by BMP4/FGF-treatment from the Hallmarks gene set. Graph shows the normalised enrichment score, padj values and size of each pathway.

We identified 40 significantly altered pathways induced by BMP4/FGF treatment in the *Nf1*$^{-/-}$*/Pten*$^{-/-}$*/P53*$^{-/-}$ tumour cells (Fig 3.2). Firstly, we observed significant positive enrichment for the TGFβ signalling pathway with a NES of 1.97 (padj = 7.91E-05) (Fig 3.2). As discussed in the introduction, there is overlap in the BMP and TGFβ signalling pathways, hence, upregulation of the TGFβ signalling pathway may also indicate upregulation of BMP signalling (Derynck et al., 2021; Gomez-Puerto et al., 2019; R. N. Wang et al., 2014).

We also observed significant negative enrichment of pathways associated with cell cycle progression. There was a significant negative enrichment for the 'E2F targets' pathway (NES = -3.81, padj = 2.50E-49), the G2M checkpoint pathway (NES = -3.44, padj = 2.28E-43), MYC targets pathway v1 (NES = -3.67 , padj = 2.50E-49), MYC targets pathway v2 (NES = -3.26, padj = 9.48E-25) and the mitotic spindle pathway (NES = -1.74, padj = 1.07E-05) (Fig 3.2). It is worth noting that the top three most negatively enriched pathways were associated with the cell cycle, highlighting that BMP4/FGF-treatment for three days is likely inducing cell cycle arrest (Fig 3.2). Interestingly, the BMP4/FGF-treated tumour cells also exhibited significant negative enrichment in DNA repair with a NES of -2.13 (padj = 6.59E-09) (Fig 3.2).

Consistent with the differential gene expression analysis, the GSEA indicated that BMP4/FGF-treatment is likely associated with a decrease in cell cycle and an

increased response to BMP signalling. Hence, to clarify further whether the BMP4/FGF-treated tumour cells were recapitulating the AC-like dormant state identified in the *Nf1*$^{-/-}$*/Pten*$^{-/-}$*/P53*$^{-/-}$ mouse model, we next compared the bulk RNAseq data with the scRNAseq data. We used a transcriptional signature of the BMP4/FGF-treated tumour cells *in vitro,* generated by Dr Wenhao Tang, who compared them to the signature of the AC-like dormant cells in the scRNAseq dataset of the *Nf1*$^{-/-}$*/Pten*$^{-/-}$*/P53*$^{-/-}$ mouse model.

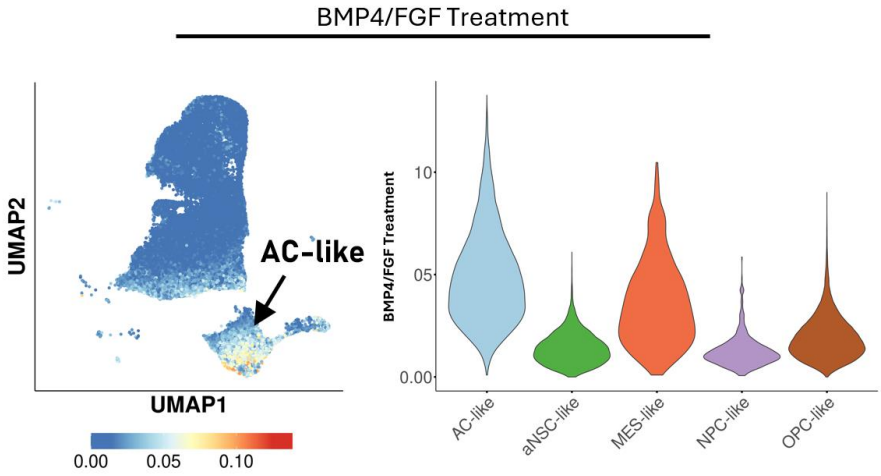

Figure 3.3 AC-like tumour cells express the BMP4/FGF-treatment signature

BMP4/FGF-treatment signature was generated by Dr Wenhao Tang from bulk RNAseq data (See Methods Chapter 7.8) of tumour cells treated with BMP4/FGF in vitro. Figure shows BMP4/FGF-treatment signature expression in the tumour clusters of the Nf1$^{-/-}$*/Pten*$^{-/-}$*/P53*$^{-/-}$ *glioblastoma mouse model as a UMAP (left) and violin plot (right).*

We found that the BMP4/FGF-treatment signature was highly expressed by the AC-like (Fig 3.3). The signature was also expressed highly by the MES-like population, whilst this signature was lowly expressed by the more proliferative aNSC-like, NPC-like and OPC-like populations (Fig 3.3). Importantly, the high expression of the BMP4/FGF-treatment transcriptional signature in the AC-like populations suggests that BMP4/FGF-treatment

likely promotes astrocytic differentiation of the *Nf1*$^{-/-}$*/Pten*$^{-/-}$*/P53*$^{-/-}$ tumour cells *in vitro*. However, this data suggests that BMP4/FGF-treatment may also promote mesenchymal-differentiation to a certain extent.

This data, together with the differential gene expression analysis and GSEA indicates that BMP4/FGF-treatment of the *Nf1*$^{-/-}$*/Pten*$^{-/-}$*/P53*$^{-/-}$ tumour cells *in vitro* may induce cell cycle arrest and likely recapitulates the AC-like dormant population identified in the *Nf1*$^{-/-}$*/Pten*$^{-/-}$*/P53*$^{-/-}$ mouse models of glioblastoma at the transcriptional level.

3.2 BMP4/FGF-treatment induces robust and reversible cell cycle arrest

In the previous section, we observed significant downregulation of pathways associated with cell cycle progression in the BMP4/FGF-treated tumour cells compared to tumour cells cultured in EGF/FGF. Next, we sought to validate these findings by assessing whether BMP4/FGF treatment for three days could significantly reduce proliferation in primary mouse *Nf1*$^{-/-}$*/Pten*$^{-/-}$*/P53*$^{-/-}$ glioblastoma cells.

To achieve this aim, the S177F (*Nf1*$^{-/-}$*/Pten*$^{-/-}$*/P53*$^{-/-}$) primary mouse cell line was used, this is a cell line isolated from a mouse with an *Nf1*$^{-/-}$*/Pten*$^{-/-}$*/P53*$^{-/-}$. The cell line was cultured with EGF/FGF to model proliferating tumour cells (Proliferating) and BMP4/FGF for three days to model the AC-like dormant population (BMP4/FGF-treated) (Fig 3.4A). Proliferation was assessed with EdU incorporation for 30 mins and subsequent

completion of the Click-iT reaction (See Methods Chapter 7.7.1). The percentage of EdU positive cells was quantified by imaging and analysed on Cell Profiler (Fig 3.4A)

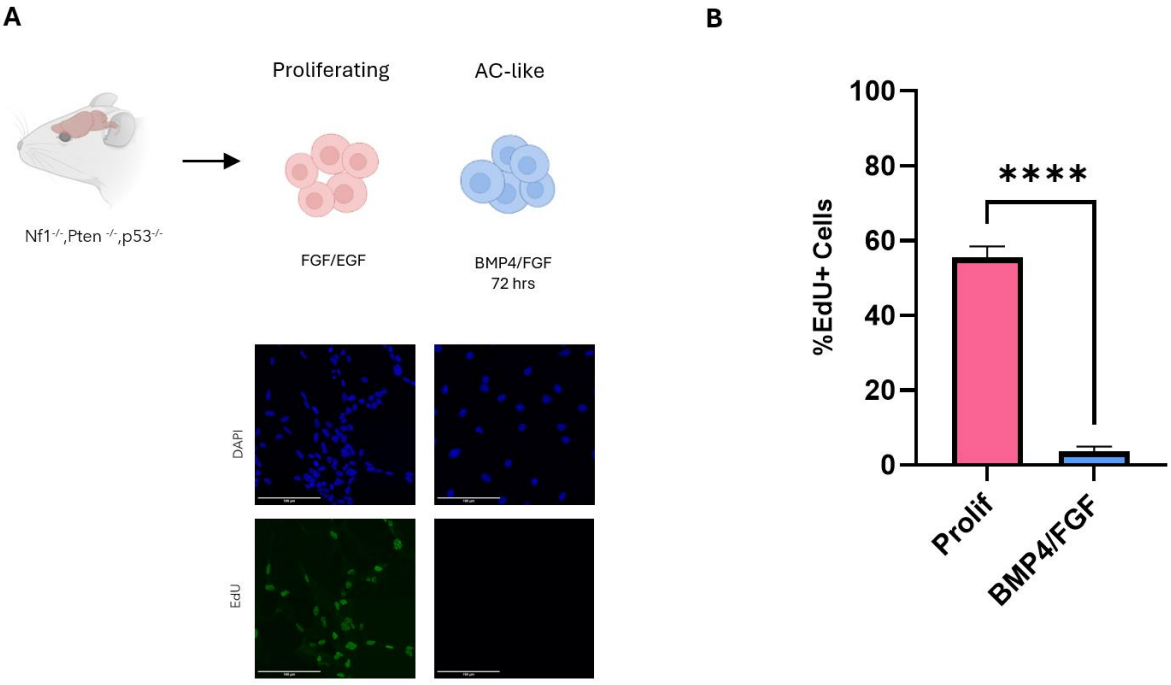

Figure 3.4 BMP4/FGF-treatment induces robust cell cycle arrest in the S177F primary mouse tumour line

*Primary mouse tumour cell line S177F was isolated and cultured in vitro for three days with either EGF/FGF to model proliferating (Prolif) conditions and with BMP4/FGF to model the AC-like dormant state (BMP4/FGF-treated). Tumour cells were incubated with EdU for 30 mins. EdU Click-iT reaction was performed with imaging as described in methods section 7.4.1. Analysis was completed using Cell Profiler. (A) Diagram of the experiment outline. (B) Representative images of EdU (Green) and nuclei with DAPI (Blue) staining (C) Bar chart showing the percentage of EdU+ cells of the proliferating and BMP4/FGF-treated tumour cells. Mean±SEM, n=3, t-test. (****p<0.0001)*

BMP4/FGF-treatment for three days significantly reduced the percentage of EdU+ cells *in vitro* (Fig 3.4B). Indeed, 54.89% of proliferating tumour cells were EdU+ whereas only 3.48% of the BMP4/FGF-treated tumour cells were EdU+ (Fig 3.4B). This data

suggests that BMP4/FGF-treatment induced a robust cell cycle arrest in the *Nf1*$^{-/-}$*/Pten*$^{-/-}$*/P53*$^{-/-}$ tumour cells *in vitro* which is consistent with the findings from the bulk RNAseq analysis.

However, tumour cell dormancy is defined as a reversible cell cycle arrest (Aguirre-Ghiso, 2007; Hadfield, 1954). Hence, in addition to measuring the cell cycle arrest induced by BMP4/FGF-treatment, we also measured the reversibility of this effect. We first induced cell cycle arrest with BMP4/FGF-treatment for three days (Fig 3.5A). Following this, the cells were washed and cultured in media with EGF/FGF for an additional three days to induce cell cycle re-entry or 're-activation' (Fig 3.5A). The levels of proliferation were measured using EdU incorporation as described above.

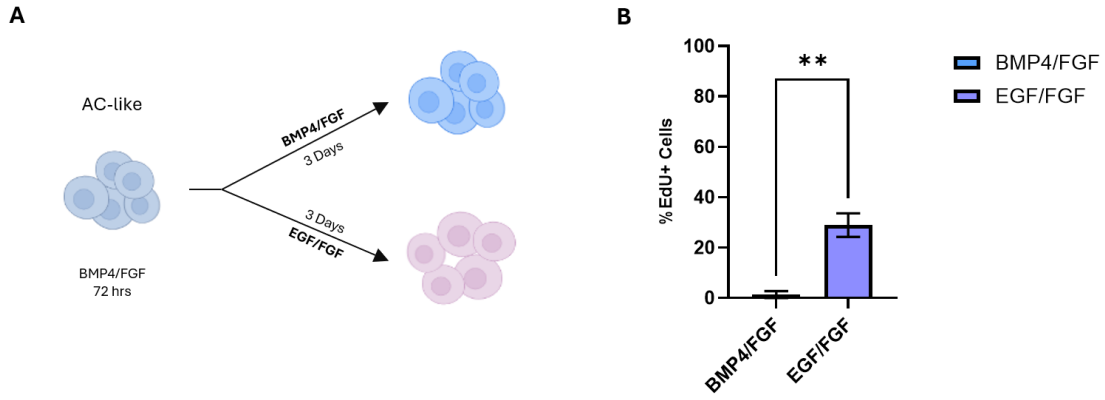

Figure 3.5 Cell cycle arrest is reversible

Primary mouse tumour cell line S177F was isolated and cultured in vitro to model the AC-like dormant state (BMP4/FGF for three days). To subsequently induce cell cycle re-entry or 'Re-activation', tumour cells were washed and cultured in media with EGF/FGF. Three days after culture in media with EGF/FGF, the tumour cells were incubated with EdU for 30 mins. EdU Click-iT reaction was performed with imaging as described in methods chapter 7.4.1. Analysis was completed using Cell Profiler. (A) Diagram of the experiment outline. (B) Bar chart showing

*the percentage of proliferating cells when maintained in BMP4/FGF compared to 're-activation' in media with EGF/FGF. Mean±SEM, n=4, t-test. (**p<0.01)*

The BMP4/FGF-treated tumour cells exhibited an increase in proliferation following 're-activation' from 1.41% when maintained in BMP4/FGF to 28.97% when cultured in EGF/FGF for three days (Fig 3.5B). Hence, this data confirms that although BMP4/FGF-treatment induced a robust cell cycle arrest, this effect is not permanent.

Furthermore, we assessed whether the robust cell cycle arrest observed in the *Nf1*$^{-/-}$*/Pten*$^{-/-}$*/P53*$^{-/-}$ tumour cells was conserved in patient-derived glioblastoma lines. Hence, we cultured four patient-derived glioblastoma lines in media with BMP4/FGF for three days and assessed the changes in proliferation. For this experiment, to quantify the percentage of proliferating tumour cells, we used EdU incorporation for two hours and performed the Click-iT reaction by FACS as described in methods chapter 7.7.1.

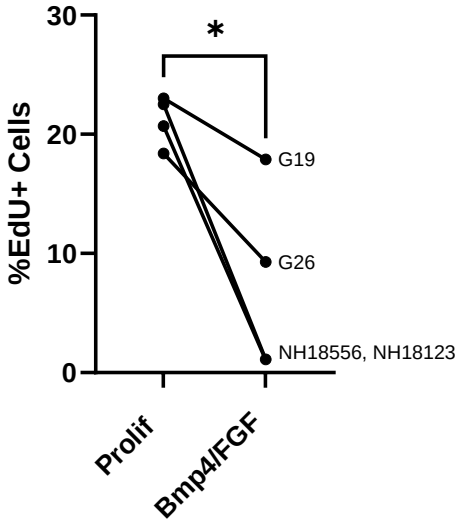

Figure 3.6 BMP4/FGF-treatment induced cell-cycle arrest in patient-derived glioblastoma lines

Patient-derived glioblastoma lines NH18556, NH18123, G19 and G26 were cultured with BMP4/FGF for three days or EGF/FGF (Prolif) for three days. Bar chart shows the percentage of

*EdU+ tumour cells in proliferating or BMP4/FGF-treated tumour cells. Mean±SEM, n=4, ratio paired t-test, (*p<0.05)*

We observed that BMP4/FGF-treatment significantly reduced proliferation in the patient-derived lines (Fig 3.6). The percentage of EdU+ cells were 21.15% in the proliferating tumour cells but were reduced to 7.34% in the BMP4/FGF-treated tumour cells (Fig 3.6). The degree of cell cycle arrest was notably variable between patient-derived glioblastoma lines, where BMP4/FGF-treatment was less effective in reducing the proliferation in the G19 and G26 cell lines (Fig 3.6). Altogether, this data suggests that the effect of BMP4/FGF-treatment on proliferation is conserved in the four patient-derived lines used in this experiment. However, it is unlikely that all patient-derived lines will exhibit a robust cell cycle arrest (Pollard et al., 2009a).

3.3 BMP4/FGF-treated tumour cells are radio-resistant

In chapter 2, we established that the AC-like dormant cells are likely radio-resistant *in vivo*. In fact, the AC-like dormant tumour cells were the only dormant population enriched one week following radiotherapy *in vivo* (Chapter 2.1). Hence, we assessed whether the BMP4/FGF-treated tumour cells were also radio-resistant *in vitro*.

To assess the radio-resistance of the proliferating and BMP4/FGF-treated tumour cells, we measured cell death three days after a single dose of radiation. Cell death was measured using Sytox Green (Invitrogen), a live cell impermeable dye (Fig 3.7B). Cells were imaged live and the percentage of dead or Sytox positive cells were quantified using Cell Profiler (See Methods Chapter 7.7.2). The nature of the dye does not capture the

early stages of cell death, nor does it identify cells which may have entered a non-proliferative state (eg. Senescence) following radiation. However, this author found that the use of Sytox Green allows for the efficient measure of cell death at these time points. While the well-established colony formation assay may have addressed these concerns, in this author's experience, the *Nf1*$^{-/-}$/*Pten*$^{-/-}$/*P53*$^{-/-}$ tumour cells did not form compact colonies which hindered accurate colony counting. Hence, Sytox Green was used to measure cell death.

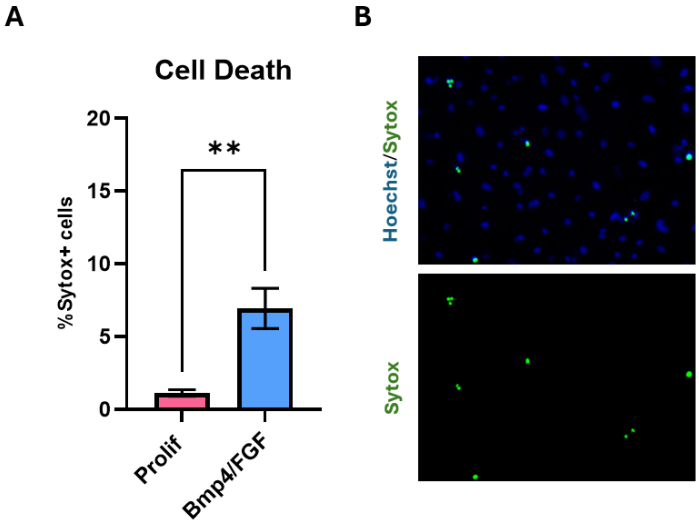

Figure 3.7 Bmp4/FGF-treated and differentiated tumour cells exhibited higher levels of cell death than proliferating tumour cells before radiation

*Cell death was measured in the unirradiated proliferating and BMP4/FGF-treated tumour cells using Sytox Green (Invitrogen), a live cell impermeable dye. (A) Bar chart shows the dead (Sytox+) cells as a percentage of total number of cells. Mean±SEM, n=4 (S177F cell line), t-test (**p< 0.01). (B) Representative images of Hoechst (blue) and Sytox (green) staining.*

Firstly, we observed significantly higher levels of cell death in the BMP4/FGF-treated tumour cells compared to the proliferating tumour cells without radiation (Fig 3.7). Without radiation, only 0.93% of the proliferating tumour cells were dead whereas

5.55% of the BMP4/FGF-treated tumour cells were dead (Fig 3.7). This observation may be due to the removal of EGF a known survival factor (Henson & Gibson, 2006).

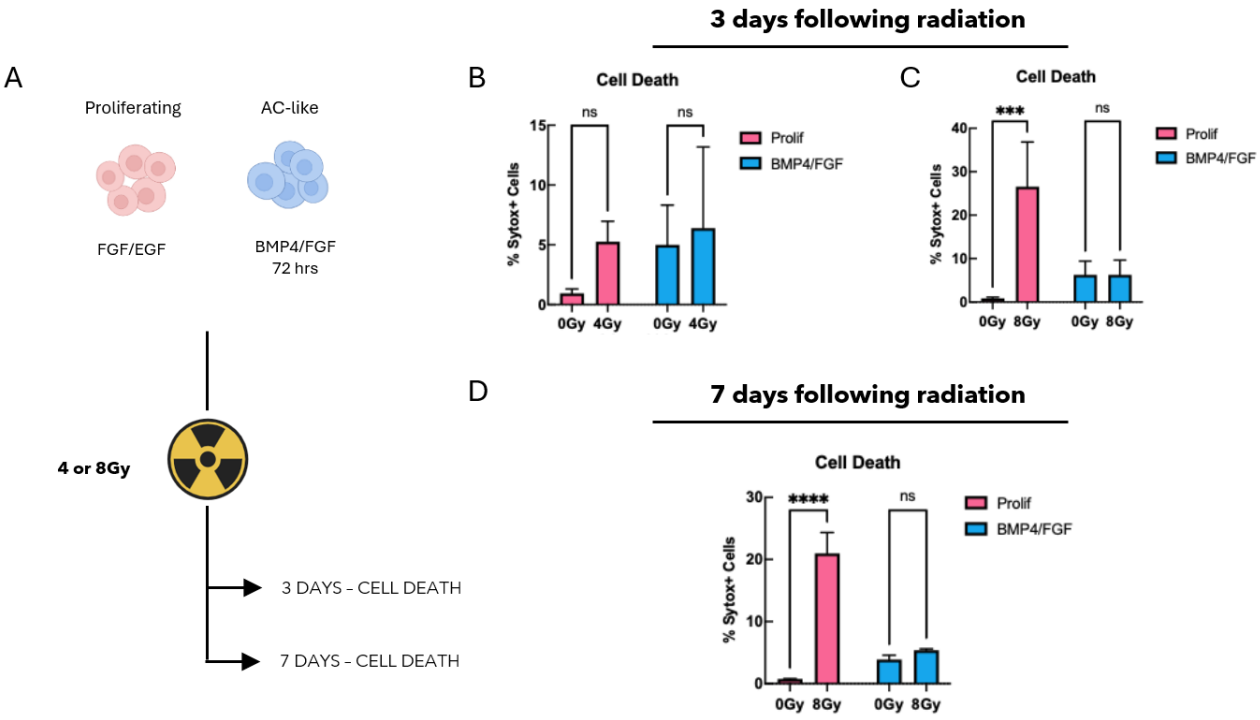

Figure 3.8 BMP4/FGF-treated tumour cells are radio-resistant compared to proliferating tumour cells

*Cell death was measured in the proliferating and BMP4/FGF-treated tumour cells three and seven days after radiation using Sytox Green (Invitrogen), a live cell impermeable dye. The percentage of Sytox+ cells was quantified with imaging and analysed on cell profiler. Fold change was calculated based on the relative unirradiated control (A) Experiment outline. (B) Cell death of tumour cells three days following 4 Gy of radiation. (C) Cell death of tumour cells three days following 8 Gy of radiation. (D) Cell death of tumour cells seven days following 8 Gy of radiation. All graphs show Mean±SEM, n=3 technical replicates of the S177F cell line. two-way ANOVA. (***p<0.001, **** p<0.0001)*

Three days following 4 Gy of radiation, there is no significant increase in cell death in either the proliferating or BMP4/FGF-treated tumour cells (Fig 3.8B). On the other hand, the proliferating tumour cells exhibited a significant increase in cell death three days after 8 Gy of radiation (Fig 3.8C). Following 8 Gy of radiation at this time point, the proliferating tumour cells show an increase in cell death from 0.83% to 26.55% (Fig 3.8C). Interestingly, the BMP4/FGF-treated tumour cells did not exhibit significantly increased levels of cell death three days after 8 Gy of radiation. Similarly, seven days after 8 Gy of radiation we observe a significant increase in cell death of the proliferating tumour cells but not the BMP4/FGF-treated tumour cells. Together, this data highlights that the BMP4/FGF-treated tumour cells are significantly more radio-resistant than the proliferating tumour cells.

However, it is known that uncontrolled cell division plays a role in radiation-induced cell death. Proliferating tumour cells likely have dysfunctional cell cycle checkpoints which may allow them to pre-maturely enter mitosis with unrepaired DNA damage (Chan et al., 1999; Vakifahmetoglu et al., 2008). This may result in mitotic death and eventual necrosis of the tumour cells. Hence, we considered whether, after radiation, the BMP4/FGF-treated tumour cells may have exhibited less cell death than the proliferating tumour cells *in vitro* solely due to their cell cycle arrest. Thus, we investigated whether the BMP4/FGF-treated tumour cells could re-enter the cell cycle without experiencing enhanced cell death following radiotherapy.

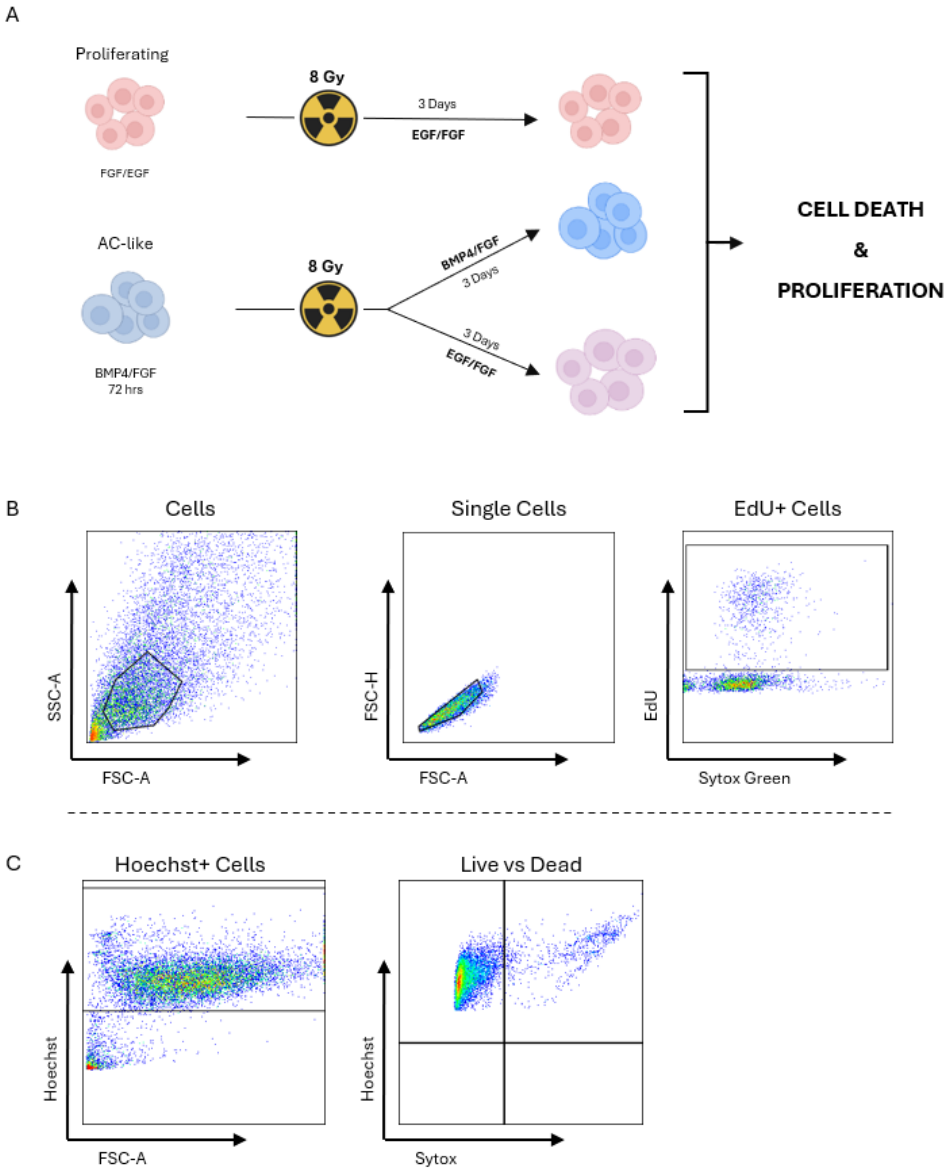

Figure 3.9 Gating Strategy and Experiment outline

(A) Diagram representing the experiment outline (B) Gating strategy to assess the percentage of EdU+ cells by FACS. (C) Gating strategy to assess the percentage of dead cells (Sytox+Hoechst+) cells by FACS.

To test this hypothesis, three different primary *Nf1*$^{-/-}$*/Pten*$^{-/-}$*/P53*$^{-/-}$ mouse tumour lines were first cultured in either proliferating conditions (EGF/FGF) or BMP4/FGF for three days before irradiation. Four hours following radiation, the BMP4/FGF-treated

tumour cells were washed with PBS and cultured with either BMP4/FGF to maintain cell cycle arrest or cultured with EGF/FGF to induce proliferation (Fig 3.9A). BMP4/FGF-treated tumour cells that were kept in BMP4/FGF following radiation will hereto be referred to as dormant BMP4/FGF-treated tumour cells (Fig 3.9A). On the other hand, BMP4/FGF-treated tumour cells that were cultured in EGF/FGF following radiation will be referred to as re-activated BMP4/FGF-treated tumour cells (Fig 3.9A). Cell death was measured three days following radiation using Sytox, the live cell impermeable dye (See chapter 7.7.2). FACS analysis was used to quantify the cell death of each condition (Fig 3.9C) (See chapter 7.7.2). In addition to cell death, we measured the percentage of proliferating cells through EdU incorporation three days following radiation to assess whether the BMP4/FGF-treated tumour cells would re-activate following radiation. The percentage of EdU+ tumour cells were quantified by FACS analysis (Fig 3.9B) (See chapter 7.7.1).

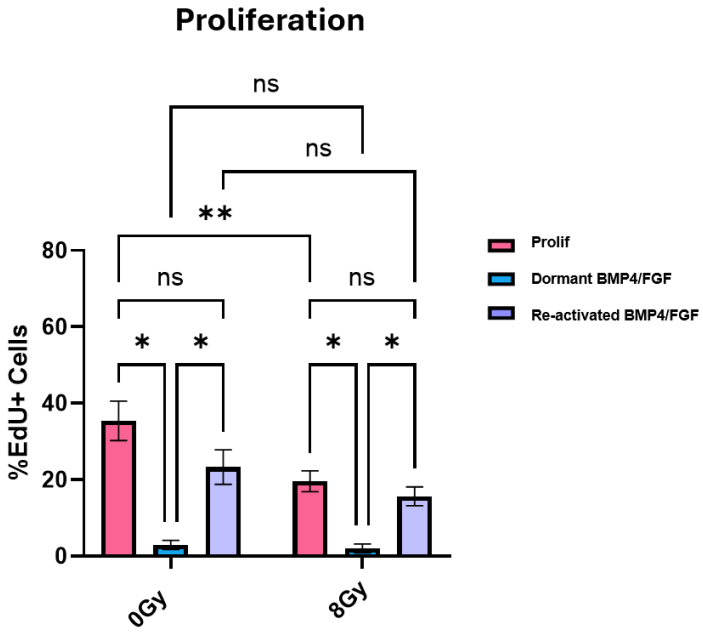

Figure 3.10 The BMP4/FGF-treated tumour cells re-activate despite radiation

*Proliferation was assessed three days following radiation (8Gy). The tumour cells were incubated with EdU for 2 hrs. EdU Click-iT reaction was performed and quantified by FACS as described in methods chapter 7.7.1. Bar chart shows the percentage of EdU+ cells. Mean ± SEM, n=3 unique biological cell lines, two-way ANOVA, Tukey's Test (*p<0.05, **p<0.01).*

Without radiation, we found that 35.41% of the proliferating tumour cells were EdU+ while only 2.88% of the dormant BMP4/FGF-treated tumour cells were EdU+ (Fig 3.10). Indeed, BMP4/FGF-treatment significantly reduced the percentage of proliferating tumour cells which is in line with previous data from the S177F line (See Chapter 3.2). In addition, the re-activated BMP4/FGF-treated tumour cells exhibited a significantly higher percentage of EdU+ cells than the dormant BMP4/FGF-treated tumour cells. Again, this is consistent with previous findings that the effect of BMP4/FGF-treatment is reversible (See Chapter 3.2).

We found that the proliferating tumour cells were less proliferative three days following radiation (Fig 3.10). Only 19.58% of the proliferating tumour cells were EdU+ after radiation (Fig 3.10). Additionally, radiation did not significantly alter the percentage of EdU+ cells in either the dormant or re-activated BMP4/FGF-treated tumour cells (Fig 3.10). Importantly, we found that there was a higher percentage of EdU+ cells in the re-activated BMP4/FGF-treated tumour cells compared to the dormant BMP4/FGF-treated tumour cells (Fig 3.10). 15.64% of the re-activated BMP4/FGF-treated were EdU+ whilst only 1.97% of the dormant BMP4/FGF-treated tumour cells were EdU+ following radiation (Fig 3.10). This data highlights that the BMP4/FGF-treated tumour cells could re-enter the cell cycle or 're-activate' when cultured with EGF/FGF despite radiation.

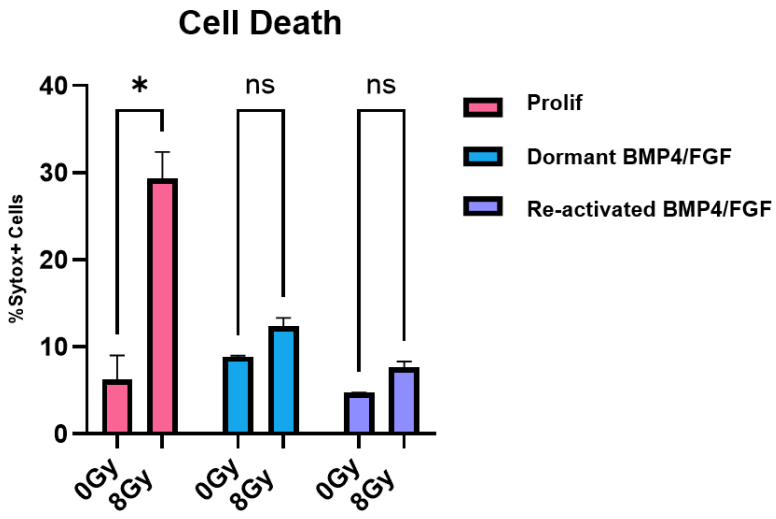

Figure 3.11 Cell cycle re-entry does not increase the cell death of BMP4/FGF-treated tumour cells

*Cell death was assessed three days following radiation (8Gy). Cell death was measured using Sytox Green (Invitrogen) and quantified by FACS as described in methods chapter 7.72. Bar chart shows the percentage of Sytox+ cells. Mean±SEM , n=3, two-way ANOVA, Sidak's test (*p<0.05).*

Next, we assessed the level of cell death of the proliferating, the dormant BMP4/FGF-treated and re-activated BMP4/FGF-treated tumour cells following radiation. In line with previous results, the proliferating tumour cells exhibited a significant increase in cell death three days following radiation (Fig 3.11). Cell death increased from 6.23% without radiation to 29.37% following radiation in these proliferating tumour cells (Fig 3.11). Importantly, the BMP4/FGF-treated tumour cells showed no significant increase in cell death following radiation (Fig 3.11). However, there was a small trend towards an increase from 8.86% without radiation to 12.33% with radiation (p=0.1892) (Fig 3.11E). Unexpectedly the reactivated BMP4/FGF-treated tumour cells exhibited less cell death compared to the dormant BMP4/FGF-treated tumour cells with and without

radiation (Fig 3.11). There was no significant difference in cell death of the re-activated BMP4/FGF-treated tumour cells with and without radiation (Fig 3.11E). However, similarly to the dormant BMP4/FGF-treated tumour cells, there was a trend towards an increase in cell death from 4.71% without radiation to 7.66% with radiation in the re-activated BMP4/FGF-treated tumour cells (p=0.1238) (Fig 3.11E).

Evidently, the BMP4/FGF-treated tumour cells can re-activate as previously shown. However, there was a trend towards lower levels of proliferation in the re-activated BMP4/FGF-treated tumour cells compared to the proliferating tumour cells. It is possible that three days is insufficient to recover pre-BMP4/FGF-treatment levels of proliferation. Nevertheless, these findings suggest that re-activation of the BMP4/FGF-treated cells following radiation did not significantly increase their cell death. This work confirms that the BMP4/FGF-treated tumour cells are indeed radioresistant.

3.4 Discussion

In this chapter we sought to determine whether BMP4/FGF-treatment for three days *in vitro* could model the AC-like dormant population identified in the *Nf1*$^{-/-}$/*Pten*$^{-/-}$/*P53*$^{-/-}$ mouse model of glioblastoma. To this effect, we established that BMP4/FGF-treated tumour cells exhibited a transcriptional profile that resembles the AC-like dormant population. Furthermore, we confirmed that BMP4/FGF-treatment induced a robust but reversible cell cycle arrest. Finally, we established that the BMP4/FGF-treated cells are more resistant to radiation than proliferating tumour cells. In conclusion, BMP4/FGF-

treatment may be a useful *in vitro* model to study the radio-resistance mechanisms of the AC-like dormant population.

We anticipated that the GSEA of the bulk RNAseq data would indicate downregulation of cell cycle associated pathways and upregulation of pathways associated with BMP signalling. On the other hand, it was somewhat surprising that epithelial to mesenchymal transition (EMT) and IFN signalling were amongst the most positively enriched pathways in the BMP4/FGF-treated tumour cells.

It is thought that glioblastoma does not undergo EMT, hence, it is interesting that the EMT was the most upregulated pathway in the BMP4/FGF-treated tumour cells (Iser et al., 2019; Iwadate, 2016; Roche, 2018). EMT describes the reversible process by which tumour cells transition from an epithelial-like state to a more mesenchymal-like state (Iwadate, 2016; Roche, 2018). Two Hallmarks of EMT are tumour cell detachment from the cell membrane and the downregulation of E-cadherin in accompanied by an upregulation of N-Cadherin (Iwadate, 2016; Roche, 2018). Yet, the CNS has no basement membrane except for the vasculature, and glioblastoma has been shown to have higher expression of N-cadherin accompanied with low E-cadherin expression (Iser et al., 2017, 2019; Iwadate, 2016; Roche, 2018). For these reasons, glioblastoma may not undergo the EMT process, but it is plausible to suggest that glioblastoma may exhibit characteristics associated with EMT. We found the leading-edge genes of the EMT pathway included *Vcam1*, *Snai2*, multiple genes encoding laminin, and multiple genes encoding collagen. Furthermore, amongst these leading-edge genes is *Cdh2*, which encodes N-cadherin. Given that these genes are thought to be upregulated in EMT, it follows that the BMP4/FGF-treated tumour cells exhibit a significant upregulation of this

pathway despite the controversial role for EMT in glioblastoma. Whilst there is little evidence describing the impact of BMP treatment on the expression of EMT-associated genes in glioblastoma, multiple studies in epithelial cancers support this observation (S. Choi et al., 2019; Kestens et al., 2016). Indeed, Choi *et al*. demonstrated that BMP4 increased the expression of fibronectin, laminin, N-Cadherin and slug in the MCF-10A breast tumour cell line (S. Choi et al., 2019). Additionally, Kestens *et al*. showed that BMP4 treatment increased the migration of oesophageal adenocarcinoma cells *in vitro* which was accompanied with significantly increased expression of the epithelial to mesenchymal associated marker Snail2 (Kestens et al., 2016). Further research is necessary to understand whether BMP signalling results in an upregulation of EMT-associated genes in glioblastoma. However, it remains unclear why BMP would induce the expression of EMT-associated genes in a tumour that is not known to undergo EMT (Iser et al., 2019; Iwadate, 2016; Roche, 2018). One possible explanation for this observation is the thought that EMT in glioblastoma resembles reactive astrocytes, a cell state by which astrocytes transform into in response to injury or insults to the CNS (Iser et al., 2019; Iwadate, 2016; C. Zhang et al., 2023). Thus, the upregulation of EMT in the BMP4/FGF-treated tumour cells may be indicative of differentiation towards a MES-like state, given that reactive astrocytes are thought to resemble MES-like tumour cells (Niklasson et al., 2019; Richards et al., 2021). This idea is supported by the fact that the MES-Plp1 population in the *Nf1*$^{-/-}$*/Pten*$^{-/-}$*/P53*$^{-/-}$ glioblastoma mouse model also expressed the BMP4/FGF-treatment signature.

In addition to the EMT pathway, IFNα signalling and IFNγ signalling were amongst the top five upregulated pathways in the BMP4/FGF-treated tumour cells. In

fact, multiple inflammation-associated Hallmark pathways were upregulated in the BMP4/FGF-treated tumour cells (Fig 3.2, Appendix Table 3.1). There was significant upregulation of the inflammatory signalling, IL2-STAT5 signalling, IL6-JAK-STAT3 signalling and the TNFα signalling pathway via NFkβ gene sets. Together these findings collectively point towards a link between BMP4/FGF-treatment and inflammation. One explanation for this finding may be the increased cell death observed in the BMP4/FGF-treated tumour cells. Furthermore, another study similarly identified an upregulation of inflammation and injury associated Hallmark gene signatures in U3065 MG cell lines following exposure to BMP4 (Niklasson et al., 2024). There is also some evidence to suggest that BMP signalling may promote the inflammatory response (Eixarch et al., 2020; X. Zhao et al., 2021). One study showed that culturing primary mouse splenocytes with BMP4 significantly increased their expression of GM-CSF, IFNγ, IL-6 and TNFα (Eixarch et al., 2020). In addition, it has been observed in patients undergoing surgery that elevated circulating levels of BMP4 were positively correlated with elevated circulating levels of IL-1β and TNFα (X. Zhao et al., 2021). We may speculate that BMP4 signalling may directly induce the upregulation of pro-inflammatory cytokines, which may account for the upregulation of multiple inflammation-associated signalling pathways in the BMP4/FGF-treated tumour cells. However, BMP4 is also known to have an anti-inflammatory effect in the context of inflammatory bowel disease (Hu et al., 2021; Ji et al., 2016). Indeed, Hu *et al.* demonstrated that BMP4 treatment alleviated dextran-sulfate-induced colitis *in vivo* (Hu et al., 2021). Further work is necessary to validate whether BMP4/FGF-treatment is associated with increased inflammation *in vitro*.

We identified that the BMP4/FGF-treatment transcriptional signature was highly expressed by the AC-like tumour cells. This suggests that the BMP4/FGF-treatment induced astrocyte-like changes were in line with previous studies that demonstrated the role for BMP4 in inducing astrocytic differentiation in patient-derived glioblastoma lines (Carén et al., 2015; Han, Cai, et al., 2022; Pollard et al., 2009a). Interestingly, this contrasts with recent work by Nikklasson *et al*. who performed bulk RNAseq on BMP4 treated U3065 MG cell line and did not observe astrocytic differentiation (Niklasson et al., 2024). One potential explanation for this may be that the astrocytic differentiation induced by BMP4 depends on cell intrinsic factors. Building on this point, Pollard *et al*. and Carén *et al*. observed variability in the degree of astrocytic differentiation in different patient lines following exposure of the tumour cells to BMP4 (Carén et al., 2015; Pollard et al., 2009a).

It is not unexpected that the patient-derived lines exhibited varying degrees of cell-cycle arrest in response to BMP4/FGF-treatment. This finding is consistent with results from Carén *et al*. who demonstrated that 2 weeks of BMP4 treatment also resulted in varying degrees of cell cycle arrest in a series of patient-derived glioblastoma lines (Carén et al., 2015). To this author's knowledge all the patient-derived tumour lines used in this experiment expressed receptors for BMP4. However, it remains unclear what determines the extent of the response to BMP4 signalling in these patient derived lines.

In addition, we observed higher levels of cell death in the BMP4/FGF-treated tumour cells compared to the proliferating tumour cells following 8 Gy of radiation. This finding is consistent with the upregulated apoptosis pathway in the BMP4/FGF-treated tumour cells as identified through GSEA of the bulk RNAseq data. The apoptosis pathway

exhibited an NES of 1.98 (padj = 2.40E-07). It is important to note that the BMP4/FGF-treated cells were cultured with less growth factors than the proliferating tumour cells. EGF, of course is a known pro-survival factor, hence, their removal in the slow-cycling models likely accounts for the higher levels of cell death (Henson & Gibson, 2006).

We demonstrated that the BMP4/FGF-treated tumour cells were more radio-resistant than the proliferating tumour cells *in vitro*. This is in line with previous findings that the AC-like dormant population were radio-resistant following fractionated radiotherapy *in vivo* (Chapter 2.1). Importantly, we confirmed that the BMP4/FGF-treated cells remain viable following radiation, given they were able to re-enter the cell cycle without a significant increase in cell death following radiation. Hence, this BMP4/FGF-treated model of the AC-like dormant population may serve as a valuable tool to determine the mechanisms underlying the radio-resistance of the AC-like dormant population.

Chapter 4. Investigating the mechanisms underlying the radio-resistance of BMP4/FGF-treated tumour cells

In chapter 3, we established that BMP4/FGF-treatment induced transcriptional changes that recapitulate the AC-like dormant cells identified in the *Nf1*$^{-/-}$/*Pten*$^{-/-}$/*P53*$^{-/-}$ mouse model of glioblastoma. Importantly, we confirmed that the BMP4/FGF-treated tumour cells are more radio-resistant than proliferating tumour cells *in vitro*. In this chapter, we sought to leverage this *in vitro* model of AC-like dormant tumour cells to investigate the mechanisms underlying their radio-resistance.

It is well established that radiotherapy targets tumour cells by inducing DNA damage (Ali et al., 2020; Boustani et al., 2019; Kuo & Yang, 2008). Hence, we characterised how the BMP4/FGF-treated and proliferating tumour cells respond to radiation-induced DNA damage. Specifically, we sought to quantify the levels of radiation-induced DNA damage and the activity of specific DSB repair mechanisms *in vitro*.

In addition to the DDR and DNA damage repair, tumour cell radio-resistance may also be mediated by a number of factors including cell cycle phase, oxygenation status, and stemness (Ali et al., 2020; Boustani et al., 2019; Ou et al., 2020). It is possible that a combination of these factors may contribute to the radio-resistance of AC-like dormant

tumour cells. Hence, we also we sought to identify potential mechanisms of radio-resistance that were independent to DDR and the DNA damage repair using a bulk RNAseq approach.

4.1 BMP4/FGF-treated cells exhibited higher levels of DNA damage immediately following radiation and likely faster DNA damage repair

Radiotherapy kills tumour cells primarily through the induction of DNA damage (Ali et al., 2020; Boustani et al., 2019; Kuo & Yang, 2008). It follows that the rapid resolution of radiation-induced DNA damage impacts tumour cell survival. Hence, we first assessed the DNA damage levels of proliferating and BMP4/FGF-treated tumour cells following a single dose of radiation.

4.1.1 BMP4/FGF-treated cells exhibited higher levels of DNA damage immediately following radiation

To assess DNA damage levels following radiation, we first utilised the alkali comet assay. This assay allowed us to measure both SSBs and DSBs, which may indicate the total level of DNA damage. The comet assay protocol used was adapted from Hartley *et al.* and is described further in methods chapter 7.7.3 (Hartley et al., 2011). To quantify peak levels of DNA damage, samples were collected 0 mins following radiation. For the 0 min timepoint, cells were first dissociated before being irradiated on ice. This ensured that the timepoint reflected close to peak levels of radiation-induced DNA damage. While this

0 min time point is called as such, it may not truly reflect 0 mins; although the DDR activity within the cells may have been slowed or stopped while on ice, during lengthy processing it is possible for some repair to occur. However, this time point still serves as an indication of peak levels of DNA damage. Additionally, the time points for the alkali comet assay extended up to 24 hrs following radiation which allowed us to compare the resolution of DNA damage in the BMP4/FGF-treated and proliferating tumour cells. The levels of DNA damage were represented by the olive tail moment, which is calculated by considering both the distribution of total DNA in the tail and the length of this tail.

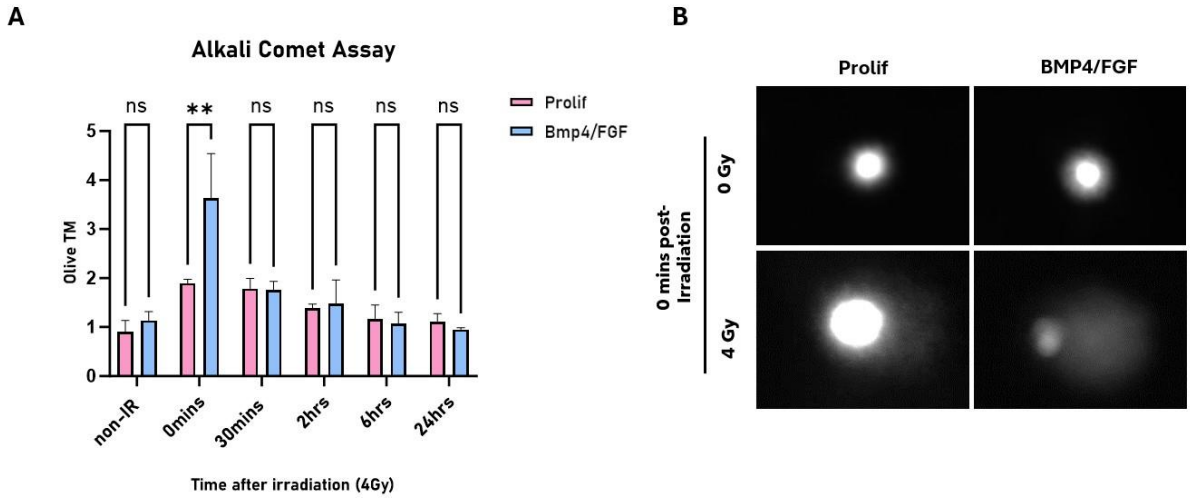

Figure 4.1 Alkali comet assay of the BMP4/FGF-treated and proliferating tumour cells following radiation

*DNA damage was quantified using the alkali comet assay (identifies both SSBs and DSBs) following radiation (4 Gy) of the BMP4/FGF-treated and proliferating tumour cells. (A) Bar graph represents the amount of DNA damage (Olive TM) using the alkali comet assay. Mean±SEM, n=3 (biological replicates), 80 cells analysed per sample. Two-way ANOVA Sidak's multiple comparison test. (**p<0.01) (B) Representative images of Alkali comet assay of proliferating and BMP4/FGF-treated tumour cells.*

In the alkali comet assay, there was no significant difference in DNA damage between the BMP4/FGF-treated and proliferating tumour cells without radiation (Fig 4.1A). Unexpectedly, the BMP4/FGF-treated tumour cells exhibited significantly more DNA damage than the proliferating tumour cells 0 mins following radiation (Fig 4.1A). The BMP4/FGF-treated tumour cells exhibited an olive tail moment of 3.63, whilst the proliferating tumour cells exhibited an olive tail moment of 1.89 (Fig 4.1A). However, 30 mins following radiation, there was no significant difference in DNA damage levels between the BMP4/FGF-treated and proliferating tumour cells (Fig 4.1A). Furthermore, there were no significant differences in DNA damage between the proliferating and BMP4/FGF-treated tumour cells from 30 mins to 24 hrs following radiation (Fig 4.1A); Indeed, the rate of DNA damage resolution was similar between the BMP4/FGF-treated and proliferating tumour cells from 30 mins to 24 hrs (Fig 4.1A).

Subsequently, we assessed DNA damage with the neutral comet assay to understand whether the higher levels of peak DNA damage exhibited by the BMP4/FGF-treated cells were due to DSBs specifically. Unlike its alkali counterpart, the neutral comet assay exclusively assesses the level of DSBs. This type of DNA damage is particularly relevant to radiation given that DSBs are considered the most cytotoxic type of DNA damage (Cantoni et al., 1994; Dahm-Daphi et al., 2000). The neutral comet assay protocol was also adapted from Hartley *et al.* and described in further detail in methods chapter 7.7.3 (Hartley et al., 2011). Consistent with the alkali comet assay, the 0 min timepoint represents the peak levels of DSBs experienced by the tumour cells. The last time point assessed by the neutral comet assay was 30 mins following radiation; this timepoint was selected since the alkali comet assay showed no significant difference in

DNA damage between the BMP4/FGF-treated and proliferating tumour cells from this time point (Fig. 4.1.1A). Again, the olive tail moment was used to represent the levels of DNA damage.

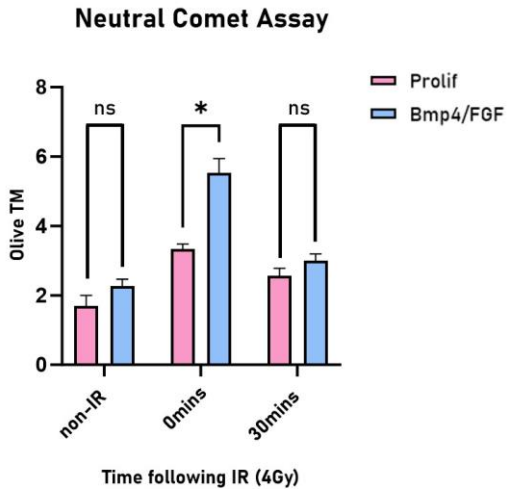

Figure 4.2 Neutral comet assay of the BMP4/FGF-treated and proliferating tumour cells following radiation

*DSBs were quantified using the neutral comet assay (DSBs only) following radiation (4 Gy) of the BMP4/FGF-treated and proliferating tumour cells. (A) Bar graph represents the amount of DNA damage (Olive TM) using the neutral comet assay. Mean±SEM, n=3 (biological replicates), 60 cells analysed per sample. Two-way ANOVA Sidak's multiple comparison test. (*p<0.05)*

Consistent with the alkali comet assay, the neutral comet assay showed that the BMP4/FGF-treated tumour cells exhibited significantly more DSBs than the proliferating tumour cells 0 mins following radiation (Fig 4.2). The BMP4/FGF-treated tumour cells exhibited an olive tail moment of 5.54, whereas the proliferating tumour cells exhibited an olive tail moment of 3.34 at this 0 min time point (Fig 4.2). However, there was no significant difference in the levels of DSBs between the BMP4/FGF-treated and proliferating tumour cells 30 mins following radiation (Fig 4.2).

These results confirm that DSBs contribute to the higher levels of peak DNA damage we observed in the BMP4/FGF-treated cells. Yet, based on this data we cannot rule out the potential contribution of SSBs to the peak levels of DNA damage. Collectively, these two assays suggest that the BMP4/FGF-treated tumour cells indeed experience more DNA damage than proliferating tumour cells following radiation. Given that there is no difference in DNA damage between the BMP4/FGF-treated and proliferating tumour cells following radiation, this implies that the BMP4/FGF-treated tumour cells may repair their DNA damage faster than the proliferating tumour cells. Additionally, we observed a small trend towards higher levels of DNA damage in the BMP4/FGF-treated tumour cells without radiation in both the alkali and neutral comet assays. However, these findings are not statistically significant. Thus, further investigation is required to determine whether BMP4/FGF-treatment plays a role in inducing DNA damage without radiation.

4.1.2 Both the BMP4/FGF-treated and proliferating tumour cells resolve radiation-induced DNA damage

The alkali and neutral comet assay are well established methods of assessing DNA damage. Additionally, the olive tail moment considers the total amount of DNA in a cell which is useful when we expect differences in DNA content. This is relevant given the BMP4/FGF-treated tumour cells are mostly in G1 and therefore have less DNA than proliferating tumour cells which may partly be in S/G2. However, it is known that the assay may be variable with changes in electrophoresis temperatures or the length of alkali treatment (Sirota et al., 2014). Hence, it is important to use another method of measuring DNA damage to confirm our results. Another consistently used marker for DSBs is phosphorylated H2AX otherwise known as γH2AX. This histone variant is

phosphorylated immediately upon DNA damage (Foster & Downs, 2005; Kuo & Yang, 2008; Rogakou et al., 1998). Furthermore, γH2AX forms foci at DSB sites, in fact, one γH2AX focus represents a single DSB (Sedelnikova et al., 2002). γH2AX also serves to recruit key factors to the site of DNA damage to initiate the DDR and DSB repair pathways. Hence, this marker could also indicate the activity of DNA repair and DDR when considered together with the comet assay data (Foster & Downs, 2005; Kuo & Yang, 2008; Podhorecka et al., 2010).

To assess the levels of γH2AX foci, the proliferating and BMP4/FGF-treated tumour cells were fixed at 30 mins, 6 hrs, 16 hrs and 24 hrs following radiation. Cells were stained with γH2AX (Fig 4.3A) and imaged using the Opera Phenix Plus. Subsequent image analysis was performed on the Harmony software in collaboration with Ok-Ryul Song. Since this analysis identified the number of γH2AX foci within each nucleus, we were limited to analysing samples 30 minutes after radiation. We found that at earlier time points, it was difficult to distinguish the foci clearly using this method.

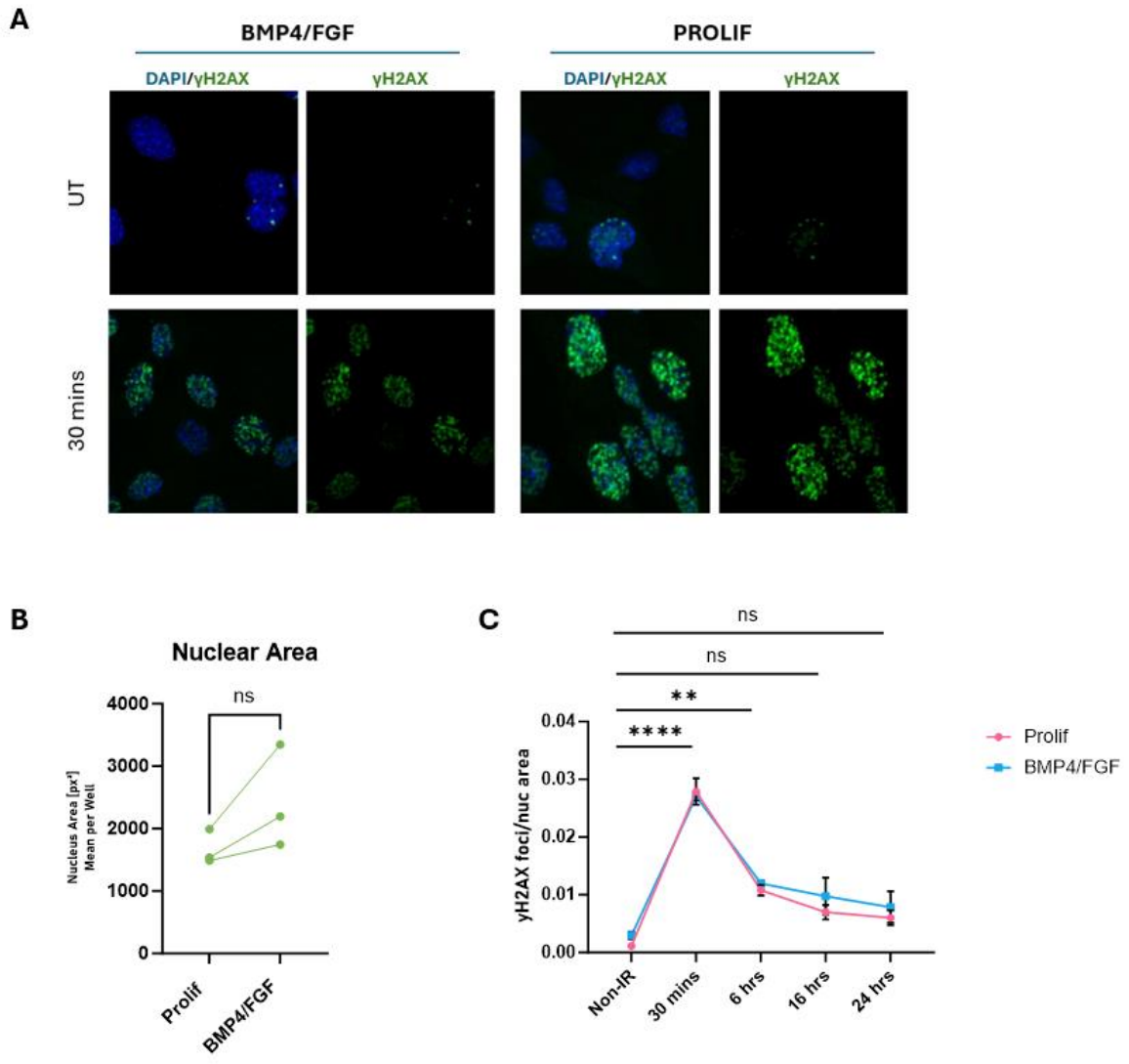

Figure 4.3 Both BMP4/FGF-treated and proliferating tumour cells repair their radiation-induced DNA damage

*DNA damage was measured by staining for γH2AX in BMP4/FGF-treated and proliferating tumour cells following radiation (4 Gy). Images of staining were acquired with the Opera Phenix in collaboration with Dr Ok-Ryul Song. (A) Sample images of γH2AX (Green) and dapi (Blue) staining for both the BMP4/FGF-treated and proliferating tumour cells (B) Line graph of average nuclear area/well. Mean±SEM, n=3, paired t-test. (C) Line graph of γH2AX foci/nucleus area. Mean±SEM, n=3, Two-way ANOVA Tukey's test. (**p<0.01, ****p<0.0001 for both Proliferating and BMP4/FGF-treated tumour cells)*

We observed that the BMP4/FGF-treated tumour cells had consistently but not significantly greater average nuclear area than the proliferating tumour cells (Fig 4.3A). The percentage increase in nuclear area was variable across the three biological cell lines used (Fig 4.3B). We reasoned that the increased nuclear area could alter the number of foci identified by the harmony analysis software if foci were too close together. Hence, to estimate the γH2AX levels in each sample, we normalised the mean number of γH2AX foci per well to the mean nuclear area per well.

We observed a trend towards higher levels of γH2AX foci in the BMP4/FGF-treated tumour cells compared to the proliferating tumour cells ($p=0.0762$) (Fig 4.3C). This result is in line with the findings from both the alkali and neutral comet assays. In both the BMP4/FGF-treated and proliferating tumour cells we observed that radiation induced peak levels at 30 mins following radiation (Fig 4.3C). This DNA damage was then resolved at a similar rate between the proliferating and BMP4/FGF-treated tumour cells from 30 mins to 24 hrs after radiation (Fig 4.3C). There was no significant difference in the γH2AX foci levels between the proliferating and BMP4/FGF-treated tumour cells at 30 mins, 6 hrs, 16 hrs and 24 hrs following radiation (Fig 4.3C). Again, this is consistent with the rate of DNA damage repair observed using the alkali and neutral comet assays.

Although the findings were not significant, the γH2AX data and both alkali and neutral comet assays suggest that BMP4/FGF-treated cells exhibit increased DNA damage without radiation. However, further research is needed to confirm whether BMP4/FGF-treatment can increase DNA damage in the *Nf1*$^{-/-}$*/Pten*$^{-/-}$*/P53*$^{-/}$ tumour cells. Indeed, this finding was unexpected given that proliferating tumour cells are thought to experience high levels of DNA damage due to factors such as replication stress or

increased metabolic activity (Gaillard et al., 2015; Hills & Diffley, 2014; Jang et al., 2013; Stanke et al., 2021).

Following radiation, there were no differences in DNA damage levels, and consequently, no differences in DNA damage repair rates between the proliferating and BMP4/FGF-treated tumour cells. This finding supports the data acquired from 30 mins after radiation through the neutral and alkali comet assays. Additionally, it implies that the DDR may be similarly activated in the BMP4/FGF-treated and proliferating tumour cells given the role of γH2AX in mediating the DDR (Foster & Downs, 2005; Kuo & Yang, 2008; Podhorecka et al., 2010). Altogether, the γH2AX and the comet assay results are consistent from 30 mins to 24 hrs.

4.2 BMP4/FGF-treatment induced higher levels of ROS

In the previous section, we established that the BMP4/FGF-treated tumour cells likely experienced more DNA damage than the proliferating tumour cells immediately after radiation. Given that radiation-induced ROS are a major source of DNA damage, we assessed differences in ROS levels between BMP4/FGF-treated and proliferating tumour cells.

To assess the differences in ROS levels between the BMP4/FGF-treated tumour cells compared to the proliferating tumour cells we first probed the bulk RNAseq data. We performed bulk RNAseq on BMP4/FGF-treated and proliferating tumour cells as described in methods chapter 7.8. QC and sequence alignment was performed by Wenhao Tang. We then performed differential gene expression analysis using the

DESeq2 package and GSEA using the fgsea package in R. We aimed to assess alterations in signalling pathways associated with ROS using the GO biological pathways gene set.

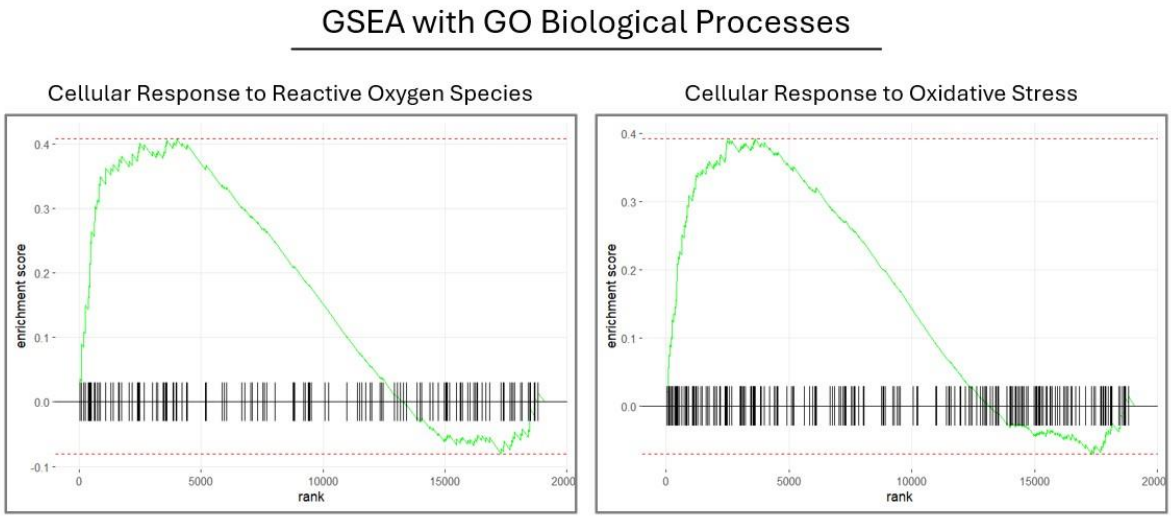

Figure 4.4 BMP4/FGF-treated tumour cells are enriched for pathways associated with ROS

Bulk RNAseq (See Methods Chapter 7.8) was performed on the $Nf1^{-/-}/Pten^{-/-}/P53^{-/-}$ tumour cells cultured in BMP4/FGF or EGF/FGF (Proliferating tumour cells) for 3 days. GSEA of bulk RNAseq data was performed using the GO Biological Processes gene set. Graphs showing enrichment scores of the following GO biological process pathways: cellular response to reactive oxygen species (Left) and cellular response to oxidative stress (Right).

We observed a significant positive enrichment for the 'cellular response to reactive oxygen species' and the 'cellular response to oxidative stress' pathways in the BMP4/FGF-treated tumour cells compared to the proliferating tumour cells (Fig 4.4). These two pathways exhibited a NES of 1.57 (padj = 1.06E-02) and 1.60 (padj = 1.60E-04) respectively (Fig 4.4) (Appendix Chapter 8.2). The observed upregulation of these

pathways suggests that the BMP4/FGF-treated tumour cells may exhibit increased levels of ROS.

In addition to these pathways, we also explored whether BMP4/FGF-treatment altered pathways or genes associated with antioxidants. Multiple genes encoding known antioxidant enzymes from the glutathione peroxidase (gpx) and glutathione-s-transferase (gst) families were upregulated in the BMP4/FGF-treated tumour cells (Appendix Chapter 8.1) (Kalinina et al., 2014; Pei et al., 2023). We observed the increased expression of *Gpx3* (2.069, padj= 1.09E-10), *Gpx4* (1.025 padj= 8.10E-09) and *Gpx8* (1.78 padj= 2.96E-15) in the BMP4/FGF-treated tumour cells (Appendix Chapter 8.1). Additionally, a series of gst enzymes were upregulated in the BMP4/FGF-treated tumour cells including *Gstm1* (log2fold change = 1.18, padj = 6.13E-03), *Gstm2* (log2fold change = 2.64, padj = 2.84E-10), *Gsta4* (log2fold change = 2.33, padj = 8.85E-13) (Appendix 1). However, GSEA found no significant alterations in the 'Cellular Oxidant Detoxification' pathway following BMP4/FGF-treatment. Thus, it remains unclear based on this analysis alone whether the BMP4/FGF-treated tumour cells have both increased levels of ROS and increased capacity to buffer ROS.

Following this analysis, we sought to quantify the actual levels of ROS in the BMP4/FGF-treated and proliferating tumour cells before and after radiation. To achieve this, the tumour cells were stained with CellRox Deep Red (Invitrogen), a dye that becomes fluorescent upon oxidation by ROS and subsequently accumulates in the cytoplasm (See Fig 4.5B). After staining, cells were fixed prior to imaging (See methods chapter 7.7.4). ROS levels were quantified using the total intensity of CellRox Deep Red normalised to the number of nuclei per well.

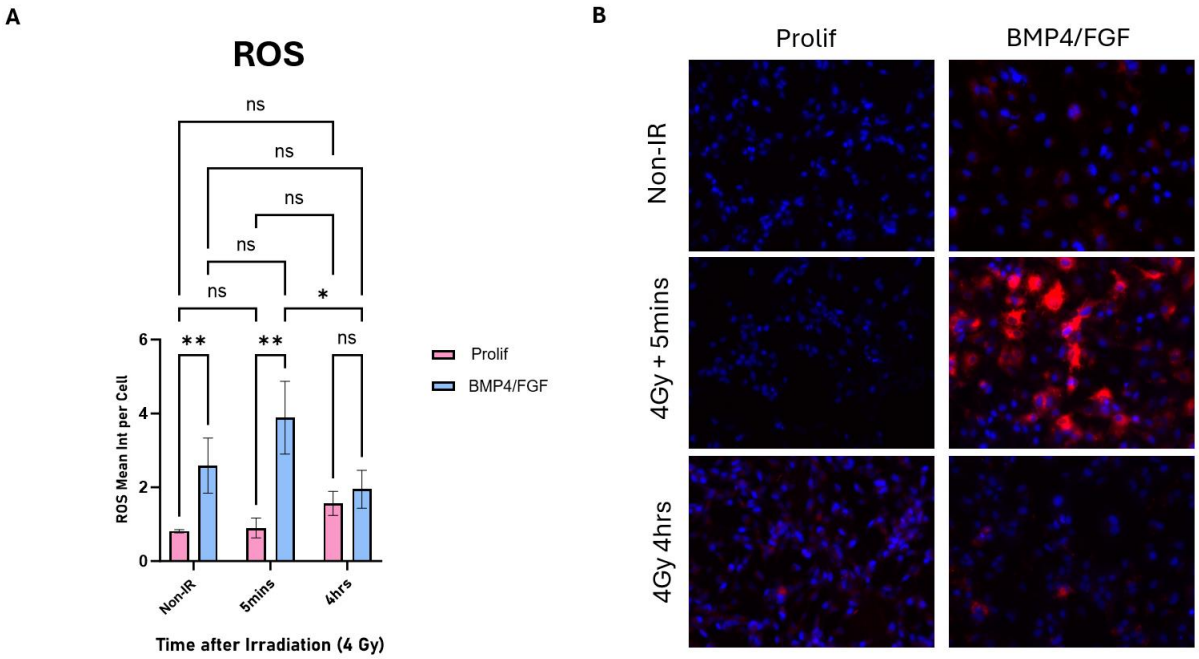

Figure 4.5 ROS levels are higher in the BMP4/FGF-treated tumour cells compared to the proliferating tumour cells

*ROS were measured by staining with CellRox Deep Red (See Methods Chapter 7.7.4), which fluoresces and deposits in the cytoplasm in the presence of ROS. Cells were fixed in 4% PFA for 15 minutes and imaged on the EVOS. (A) Bar chart shows the mean ROS intensity per cell of proliferating or BMP4/FGF-treated mouse cells which are non-IR, 5mins after radiation (4 Gy) or 4 hrs after radiation (4 Gy). (B) Representative images of ROS staining. Mean±SEM. n=3 (biological replicates), >500 cells analysed per sample. Two-way ANOVA, Sidak's multiple comparison test. (**p<0.01)*

The BMP4/FGF-treated tumour cells exhibited significantly higher levels of ROS than the proliferating tumour cells without radiation (Fig 4.5A). The BMP4/FGF-treated tumour cells exhibited a mean ROS intensity of 2.59 arbitrary units (a.u.), whereas the proliferating tumour cells exhibited a mean ROS intensity of 0.81 a.u. (Fig 4.5A). Interestingly, there were also significantly higher levels of ROS in the BMP4/FGF-treated tumour cells compared to the proliferating tumour cells 5 mins after radiation (Fig 4.5A).

At this time point, the BMP4/FGF-treated tumour cells exhibited a mean ROS intensity of 3.89 a.u. whereas the proliferating tumour cells exhibited a mean ROS intensity of 0.90 a.u. (Fig 4.5A). However, 4 hrs following radiation, there was no significant difference observed between the BMP4/FGF-treated tumour cells and the proliferating tumour cells ($p=0.366$) (Fig 4.5A).

Additionally, we observed a consistent but insignificant increase in ROS levels in the BMP4/FGF-treated tumour cells from non-irradiated to 5 mins following radiation ($p=0.057$) (Fig 4.5A). These ROS levels were then significantly reduced in the BMP4/FGF-treated tumour cells from 5 mins to 4 hrs following radiation (*$p=0.015$) (Fig 4.5A). Interestingly, the proliferating tumour cells showed no significant difference in ROS levels from non-irradiated to 5 mins following radiation ($p=0.972$) (Fig 4.5A). However, there was a trend towards increased levels of ROS from 5 mins to 4 hrs after radiation for the proliferating tumour cells ($p=0.26$) (Fig 4.5A).

This data suggests that BMP4/FGF-treatment for 3 days is associated with increased ROS levels in tumour cells. This is consistent with our observations of increased levels of DNA damage associated with BMP4/FGF-treatment without radiation (See Chapter 4.1). Additionally, this data suggests that the BMP4/FGF-treated tumour cells may experience higher peak levels of ROS following radiation. However, it is unclear whether the proliferating tumour cells accumulate ROS from 5 mins to 4 hrs following radiation or if the time points used in this experiment did not capture the peak levels of ROS experienced by the proliferating tumour cells. Importantly, we observed that whilst the BMP4/FGF-treated cells may experience more ROS 5 mins following radiation they can resolve the high levels of ROS within 4 hrs.

4.3 BMP4/FGF-treatment is associated with decreased levels of NHEJ and HR

We have previously established that BMP4/FGF-treated tumour cells experienced more DNA damage than proliferating tumour cells immediately after radiation. In addition, the BMP4/FGF-treated tumour cells likely repair this DNA damage faster than proliferating tumour cells (See Chapter 4.1.1). Following this, it is possible that the DDR and DNA repair mechanisms is altered in the BMP4/FGF-treated tumour cells. Hence, we next sought to identify differences in the DSB repair pathways utilised by the BMP4/FGF-treated and proliferating tumour cells to repair radiation-induced DNA damage.

To probe for potential alterations of DSB repair pathways in the BMP4/FGF-treated and proliferating tumour cells we assessed the bulk RNAseq data for transcriptional changes associated with DNA damage repair. Bulk RNAseq was performed as described in the previous section (Chapter 4.2) and described in further detail in methods chapter 7.8.

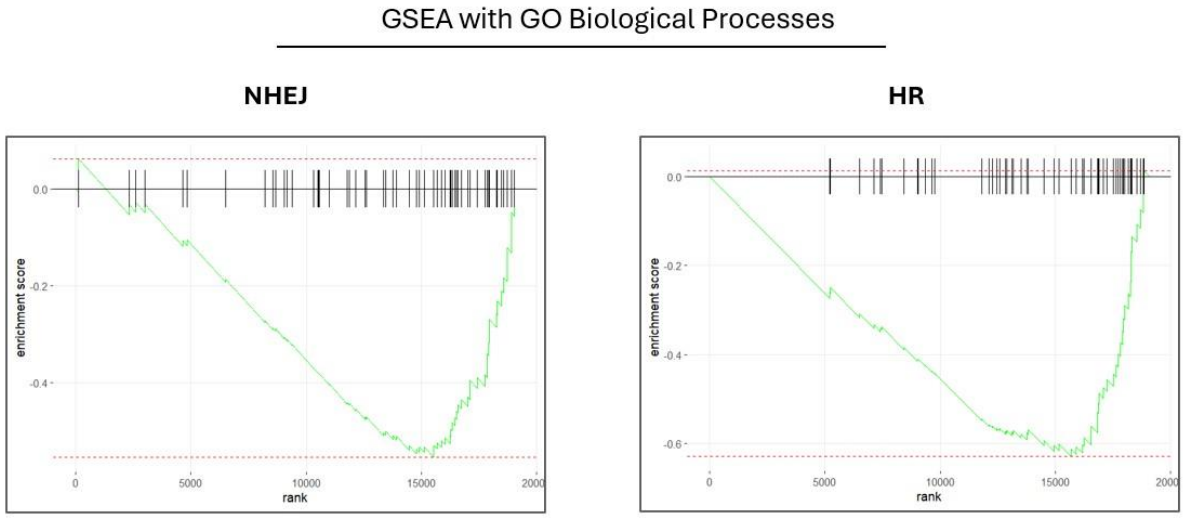

Figure 4.6 BMP4/FGF-treated tumour cells exhibited downregulated NHEJ and HR

Bulk RNAseq (See Methods Chapter 7.8) was performed on the Nf1$^{-/-}$/Pten$^{-/-}$/P53$^{-/-}$ tumour cells cultured in BMP4/FGF or EGF/FGF (Proliferating tumour cells) for 3 days. GSEA of bulk RNAseq data was performed using the GO Biological Processes gene set. Graphs showing enrichment scores of the following GO biological process pathways for NHEJ (Left) and HR (Right).

In the previous chapter, we found that the Hallmark DNA damage repair pathway was downregulated in the BMP4/FGF-treated tumour cells compared to the proliferating tumour cells (See Chapter 3.1). To explore alterations in specific DSB repair pathways we utilised the GO biological processes gene set which had specific pathways for NHEJ and HR. Although there was no pathway specifically for MMEJ, we instead assessed for alterations in the expression of *Polq*. This gene encodes Polymerase Q, also known as POLθ, which plays a critical role in MMEJ (Ceccaldi et al., 2015; Mateos-Gomez et al., 2015).

This analysis revealed a significant negative enrichment of both the NHEJ and HR DSB repair pathways in the BMP4/FGF-treated tumour cells compared to the proliferating tumour cells (Fig 4.6). The NHEJ and HR pathways exhibited an NES of -2.17 (padj=1.43E-05) and -2.43 (padj = 1.52E-08) respectively (Appendix Chapter 8.2). In addition, we observed a significant reduction in *Polq* expression in the BMP4/FGF-treated tumour cells compared to the proliferating tumour cells. *Polq* exhibited a log2foldchange of -1.11 (padj = 2.58E-04) (Appendix Chapter 8.1).

This GSEA of the bulk RNAseq data suggests that the NHEJ and HR DSB repair pathways are likely downregulated in the BMP4/FGF-treated tumour cells compared to the proliferating tumour cells. It was somewhat expected that HR would be downregulated in the BMP4/FGF-treated cells given they are arrested in G1 given the

necessity of a sister chromatid to complete HR (Mao et al., 2008; Rothkamm et al., 2003); However, it was unexpected that the NHEJ pathway was also downregulated since it is thought to be available at all stages of the cell cycle (Karanam et al., 2012; Mao et al., 2008; Rothkamm et al., 2003). Additionally, the downregulation of *Polq* in the BMP4/FGF-treated tumour cells also implies that MMEJ may be downregulated. Collectively, these results indicate that all DSB repair pathways may be downregulated following BMP4/FGF-treatment. However, the DDR and thus DNA damage repair is mediated by a series of protein kinases, hence, transcriptional changes may not accurately reflect the activity of the different DSB repair pathways *in vitro* (Jackson & Bartek, 2009; Jurkovicova et al., 2022; Majd et al., 2021). We next sought to functionally determine the activity of the different DSB repair pathways in the BMP4/FGF-treated and proliferating tumour cells.

We utilised a dual luciferase reporter assay system to assess the activity of the specific DSB repair pathways HR, NHEJ and MMEJ in the BMP4/FGF-treated and proliferating tumour cells. For this experiment up to seven different primary mouse cell lines were used to check for variability in HR, NHEJ and MMEJ across cell lines. This reporter system functions by transfecting the tumour cells with a control plasmid that encodes the firefly luciferase, this indicates transfection efficiency per well. The control plasmid was transfected in combination with plasmids specific for HR, NHEJ and MMEJ respectively that each encoded Nano luciferase (proprietary plasmids provided by ARTIOS therapeutics). The DSB repair pathway-specific plasmids underwent restriction digestion prior to transfection. Once transfected, the plasmids would be recircularized by its respective DSB repair pathway. The Nano luciferase signal was normalised to the

firefly signal in this experiment to indicate the average activity of the HR, NHEJ or MMEJ pathways in wells of the BMP4/FGF-treated and proliferating tumour cells. Transfection was performed as described in methods chapter 7.7.5, 24 hrs prior to performing the dual luciferase assay.

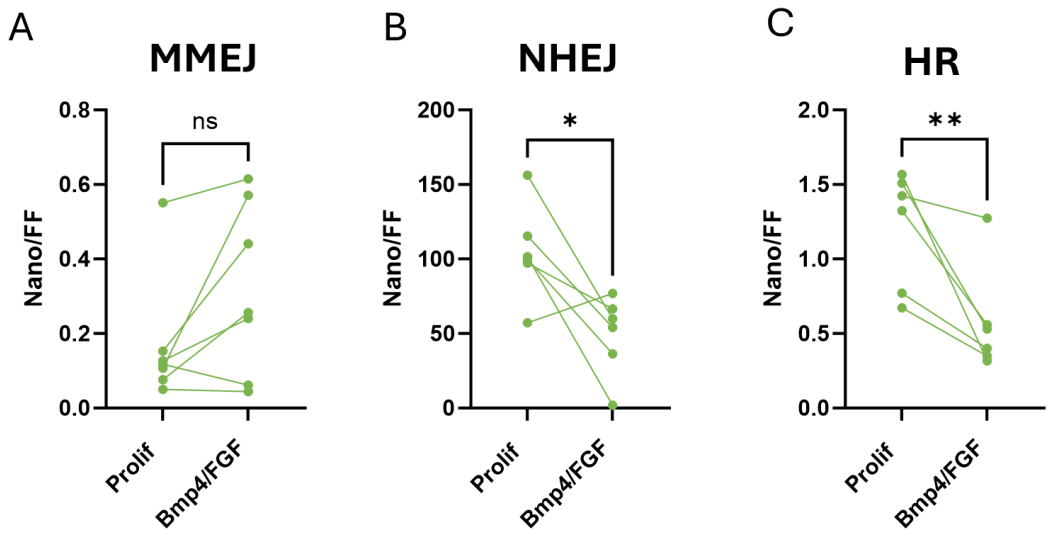

Figure 4.7 BMP4/FGF-treated tumour cells exhibited decreased activity of the NHEJ and HR DSB repair pathways

*MMEJ, NHEJ and HR activity were quantified using a dual luciferase reporter system to readout DSB repair pathway activity (NanoLuc) and transfection efficiency (Firefly (FF)). Bars represent DSB repair pathway activity (Nanoluc) activity normalised to transfection efficiency (FF). Transfection and dual luciferase reporter assay were completed as described in method chapter 7.7.5. Line graphs show (A) MMEJ activity, (B) NHEJ activity, and (C) HR activity. Mean±SEM, n=6, except MMEJ where n=7, paired t-test (*p<0.05, **p<0.01).*

We observed that BMP4/FGF-treatment induced a trend towards increased MMEJ activity (Fig 4.7A). On average, the proliferating tumour cells exhibited an MMEJ activity signal of 0.17 a.u., whereas the BMP4/FGF-treated tumour cells exhibited an MMEJ

activity signal of 0.32 a.u. (p=0.070) (Fig 4.7A). This trend was not consistent across all cell lines, in fact, there were 2 cell lines which exhibited a decrease in MMEJ activity following BMP4/FGF-treatment (Fig 4.7A). The MMEJ activity in cell line 1 exhibited a decrease from 0.12 (proliferating) to 0.06 (BMP4/FGF-treated), whereas cell line 2 exhibited a decrease from 0.051 (proliferating) to 0.044 (BMP4/FGF-treated) (Fig 4.7A).

In parallel, we observed a significant decrease in the level of NHEJ activity in the BMP4/FGF-treated tumour cells compared to the proliferating tumour cells (Fig 4.7B). BMP4/FGF-treatment significantly reduced NHEJ activity by 63%, from 104.6 a.u. in the proliferating tumour cells to 49.28 a.u. in the BMP4/FGF-treated tumour cells (Fig 4.7C). However, there was one cell line that exhibited an increase in NHEJ activity following BMP4/FGF-treatment (Fig 4.7C). As we expected, the level of HR activity was consistently decreased in the BMP4/FGF-treated tumour cells compared to the proliferating tumour cells (Fig 4.7C). Indeed, BMP4/FGF-treatment significantly reduced HR activity by 63%, from 1.21 a.u. in the proliferating tumour cells, to 0.57 a.u. in the BMP4/FGF-treated tumour cells (Fig 4.7C).

Collectively the data from this assay and the bulk RNAseq analysis suggests that BMP4/FGF-treatment may decrease the activity of HR and NHEJ. On the other hand, whilst *Polq* expression was downregulated in the BMP4/FGF-treated tumour cells, the luciferase data indicates that there is no difference in MMEJ activity between the BMP4/FGF-treated and proliferating tumour cells. Given that the activity of all of DSB repair pathways were decreased except for MMEJ, it is possible that the BMP4/FGF-treated tumour cells may depend more on MMEJ for their DSB repair rather than NHEJ or HR. In the previous sections we found that the BMP4/FGF-treated tumour cells could

achieve a similar rate of DNA repair as the proliferating tumour cells. In light of the findings from the luciferase assays, it's possible that MMEJ compensates for the decreased activity of HR and NHEJ in the BMP4/FGF-treated tumour cells. However, it is important to note that the dual luciferase assay cannot directly compare the activity of NHEJ, HR or MMEJ within the BMP4/FGF-treated or the proliferating tumour cells. Indeed, further work is needed to validate whether MMEJ activity contributes to the radio-resistance of the BMP4/FGF-treated tumour cells.

4.4 BMP4/FGF-treated and proliferating tumour cells undergo similar transcriptional changes following radiation

Whilst the data above suggests that MMEJ activity may play a role in the radio-resistance of BMP4/FGF-treated tumour cells, we also sought to characterise radio-resistance mechanisms independent of the tumour cell response to DNA damage. Hence, we assessed radiation-induced transcriptional changes *in vitro* to identify potential DDR and DSB repair independent mechanisms involved in the radio-resistance of the BMP4/FGF-treated tumour cells.

To meet this objective, bulk RNAseq was performed on BMP4/FGF-treated and proliferating tumour cells (See Methods Chapter 7.8). We collected samples for bulk RNAseq 6 hrs and 24 hrs following radiation to identify radiation-induced transcriptional changes in these cells. 6 hrs following radiation was chosen to capture immediate transcriptional changes, whilst 24 hrs following radiation was chosen to capture later transcriptional changes. In addition, these later transcriptional changes were unlikely to be impacted by the population

changes incurred by radiation-induced cell death. Unirradiated proliferating and BMP4/FGF-treated cells were collected for bulk RNAseq at both 6 hrs and 24 hrs following radiation to serve as relative controls for each time point. We first explored what genes were differentially expressed in the BMP4/FGF-treated and proliferating tumour cells following radiation using the DEseq2 package on R.

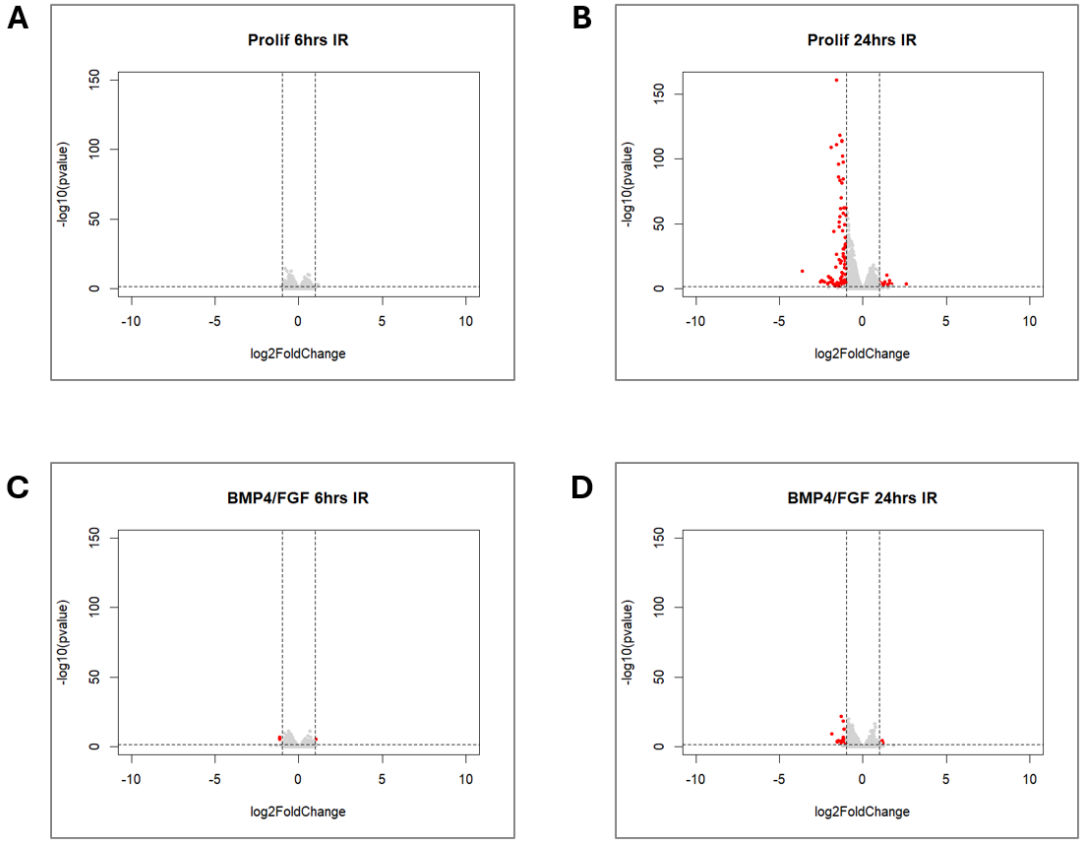

Figure 4.8 Differentially expressed genes in the BMP4/FGF-treated and proliferating tumour cells following radiation

Bulk RNAseq (See Methods Chapter 7.8) was performed on the BMP4/FGF-treated or proliferating tumour cells 6 hrs and 24 hrs following radiation (4 Gy). Unirradiated BMP4/FGF-treated and proliferating tumour cells were also collected at 6hrs and 24hrs to serve as the relative control for each time point. Differential gene expression was assessed using the DEseq2 package on R. The volcano plots illustrate the genes altered in the proliferating tumour cells 6hrs (A) and 24hrs (B)

following radiation. In addition, the volcano plots illustrate the genes altered in the BMP4/FGF-treated tumour cells 6hrs (C) and 24hrs (D) following radiation. The red dots represent genes with padj < 0.05 and log2foldchange greater or less than 1.

6 hrs following radiation, we identified 158 differentially expressed genes in the proliferating tumour cells (Fig 4.8A). The volcano plot illustrates that amongst these differentially expressed genes there were none that exhibited a log2fold change greater or less than 1 (Fig 4.8A). This highlights that there were no meaningful transcriptional changes induced by radiation in the proliferating cells 6 hrs following radiation.

In contrast, the proliferating tumour cells exhibited more transcriptional changes 24 hrs following radiation. 1501 genes were significantly upregulated, and 1352 genes were significantly downregulated (Fig 4.8B). Amongst these differentially expressed genes, 147 exhibited a log2fold change greater or less than one (Appendix Chapter 8.3). We observed significant downregulation of multiple genes associated with cell cycle, as anticipated given that the proliferating tumour cells are likely to undergo cell cycle arrest following radiation. Indeed, the common cell cycle marker *Ki67* was significantly downregulated with a log2fold change of -1.67 (padj = 2.82E-08) (Appendix Chapter 8.3) (Uxa et al., 2021). Multiple DDR genes were also significantly downregulated 24 hrs following radiation (Appendix Chapter 8.3). In addition, multiple genes associated with cytoskeletal organisation were downregulated at this time point (Appendix Chapter 8.3). Multiple inflammation or stress associated genes were also significantly upregulated (Appendix Chapter 8.3). Interestingly, we observed significant downregulation of *Erbb4* and *Lrp1*, with a log2fold change of -1.33 (padj = 4.14E-18) and -1.24 (padj = 9.2E-100)

(Appendix 3). Both *Erbb4* and *Lrp1* are implicated in oligodendrocyte differentiation (Hennen et al., 2013; Ortega et al., 2012).

Differential gene expression analysis of the BMP4/FGF-treated cells identified only 117 significantly altered genes 6 hrs following radiation (Fig 4.8C). Of these significantly altered genes, three exhibited a log2fold change less than or greater than one: *Pr2x1*, *Pmp2* and *Hes5* (Appendix 4). To this author's knowledge, there are no studies that link *Pr2x1* and *Pmp2* to cellular radiation response. On the other hand, *Hes5* encodes a transcription factor that is part of the basic helix-loop-helix family of transcriptional repressors. *Hes5* is in fact a downstream effector of the Notch pathway, which has been linked to radio-resistance in glioblastoma (W. Shen et al., 2022; J. Wang et al., 2010). Interestingly, this transcription factor has also been implicated in astrocytic differentiation (Nakashima et al., 2001).

24 hrs following radiation, we observed a total of 775 differentially expressed genes in the BMP4/FGF-treated tumour cells (Fig 4.8D). Amongst these significantly altered genes, 36 exhibited a log2fold change greater than one (Appendix Chapter 8.4). In this subset of genes, only 4 were upregulated, one of which was *Fhl2* with a log2foldchange of 1.04 (padj = 0.041) (Appendix 8.4). *Fhl2* also known as Lim domain 2 protein, is a member of the FHL protein family and is thought to participate in multiple signalling pathways (J. Zhang et al., 2023). The expression of *Fhl2* has been previously linked with radio-resistance in pancreatic, nasopharyngeal and breast cancer (G.-F. Wang et al., 2021; Zeng et al., 2024; Zienert et al., 2015). Interestingly, the BMP4/FGF-treated tumour cells also exhibited significant downregulation of multiple genes associated with oligodendrocyte differentiation; the genes *Sox10*, *Myt1* and *Lrp1*

exhibited a log2foldchange of -1.17 (padj = 1.82E-03), -1.85 (padj = 1.58E-07) and -1.18 (padj = 9.55E-05) respectively (Appendix 8.4) (García-León et al., 2018; Hennen et al., 2013; Nielsen et al., 2004).

Given the numerous significantly altered genes in both BMP4/FGF-treated and proliferating tumour cells 24 hrs after radiation, we performed GSEA on this time point to identify what signalling pathways these genes converge on. For this analysis, we utilised the Hallmarks gene set and the fgsea package on R.

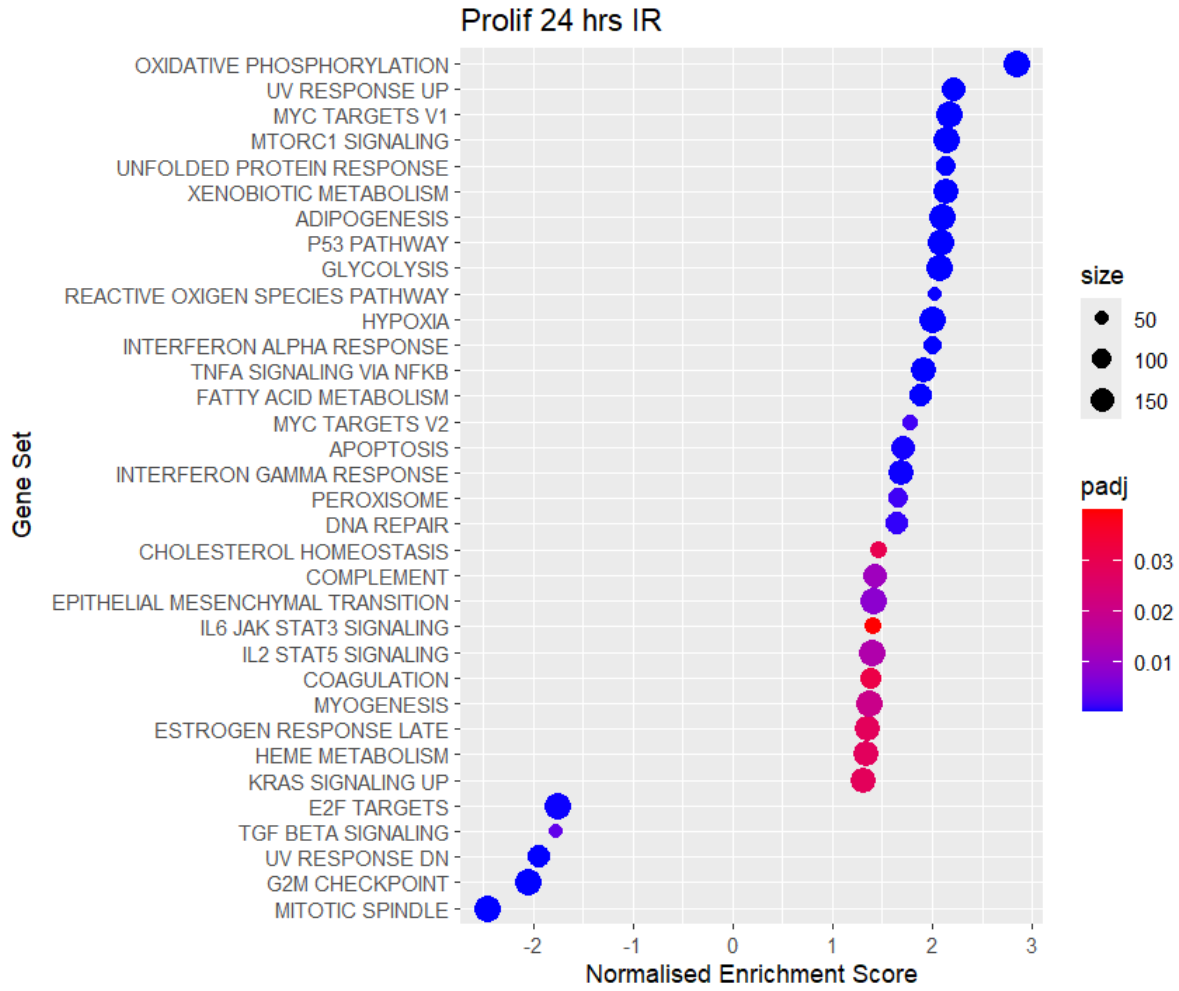

Figure 4.9 Significantly altered pathways in the proliferating tumour cells 24 hrs after radiation

Bulk RNAseq (See Methods Chapter 7.8) was performed on the proliferating tumour cells 24 hrs following radiation. Unirradiated proliferating tumour cells were also collected at this time point

to serve as relative controls. GSEA was performed using the hallmarks gene set and the fgsea package on R. The bubble plot above illustrates the pathways significantly (padj < 0.05) altered following radiation.

In the proliferating tumour cells, we observed negative enrichment of multiple pathways associated with the cell cycle. Indeed, the E2F target pathway, G2M checkpoint pathway and mitotic spindle pathway were amongst the top five most downregulated pathways following radiation (Fig 4.9). This finding is anticipated since it is known that radiation may induce cell cycle arrest (Boustani et al., 2019). We also observed the positive enrichment of numerous pathways associated with the cellular response to radiation; the DNA repair, apoptosis and ROS pathways were all upregulated in the proliferating tumour cells following radiation (Fig 4.9). The upregulation of these pathways was expected given that radiation is known to induce DNA damage and generate ROS, both of which may trigger apoptosis (Boustani et al., 2019; Steel et al., 1989; Yamaguchi et al., 2005; Yokoya et al., 2008). In addition to these pathways, multiple inflammatory associated pathways were upregulated following radiation including IFN signalling, interleukin activated JAK/STAT signalling, and TNFα signalling pathways (Fig 4.9).

Furthermore, we also detected the upregulation of the EMT pathway in the proliferating tumour cells following radiation (Fig 4.9). As discussed in the previous chapter, this pathway may implicate a transition towards a more MES-like state (Iser et al., 2019; Iwadate, 2016; J. Zhang et al., 2023).

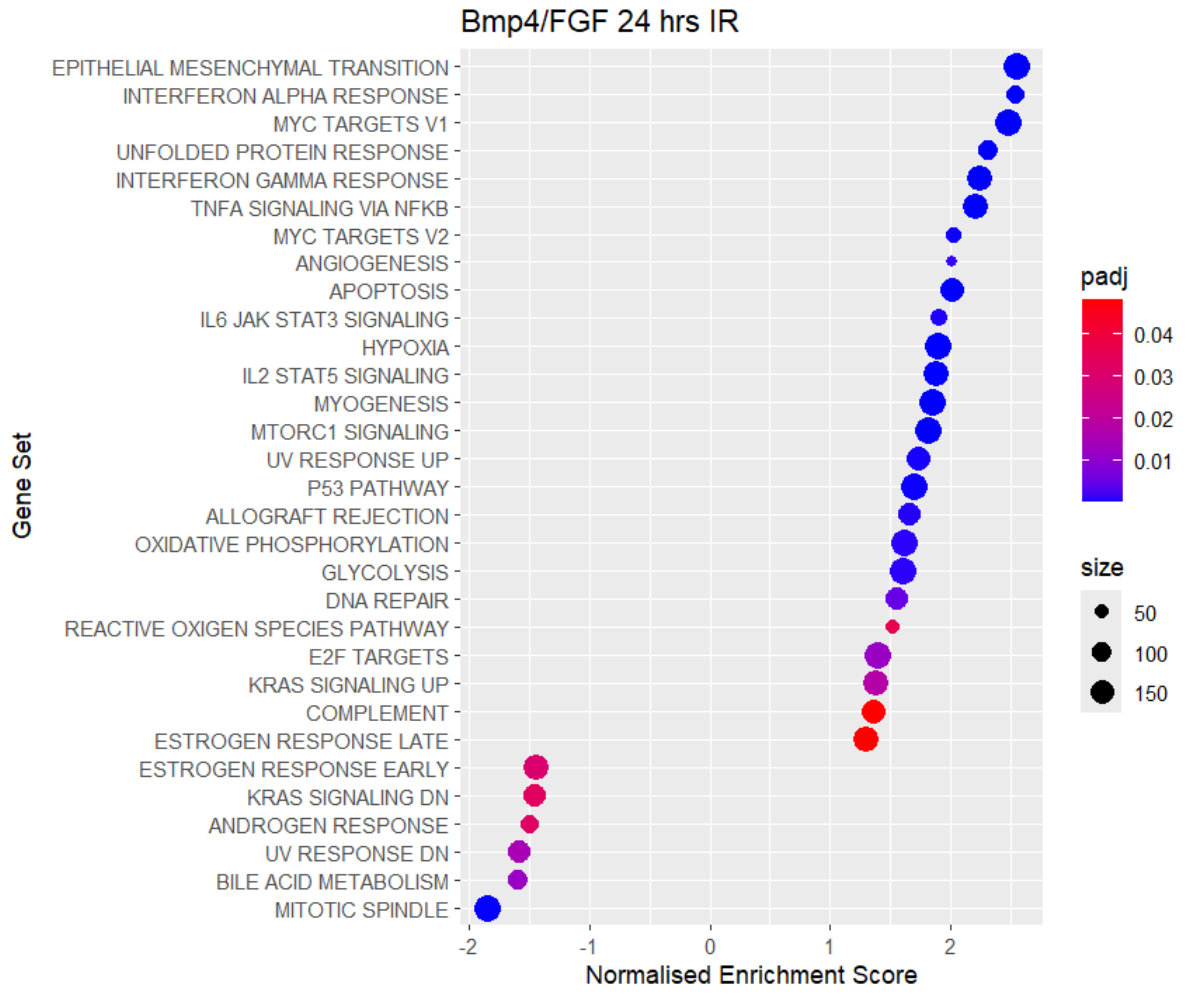

Figure 4.10 Significantly altered pathways in the BMP4/FGF-treated tumour cells 24 hrs after radiation

Bulk RNAseq (See Methods Chapter 7.8) was performed on the BMP4/FGF-treated tumour cells 24 hrs following radiation. Unirradiated BMP4/FGF-treated tumour cells were also collected at this time point to serve as relative controls. GSEA was performed using the hallmarks gene set and the fgsea package on R. The bubble plot above illustrates the pathways significantly (padj < 0.05) altered following radiation.

Consistent with the proliferating tumour cells, the BMP4/FGF-treated tumour cells exhibited significant positive enrichment of the DNA repair, ROS and apoptosis pathways following radiation (Fig 4.10). This suggests that like the proliferating tumour

cells, the BMP4/FGF-treated tumour cells exhibited the expected response to radiation. In fact, inflammatory associated signalling pathways were also upregulated in the BMP4/FGF-treated tumour cells; again, we observed positive enrichment of the IFN signalling, interleukin activated JAK/STAT signalling, and TNFα signalling pathways. In contrast to the proliferating tumour cells, however, the impact of radiation on cell cycle associated pathways is unclear in the BMP4/FGF-treated tumour cells. Here, we observed significant downregulation of the mitotic spindle pathway whereas the E2F signalling pathway was upregulated (Fig 4.10). We have previously shown that the BMP4/FGF-treated tumour cells undergo robust cell cycle arrest that is unchanged three days following radiation (See Chapter 3.5). Hence, these transcriptional changes in the BMP4/FGF-treated tumour cells may not have functional implications. In addition, the EMT pathway was the most upregulated pathway in the BMP4/FGF-treated tumour cells following radiation (Fig 4.10). Given that the BMP4/FGF-treatment was already associated with upregulation of the EMT pathway without radiation, it is interesting to find this effect amplified further by radiation (See Chapter 3.1).

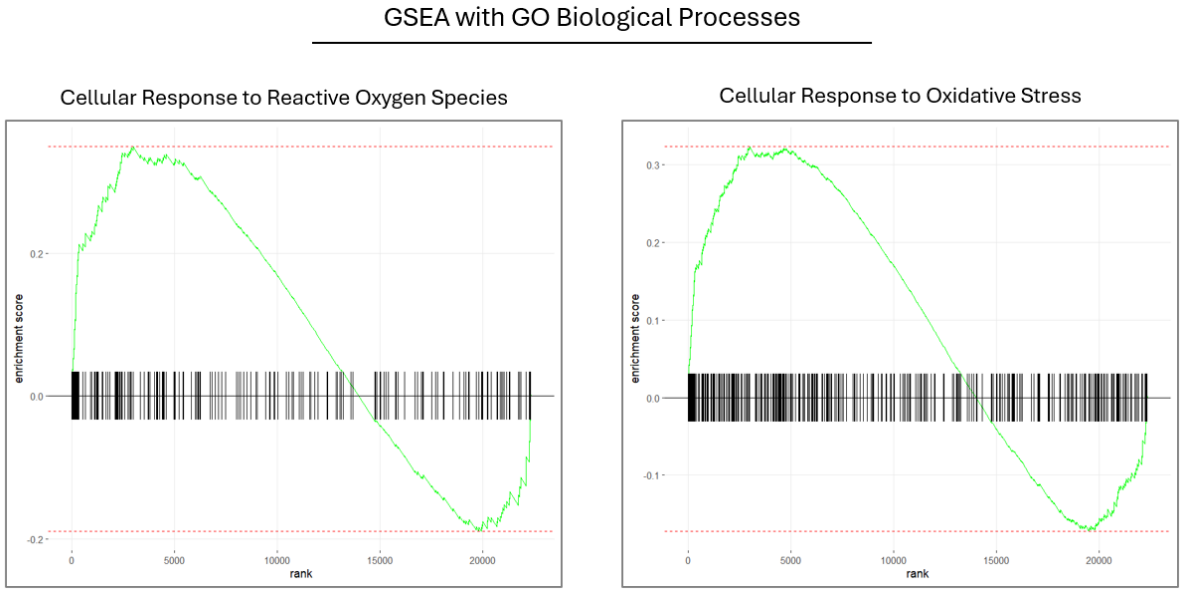

Figure 4.11 Proliferating tumour cells exhibited upregulation of ROS associated pathways following radiation

Bulk RNAseq (See Methods Chapter 7.8) was performed on the proliferating tumour cells 24 hrs following radiation. Unirradiated proliferating tumour cells were also collected at this time point to serve as relative controls. GSEA was performed using the GO Biological Processes gene set and the fgsea package on R. Graphs showing enrichment scores of the following GO biological process pathways for Cellular Response to Reactive Oxygen Species (Left) and Cellular Response to Oxidative Stress (Right).

This analysis utilising the Hallmarks gene sets highlighted that ROS levels may be upregulated in both the BMP4/FGF-treated and proliferating tumour cells 24 hrs following radiation. However, further GSEA using the GO biological processes gene sets revealed that the 'Response to Reactive Oxygen Species' and 'Response to Oxidative Stress' pathways were positively enriched only in the proliferating tumour cells (See Fig 4.11). The 'Response to Reactive Oxygen Species' pathway exhibited an NES of 1.45 (padj = 1.95E-02), whilst the 'Response to Oxidative Stress' pathway exhibited an NES of 1.43

(padj = 2.24E-02) (See Fig 4.11). Although the ROS levels we previously measured *in vitro* using CellRox up suggested that there were low levels of radiation-induced ROS 4 hrs following radiation, one may speculate that the transcriptional changes induced by ROS may be delayed, or the ROS levels may have increased 24 hrs following radiation. Measuring ROS levels *in vitro* up to 24 hrs post-radiation may be necessary to understand the ROS dynamics in the BMP4/FGF-treated and proliferating tumour cells.

Collectively, this data suggests that both the BMP4/FGF-treated and proliferating tumour cells may be shifting towards the MES-like state in response to radiation. Further work is necessary to determine whether these transcriptional changes resulted in a phenotypic change towards the MES-like state. However, this transition to the more MES-like state would be in line with previous studies that have previously demonstrated the effect *in vitro* and *in vivo* (Bhat et al., 2013; Halliday et al., 2014). Furthermore, we also observed a loss of genes associated with oligodendrocyte differentiation in both the BMP4/FGF-treated and proliferating tumour cells 24 hrs following radiation. However, it remains unclear whether this loss in oligodendrocyte genes represents the death of OPC-like or oligodendrocyte-like tumour cells or perhaps the shift of these cells towards a different cell fate. Importantly, this analysis highlights that the transcriptional changes induced by radiation were similar in both the BMP4/FGF-treated and proliferating tumour cells, which suggests that the radio-resistance mechanisms of the BMP4/FGF-treated tumour cells may lie beyond transcriptional changes.

4.5 Discussion

In this chapter, we sought to characterize the potential mechanisms underlying the radio-resistance of BMP4/FGF-treated tumour cells. To this end, we observed that BMP4/FGF-treated tumour cells experienced more DNA damage than proliferating tumour cells immediately after radiation. Interestingly, this increased DNA damage corresponded to higher levels of ROS in the BMP4/FGF-treated tumour cells. The resolution of DNA damage measured using multiple assays suggests that the BMP4/FGF-treated tumour cells may repair their radiation-induced DNA damage faster than the proliferating tumour cells. Further assessment of the activity of specific DSB repair pathways revealed that the activity of all pathways was downregulated except for MMEJ. This finding suggests the BMP4/FGF-treated tumour cells may be more dependent on MMEJ to repair radiation-induced DNA damage. The analysis of radiation-induced transcriptional changes in the BMP4/FGF-treated and proliferating tumour cells after radiation revealed no unique changes in the BMP4/FGF-treated tumour cells that may promote their radio-resistance. With the context of this analysis, further research should focus on assessing the role of the MMEJ pathway in the radio-resistance of the BMP4/FGF-treated tumour cells.

It was unexpected that BMP4/FGF-treated cells exhibited higher levels of ROS without radiation, given that proliferating tumour cells are thought to have higher levels of ROS due to their increased metabolic activity (Jang et al., 2013; Stanke et al., 2021). However, another study also suggests that BMP4 may increase ROS levels in glioblastoma *in vitro* (Niklasson et al., 2024). Niklasson *et al*. performed bulk RNAseq on the human glioblastoma cell line (U3065MG) that was cultured with BMP4, EGF and FGF

for two weeks (Niklasson et al., 2024). Their analysis identified the upregulation of genes associated with the ROS (Niklasson et al., 2024). In fact, there is evidence to suggest that BMP signalling contributes to elevated ROS by increasing the expression or activity of NADPH oxidases (NOX), which are ROS producing enzymes (Chandrasekaran et al., 2015; Simone et al., 2012; Sorescu et al., 2004). Simone *et al*. showed that treating adult renal progenitor cells with BMP2 *in vitro* resulted in elevated ROS associated with increased NOX activity (Simone et al., 2012). Furthermore, one study showed that BMP4 treatment for 1 to 4 hrs significantly upregulated *Nox1* expression in endothelial cells (Sorescu et al., 2004). Additionally, Chandrasekeran *et al*. found that BMP7 upregulates *Nox2* expression in Rat sympathetic neurons (Chandrasekaran et al., 2015). Together these results suggest the elevated ROS levels observed in the BMP4/FGF-treated tumour cells without radiation may be a direct result of BMP4 treatment.

It is also worth noting that the alkali comet assay, neutral comet assay and γH2AX data all showed that BMP4/FGF-treated tumour cells exhibited a small but consistent increase in DNA damage. Whilst these observations were not significant, the higher levels of ROS without radiation may account for the increased DNA damage we consistently observed. Indeed, there is some evidence to suggest that *in vitro,* induced dormant tumour cells exhibit equal or greater levels of DNA damage than proliferating tumour cells (Warters et al., 1985; Wilson & Keng, 1989). Additionally, the BMP4/FGF-treated tumour cells exhibited decreased activity of both HR and NHEJ, which could account for the accumulation of DNA damage in the BMP4/FGF-treated tumour cells without radiation.

Whilst the higher levels of ROS may explain the increased levels of DNA damage in the BMP4/FGF-treated tumour cells at baseline, it is unclear why the BMP4/FGF-treated tumour cells experienced higher levels of both DNA damage and ROS immediately after radiation. It is well established that the ROS generated by radiation induces DNA damage (Balasubramanian et al., 1998; Dahm-Daphi et al., 2000; Schraufstätter et al., 1988). Thus, the increased DNA damage immediately after radiation may simply be a consequence of the higher levels of ROS at this time point. However, it is still unclear why significantly more ROS is generated in the BMP4/FGF-treated tumour cells than the proliferating tumour cells immediately after radiation. Another factor to consider is that DNA damage has also been shown to induce ROS levels. Multiple studies in *Saccharomyces cerevisiae* showed that the accumulated DNA damage in strains deficient for base excision repair and nucleotide excision repair resulted in significantly increased ROS levels (Evert et al., 2004; Rowe et al., 2008). Additionally, one study using epithelial cell lines found that γH2AX may contribute to increased ROS levels by indirectly activating NOX1, a ROS producing enzyme (Kang et al., 2012). Hence, it is possible that there is a positive feedback loop between increased DNA damage and ROS in the BMP4/FGF-treated tumour cells. This potential interaction between DNA and ROS induction would be interesting to study further given the potential role for ROS in activating the DDR (Srinivas et al., 2019).

In this chapter, we observed the downregulation of both the HR and NHEJ DSB repair pathways in the BMP4/FGF-treated tumour cells. The downregulation of HR in the G1-arrested BMP4/FGF-treated tumour cells was anticipated since a template strand is necessary for HR, which restricts its activity to the S and G2 phases of the cell cycle

(Bunting et al., 2010; Escribano-Díaz et al., 2013; Xu et al., 2018). On the other hand, NHEJ is known to be active throughout the cell cycle which made its downregulation in the BMP4/FGF-treated tumour cells unexpected (Karanam et al., 2012; Mao et al., 2008; Rothkamm et al., 2003). Yet, these dormant BMP4/FGF-treated tumour cells repaired their radiation-induced DNA damage at the same rate as the proliferating tumour cells, if not faster. It follows that the BMP4/FGF-treated tumour cells must compensate for the decreased activity of HR and NHEJ to resolve the DSBs. Given that MMEJ activity was not significantly altered by BMP4/FGF-treatment, this implies that the BMP4/FGF-treated tumour cells may depend on this pathway for their DSB repair. MMEJ has been shown to be upregulated in cancers compared to normal cells, making it a favourable mechanism to inhibit in order to target the radio-resistant BMP4/FGF-treated tumour cells (Ceccaldi et al., 2015). Further investigation is necessary to determine the potential of MMEJ inhibition in radio-sensitising the BMP4/FGF-treated tumour cells. It is worth noting that the activity of the DSB repair pathways were measured in unirradiated BMP4/FGF-treated and proliferating tumour cells. It is also possible that radiation would alter the activity of these pathways *in vitro*.

There were few significant transcriptional changes observed 6 hrs following radiation. Given the numerous gene alterations observed 24 hrs following radiation, 6 hrs may have been too early to detect radiation-induced transcriptional changes in the *Nf1*$^{-/-}$*/Pten*$^{-/-}$*/P53*$^{-/-}$ tumour cells. This is in contrast to previous work by Halliday *et al.* showed that a single dose of radiation induced significant transcriptional changes 6 hrs following radiation in a *de novo* mouse model of glioblastoma (Halliday et al., 2014). In this study, the tumour cells exhibited significant enrichment for pathways associated with

apoptosis and negative regulation of cell growth as one would expect from irradiated tumour cells (Halliday et al., 2014). However, Halliday *et al*. used a P53 wildtype mouse model (Halliday et al., 2014). Given the central role of P53 in mediating the effects of the DDR, it provides a plausible explanation for why we observed no meaningful transcriptional changes at this time point (Abuetabh et al., 2022).

The bulk RNAseq analysis revealed that multiple genes linked to oligodendrocyte differentiation were downregulated in the BMP4/FGF-treated and proliferating tumour cells 24 hrs after radiation. It is well known that oligodendrocytes and their precursors are sensitive to oxidative stress (Husain & Juurlink, 1995; Mitrovic et al., 1994; Thorburne & Juurlink, 1996). In fact, one study has demonstrated that exposure to oxidative stress for 24 hrs induced the downregulation of genes associated with oligodendrocyte differentiation including Sox10 and Shh (French et al., 2009). Given the sensitivity of oligodendrocytes and their precursor cells to ROS, it is possible that these cells are radioresistant. Indeed, prior studies have reported the increased sensitivity of OPCs to radiation compared to other glial cells (Barbarese & Barry, 1989; R. X. Lee & Tang, 2022). As mentioned above, the loss of genes associated with oligodendrocyte differentiation may indicate that the oligo-like cells have been rapidly terminated by radiation, or that the tumour cells are shifting away from this cell fate, towards other cell fates. However, further research is necessary to determine the degree of oligodendrocyte-like or OPC-like differentiation present in either the proliferating or BMP4/FGF-treated tumour cells before and after radiation.

In addition to these findings, we also found the EMT pathway to be significantly upregulated in both the BMP4/FGF-treated and proliferating tumour cells 24 hrs after

radiation. As previously discussed in Chapter 3, the upregulation of EMT in glioblastoma may indicate upregulation of the MES-like state. There is evidence that reactive astrocytes exhibit transcriptional and phenotypical characteristics that resemble EMT (Iser et al., 2019; Iwadate, 2016; C. Zhang et al., 2023). Astrocytes transition into the reactive astrocyte state in response to CNS injury or inflammation (Sofroniew, 2020). However, there is also evidence that the MES-like state in glioblastoma resembles this reactive astrocyte state astrocytes (Niklasson et al., 2019; Richards et al., 2021). Taking this into consideration, one may speculate that upregulation of the EMT pathways indicates a shift towards the MES-like state in response to radiation. Indeed, the radiation-induced transition to the MES-like state is well established in glioblastoma (Bhat et al., 2013; Halliday et al., 2014; Phillips et al., 2006; Q. Wang et al., 2017). There is evidence to suggest that the MES-like state is associated with radioresistance (Bhat et al., 2013; Halliday et al., 2014; Neftel et al., 2019; Phillips et al., 2006; Q. Wang et al., 2017). It follows that the BMP4/FGF-treated and proliferating tumour cells may upregulate characteristics of the MES-like state as a radio-resistance mechanism. Interestingly, Halliday *et al.* previously demonstrated a central role for P53 in mediating the transcriptional changes associated with adopting the MES-like phenotype following radiation (Halliday et al., 2014). However, the model used in this thesis is *P53*$^{-/-}$ (Garcia-Diaz et al., 2023). We may speculate that the potential transition to the MES-like state in this model was mediated by P53 independent mechanisms. However, further analysis is required to compare the MES-like state characteristics induced by radiotherapy in this model, and the MES-like state characteristics achieved in a P53-wildtype model.

Chapter 5. Sensitizing AC-like Dormant Cells to Radiotherapy Through Inhibition of Double-Strand Break Repair Pathways

In the previous chapter, we identified that the BMP4/FGF-treated tumour cells experienced higher levels of DNA damage compared to proliferating tumour cells upon radiation; the BMP4/FGF-treated cells were capable of rapidly repairing this DNA damage. Hence, this chapter sought to assess the potential of DNA damage repair inhibition as a strategy to target the radioresistant astrocyte-like dormant population in glioblastoma.

Indeed, inhibition of DNA damage repair is an established strategy in cancer therapy. For example, PARP inhibition has achieved clinical success in multiple solid tumours including ovarian, breast and prostate cancer (Groelly et al., 2023; Morganti et al., 2024; R. Wang et al., 2023). To this end, four PARP inhibitors have been approved for clinical use. Additionally, multiple inhibitors targeting DNA-PK, ATM and ATR have also reached clinical trials for various solid tumours, including glioblastoma (Groelly et al., 2023; Jurkovicova et al., 2022; R. Wang et al., 2023). The use of DDR inhibitors in glioblastoma is a promising strategy to leverage the DNA damage induced by radiotherapy and temozolomide, the current mainstays of treatment.

Given that HR and NHEJ activity was downregulated in the BMP4/FGF-treated tumour cells compared to proliferating tumour cells, it is possible that the BMP4/FGF-treated tumour cells depend on MMEJ to repair their DNA damage. Additionally, it has been shown that MMEJ may predominate in solid tumours with HR aberrations (Chatterjee & Starrett, 2024). Hence, we

hypothesised that specifically inhibiting the MMEJ DSB repair pathway combined with radiotherapy may indeed target the radioresistant BMP4/FGF-treated cells.

In this chapter, we aimed to assess the effect of MMEJ inhibition on the radiosensitivity of the BMP4/FGF-treated and proliferating tumour cells *in vitro* and, should the results prove promising, *in vivo*.

5.1 *In vitro* inhibition of MMEJ activity through inhibition of POLθ

To assess whether MMEJ inhibition can increase the radiosensitivity of the BMP4/FGF-treated tumour cells *in vitro* we must first determine if the POLθ inhibitors, ART-558 and ART-6043 (proprietary small molecules provided by ARTIOS therapeutics) can sufficiently inhibit MMEJ in the proliferating and BMP4/FGF-treated cells. The novel inhibitor of POLθ, ART-558 has been previously demonstrated to reduce the activity of isolated POLθ enzyme to <5% at 1 μM (Zatreanu et al., 2021). However, the activity of ART-558 or ART-6043 has yet to be tested in glioblastoma cells.

Thus, in order to determine the effect of ART-558 and ART-6043 on POLθ activity, we utilised the dual luciferase reporter assay system to measure MMEJ activity *in vitro* (See Methods Chapter 7.7.5). The inhibitors were added to the culture media 2 hrs prior to transfection, to allow enough time for ART-558 or ART-6043 to inhibit POLθ enzyme activity in the cells. Specifically for ART-558, the dual luciferase assay was collected in collaboration with Anni Poysti. MMEJ activity was measured 24 hrs after transfection as described in methods chapter 7.7.5.

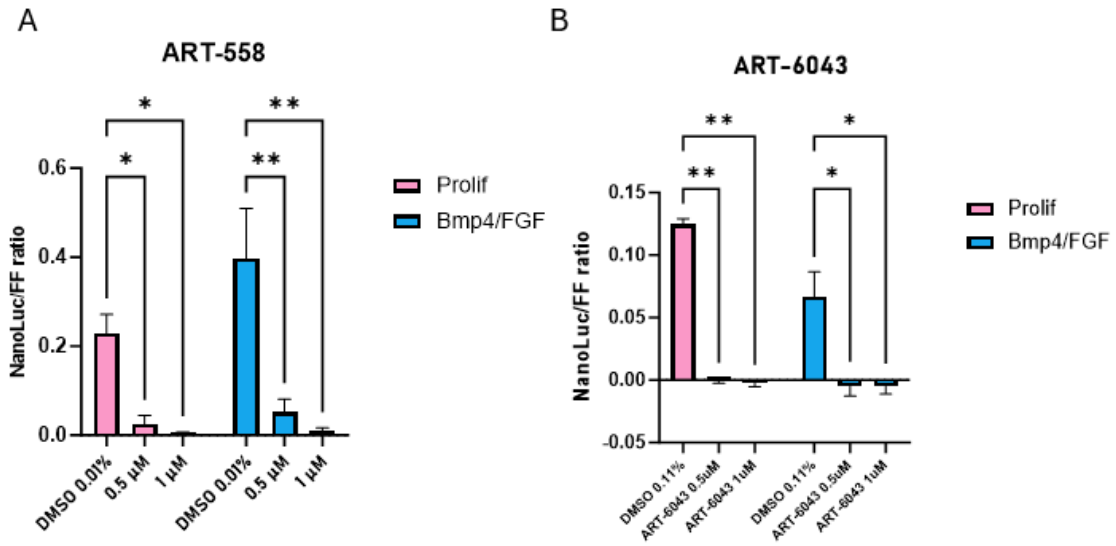

Figure 5.1 In vitro inhibition of MMEJ activity using ART-558 and ART-6043 without radiation

*MMEJ activity was quantified using a dual-luciferase reporter system to readout MMEJ activity (NanoLuc) and transfection efficiency (Firefly (FF)). Bars represent MMEJ activity normalised to transfection efficiency. Transfection and dual-luciferase reporter assay were completed as described in method section 7.7.5. (A) Bar graph shows that 0.5 µM and 1 µM of ART-558 significantly reduces the activity of MMEJ. Mean±SEM, n=3 biological cell lines, Two-way ANOVA with Dunnett's multiple comparison test was performed. Data was collected in collaboration with Anni Poysti.) (B) Bar graph shows that 0.5 µM and 1 µM of ART-6043 significantly reduces the activity of MMEJ. Mean±SEM. n=3, Two-way ANOVA with Dunnet's multiple comparison test was performed. DMSO vs 0.5 µM ART-6043. (** p<0.01, * p<0.05)*

In the proliferating tumour cells, we found that MMEJ activity was decreased from 0.23 a.u. (DMSO 0.01%) to 0.024 a.u. with 0.5 µM of ART-558, and further lowered to 0.006 a.u. with 1 µM of ART-558 (Fig 5.1A). ART-558 had a similar impact on the BMP4/FGF-treated tumour

cells, where 0.5 μM and 1 μM of ART-558 reduced MMEJ activity from 0.4 a.u. (DMSO 0.01%) down to 0.052 a.u. and 0.009 a.u. respectively (Fig 5.1A). Likewise, we found that ART-6043 also significantly reduced MMEJ activity in both the proliferating and BMP4/FGF-treated tumour cells (Fig 5.1B). In the proliferating tumour cells, 0.5 μM of ART-6043 reduced MMEJ activity from 0.12 a.u. (DMSO 0.1%) to 0.00 a.u. whilst 1 μM of ART-6043 reduced MMEJ activity to −0.002 a.u. (Fig 5.1B). Additionally, in the BMP4/FGF-treated tumour cells, 0.5 μM and 1 μM of ART-6043 decreased MMEJ activity from 0.06 a.u. (DMSO 0.1%) to −0.005 a.u. and −0.0048 a.u. respectively (Fig 5.1B).

Collectively, this data validates that ART-558 and ART-6043 effectively inhibit MMEJ activity in both the proliferating and BMP4/FGF-treated tumour cells. The effectiveness of ART-558 is in line with previous findings on isolated POLθ enzyme, where 1 μM of ART-558 reduced MMEJ activity to < 5% (Zatreanu et al., 2021). Indeed, in this assay 1 μM of ART-558 and ART-6043 reduced the activity of MMEJ to < 3% of the activity observed with DMSO treatment. In addition, this data suggests that of the two POLθ inhibitors, ART-6043 may be more effective.

5.2 MMEJ inhibition impacts the radiosensitivity of BMP4/FGF-treated and proliferating tumour cells *in vitro*

Assessment of the activity of specific DSB repair pathways *in vitro* revealed that both NHEJ and HR were downregulated following BMP4/FGF-treatment (See Chapter 4.3). In spite of this, the BMP4/FGF-treated tumour cells effectively repaired their radiation-induced DNA damage (See Chapter 4.1). Thus, we reasoned that these dormant cells may be more dependent on MMEJ

for their DNA damage repair. Following this, we hypothesised that inhibition of POLθ may increase the radiosensitivity of the dormant BMP4/FGF-treated tumour cells. Since both the POLθ inhibitors, ART-558 and ART-6043, reduced MMEJ activity to < 3% *in vitro*, we next assessed their impact on cell death in combination with radiation.

To assess the effect of the POLθ inhibitors on cell death in combination with radiation, the inhibitors were added 2 hrs prior to radiation (8 Gy) to allow time for the POLθ inhibitors to inhibit MMEJ activity. Cell death was measured 3 days following radiotherapy using Sytox green (a live cell impermeable dye) to identify the dead cells (See Methods Chapter 7.7.2). This was quantified using imaging for ART-558 and FACS for ART-6043. The gating strategy to quantify the percentage of Sytox positive cells was previously shown in Chapter 3.3.

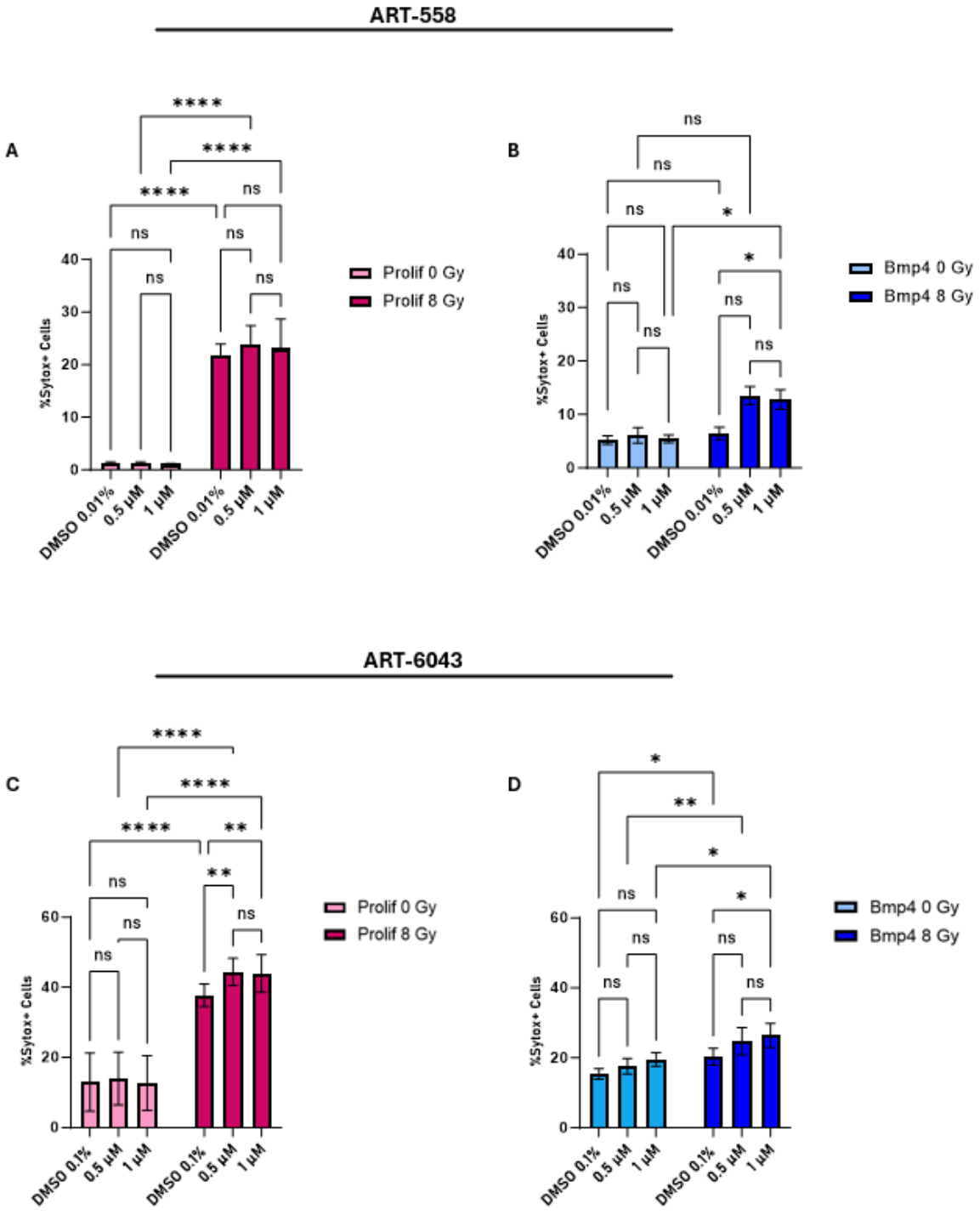

Figure 5.2 Assessing the effect of ART-558 and ART-6043 on the cell death of proliferating and BMP4/FGF-treated tumour cells following radiation

*2 hrs prior to radiation, ART-558/ART-6043 or DMSO were added to the proliferating and BMP4/FGF-treated tumour cells. Cell death was measured using Sytox, a live cell impermeable dye, 3 days following radiation (8 Gy) (See Methods Chapter 7.7.2). (A, B) Bar graphs showing the percentage of Sytox positive (%Sytox+) cells in proliferating (A) or BMP4/FGF-treated (B) tumour cells when treated with 0.01% of DMSO, 0.5 μM, and 1 μM of ART-558, with and without radiation. For both A and B, Mean±SEM, n=5. (C, D) Bar graphs showing the percentage of Sytox positive (%Sytox+) cells in proliferating (C) or BMP4/FGF-treated (D) tumour cells when treated with 0.1% of DMSO, 0.5 μM, and 1 μM of ART-6043., with and without radiation. For C and D, Mean±SEM, n=3. (A-D) Two-way ANOVA with Tukey's multiple comparison test was performed (*p<0.05, **p<0.01, ****p<0.0001).*

We observed that ART-558 alone did not increase cell death in either the proliferating or BMP4/FGF-treated cells (Fig 5.2A, B). Additionally, ART-558 in combination with radiation did not significantly impact the cell death of the proliferating tumour cells (Fig 5.2A). On the other hand, in the irradiated BMP4/FGF-treated tumour cells, there was a trend towards an increase in cell death from 6.44% when treated with DMSO 0.01% to 13. 52% with 0.5 μM of ART-558 (p=0.0775) (Fig. 5.2B). Finally, we found that 1 μM of ART-558 in combination with radiation significantly increased cell death from 6.44% (DMSO 0.01%) to 12.81% (Fig 5.2B). This data suggests that 0.5 μM and 1 μM of ART-558 induces a 2.1-fold and 1.98-fold increase in cell death in the BMP4/FGF-treated tumour cells respectively.

Consistent with ART-558, ART-6043 without radiation did not increase cell death in the proliferating or BMP4/FGF-treated tumour cells (Fig 5.2C, D). However, in combination with radiation we found that 0.5 μM and 1 μM of ART-6043 significantly increased cell death in the proliferating tumour cells, from 37.7% (DMSO 0.1%) to 44.36% and 43.9% respectively (Fig 5.2C). Whilst the irradiated BMP4/FGF-treated tumour cells exhibited a significant increase in

cell death from 20.3% when treated with DMSO 0.1% to 26.4% with 1 μM of ART-6043 (Fig 5.2D). It should be noted that the baseline levels of cell death of the proliferating and BMP4/FGF-treated cells are higher than that observed in the ART-558 experiment. It is likely that processing the cells for FACS in the ART-6043 experiment may have increased the baseline level of cell death. However, the effect of MMEJ inhibition on increasing cell death is conserved.

These results show that MMEJ inhibition combined with a single dose of radiation can induce a small but consistent increase in cell death in the BMP4/FGF-treated tumour cells that is statistically significant. In the case of ART-6043, this consistent effect also extends to the proliferating tumour cells. It has been previously shown that ART-558 is more effective in inducing cell death with fractionated doses of radiotherapy (Rodriguez-Berriguete et al., 2023; Zatreanu et al., 2021). Thus, it is possible that the small effect exhibited here is due to a single dose of radiation used. Although the proliferating tumour cells exhibited higher activity in the HR and NHEJ double-strand break repair pathways, the inhibition of MMEJ had a similar effect in the proliferating and BMP4/FGF-treated tumour cells. This suggests that MMEJ inhibition does not specifically impact the cell death of the BMP4/FGF-treated tumour cells but may be able to improve the radiosensitivity of these radioresistant dormant tumour cells.

5.3 Inducing cell cycle re-entry of the BMP4/FGF-treated tumour cells does not improve the effect of ART-6043 in combination with radiation

Proliferating tumour cells are thought to be sensitive to radiotherapy due to their rapid cell cycle progression accompanied often by dysfunctional cell cycle checkpoints. These features are disadvantageous for efficient and high-fidelity DNA repair, thus the extended presence of unrepaired DNA damage may trigger the cell death of these tumour cells following radiation (Abuetabh et al., 2022; Y. Zhou et al., 2021). It follows that dormant tumour cells may be sensitized to radiation if they re-enter the cell cycle. Hence, we sought to understand whether inducing cell cycle re-entry of the BMP4/FGF-treated tumour cells following radiation could impact the effectiveness of MMEJ inhibition.

To test this hypothesis, tumour cells were first treated with BMP4/FGF to induce dormancy. The BMP4/FGF-treated cells were then irradiated (8Gy), and 4 hrs following radiation the BMP4/FGF media was replaced with EGF/FGF media to induce cell cycle re-entry. This condition will be described as the ‘re-activated’ BMP4/FGF-treated tumour cells. The re-activated BMP4/FGF-treated tumour cells were cultured in the EGF/FGF-media for 3 days following radiotherapy and cell death was measured as previously described in section 5.2 and quantified by FACS. Tumour cells that were treated with BMP4/FGF for 3 days before radiation and maintained in BMP4/FGF after radiation were used as a control for this experiment. This condition will be described as the ‘dormant’ BMP4/FGF-treated tumour cells.

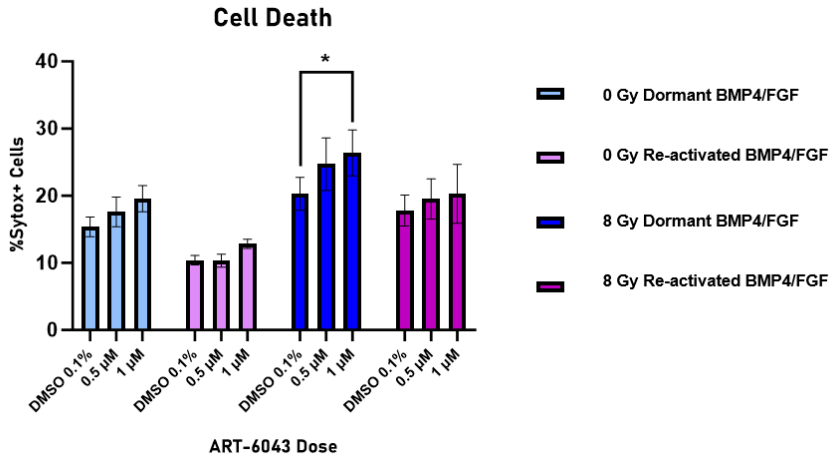

Figure 5.3 Assessing the effect of cell cycle re-entry on the response of BMP4/FGF-treated tumour cells to ART-6043 in combination with radiotherapy

*2 hrs prior to radiation, ART-6043 or DMSO 0.1% were added to the proliferating and BMP4/FGF-treated tumour cells. Cell death was measured using Sytox, a live cell impermeable dye, 3 days following radiation (8 Gy) (See Methods Chapter 7.7.2). FACS was used to quantify the cell death. (A) Gating strategy. (B) Bar chart showing the percentage of dead (Sytox+) cells. Mean±SEM, n=3. Three-way ANOVA with Tukey's multiple comparison test. (*p<0.05)*

Firstly, we observed less cell death in the re-activated BMP4/FGF-treated tumour cells than the dormant BMP4/FGF-treated tumour cells both with and without radiation (Fig 5.3B). This was likely due to the addition of EGF, a mitogen and pro-survival factor, to the re-activated BMP4/FGF-treated cells. Importantly, 1 µM of ART-6043 showed a small but significant increase in cell death of the dormant BMP4/FGF-treated cells in combination with radiation (Fig 5.3B). Surprisingly, 1 µM of ART-6043 did not significantly increase cell death in the re-activated BMP4/FGF-treated cells (Fig 5.3B). Although, combined with radiation, there was a trend towards a small increase in cell death (Fig 5.3B).

These results suggest that inducing cell cycle re-entry of the BMP4/FGF-treated cells does not improve the effect of ART-6043 in combination with radiotherapy. However, this experiment was performed with a single dose of radiation, fractionated radiotherapy may be more effective as previously discussed.

5.4 NHEJ inhibition impacts the radiosensitivity of BMP4/FGF-treated and proliferating tumour cells *in vitro*

Whilst MMEJ was the most likely DSB repair mechanism involved in the DNA damage repair of the BMP4/FGF-treated tumour cells, it remains that NHEJ is not completely abrogated in the BMP4/FGF-treated tumour cells (See Chapter 4.3). Indeed, NHEJ activity was significantly reduced in the BMP4/FGF-treated tumour cells compared to the proliferating tumour cells, however, the dual luciferase assay does not allow for direct comparison of MMEJ and NHEJ activity (See Chapter 4.3). Thus, the relative levels of NHEJ activity and MMEJ activity within the BMP4/FGF-treated or proliferating tumour cells remain unknown. Furthermore, DSB repair mediated by NHEJ is thought to occur throughout the cell cycle (Groelly et al., 2023; Jurkovicova et al., 2022; R. Wang et al., 2023). For these reasons, we also sought to explore the potential role of NHEJ inhibition on the radio-resistance of BMP4/FGF-treated and proliferating tumour cells.

To achieve this aim, we assessed the impact of NHEJ inhibition on cell death in combination with radiation, by utilising Nu7441. This inhibitor targets DNA-PK, a key enzyme in the NHEJ pathway (Blackford & Jackson, 2017; Tavecchio et al., 2012). Nu7441 was added

directly to the media 2 hrs prior to radiation to allow time for Nu7441 to inhibit NHEJ activity. Cell death was measured as described in section 5.2, and it was quantified by imaging.

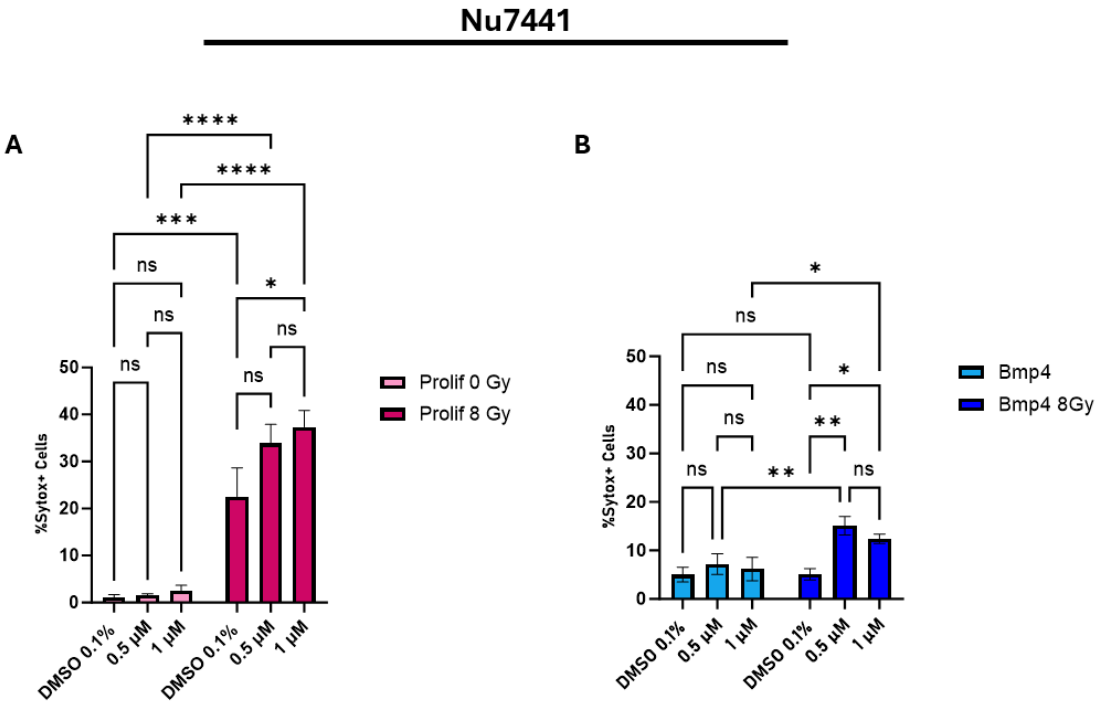

Figure 5.4 Assessing the effect of Nu7441 on the cell death of proliferating and BMP4/FGF-treated tumour cells

*2 hrs prior to radiation, Nu7441 or DMSO 0.01% was added to the proliferating and BMP4/FGF-treated tumour cells. Cell death was measured using Sytox, a live cell impermeable dye, 3 days following radiation (8 Gy) (See Methods Chapter 7.7.2). Cell death was quantified via imaging. Bar chart shows the percentage of dead (Sytox+) cells in the Proliferating (A) and BMP4/FGF-treated (B) tumour cells. Mean±SEM, n=3. Two-way ANOVA with Tukey's test. (*p<0.05, **p<0.01, ***p<0.001, ****p<0.0001)*

We observed that the addition of Nu7441 without radiation did not significantly increase cell death in the proliferating or BMP4/FGF-treated tumour cells (Fig 5.4A, B). On the other hand, 0.5 µM and 1 µM of Nu7441 in combination with radiation, significantly increased the level of

cell death in the proliferating tumour cells (Fig 5.4A). Indeed, combined with radiation cell death was increased from 22.57% (DMSO 0.01%) to 33.84% with 0.5 μM of Nu7441, and increased to 37.33% with 1 μM of Nu7441 (Fig 5.4A). In the BMP4/FGF-treated tumour cells, we found that Nu7441 in combination with radiation significantly increased cell death from 5.1% (DMSO 0.01%) to 15.09% with 0.5 μM of Nu7441 and to 12.41% with 1 μM of Nu7441 (Fig 5.4B).

These results demonstrate that when combined with radiation, inhibition of NHEJ, likewise with MMEJ inhibition, has a small but statistically significant effect on cell death of both proliferating and BMP4/FGF-treated tumour cells. DNA-PK inhibitors are thought to be highly potent radiosensitisers, with some studies showing up to ten-fold decrease in survival of glioblastoma cell lines when combining DNA-PK inhibitors with radiation (Timme et al., 2018). As this was not observed in this experiment, it is possible that the *Nf1*$^{-/-}$*/Pten*$^{-/-}$*/P53*$^{-/-}$ cell lines used in this experiment have higher levels of radioresistance or may be particularly resistant to the Nu7441 DNA-PK inhibitor. In future, it would be interesting to assess the effect of other available DNA-PK inhibitors or to assess the combination of Nu7441 with different doses of radiation. Collectively this data suggests that BMP4/FGF-treated tumour cells are reliant on both MMEJ and NHEJ to repair DNA following radiation. Additionally, it suggests that while BMP4/FGF-treatment significantly decreased NHEJ activity in the *Nf1*$^{-/-}$*/Pten*$^{-/-}$*/P53*$^{-/-}$ tumour cells, this may not reflect the absolute levels of NHEJ activity (See Chapter 4.3).

5.5 Assessing the effect of ART-6043 on the survival of tumour bearing mice

In this chapter, we have established that MMEJ inhibition by ART-6043 combined with radiation consistently increased cell death in the proliferating and BMP4/FGF-treated tumour cells with a single dose of radiation. Whilst the effect of ART-6043 combined with a single dose of radiation on cell death was small, we speculated that this effect may increase with fractionated doses of radiation as shown in other solid tumours (Rodriguez-Berriguete et al., 2023). Thus, we explored whether targeting this pathway may yet sensitise the radio-resistant AC-like dormant population *in vivo*.

Although we discovered that both MMEJ and NHEJ inhibition increased the radiosensitivity of the BMP4/FGF-treated tumour cells, the upregulation of MMEJ in cancers compared to normal tumour cells make it a favourable therapeutic target (Ceccaldi et al., 2015; Higgins et al., 2010; Lemée et al., 2010). Indeed, Lemée *et al.* found through real time PCR of tumour and non-tumour samples from breast cancer patients that POLθ is upregulated in the tumour tissue (Lemée et al., 2010). This is further supported by Higgins *et al.* who also found that POLθ is overexpressed in multiple breast tumour samples (Higgins et al., 2010). Additionally, Ceccaldi *et al.* compared datasets of tumour and non-tumour tissues and found that POLθ is upregulated in multiple cancers including breast, ovarian, lung and colorectal cancer (Ceccaldi et al., 2015). Based on these studies, we decided to focus on targeting MMEJ since it may allow for a therapeutic window to preferentially target radioresistant tumour cells without increasing toxicity to normal tissues.

For this experiment, we investigated the effectiveness of MMEJ in combination with both fractionated radiotherapy and temozolomide, as this would be clinically relevant given that chemoradiotherapy is the current standard of treatment for glioblastoma (Louis et al., 2021; Obrador et al., 2024; Stupp et al., 2005). To achieve this aim, we assessed the potential for ART-6043 to cross the BBB, its impact on tumour progression and importantly, its impact on survival.

5.5.1 ART-6043 crosses the blood brain barrier

The BBB consists of endothelial cells with tight junctions, and it is known to tightly regulate the movement of molecules, ions, and cells into the CNS (Daneman & Prat, 2015; Hersh et al., 2016; Wu et al., 2023). Whilst this serves to protect the CNS from toxins or pathogens in normal physiology, it has posed a significant challenge to treating CNS tumours. In fact, it is thought that the BBB excludes the majority of small molecule inhibitors (Hersh et al., 2016). Hence, it is important to first check whether ART-6043 can penetrate the BBB *in vivo* when administered via oral gavage either alone or in combination with temozolomide.

Non-tumour bearing C57BL/6 mice were dosed with ART-6043 alone or ART-6043 in combination with temozolomide via oral gavage as outlined in Fig 5.7A. The treatment course lasted 6 days (5 days bi-daily, with 1 day 1 dose) to assess the ability of ART-6043 to cross the BBB when administered alone or with temozolomide. In this pilot study, temozolomide alone was also administered via i.p. injection, to compare whether administration of temozolomide in combination with ART-6043 via oral gavage impacted temozolomide levels in the brain. The mouse brain and blood samples were collected 2 hrs following the last dose and processed for

pharmacokinetic (PK) analysis. The administration of treatment and sample collection was completed in collaboration with Dr Anni Poysti, Rachel Lindsay and Dr Lucy Brooks. The PK analysis of the samples was then completed by ARTIOS. In addition, the subsequent data analysis and graphs were generated by Dr Jayesh Majithiya of ARTIOS.

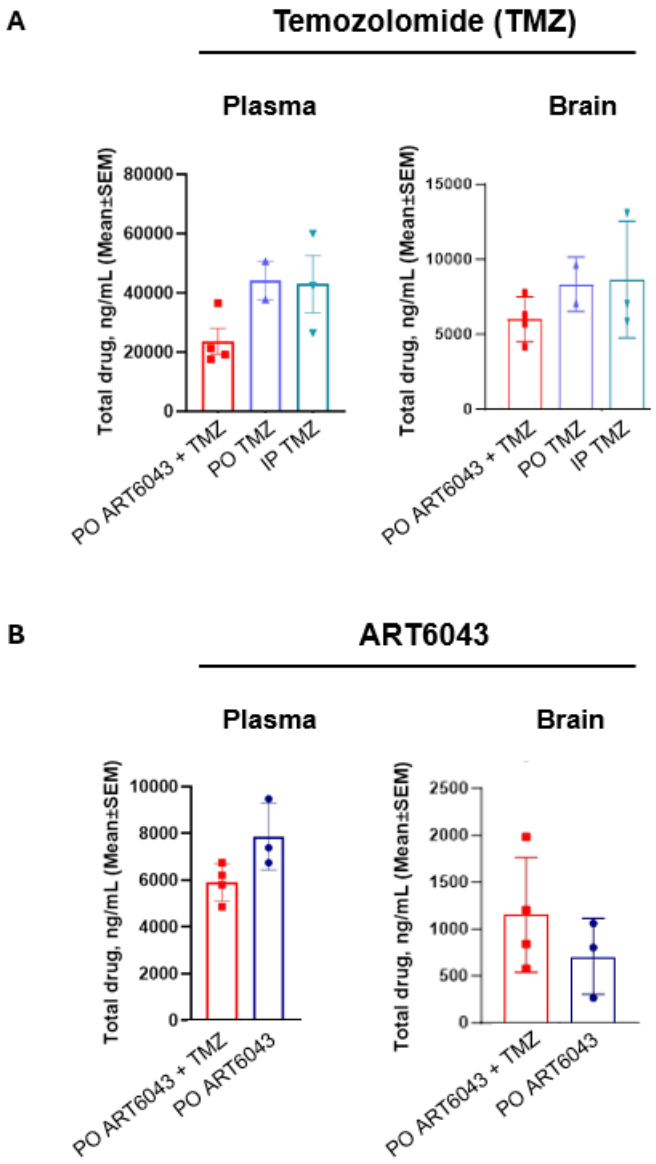

Figure 5.5 Accumulation of ART-6043 and Temozolomide in the brain

PK analysis was performed on mouse brain and blood samples by ARTIOS, the subsequent data analysis and graphs were generated by Dr Jayesh Majithiya. (A) Bar charts illustrating the concentration (ng/ml) of temozolomide in the plasma (left) and in the brain (right). (n= 4 PO ART6043 + TMZ, n=2 PO TMZ, n=3 IP TMZ) (B) Bar charts of the concentration (ng/ml) of ART-6043, in the plasma (left) and in the brain (right). Mean±SD, n=3, Students t-test. PO = oral gaveage, IP = intraperitoneal injection. (n=3 PO ART6043 + TMZ, n=3 PO ART6043).

Firstly, administration of temozolomide alone, via oral gavage (PO) or via intraperitoneal injection (IP), did not appear to alter its accumulation in either the plasma or the brain (Fig 5.5A). Similarly, there was no significant difference in the levels of ART-6043 in the brain when administered alone or in combination with temozolomide (Fig 5.5B). In this PK analysis, we found that approximately 20000 ng/ml of temozolomide was available in the plasma, whilst 5000 ng/ml of temozolomide was observed in the brain (Fig 5.5A). This data suggests approximately 25% of temozolomide crossed the BBB and accumulated in the brain when administered with ART6043 via oral gavage. We observed approximately 6000 ng/ml of ART6043 in the plasma, whilst only approximately 1000 ng/ml of the free plasma concentration of the drug accumulated in the brain (Fig 5.5B). This data indicates that 17% of the available ART6043 crossed the BBB to accumulate in the brain. In fact, a concentration of approximately 1000 ng/ml of ART6043 in the brain approximates to 0.2 μM.

Whilst these results confirm that ART-6043 can cross an intact BBB, the concentration of ART-6043 is below the effective dose *in vitro* (1 μM of ART-6043). Additionally, this measurement was taken where we expect the peak levels of ART-6043 after administration (2 hrs following administration), this does not indicate the potential fluctuations of ART-6043 levels throughout the day. However, it is important to note that this study was performed using

non-tumour bearing mice, given that glioblastoma is thought to disrupt the BBB, it is possible that tumour bearing mice may exhibit greater accumulation of ART-6043 in the CNS (Hersh et al., 2016; Rosińska & Gavard, 2021; Wu et al., 2023). Additionally, since glioblastoma-related BBB disruption could affect drug distribution, this analysis which was performed on whole brain samples may not reflect the potential differences in accumulation between tumour and non-tumour sections. Furthermore, the tumour mice would receive a fractionated dose of radiation which may work to counteract the lower dose of ART-6043 that accumulates in the brain.

The accumulation of temozolomide in the CNS was in line with previous studies in rats and rhesus monkeys where 30% of the free plasma concentration of temozolomide accumulated in the CNS (Agarwala & Kirkwood, 2000). Importantly, we confirm that administration of ART-6043 with temozolomide did not have any impact on the BBB penetration of either ART-6043 or temozolomide.

5.5.2 ART-6043 combined with chemoradiotherapy extends survival in tumour bearing mice compared to standard treatment alone

To assess the impact of ART-6043 on survival *in vivo,* immunocompetent mouse models of glioblastoma with *Nf1*$^{-/-}$*/Pten*$^{-/-}$*/P53*$^{-/-}$ deletions were used (Clements et al., 2024; Garcia-Diaz et al., 2023). Whilst this model of glioblastoma provides the benefit of modelling tumour initiation and progression, we expected some degree of variability in the size and location of these *de novo* tumours. Hence, to ensure that there was no bias amongst the different

treatment groups we used the luciferase signal, which was indicative of tumour size, from each mouse to randomise the groups. The luciferase signal from each mouse's tumour was quantified using IVIS as described in methods chapter 7.1.4. The four treatment groups were as follows: no treatment control (Control), ART-6043 alone, radiotherapy and temozolomide, and radiotherapy and temozolomide combined with ART-6043 (5.6B). Briefly, the treatment regimen involved radiotherapy (5 days x 2 Gy), temozolomide (5 days x 50 mg/kg once per day), and ART-6043 (7 days x 100 mg/kg twice per day) (See methods section 7.1.3). Mice were culled at terminal disease stage. For this study, survival was measured in days following the end of the treatment course.

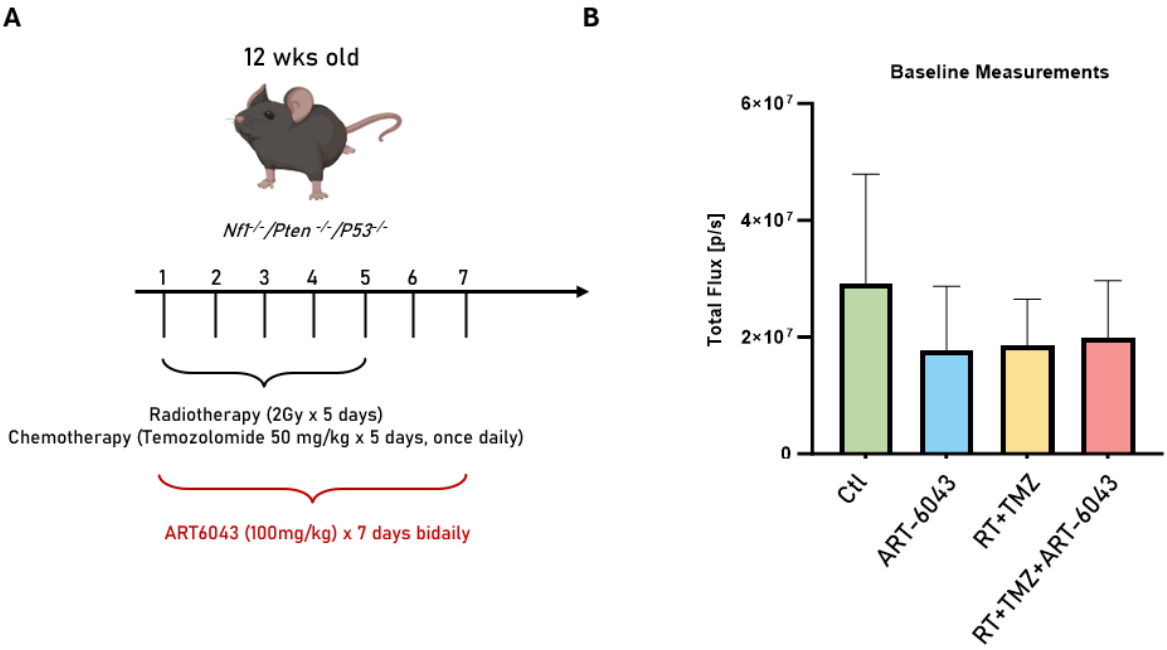

Figure 5.6 Nf1$^{-/-}$/Pten$^{-/-}$/P53$^{-/-}$ tumour bearing mice were randomised into four treatment arms

(A) Diagram outlining the treatment regimen for the survival study. Mice were either given no treatment, ART6043 (100mg/kg) alone for 7 days bidaily via oral gavage, or administered ART6043 in combination with radiotherapy (RT) (5 days x 2Gy) and temozolomide (TMZ) (once daily 50mg/kg). (B) Bar graph shows the luciferase signal of the mice in each treatment arm for the survival study. (n: Ctl=10, ART-6043 only =7, RT+TMZ=8, RT+TMZ+ART-6043 = 10). Mean±SEM. One-way ANOVA was performed.

Following the end of treatment, we found that the median survival of the control group was 22 days (Fig 5.7). There was no significant difference in median survival between the control group and the ART-6043 alone group (Fig 5.7). Consistent with previous studies, combined radiotherapy and temozolomide significantly extended survival compared to that of the control group; this group exhibited a median survival of 43 days (Fig 5.7). Combined radiotherapy and temozolomide with ART-6043 significantly extended survival, where median survival was 51 days in this treatment arm (Fig 5.7). No mice were cured of glioblastoma in any treatment arm.

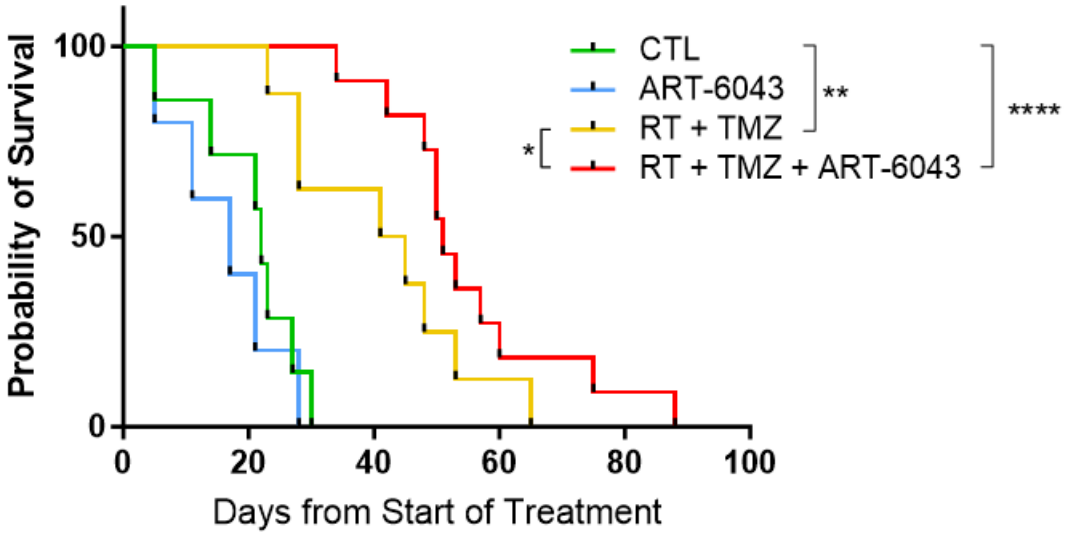

Figure 5.7 ART-6043 in combination with radiotherapy and temozolomide extended survival compared to radiotherapy and temozolomide alone

*Kaplan-Meier shows the survival for the four treatment arms: control, ART-6043 alone, radiotherapy and temozolomide (RT+TMZ), and radiotherapy and temozolomide combined with ART-6043 (RT+TMZ+ART-6043).(n: Ctl=7, POLQ only =5, RT+TMZ=8, RT+TMZ+ART-6043 = 11). Gehan-Beslow-Wilcoxon test was performed (*p<0.05, **p<0.01, ****p<0.0001).*

This data suggests that combined with radiotherapy and temozolomide, MMEJ inhibition by the novel POLθ inhibitor ART-6043 significantly improved survival in the *Nf1*$^{-/-}$ */Pten*$^{-/-}$*/P53*$^{-/-}$ glioblastoma mouse model compared to radiotherapy and temozolomide alone. The combination of radiotherapy, temozolomide and ART-6043 significantly extended survival by 8 days compared to the radiotherapy and temozolomide treatment group, and by 29 days compared to the control group (Fig 5.7). This observation suggests that targeting the MMEJ DSB repair pathway could be an effective strategy to improve the efficacy of current treatment in glioblastoma.

Chapter 6. Discussion

Summary of Findings

Radiotherapy plays a crucial role in treating glioblastoma, but its effectiveness is limited in part by tumour cell dormancy (Stupp et al., 2005). To address this problem, we sought to elucidate the mechanisms underlying the radio-resistance of dormant tumour cells in glioblastoma.

In this process, we first recognised that the dormant population within glioblastoma was comprised of cells in different states; a dormant AC-like and a dormant MES-like state were identified in an *Nf1*$^{-/-}$*/Pten*$^{-/-}$*/P53*$^{-/-}$ mouse model of glioblastoma. Of these different dormant states only the AC-like tumour cells were enriched one week after radiation *in vivo*, suggesting this fate was likely radio-resistant. This finding prompted us to investigate what signalling pathways may drive tumour cells towards this cell fate. Through combined scRNAseq analysis and RNAscope validation in the tumour tissue, we identified tumour-derived BMP signalling as an important regulator of the dormant AC-like population. Specifically, we found the Enpp6+ OPC-like tumour cells as the likely source of this BMP signalling. With this added context, we then modelled the dormant AC-like population *in vitro* by treating primary *Nf1*$^{-/-}$*/Pten*$^{-/-}$*/P53*$^{-/-}$ mouse lines with BMP4/FGF (Blomfield et al., 2019; Sachdeva et al., 2019).

Next, we leveraged this *in vitro* model to further investigate the radio-resistance mechanisms of the dormant AC-like population. As one might expect, BMP4/FGF-treated tumour cells were indeed more radio-resistant than the proliferating tumour cells. However,

the BMP4/FGF-treated tumour cells surprisingly exhibited higher levels of both DNA damage and ROS immediately after radiation. Although the factors responsible for this observed increase in DNA damage remain unknown, the BMP4/FGF-treated tumour cells were able to resolve the increased levels of DNA damage and ROS without consequence to their survival.

Further investigation into the mechanisms underpinning DNA repair within BMP4/FGF-treated tumour cells showed that the activity of all DSB repair pathways were downregulated with the exception of MMEJ. Since these dormant cells repaired DNA damage effectively despite reduced HR and NHEJ activity, we hypothesized they rely on the MMEJ pathway for DSB repair. Indeed, we found that targeting MMEJ with a novel inhibitor of POLθ, a key component of this DSB repair pathway, increased the cell death of the BMP4/FGF-treated tumour cells after radiation (Ceccaldi et al., 2015; Thyme & Schier, 2016). The POLθ inhibitor also enhanced cell death in proliferating tumour cells, which was unexpected given their higher levels of NHEJ and HR that we assumed would compensate for MMEJ deficiencies. Nonetheless, these results suggest that MMEJ inhibition could effectively increase radiosensitivity in both proliferating and radio-resistant dormant tumour cells. Additionally, since MMEJ activity is thought to be upregulated in cancers compared to normal tissue, its inhibition may yet improve glioblastoma radiosensitivity whilst sparing normal cells (Ceccaldi et al., 2015; Higgins et al., 2010). For these reasons, we further investigated the impact of MMEJ inhibition in combination with radiation and chemotherapy with temozolomide in a *Nf1*$^{-/-}$*/Pten*$^{-/-}$*/P53*$^{-/-}$ mouse model of glioblastoma. Ultimately, we found that combining MMEJ inhibition with chemoradiotherapy led to longer survival in tumour-bearing mice compared to those treated with chemoradiotherapy alone.

Final Remarks

In this thesis, we have demonstrated that the AC-like dormant population within *Nf1*$^{-/-}$*/Pten*$^{-/-}$*/P53*$^{-/-}$ tumours was enriched following radiation, warranting the investigation of their radio-resistance mechanisms. However, the contribution of this population to tumour recurrence remains to be determined. The AC-like population highly expressed the quiescence signature from Xie *et al*. which were derived from a dormant population that was implicated in tumour recurrence (J. Chen et al., 2012; Xie et al., 2022). It is possible that the AC-like dormant population identified in this thesis is the same population identified by the Parada group, which points towards the potential role for this radio-resistant population in tumour recurrence. Experimentally, ablation of the AC-like population post-treatment *in vivo* could be explored to assess whether AC-like dormant tumour cells affect tumour progression and survival.

Given the potential radio-resistance of the AC-like tumour cells, we sought to further investigate the signalling pathways regulating this cell state. Our findings demonstrated that BMP signalling plays a key role in this process. BMP signalling plays a well-established role in promoting both dormancy and astrocyte differentiation in glioblastoma (Blomfield et al., 2019; Carén et al., 2015; Han, Cai, et al., 2022; Huchedé et al., 2024; Mira et al., 2010; Pollard et al., 2009b; Rampazzo et al., 2017; Sachdeva et al., 2019; H. Sun et al., 2023). However, the source of BMP in glioblastoma is unclear. Unexpectedly, we found the tumour itself to be the primary source of BMP signalling in this tumour model (See Chapter 2.3). Whilst the observation of tumour-derived BMP was interesting, further work is needed to validate whether tumour-derived BMP promotes the dormant AC-like state *in vivo*. One approach to explore this

phenomenon experimentally would be to abrogate BMP production or BMP receptor expression in the tumour cells and assess for changes in the AC-like population.

Nonetheless, this finding raises the question of why certain tumour cells might produce BMP. Combined scRNAseq analysis and RNAscope validation identified Enpp6+ OPC-like tumour cells as the likely source of BMP4. However, there is limited evidence that normal CNS glial cells express BMP, except for reports that non-malignant astrocytes may produce BMP4 (Lim et al., 2016; Mikawa et al., 2006; Peretto et al., 2002). It is also interesting that BMP4 expression was likely restricted to the Enpp6+ subset of OPC-like tumour cells. With this in mind, further work may seek to characterise, more broadly, the population of BMP4 producing tumour cells. Additionally, this thesis focused specifically on BMP4 given its known role in regulating dormancy and astrocyte differentiation in glioblastoma, however, it is possible that BMP2 and BMP7 may also contribute to these processes (Huchedé et al., 2024; Savary et al., 2013). Since the scRNAseq analysis suggests that BMP2 and BMP7 may also be expressed by the tumour cells, it is possible that these BMPs act in concert to regulate the AC-like tumour state. Thus, it would be interesting to expand this research to explore the roles of multiple BMPs.

The significance of the observations described above lies in the implication that the tumour itself maintains a radio-resistant proportion of dormant tumour cells through BMP expression. This finding naturally leads us to question the role of tumour-derived BMP in the treatment response of this disease. Firstly, increased BMP levels after radiation could drive more tumour cells towards the likely radio-resistant AC-like fate. On the other hand, treatment-induced BMP loss may allow the dormant AC-like tumour cells to escape cell-cycle arrest and contribute to tumour progression. This is particularly relevant given the evidence

that the OPC-like tumour population, which we found highly expressed BMP4, was decreased one week following radiation (See Chapter 2.1). Hence, it would be valuable to explore BMP level changes after radiation and their potential impact on the dormant AC-like population.

In order to elucidate the radio-resistance mechanisms of the dormant AC-like state, we modelled this population through BMP4/FGF-treatment of primary *Nf1*$^{-/-}$/*Pten*$^{-/-}$/*P53*$^{-/-}$ mouse cells. Utilising this model, we discovered that radiation induced higher levels of DNA damage in these dormant tumour cells compared to their more proliferative counterparts (See Chapter 4.1). Further investigation revealed that higher levels of DNA damage in the BMP4/FGF-treated tumour cells were associated with higher levels of radiation-induced ROS (See Chapter 4.2); This may underly the elevated levels of DNA damage given that ROS induce DSBs through their interaction with DNA (Balasubramanian et al., 1998; Dahm-Daphi et al., 2000; Schraufstätter et al., 1988) . Yet, the BMP4/FGF-treated tumour cells resolved the ROS within four hours of radiation (See Chapter 4.2). Whilst the cause behind the higher levels of radiation-induced ROS in the BMP4/FGF-treated tumour cells remain unclear, this observation raises the possibility that interfering with their clearance of ROS could increase their radiosensitivity (Balasubramanian et al., 1998; Dahm-Daphi et al., 2000; Schraufstätter et al., 1988). ROS clearance is known to be mediated by a combination of noncatalytic small molecules, antioxidant enzymes and the transcription factor NRF2, which regulates the expression of multiple antioxidant enzymes (Panieri & Santoro, 2016; Xue et al., 2020). It would be valuable to understand which strategies are utilised by the BMP4/FGF-treated tumour cells to rapidly clear their radiation-induced ROS (See Chapter 4.2).

Since the BMP4/FGF-treated tumour cells were remarkably capable of repairing their elevated levels of radiation-induced DNA damage, we focused on elucidating their

mechanisms of DSB repair in this thesis. Interestingly, combined transcriptional analysis and DSB activity reporter assays suggested that BMP4/FGF-treatment reduced the activity of both HR and NHEJ, whilst MMEJ activity remained unchanged. Given the availability of reliable inhibitors for NHEJ and MMEJ, we assessed the impact of inhibiting these DSB repair pathways on the radiosensitivity of both the proliferating and BMP4/FGF-treated tumour cells.

Although BMP4/FGF-treatment reduced NHEJ activity, inhibition of this pathway increased the radiosensitivity of these dormant tumour cells. Whilst this finding might initially seem counterintuitive, it is important to note that the dual-luciferase assay used to compare the activity of these DSB repair pathways in the BMP4/FGF-treated and proliferating tumour cells cannot report on the relative activity of MMEJ, NHEJ, and HR (Grande et al., 2024). Thus, these findings collectively suggest that despite the decreased NHEJ activity in the BMP4/FGF-treated tumour cells, this pathway still plays a role in the DSB repair of this tumour population.

On the other hand, it was reasonable to speculate that the higher levels of HR and NHEJ in the proliferating tumour cells may exclude them from the impact of MMEJ inhibition. Yet, inhibition of MMEJ in the proliferating tumour cells increased their radiosensitivity. Given that MMEJ also increased the radiosensitivity of the BMP4/FGF-treated tumour cells, we may argue that the MMEJ pathway plays a role in the DSB repair of both the dormant and proliferating tumour cells. This finding leant itself to the idea that MMEJ inhibition may prove to be a valuable strategy to improve the radiosensitivity of glioblastoma, by targeting both proliferating tumour cells and the radio-resistant dormant tumour population. In addition, MMEJ is known to be upregulated in cancers compared to normal cells which encouraged us to assess the impact of MMEJ on glioblastoma radiosensitivity *in vivo* (Ceccaldi et al., 2015; Higgins et al., 2010).

Indeed, we observed that inhibition of MMEJ with the novel POLθ inhibitor ART-6043, when combined with chemoradiotherapy significantly extended the survival of *Nf1*$^{-/-}$*/Pten*$^{-/-}$*/P53*$^{-/-}$ glioblastoma bearing mice compared to chemoradiotherapy alone. This observation is in line with previous studies on colorectal cancer xenografts, where treatment with ART-6043, unconstrained by the BBB and administered for a longer duration, also showed significant efficacy (Rodriguez-Berriguete et al., 2023). Whilst this finding is interesting, it remains unknown what populations were targeted by ART-6043 in combination with chemoradiotherapy *in vivo*. Although the *in vitro* data suggests the AC-like and proliferative tumour populations may be targeted by the MMEJ inhibition, further assessment of population changes following therapy would be valuable in characterising the impact of MMEJ inhibition on the tumour.

Importantly, no mice were cured of their disease following combined ART-6043 and chemoradiotherapy. This finding points towards a potential inherent or acquired resistance to MMEJ inhibition. In future, it would be interesting to explore whether this resistance is specific to different tumour populations or if the tumour cells overcome ART-6043 inhibition of MMEJ. This would be a valuable avenue of research given the fact that current therapies for glioblastoma are not curative (Hanif et al., 2017; Stupp et al., 2005).

Collectively, this work points towards the potential for targeting the MMEJ pathway to improve the efficacy of the current standard of treatment in glioblastoma. However, even though the *Nf1*$^{-/-}$*/Pten*$^{-/-}$*/P53*$^{-/-}$ glioblastoma mouse model is well-established to recapitulate characteristics of human disease, it remains to be seen whether the impact of MMEJ inhibition will be conserved in glioblastoma patients (J. Chen et al., 2012; Garcia-Diaz et al., 2023). Thus,

further experiments to assess the impact of MMEJ inhibition combined with chemoradiotherapy in patient samples is paramount.

Chapter 7. Materials and Methods

7.1 *In vivo* protocols

7.1.1 Animals

All procedures were performed in compliance with the Animal Scientific Procedures Act, 1986 and approved by the UCL Animal Welfare and Ethical Review Body (AWERB) in accordance with the international guidelines of the Home Office (UK). Mice were housed with a 12-hour light dark cycle and access to food and water ad libitum. C57Bl6 (Strain code 027) and FVB (Strain code 207) mouse lines were used and purchased from Charles River. All animal work was performed under project license PP5770663.

7.1.2 De novo model generation

Immunocompetent *Nf1*$^{-/-}$*/Pten*$^{-/-}$*/P53*$^{-/-}$ models of glioblastoma were generated as previously described (Clements et al., 2024; Garcia-Diaz et al., 2023). Firstly, P2 mouse pups (C57BL/6 or FVB) were anesthetised with 3% isoflurane. The plasmid mixture with PiggyBac (encoding *Nf1*$^{-/-}$*, Pten*$^{-/-}$*, P53*$^{-/-}$, luciferase, and either tdTomato or tgBFP) and PiggyBase (encoding the CRISPR/CAS9) was injected into the right lateral ventricle, to target the neural stem cells of the sub-ventricular zone. Gel-covered tweezertrodes were placed on either side of the pup's head and 5 pulses were delivered. These models constitutively expressed luciferase and tdTomato or tgBFP in the cytoplasm to identify the transformed cells. All injections were performed by Melanie Clements. Following this procedure, all injected pups are expected to develop

tumours with >98% penetrance (Clements et al., 2024). Additionally, the expected latency of these tumours is from 15-18 weeks (Clements et al., 2024). An example image of a full-blown tumour is shown below.

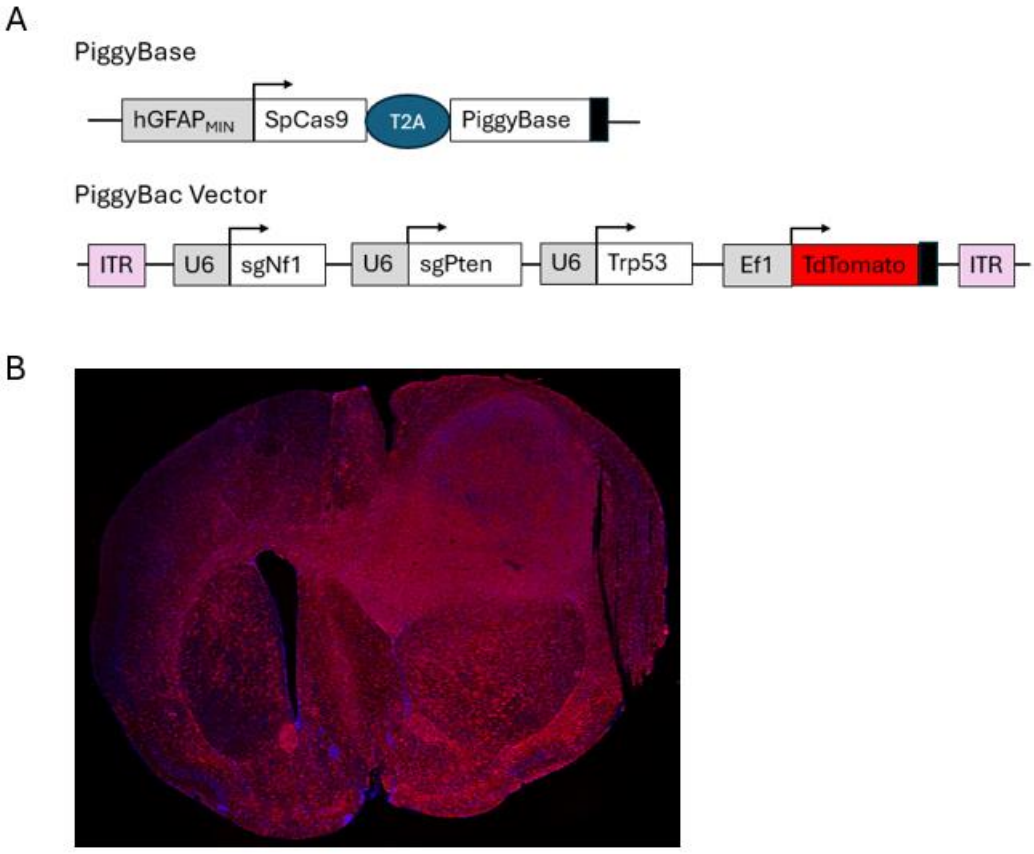

Figure 7.1 De novo mouse model of glioblastoma

(A) Diagram outlining the vector map of the piggybac and piggybase utilised to generate the Nf1$^{-/-}$/Pten$^{-/-}$/P53$^{-/-}$ mouse models of glioblastoma (Clements et al., 2024; Garcia-Diaz et al., 2023). Promoters are shown in grey boxes for the respective genes. (B) Fluorescent image of a coronal section of a mouse (13-weeks old) with a full-blown Nf1$^{-/-}$/Pten$^{-/-}$/P53$^{-/-}$ tumour. This image shows the tdtomato positive tumour cells (Shown in red) with dapi (Shown in blue).

7.1.3 Delivery of Radiotherapy, Temozolomide and ART-6043

7.1.3.1 Radiotherapy

To deliver radiotherapy to a targeted section of the brain, a computer tomography scan was performed on each mouse. Radiotherapy (5 days x 2 Gy) was delivered to a targeted area of the brain, avoiding sensitive oral tissue using a 10x10cm collimator. All radiotherapy was delivered using the SARRP (Xstrahl). With regards to the radiotherapy delivered for the survival study, irradiation was initiated once the tumour mice were 12 weeks old. This time point was selected based on prior experience that the tumours should be of moderate size and suitable for treatment. The presence of a tumour was confirmed by assessing the tumour luciferase signal.

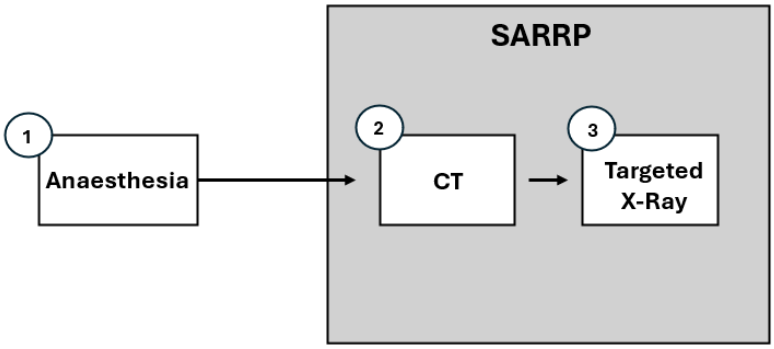

Figure 7.2 Overview of SARRP treatment plan

The diagram provides an overview of the SARRP treatment plan. Mice are first placed under anaesthesia before being secured in the SARRP. Once the mouse is secured, a CT scan is performed. The subsequent CT scan is utilised to ensure the X-Ray beams specifically target the whole brain. Care is taken to avoid the soft tissues of the mouth and the to avoid the brain stem.

7.1.3.2 Temozolomide

Temozolomide (Sigma, T2577) was administered at 50 mg/kg once daily for 5 days by intraperitoneal injection or oral gavage. Temozolomide powder was resuspended first in 100% DMSO and incubated in a shaking heat block at 90°C for 1 min. The final temozolomide solution was made-up with pre-warmed PBS or pre-warmed 1% solutol in if delivered alone or in combination with ART-6043 respectively. The solution was returned to the pre-warmed heatblock until injection. Daily intraperitoneal injections were administered on alternating sides of the mouse abdomen.

7.1.3.3 ART-6043

ART-6043 (ARTIOS) was administered at 100 mg/kg bi-daily (at 9am and 5pm) for 7 days by oral gavage. ART-6043 was administered alone or in solution with temozolomide. ART-6043 powder was first resuspended in 100% DMSO before being vortexed for 5 mins and sonicated in a water bath for 10 mins. The ART-6043 suspension was added to 1% solutol in dH2O drop by drop, vortexing constantly to ensure adequate resuspension. For the first 5 days of treatment, morning doses of ART-6043 were given a minimum of 2 hrs prior to radiotherapy, afternoon doses of ART-6043 were administered with temozolomide.

Time	Day 1	Day 2	Day 3	Day 4	Day 5	Day 6	Day 7
9am	ART-6043 (100mg/kg)	ART-6043 (100mg/kg)	ART-6043 (100mg/kg)	ART-6043 (100mg/kg)	ART-6043 (100mg/kg)	ART-6043 (100mg/kg)	ART-6043 (100mg/kg)
11am	Radiotherapy (2Gy)	Radiotherapy (2Gy)	Radiotherapy (2Gy)	Radiotherapy (2Gy)	Radiotherapy (2Gy)		
5pm	ART-6043 (100mg/kg) Temozolomide (50mg/kg)	ART-6043 (100mg/kg) Temozolomide (50mg/kg)	ART-6043 (100mg/kg) Temozolomide (50mg/kg)	ART-6043 (100mg/kg) Temozolomide (50mg/kg)	ART-6043 (100mg/kg) Temozolomide (50mg/kg)	ART-6043 (100mg/kg)	ART-6043 (100mg/kg)

Table 7-1 Outline of treatment schedule for the in vivo survival study

7.1.4 Animal monitoring, endpoints and tissue collection

Following tumourigenesis, animals were weighed weekly and monitored for signs of pain, distress, seizures, lethargy, or a general loss of body conditioning. If mice exhibit weight loss >10% they were weighed and monitored daily, if weight loss exceeded 15% mice were sacrificed. Mice were sacrificed if sufficient signs encompassing pain, distress, seizures, lethargy, or a loss in body conditioning were observed according to the animal license. If fresh tissue was required, animals were sacrificed by cervical dislocation without anaesthesia. If fixed tissue was required, animals were either sacrificed by cervical dislocation without anaesthesia with the brain drop-fixed into 4% PFA or animals were transcardially perfused with 1x PBS followed by 4% PFA under terminal anaesthesia.

7.1.5 IVIS

Mice were anesthetised with isofluorane and the area over the brain was shaved. Next, the mice were injected with 25 mg/kg of luciferin. The IVIS Spectrum was used to measure the luciferase signal 10 mins after the injection of luciferin. Total flux [p/s] was measured over 5 mins.

7.2 Single Cell RNA Sequencing

For scRNAseq of the *Nf1*$^{-/-}$, *Pten*$^{-/-}$, *P53*$^{-/-}$ mouse model, mouse brains were harvested and immediately placed in ice-cold HBSS medium. The brains were sectioned into 1 mm thick

slices using a brain matrix (WPI, RBMS200C). Tumour regions were dissected out and cut into smaller fragments. Cells were isolated by papain dissociation and RNA libraries were prepared using the Chromium Next GEM Chip G Single Cell Kit (10x 1365 genomics; 1000127) and sequenced on Nova Seq X Plus PE 150. Reads were pre-processed and aligned to the mm10-2020-A mouse genome using 10x Genomics Cell Ranger 7.0.1. The TdTomato sequence, which was expressed by the tumour cells, was incorporated into this reference genome.

Further scRNAseq analysis was completed by Dr Wenhao Tang. Cells with zero UMI count of the 4 red blood cell markers Hbb-bs, Hba-a1, Hba-a2 and Hbb-bt and with either tdTomato expression$= 0$ (likely to be microenvironment cells) or tdTomato ≥ 5 (likely to be tumour cells) were kept for further analysis. Cells with proportion of mitochondria genes below 0.25 and $\log_2$ total counts between 9 and 15 were kept for further analysis. Genes with non-zero UMI counts in at least 0.1% of cells were kept for further analysis. As a result, the dataset presented in this study consists of 6560 non-tumor and 59520 tumor cells respectively, and of a total of 17957 genes. Cells with tdTomato ≥5 or predicted to be aneuploid by R package copyKat (Ximerakis et al., 2019). and with UMI count for the Ptprc and Cd68 genes = 0 were identified as tumor cells. While cells with tdTomato $= 0$ and predicted to be diploid by R package copyKat (Ximerakis et al., 2019) . were identified as non-tumor cells. Tumour and non-tumour cells were integrated and clustered separately using Harmony and Seurat (Hao et al., 2024; Korsunsky et al., 2019). Clustering was performed using the Louvain approach in Harmony space (Korsunsky et al., 2019). Clusters were annotated using lineage markers and the gene enrichment analysis package fgsea. Cluster annotation was finally checked manually for accuracy.

7.3 CyTOF

Mouse brains were collected in Hibernate-A on ice and micro-dissected under fluorescence to isolate the tumour tissue. Tumour pieces (~0.5 mm^2) were dissociated using papain and DNase for 30 minutes with gentle agitation. The samples were thereafter demyelinated using Myelin removal beads II (Miltenyi) and the magnetic field of the MACS separator. Cells were incubated with 0.5 µM of cisplatin for 1 min on ice to label dead cells, then washed once with 1x PBS + 10% BSA, and twice with 1x PBS. For fixation, 4% PFA for 15 mins at room temperature was performed. To complete TOBis barcoding, samples were incubated with the barcodes (1:10) for 2 hrs at 4°C. The cells were subsequently washed in 1mM GSH in cell staining buffer (CSB) on a rocker for 10 mins at room temperature. This step was repeated twice, before another two washes were completed with 1x PBS. The barcoded samples were then resuspended in EDTA in CSB before being combined into one tube. The sample was filtered through a 70 µm strainer before a maximum of $3x10^6$ cells were stained. Extracellular staining was achieved through resuspension in the antibody cocktail for 30 mins at room temperature. Cells were then washed with 800g for 5 mins in 1 ml of EDTA in CSB. The stained cells were fixed with Fix/Perm buffer (eBiosciences) for 60 mins at 4°C. Once the samples were fixed, they were incubated with the intracellular antibody cocktail for 60 mins at 4°C. The cells were washed twice with perm buffer and subsequently incubated with 1.6% methanol-free formaldehyde solution and 1x intercalator overnight. The intercalator was removed and cells were sequentially washed in CSB, 1x PBS and MaxPar H2O. Total protein staining was then completed with 25 µg/ml ASCQ_Ru (96631, Sigma) in 0.1 m NaHCO3 solution for 10 min at room temperature. The previous wash step with CSB, 1x PBS and MAxPar H2O was repeated. The cells were washed

in 2 mls of CAS plus (Fluidigm) and resuspended at a concentration of 0.5-0.8x10^6 cells/ml for acquisition. EQ6 beads were added to the samples in a 1:6 ration, and EDTA solution added for a final concentration of 1mM. Finally, the samples were filtered through a 70 µm strainer before acquisition on the mass cytometer (Helios XT). This acquisition process allows for the single cell analysis of each sample. The following is a list of the markers used in this experiment: SPARCL1 (R&D Systems), RFP (Rockland), OLIG2 (Sigma), SOX2 (Abcam), SLC4A4 (Proteintech), Nestin (Std biotools), BLBP (abcam), SOX10 (Abcam), GFAP (Aglient), DCX (Abcam), cPARP [D214] (CST), pCHK1 [S345] (CST), Cyclin B1 (BD Biosciences), pBAD [S112] (CST), pHistone H2A.X [S139] (CST), cCaspase 3 [D175] (Std biotools), CD44 (BioLegend), OLIG2 (Sigma),

7.4 RNA Scope

For RNAscope analysis, mice were transcardially perfused with 1x PBS for 5 mins followed by 4% PFA for 5 mins. The brain was post-fixed in 4% PFA overnight at 4°C and stored in 1x PBS until they were embedded in paraffin. 3 µm sections were taken from these brains.

In preparation for the RNAscope assay the sections were baked at 60°C for 1.5 hrs and deparraffinised according to the RNAscope protocol. Antigen retrieval was performed using a steamer. The antigen retrieval buffer (Akoya) was preheated in the steamer for 15 mins before the slides were added. The slides were steamed in the antigen retrieval buffer for 15 mins, a time point optimised for brain tissue. The slides were then washed in dH2O for 3 mins, twice before being submerged into 100% EtOH for a further 3 mins. Slides were allowed to dry at room temperature overnight. The tissue was incubated with protease plus at 40°C for 30 mins before the RNAscope assay was performed according to the RNAscope Multiplex Fluorescent

Reagent Kit v2 manual. The RNAscope assay was completed for the probes listed in table 7.2. The Opal 420, 570, 690 and 780 were used to develop the signals for each probe. Once the RNAscope assay was completed, the sections were then stained for TdTomato expression using the antibody for RFP (AA234 (ABIN129578)).

Target	Probe	Catalogue Number
Slc4a4	Mm-Slc4a4	Cat No. 452981
Bmp4	Mm-Bmp4	Cat No. 401301
Ki67	Mm-Mki67-C2	Cat No. 416771-C2
Id3	Mm-Id3-C2	Cat No. 445881-C2
Enpp6	Mm-Enpp6-C2	Cat No. 511021-C2

Table 7-2 Probes used for RNAScope Assay

To stain for protein, the slides were first washed 3 times with 1x TBST buffer for 5 mins. Following this, the sections were blocked in 10% donkey serum in 1x TBST for 30 mins. The primary antibody was prepared in the blocking solution and added to the sections. The sections were incubated with the primary antibody overnight at 4°C. The slides were then washed in 1x TBST three times for 5 mins. This was followed by secondary antibody staining using an appropriate HRP secondary antibody for 30 mins at room temperature. The secondary antibody was prepared in blocking solution. Next, the slides were washed in 1x TBST three times for 5 mins.

To develop the antibody signal with Opal 780, the slides were first incubated with TSA-DIG for 30 mins at room temperature. The slides were subsequently washed with 1x TBST three times. Next, the slides were incubated with Opal 780 for 10 mins at room temperature. The slides were then washed with. The slides were then incubated with HRP-block for 15 mins at 30°C. The slides were then washed with 1x TBST. Finally, the slides were counterstained with the RNAscope provided DAPI for 30 secs before they were mounted.

All slides were imaged at 40X magnification using the PhenoImager HT (Akoya Biosciences). Each image was uploaded to QuPath (Bankhead et al., 2017). Image analysis was performed in collaboration with Dr Simon Castillo. Tissue was first segmented and subsequent single cell detection was performed on the DAPI channel and cell expansion of 2 µm employed from the nucleus boundary to denote the cell. For every individual cell, a set of features were extracted for each probe including the minimum, maximum, mean, and standard deviation values of the probe intensity. Based on manual phenotype annotations we provided, Dr Simon Castillo optimised automatic classification of all cells in QuPath. The mean and maximum expression of each probe was scaled (z-transformation) across all cells for each slide. A priori, the classification criteria consisted of setting probe^{+} for z-transformed expression > 0, and probe^{-} for z-transformed expression < 0. Each biological replicate had two tissue sections digitized and mounted on the same slide. To avoid averaging cell abundance metrics across samples and losing intra-individual variability, both tissue sections were considered as observations statistically nested in the experimental unit (mice). Therefore, we used generalized mixed models, with a nested structure, with the individual ID as a random factor.

7.5 Immunofluorescence

For *in vitro* immunofluorescence, cells were fixed with 4% PFA for 15 mins at room temperature. They were permeabilized in 0.5% tritonX-100 and blocked with 3% BSA prior to incubation with the primary antibody overnight at 4 °C. The primary antibody γH2AX (05-636, Millipore) was used at 1:2000. Cells were washed with 1X PBS 4 times before incubation with

the secondary antibody (1:1000) and DAPI (1 in 50000) for 1 hr. Cells were washed in 1x PBS 4 times before mounting (if using coverslips) or cells were kept in 1x PBS (if using plates). Primary and secondary antibodies were diluted in 3% BSA.

7.6 Cell Culture

Primary tumour cell isolation

Mice were sacrificed by cervical dislocation and the brain micro dissected to isolate the striatum and corpus callosum in ice-cold Hibernate A (Sigma). The collected tissue was incubated with papain (20 units/ml) and DNAse (0.005%) for 30mins at 37°C. EBSS was added to the solution and centrifuged at 300g for 3 mins. Digestion was terminated with ovomucoid inhibitor (10 mg/ml), albumin (10mg/ml) and DNase (0.005%) in EBSS. The dissociated cells were centrifuged and resuspended in serum-free GSC media (N2 (1/200), B27 (1/100) (Life Technologies), 1 mg/ml laminin (Sigma), 10 ng/mL EGF and FGF-2 (Peprotech), 1× MEM NEAA (Gibco), 0.1 mM betamercaptoethanol, 0.012% BSA (Gibco), 0.2 g/L glucose (Sigma), 1000 U/ml penicillin-streptomycin (Sigma)). To model the dormant AC-like tumour population, the tumour cells were cultured without EGF, and with 20ng/ml of BMP4 (Proteintech) and 10 ng/ml FGF (peprotech).

In vitro DNA repair inhibitors

For experiments involving *in vitro* treatment with DNA damage repair inhibitors ART-558, ART-6043 and Nu7441, all drugs were dissolved in 100% DMSO and added directly to cell media.

In vitro irradiation

In vitro irradiations were performed using the stage attachment of the SARRP (Xstrahl). Irradiations were performed open field using the copper filter.

7.7 In vitro Assays

7.7.1 Click-it EdU

The Invitrogen kit was used to complete Click-it EdU imaging. Cells were cultured on coverslips or in plastic plates. Next, cells were incubated with EdU for 1:1000 for 2 hrs, unless specified otherwise. Cells were washed 3 times in 1x PBS before proceeding with the Click-it reaction protocols for imaging (Thermofisher, C10337) or for FACS analysis (Thermofisher, C10420).

7.7.1.1 Imaging

Cells were washed 3 times in 1x PBS before fixation in 4% PFA for 15 mins at room temperature. To permeabilise the cells, the cells were incubated with 1% Triton-X and 3% BSA for 30 mins at room temperature. Primary antibody staining was performed at 4 °C overnight as described in the Immunostaining section above if required. Subsequent secondary antibody and DAPI (1

µg/ml) staining was performed according to the immunostaining protocol. Cells were washed 3 times in 1x PBS, as much of the PBS was removed as possible prior to staining with the click-it reaction kit. The click-it reaction was prepared as described in table 7.3. Either A647 or A488 were used in the reaction. Cells were incubated with the click-it for 30 mins and subsequently washed 3 times in 1x PBS. Cells were left in a volume of PBS appropriate to the well size, unless the cells were cultured on coverslips, here they were mounted onto slides.

Reagent	**Volume for a 10ul reaction (Scale up as necessary)**
(A) 1X Click-It Reaction Buffer	8.8
CuSO4	0.2
A647 or A488	0.024
(B) Rxn Buffer Additive	1

Table 7-3 Volumes used for the Click-iT Imaging reaction

7.7.1.2 Flow

Cells were accutased and washed once in 1% BSA in 1x PBS. Cells were subsequently fixed in 4% PFA for 15 mins at room temperature and washed once in 1% BSA in 1xPBS. Next, the cells were permeabilised in 1% Triton-X100 (Sigma) for 15 mins at room temperature. The cells were spun down and the supernatant removed as much as possible prior to the Click-it reaction. The Click-it reaction was prepared according to table 7.4. Once the cells were permeabilised, they were incubated in 100ul of the Click-it reaction for 30 mins. The cells were then washed in 1% BSA in 1x PBS before they were finally resuspended in DAPI at 1 µg/ml + 0.5% Tx in PBS. The cells were then analysed by FACS.

Reagent	100 µl Reaction
1X PBS	87.6
CuSO4	2
A647*	0.5
1X Rxn Buffer Additive	10

Table 7-4 Volumes used for the Click-iT FACS reaction

7.7.2 Cell Death

To measure cell death *in vitro* Sytox Green (Invitrogen) was used. Tumour cells were incubated with Sytox Green (Invitrogen, S7020) at 0.1 µM (or 1:50000 of the stock concentration) and Hoechst 33342 (Thermofisher, H3570) at 2 µg/ml for 5 mins before being processed for imaging or FACS. For imaging analysis, cells were subsequently imaged live on the EVOS. For FACS analysis cells were accutased at 37 °C and kept on ice until the sample was collected for FACS. Excess washing was avoided to prevent the loss of dead cells.

7.7.3 Comet

This protocol was adapted from the 2011 Hartley protocol (Hartley et al., 2011). Tumour cells were accutased and washed once in 1x PBS. The tumour cells were then resuspended in 500 µl of ice-cold PBS and counted. A concentration of 3 x 10^6 cells per ml in 1x PBS was achieved. To embed the tumour cells in agarose in preparation for the comet assay, 500 µl of the tumour cell suspension was mixed with 1 ml of low-grade temperature agarose (Invitrogen). 1 ml of the cell suspension-agarose mixture was added to a slide (60 cm x 40 cm) that was pre-coated with 1% agarose the night before. A coverslip (60 cm x 40 cm) was placed over the cell

suspension-agarose mixture and allowed to set on ice. Once all the samples were set in the agarose gels, they were covered with lysis buffer and incubated on ice for 1 hr. The slides were then processed for either the alkali or neutral comet assays.

7.7.3.1 Alkali Comet Assay

The slides were washed three times in dH2O for 15 mins each time. Next, the slides were placed into an electrophoresis tank and incubated in the alkali buffer for 45 mins. The electrophoresis chamber was run at 21 volts for 25 mins. The cells were subsequently removed from the chamber and washed with 1 ml of neutralisation buffer for 10 mins. The slides were washed in 1x PBS three times for 10 mins each before being allowed to dry at 60 °C.

7.7.3.2 Neutral Comet Assay

For the neutral comet assay the slides were washed three times in neutral assay buffer for 10 mins each time. The slides were then placed into the electrophoresis chamber and covered with fresh neutral assay buffer. The electrophoresis was run for 25 volts for 60 mins (1 volt/cm). Once the run was finished, the slides were removed from the chamber and washed with 70% EtOH twice for 10 mins each time. The slides were finally washed x2 with 1x PBS for 20 mins before they were allowed to dry at 60 °C.

7.7.3.3 Staining and Imaging

The following day or once the slides had completely dried, the slides were re-hydrated in 1 ml of dH2O for 30 mins. The slides were incubated with 1 ml of propidium iodide (2.5 µg/ml) for 30

mins. This step was repeated once more. Once staining with propidium iodide was complete, the slides were washed in dH2O once for 10 mins. The slides were washed further in dH2O for 30 mins before being allowed to dry at 60°C. Once staining was completed the comets were imaged using the Open Comet software, images of the comets were acquired using a 20x magnification.

7.7.4 ROS

In 96 well plates, tumour cells were cultured in media with EGF/FGF or BMP4/FGF for 3 days. To measure the levels of ROS, CellRox Deep Red (Invitrogen) was added to the media at a final concentration of 5 µM and incubated at 37°C for 30 mins. Cells were subsequently washed 3 times in 1x PBS and then fixed in 4% PFA for 15 mins at room temperature. Cells were counterstained with Hoechst 33342 (Thermofisher, H3570) at 2 µg/ml for 5 mins once they were fixed.

To measure the levels of ROS following 5 mins of radiation cells were incubated with CellRox Deep Red for 25 mins prior to radiation (4 Gy) on the SARRP (Xstrahl). The cells were washed and fixed as described above 5 mins later. To assess ROS levels following 30 mins or more after radiation (4 Gy), cells were first irradiated before the CellRox Deep Red dye was added to the media.

The EVOS (Thermofisher) was used to image the cells. The fluorescence intensity of the CellRox Deep Red and the number of nuclei were quantified for each image in Fiji. The fluorescence intensity normalised to the number of nuclei was used to indicate the level of ROS.

7.7.5 DSB Repair

Plasmid Preparation

The MMEJ, NHEJ and HR DSB reporter plasmids were gifted by ARTIOS. Prior to transfection both the NHEJ and HR plasmids were linearized by I-SceI (NEB) digestion. On the other hand, the MMEJ core plasmid required linearization with HindIII-HF and Xhol. Prior to transfection, the linearized MMEJ core plasmid was further modified. Specifically, pre-annealed oligonucleotide caps were ligated to the cut ends of the MMEJ core plasmid.

Transfection

Transfection of the control firefly plasmid and the linearized MMEJ, NHEJ or HR plasmids were performed using FuGene HD transfection reagent (Promega) according to the manufacturer's protocol. A 1:1 ratio of plasmid mix:fugene reagent was used. The amounts of each plasmid transfected per well are outlined below.

Plasmid	ng added per well
Firefly	20
MMEJ	15
non-blunt NHEJ	15
long HR	30

Table 7-5 Plasmids used for DSB activity assays

Dual Luciferase Assay

24 hrs following transfection, the dual luciferase assay was performed with the Dual-Glo luciferase kit (Promega). Cells, seeded in a 96 well plate, were washed twice in 1x PBS before

the reactions. First, 60 µl of the ONE-Glo EX substrate was added to each well. The plate was shaken at 450 rpm in the dark for 3 mins. The Firefly signal was subsequently measured on the Variosakn LUX (Thermofisher). Next, 60 µl of the Stop & Glo substrate was added to each well. The plate was shaken at 450 rpm for 3 mins in the dark, then incubated for 7 mins at room temperature. The NanoLuc signal was subsequently measured using the Varioskan LUX (Thermofisher).

7.8 Bulk RNA Sequencing

Cells were first accutased and washed once in 1x PBS. The RNA was then extracted from the cells using the NEB monarch RNA extraction kit (New England Biolabs). Once the RNA was extracted the purity and integrity of the RNA was assessed with the nanodrop. Once the RNA met sufficient standards, with an A260/280 ratio within 1.9–2.1, and an A260/230 ratio within 2.0–2.2, the samples were accepted for the next stage. RNA libraries were prepared, and sequencing performed by Novogene. The QC was performed by Novogene. The RNAseq alignment was performed with the mm10-2020-A mouse genome, matrices generation and PCA were performed by Dr Wenhao Tang. In addition, Wenhao Tang acquired the transcriptional signature from the BMP4/FGF-treated tumour cells. Subsequent differential gene expression analysis was performed on R with the DEseq2 package, and the Gene set enrichment analysis was performed on R with the fgsea package.

7.9 Statistical Analysis

Statistical analyses were performed using Prism (GraphPad, ver10), FACS analysis was completed using Flowjo. Statistical tests and significance are described in figure legends, otherwise, *P* values equal ns > 0.05; * <0.05; ** <0.01; *** < 0.001; ****<0.000

Chapter 8. Appendix

8.1 Significantly Altered Genes induced by BMP4/FGF

Genes (UP)	log2FoldChange	padj	Genes (Down)	log2FoldChange	padj
Fmod	15.270	1.58E-21	**Klrb1c**	-8.058	9.55E-07
Myoc	11.144	4.73E-05	**Izumo1r**	-7.868	2.71E-06
Hmgcs2	10.344	3.87E-14	**A330049N07Rik**	-6.842	5.97E-04
Gfap	9.246	3.65E-10	**Gm2824**	-6.545	1.39E-05
Aqp4	8.963	3.12E-22	**C030029H02Rik**	-6.439	2.42E-05
Nog	8.831	1.53E-108	**Zfp488**	-6.428	1.37E-02
Islr	8.812	7.91E-19	**Gm34776**	-6.032	8.55E-03
Bgn	8.724	1.88E-11	**Colec10**	-5.847	8.87E-05
Aspg	8.622	6.25E-08	**Egr4**	-5.829	1.09E-03
Omd	8.419	1.71E-07	**Spo11**	-5.807	2.41E-02
Gm50048	8.375	1.09E-07	**Magel2**	-5.712	5.91E-04
Ltbp2	7.811	2.32E-36	**Barx2**	-5.500	3.83E-15
Hrc	7.463	1.87E-06	**Adamts19**	-5.409	3.86E-16
Sncg	7.270	1.36E-08	**Thbd**	-5.362	2.30E-06
Ehf	7.247	1.94E-04	**Olfr549**	-5.290	5.30E-03
Gm39323	7.237	7.16E-05	**Lrmp**	-5.253	2.08E-02
Cd164l2	7.159	6.29E-04	**Nts**	-5.231	4.64E-02
H2-DMb1	7.132	6.66E-04	**1700036A12Rik**	-5.166	1.49E-02
Slit3	7.039	1.26E-35	**Gm28578**	-5.165	2.29E-02
Aldh1a1	7.027	1.06E-09	**Kcnv1**	-5.133	1.17E-05
Ablim2	6.978	2.25E-17	**Myt1**	-4.976	9.43E-03
Foxi2	6.971	1.30E-03	**Klrb1a**	-4.964	1.59E-02
Oas2	6.969	8.02E-04	**Egr3**	-4.886	3.25E-13
Cbr2	6.940	1.25E-06	**4930502A04Rik**	-4.861	5.58E-03
Atp1a4	6.916	1.36E-03	**Olfr550**	-4.791	2.19E-02
Mal	6.893	6.08E-07	**F2rl2**	-4.715	1.38E-04
Ifi47	6.882	1.50E-09	**Gm19500**	-4.706	4.76E-02
Cidea	6.854	1.63E-03	**Grap2**	-4.690	2.63E-02
Inpp5j	6.797	5.99E-75	**Egr1**	-4.671	1.93E-40
Gm49807	6.796	2.57E-03	**Acod1**	-4.598	1.52E-02
Atp1a2	6.767	4.48E-10	**Ccl12**	-4.575	3.90E-02
Fam167b	6.763	1.94E-03	**Car3**	-4.468	4.06E-08

Genes (UP)	log2FoldChange	padj	Genes (Down)	log2FoldChange	padj
Fabp4	6.762	1.14E-03	**Nr5a2**	-4.464	3.50E-16
Shbg	6.750	2.73E-03	**Col28a1**	-4.389	4.42E-02
Gja3	6.715	1.10E-14	**Sv2c**	-4.300	4.03E-60
Podn	6.691	6.26E-06	**Pou4f2**	-4.279	2.65E-02
Icos	6.653	1.90E-03	**Vgll2**	-4.172	3.45E-04
4921539H07Rik	6.641	3.50E-03	**Cd93**	-4.014	7.74E-48
Zbp1	6.608	2.43E-07	**Cpne7**	-4.012	1.90E-27
Stum	6.597	3.27E-16	**Gm19541**	-3.968	3.38E-07
Myom3	6.587	4.62E-03	**A930003A15Rik**	-3.891	1.32E-05
1700019L13Rik	6.575	4.58E-03	**Egr2**	-3.867	1.30E-13
4933400C23Rik	6.573	4.28E-03	**Rab17**	-3.849	3.13E-03
Ggt1	6.539	4.20E-04	**Pcdh15**	-3.816	2.08E-08
Gjb4	6.508	5.23E-08	**Mpped1**	-3.681	1.91E-03
Bmp15	6.500	1.28E-05	**Tmc3**	-3.677	5.63E-33
Cldn9	6.480	3.72E-03	**Fetub**	-3.662	7.21E-08
Ankrd55	6.398	1.15E-02	**Zcchc12**	-3.595	1.43E-35
Apol9b	6.396	3.55E-19	**Trp53i11**	-3.583	7.07E-63
Snai2	6.298	1.75E-05	**B230334C09Rik**	-3.480	2.68E-15
Gbp10	6.291	1.58E-02	**Arc**	-3.475	7.51E-07
P2rx1	6.290	7.68E-14	**I730030J21Rik**	-3.457	1.62E-03
Wif1	6.271	1.23E-07	**Pf4**	-3.420	2.01E-02
Cpne6	6.253	4.69E-05	**Tacr3**	-3.408	1.68E-06
A830021F12Rik	6.244	7.41E-03	**Itga4**	-3.397	2.50E-43
Serpind1	6.204	3.85E-03	**Vwc2**	-3.363	1.96E-24
Scrg1	6.199	6.95E-07	**Tmem178**	-3.361	1.65E-11
Ccl20	6.186	1.05E-02	**Trim71**	-3.361	4.74E-13
Ifit3b	6.182	7.49E-45	**Dusp2**	-3.351	1.27E-05
Cfh	6.175	7.22E-05	**Fgf5**	-3.341	4.14E-02
Kndc1	6.142	5.47E-04	**Lrrn4**	-3.328	2.88E-07
Defb42	6.127	2.87E-04	**Elavl4**	-3.320	1.52E-09
Cav3	6.114	1.14E-05	**Cldn11**	-3.304	3.82E-17
Gm12324	6.112	2.48E-02	**Nptx2**	-3.278	1.38E-06
Oas1c	6.097	9.31E-03	**Rab3b**	-3.237	5.20E-29
Gjc2	6.097	9.39E-11	**Rab26**	-3.230	2.70E-15
Vnn3	6.068	2.23E-02	**Lpo**	-3.214	4.77E-20
Trim30a	6.034	8.76E-11	**Pstpip2**	-3.202	1.66E-03
Mymk	6.030	1.80E-02	**Gm44632**	-3.189	4.37E-03
Fgd2	6.026	2.84E-03	**E330013P04Rik**	-3.177	3.32E-05
Ggt5	6.011	4.01E-04	**Rbp4**	-3.157	3.51E-02
Fbp1	5.975	6.13E-07	**Aldh1a3**	-3.156	8.82E-39
Hrct1	5.970	3.68E-02	**Gpr17**	-3.153	6.96E-04
Fer1l6	5.967	7.07E-04	**Arap3**	-3.050	2.32E-02
A730036I17Rik	5.963	3.47E-02	**Bcl6b**	-3.048	3.88E-16

Genes (UP)	log2FoldChange	padj	Genes (Down)	log2FoldChange	padj
Gm49306	5.958	3.14E-02	**Mlip**	-3.031	7.89E-06
Kcnj6	5.951	7.41E-03	**2010204K13Rik**	-3.016	1.49E-04
Prss50	5.924	2.84E-02	**Gm29502**	-3.006	9.46E-03
Lrtm2	5.905	1.52E-05	**Filip1**	-3.006	1.11E-07
Cpvl	5.890	4.98E-05	**AI504432**	-2.989	3.81E-08
Gm12092	5.889	2.62E-03	**Opalin**	-2.950	3.87E-02
Slc22a2	5.862	3.24E-02	**Gm34804**	-2.931	1.63E-02
Scube3	5.858	1.82E-72	**Nrap**	-2.884	6.99E-06
Ass1	5.845	3.99E-42	**Nefm**	-2.882	1.21E-06
2810032G03Rik	5.837	1.19E-03	**Elfn2**	-2.845	2.71E-16
Fxyd1	5.831	4.66E-04	**Vwa5b1**	-2.835	9.24E-04
Fam180a	5.815	2.33E-03	**Fbn2**	-2.815	1.18E-30
Slc22a12	5.797	2.10E-04	**Sox10**	-2.795	8.63E-06
Rtp1	5.789	2.43E-03	**4930429F24Rik**	-2.787	3.14E-02
Slc6a4	5.781	5.87E-04	**Slc35d3**	-2.766	2.30E-02
Gm36356	5.780	5.41E-11	**Bmp7**	-2.764	5.15E-10
Ptprtos	5.751	4.42E-02	**T**	-2.741	2.22E-02
Gm4951	5.733	5.86E-05	**Neurod1**	-2.731	4.75E-02
Eprn	5.732	3.92E-02	**Camk2b**	-2.718	5.93E-11
Npy	5.729	4.05E-04	**Gm11872**	-2.717	1.63E-02
Wfdc1	5.718	6.82E-04	**Inka2**	-2.704	2.10E-08
Rian	5.685	3.13E-03	**Foxr2**	-2.691	2.81E-05
Olfml1	5.680	5.12E-09	**Prr18**	-2.667	1.24E-11
Col1a1	5.612	4.07E-24	**Nrgn**	-2.666	4.16E-17
Hpse	5.610	4.01E-03	**1700016P03Rik**	-2.638	1.53E-02
Gm34684	5.601	2.10E-08	**Hydin**	-2.637	2.31E-02
B4galnt3	5.589	3.08E-03	**Kcnn4**	-2.604	1.82E-03
Chil1	5.583	1.26E-06	**Hcrtr2**	-2.593	2.02E-02
Rtl3	5.576	3.34E-03	**Lgr5**	-2.586	9.94E-06
2210011C24Rik	5.572	7.42E-03	**Ube2ql1**	-2.548	5.80E-16
Fibcd1	5.543	4.54E-04	**Gsx1**	-2.539	4.72E-03
Tnn	5.542	2.64E-40	**Lmo3**	-2.517	3.63E-13
Sostdc1	5.494	1.24E-02	**Ccbe1**	-2.515	1.42E-23
Clca3a2	5.478	4.36E-02	**Prdm8**	-2.497	3.85E-02
Slc22a18	5.477	1.19E-02	**Gm45552**	-2.482	1.01E-02
Ifit3	5.443	6.57E-21	**Crispld2**	-2.464	3.91E-10
Sgca	5.442	2.08E-05	**Ankrd33b**	-2.457	6.44E-08
Ptgs1	5.425	2.87E-03	**Tafa4**	-2.440	1.66E-06
Gm536	5.410	4.45E-03	**Dleu7**	-2.423	7.34E-04
Gm17455	5.404	1.65E-02	**Dhh**	-2.420	2.22E-03
4930540M05Rik	5.397	1.99E-03	**Lrrc7**	-2.408	2.81E-10
Gucy2c	5.397	4.58E-02	**Stc1**	-2.397	3.25E-08
Defb1	5.395	3.64E-12	**Cyp26a1**	-2.393	1.58E-02

Genes (UP)	log2FoldChange	padj	Genes (Down)	log2FoldChange	padj
Slc4a5	5.379	6.47E-03	**Lor**	-2.385	2.99E-08
Ccl6	5.323	1.05E-02	**Chrm3**	-2.361	5.86E-23
Pdgfrl	5.303	3.53E-29	**Myb**	-2.360	2.97E-10
Cnn1	5.302	5.06E-03	**Eya2**	-2.358	9.21E-08
Disp3	5.272	3.22E-05	**A830011K09Rik**	-2.350	1.21E-02
Diras2	5.257	1.64E-19	**Crb1**	-2.349	4.52E-02
Heph	5.257	5.92E-03	**Scml4**	-2.334	3.00E-05
Nmrk2	5.242	2.01E-02	**Dact1**	-2.332	3.80E-25
Trp63	5.227	1.30E-02	**Lingo3**	-2.327	2.77E-10
Gm19935	5.224	8.05E-03	**Rcor2**	-2.320	6.20E-21
Zbtb8b	5.221	1.06E-02	**Adm**	-2.319	4.05E-12
Kif26b	5.219	1.85E-44	**Kcna3**	-2.317	2.61E-03
Olfm3	5.205	1.03E-02	**Rfx4**	-2.306	7.86E-07
Lrrc75b	5.204	4.13E-45	**Peg12**	-2.297	7.83E-33
Fam43b	5.199	1.34E-02	**Pou3f1**	-2.291	1.22E-21
Lctl	5.188	3.37E-06	**Tspan8**	-2.280	2.50E-06
Iigp1	5.181	1.23E-09	**Zfp820**	-2.267	3.15E-02
Pmp2	5.178	2.19E-09	**Sorcs3**	-2.248	3.49E-02
Gm47400	5.177	1.36E-02	**Shcbp1l**	-2.236	2.42E-02
Gm49694	5.175	2.47E-02	**Syt7**	-2.235	8.57E-07
Abca8a	5.164	1.46E-07	**Syt6**	-2.234	2.76E-07
Myh8	5.164	1.55E-05	**Gap43**	-2.224	1.60E-34
Tmie	5.156	1.41E-12	**Chrna7**	-2.221	9.71E-08
Mrc1	5.144	8.61E-03	**Necab2**	-2.219	4.41E-09
Col17a1	5.140	6.21E-03	**Dll1**	-2.217	4.65E-10
Ctf2	5.137	3.40E-02	**Gm38414**	-2.214	6.91E-03
Gm38477	5.114	3.87E-02	**Sptbn2**	-2.212	1.43E-06
Gm13431	5.106	1.16E-02	**Prdm1**	-2.210	8.71E-08
Gm48898	5.103	4.13E-02	**Dusp9**	-2.208	7.51E-03
Gm15410	5.096	1.71E-02	**Mir17hg**	-2.208	4.96E-07
Fam20a	5.093	3.34E-10	**Brsk2**	-2.205	1.23E-07
Edn1	5.090	1.03E-21	**Hic1**	-2.205	1.11E-23
Cox4i2	5.076	5.33E-03	**Doc2b**	-2.199	1.21E-02
Fut7	5.076	2.16E-02	**A430106G13Rik**	-2.195	4.85E-02
Gm30373	5.073	7.04E-05	**Gm7457**	-2.195	3.08E-03
Ifit1	5.073	4.41E-03	**Vav3**	-2.189	1.53E-11
Adap1	5.063	9.54E-26	**Cdh4**	-2.170	3.86E-07
Dlx4	5.060	4.17E-02	**C030034L19Rik**	-2.165	2.15E-02
Serpinf1	5.056	2.01E-47	**Gm11549**	-2.165	9.45E-05
Gm12052	5.043	3.31E-02	**Rassf3**	-2.162	1.53E-13
Slc36a2	5.033	5.62E-04	**Dna2**	-2.157	1.13E-09
Rnase10	5.026	6.33E-07	**Vsig8**	-2.155	6.85E-04
Dock8	5.022	2.90E-19	**Syt4**	-2.145	1.94E-06

Genes (UP)	log2FoldChange	padj	Genes (Down)	log2FoldChange	padj
Ifitm10	5.021	1.55E-14	**H2-Q7**	-2.143	4.00E-04
Col6a1	5.012	1.46E-22	**Pgm2l1**	-2.101	1.01E-07
Slc22a14	4.997	1.34E-02	**Ccdc194**	-2.094	1.42E-02
Scg5	4.990	1.43E-02	**Creb5**	-2.093	9.06E-09
Susd5	4.972	3.06E-13	**Spsb4**	-2.089	4.36E-11
Fbxo2	4.970	6.26E-40	**Bex2**	-2.085	6.14E-15
Hsd11b1	4.953	1.77E-05	**Erich3**	-2.064	2.45E-05
A530001N23Rik	4.947	3.39E-02	**Fam181a**	-2.050	1.40E-02
Dlk2	4.943	1.20E-19	**Plppr1**	-2.046	6.57E-05
Ankrd35	4.929	4.17E-04	**Cecr2**	-2.037	8.73E-04
9130213A22Rik	4.906	1.90E-06	**Gad1**	-2.026	2.76E-07
Ifi27l2a	4.892	9.23E-15	**Calhm4**	-2.018	2.83E-02
Ifi44	4.886	6.81E-12	**Slco5a1**	-2.012	3.38E-04
P2rx6	4.872	1.54E-04	**Tle6**	-2.008	1.18E-15
Crybb1	4.857	1.63E-08	**Tmem173**	-2.003	7.14E-17
Mgp	4.856	9.71E-08	**B9d1os**	-1.989	2.91E-04
Klhdc8a	4.852	2.11E-03	**Nes**	-1.988	7.36E-09
Ablim3	4.818	7.85E-08	**Nptx1**	-1.979	2.89E-05
Ephx2	4.813	1.12E-03	**Klhl34**	-1.955	9.45E-05
Gm34425	4.809	4.61E-02	**Olfr77**	-1.952	3.86E-02
Fam107a	4.809	8.11E-10	**Synj2**	-1.951	1.87E-12
Gm32027	4.801	7.18E-03	**Sox3**	-1.947	1.02E-09
H19	4.799	4.77E-15	**Sms**	-1.943	8.95E-11
Gpr26	4.796	6.00E-05	**Tmem51**	-1.940	4.92E-04
Gm9949	4.791	4.09E-02	**Spry4**	-1.927	9.79E-29
Lox	4.781	5.53E-09	**E2f2**	-1.923	1.18E-11
Smad6	4.778	3.31E-42	**Dll3**	-1.919	7.15E-03
Gm13470	4.776	1.66E-02	**P2ry12**	-1.918	1.12E-02
Lmntd2	4.765	3.19E-02	**E030013I19Rik**	-1.915	2.29E-02
Padi2	4.751	1.42E-15	**Shmt1**	-1.914	5.49E-14
C3	4.749	2.71E-08	**Rims4**	-1.913	2.67E-11
Oasl2	4.746	2.47E-23	**Nkain1**	-1.910	7.21E-10
Lyz2	4.733	6.19E-12	**Clic5**	-1.903	7.01E-09
Plscr2	4.732	7.49E-16	**Fam71f1**	-1.900	4.58E-02
Col11a2	4.723	5.36E-26	**Rrp1b**	-1.895	1.34E-10
Phf11b	4.722	8.05E-03	**Syt13**	-1.895	3.01E-05
Tie1	4.714	3.14E-06	**Adam19**	-1.886	9.13E-12
Slc26a7	4.691	1.41E-42	**Sinhcaf**	-1.883	3.92E-08
Ifitm6	4.690	2.08E-03	**Usp44**	-1.883	1.63E-04
Tceal5	4.688	3.23E-06	**Ptgds**	-1.870	3.50E-03
Usp18	4.685	1.66E-03	**Ppp1r16b**	-1.858	1.82E-05
Gbp6	4.682	9.52E-09	**Camkv**	-1.853	1.40E-03
Mmd2	4.681	8.44E-26	**Nme4**	-1.852	3.02E-11

Genes (UP)	log2FoldChange	padj	Genes (Down)	log2FoldChange	padj
Kng2	4.679	1.82E-02	**Ceacam1**	-1.838	2.44E-03
Pdgfd	4.668	1.32E-06	**Gm8251**	-1.833	1.03E-02
Fam186a	4.647	9.36E-03	**Osbp2**	-1.831	2.09E-06
Ces1g	4.642	2.30E-02	**Frmd7**	-1.824	9.73E-03
Gm44672	4.641	3.49E-02	**Cdon**	-1.815	1.22E-15
Aplnr	4.631	3.17E-02	**Ets2**	-1.812	2.01E-06
Col6a2	4.606	2.74E-26	**Hmga1**	-1.807	8.04E-09
Vnn1	4.605	4.83E-02	**Gm13889**	-1.803	6.74E-04
Cryab	4.601	2.00E-22	**Morc4**	-1.797	1.44E-05
Sla	4.594	4.44E-03	**Tafa1**	-1.794	2.39E-04
Slc1a2	4.591	3.32E-80	**Rnf165**	-1.786	8.42E-07
Sox1ot	4.585	5.39E-20	**N4bp3**	-1.769	5.04E-06
Rspo3	4.576	3.36E-03	**Mfng**	-1.768	8.54E-04
Stard8	4.571	6.52E-42	**6430562O15Rik**	-1.761	1.33E-03
Col23a1	4.568	6.02E-24	**Gm17300**	-1.758	2.59E-02
Fcgrt	4.566	2.27E-37	**Celf3**	-1.751	9.10E-03
Kcnq3	4.559	1.16E-53	**Igsf21**	-1.746	1.60E-05
Ngfr	4.559	3.70E-18	**Srm**	-1.743	4.78E-07
Igfbp7	4.555	3.13E-20	**Arhgdig**	-1.743	3.89E-02
Xaf1	4.537	3.42E-12	**Fam110c**	-1.742	1.86E-02
Slc25a34	4.528	1.38E-02	**Onecut2**	-1.736	5.57E-03
Gm36001	4.524	3.29E-02	**Nup210**	-1.727	6.83E-11
Sncb	4.513	1.04E-03	**Cd37**	-1.726	4.35E-02
Ddx60	4.508	6.96E-07	**Traf4**	-1.722	1.30E-10
Ndrg2	4.506	9.31E-22	**Snhg15**	-1.707	7.39E-04
Plk5	4.499	2.60E-02	**Pidd1**	-1.706	3.00E-09
Vit	4.492	2.44E-05	**Ifrd2**	-1.702	1.39E-08
Gm29417	4.489	8.90E-04	**Sh3gl3**	-1.701	2.60E-04
2900052N01Rik	4.481	8.81E-03	**Gm16010**	-1.695	3.13E-02
Lcat	4.476	3.48E-05	**Mreg**	-1.695	6.47E-04
Marveld3	4.469	5.63E-03	**Tagln2**	-1.685	4.99E-04
Als2cl	4.462	1.38E-26	**Tfap4**	-1.679	3.52E-04
Atoh8	4.455	4.47E-30	**Plekhh1**	-1.678	5.69E-08
Aox3	4.452	2.06E-02	**Hmga2**	-1.673	3.97E-14
Atp13a4	4.445	1.36E-04	**Rtkn2**	-1.670	1.82E-09
Jaml	4.428	2.71E-04	**Unc5a**	-1.670	8.34E-05
A930001A20Rik	4.420	2.00E-04	**Oacyl**	-1.665	1.61E-02
Tmem63c	4.417	2.51E-03	**Dctpp1**	-1.659	7.34E-08
Gm50147	4.413	1.37E-06	**Qtrt1**	-1.656	9.18E-06
Gm16325	4.411	4.71E-03	**Dctd**	-1.654	9.06E-05
Igtp	4.401	5.48E-07	**Irf8**	-1.653	2.12E-02
Acta2	4.392	1.99E-40	**Grm5**	-1.632	7.73E-03
Kcnc4	4.392	4.91E-21	**Smpdl3b**	-1.630	5.06E-08

Genes (UP)	log2FoldChange	padj	Genes (Down)	log2FoldChange	padj
Plac8	4.387	2.85E-02	**Radx**	-1.626	1.11E-03
Slc13a4	4.386	4.98E-07	**Ppp1r14b**	-1.624	4.19E-20
Stra6	4.386	2.38E-08	**A930024E05Rik**	-1.624	5.30E-06
Ptx3	4.386	8.59E-20	**Smagp**	-1.623	1.28E-02
Col2a1	4.385	3.32E-29	**Snhg5**	-1.621	9.46E-04
Trim30d	4.366	1.15E-06	**Rem2**	-1.620	1.27E-02
Cstad	4.365	2.30E-02	**Rmi2**	-1.619	2.31E-05
H2-T23	4.350	7.49E-45	**Dscam**	-1.616	7.61E-03
Eef1a2	4.342	6.77E-15	**Sall3**	-1.615	4.26E-17
Atp2a3	4.340	3.53E-24	**Suv39h2**	-1.601	3.59E-10
Itgb3	4.338	2.38E-25	**Prkcb**	-1.598	2.33E-05
Trim12c	4.337	8.82E-05	**Lmo1**	-1.597	7.95E-13
Dclk3	4.331	7.90E-06	**Phex**	-1.596	9.89E-06
Tshr	4.325	1.60E-09	**Moxd1**	-1.596	5.40E-07
Ccdc80	4.321	1.35E-103	**Bok**	-1.590	1.56E-04
Gm15688	4.318	4.83E-02	**Plcl2**	-1.587	1.16E-09
Casq1	4.305	1.59E-50	**Nle1**	-1.587	1.84E-08
9130015G15Rik	4.290	4.39E-05	**Tesc**	-1.585	4.00E-04
Fyb2	4.286	1.97E-02	**Fut4**	-1.584	1.27E-03
Gpr141	4.285	1.51E-05	**Cbx2**	-1.579	7.85E-08
Pdzk1ip1	4.264	1.94E-04	**Ccnjl**	-1.576	1.32E-06
Serpinb1a	4.262	2.95E-08	**Abca4**	-1.575	4.90E-05
Otof	4.257	4.23E-02	**Asb4**	-1.567	3.47E-02
Apoh	4.257	1.42E-03	**Ccl2**	-1.567	5.93E-06
Smad9	4.254	2.25E-47	**Uhrf1**	-1.560	1.49E-07
Ddo	4.250	1.09E-03	**Cdc6**	-1.558	5.48E-07
Notum	4.229	2.63E-05	**Bcat1**	-1.555	6.84E-03
Isg15	4.223	5.48E-03	**Cmss1**	-1.553	2.26E-07
Ifitm1	4.212	1.81E-02	**Acvr2b**	-1.549	5.93E-04
Sema3b	4.212	5.63E-33	**Ptger4**	-1.548	4.76E-02
Xirp1	4.211	1.49E-02	**Lyar**	-1.548	6.92E-08
Adgrg2	4.210	5.63E-33	**Tlx3**	-1.545	6.85E-05
A730020M07Rik	4.202	1.08E-02	**Rpia**	-1.542	5.87E-09
Car10	4.197	1.68E-04	**Dkc1**	-1.536	7.82E-07
2610027K06Rik	4.195	2.43E-02	**Megf6**	-1.534	9.78E-12
Ncan	4.185	1.23E-71	**Ung**	-1.533	1.60E-09
Faim2	4.183	1.59E-53	**Fam72a**	-1.529	4.61E-06
Svep1	4.178	8.19E-21	**Mcm2**	-1.529	6.67E-06
Hspb8	4.168	1.97E-11	**Orc1**	-1.527	5.80E-05
Lax1	4.159	1.03E-02	**Cxadr**	-1.526	1.98E-06
Npvf	4.149	1.03E-05	**Sh2b3**	-1.524	1.17E-12
Shh	4.147	3.28E-08	**Atg9b**	-1.521	6.84E-03
Gm38398	4.146	4.16E-02	**Hmgb2**	-1.520	1.45E-13

Genes (UP)	log2FoldChange	padj	Genes (Down)	log2FoldChange	padj
Tgtp2	4.099	8.14E-03	**Nr4a1**	-1.519	2.62E-09
Atp1b2	4.093	9.06E-29	**Kcng1**	-1.519	4.58E-06
Fgfr4	4.092	5.85E-09	**Rbfox3**	-1.519	2.60E-02
Hacd4	4.089	1.31E-16	**Gm42595**	-1.516	9.07E-04
Cntn5	4.083	4.06E-02	**Cdc25a**	-1.515	5.44E-09
Folh1	4.058	4.28E-02	**Dcc**	-1.512	1.34E-06
C4b	4.056	1.65E-06	**Myc**	-1.512	5.40E-10
Rpe65	4.043	2.49E-02	**Cdc7**	-1.508	8.80E-08
Gm47096	4.041	8.79E-03	**Gnl3**	-1.508	1.74E-04
Acox2	4.029	9.46E-04	**Ivns1abp**	-1.499	1.66E-10
Ndst3	4.027	1.41E-05	**Csgalnact1**	-1.496	5.82E-06
Chrdl2	4.023	1.30E-02	**Rcc1**	-1.496	5.08E-07
Pth1r	4.015	1.25E-20	**Whrn**	-1.494	6.60E-12
Sntb1	4.009	7.11E-39	**Nnat**	-1.490	1.55E-07
Gm36315	4.005	7.00E-04	**Vash1**	-1.490	1.16E-03
Col14a1	3.995	1.54E-04	**Cad**	-1.489	1.51E-07
Gsg1l	3.995	8.77E-06	**Liph**	-1.485	5.69E-03
Cyp4f14	3.991	4.53E-15	**Vrk1**	-1.484	2.95E-12
Parp10	3.990	1.54E-18	**4933415A04Rik**	-1.482	8.81E-03
Lgals3bp	3.984	5.10E-14	**Hectd2os**	-1.482	3.80E-02
Rgs8	3.979	2.51E-19	**Mybl2**	-1.482	3.27E-05
Pla2g5	3.970	7.23E-04	**Arhgap26**	-1.478	4.65E-05
Cend1	3.968	2.85E-21	**AI593442**	-1.476	3.27E-02
P4ha3	3.957	6.01E-03	**Recql4**	-1.475	1.58E-04
Scn4a	3.954	1.90E-02	**Hectd2**	-1.471	1.52E-05
Slc12a3	3.933	2.85E-03	**Wdhd1**	-1.469	2.99E-08
Ifit1bl2	3.922	3.11E-06	**Gjc1**	-1.468	5.91E-04
Kcnn2	3.922	2.00E-09	**Gins1**	-1.468	9.73E-08
Smad7	3.914	3.50E-45	**Mmp15**	-1.462	3.91E-05
Pappa	3.907	2.46E-03	**Chek1**	-1.462	2.18E-05
Ifit1bl1	3.897	1.33E-05	**Lmnb1**	-1.462	1.95E-14
Adra1d	3.893	7.50E-14	**Tox2**	-1.460	5.22E-03
Mfrp	3.884	1.81E-02	**Plk2**	-1.459	1.82E-05
Oxtr	3.883	3.12E-12	**Cdr2l**	-1.454	1.75E-11
Ecrg4	3.875	1.24E-43	**Lbr**	-1.453	2.04E-06
Gask1b	3.867	2.88E-04	**Lmnb2**	-1.452	4.98E-08
Atp6v0a4	3.866	2.46E-02	**Nab2**	-1.447	4.93E-06
Csmd1	3.865	4.89E-02	**Six2**	-1.443	1.88E-02
Nrxn3	3.857	4.18E-10	**Lypla2**	-1.442	1.74E-11
Phf11d	3.843	1.21E-05	**Dgkk**	-1.442	3.81E-02
Mfsd4b5	3.838	2.13E-02	**Kcnip1**	-1.437	1.01E-02
Id1	3.834	4.43E-23	**Hnrnpa3**	-1.436	2.44E-13
Irf7	3.817	5.25E-11	**Adcyap1r1**	-1.435	2.14E-02

Genes (UP)	log2FoldChange	padj	Genes (Down)	log2FoldChange	padj
Gm43674	3.813	1.20E-02	**Cdt1**	-1.433	1.62E-05
Papss2	3.803	8.96E-03	**Tmod1**	-1.432	1.78E-02
Sphk1	3.802	1.10E-14	**Ggct**	-1.430	1.20E-03
Gm11961	3.791	1.65E-02	**Lrrtm2**	-1.427	4.04E-03
Adamts2	3.778	1.96E-04	**Dyrk3**	-1.426	1.94E-04
Gm33027	3.774	2.58E-02	**Mcm10**	-1.426	5.46E-05
Plaat1	3.773	4.32E-05	**Pvt1**	-1.425	4.51E-06
Irgm2	3.760	2.71E-08	**Gpatch4**	-1.423	8.53E-05
Fgf9	3.747	3.65E-02	**Chaf1b**	-1.420	5.22E-07
A330048O09Rik	3.739	3.72E-03	**Ovgp1**	-1.419	3.99E-03
F630040K05Rik	3.734	1.17E-02	**Bin1**	-1.417	1.11E-10
Rhbg	3.728	8.61E-03	**Gm28229**	-1.417	4.34E-02
Masp1	3.728	3.92E-15	**Ptpn5**	-1.416	2.00E-02
Kcna4	3.724	2.04E-06	**Pak6**	-1.414	2.37E-05
Id4	3.715	8.44E-26	**Polr1b**	-1.413	7.86E-07
Chst8	3.710	2.55E-09	**Gabra2**	-1.413	1.57E-03
Pappa2	3.697	6.02E-03	**Pdzrn4**	-1.411	3.61E-02
Fmo1	3.679	1.59E-06	**Ing5**	-1.410	1.81E-05
Calr4	3.675	6.84E-03	**Rnf122**	-1.409	2.14E-04
Bmp4	3.666	3.10E-04	**Esrrb**	-1.408	1.99E-02
Gm19522	3.663	2.39E-02	**Hells**	-1.406	3.04E-05
Dock2	3.663	2.96E-02	**Cdca7**	-1.404	9.58E-11
Crlf1	3.661	1.53E-06	**Pold1**	-1.403	1.13E-07
Clu	3.643	9.05E-13	**Insm1**	-1.403	6.48E-06
Vgll3	3.632	2.49E-03	**Depdc1b**	-1.401	9.16E-07
Gm13293	3.630	9.84E-04	**Btbd11**	-1.400	3.33E-07
Hmcn2	3.630	5.42E-04	**Iqgap2**	-1.399	1.53E-06
Gm9939	3.626	4.03E-02	**Mpp3**	-1.398	9.83E-03
Angptl4	3.621	5.63E-03	**Hk2**	-1.397	1.19E-03
Dock5	3.616	7.87E-10	**3110082I17Rik**	-1.390	3.60E-04
E130310I04Rik	3.615	2.57E-02	**Grwd1**	-1.390	2.29E-05
Scg2	3.611	1.66E-22	**Sdad1**	-1.389	3.60E-05
D630023F18Rik	3.611	1.85E-03	**Calcrl**	-1.389	1.93E-03
Gm12108	3.598	8.35E-06	**Gar1**	-1.385	5.42E-07
Ppp3r2	3.595	1.58E-03	**Fblim1**	-1.385	7.42E-03
Traf1	3.590	3.74E-02	**Nop56**	-1.385	2.03E-04
Cav1	3.586	2.00E-37	**Arap2**	-1.384	6.96E-03
Adamtsl3	3.585	6.82E-18	**St8sia1**	-1.382	2.42E-06
Ttc22	3.583	2.26E-02	**Ercc8**	-1.382	4.29E-07
A930012L18Rik	3.576	3.00E-02	**Nol9**	-1.379	2.45E-07
Timp4	3.575	5.91E-13	**Ccnb1ip1**	-1.378	3.84E-02
Art3	3.571	2.03E-05	**Fbxo5**	-1.375	7.13E-06
Col4a3	3.570	1.15E-02	**Ybx3**	-1.375	1.58E-10

Genes (UP)	log2FoldChange	padj	Genes (Down)	log2FoldChange	padj
Cemip	3.569	9.02E-15	**Wdr90**	-1.374	4.01E-09
Parp14	3.565	3.88E-13	**Thg1l**	-1.374	3.77E-04
Lcn2	3.557	2.91E-02	**Tle2**	-1.373	5.42E-07
6530411M01Rik	3.555	1.26E-08	**Csrnp3**	-1.370	2.84E-04
Tulp2	3.553	4.04E-02	**Phlda1**	-1.370	9.87E-07
Aldh1a7	3.549	3.63E-12	**Espl1**	-1.367	2.31E-06
2900072N19Rik	3.541	2.74E-02	**Exo1**	-1.366	3.35E-06
Dlk1	3.534	9.59E-03	**Kti12**	-1.365	2.18E-07
Pygm	3.529	1.18E-02	**Lancl3**	-1.364	8.03E-04
Crtac1	3.524	2.70E-04	**Npm3**	-1.364	8.23E-07
Hist2h2ac	3.524	5.80E-03	**C530008M17Rik**	-1.364	6.73E-07
Tap1	3.513	1.96E-06	**1110038B12Rik**	-1.364	2.26E-04
4932438H23Rik	3.511	8.20E-06	**Aunip**	-1.363	2.59E-05
Cnmd	3.510	1.40E-02	**Ptgfr**	-1.363	1.14E-02
Gm46614	3.473	3.25E-02	**Wdr55**	-1.361	3.02E-06
Draxin	3.467	4.07E-40	**2610318N02Rik**	-1.360	3.35E-03
Pstpip1	3.460	1.52E-23	**Pdss1**	-1.360	1.74E-05
Dipk1c	3.459	8.53E-05	**Kcnj2**	-1.358	3.62E-02
Wnt5b	3.457	7.46E-14	**Slc6a11**	-1.357	1.19E-02
Hs3st3a1	3.450	1.26E-10	**Slc29a4**	-1.356	5.56E-06
Slc14a1	3.439	3.54E-05	**BC030867**	-1.356	8.92E-06
Trim29	3.438	3.32E-02	**Trip13**	-1.355	7.43E-04
Klhl30	3.436	3.41E-11	**Pimreg**	-1.350	8.75E-05
Insyn2b	3.430	4.88E-04	**Znrf2**	-1.350	8.48E-09
Igf2	3.424	2.11E-13	**BC055324**	-1.350	3.78E-07
Wdr72	3.423	1.34E-03	**Srpk3**	-1.349	3.97E-02
Cldn19	3.413	9.27E-06	**Snhg17**	-1.348	6.03E-05
Bhlhe41	3.412	2.84E-17	**Sox11**	-1.347	6.51E-10
S100a6	3.410	1.51E-11	**Slc4a7**	-1.346	9.20E-09
Cyp1b1	3.405	6.73E-10	**Nemp1**	-1.345	3.05E-08
Abca9	3.401	3.46E-11	**Olfml3**	-1.344	1.06E-04
Dmrtc1a	3.395	1.94E-02	**Ttc39aos1**	-1.344	1.18E-02
Mroh7	3.385	4.11E-02	**Gm16638**	-1.339	2.31E-03
Gm15222	3.377	1.50E-02	**Pou3f2**	-1.339	1.34E-03
Car5b	3.371	4.03E-31	**Hirip3**	-1.339	3.48E-05
Cyp2b13	3.363	4.77E-02	**Fbln2**	-1.338	1.24E-09
Gbgt1	3.358	1.08E-02	**Smtn**	-1.335	2.30E-03
AB124611	3.357	2.01E-02	**1700019D03Rik**	-1.334	2.27E-03
Rtp4	3.357	1.03E-05	**Npr1**	-1.333	2.79E-04
Rassf4	3.357	2.51E-02	**Mcm7**	-1.332	2.51E-06
Aqp5	3.355	5.76E-05	**E2f8**	-1.332	5.21E-06
Iapp	3.353	2.34E-02	**Zyx**	-1.325	1.00E-10
Gcnt1	3.348	1.63E-07	**Gm10791**	-1.324	7.61E-03

Genes (UP)	log2FoldChange	padj	Genes (Down)	log2FoldChange	padj
Miat	3.348	2.45E-05	**Mgat5b**	-1.324	4.19E-02
Fbln5	3.347	9.34E-09	**Ddx11**	-1.322	9.18E-07
Ppp2r2b	3.346	6.69E-03	**Gm49774**	-1.319	2.86E-02
Lgi4	3.346	1.30E-03	**Ankle1**	-1.319	1.77E-06
A330033J07Rik	3.344	6.66E-03	**Birc5**	-1.318	2.09E-05
Fgf2	3.342	2.87E-16	**Vars**	-1.317	3.60E-05
Parm1	3.328	2.68E-22	**Nolc1**	-1.316	1.07E-06
Entpd2	3.325	3.04E-03	**Mcm3**	-1.315	1.24E-08
Cyp4v3	3.324	3.70E-22	**Rpusd2**	-1.313	1.53E-05
Wnt8b	3.323	2.67E-02	**Fbl**	-1.312	5.29E-05
Tmem108	3.322	1.10E-16	**Nhp2**	-1.311	1.92E-05
Rcsd1	3.319	4.43E-03	**Olig2**	-1.310	6.38E-04
S100b	3.307	3.06E-10	**Syp**	-1.307	3.90E-02
Sdsl	3.306	8.20E-03	**Dusp6**	-1.307	5.29E-05
Trim12a	3.304	3.86E-03	**Rnf225**	-1.306	5.32E-03
Nrcam	3.304	2.48E-45	**Gm17491**	-1.306	8.60E-03
Baalc	3.302	4.98E-15	**Taf5**	-1.306	1.95E-06
Mgll	3.302	4.36E-03	**Elavl2**	-1.305	3.93E-05
Insyn2a	3.296	4.69E-06	**Ier2**	-1.304	1.61E-07
Gm31135	3.295	1.89E-02	**Tnik**	-1.304	2.17E-05
Cd200	3.287	1.43E-13	**Nt5dc2**	-1.303	4.35E-10
Clstn3	3.285	2.63E-08	**Nup205**	-1.299	2.94E-04
AC109619.1	3.281	9.83E-03	**Adamts20**	-1.299	1.73E-02
Tacr1	3.276	1.06E-02	**Tcof1**	-1.298	9.90E-05
Hephl1	3.275	2.88E-03	**Lrr1**	-1.298	2.37E-03
Pdk4	3.265	5.32E-10	**Esm1**	-1.298	4.63E-02
Kpna7	3.265	5.64E-03	**Itga8**	-1.297	4.40E-10
Prph	3.263	6.81E-10	**Slc25a24**	-1.296	6.34E-05
Samd9l	3.255	3.22E-14	**Mybbp1a**	-1.294	1.32E-04
Alx4	3.244	9.97E-12	**Ppat**	-1.293	4.41E-07
Pcp4	3.241	1.99E-06	**Zfhx2**	-1.293	2.91E-04
Plxdc2	3.236	7.34E-13	**Sep-03**	-1.292	6.89E-09
Hspb7	3.233	8.43E-03	**Rpp40**	-1.286	2.32E-03
Srgn	3.228	4.28E-02	**Mcm5**	-1.284	4.23E-07
4932435O22Rik	3.217	3.52E-02	**Noc2l**	-1.281	9.78E-06
Fam83h	3.215	4.07E-02	**3010003L21Rik**	-1.280	2.65E-02
Armh1	3.213	1.53E-02	**Slc35g1**	-1.276	8.28E-04
Nat1	3.211	3.16E-02	**Mrps27**	-1.276	5.20E-07
Atp2b3	3.210	4.01E-02	**Wdr76**	-1.272	1.09E-05
Ccn1	3.209	2.01E-03	**Lig1**	-1.270	3.19E-07
Gucy1a1	3.204	3.97E-10	**Exosc8**	-1.270	2.84E-04
Smim1	3.202	7.56E-09	**Ddx21**	-1.266	1.95E-04
C030014I23Rik	3.199	3.14E-03	**Nop16**	-1.266	1.12E-03

Genes (UP)	log2FoldChange	padj	Genes (Down)	log2FoldChange	padj
Bfsp2	3.195	2.59E-05	**Usp31**	-1.266	4.99E-06
Bcam	3.195	8.72E-27	**Atad5**	-1.264	1.76E-05
Col12a1	3.191	5.25E-03	**Prr22**	-1.263	2.30E-02
Ccn2	3.182	2.99E-16	**Ptma**	-1.262	2.98E-07
Sema3f	3.181	1.29E-19	**Mpped2**	-1.260	1.87E-07
Chodl	3.181	1.25E-08	**Fam169a**	-1.260	1.11E-03
Slfn8	3.176	3.45E-03	**Faah**	-1.259	7.19E-06
Ackr4	3.173	1.29E-10	**Ppan**	-1.259	1.29E-05
D730045B01Rik	3.158	1.18E-05	**Duxbl1**	-1.259	4.78E-02
C1rl	3.152	1.15E-09	**Dact2**	-1.258	4.33E-02
Cd36	3.152	8.73E-07	**Dnmt3b**	-1.257	1.90E-03
Adra2a	3.152	8.85E-04	**Ttk**	-1.256	3.36E-05
Agt	3.150	1.09E-07	**Ntng1**	-1.255	1.20E-03
S100a4	3.137	4.26E-07	**C1qbp**	-1.255	5.29E-06
Hes7	3.137	3.12E-04	**Dnmt1**	-1.255	9.93E-08
Zfp185	3.137	5.16E-04	**Osr2**	-1.254	2.71E-02
Hopx	3.131	1.25E-26	**Clcn5**	-1.253	6.77E-09
Kcnab1	3.127	4.13E-04	**Gprin1**	-1.252	3.38E-07
Col8a2	3.124	4.25E-02	**Nasp**	-1.251	1.06E-09
Itga11	3.124	1.19E-04	**Gm21887**	-1.250	7.72E-06
4930599N23Rik	3.123	3.04E-02	**Npm1**	-1.249	1.89E-04
Jph2	3.121	9.92E-03	**Arhgef39**	-1.249	6.07E-04
1700112J16Rik	3.117	4.18E-02	**Tgfbi**	-1.246	6.01E-03
Postn	3.115	2.47E-11	**Ccnf**	-1.245	6.96E-07
Fibin	3.113	3.02E-02	**Slc16a2**	-1.240	3.18E-08
Dmp1	3.110	9.57E-04	**Ttll4**	-1.239	1.60E-05
Angpt1	3.105	5.90E-31	**Sars2**	-1.239	1.65E-07
Mt2	3.098	1.43E-05	**Nop58**	-1.238	2.60E-04
Islr2	3.096	2.89E-09	**Rrp12**	-1.237	1.31E-03
2610300M13Rik	3.090	5.72E-08	**Blm**	-1.236	3.44E-05
Mar-03	3.083	1.81E-09	**Nup43**	-1.235	3.22E-04
Lrrc2	3.082	3.75E-03	**Ddx39**	-1.234	6.56E-04
Lbp	3.082	2.35E-05	**Taf1d**	-1.234	4.21E-04
Itih3	3.080	7.54E-04	**Bcar3**	-1.234	1.26E-06
Clec2d	3.077	7.47E-05	**Mdn1**	-1.233	5.08E-04
Pdgfrb	3.070	2.13E-22	**Rbm38**	-1.233	3.04E-07
Rapsn	3.069	3.12E-03	**Fam111a**	-1.232	5.39E-04
Gpr153	3.067	2.23E-13	**Nup107**	-1.229	9.00E-05
Kcne1l	3.055	4.86E-02	**Ube2cbp**	-1.228	2.25E-03
Chdh	3.053	1.85E-03	**Gcat**	-1.226	2.41E-09
Cadm3	3.048	6.09E-04	**Gm49322**	-1.225	4.76E-02
D630003M21Rik	3.047	9.68E-14	**Gm47283**	-1.224	3.68E-05
Pea15a	3.045	5.24E-69	**Baz1a**	-1.223	3.96E-05

Genes (UP)	log2FoldChange	padj	Genes (Down)	log2FoldChange	padj
Cd59a	3.043	3.06E-04	**Gen1**	-1.222	2.84E-04
Col1a2	3.040	1.39E-11	**Timeless**	-1.222	1.75E-06
Thy1	3.037	3.30E-10	**Ccnyl1**	-1.222	1.76E-02
C230024C17Rik	3.036	2.24E-02	**Hnrnpab**	-1.222	1.38E-06
C1s1	3.033	4.05E-08	**Xylb**	-1.221	4.23E-03
Msx2	3.032	1.12E-09	**Zfp773**	-1.220	2.15E-02
Man1c1	3.031	7.39E-33	**Trim9**	-1.218	1.93E-02
Apoe	3.029	2.47E-09	**Dock10**	-1.217	2.79E-09
Gm12925	3.029	2.02E-03	**Stambpl1**	-1.217	1.57E-03
Spock2	3.025	1.98E-07	**Arhgap19**	-1.216	2.10E-08
Pitpnm3	3.022	3.97E-07	**Mtf2**	-1.216	7.49E-07
Fn1	3.021	6.69E-03	**Kcnj16**	-1.215	1.23E-03
Hspb2	3.020	9.87E-03	**Naa16**	-1.215	4.97E-07
Matn4	3.018	7.96E-05	**Paqr9**	-1.215	1.77E-03
Aqp1	3.018	5.27E-08	**Ccdc184**	-1.213	1.79E-04
Hapln2	3.017	3.02E-03	**Trub1**	-1.213	1.73E-06
Tmem132b	3.013	4.41E-04	**Magohb**	-1.211	1.17E-03
Sstr2	3.013	1.52E-09	**5430416N02Rik**	-1.209	8.54E-04
Prrx2	3.011	1.66E-03	**Hmcn1**	-1.209	3.01E-02
Ppef1	3.010	8.06E-03	**Kif11**	-1.208	3.42E-07
Ush1g	3.009	1.15E-02	**Dpf1**	-1.207	3.26E-06
Parp9	3.007	1.16E-07	**Armcx4**	-1.207	1.32E-07
Slc39a12	3.004	2.17E-03	**E2f7**	-1.207	3.72E-04
Adam23	3.001	5.39E-10	**Gemin5**	-1.205	2.30E-05
Gm47414	2.999	1.79E-02	**Chd7**	-1.203	2.08E-05
Txnip	2.998	6.10E-16	**Gas1**	-1.203	2.76E-06
Gm41492	2.996	2.44E-02	**Gm50322**	-1.200	1.43E-02
Hmgcll1	2.988	3.04E-03	**Cdc45**	-1.198	5.69E-04
9530082P21Rik	2.988	6.17E-05	**Mroh2a**	-1.196	2.16E-04
Psmb8	2.987	8.51E-03	**Cenpv**	-1.195	1.82E-05
Rgs9	2.984	3.66E-21	**Nup85**	-1.195	5.06E-06
Cib3	2.984	3.85E-02	**Aoc2**	-1.194	1.41E-03
Ifi35	2.983	1.02E-09	**Rpf2**	-1.192	9.71E-08
Cytip	2.982	1.40E-02	**Epn2**	-1.191	2.66E-04
Pde11a	2.981	1.46E-06	**Nkain2**	-1.190	3.25E-02
Eepd1	2.981	3.43E-11	**Dut**	-1.188	9.42E-05
Mia	2.976	1.30E-04	**Panx1**	-1.187	6.34E-04
Slc7a2	2.976	2.09E-28	**Rif1**	-1.186	1.19E-04
Kank1	2.974	1.26E-35	**Cntnap4**	-1.184	4.74E-02
Necab1	2.973	4.33E-04	**Kcnab3**	-1.184	1.01E-03
Cyp24a1	2.972	2.60E-02	**Cdr2**	-1.183	8.43E-07
Casp4	2.965	1.05E-02	**Tube1**	-1.183	1.07E-04
Ogn	2.963	6.90E-10	**Umps**	-1.182	4.11E-06

Genes (UP)	log2FoldChange	padj	Genes (Down)	log2FoldChange	padj
Gm20743	2.961	2.70E-03	**Aurkb**	-1.181	1.41E-04
Fstl5	2.955	2.52E-03	**Gk5**	-1.181	6.79E-03
Cst3	2.947	3.64E-24	**Coro1c**	-1.181	2.09E-08
A730049H05Rik	2.942	4.01E-04	**Heatr1**	-1.180	2.44E-04
Gpr88	2.941	1.23E-09	**Mast1**	-1.180	4.28E-02
Ak5	2.939	1.35E-11	**Prmt7**	-1.180	1.78E-05
Klkb1	2.934	3.41E-02	**Zmynd19**	-1.180	1.52E-04
Serping1	2.932	1.65E-04	**Mrto4**	-1.179	4.72E-05
Fkbp1b	2.931	2.28E-04	**Kif15**	-1.177	9.37E-05
4632428C04Rik	2.931	1.19E-02	**Prkcq**	-1.174	3.82E-04
Grin3a	2.925	6.07E-19	**H2afz**	-1.174	1.12E-09
Abca1	2.919	1.51E-02	**Ercc6l**	-1.173	9.71E-05
Trpv2	2.914	7.14E-05	**Brca2**	-1.173	3.23E-05
Gm29695	2.910	1.43E-03	**Pclaf**	-1.172	2.99E-06
Cp	2.910	1.07E-13	**Lsm2**	-1.172	5.69E-07
Gm6277	2.906	7.59E-04	**Yars2**	-1.171	3.12E-04
Ldlrad4	2.903	2.00E-05	**Mtfr2**	-1.170	9.89E-04
Gm16793	2.903	4.67E-02	**Prmt1**	-1.170	5.52E-06
Alpl	2.901	3.63E-12	**Tex30**	-1.169	3.20E-04
Nacc2	2.900	1.22E-26	**Rfc4**	-1.168	3.10E-05
Plxna4	2.900	1.23E-26	**Wscd1**	-1.166	4.74E-05
Myl4	2.892	1.52E-09	**Pole**	-1.166	4.15E-05
Abca13	2.890	1.95E-06	**Melk**	-1.166	1.55E-04
Spon2	2.889	1.87E-06	**Prim1**	-1.165	5.32E-05
Wnt9a	2.889	2.83E-03	**Exosc1**	-1.165	4.38E-05
Ahnak	2.888	1.36E-17	**Plekha1**	-1.164	3.43E-06
Ankrd34a	2.886	1.64E-09	**Fam102b**	-1.162	3.56E-05
Mkln1os	2.885	5.18E-05	**Kif14**	-1.162	8.83E-05
Coq8a	2.883	2.59E-05	**Rrp15**	-1.161	3.23E-04
Slc25a48	2.882	2.18E-06	**Mis18a**	-1.160	1.67E-05
Cys1	2.882	1.56E-05	**Mrps18b**	-1.159	3.74E-04
Gm15411	2.878	2.52E-02	**Cnpy1**	-1.158	1.04E-03
Dbp	2.874	1.67E-10	**Cth**	-1.154	1.39E-02
B230206L02Rik	2.873	2.43E-02	**Smyd2**	-1.154	3.72E-05
Lgals9	2.870	3.44E-11	**Nsl1**	-1.154	1.80E-04
Selenom	2.868	1.77E-18	**Neil3**	-1.153	1.47E-03
Nebl	2.867	8.61E-06	**Dhfr**	-1.151	2.42E-04
Uba7	2.865	2.87E-04	**Trim27**	-1.151	3.75E-07
Arhgef33	2.865	5.52E-08	**Gfpt2**	-1.150	1.57E-03
Mfap5	2.863	8.63E-07	**Sapcd2**	-1.150	3.42E-03
Aass	2.862	1.50E-04	**Eif1a**	-1.149	5.87E-03
Mmp19	2.861	6.06E-13	**Skp2**	-1.148	5.58E-08
9430041J12Rik	2.858	4.16E-02	**Dach1**	-1.148	3.43E-02

Genes (UP)	log2FoldChange	padj	Genes (Down)	log2FoldChange	padj
Sugct	2.858	8.76E-04	**Mak16**	-1.147	1.16E-05
Gadd45b	2.857	5.02E-21	**Igfbp4**	-1.146	3.07E-04
Rab27b	2.856	9.45E-05	**Lsm7**	-1.145	6.87E-04
Ldhd	2.849	3.60E-04	**Tha1**	-1.144	2.10E-02
Ccdc3	2.844	4.55E-05	**Mettl1**	-1.144	1.33E-02
Gm20544	2.842	4.60E-03	**Tmpo**	-1.143	8.24E-07
Col5a2	2.839	4.42E-03	**Ppp1r2**	-1.143	2.25E-07
Ttyh1	2.838	3.23E-20	**Mthfd2**	-1.143	9.23E-03
Cdh11	2.836	6.60E-16	**Mthfd1l**	-1.142	1.90E-03
Gpr179	2.833	5.38E-18	**Spty2d1**	-1.142	6.92E-08
Plin5	2.827	2.65E-02	**H2afy**	-1.141	5.24E-10
Axl	2.826	1.12E-35	**Mis18bp1**	-1.139	1.02E-04
Oit3	2.818	7.46E-03	**Tma16**	-1.138	8.19E-04
Gm15743	2.812	1.43E-02	**Ebna1bp2**	-1.138	2.34E-04
Gm26512	2.811	2.33E-02	**Pold3**	-1.138	2.43E-07
Nxph4	2.810	5.00E-06	**Cacna1b**	-1.137	5.65E-06
Cyp46a1	2.806	3.37E-11	**Nob1**	-1.137	8.84E-07
Fmo5	2.805	4.34E-06	**Mcm6**	-1.136	2.94E-05
Casp12	2.804	1.66E-14	**Serpini1**	-1.136	1.20E-03
Ddx58	2.803	6.56E-14	**Gm41442**	-1.135	3.11E-02
Rassf10	2.802	5.55E-03	**Pwp2**	-1.133	1.55E-04
Tmem217	2.792	3.54E-02	**Tbrg4**	-1.133	4.33E-06
Mmp28	2.781	3.31E-10	**Tk1**	-1.133	1.09E-03
Ckmt1	2.781	3.80E-03	**Haspin**	-1.132	6.14E-04
Xdh	2.779	1.10E-06	**Eya1**	-1.132	1.98E-02
Loxl3	2.777	3.23E-06	**Ddx20**	-1.131	7.23E-05
Atxn1	2.765	2.07E-10	**Ranbp1**	-1.131	7.02E-04
Pcsk6	2.764	2.67E-27	**Rad54l**	-1.128	4.55E-06
Atp2b4	2.758	2.81E-17	**Pus1**	-1.128	1.70E-05
Itga3	2.756	1.16E-29	**Pif1**	-1.127	5.03E-04
Slc24a3	2.755	1.08E-33	**Plk4**	-1.127	7.64E-04
Fgf7	2.753	3.87E-03	**Gm37422**	-1.126	9.61E-04
Psmb9	2.750	2.00E-02	**Rrm2**	-1.126	1.75E-04
Tap2	2.749	1.66E-05	**Dtl**	-1.125	2.74E-04
Ssc5d	2.748	2.66E-11	**Ruvbl2**	-1.124	7.92E-05
Dtx3l	2.745	4.38E-05	**Magi1**	-1.124	1.46E-06
Fam129b	2.744	2.81E-22	**Rtn2**	-1.124	1.51E-06
Tapbp	2.735	6.34E-36	**Wdr46**	-1.123	2.90E-05
Dlx5	2.732	1.58E-03	**4931428F04Rik**	-1.123	1.85E-05
Slc41a3	2.731	3.90E-15	**Ankrd13b**	-1.123	1.32E-06
Rnd1	2.729	6.35E-06	**Arid3b**	-1.122	1.55E-02
Trpm3	2.726	1.12E-13	**Qtrt2**	-1.118	2.49E-04
Nuak1	2.723	8.95E-11	**Kif2c**	-1.118	2.54E-04

Genes (UP)	log2FoldChange	padj	Genes (Down)	log2FoldChange	padj
Ecm1	2.723	1.15E-17	**Slc29a2**	-1.117	1.63E-03
Gm35721	2.721	2.22E-02	**Ube2c**	-1.117	1.13E-03
Lynx1	2.711	2.45E-28	**Rnaseh2a**	-1.116	2.45E-05
Plppr4	2.710	5.35E-05	**Rsl1d1**	-1.115	6.60E-05
Irf5	2.704	2.71E-02	**Wdr43**	-1.115	8.66E-04
Lypd1	2.703	2.85E-02	**Stil**	-1.115	6.90E-04
Ifi204	2.700	4.66E-03	**Slc10a7**	-1.114	9.21E-06
Adamtsl5	2.699	2.40E-07	**Trmt61a**	-1.114	2.96E-04
Loxl1	2.691	1.57E-06	**Schip1**	-1.113	4.67E-07
Fgfr3	2.683	4.77E-02	**Grasp**	-1.113	1.26E-03
Duoxa1	2.672	8.44E-03	**Mex3a**	-1.110	1.79E-05
Tbx2	2.665	5.08E-07	**Gm20667**	-1.110	1.08E-02
Chadl	2.662	5.04E-15	**Slc1a5**	-1.110	1.70E-02
Scube1	2.659	8.49E-11	**Ccnb1**	-1.110	8.41E-04
Dkk3	2.657	2.14E-09	**Nsun2**	-1.110	1.17E-03
Astn2	2.655	2.85E-08	**Nfil3**	-1.109	1.17E-02
Efcab12	2.646	7.13E-04	**Cenpu**	-1.108	9.62E-04
Gstm2	2.645	2.84E-10	**Exosc2**	-1.108	4.11E-04
Sorbs1	2.644	1.10E-16	**Mms22l**	-1.107	6.48E-04
C1ra	2.639	1.17E-09	**Ddx51**	-1.106	9.61E-06
Ifi27	2.637	3.83E-09	**Polq**	-1.105	2.58E-04
Epas1	2.636	9.39E-11	**Mtap**	-1.105	4.73E-03
Gm20597	2.635	2.24E-02	**Alkbh1**	-1.105	1.25E-04
Cygb	2.635	1.06E-04	**Wdr75**	-1.104	1.55E-04
Myo1d	2.633	5.47E-11	**Eldr**	-1.104	7.27E-03
Slc4a10	2.631	1.47E-03	**Lsm8**	-1.102	2.62E-04
Daam2	2.631	4.28E-14	**Fbxo48**	-1.102	2.01E-02
Tuba8	2.628	2.47E-03	**Rad51c**	-1.101	1.66E-04
Lrrc75a	2.627	2.59E-20	**Epb41l4aos**	-1.100	1.76E-02
Paqr8	2.624	8.82E-08	**Il6ra**	-1.100	1.06E-03
Susd2	2.622	4.22E-07	**Ran**	-1.099	3.60E-04
Gpc4	2.618	1.11E-17	**Pold2**	-1.098	6.52E-05
Ramp1	2.607	6.33E-17	**Pprc1**	-1.097	2.97E-04
Csf1	2.603	8.95E-10	**Nrm**	-1.097	2.40E-05
Nedd9	2.602	9.31E-22	**Pak1**	-1.097	1.54E-03
Flrt1	2.602	6.93E-09	**Pa2g4**	-1.095	1.36E-04
Kctd4	2.602	2.04E-03	**Arl5b**	-1.095	2.12E-04
Gna14	2.602	1.06E-04	**Srsf7**	-1.094	7.20E-07
Aqp11	2.601	1.97E-07	**Cdca4**	-1.093	3.40E-03
1110032F04Rik	2.596	7.33E-04	**Dhodh**	-1.093	2.08E-04
Vasn	2.593	8.27E-26	**Naaladl1**	-1.092	8.58E-03
Casq2	2.593	7.22E-04	**Snhg12**	-1.091	1.43E-02
Synpo2	2.592	2.13E-07	**Kbtbd8**	-1.091	8.15E-05

Genes (UP)	log2FoldChange	padj	Genes (Down)	log2FoldChange	padj
Vwa1	2.587	8.41E-11	**Cpsf4**	-1.089	2.75E-05
Sema6b	2.583	3.05E-25	**Utp20**	-1.089	4.87E-03
Hpx	2.578	1.69E-04	**Incenp**	-1.089	1.92E-05
Hcfc1r1	2.578	6.26E-30	**Fam118a**	-1.087	1.59E-06
Ak1	2.574	3.61E-17	**Palb2**	-1.087	1.22E-03
Pdk2	2.574	2.09E-08	**Kdm2b**	-1.085	1.61E-07
1700020L24Rik	2.572	1.26E-06	**Tgfbr1**	-1.085	9.59E-07
Pygb	2.571	6.42E-15	**Wdr77**	-1.085	2.51E-04
Fas	2.569	8.20E-05	**Lsm11**	-1.085	7.51E-07
Nfasc	2.567	3.13E-07	**Net1**	-1.085	4.08E-05
Rp1l1	2.565	1.79E-02	**Upp1**	-1.084	5.04E-04
Nipal3	2.563	1.98E-08	**Map4k3**	-1.084	1.00E-05
Mylk3	2.563	2.07E-03	**Snrpd1**	-1.084	1.08E-04
Tmem151a	2.563	3.35E-02	**Polr1a**	-1.082	2.32E-04
Phyhipl	2.563	2.95E-26	**Ebf1**	-1.082	1.19E-02
Stat1	2.560	9.16E-08	**Ears2**	-1.081	1.48E-03
Calml4	2.558	1.90E-03	**Dusp10**	-1.081	4.68E-03
Rorc	2.556	3.20E-04	**Iffo2**	-1.080	2.86E-03
Kcnq4	2.551	1.06E-05	**Ezh2**	-1.080	4.05E-04
Fhdc1	2.550	2.05E-10	**Knl1**	-1.079	3.69E-04
Ccdc85a	2.548	4.46E-18	**Hecw2**	-1.079	1.12E-03
Gm45495	2.542	4.86E-03	**Dnph1**	-1.078	1.12E-03
Shisa9	2.541	3.28E-04	**Cep135**	-1.078	4.57E-05
Tmem119	2.541	2.40E-04	**Noc4l**	-1.078	2.90E-04
Eml2	2.540	1.79E-03	**Rgs7**	-1.078	1.53E-02
Cpxm2	2.536	5.01E-12	**Slc27a6**	-1.077	1.71E-02
Itga1	2.536	5.45E-08	**Ddx18**	-1.077	1.16E-04
Unc5c	2.535	1.42E-11	**Igsf9**	-1.076	5.59E-03
Slco1a5	2.534	4.03E-02	**Dimt1**	-1.075	2.92E-03
Cadm2	2.531	8.54E-08	**Hmgn5**	-1.075	4.71E-05
Adra2c	2.530	1.22E-03	**Egfr**	-1.073	6.27E-03
Wnt4	2.526	5.73E-03	**Pola2**	-1.073	1.52E-07
Gm11613	2.522	2.55E-05	**Rbm19**	-1.072	4.39E-05
Myl9	2.521	1.46E-06	**Faxc**	-1.072	7.39E-06
Gm49165	2.517	1.03E-03	**Epop**	-1.072	6.73E-05
Abhd3	2.509	9.61E-06	**Gga2**	-1.071	1.45E-05
Dlx6	2.506	6.85E-04	**Selenoh**	-1.071	3.27E-08
Aldoc	2.501	3.91E-25	**Ncapg**	-1.070	1.40E-04
Isg20	2.497	2.44E-03	**Tnfaip6**	-1.069	1.43E-05
Col8a1	2.496	1.05E-06	**Pole2**	-1.069	1.54E-04
Kcnh5	2.496	1.45E-02	**Gm35040**	-1.067	6.02E-03
Fam131c	2.495	2.80E-02	**Slc38a4**	-1.067	1.99E-02
Apcdd1	2.491	1.47E-12	**Seh1l**	-1.067	2.15E-08

Genes (UP)	log2FoldChange	padj	Genes (Down)	log2FoldChange	padj
Cbln3	2.489	1.13E-07	**Cdca7l**	-1.065	4.02E-04
Psd2	2.485	7.94E-06	**Ftsj3**	-1.065	1.72E-03
Cdkl2	2.481	6.19E-08	**B3gnt5**	-1.065	3.38E-05
Fndc5	2.480	3.22E-04	**Adat1**	-1.064	1.25E-03
Reln	2.477	4.24E-07	**Zfp566**	-1.064	2.42E-02
1810021B22Rik	2.475	2.88E-03	**Efhd2**	-1.063	9.38E-04
Naaladl2	2.474	6.19E-06	**Cdca5**	-1.063	7.31E-04
Pltp	2.473	5.62E-05	**Inpp4b**	-1.062	3.91E-02
Grid2	2.461	7.85E-17	**Ccp110**	-1.061	4.65E-06
Mrvi1	2.461	1.00E-02	**C77080**	-1.059	6.96E-07
Kazald1	2.458	1.20E-04	**Fsd1l**	-1.059	6.63E-04
Cyp26b1	2.458	8.74E-12	**Adamts6**	-1.059	5.72E-04
Parp12	2.455	8.79E-07	**Arv1**	-1.058	2.30E-02
Snta1	2.454	5.19E-14	**Atad2**	-1.058	2.35E-04
Hgf	2.451	2.05E-02	**Clspn**	-1.058	5.80E-04
Clec18a	2.451	1.07E-03	**Mapk12**	-1.057	8.97E-04
Hspb1	2.447	7.47E-09	**Smc2**	-1.057	6.09E-05
Fmnl1	2.444	1.36E-10	**Msh6**	-1.057	1.85E-05
Tnr	2.444	1.90E-05	**Eif2b3**	-1.057	1.06E-03
Prkca	2.442	1.13E-17	**Eme1**	-1.057	7.69E-03
Kcna6	2.440	4.49E-09	**Ttc7b**	-1.056	2.70E-03
Steap4	2.440	4.22E-02	**Slc19a2**	-1.055	4.65E-04
Ccn4	2.440	1.51E-06	**Pdxp**	-1.054	2.10E-04
Timp3	2.435	5.32E-06	**Bora**	-1.054	7.43E-04
Samd5	2.433	3.13E-14	**Set**	-1.053	1.10E-04
Epha4	2.432	1.58E-07	**Lif**	-1.053	2.03E-02
Tnfrsf11b	2.428	3.66E-02	**Rbmxl1**	-1.053	1.13E-06
Tceal3	2.428	6.65E-12	**Rbp1**	-1.052	9.32E-05
Cacna1g	2.424	1.83E-29	**Shq1**	-1.052	2.52E-04
Hepacam	2.423	1.50E-16	**Rad51ap1**	-1.052	3.07E-05
Tmem53	2.420	4.46E-04	**Chn1**	-1.052	1.51E-05
Irgm1	2.417	1.47E-04	**Ncapg2**	-1.052	4.79E-05
Grik4	2.412	6.78E-14	**Cttnbp2nl**	-1.051	8.82E-04
S100a11	2.410	6.84E-08	**Polr3k**	-1.049	1.90E-07
Vstm4	2.405	8.13E-05	**Fam181b**	-1.048	6.99E-03
Cfap61	2.405	6.24E-04	**Ticrr**	-1.048	5.46E-05
Lzts1	2.404	2.47E-05	**H2afx**	-1.047	5.69E-08
Phyh	2.400	1.21E-10	**Stk10**	-1.047	1.38E-02
Hc	2.387	1.42E-03	**Itpripl1**	-1.046	8.21E-03
Efhc1	2.386	1.25E-04	**Sgf29**	-1.045	8.66E-04
Igsf11	2.386	4.34E-15	**Rps6ka6**	-1.045	5.22E-07
Gata3	2.383	2.03E-02	**Smyd5**	-1.044	5.02E-03
Endod1	2.382	5.20E-29	**Cacng5**	-1.044	2.21E-04

Genes (UP)	log2FoldChange	padj	Genes (Down)	log2FoldChange	padj
Gdpd2	2.380	5.45E-08	**Mcm4**	-1.042	2.23E-05
Calhm2	2.377	6.22E-04	**Tfdp1**	-1.041	5.60E-05
Gm7854	2.377	2.51E-02	**Fen1**	-1.038	1.82E-02
Ccdc74a	2.376	1.01E-07	**Hspa12b**	-1.035	3.93E-03
Trim47	2.372	1.65E-10	**Eif4a1**	-1.035	3.94E-05
Igfbp5	2.370	1.12E-16	**Rpa2**	-1.034	1.78E-04
Nkd1	2.368	3.00E-05	**Kif18a**	-1.034	1.01E-04
Mras	2.366	4.17E-15	**Zbtb46**	-1.034	4.05E-03
Chrm2	2.360	3.25E-02	**Klf12**	-1.033	2.22E-03
Nfatc4	2.360	1.34E-04	**Efs**	-1.033	1.24E-03
Cmya5	2.350	2.39E-04	**Usp1**	-1.032	8.07E-05
Klhl6	2.348	3.78E-02	**Aurka**	-1.032	9.80E-03
Dnaic1	2.347	6.85E-05	**Ccnj**	-1.031	9.38E-04
Tlr2	2.345	1.76E-07	**Jade3**	-1.030	2.58E-03
Gm4876	2.344	4.61E-08	**Camkk2**	-1.030	3.30E-03
Hcrtr1	2.342	1.20E-04	**Cep55**	-1.029	9.79E-03
Nsg2	2.342	2.97E-06	**Naa25**	-1.029	9.54E-04
Cdh22	2.339	5.20E-29	**Tipin**	-1.028	1.14E-04
Spn	2.337	4.40E-04	**Alyref**	-1.026	3.82E-05
Ngf	2.333	1.65E-02	**Nin**	-1.026	2.80E-04
Gm2115	2.332	1.39E-08	**Sfmbt1**	-1.026	1.96E-04
Cebpa	2.331	2.74E-06	**Nmral1**	-1.026	4.57E-05
Efhd1	2.331	7.39E-04	**Wnt7a**	-1.026	1.53E-02
Mt3	2.328	2.06E-08	**Prmt5**	-1.025	2.18E-04
Gm17396	2.327	1.74E-05	**Sgo1**	-1.024	2.03E-03
Dmtn	2.327	3.35E-06	**Cdca8**	-1.023	1.43E-03
Mamdc2	2.326	7.30E-25	**Aarsd1**	-1.023	1.74E-07
Gsta4	2.325	8.85E-13	**Anp32b**	-1.023	1.73E-05
Prelp	2.322	1.95E-05	**Depdc1a**	-1.023	6.16E-04
2310001H17Rik	2.320	2.89E-02	**Dph2**	-1.023	8.83E-05
Nrp1	2.316	4.77E-13	**Snhg1**	-1.022	1.03E-02
Prkar1b	2.312	5.26E-08	**Tmem199**	-1.022	2.50E-05
Kank4	2.312	2.00E-07	**Bola1**	-1.022	5.99E-06
Ranbp3l	2.308	8.20E-03	**Adgre5**	-1.021	1.20E-02
Plpp1	2.307	1.31E-17	**Ap1g2**	-1.021	6.82E-03
Sema4f	2.305	2.82E-02	**Sfrp2**	-1.020	1.13E-03
Echdc3	2.304	3.04E-02	**Chaf1a**	-1.020	1.82E-03
Tpm2	2.302	2.16E-05	**Zfhx2os**	-1.019	3.08E-02
Ctso	2.302	1.27E-11	**Suv39h1**	-1.016	9.40E-05
A930012O16Rik	2.300	2.93E-02	**Tet1**	-1.015	1.32E-02
Sult1a1	2.296	5.95E-03	**Eri2**	-1.015	5.36E-05
Dusp27	2.294	2.04E-03	**Spata5l1**	-1.014	7.46E-05
Retreg1	2.291	2.80E-07	**Kifc5b**	-1.014	5.64E-03

Genes (UP)	log2FoldChange	padj	Genes (Down)	log2FoldChange	padj
Adcy1	2.287	5.05E-14	**Ywhaq**	-1.013	3.50E-05
4930556M19Rik	2.285	6.71E-03	**Serinc5**	-1.012	7.36E-03
Osmr	2.284	2.85E-02	**mt-Nd3**	-1.012	1.04E-02
Gal3st4	2.281	7.02E-04	**Mutyh**	-1.012	1.65E-02
Gpat3	2.281	1.79E-02	**Taf5l**	-1.012	1.89E-05
Kcnj9	2.281	5.53E-03	**Lrrfip1**	-1.011	1.03E-03
9530052C20Rik	2.281	3.01E-03	**Ncaph**	-1.011	1.90E-05
Chl1	2.280	2.99E-17	**Ttc39a**	-1.011	6.16E-03
Apc2	2.274	1.94E-08	**Snrpg**	-1.011	7.48E-04
Slc45a1	2.274	3.38E-02	**Hyls1**	-1.010	2.38E-03
Kcnh3	2.271	1.55E-02	**Cgas**	-1.010	2.09E-02
Pdgfb	2.268	4.59E-03	**Pus7l**	-1.010	9.40E-05
Vwa5a	2.268	1.36E-06	**Psmc3ip**	-1.009	4.81E-03
Lurap1l	2.267	8.03E-04	**Zbtb12**	-1.009	5.23E-04
Slc8a1	2.266	2.41E-12	**Actl6a**	-1.009	3.89E-05
Prss16	2.265	2.34E-02	**Troap**	-1.009	1.01E-02
Gm9908	2.263	9.39E-03	**Mrps22**	-1.008	1.49E-05
Ptprt	2.262	1.42E-06	**Sipa1**	-1.006	2.13E-03
A330040F15Rik	2.261	1.02E-02	**Bysl**	-1.005	2.73E-05
Tspan17	2.258	3.63E-12	**Arntl2**	-1.004	3.38E-02
4933412E12Rik	2.253	7.61E-06	**Dscc1**	-1.003	3.14E-03
Cd274	2.252	3.53E-03	**Cst6**	-1.003	3.24E-02
Slc43a3	2.248	5.35E-05	**Plk3**	-1.001	1.14E-02
Vamp5	2.241	7.23E-06	**Fxn**	-1.001	2.58E-04
Gm4544	2.239	2.41E-04	**Polr3g**	-1.001	1.69E-03
Ltbp3	2.235	9.67E-30	**Mapk11**	-0.999	4.67E-03
Sstr3	2.230	2.78E-02	**Zfas1**	-0.998	6.96E-03
Lpar1	2.230	2.16E-05	**Mtfp1**	-0.997	9.25E-03
Dnah10	2.227	1.79E-05	**Kif24**	-0.997	1.06E-03
Cacna2d2	2.223	4.50E-05	**Arhgap6**	-0.997	1.45E-03
Serpinb8	2.223	2.25E-07	**Peg10**	-0.995	2.20E-02
Rgs6	2.223	3.20E-06	**Nat10**	-0.993	4.02E-04
Pax8	2.221	2.41E-02	**Setd4**	-0.993	1.78E-02
Col6a3	2.220	3.69E-05	**Cks2**	-0.993	2.65E-03
Dgki	2.219	3.15E-06	**Dek**	-0.992	2.81E-05
Ston2	2.215	1.03E-14	**Nifk**	-0.992	1.60E-04
Lgals8	2.214	1.13E-09	**Tsr1**	-0.992	1.66E-03
C130026L21Rik	2.214	2.01E-04	**Utp15**	-0.991	2.33E-04
Anxa2	2.213	1.30E-13	**Bend3**	-0.991	3.42E-04
1010001B22Rik	2.212	1.44E-02	**Klhl13**	-0.990	1.72E-03
Pld5	2.210	3.15E-02	**Plk1**	-0.990	5.58E-03
Ntsr2	2.209	1.90E-02	**Nxt1**	-0.989	1.01E-04
Gm16565	2.206	1.37E-04	**Cip2a**	-0.989	2.90E-03

Genes (UP)	log2FoldChange	padj	Genes (Down)	log2FoldChange	padj
Adhfe1	2.206	1.67E-08	**Pkmyt1**	-0.989	4.29E-03
Gm9922	2.201	2.14E-03	**Utp14a**	-0.989	3.80E-03
Tmem40	2.200	8.54E-08	**Igsf9b**	-0.988	1.65E-05
Ahr	2.199	4.38E-04	**Tead2**	-0.988	7.36E-05
Hr	2.197	4.90E-05	**Rnf227**	-0.988	1.48E-02
Gm20633	2.196	1.66E-05	**Snrnp40**	-0.987	2.04E-06
Tuba4a	2.194	5.10E-03	**Pcna**	-0.987	6.76E-05
Scd4	2.185	2.41E-02	**Nudcd1**	-0.987	8.78E-03
Adrb2	2.183	3.07E-04	**Wdr36**	-0.986	5.17E-04
Nrxn1	2.182	5.02E-13	**Pom121**	-0.984	5.86E-05
Sh3gl2	2.179	2.22E-07	**Zfp472**	-0.984	1.17E-03
Rnf112	2.178	6.84E-05	**Psmg1**	-0.984	2.52E-04
Col9a2	2.177	5.31E-03	**Tubb5**	-0.984	2.02E-04
Cep170b	2.177	8.75E-12	**Gtpbp4**	-0.983	1.09E-03
Strc	2.175	9.74E-11	**Gm38394**	-0.983	1.94E-02
Nalcn	2.174	1.12E-03	**Spc24**	-0.983	1.96E-03
9330160F10Rik	2.174	2.30E-02	**Ptbp1**	-0.983	2.55E-03
Gm30122	2.172	2.98E-02	**Slf1**	-0.983	7.12E-04
Esr1	2.171	2.98E-08	**Dnaaf2**	-0.982	4.24E-05
Abat	2.167	3.34E-06	**Agk**	-0.981	4.90E-05
Apobr	2.166	1.76E-07	**Zcchc10**	-0.980	2.24E-03
Gm34934	2.164	3.43E-06	**Cenpw**	-0.980	3.02E-02
Gprin2	2.161	1.71E-09	**Kat2a**	-0.980	6.62E-04
Adamtsl1	2.160	3.75E-05	**Apex1**	-0.980	2.68E-04
Ctnnal1	2.158	1.44E-24	**Yrdc**	-0.979	3.70E-03
Hist2h3c2	2.156	9.30E-07	**G3bp1**	-0.978	7.71E-05
Fhl1	2.149	2.68E-22	**Dus1l**	-0.978	1.75E-06
Fkbp10	2.149	1.00E-21	**Igf2bp3**	-0.977	2.65E-04
Tgm2	2.145	2.86E-15	**Nanos1**	-0.977	1.38E-03
Wipi1	2.145	2.53E-07	**Parp1**	-0.977	2.99E-05
Ecel1	2.144	7.00E-04	**Hjurp**	-0.976	1.42E-05
Tcp11l2	2.143	2.18E-04	**Polr3e**	-0.976	1.14E-04
Sez6	2.139	1.08E-23	**Tacc2**	-0.976	4.40E-05
Emb	2.138	1.75E-06	**Nip7**	-0.974	1.58E-03
2900060B14Rik	2.136	4.36E-02	**Esco2**	-0.974	4.16E-04
Id2	2.133	1.10E-06	**Cenpf**	-0.973	2.87E-04
Camsap3	2.130	1.17E-03	**Ltv1**	-0.972	8.12E-04
Lrrn2	2.125	6.03E-23	**Utp4**	-0.972	1.25E-03
Aqp9	2.124	7.76E-03	**Kif22**	-0.972	1.52E-04
Rec8	2.124	9.19E-03	**Zc3hav1l**	-0.971	3.22E-04
Trim17	2.122	7.55E-03	**Snhg6**	-0.970	1.81E-02
Eno3	2.121	5.49E-14	**Carm1**	-0.970	9.77E-05
Sema3c	2.119	1.52E-09	**Cenpn**	-0.970	2.40E-04

Genes (UP)	log2FoldChange	padj	Genes (Down)	log2FoldChange	padj
Cacnb4	2.119	5.83E-04	**Prps1**	-0.970	9.03E-04
Upp2	2.119	1.81E-05	**Ddias**	-0.970	1.80E-03
Slc6a8	2.115	3.76E-18	**Dusp16**	-0.970	9.54E-04
4930426L09Rik	2.114	1.19E-02	**Ddx25**	-0.970	2.12E-04
Eln	2.114	8.67E-09	**Cep152**	-0.970	9.61E-03
Vamp8	2.113	9.34E-04	**Nubp1**	-0.970	1.86E-04
Cyp7b1	2.113	3.79E-08	**Smarcc1**	-0.969	6.08E-06
Agrn	2.112	1.41E-29	**Nme1**	-0.968	5.22E-04
5033430I15Rik	2.111	7.00E-03	**Inka1**	-0.967	3.77E-02
Notch3	2.110	2.76E-19	**Wdr4**	-0.967	2.40E-03
Gm20515	2.110	1.83E-03	**Mad2l1**	-0.966	1.55E-04
Cd247	2.106	1.10E-03	**Col26a1**	-0.966	2.19E-02
Nid2	2.102	2.66E-05	**Poc1b**	-0.965	6.06E-06
Gm10134	2.099	4.23E-02	**Lrrtm3**	-0.965	4.20E-02
Vdr	2.094	4.79E-05	**Pfas**	-0.965	1.59E-06
Sync	2.092	4.35E-03	**Nelfa**	-0.964	2.13E-06
Gpr146	2.092	8.95E-11	**Timm8a1**	-0.963	2.69E-03
Myh3	2.090	4.35E-02	**Atp23**	-0.963	1.35E-03
C230037L18Rik	2.088	2.73E-02	**Gtse1**	-0.963	3.30E-03
Pde4a	2.087	3.29E-05	**Nup37**	-0.963	1.02E-03
Stbd1	2.086	2.60E-04	**Shcbp1**	-0.962	1.39E-03
Eng	2.084	7.70E-03	**Pola1**	-0.962	9.87E-04
Nfix	2.081	8.59E-28	**Hspd1**	-0.962	8.28E-04
Chgb	2.072	1.05E-02	**Impdh2**	-0.961	8.93E-04
Gpx3	2.070	1.09E-10	**Gfer**	-0.961	1.01E-04
Gm6145	2.068	1.18E-05	**Dbf4**	-0.960	3.12E-03
Tmem221	2.066	2.10E-03	**Wdr3**	-0.960	1.05E-03
Cda	2.066	3.63E-02	**Sox13**	-0.959	2.87E-05
Gbp2	2.066	5.33E-07	**Pbk**	-0.959	1.12E-03
Gm9484	2.065	3.38E-02	**Dleu2**	-0.959	6.99E-04
Tlx1	2.065	1.06E-04	**Hnrnpd**	-0.958	1.37E-06
Gm47015	2.063	3.29E-03	**Tbl3**	-0.958	5.49E-05
Coro6	2.062	1.28E-02	**Cep76**	-0.956	1.04E-03
Kdm4d	2.058	2.61E-02	**Grik3**	-0.956	2.23E-02
Frem2	2.057	2.50E-10	**Fndc3c1**	-0.956	4.42E-04
Arhgef6	2.056	1.15E-07	**Zeb1**	-0.955	7.59E-04
Foxf2	2.054	1.40E-02	**Gmip**	-0.954	3.72E-03
Nrip3	2.054	8.34E-05	**4930452B06Rik**	-0.954	8.82E-05
D830050J10Rik	2.051	5.40E-03	**Ccdc163**	-0.954	6.71E-03
Ackr3	2.050	3.39E-10	**Pmf1**	-0.954	4.61E-04
Gm20559	2.050	2.37E-02	**Cnksr2**	-0.953	1.30E-03
Adam22	2.049	2.69E-21	**Rnaseh2b**	-0.952	1.13E-05
Spsb1	2.041	6.57E-12	**Bub1**	-0.952	9.44E-03

Genes (UP)	log2FoldChange	padj	Genes (Down)	log2FoldChange	padj
Gm26581	2.041	1.10E-02	**Pkn3**	-0.951	6.69E-03
Sned1	2.038	1.42E-04	**D10Wsu102e**	-0.951	1.26E-04
Arhgef26	2.036	2.38E-07	**Cdkn2aipnl**	-0.950	1.12E-02
Sorl1	2.031	2.01E-11	**Hip1**	-0.949	4.10E-06
Thrsp	2.029	1.95E-03	**Zbtb10**	-0.949	6.53E-06
Fzd10os	2.029	2.52E-03	**Eef1akmt4**	-0.947	5.90E-03
Slc44a1	2.025	1.07E-05	**Pus10**	-0.946	3.06E-03
Nkx6-2	2.022	1.03E-06	**Inip**	-0.944	6.43E-04
Nynrin	2.021	8.33E-06	**Sf3a2**	-0.943	1.65E-04
Adamtsl4	2.021	1.53E-03	**E130309D02Rik**	-0.943	1.95E-06
Rtn4r	2.018	3.10E-03	**Btg2**	-0.942	5.40E-03
Fzd6	2.018	2.52E-09	**Nsun5**	-0.942	2.83E-03
Lrp1	2.016	1.43E-28	**Apln**	-0.942	4.37E-02
Rtn4rl1	2.013	1.10E-04	**Usp10**	-0.942	5.36E-05
Ldb3	2.011	2.39E-04	**Kpna2**	-0.942	5.03E-04
Fstl1	2.009	3.65E-19	**Ppid**	-0.941	7.67E-04
Acot11	2.007	7.85E-08	**Hmgb3**	-0.941	7.29E-06
Lef1	2.007	1.39E-04	**Ak6**	-0.941	1.91E-02
Mmp11	2.004	9.66E-09	**Tonsl**	-0.941	3.55E-03
Smyd1	2.003	5.84E-03	**Nemp2**	-0.940	9.24E-03
Aldh6a1	2.000	1.17E-09	**Ctu1**	-0.940	4.92E-05
Ifih1	2.000	2.15E-03	**Ccna2**	-0.939	1.62E-03
Tinagl1	1.998	2.39E-03	**Mxd3**	-0.939	1.81E-03
Ikzf2	1.998	2.42E-13	**Snapc4**	-0.939	1.39E-03
Pth2r	1.995	1.72E-02	**Ppa1**	-0.937	1.89E-03
Mdfi	1.992	8.54E-18	**Znhit3**	-0.936	1.44E-04
Acvrl1	1.991	7.33E-06	**Shmt2**	-0.936	6.25E-03
Pik3ip1	1.991	1.38E-08	**Haus5**	-0.936	2.04E-03
S1pr1	1.989	6.91E-04	**Ncl**	-0.935	3.22E-03
Thrb	1.988	3.79E-05	**Nup188**	-0.934	2.81E-04
Gcnt2	1.988	1.38E-09	**Hnrnpdl**	-0.934	3.20E-06
Extl1	1.988	9.23E-05	**Adgrl2**	-0.933	3.45E-04
Sds	1.986	4.27E-02	**Rcc2**	-0.933	6.50E-04
Ky	1.984	4.02E-04	**Cenps**	-0.932	1.87E-02
Grhl1	1.984	7.66E-05	**Pcolce2**	-0.932	1.38E-02
Gm5089	1.983	2.07E-02	**Pes1**	-0.931	7.13E-04
Cmpk2	1.983	1.26E-06	**Pla2g4b**	-0.930	1.67E-02
Ctsd	1.983	1.77E-18	**Riox1**	-0.930	2.25E-03
Prss35	1.981	5.23E-05	**Chchd4**	-0.929	2.85E-03
Emp2	1.980	1.58E-17	**Nfya**	-0.929	1.07E-04
9630014M24Rik	1.979	2.34E-02	**Rrp9**	-0.929	8.17E-03
Phyhd1	1.979	1.27E-06	**Gm49336**	-0.928	4.04E-04
Sod3	1.978	1.02E-05	**Fastkd3**	-0.928	4.81E-04

Genes (UP)	log2FoldChange	padj	Genes (Down)	log2FoldChange	padj
C130074G19Rik	1.977	4.25E-04	**Cenpa**	-0.927	8.35E-04
Gabrb2	1.974	2.77E-05	**Gemin6**	-0.927	4.24E-03
Mr1	1.972	4.57E-07	**Jade1**	-0.927	4.62E-03
B930059L03Rik	1.972	1.32E-02	**Rcc1l**	-0.926	7.32E-04
Gata2	1.969	1.15E-07	**Akap8**	-0.926	2.48E-04
Gm26782	1.967	2.07E-03	**Hnrnpa1**	-0.926	1.17E-03
Ezr	1.966	1.01E-07	**Kif18b**	-0.925	1.65E-03
Ajm1	1.965	2.79E-06	**Emg1**	-0.925	1.66E-06
Catip	1.963	1.50E-02	**Tet3**	-0.925	5.28E-06
Slc39a4	1.962	2.94E-02	**Nup62**	-0.923	1.75E-03
Cmtm5	1.962	2.95E-02	**Cdca2**	-0.922	1.40E-02
Lgmn	1.954	4.80E-14	**Meaf6**	-0.922	8.06E-05
Gm6556	1.953	2.88E-03	**Pum3**	-0.921	4.08E-04
Lama3	1.953	1.30E-02	**Rtl5**	-0.920	2.60E-03
Cited4	1.953	6.71E-03	**Neil1**	-0.920	1.78E-02
Tmem25	1.952	8.15E-05	**Top2a**	-0.920	8.73E-04
Carmil1	1.952	3.82E-17	**Ppih**	-0.920	1.52E-03
Trpv4	1.950	2.57E-02	**Ccdc58**	-0.919	1.87E-03
Rsad2	1.948	2.18E-04	**Fjx1**	-0.919	1.66E-03
Gm11266	1.948	4.12E-03	**Cmtr2**	-0.919	3.39E-04
Zcchc18	1.947	7.04E-08	**Tle4**	-0.918	7.42E-05
Rgs2	1.946	1.55E-06	**Traip**	-0.918	1.34E-02
Itpk1	1.945	2.64E-09	**Wdr74**	-0.918	3.74E-03
Cfap100	1.944	3.80E-03	**Nphp4**	-0.917	4.09E-03
Adamts15	1.942	2.24E-07	**Banf1**	-0.915	5.98E-04
F3	1.939	1.48E-11	**Spdl1**	-0.915	9.20E-03
Susd6	1.937	6.42E-15	**Brip1**	-0.915	3.31E-03
Zfr2	1.937	9.98E-05	**Nop2**	-0.915	7.27E-04
Enpp5	1.935	2.90E-19	**Slc7a1**	-0.914	2.25E-02
Cmbl	1.935	1.44E-05	**Cenpe**	-0.914	1.13E-03
Cdh10	1.935	4.69E-15	**Sf3a3**	-0.913	5.42E-04
Lipa	1.935	2.45E-07	**Lgi2**	-0.913	1.91E-03
Parp3	1.935	1.19E-18	**Mbtd1**	-0.912	3.59E-03
Tep1	1.934	1.17E-04	**Gcfc2**	-0.912	1.32E-02
Zfp697	1.933	3.10E-12	**Hat1**	-0.911	3.74E-03
Celsr1	1.930	8.22E-09	**Lbhd1**	-0.910	1.02E-02
Lipg	1.925	2.89E-05	**Rad51**	-0.909	2.51E-03
Ankrd45	1.922	3.49E-03	**C1ql3**	-0.908	4.29E-02
Irf9	1.921	2.48E-04	**Cdk8**	-0.908	9.78E-04
Acan	1.921	5.80E-04	**Fbln1**	-0.908	8.38E-05
Gdnf	1.918	2.60E-04	**Dnajc21**	-0.908	8.59E-03
Sema4a	1.911	1.13E-03	**Rab3gap2**	-0.907	4.99E-04
Aspa	1.910	2.44E-02	**Dis3**	-0.907	2.42E-03

Genes (UP)	log2FoldChange	padj	Genes (Down)	log2FoldChange	padj
Tgfb1	1.910	2.76E-04	**Lsm5**	-0.906	2.09E-03
Nkx2-2os	1.908	2.34E-02	**Srsf3**	-0.906	2.35E-05
Nrxn2	1.908	2.47E-16	**Topbp1**	-0.906	1.45E-03
Npnt	1.902	7.86E-04	**Sf3b4**	-0.904	1.62E-06
D030068K23Rik	1.902	4.69E-03	**Pip5k1b**	-0.904	1.86E-03
Fbxl21	1.901	7.05E-03	**Polr1e**	-0.904	7.37E-04
Emp1	1.898	2.87E-11	**Zfp692**	-0.904	1.15E-03
Hist2h3c1	1.897	2.76E-06	**Rcl1**	-0.903	7.33E-04
Adamtsl2	1.896	4.18E-02	**Dlgap5**	-0.903	1.16E-02
Rtn4rl2	1.896	4.97E-05	**Tsfm**	-0.903	3.21E-05
S100a1	1.894	9.92E-04	**Hira**	-0.902	5.98E-06
Tmem100	1.893	7.66E-04	**Rbl1**	-0.902	6.32E-04
Pxmp4	1.892	2.20E-11	**Slc12a2**	-0.902	5.98E-03
Scx	1.891	3.06E-02	**Gins2**	-0.902	1.60E-02
Zdhhc23	1.891	3.59E-03	**Mbtps2**	-0.901	6.22E-04
Slc38a3	1.890	6.18E-05	**Asf1b**	-0.901	3.19E-02
Vcam1	1.887	3.16E-22	**Chd1**	-0.899	1.88E-03
Scn3b	1.886	1.68E-02	**Gpn3**	-0.899	4.32E-03
Gm45447	1.884	4.35E-02	**Thop1**	-0.898	5.42E-04
Snhg18	1.883	2.30E-04	**Uchl5**	-0.898	1.82E-03
Gm20632	1.883	2.43E-05	**Rnaseh2c**	-0.898	1.45E-03
D130020L05Rik	1.882	4.30E-03	**Casp8ap2**	-0.897	1.36E-03
Insyn1	1.882	4.82E-17	**Ebf3**	-0.896	1.40E-03
Ttc9b	1.880	1.47E-02	**Nfxl1**	-0.894	8.95E-04
Nkd2	1.879	4.43E-03	**Ndc1**	-0.894	1.33E-03
Nacad	1.878	1.04E-06	**Mogs**	-0.893	1.13E-03
Enpep	1.878	2.44E-02	**Zfp850**	-0.893	8.42E-03
Frmpd1	1.877	1.36E-08	**Cdk4**	-0.892	1.21E-06
Cox6a2	1.876	1.48E-02	**Mtrr**	-0.891	6.95E-03
Lamc2	1.876	2.58E-08	**Lsm3**	-0.891	4.58E-03
Idua	1.875	3.96E-07	**Pusl1**	-0.891	1.23E-03
Adgra1	1.872	4.86E-09	**Tbc1d16**	-0.890	2.72E-02
Rnf213	1.870	1.33E-03	**Acap3**	-0.890	5.28E-06
L1cam	1.869	1.17E-02	**Phykpl**	-0.890	1.48E-03
Cdo1	1.868	1.01E-04	**Cerk**	-0.889	1.28E-02
Tril	1.867	1.47E-07	**Suclg2**	-0.889	1.98E-05
Erap1	1.866	1.37E-06	**Cnbp**	-0.888	2.61E-04
Pmp22	1.864	6.60E-09	**Sppl2b**	-0.888	4.18E-06
Sytl5	1.864	1.02E-02	**Rpf1**	-0.888	6.50E-04
Igfbp2	1.863	2.26E-09	**Kcnip3**	-0.887	1.55E-02
Man2b2	1.862	4.29E-10	**Atic**	-0.887	1.37E-02
Frk	1.861	1.65E-02	**Cenpi**	-0.887	6.35E-03
Serpinh1	1.861	3.04E-09	**Nepro**	-0.887	2.81E-02

Genes (UP)	log2FoldChange	padj	Genes (Down)	log2FoldChange	padj
Mxra8	1.861	2.68E-21	**Naa10**	-0.887	5.94E-03
Tmem106a	1.861	3.25E-03	**Spry1**	-0.886	2.46E-04
Paqr7	1.860	2.58E-04	**Camk2n2**	-0.886	2.64E-03
Gm48550	1.856	2.61E-02	**Fignl1**	-0.886	1.46E-04
Tmtc1	1.853	4.33E-03	**G2e3**	-0.886	2.48E-04
S100a3	1.851	1.92E-02	**Brca1**	-0.886	9.33E-04
Zfp423	1.847	4.19E-10	**Fkbp4**	-0.885	1.48E-04
Dok5	1.845	5.79E-06	**Elmo1**	-0.883	1.25E-03
Rph3al	1.842	4.63E-03	**Akna**	-0.882	4.27E-03
Spata17	1.842	4.67E-02	**Cnot6**	-0.881	3.44E-05
Slc1a3	1.841	9.89E-08	**2310057M21Rik**	-0.880	1.90E-03
Gstt3	1.837	1.18E-02	**Mpp6**	-0.880	9.96E-04
Gm7628	1.837	8.81E-03	**Wdr89**	-0.879	2.30E-02
Sorbs2	1.836	6.85E-04	**Kbtbd6**	-0.879	9.32E-03
Cdc42ep3	1.834	2.83E-03	**Isl2**	-0.879	2.46E-02
Gm43672	1.833	3.14E-06	**Alad**	-0.879	4.08E-03
Pcdh7	1.831	1.26E-17	**Tmem39b**	-0.879	3.49E-03
Gm2a	1.831	1.99E-09	**Srsf2**	-0.878	3.65E-05
Gm3693	1.830	3.31E-02	**Rnf128**	-0.878	7.15E-03
Gbp4	1.829	3.03E-02	**Dynlt1f**	-0.877	4.65E-05
Cnn2	1.827	4.04E-22	**Sart3**	-0.877	1.12E-04
Htra1	1.826	1.28E-10	**Zcchc9**	-0.876	2.97E-04
Gm10642	1.825	2.77E-02	**Cse1l**	-0.876	2.21E-03
Psd4	1.824	2.19E-03	**Cct5**	-0.876	6.10E-04
P2ry1	1.823	4.95E-07	**Rtel1**	-0.875	3.60E-04
Adcy5	1.821	1.88E-11	**Gabpb1**	-0.872	4.17E-04
Gstm4	1.819	2.32E-02	**Rbpms2**	-0.872	6.15E-04
Rinl	1.818	3.04E-02	**Tarbp1**	-0.871	4.66E-04
Ptprk	1.818	7.49E-09	**Atp11c**	-0.870	6.49E-04
Enpp2	1.818	4.64E-03	**Nol12**	-0.869	3.12E-04
Svip	1.818	1.75E-06	**Thoc3**	-0.869	1.55E-04
Mef2b	1.816	2.60E-04	**Cdc25c**	-0.869	1.86E-02
Arhgef19	1.816	7.53E-07	**Rttn**	-0.868	6.15E-03
Lrrc32	1.814	2.41E-04	**Kif20b**	-0.868	1.34E-02
AI849053	1.812	2.01E-04	**Dck**	-0.868	1.03E-03
Cfap97d2	1.812	2.51E-02	**Eed**	-0.868	1.45E-03
Hist1h2be	1.808	6.12E-04	**Abce1**	-0.868	2.15E-03
Sv2a	1.808	5.07E-04	**U2af1**	-0.868	1.17E-04
Mdga1	1.806	4.28E-12	**Myo1b**	-0.868	3.51E-03
Fzd9	1.806	3.03E-10	**Aaas**	-0.867	1.70E-04
Speg	1.800	1.20E-07	**Rrs1**	-0.867	8.15E-05
Htra3	1.797	2.71E-03	**Helq**	-0.867	8.71E-04
Snai1	1.797	1.41E-02	**Isoc1**	-0.867	1.64E-05

Genes (UP)	log2FoldChange	padj	Genes (Down)	log2FoldChange	padj
Plpp3	1.797	5.02E-10	**Slbp**	-0.867	4.41E-05
Gm34256	1.790	5.73E-03	**Kifc1**	-0.866	5.74E-03
Col4a6	1.789	1.09E-04	**Gsr**	-0.866	4.22E-03
Ppp1r1a	1.789	6.20E-10	**Tcp1**	-0.865	1.36E-03
1190005I06Rik	1.787	2.38E-03	**Ccdc57**	-0.865	1.71E-02
Dlgap1	1.784	3.86E-03	**Tinf2**	-0.865	8.80E-03
Lnx1	1.784	1.78E-02	**Mto1**	-0.864	2.75E-04
Rab32	1.783	1.02E-07	**Rarb**	-0.863	1.77E-03
Gpx8	1.781	2.96E-15	**Fam110a**	-0.863	1.32E-02
Pcdhac2	1.780	3.48E-11	**Gm12940**	-0.863	2.86E-02
Runx2	1.779	1.66E-05	**Hmgb1**	-0.863	3.39E-05
Dhrs1	1.779	2.24E-17	**Rbmx2**	-0.862	7.16E-03
Megf10	1.778	1.35E-07	**Ahcy**	-0.862	1.60E-02
Frzb	1.777	2.06E-03	**Zfp568**	-0.861	3.55E-02
Nat8f1	1.776	3.90E-03	**Thumpd1**	-0.860	3.92E-03
Arhgef10	1.773	7.95E-12	**Mif**	-0.859	1.19E-03
Tnfrsf13c	1.773	1.17E-02	**Flvcr1**	-0.859	1.79E-03
Rora	1.771	2.46E-04	**Pdcd11**	-0.859	2.03E-03
Slc16a9	1.770	9.30E-07	**Nop10**	-0.859	5.24E-03
Lmod1	1.769	3.67E-02	**Utp25**	-0.858	1.84E-03
Rapgef5	1.769	1.32E-06	**Mrps5**	-0.858	2.94E-05
Fam160a1	1.769	1.23E-06	**Bub1b**	-0.858	7.10E-05
Cilp2	1.769	9.38E-04	**Abcb7**	-0.858	4.86E-04
Ccnd2	1.765	6.51E-10	**Prag1**	-0.858	3.55E-03
Gnao1	1.765	1.77E-08	**Arrb2**	-0.858	2.02E-04
Gm973	1.765	1.12E-03	**Pwp1**	-0.857	8.07E-04
Pcdh17	1.763	4.87E-09	**Lpar6**	-0.857	2.83E-02
Dpysl3	1.763	9.06E-10	**Tango6**	-0.857	2.43E-04
Tcirg1	1.762	2.30E-07	**Farsb**	-0.857	9.80E-03
Klhl32	1.762	3.80E-05	**Tex10**	-0.856	3.08E-03
Zbtb4	1.756	7.39E-09	**Sema4c**	-0.856	7.74E-05
Hist1h3d	1.751	2.65E-02	**Rpusd4**	-0.856	4.75E-04
Prnp	1.750	6.24E-13	**Rbm14**	-0.856	8.31E-04
Ppp1r1b	1.749	9.84E-04	**Phf20**	-0.856	3.32E-05
Slc13a3	1.748	4.91E-09	**Exosc7**	-0.856	1.24E-02
Vmac	1.746	3.82E-09	**Ska3**	-0.856	1.33E-02
Rgs4	1.745	1.94E-02	**Nr6a1**	-0.856	1.26E-02
Id3	1.744	2.76E-13	**Nup153**	-0.855	5.07E-04
Rbm46	1.744	1.84E-02	**Cd1d1**	-0.855	7.75E-03
Gm26645	1.743	3.17E-03	**Zik1**	-0.854	9.93E-03
Gcnt4	1.743	1.27E-08	**Taf4b**	-0.854	1.19E-02
Pld2	1.741	2.01E-06	**Abcb6**	-0.854	9.59E-03
Ficd	1.741	4.35E-10	**Tomm70a**	-0.853	1.66E-04

Genes (UP)	log2FoldChange	padj	Genes (Down)	log2FoldChange	padj
Tspan7	1.740	7.32E-06	**Limd2**	-0.853	2.35E-03
Rasgef1b	1.739	1.34E-02	**Isy1**	-0.853	1.01E-03
Hist1h4h	1.737	6.75E-03	**Eef1e1**	-0.853	7.34E-03
Inca1	1.736	1.43E-02	**Nek2**	-0.852	1.38E-02
Per3	1.736	1.84E-06	**Timm50**	-0.852	1.04E-03
Adgrf4	1.735	4.75E-02	**Fam222a**	-0.852	4.51E-02
4430402I18Rik	1.735	2.22E-02	**Mki67**	-0.852	3.36E-03
Synpr	1.734	1.76E-03	**Arhgap11a**	-0.851	5.02E-03
Serpina3n	1.733	3.22E-06	**Srsf9**	-0.851	3.04E-05
Lamb2	1.731	4.76E-10	**Haus6**	-0.851	2.62E-03
Ank	1.731	1.38E-03	**Nxf1**	-0.851	1.10E-04
Pde8b	1.729	5.25E-04	**Atad3a**	-0.850	9.53E-05
Bmper	1.729	3.27E-03	**Ipo7**	-0.850	7.05E-03
2700054A10Rik	1.729	4.11E-04	**Dennd2a**	-0.850	2.00E-05
Slc15a2	1.729	3.12E-10	**Ncbp1**	-0.850	7.71E-05
Kcnn1	1.728	5.97E-04	**Impdh1**	-0.849	3.50E-04
Asap3	1.725	2.40E-11	**Sfpq**	-0.849	1.32E-04
Kifc2	1.724	5.28E-05	**Tgif2**	-0.849	1.28E-02
Rgma	1.723	7.13E-06	**Clp1**	-0.848	2.28E-02
Rnd2	1.723	3.38E-15	**Wbp11**	-0.848	1.77E-03
Tmsb15b2	1.721	2.16E-03	**Kntc1**	-0.846	3.26E-02
Gpm6b	1.721	3.39E-06	**Eif1ad**	-0.846	3.64E-05
Met	1.721	1.95E-09	**Aen**	-0.846	1.98E-02
Pdcd4	1.718	9.20E-04	**Gpn1**	-0.846	8.23E-04
Wnt5a	1.718	2.58E-04	**Zpr1**	-0.845	8.74E-03
Slc7a8	1.718	1.45E-02	**Chst11**	-0.845	3.09E-02
Rgs5	1.716	4.14E-03	**Ppip5k2**	-0.844	4.06E-04
Bmf	1.715	3.20E-04	**Mast4**	-0.844	5.04E-03
Olfm2	1.714	5.72E-08	**Dhx15**	-0.843	1.29E-03
Mylip	1.714	7.00E-08	**Rnf219**	-0.843	3.34E-04
Itgb5	1.713	3.15E-12	**Aatf**	-0.843	2.04E-02
Arfgef3	1.711	2.84E-02	**Gstcd**	-0.843	5.47E-03
Slc2a4	1.711	2.95E-02	**Ddx31**	-0.843	7.61E-03
Armc2	1.710	1.08E-02	**Snrnp35**	-0.843	4.11E-03
Ptgr2	1.709	1.10E-07	**Pabpc4**	-0.842	1.59E-02
Gm15050	1.708	2.89E-05	**Cdk1**	-0.842	1.75E-02
Khk	1.707	8.86E-05	**Ppwd1**	-0.842	1.59E-03
AW011738	1.705	9.23E-03	**Tardbp**	-0.841	1.70E-04
Rubcnl	1.704	9.36E-03	**Taf1a**	-0.839	1.33E-02
Ctf1	1.704	5.24E-05	**Nif3l1**	-0.839	1.44E-03
Gmpr	1.702	1.29E-05	**Camta1**	-0.838	3.50E-03
Fgfrl1	1.701	1.64E-07	**Ccne2**	-0.838	1.57E-02
Gm8098	1.700	4.37E-02	**Rpp30**	-0.838	1.17E-03

Genes (UP)	log2FoldChange	padj	Genes (Down)	log2FoldChange	padj
Xlr	1.699	3.68E-03	**Gas5**	-0.838	2.87E-02
Kcnj10	1.698	1.39E-03	**Sh2b2**	-0.837	8.81E-03
Foxo3	1.698	1.30E-12	**Cks1b**	-0.837	2.32E-02
S100a13	1.697	1.21E-07	**Rps25**	-0.837	8.45E-04
Rgs16	1.696	8.60E-17	**Klf10**	-0.836	1.23E-03
Icam5	1.695	1.80E-02	**Bard1**	-0.836	3.55E-02
Usp53	1.692	1.09E-07	**Ercc1**	-0.835	3.35E-03
Mef2c	1.692	5.83E-12	**Thada**	-0.835	6.42E-03
Gm47863	1.691	1.14E-02	**Prmt3**	-0.835	8.02E-03
H2-Ab1	1.690	4.69E-02	**Kars**	-0.835	3.05E-03
Aldh1l1	1.689	4.58E-04	**Lrwd1**	-0.834	8.24E-05
Enpp6	1.689	3.93E-02	**Pop5**	-0.834	3.33E-04
Slc2a13	1.688	5.00E-03	**Gadd45gip1**	-0.833	1.50E-02
Gm35021	1.688	3.43E-02	**Idh2**	-0.833	8.57E-05
Hfe	1.688	1.06E-08	**Dgkd**	-0.833	3.00E-05
Myl6b	1.687	6.44E-14	**Gas7**	-0.833	7.31E-03
Ccdc183	1.687	2.16E-02	**Rnf126**	-0.832	2.38E-03
Pparg	1.686	1.15E-07	**Tdp2**	-0.832	7.84E-04
Timp2	1.684	4.73E-17	**Brix1**	-0.831	5.11E-04
Plekhg1	1.684	3.97E-08	**Rps8**	-0.831	1.86E-03
Gria4	1.682	3.41E-04	**Ddx27**	-0.831	2.17E-03
Limch1	1.681	3.06E-16	**Urb2**	-0.831	8.57E-03
Hhipl1	1.678	2.80E-04	**Wdr12**	-0.831	6.96E-03
Srgap3	1.677	1.03E-16	**Zbed4**	-0.831	1.14E-04
Anxa4	1.676	1.57E-06	**Tcerg1**	-0.830	1.79E-03
Glipr1	1.675	4.88E-02	**Cwf19l1**	-0.829	2.05E-03
Lrrc3	1.674	1.57E-02	**Mrpl19**	-0.829	9.71E-03
Dio2	1.674	1.66E-02	**Tmem97**	-0.828	5.95E-03
Plec	1.673	2.71E-05	**Bcor**	-0.828	3.34E-03
Lrrc4	1.673	6.33E-11	**Dph6**	-0.827	1.19E-03
Tmem159	1.672	6.35E-03	**Gart**	-0.827	2.42E-03
Gm47939	1.670	9.07E-03	**Zfp41**	-0.827	1.20E-03
Sh2d3c	1.670	3.80E-03	**Aspm**	-0.827	4.46E-03
Hist1h2ac	1.668	1.17E-03	**Atm**	-0.827	1.34E-02
Sspn	1.666	1.10E-12	**Surf6**	-0.827	4.56E-03
Cavin3	1.665	8.54E-08	**Fam136a**	-0.826	1.45E-03
Slc7a4	1.664	5.57E-03	**Zfp81**	-0.826	7.82E-03
Rarres1	1.663	2.89E-03	**Eif3b**	-0.826	2.49E-03
Fabp5	1.661	2.38E-22	**Msantd2**	-0.825	2.49E-03
Jak3	1.661	1.80E-02	**5031439G07Rik**	-0.825	2.14E-03
Rassf5	1.660	2.92E-03	**Arl6ip6**	-0.825	8.66E-04
3830403N18Rik	1.660	4.47E-02	**Polg**	-0.825	1.35E-02
Lgi3	1.660	3.71E-03	**Prr11**	-0.824	8.99E-03

Genes (UP)	log2FoldChange	padj	Genes (Down)	log2FoldChange	padj
Nyap1	1.659	7.93E-08	**Rbbp8**	-0.824	6.34E-03
Dop1b	1.659	1.46E-08	**Trim28**	-0.824	5.93E-04
2810414N06Rik	1.657	8.81E-03	**Pdik1l**	-0.824	3.35E-03
Slc4a4	1.657	5.17E-09	**Syne1**	-0.824	5.15E-03
Alpk1	1.655	2.67E-04	**Crip2**	-0.824	8.57E-05
Fat1	1.654	1.52E-15	**Dhps**	-0.823	4.33E-04
Thra	1.652	5.19E-14	**Rffl**	-0.823	2.15E-02
Xrra1	1.650	1.90E-02	**Enkd1**	-0.823	3.97E-03
Tiam2	1.650	2.38E-08	**Prpf4**	-0.823	1.32E-03
Crabp1	1.649	2.00E-04	**Alg13**	-0.823	1.86E-03
Ntrk2	1.648	2.98E-03	**Nup160**	-0.822	3.66E-03
Pdgfc	1.648	6.85E-11	**Stoml2**	-0.821	1.37E-04
Arhgap15	1.648	4.00E-02	**0610010F05Rik**	-0.820	8.80E-04
Pwwp2b	1.646	6.13E-07	**Reps2**	-0.819	1.21E-02
A930007I19Rik	1.645	4.20E-02	**Etaa1**	-0.819	4.70E-03
Il17rc	1.644	3.51E-06	**Cenpm**	-0.819	2.10E-03
6330403K07Rik	1.643	8.05E-03	**Taf3**	-0.818	9.11E-04
Parp4	1.642	2.23E-12	**Syne2**	-0.818	3.47E-02
Boc	1.641	4.61E-12	**Tuba1b**	-0.817	2.57E-02
Nid1	1.639	2.51E-06	**Cep78**	-0.817	1.14E-03
Ldb2	1.639	2.07E-03	**Madd**	-0.817	4.79E-03
Lats2	1.638	2.15E-08	**Crmp1**	-0.816	3.99E-05
Gm15608	1.638	6.37E-03	**Nmd3**	-0.816	3.05E-03
Ache	1.638	2.10E-03	**Pot1b**	-0.816	4.28E-03
Cpeb3	1.637	4.56E-06	**Iars**	-0.816	1.44E-02
Drp2	1.635	2.74E-08	**Tmem265**	-0.816	1.55E-02
Amz1	1.633	4.49E-03	**Ints2**	-0.816	1.09E-03
Lipo3	1.632	6.43E-04	**Spc25**	-0.816	1.31E-03
Cds1	1.631	1.39E-04	**Fubp1**	-0.815	2.59E-04
Cpxm1	1.629	9.37E-07	**Eml4**	-0.814	8.81E-05
Maged2	1.627	3.89E-08	**Mphosph10**	-0.814	6.84E-03
Tst	1.625	9.99E-08	**Dcaf15**	-0.814	1.19E-03
Crebrf	1.624	4.56E-03	**Kcnc1**	-0.813	2.55E-03
Col4a5	1.623	5.61E-06	**Mphosph6**	-0.813	1.69E-04
Smpd1	1.623	4.64E-12	**Kmt5a**	-0.813	2.55E-02
B3galt2	1.622	1.05E-03	**Rrm1**	-0.813	1.96E-03
1700084E18Rik	1.621	3.52E-02	**Tsr2**	-0.813	5.48E-03
Plekhg3	1.620	1.28E-02	**Wdr5**	-0.813	4.74E-04
Gria1	1.618	3.79E-02	**Uaca**	-0.813	3.66E-03
Ptprj	1.617	3.54E-08	**Jpt2**	-0.812	2.84E-02
Lrp2	1.617	2.80E-03	**Srrt**	-0.812	1.24E-03
AV356131	1.614	5.02E-04	**Terf1**	-0.812	1.97E-02
Fgf11	1.613	1.71E-05	**Zfp280c**	-0.812	1.68E-02

Genes (UP)	log2FoldChange	padj	Genes (Down)	log2FoldChange	padj
Tmem158	1.611	1.17E-07	**Ddx56**	-0.812	8.29E-03
Slain1	1.610	2.21E-08	**Hmmr**	-0.811	5.11E-03
Lhfp	1.610	2.56E-16	**Gmnn**	-0.810	2.42E-02
Prune2	1.609	3.25E-15	**Ccdc86**	-0.810	4.58E-03
Peli3	1.609	3.98E-04	**Slc7a11**	-0.809	1.04E-04
Slc25a35	1.609	3.64E-03	**Urb1**	-0.809	2.05E-03
Il11ra1	1.609	6.85E-07	**Hnrnpa0**	-0.808	9.27E-06
Pmepa1	1.608	1.30E-03	**Rpl12**	-0.808	2.16E-02
Pcsk1n	1.607	2.02E-04	**Siva1**	-0.807	2.70E-03
Carns1	1.607	1.56E-02	**Pus7**	-0.807	3.64E-03
Slc25a42	1.606	1.38E-02	**Sox9**	-0.806	1.08E-02
Gm44899	1.606	1.39E-02	**Dffb**	-0.806	1.68E-02
Kcnmb4	1.605	1.33E-04	**Supt16**	-0.806	7.89E-04
B230311B06Rik	1.604	1.78E-03	**Psrc1**	-0.806	2.24E-03
Igsf3	1.604	5.70E-13	**Cpsf6**	-0.805	2.28E-04
Myo6	1.603	7.90E-06	**Mapk1ip1l**	-0.805	1.62E-04
Zbtb7c	1.602	6.10E-05	**Atp10a**	-0.805	4.68E-02
Ramp3	1.601	3.77E-02	**Paxip1**	-0.804	2.16E-04
Tmco3	1.601	6.66E-05	**Sass6**	-0.804	6.84E-03
Tdrp	1.600	2.00E-04	**Mrpl12**	-0.804	6.40E-04
Lmo7	1.598	1.14E-03	**Prep**	-0.803	6.35E-03
A730056A06Rik	1.594	4.60E-02	**Dnajc2**	-0.803	1.24E-03
Mcf2l	1.593	4.86E-09	**Rps11**	-0.803	5.27E-03
Gpc6	1.592	4.31E-08	**Nova1**	-0.801	4.58E-02
Map1a	1.592	1.59E-11	**Mrm3**	-0.801	6.27E-03
Kirrel3	1.591	1.84E-07	**Tmem41a**	-0.801	1.64E-02
Slit2	1.588	1.24E-02	**Lyn**	-0.801	3.95E-04
Slc43a2	1.588	2.94E-09	**Lin9**	-0.800	1.37E-02
Ggact	1.587	1.89E-07	**Wiz**	-0.800	9.88E-05
Tspo	1.584	1.37E-03	**Pask**	-0.799	6.66E-04
Coch	1.583	3.27E-03	**Krr1**	-0.798	1.01E-03
Tmem200a	1.581	5.93E-10	**Hic2**	-0.797	1.41E-02
AW047730	1.580	2.27E-06	**Rps5**	-0.797	3.50E-03
Etl4	1.578	1.44E-05	**Eif5a**	-0.797	1.55E-02
Oaf	1.576	1.72E-04	**Sf3b3**	-0.796	4.72E-03
Arsa	1.576	1.53E-06	**Lsm4**	-0.796	1.80E-04
Fmn1	1.576	1.08E-02	**Ipo5**	-0.795	2.36E-03
Igfbp3	1.575	3.96E-13	**Gm9844**	-0.793	3.08E-02
Cabp1	1.573	1.93E-02	**Frmd4a**	-0.793	4.66E-04
Jakmip3	1.572	4.60E-03	**Rpl7a**	-0.792	3.96E-04
Trmt9b	1.571	1.24E-03	**Plch1**	-0.792	4.81E-02
Nr1d1	1.569	4.43E-11	**Ndc80**	-0.792	2.82E-02
Zhx1	1.567	7.20E-10	**Txnrd1**	-0.792	4.42E-05

Genes (UP)	log2FoldChange	padj	Genes (Down)	log2FoldChange	padj
Dnm3	1.564	2.08E-02	**Rpl3**	-0.792	1.78E-03
Crim1	1.564	1.29E-12	**Stk40**	-0.792	7.15E-04
Cpt1c	1.563	1.70E-04	**Nab1**	-0.791	1.62E-03
Gm11734	1.563	7.34E-03	**Slc7a6**	-0.791	1.57E-03
Slco2a1	1.562	1.11E-02	**Nufip1**	-0.791	7.98E-03
Gm32618	1.561	4.65E-03	**Rfc5**	-0.791	1.26E-02
Entpd5	1.559	2.94E-05	**Ruvbl1**	-0.790	1.86E-02
Kcnmb4os2	1.559	5.16E-07	**Atf1**	-0.790	3.05E-03
Hs6st3	1.558	3.24E-02	**Sh3bgrl2**	-0.789	3.40E-02
Rb1	1.558	2.21E-09	**Hnrnph1**	-0.789	4.14E-03
Pla2g3	1.556	1.68E-03	**Rexo1**	-0.789	3.28E-05
Fhl4	1.556	2.22E-03	**Prelid3a**	-0.789	2.25E-02
Mn1	1.554	1.84E-11	**Zfp704**	-0.789	3.64E-02
Cdc42ep2	1.554	2.39E-02	**Zfp536**	-0.789	1.58E-02
Plscr4	1.553	6.47E-06	**E2f4**	-0.788	1.66E-04
Scd1	1.551	4.68E-10	**Specc1**	-0.788	1.26E-03
Fstl3	1.549	4.58E-02	**Uba2**	-0.788	1.20E-03
Itm2a	1.549	3.52E-04	**Ttc27**	-0.788	2.56E-03
Scn1b	1.548	7.05E-03	**Mrps30**	-0.788	7.10E-03
Trank1	1.547	2.19E-02	**Cdk2**	-0.788	7.59E-04
Unc13d	1.547	4.11E-03	**Mrps10**	-0.788	3.34E-03
Ablim1	1.547	5.49E-14	**Msh2**	-0.788	7.26E-04
Myh7b	1.546	2.72E-02	**Phf5a**	-0.787	4.20E-03
Ampd3	1.546	1.85E-06	**Hspe1**	-0.787	6.05E-03
Gbp9	1.543	1.04E-03	**Kyat3**	-0.786	4.18E-02
Cers1	1.542	4.02E-05	**Mrpl38**	-0.785	8.78E-03
Prkcd	1.542	2.16E-03	**Tyms**	-0.784	1.68E-02
Polr3gl	1.541	1.10E-06	**Cdc14a**	-0.784	1.76E-02
Stab1	1.540	3.94E-02	**Scrib**	-0.783	2.26E-04
Fras1	1.539	3.29E-06	**Haus4**	-0.783	1.36E-03
Epb41l3	1.539	3.34E-03	**Rfwd3**	-0.783	6.25E-04
Rab3il1	1.538	1.60E-06	**Rad54l2**	-0.783	1.60E-03
BC029722	1.538	4.95E-07	**Rnps1**	-0.783	3.70E-04
Plpp4	1.536	9.89E-03	**Psme3**	-0.783	1.66E-04
Eps8l1	1.535	7.98E-03	**Polr1c**	-0.783	5.82E-03
Bco2	1.534	1.32E-02	**Exosc3**	-0.783	5.00E-03
Aff3	1.533	2.02E-08	**Nudt5**	-0.783	1.37E-03
Rims1	1.532	7.76E-06	**Tut4**	-0.783	2.27E-04
Ptchd4	1.531	5.91E-03	**Gm9833**	-0.782	3.72E-03
Rom1	1.531	7.93E-04	**Slc25a30**	-0.782	1.92E-02
Ptprd	1.530	1.37E-04	**Sacs**	-0.782	3.48E-02
Helz2	1.530	1.55E-02	**Wdr73**	-0.782	4.70E-03
Isoc2b	1.529	5.30E-03	**Leo1**	-0.781	1.25E-04

Genes (UP)	log2FoldChange	padj	Genes (Down)	log2FoldChange	padj
Cebpd	1.526	4.66E-05	**Dgcr8**	-0.781	1.42E-03
B4galt1	1.526	3.60E-05	**Rpl22l1**	-0.780	1.42E-02
Abcc12	1.525	5.78E-09	**Rad54b**	-0.780	3.82E-02
Ddah1	1.524	1.35E-04	**Inpp5f**	-0.780	4.76E-04
Gria3	1.523	4.72E-06	**2810004N23Rik**	-0.780	3.22E-03
Grid2ip	1.522	1.02E-02	**Snx30**	-0.779	7.74E-03
Il6st	1.521	2.12E-10	**Pdcd2l**	-0.779	1.46E-02
Oplah	1.521	2.18E-04	**Cep97**	-0.779	2.76E-03
Copz2	1.520	1.23E-09	**Zfp141**	-0.779	4.01E-02
Ctsh	1.520	6.20E-04	**Otud4**	-0.779	5.15E-03
Syn2	1.519	1.03E-06	**Dpy30**	-0.778	6.44E-03
Chrm4	1.519	3.78E-02	**Gars**	-0.778	1.39E-02
Ntng2	1.518	6.94E-07	**Snrpe**	-0.777	2.10E-03
Ptpre	1.517	4.18E-02	**Elac2**	-0.777	6.73E-04
3110039M20Rik	1.515	6.80E-03	**Pms1**	-0.777	1.50E-02
Rnf182	1.514	1.39E-02	**Hoxa4**	-0.776	3.46E-03
Nqo1	1.514	1.74E-02	**Ipo4**	-0.776	1.49E-02
Abhd4	1.513	1.09E-05	**Polr3d**	-0.776	1.04E-02
2810430I11Rik	1.509	4.98E-02	**Msh3**	-0.775	2.27E-03
2010001A14Rik	1.508	1.63E-03	**Dcps**	-0.775	1.52E-03
Tmem141	1.507	1.95E-02	**Sf3a1**	-0.775	4.82E-04
Caps2	1.506	4.44E-02	**Homer1**	-0.774	9.61E-04
Sgcb	1.506	6.13E-09	**Lcor**	-0.774	2.18E-02
Hsd3b7	1.504	4.29E-06	**Rps26**	-0.774	7.93E-03
Htr2a	1.503	2.06E-03	**Ilf2**	-0.774	3.09E-03
Lix1l	1.503	8.06E-15	**Hes1**	-0.774	7.03E-03
Igdcc4	1.500	8.06E-03	**Mios**	-0.772	4.76E-03
Igf1	1.499	2.46E-02	**Slc25a25**	-0.772	1.08E-02
Acad12	1.494	3.87E-05	**Tnpo1**	-0.770	8.14E-03
Npr2	1.494	1.55E-07	**Smarca5**	-0.770	6.58E-04
Socs1	1.492	8.99E-03	**Orc2**	-0.769	3.86E-03
Hsdl2	1.492	7.18E-05	**Utp18**	-0.769	1.77E-03
Serpinb6a	1.492	3.89E-11	**Prr5**	-0.768	3.29E-02
Zfpm1	1.488	5.24E-06	**Sf1**	-0.767	1.25E-03
Iqsec1	1.488	6.96E-15	**Suz12**	-0.767	1.26E-03
Mmgt2	1.488	7.10E-06	**Wdr54**	-0.766	3.44E-02
Bambi	1.486	1.76E-07	**Nckap5l**	-0.766	2.63E-04
Baiap2l1	1.484	2.31E-02	**Sdc1**	-0.766	2.30E-02
Lama2	1.481	1.44E-03	**Jpt1**	-0.766	3.32E-03
Stom	1.479	1.02E-10	**Ing1**	-0.765	1.33E-04
Tgfb3	1.479	2.70E-03	**Rps18**	-0.765	1.32E-02
Ndrg1	1.478	5.97E-03	**Snu13**	-0.765	2.10E-03
Robo2	1.477	1.59E-02	**Nup133**	-0.764	5.46E-04

Genes (UP)	log2FoldChange	padj	Genes (Down)	log2FoldChange	padj
Il13ra1	1.477	1.01E-03	**Arhgap10**	-0.764	2.26E-02
Fads6	1.476	1.06E-06	**Fam204a**	-0.764	9.25E-04
Mertk	1.476	6.03E-03	**Fnip2**	-0.764	3.65E-03
Me3	1.476	7.66E-04	**Abt1**	-0.763	2.12E-03
Shpk	1.475	1.29E-03	**Zfp292**	-0.763	1.36E-02
Dmpk	1.471	1.27E-02	**Trp53rkb**	-0.763	1.07E-02
Slc12a5	1.469	2.70E-03	**Zfp770**	-0.762	9.14E-04
Ankrd29	1.468	8.40E-06	**Cntrl**	-0.762	1.26E-03
Epb41l4b	1.467	1.59E-11	**Etf1**	-0.762	5.35E-03
Mro	1.467	1.36E-08	**Nudc**	-0.762	3.45E-03
Col5a3	1.463	6.49E-06	**Adamts7**	-0.760	2.59E-02
C920021L13Rik	1.462	2.52E-02	**Lsm14b**	-0.760	1.24E-03
Tnfrsf23	1.462	5.21E-06	**Nsd2**	-0.760	3.55E-03
Irak2	1.461	6.56E-04	**Srsf1**	-0.759	5.42E-04
Msrb3	1.461	6.60E-12	**Auts2**	-0.759	3.55E-03
Myrip	1.460	6.04E-04	**Cfap298**	-0.759	2.32E-02
Ndrg4	1.458	2.47E-03	**Cct2**	-0.759	7.40E-03
Atp9a	1.457	1.40E-04	**Coa7**	-0.758	8.04E-03
Nrep	1.456	4.95E-04	**Map3k3**	-0.758	1.38E-02
Trim25	1.455	2.55E-03	**Trmt10c**	-0.758	1.84E-02
Glul	1.455	3.99E-06	**Rfc2**	-0.758	9.38E-04
Grina	1.454	1.55E-06	**Cenpq**	-0.757	3.93E-03
Pdzd2	1.451	3.49E-02	**Rsl24d1**	-0.757	1.65E-03
Capn1	1.451	3.29E-06	**Rps13**	-0.757	1.12E-02
Gm4285	1.450	2.42E-02	**Mars2**	-0.757	6.14E-03
Cadm4	1.449	7.49E-07	**AI506816**	-0.757	8.48E-05
Hsd17b11	1.449	1.95E-02	**Hprt**	-0.757	4.23E-02
Tifa	1.448	7.72E-05	**Zfp930**	-0.757	2.58E-02
Prkag2	1.445	1.70E-09	**Rpl13a**	-0.756	1.87E-02
Fam241a	1.444	1.19E-06	**Fastkd2**	-0.756	6.39E-03
Mxd4	1.442	1.06E-04	**Mdc1**	-0.755	9.11E-04
Herc6	1.442	1.43E-02	**Plvap**	-0.755	8.80E-03
A330074K22Rik	1.441	2.21E-02	**Nudcd2**	-0.755	6.38E-04
Adam9	1.441	2.10E-08	**Antxr2**	-0.755	2.21E-02
Srrm3	1.440	1.02E-02	**Ddx41**	-0.755	6.71E-04
Dnase1l1	1.440	6.05E-03	**Dot1l**	-0.755	1.07E-04
Dtx1	1.437	4.19E-04	**Rad18**	-0.754	2.62E-03
Celrr	1.434	5.43E-04	**Clpp**	-0.754	1.63E-03
Klf4	1.433	7.34E-04	**Rpl14**	-0.753	1.40E-02
Rnf180	1.433	1.09E-07	**Aimp2**	-0.753	2.26E-02
Foxc2	1.433	2.82E-02	**Dusp4**	-0.752	7.13E-04
Eif2ak2	1.430	1.72E-04	**Eif4ebp2**	-0.752	1.25E-02
Cpeb2	1.429	3.22E-05	**Chchd1**	-0.752	4.61E-03

Genes (UP)	log2FoldChange	padj	Genes (Down)	log2FoldChange	padj
Fam184b	1.429	3.70E-03	**Nup88**	-0.752	2.34E-04
Fbxo41	1.428	9.36E-03	**Trnt1**	-0.752	1.19E-03
Ttc30b	1.424	3.46E-04	**Rps27a**	-0.752	1.17E-02
E530011L22Rik	1.422	5.81E-03	**Riok2**	-0.751	8.10E-03
Cx3cl1	1.420	1.10E-07	**Ipo11**	-0.751	5.04E-03
C2	1.420	2.30E-02	**Rps6**	-0.750	9.68E-03
Myof	1.419	1.99E-06	**Epb41**	-0.750	2.60E-04
Nuak2	1.418	4.68E-02	**Xpo4**	-0.750	3.63E-03
Cdc42ep4	1.417	8.62E-09	**Arhgap29**	-0.749	4.80E-03
Ppargc1a	1.417	1.75E-05	**Ccnb2**	-0.749	1.22E-02
Adra1b	1.416	1.51E-06	**Snrpb**	-0.748	4.51E-03
Nkpd1	1.414	3.90E-02	**Zfp553**	-0.748	3.60E-04
Slc35f1	1.412	1.21E-04	**Haus1**	-0.748	9.93E-03
Minar2	1.412	2.85E-03	**Ska2**	-0.747	5.46E-03
Sidt2	1.412	1.33E-08	**Prdm15**	-0.747	5.18E-03
Kcnd1	1.411	6.10E-04	**Tra2b**	-0.746	9.63E-04
Ppp1r14c	1.410	8.63E-06	**Rars**	-0.746	1.29E-02
Hyal1	1.410	7.72E-04	**Naa15**	-0.745	1.16E-02
Gm49708	1.409	1.77E-02	**Lrrc59**	-0.745	2.32E-02
Ctsf	1.408	1.22E-04	**Rpl27a**	-0.745	2.15E-02
Grid1	1.407	2.31E-06	**Fanca**	-0.745	2.18E-02
Trim21	1.406	2.05E-02	**Serbp1**	-0.744	6.00E-04
Pxdc1	1.405	4.72E-06	**2610021A01Rik**	-0.744	4.03E-02
Frem1	1.404	1.88E-02	**Twistnb**	-0.744	2.06E-02
Strip2	1.404	1.19E-03	**Zfp143**	-0.743	4.12E-03
C130021I20Rik	1.403	1.73E-02	**Ugt8a**	-0.743	1.99E-02
5730409E04Rik	1.402	6.17E-04	**Rps23**	-0.743	2.41E-02
Plod1	1.402	7.53E-08	**Ctcf**	-0.743	2.78E-04
Sema4d	1.401	1.42E-10	**Lrpprc**	-0.743	4.32E-03
1600014C10Rik	1.399	8.38E-06	**Saal1**	-0.742	1.55E-03
D130058E05Rik	1.399	1.33E-03	**Prom1**	-0.742	2.30E-03
Patj	1.399	1.36E-05	**Tsen54**	-0.742	4.47E-03
Fam214a	1.398	4.66E-04	**Esf1**	-0.741	1.12E-02
Pink1	1.394	9.41E-07	**Tmeff1**	-0.741	2.44E-03
Anxa7	1.394	3.76E-06	**Jmjd7**	-0.741	6.78E-03
Glud1	1.393	2.40E-04	**Slc39a10**	-0.741	6.39E-03
Tmeff2	1.390	9.17E-08	**Ccdc88c**	-0.740	3.70E-02
Cxxc5	1.390	1.09E-08	**Ano8**	-0.739	1.15E-04
Gabre	1.390	1.86E-04	**Plekha5**	-0.739	1.78E-03
Sytl4	1.388	7.96E-06	**Gle1**	-0.739	3.91E-03
Pfn4	1.386	3.16E-03	**Calm1**	-0.738	1.86E-04
Efnb2	1.386	5.47E-05	**Prps1l3**	-0.737	2.03E-03
Tgfb2	1.385	1.61E-07	**Frat2**	-0.737	3.58E-02

Genes (UP)	log2FoldChange	padj	Genes (Down)	log2FoldChange	padj
Sema3a	1.385	2.00E-05	**Sac3d1**	-0.737	1.77E-02
Hapln4	1.384	4.95E-11	**Nbn**	-0.737	9.60E-04
Arhgap20	1.383	4.35E-10	**Mthfd1**	-0.737	4.58E-04
Rsph9	1.382	1.80E-03	**Pde7a**	-0.737	1.91E-03
Ppm1h	1.382	7.16E-05	**Top3a**	-0.736	2.28E-02
D330050G23Rik	1.380	3.62E-03	**Ppp5c**	-0.736	3.23E-04
Cpt1a	1.379	1.32E-06	**Celf1**	-0.736	1.67E-03
Fgf1	1.379	3.77E-08	**Nfyb**	-0.736	4.63E-03
Tcf7l1	1.378	1.55E-07	**BC052040**	-0.735	2.66E-02
Fbxl2	1.378	4.51E-04	**Vps16**	-0.735	5.23E-04
Fbxl7	1.378	1.07E-03	**Bud23**	-0.734	2.85E-03
Epb41l2	1.378	4.48E-10	**Nol11**	-0.734	4.98E-03
Tnfaip3	1.375	1.04E-02	**Fancf**	-0.734	1.39E-02
Mmp14	1.372	1.76E-06	**B3galnt2**	-0.734	1.07E-02
Myh14	1.372	5.71E-07	**Rev1**	-0.734	3.53E-03
Fzd5	1.370	9.10E-08	**Ing2**	-0.733	3.34E-03
Znfx1	1.369	3.63E-11	**Ctu2**	-0.733	4.54E-03
Nat8f4	1.369	1.82E-03	**Usp37**	-0.733	3.36E-03
Plxnc1	1.367	1.79E-03	**Fbxl14**	-0.732	1.08E-03
Izumo4	1.365	3.85E-05	**Edc3**	-0.732	6.32E-04
Psmb10	1.363	1.81E-10	**Phf6**	-0.732	1.65E-03
Snapin	1.362	7.91E-09	**Tmem186**	-0.732	5.90E-03
Tapbpl	1.361	3.81E-03	**Nup155**	-0.731	1.24E-02
Mgat4a	1.361	1.17E-04	**Prpf31**	-0.731	8.59E-03
Dnajb9	1.361	3.00E-04	**Gpsm2**	-0.730	1.66E-03
Tcaf2	1.358	4.96E-03	**Arrb1**	-0.730	3.36E-03
Hist1h2bg	1.358	3.01E-02	**Cct6a**	-0.729	1.92E-02
Prickle1	1.357	7.07E-05	**Morc2a**	-0.729	1.44E-03
Chrna4	1.357	8.66E-03	**Poglut2**	-0.729	6.63E-03
Bnip3	1.355	1.65E-05	**Dhx9**	-0.728	3.53E-03
Serpinb5	1.355	1.59E-03	**Srgap2**	-0.728	1.38E-04
Nipa1	1.354	3.14E-06	**Ppp2r1b**	-0.727	5.31E-03
Plaat3	1.353	1.22E-02	**Nusap1**	-0.726	3.55E-03
0610009L18Rik	1.353	3.10E-02	**Rnmt**	-0.725	9.08E-04
Ikbke	1.352	7.68E-03	**Gal3st3**	-0.725	4.99E-03
Tubb3	1.351	1.54E-04	**Dsn1**	-0.725	5.82E-03
Ankrd44	1.351	1.05E-02	**Snrpd3**	-0.725	1.18E-02
Cd248	1.351	2.21E-03	**Csnk1e**	-0.724	4.86E-04
Itm2b	1.351	1.87E-07	**Marcksl1**	-0.724	9.97E-05
Loxl2	1.350	1.67E-05	**Isg20l2**	-0.724	5.17E-04
Anxa3	1.348	8.66E-03	**Bop1**	-0.724	3.77E-02
Cpne2	1.347	1.01E-02	**Fzr1**	-0.724	1.43E-03
Fah	1.347	3.14E-03	**Gldc**	-0.723	3.51E-04

Genes (UP)	log2FoldChange	padj	Genes (Down)	log2FoldChange	padj
2410022M11Rik	1.347	1.33E-04	**Prpf38a**	-0.723	2.47E-03
Tgfb1i1	1.346	4.70E-04	**Dnajc9**	-0.723	4.23E-04
Wwc2	1.345	9.49E-12	**Nol10**	-0.722	8.30E-03
Grn	1.343	2.10E-10	**Orc6**	-0.722	6.90E-03
Gm49164	1.343	1.86E-02	**Ttc26**	-0.722	2.83E-02
2900093K20Rik	1.341	2.71E-02	**Polr2h**	-0.722	1.36E-02
Ripor2	1.339	4.86E-03	**Rpl10a**	-0.721	7.40E-03
Inf2	1.339	3.83E-10	**Tmed8**	-0.720	5.23E-03
1500009C09Rik	1.338	2.04E-03	**Alg3**	-0.720	2.52E-03
Rcn3	1.338	1.06E-04	**Pot1a**	-0.720	3.36E-03
Cables1	1.337	3.19E-04	**Tomm40**	-0.720	4.58E-03
H2-T22	1.336	3.74E-05	**Zfp146**	-0.720	9.36E-04
Mgst1	1.336	1.61E-07	**Cplx2**	-0.719	9.89E-03
Camk2d	1.336	2.49E-11	**Utp6**	-0.719	2.78E-03
Capn5	1.336	2.19E-02	**Mettl4**	-0.719	7.39E-03
Epb41l1	1.334	1.40E-03	**Mrpl50**	-0.719	2.80E-03
Fam20c	1.332	1.92E-05	**Ctif**	-0.718	1.01E-03
Notch4	1.331	5.05E-03	**Zbtb39**	-0.718	4.23E-03
Lingo4	1.331	1.37E-03	**Angptl2**	-0.717	1.28E-02
Actn1	1.328	1.89E-04	**Rpl4**	-0.717	7.52E-03
Nrg1	1.326	7.10E-04	**Rpl5**	-0.717	2.80E-03
Mkx	1.323	4.44E-02	**Rps2**	-0.717	4.65E-02
Nudt7	1.323	7.92E-04	**Rap2c**	-0.717	8.12E-03
Hacl1	1.322	9.41E-05	**Zfp451**	-0.716	1.66E-03
Vsig10l	1.321	1.05E-03	**Btaf1**	-0.716	5.23E-03
Ehhadh	1.321	1.79E-02	**Miip**	-0.715	2.93E-02
Zfp791	1.320	3.43E-02	**Pycr2**	-0.715	5.58E-03
Itga10	1.319	1.57E-02	**Map2**	-0.715	4.40E-04
2610035D17Rik	1.319	3.12E-03	**Hnrnph3**	-0.715	9.71E-04
Pdk1	1.316	6.36E-05	**Snrpa1**	-0.714	2.05E-03
Abhd14b	1.316	6.61E-03	**Phf10**	-0.714	1.03E-03
Gsn	1.315	6.34E-04	**Pnn**	-0.714	9.79E-04
Emc9	1.315	1.03E-02	**Ptcd3**	-0.713	2.50E-03
Tln2	1.314	8.23E-11	**Sec11c**	-0.713	1.11E-03
Gm42067	1.314	8.79E-03	**Zfp101**	-0.713	1.21E-02
Cpeb1	1.313	4.41E-03	**Ppp1r8**	-0.713	2.04E-03
Agl	1.313	1.08E-06	**Cdc20**	-0.712	4.15E-02
Klhl29	1.312	3.12E-05	**Ssh2**	-0.712	5.64E-03
D330023K18Rik	1.312	2.51E-02	**Trap1**	-0.711	1.42E-03
Ppp1r3c	1.311	4.54E-03	**Trio**	-0.711	1.13E-02
Nod1	1.310	3.59E-03	**Cct8**	-0.711	5.77E-03
Erc2	1.309	2.27E-07	**Ankrd10**	-0.711	1.65E-03
Rps6ka5	1.308	7.36E-05	**Pgm2**	-0.711	8.86E-04

Genes (UP)	log2FoldChange	padj	Genes (Down)	log2FoldChange	padj
Mcc	1.307	5.36E-05	**Gmeb2**	-0.710	2.93E-03
Plce1	1.307	1.37E-06	**Ahsa1**	-0.710	2.35E-03
Brinp2	1.306	1.68E-02	**Ibtk**	-0.710	4.18E-03
Sfrp1	1.304	4.62E-06	**Arfrp1**	-0.710	5.15E-03
Gm10643	1.303	2.38E-02	**Btbd8**	-0.710	4.82E-02
Rab11fip5	1.303	2.14E-08	**Plagl2**	-0.710	2.02E-02
Pdzd7	1.302	7.48E-03	**Rps28**	-0.709	3.74E-02
4930402H24Rik	1.301	3.54E-03	**Tdg**	-0.709	3.12E-03
Gbx2	1.299	3.95E-02	**Akap1**	-0.709	2.47E-03
Glt8d2	1.298	6.37E-03	**Zfp365**	-0.709	8.66E-03
Rab3d	1.295	6.72E-04	**Fanci**	-0.709	1.58E-02
Aatk	1.294	1.13E-05	**Pop1**	-0.709	1.97E-03
Gm30025	1.293	3.46E-03	**Hgh1**	-0.708	2.44E-02
Tcta	1.293	2.24E-06	**Knstrn**	-0.708	4.33E-02
1700096K18Rik	1.293	7.10E-03	**Mettl2**	-0.708	1.14E-02
Sfxn5	1.290	3.82E-04	**Dtymk**	-0.708	2.29E-03
Hist1h1e	1.287	1.33E-02	**Riox2**	-0.708	4.07E-02
Aph1c	1.285	2.66E-02	**A430005L14Rik**	-0.707	9.24E-03
Nr4a2	1.285	3.52E-04	**Rrp7a**	-0.707	1.76E-02
Lratd1	1.285	4.65E-02	**Tasor2**	-0.707	1.48E-02
Pdp1	1.284	8.96E-04	**Itpa**	-0.707	9.64E-03
Kcnt1	1.284	6.98E-04	**Cpox**	-0.706	2.65E-03
Zmat1	1.284	1.00E-04	**Luc7l**	-0.706	3.41E-04
Steap1	1.284	3.55E-03	**Rpl18**	-0.706	6.58E-03
Nos1	1.284	7.30E-03	**Nup54**	-0.705	8.72E-03
Gpr155	1.283	8.19E-05	**Ado**	-0.705	1.31E-03
Hs3st3b1	1.282	2.11E-02	**Rnf220**	-0.704	2.56E-03
Apba1	1.282	2.76E-02	**Gls**	-0.703	1.01E-02
Lgalsl	1.282	2.96E-11	**Smc4**	-0.703	1.56E-02
Sel1l3	1.280	5.68E-03	**Arhgap18**	-0.703	5.48E-03
2010315B03Rik	1.280	1.14E-04	**Hmgn2**	-0.703	1.06E-03
Cav2	1.278	2.65E-05	**Wsb1**	-0.703	1.87E-03
Ccdc122	1.278	1.34E-03	**Med10**	-0.703	3.76E-02
Itprid2	1.277	5.02E-10	**1110059E24Rik**	-0.702	9.35E-03
Sqor	1.277	1.97E-04	**Nkrf**	-0.702	6.65E-03
Klhdc8b	1.276	1.27E-03	**Prkd3**	-0.702	5.48E-03
Sipa1l1	1.276	3.63E-12	**Myef2**	-0.702	1.84E-03
Slc37a2	1.276	3.55E-03	**Tcf12**	-0.702	6.30E-04
Cdk6	1.273	9.64E-04	**Rps20**	-0.701	1.46E-02
Bmpr1a	1.273	1.31E-04	**Tada2a**	-0.700	5.51E-03
Artn	1.272	1.86E-02	**Pwwp2a**	-0.699	1.53E-03
Ephb2	1.272	7.12E-12	**Cit**	-0.699	2.47E-03
Zfp521	1.272	2.01E-10	**Rhno1**	-0.698	1.15E-02

Genes (UP)	log2FoldChange	padj	Genes (Down)	log2FoldChange	padj
Ebf4	1.272	2.01E-03	**Xrcc1**	-0.697	5.94E-03
Spon1	1.272	8.18E-04	**Ncapd3**	-0.697	9.16E-03
Itgav	1.270	3.74E-09	**C2cd5**	-0.697	6.44E-03
Car13	1.269	2.58E-03	**Nabp2**	-0.697	1.61E-02
Camk1g	1.267	1.61E-03	**Ints7**	-0.697	9.03E-04
Tmem229b	1.266	6.19E-07	**Xrcc3**	-0.696	2.23E-02
Galt	1.265	8.87E-05	**Rbm10**	-0.696	5.93E-03
Ypel3	1.265	4.33E-03	**Psmg4**	-0.696	7.52E-03
Perm1	1.264	4.34E-02	**Hpf1**	-0.696	3.99E-03
Mgst3	1.262	7.36E-05	**Lin54**	-0.696	2.39E-02
Foxj1	1.261	2.91E-04	**Mapk7**	-0.696	5.15E-03
Enho	1.261	2.96E-05	**Dph5**	-0.696	8.44E-03
Mar-02	1.261	5.33E-04	**Prim2**	-0.695	4.90E-03
Myorg	1.260	1.98E-10	**Bag4**	-0.695	4.20E-03
Lncppara	1.259	1.84E-02	**Dab1**	-0.695	4.65E-03
Cers4	1.258	6.02E-04	**Elp6**	-0.695	2.82E-02
Gm12473	1.258	1.75E-02	**Ccdc14**	-0.694	3.06E-02
Crebl2	1.256	7.57E-04	**Foxp4**	-0.694	1.94E-02
Kazn	1.256	6.50E-06	**Rae1**	-0.694	1.89E-02
Tsc22d3	1.256	1.66E-06	**Actr5**	-0.693	1.03E-02
Casp1	1.256	3.24E-03	**Gnpat**	-0.693	1.82E-03
Gpr157	1.255	3.20E-02	**Tacc3**	-0.693	7.81E-03
Dzank1	1.255	2.64E-02	**Zbtb17**	-0.693	1.16E-03
Tlr6	1.255	7.31E-03	**Rack1**	-0.693	1.34E-02
Dynlt3	1.253	1.32E-06	**Casp2**	-0.693	2.37E-03
Tex264	1.252	2.43E-07	**Naa40**	-0.692	1.60E-03
Bvht	1.252	4.17E-02	**Pelp1**	-0.692	1.67E-03
Tex2	1.252	2.99E-07	**Eri1**	-0.692	1.04E-03
Pyroxd2	1.251	3.42E-03	**Rapgef3**	-0.691	4.90E-02
Fam234a	1.249	1.17E-04	**Rpl6**	-0.691	1.32E-02
Tns1	1.249	5.60E-03	**Smn1**	-0.691	3.19E-02
Agpat3	1.248	8.98E-09	**Zfp958**	-0.691	4.32E-02
Gpc3	1.248	4.76E-02	**Ndufaf4**	-0.691	7.40E-03
Arrdc4	1.247	7.95E-05	**Cct7**	-0.691	1.87E-02
Cyp2j9	1.247	5.04E-03	**Ak2**	-0.691	7.49E-04
Mvp	1.246	6.27E-06	**Tubg1**	-0.691	2.24E-03
Sybu	1.245	3.16E-07	**Pgam5**	-0.690	2.98E-03
Tlr4	1.245	1.35E-04	**Bud13**	-0.689	1.62E-02
Usp35	1.245	7.71E-05	**Gatb**	-0.689	1.27E-02
Abca7	1.244	4.43E-06	**Pds5a**	-0.689	1.19E-02
Rasl10b	1.244	1.26E-04	**Ppm1g**	-0.689	3.89E-03
Gm49492	1.243	3.51E-02	**Zgrf1**	-0.688	3.02E-02
Pex11a	1.242	6.30E-04	**Dcaf1**	-0.688	2.14E-02

Genes (UP)	log2FoldChange	padj	Genes (Down)	log2FoldChange	padj
Rab11fip4	1.242	9.86E-03	**Eif2s1**	-0.688	1.16E-02
Dap	1.241	9.02E-06	**Piga**	-0.688	4.69E-03
Dok4	1.240	1.52E-04	**Farsa**	-0.688	2.66E-03
Ston1	1.240	4.43E-03	**Gtf2h2**	-0.688	2.50E-02
Tmem86a	1.240	3.82E-04	**Mdm4**	-0.688	4.76E-03
Col25a1	1.239	9.97E-04	**Tmsb10**	-0.688	1.96E-03
Thbs3	1.238	6.28E-10	**Surf2**	-0.687	1.53E-02
Suox	1.237	3.16E-04	**H1f0**	-0.687	3.66E-03
Slc49a4	1.237	1.75E-10	**E2f3**	-0.687	1.54E-03
Gm4524	1.237	3.32E-02	**Hist1h4i**	-0.687	5.42E-03
Prickle2	1.236	4.27E-03	**Ammecr1**	-0.687	1.05E-02
Kctd21	1.235	3.33E-04	**Ppp1r35**	-0.686	1.20E-02
Tspan11	1.234	3.06E-04	**Aif1l**	-0.686	3.22E-03
B3gnt2	1.233	1.61E-07	**Znrd2**	-0.686	1.94E-02
C1ql1	1.231	4.13E-02	**Rps19**	-0.685	3.86E-02
Nav1	1.231	6.81E-10	**Eif3g**	-0.685	1.70E-02
Nbl1	1.231	1.34E-02	**Fbxo31**	-0.685	9.86E-03
Gldn	1.230	3.64E-02	**Anp32e**	-0.684	2.78E-03
Epm2a	1.229	6.43E-04	**Cdc42se2**	-0.684	1.14E-02
Smim14	1.228	5.89E-07	**Nudcd3**	-0.683	9.46E-04
Fyco1	1.227	1.39E-07	**Pin1**	-0.683	2.19E-02
Lrig1	1.226	1.31E-03	**Pym1**	-0.682	4.73E-03
Klf11	1.226	6.69E-03	**Rev3l**	-0.682	1.74E-02
Plekhb2	1.226	3.96E-06	**H2afy2**	-0.681	5.09E-03
Ctnna2	1.226	1.02E-03	**Rpl30**	-0.681	2.33E-02
Mylk	1.225	4.10E-02	**Fancd2**	-0.681	3.58E-03
Atg10	1.224	2.77E-03	**Pcgf6**	-0.681	5.15E-03
Vegfc	1.224	1.69E-02	**Ap1m1**	-0.680	4.70E-04
Pdlim2	1.221	2.61E-02	**Smg9**	-0.680	3.73E-03
Pax2	1.221	1.42E-04	**Gtf2e2**	-0.679	1.53E-03
Zbtb20	1.219	7.69E-03	**Rrn3**	-0.678	4.85E-03
Grik5	1.219	2.25E-07	**Nvl**	-0.678	1.17E-02
Tspoap1	1.219	2.42E-03	**Gmps**	-0.677	2.40E-02
Dlgap3	1.218	1.10E-05	**Rps3a1**	-0.677	4.67E-03
Hspa12a	1.218	9.38E-04	**Tamm41**	-0.677	9.48E-03
Slc6a6	1.217	1.34E-10	**Ssbp1**	-0.677	3.52E-02
Hs3st1	1.216	3.68E-02	**Fkbp1a**	-0.677	3.33E-03
Itfg1	1.216	4.61E-08	**Gypc**	-0.676	4.46E-02
Peli2	1.215	1.74E-09	**Gtpbp3**	-0.676	1.17E-03
Gprc5b	1.215	9.75E-04	**Zc3h18**	-0.676	1.55E-03
6330403L08Rik	1.213	1.24E-05	**Ccdc50**	-0.676	3.34E-03
Tspan9	1.213	6.90E-09	**Gtpbp10**	-0.676	1.59E-02
Slc26a1	1.212	4.50E-03	**Nsmce4a**	-0.676	9.29E-04

Genes (UP)	log2FoldChange	padj	Genes (Down)	log2FoldChange	padj
Neu3	1.212	3.49E-03	**Cdca3**	-0.675	2.93E-03
Sesn3	1.210	1.11E-03	**Acin1**	-0.675	3.83E-03
Rida	1.210	6.04E-04	**Kif4**	-0.675	4.56E-02
Tmem9b	1.210	4.32E-05	**Bzw2**	-0.675	2.13E-03
Klf8	1.208	1.33E-02	**Agap1**	-0.675	3.03E-02
Cdsn	1.207	1.25E-03	**Arhgap39**	-0.675	1.58E-02
Acox1	1.206	1.44E-05	**Gm10282**	-0.674	5.30E-03
Col11a1	1.206	9.83E-10	**Ankrd54**	-0.674	8.39E-03
Gria2	1.206	4.33E-06	**Noa1**	-0.674	3.08E-02
Syt11	1.206	1.88E-04	**Ythdf2**	-0.674	2.49E-03
Chrnb1	1.205	2.80E-02	**Gas2l3**	-0.673	2.11E-02
Slc26a2	1.205	1.10E-08	**Fancb**	-0.673	2.16E-02
Zfp108	1.204	5.51E-03	**Syncrip**	-0.673	7.19E-03
Acadsb	1.204	2.56E-05	**Spata24**	-0.673	1.98E-02
Nagk	1.203	2.15E-04	**Usp7**	-0.673	3.80E-03
Pfkm	1.203	3.99E-05	**Dhrs13**	-0.673	5.40E-03
Borcs8	1.200	2.07E-07	**Cct3**	-0.673	5.50E-03
Zfp949	1.200	7.21E-04	**Wrnip1**	-0.672	1.70E-02
Col4a2	1.198	1.55E-07	**Soga1**	-0.672	7.72E-03
Fam43a	1.198	1.20E-02	**Polr2f**	-0.672	4.61E-03
Aox1	1.198	1.11E-03	**2410002F23Rik**	-0.671	1.46E-03
Appl2	1.198	9.62E-04	**Phb2**	-0.670	1.84E-03
Hbegf	1.197	4.68E-05	**Mrpl39**	-0.670	5.45E-03
Crb2	1.197	3.70E-03	**Pdap1**	-0.670	2.60E-02
Csrp1	1.196	2.38E-04	**Spata13**	-0.670	1.30E-02
Akap6	1.196	1.15E-03	**Xylt1**	-0.670	2.30E-02
Dstyk	1.195	7.46E-03	**Srek1**	-0.670	2.24E-03
Sfxn4	1.195	7.05E-03	**Dph1**	-0.670	8.10E-03
Tmem150a	1.194	2.51E-06	**Rpl18a**	-0.670	9.15E-03
Cryl1	1.194	2.80E-03	**Ptcd2**	-0.670	3.23E-03
2310022B05Rik	1.194	2.07E-06	**Donson**	-0.669	8.16E-03
Csrnp1	1.193	6.84E-07	**Bche**	-0.669	1.97E-02
Dlx2	1.193	2.09E-03	**Trmt6**	-0.668	7.92E-03
Frg2f1	1.193	7.85E-03	**Grpel2**	-0.668	7.60E-03
Ephb1	1.192	9.45E-08	**Nup50**	-0.668	1.92E-03
Prdx5	1.191	9.56E-07	**Det1**	-0.668	1.87E-02
Spns2	1.191	9.44E-03	**Ttf2**	-0.668	4.20E-02
Acbd5	1.190	3.56E-06	**Rfx7**	-0.667	4.28E-03
Fam71e1	1.190	4.20E-03	**Trmt10a**	-0.667	4.04E-02
Ntn3	1.189	5.60E-06	**Xndc1**	-0.667	2.75E-02
Card19	1.189	6.42E-04	**Magoh**	-0.665	1.41E-02
Bcan	1.189	5.73E-05	**Eif4e**	-0.665	4.99E-03
Samd4	1.186	2.93E-09	**Bms1**	-0.665	7.48E-03

Genes (UP)	log2FoldChange	padj	Genes (Down)	log2FoldChange	padj
Tcn2	1.185	1.34E-05	**Rpl28**	-0.665	1.29E-02
Grk4	1.183	3.86E-04	**Tlnrd1**	-0.664	4.60E-03
Mtmr7	1.182	1.53E-02	**Larp1**	-0.664	3.19E-02
D630045J12Rik	1.181	7.15E-03	**Ndufc2**	-0.663	4.14E-03
Cntnap1	1.180	1.73E-02	**Mex3d**	-0.663	6.84E-03
Gstm1	1.180	6.13E-03	**Rtkn**	-0.663	6.05E-03
Aktip	1.180	1.22E-08	**Zcchc8**	-0.663	6.27E-03
Ikzf4	1.179	3.28E-02	**Hist3h2ba**	-0.663	4.74E-02
Trp53inp2	1.179	8.81E-04	**Snrpb2**	-0.663	1.95E-03
Tspan4	1.178	2.00E-03	**mt-Nd1**	-0.663	6.84E-03
Cyp2u1	1.178	3.13E-03	**Lrrc8b**	-0.662	3.43E-02
Itga2	1.176	9.38E-04	**Ddx55**	-0.662	1.36E-02
Hspb6	1.176	7.97E-04	**Siah1b**	-0.662	1.87E-02
P2rx3	1.173	5.31E-03	**Nme6**	-0.662	3.97E-02
Mthfs	1.172	2.60E-02	**Ugcg**	-0.661	2.79E-02
Bace2	1.169	1.92E-02	**Nedd1**	-0.661	2.82E-02
Rnasel	1.168	1.01E-02	**Pms2**	-0.661	1.81E-02
Kit	1.167	2.71E-03	**Tfrc**	-0.661	7.98E-04
Tceal1	1.167	1.32E-04	**Ddx10**	-0.660	3.99E-02
Abcb9	1.167	4.09E-03	**Mtmr12**	-0.660	6.85E-03
Arhgef4	1.166	9.14E-06	**Mrpl58**	-0.660	4.11E-03
Emp3	1.165	1.62E-02	**Elp1**	-0.660	7.50E-03
H2-Q4	1.164	1.45E-02	**Creb1**	-0.659	1.17E-02
Tor3a	1.162	3.54E-03	**Jmjd6**	-0.658	1.69E-02
Map1lc3a	1.162	2.39E-05	**Cenpx**	-0.658	1.03E-02
Lrch1	1.161	7.24E-03	**Hsp90aa1**	-0.658	6.50E-03
Hspa1a	1.161	3.61E-02	**Mrps35**	-0.657	3.82E-03
Tmem205	1.161	2.92E-05	**Neto1**	-0.657	7.40E-03
Mapk10	1.160	2.23E-03	**Tbc1d1**	-0.657	6.95E-03
Sdc4	1.160	1.44E-02	**Smarcd1**	-0.657	1.34E-03
Pbxip1	1.160	4.06E-06	**Kpnb1**	-0.657	4.30E-02
Sema3d	1.160	8.25E-04	**St3gal4**	-0.657	1.49E-02
Fgfbp3	1.158	1.13E-03	**Smc3**	-0.657	4.20E-03
Rasl11b	1.157	6.91E-04	**Gale**	-0.656	5.99E-03
Psen2	1.156	1.29E-03	**Srsf10**	-0.656	3.12E-03
Ddr1	1.155	2.27E-07	**Dhx33**	-0.655	3.24E-03
Abca5	1.155	2.87E-02	**Sirt1**	-0.655	4.68E-02
Rin2	1.154	4.52E-05	**Ppie**	-0.655	1.53E-02
Kcnn3	1.153	7.70E-03	**Ctdp1**	-0.655	2.04E-02
Acad11	1.152	2.77E-05	**Rrp8**	-0.655	3.59E-02
Snca	1.152	2.78E-04	**Arl6ip4**	-0.654	4.09E-02
Galnt10	1.152	2.73E-09	**Hmg20a**	-0.654	7.57E-03
AA986860	1.152	4.41E-02	**Naca**	-0.654	1.30E-02

Genes (UP)	log2FoldChange	padj	Genes (Down)	log2FoldChange	padj
Pakap	1.151	4.56E-02	**Vac14**	-0.654	8.89E-03
Tns3	1.151	4.90E-05	**Chtf18**	-0.654	3.70E-02
Osbpl3	1.150	2.88E-07	**Oard1**	-0.653	1.98E-02
Optn	1.150	1.47E-04	**Sgo2a**	-0.653	4.49E-02
Sdr42e1	1.149	1.42E-02	**Tbpl1**	-0.651	1.25E-02
C330011M18Rik	1.149	1.49E-02	**Rpl17**	-0.651	3.21E-02
Ccpg1	1.145	5.23E-03	**Fance**	-0.651	7.75E-03
Sat1	1.144	1.42E-02	**Cnot3**	-0.651	1.52E-03
Itpkb	1.141	1.26E-03	**Cep57**	-0.651	1.75E-02
Apobec3	1.141	2.82E-02	**Cenpl**	-0.651	2.58E-02
Bmpr2	1.141	1.18E-04	**Srrm1**	-0.650	5.01E-03
Ikbip	1.140	2.31E-07	**L2hgdh**	-0.650	9.25E-03
2500004C02Rik	1.139	6.08E-03	**Yeats4**	-0.649	3.04E-03
Hspg2	1.139	6.44E-06	**Eif3e**	-0.649	1.47E-02
Myl6	1.139	5.82E-06	**Imp3**	-0.648	3.21E-03
Neat1	1.137	1.24E-02	**Rpl7l1**	-0.648	5.35E-03
Ctsb	1.135	5.18E-06	**Abcc4**	-0.647	5.73E-03
Bcl6	1.135	4.89E-06	**Mipep**	-0.647	1.16E-02
Eml1	1.135	1.55E-06	**Thoc5**	-0.647	3.59E-03
Hotairm1	1.134	4.65E-05	**Hmgn1**	-0.647	1.11E-02
Hbp1	1.133	1.28E-03	**Cenpj**	-0.647	4.58E-02
Asphd2	1.133	1.49E-07	**Vps36**	-0.646	1.53E-03
Tpcn1	1.133	9.38E-04	**Alg10b**	-0.646	7.82E-03
Chpt1	1.132	2.19E-03	**Dennd5b**	-0.646	1.84E-02
Rnf135	1.131	6.68E-03	**Coil**	-0.646	7.20E-03
C1qtnf1	1.131	2.27E-04	**Med18**	-0.645	3.74E-02
Eva1c	1.131	1.43E-02	**Pde12**	-0.645	9.39E-03
Gm5617	1.128	4.13E-03	**Wrap53**	-0.645	1.30E-02
Zrsr1	1.128	4.75E-06	**Phc2**	-0.645	1.12E-03
Gpr156	1.128	3.91E-02	**Casp3**	-0.644	1.27E-03
Zfp651	1.127	7.89E-06	**Abhd17b**	-0.644	2.35E-03
Smarca2	1.127	2.38E-05	**Rpl10**	-0.644	4.42E-02
Cdkn2b	1.127	1.47E-03	**Srsf6**	-0.644	3.63E-03
Palld	1.127	2.94E-09	**Matr3**	-0.644	2.46E-03
Cd9	1.127	2.16E-06	**Hmgxb4**	-0.644	6.84E-03
Ddit4l	1.127	6.78E-03	**Tagap1**	-0.644	6.45E-03
Aga	1.124	4.82E-06	**Fam122b**	-0.643	1.00E-02
Nucb1	1.123	1.87E-07	**Glrx3**	-0.643	7.80E-03
Gpr27	1.121	8.68E-03	**Rps17**	-0.643	2.01E-02
Arvcf	1.120	3.43E-03	**Cep295**	-0.643	3.84E-02
Chst15	1.120	1.24E-03	**Champ1**	-0.642	4.67E-03
Cetn4	1.119	6.39E-03	**Hspa14**	-0.642	8.81E-03
Maf	1.118	4.25E-06	**Bckdhb**	-0.642	1.38E-02

Genes (UP)	log2FoldChange	padj	Genes (Down)	log2FoldChange	padj
Slc25a45	1.117	1.61E-02	**Tbc1d9**	-0.641	6.82E-03
Stat2	1.115	1.25E-02	**Cep83**	-0.641	1.16E-02
Adgrb3	1.115	2.38E-05	**Kdm8**	-0.641	4.23E-02
Usp2	1.114	9.07E-06	**Gtf3a**	-0.639	4.12E-02
S100a16	1.114	8.61E-04	**Dbr1**	-0.639	2.91E-02
Cyp4f17	1.114	1.81E-03	**Rpap3**	-0.639	5.95E-03
Fads3	1.114	1.14E-02	**Pgls**	-0.638	3.49E-03
Gmds	1.114	1.02E-02	**Khsrp**	-0.638	5.83E-03
St6galnac4	1.113	1.28E-05	**Ssb**	-0.638	1.01E-02
Trpm5	1.113	4.55E-02	**Ube2s**	-0.637	2.31E-02
Ppfibp2	1.112	1.13E-03	**Pwwp3a**	-0.637	2.05E-02
Frmd5	1.111	7.31E-03	**Stim2**	-0.637	8.53E-03
Spryd3	1.111	1.35E-05	**Nucks1**	-0.636	1.65E-03
Foxo1	1.111	3.58E-05	**Ncapd2**	-0.636	4.48E-03
Ptn	1.106	3.52E-04	**Hnrnpf**	-0.636	8.73E-04
Bcas3	1.106	2.62E-03	**Ptk2**	-0.636	5.77E-03
Acot6	1.105	1.63E-03	**Llph**	-0.635	1.91E-02
Gm50240	1.105	7.36E-03	**Rbm27**	-0.635	7.60E-03
Prdx6	1.100	2.53E-03	**Pabpn1**	-0.635	4.13E-03
Calcoco1	1.100	6.86E-04	**Nrf1**	-0.635	9.34E-03
Mroh1	1.100	3.44E-06	**Ino80e**	-0.635	2.39E-02
Prpsap1	1.099	1.43E-03	**Smarca4**	-0.634	2.02E-03
Prss23	1.098	6.98E-04	**Pdlim4**	-0.634	2.43E-02
Socs2	1.098	1.39E-02	**Mrps2**	-0.634	5.68E-03
Npc1	1.097	1.18E-05	**Ahctf1**	-0.634	2.69E-02
Pcx	1.097	8.32E-03	**Ccar2**	-0.634	2.37E-03
Slc8a2	1.096	3.31E-03	**Hnrnpa2b1**	-0.634	1.30E-03
Scn2a	1.095	1.12E-04	**Eif4b**	-0.633	3.53E-03
Fez2	1.094	2.39E-08	**Rpl35a**	-0.633	4.70E-02
Rtl8c	1.094	1.68E-06	**Ybx1**	-0.633	4.81E-03
Erc1	1.092	2.18E-08	**Heatr3**	-0.632	1.88E-02
Rfxank	1.092	4.74E-04	**Setdb1**	-0.632	8.43E-03
Tmem106b	1.092	1.31E-03	**Cstf1**	-0.632	1.21E-02
Astn1	1.092	7.78E-05	**Hcfc1**	-0.631	4.60E-03
Tmem240	1.090	3.20E-02	**Ddx3x**	-0.631	1.32E-02
Kif5c	1.089	3.95E-07	**Mtrex**	-0.630	1.65E-02
Bphl	1.089	4.00E-03	**Prpf3**	-0.629	2.84E-02
Cubn	1.088	8.16E-03	**Rbm25**	-0.629	2.05E-03
Ap3b2	1.087	8.11E-03	**Plxna3**	-0.629	2.17E-03
Ccdc28a	1.087	3.99E-02	**B230118H07Rik**	-0.629	1.55E-02
Papln	1.085	6.19E-03	**Tpx2**	-0.629	4.46E-02
Nrbp2	1.085	3.00E-05	**Calm2**	-0.629	8.55E-03
Naaa	1.084	8.86E-03	**Rpl36al**	-0.629	1.04E-02

Genes (UP)	log2FoldChange	padj	Genes (Down)	log2FoldChange	padj
4931406P16Rik	1.083	9.97E-05	**Rad23a**	-0.628	6.24E-03
H2-DMa	1.083	1.79E-03	**Gtf2h4**	-0.628	9.89E-03
1110032A03Rik	1.083	6.59E-03	**Prdm10**	-0.628	8.67E-03
Cd82	1.081	4.54E-03	**Sae1**	-0.627	1.18E-02
Pcdhga7	1.081	1.18E-02	**Cnot9**	-0.627	3.45E-03
Fgfr2	1.080	2.65E-02	**Smc1a**	-0.626	1.05E-02
Klhl36	1.079	2.48E-04	**Taf1c**	-0.626	1.18E-02
Prkce	1.079	1.55E-06	**Ttc37**	-0.626	1.92E-02
Kif5a	1.078	3.64E-03	**Iws1**	-0.625	8.81E-03
Csdc2	1.078	1.36E-03	**Timm10**	-0.625	2.51E-02
Prrg2	1.077	6.70E-05	**Polr2c**	-0.624	1.82E-02
Hist1h1c	1.076	2.29E-03	**Tfam**	-0.624	7.05E-03
Nlgn1	1.074	6.84E-04	**Tedc2**	-0.624	2.49E-02
Gpd2	1.074	2.19E-03	**Ilf3**	-0.624	6.53E-03
Il18	1.073	9.95E-04	**Ube2i**	-0.624	4.07E-03
Cep83os	1.072	2.24E-02	**Rpl27**	-0.624	4.27E-02
B2m	1.072	6.84E-03	**Rpl8**	-0.624	2.11E-02
Shf	1.072	5.91E-03	**Hnrnpu**	-0.624	3.35E-03
Cyld	1.072	1.76E-07	**Fam98b**	-0.623	6.57E-03
Gm45847	1.071	6.49E-03	**Ecsit**	-0.623	1.05E-02
Gm26737	1.071	5.77E-03	**Hdac2**	-0.623	4.24E-03
Abcd1	1.071	3.73E-06	**Brd8**	-0.623	2.84E-02
Mindy2	1.070	6.38E-04	**Zfp131**	-0.623	5.95E-03
Slc2a8	1.070	7.16E-04	**Eif4a3**	-0.622	1.27E-03
Mlxip	1.070	2.38E-08	**Cwc22**	-0.622	1.40E-02
Pls3	1.069	9.68E-05	**Ccdc43**	-0.622	6.37E-03
Cd99l2	1.069	1.70E-06	**Prpf40a**	-0.621	1.77E-02
Fat4	1.068	5.17E-04	**Rbm28**	-0.620	8.64E-03
Ttbk1	1.066	8.31E-05	**Adamts14**	-0.620	4.98E-03
Tef	1.065	6.74E-05	**Stag2**	-0.619	1.97E-02
Hacd2	1.065	3.53E-06	**Ddx52**	-0.619	1.70E-02
Btd	1.065	3.17E-04	**Lta4h**	-0.618	3.97E-03
B3galt5	1.064	6.14E-06	**Selenoi**	-0.618	9.93E-03
Evi5	1.064	4.74E-04	**Ssrp1**	-0.618	2.88E-02
Scrn1	1.064	3.57E-07	**Top1**	-0.617	7.05E-03
Armcx6	1.061	4.76E-03	**Smc6**	-0.617	1.31E-02
Lingo1	1.061	1.53E-04	**Mmachc**	-0.616	1.29E-02
P4ha1	1.060	6.52E-05	**Slc25a5**	-0.616	6.84E-03
Sgce	1.060	3.17E-05	**Hmbs**	-0.616	4.51E-03
Fam189a2	1.060	2.40E-02	**Tnpo3**	-0.616	1.28E-02
Cib2	1.060	4.38E-05	**Rpl23**	-0.615	2.98E-02
Tshz3	1.059	3.15E-03	**Cpsf2**	-0.614	9.36E-03
Qsox1	1.058	8.31E-05	**Ppil1**	-0.613	3.88E-02

Genes (UP)	log2FoldChange	padj	Genes (Down)	log2FoldChange	padj
Eya4	1.057	3.88E-03	**Jun**	-0.613	1.68E-03
Saraf	1.056	1.37E-07	**Dnajc11**	-0.613	1.05E-02
Col5a1	1.055	1.20E-08	**Zfp948**	-0.613	2.38E-02
Man2a2	1.054	3.41E-04	**Gins3**	-0.613	2.25E-02
Atcay	1.054	8.45E-05	**Wdr82**	-0.613	2.98E-03
Pcdhb9	1.054	3.25E-02	**Snx9**	-0.612	7.48E-03
Ndp	1.054	1.25E-03	**Adamts4**	-0.612	4.55E-02
Clba1	1.053	3.92E-03	**Gtf3c2**	-0.612	3.32E-03
Ptpru	1.052	6.84E-03	**Maml1**	-0.612	6.35E-03
Tlcd1	1.051	1.46E-06	**Fcf1**	-0.612	9.67E-03
Garem1	1.050	4.41E-05	**Cebpz**	-0.612	2.37E-02
Rgs7bp	1.050	2.66E-04	**Ccdc22**	-0.612	1.40E-02
Pdlim5	1.050	3.01E-08	**Map2k7**	-0.611	3.30E-03
Dpysl4	1.050	8.40E-05	**U2surp**	-0.611	6.68E-03
Cited2	1.048	1.40E-02	**Pspc1**	-0.610	5.33E-03
Mapre3	1.048	1.18E-05	**Lrfn1**	-0.610	2.04E-02
Rab6b	1.046	2.61E-06	**Fam118b**	-0.609	7.40E-03
Fuca2	1.046	2.68E-05	**Gnaz**	-0.609	3.01E-02
Fggy	1.045	3.06E-02	**Oxr1**	-0.609	2.49E-02
Dlg3	1.045	1.42E-03	**Gm43566**	-0.609	3.62E-02
Fam120c	1.045	5.23E-03	**Hsf2**	-0.609	4.95E-03
Ninj1	1.044	7.61E-04	**L3mbtl2**	-0.608	5.49E-03
Abcg2	1.044	2.57E-06	**Nkap**	-0.607	3.01E-02
Gpnmb	1.044	3.74E-03	**Ddx39b**	-0.607	2.20E-03
Sparc	1.043	2.58E-08	**Exosc9**	-0.607	3.15E-02
Ptprm	1.042	2.16E-03	**Smpd4**	-0.607	9.97E-03
Zfp438	1.042	8.58E-03	**Edrf1**	-0.606	3.79E-02
Cd47	1.042	1.80E-07	**Oxsr1**	-0.606	7.15E-03
Cdk14	1.041	4.73E-06	**Setd1a**	-0.606	1.15E-02
4933421O10Rik	1.040	7.43E-03	**Cct4**	-0.606	2.36E-02
Fam161b	1.040	1.49E-02	**Dnajc7**	-0.606	9.41E-03
Sfn	1.038	2.63E-02	**Rpl21**	-0.606	3.40E-02
Efemp2	1.038	9.33E-04	**Exog**	-0.606	3.07E-02
A330035P11Rik	1.038	2.93E-02	**Spats2**	-0.605	3.22E-03
Ebpl	1.037	1.95E-03	**Pphln1**	-0.605	1.27E-02
Pbx1	1.036	1.84E-06	**Atg4d**	-0.605	7.44E-03
Notch2	1.035	2.24E-06	**0610010K14Rik**	-0.605	1.22E-02
Rdh10	1.035	5.33E-05	**Fus**	-0.604	8.57E-03
Cyb5r3	1.035	2.38E-06	**Acat2**	-0.604	5.34E-03
Ccng1	1.035	2.61E-04	**Mri1**	-0.604	1.67E-02
Acox3	1.034	4.69E-03	**Fiz1**	-0.603	4.79E-03
Nos1ap	1.034	3.56E-02	**Mphosph9**	-0.603	7.61E-03
Akr1b10	1.032	4.40E-05	**Ssr1**	-0.603	3.28E-03

Genes (UP)	log2FoldChange	padj	Genes (Down)	log2FoldChange	padj
Tmem47	1.032	2.60E-07	**Prpf19**	-0.602	4.47E-03
9330102E08Rik	1.031	1.44E-02	**Timm13**	-0.602	2.14E-02
Fam214b	1.031	4.66E-05	**Cables2**	-0.602	4.63E-02
Rbm20	1.031	1.42E-05	**Crebzf**	-0.602	1.02E-02
Mospd2	1.031	6.43E-06	**Adsl**	-0.601	2.01E-02
Ttc39b	1.030	2.66E-04	**Rps4x**	-0.601	5.55E-03
Zc2hc1c	1.030	1.28E-02	**Ppp4r3a**	-0.601	2.11E-02
Gm46620	1.029	1.20E-03	**Rbm34**	-0.600	1.18E-02
Ctsl	1.028	9.04E-07	**Usp36**	-0.600	7.75E-03
Ncam1	1.027	6.51E-03	**Elavl1**	-0.600	1.15E-02
Tead3	1.026	5.61E-04	**Zfp623**	-0.600	1.99E-02
Atl1	1.025	4.04E-03	**Zbtb45**	-0.600	1.18E-02
Gpx4	1.025	8.10E-09	**Pald1**	-0.599	1.54E-02
Trpm4	1.024	7.16E-03	**Slc25a37**	-0.599	4.50E-02
Mid1ip1	1.024	9.14E-04	**Chordc1**	-0.599	2.25E-02
Gdf15	1.023	6.55E-03	**Srsf4**	-0.599	1.61E-02
Fbxl20	1.022	5.86E-03	**Bccip**	-0.598	2.27E-02
Fbxo44	1.022	9.21E-04	**Lyrm9**	-0.598	4.14E-02
Ilvbl	1.020	4.13E-06	**Pak1ip1**	-0.598	3.08E-02
Pdgfa	1.019	4.78E-03	**Mrps31**	-0.598	1.42E-02
Iqsec2	1.018	5.93E-06	**Snrpd2**	-0.598	1.21E-02
Npas3	1.017	5.48E-06	**Rps3**	-0.598	3.85E-02
Tesk2	1.017	1.36E-03	**Dalrd3**	-0.597	1.18E-02
Layn	1.016	4.73E-03	**Prpf38b**	-0.596	2.52E-02
Col4a1	1.016	2.20E-05	**Kdm6b**	-0.596	7.02E-03
Ttc12	1.014	1.58E-02	**Slc38a2**	-0.596	3.63E-02
Tes	1.013	1.47E-02	**Thoc1**	-0.596	4.88E-02
Ech1	1.013	5.03E-03	**Mier2**	-0.596	4.29E-02
Nav2	1.012	1.61E-06	**Ddx49**	-0.595	2.72E-02
Mapk3	1.010	8.35E-06	**Slc7a6os**	-0.595	1.57E-02
Slc12a4	1.010	2.30E-03	**Tbc1d8**	-0.594	3.79E-02
Mcu	1.010	6.33E-04	**Erh**	-0.594	1.16E-02
Agtrap	1.010	5.23E-06	**Pcbp1**	-0.594	4.55E-03
A2m	1.008	5.63E-04	**Snrnp48**	-0.594	2.88E-02
Dzip1	1.008	1.56E-04	**Stk39**	-0.593	1.03E-02
Smim19	1.007	2.05E-03	**Rps15a**	-0.593	3.41E-02
Lamp1	1.006	2.28E-05	**Ddi2**	-0.593	8.49E-03
Lrp10	1.005	2.33E-06	**Srd5a1**	-0.593	3.40E-02
Plin3	1.003	4.58E-02	**Rpl26**	-0.593	1.98E-02
Mettl27	1.003	2.64E-02	**Zfp275**	-0.592	2.34E-02
Dipk1b	1.003	2.44E-04	**Ythdf1**	-0.591	6.58E-03
Cul9	1.002	9.25E-03	**Taf4**	-0.591	1.34E-02
Ccdc189	1.001	1.46E-02	**Grk6**	-0.591	2.54E-02

Genes (UP)	log2FoldChange	padj	Genes (Down)	log2FoldChange	padj
Gpr137b	1.001	5.88E-05	**Ccdc9**	-0.590	2.44E-02
Rab29	1.001	8.61E-04	**Rbm33**	-0.590	1.43E-02
Taf9b	1.001	7.11E-04	**Bclaf1**	-0.590	1.82E-02
Cdkl5	0.998	1.01E-03	**Fnbp4**	-0.589	1.72E-02
Pdpn	0.997	6.90E-05	**Lsg1**	-0.589	1.47E-02
Nudt18	0.997	2.65E-03	**Gas2**	-0.589	4.93E-02
Fkbp9	0.996	9.02E-06	**Ints11**	-0.588	2.36E-02
Tnrc18	0.995	9.96E-07	**Trub2**	-0.588	1.03E-02
Snx7	0.995	5.68E-04	**Aimp1**	-0.588	4.11E-02
Parva	0.995	1.72E-07	**Dtx4**	-0.588	3.64E-02
Slc48a1	0.994	6.85E-04	**Ahsa2**	-0.588	1.78E-02
Ckap4	0.994	3.63E-05	**Mrps9**	-0.588	1.80E-02
Plcl1	0.993	1.76E-02	**Ampd2**	-0.587	9.61E-03
Cyp4f13	0.992	2.59E-03	**Foxk2**	-0.587	1.00E-02
Ccdc177	0.992	2.43E-02	**Fam133b**	-0.587	2.84E-02
Adrb1	0.992	5.89E-05	**Fbxo45**	-0.587	6.81E-03
Lmna	0.992	1.18E-02	**Ubqln4**	-0.587	3.05E-02
Wnk2	0.991	9.92E-04	**Rabggtb**	-0.587	3.54E-02
Serhl	0.991	1.65E-02	**Phf8**	-0.587	2.15E-02
Pcdhb17	0.989	6.26E-03	**Zfp334**	-0.586	1.99E-02
Ezh1	0.989	1.47E-03	**Pde2a**	-0.586	4.91E-02
Gpr37l1	0.989	4.76E-02	**Fam168b**	-0.585	7.76E-03
Aopep	0.988	4.94E-05	**Tmx1**	-0.585	2.72E-03
Dnajb14	0.986	1.83E-03	**Zbtb48**	-0.585	4.28E-02
Gpr85	0.986	6.48E-04	**Gtpbp1**	-0.585	4.11E-03
Fgfr1	0.984	4.30E-03	**Safb**	-0.584	8.22E-03
Neo1	0.983	4.61E-05	**Ccdc115**	-0.584	3.33E-02
D130017N08Rik	0.983	7.78E-04	**Prrg3**	-0.584	6.26E-03
Shisa7	0.982	3.28E-02	**Slc20a1**	-0.584	5.96E-03
Srcin1	0.981	5.30E-03	**Ddx46**	-0.583	9.26E-03
Anxa1	0.981	2.31E-03	**Mrpl22**	-0.583	1.46E-02
Snap47	0.981	5.64E-06	**Mrps7**	-0.583	2.66E-02
Spats2l	0.979	2.80E-06	**Xrcc2**	-0.582	2.74E-02
Plbd2	0.979	1.16E-04	**Alkbh8**	-0.582	1.47E-02
Phlda3	0.979	1.21E-02	**Snrnp25**	-0.582	2.73E-02
2810013P06Rik	0.978	6.96E-03	**Wdr18**	-0.582	3.59E-02
Manea	0.978	4.19E-05	**Srf**	-0.582	9.21E-03
Zdhhc2	0.977	1.26E-04	**Ing3**	-0.582	1.59E-02
Tcp11l1	0.977	1.50E-04	**Rps10**	-0.581	3.36E-02
Klhl5	0.976	8.92E-06	**Zcchc4**	-0.581	4.09E-02
Pkp2	0.976	3.34E-02	**Mex3b**	-0.581	1.16E-02
Galnt17	0.976	1.83E-02	**Coq4**	-0.581	4.86E-02
Pim3	0.975	3.90E-02	**Ptges3**	-0.581	2.22E-02

Genes (UP)	log2FoldChange	padj	Genes (Down)	log2FoldChange	padj
Herc3	0.975	1.46E-05	**Zfp598**	-0.581	2.94E-02
Gm14597	0.974	1.12E-03	**Exosc10**	-0.581	8.95E-03
Rtl6	0.972	4.92E-05	**Nap1l1**	-0.580	3.62E-02
Pcdhb3	0.972	6.75E-03	**Lca5**	-0.578	3.96E-02
Rab31	0.971	5.84E-04	**Usp39**	-0.578	4.12E-02
Mtch1	0.971	1.82E-03	**Senp2**	-0.578	9.01E-03
Stat5a	0.970	4.21E-03	**Zfp180**	-0.577	4.31E-02
Shisa4	0.970	3.44E-04	**Btf3**	-0.576	1.40E-02
Col16a1	0.969	2.66E-02	**Golph3**	-0.576	2.34E-02
Rai14	0.969	1.08E-02	**Spout1**	-0.576	1.85E-02
Pigs	0.969	2.46E-04	**Las1l**	-0.576	3.90E-02
Trip6	0.969	3.23E-03	**Hnrnpm**	-0.575	8.11E-03
Zfp931	0.968	4.41E-02	**Zbtb34**	-0.575	1.80E-02
Mtfr1l	0.968	3.10E-04	**Mta1**	-0.574	1.36E-02
Gatm	0.967	3.27E-04	**Cntrob**	-0.574	1.88E-02
Shank1	0.967	3.17E-02	**Thoc2**	-0.574	2.78E-02
Cacng7	0.967	1.83E-03	**L3mbtl3**	-0.574	1.68E-02
Steap2	0.966	5.25E-06	**Rhoj**	-0.574	2.65E-02
Sema6c	0.964	1.39E-02	**Tdrkh**	-0.573	3.52E-02
Npdc1	0.964	4.57E-07	**Luc7l3**	-0.573	8.45E-03
Gm5577	0.964	8.95E-03	**Trmt1**	-0.572	4.77E-02
Slc8b1	0.963	3.30E-02	**Tmem39a**	-0.572	2.93E-02
Dag1	0.963	2.28E-07	**Polr2e**	-0.572	1.63E-02
Slc22a5	0.963	9.73E-03	**Fam83d**	-0.571	4.89E-02
Rdh14	0.962	4.21E-03	**Mrpl53**	-0.570	4.20E-02
B3galt1	0.961	1.80E-02	**Hoxa3**	-0.570	2.08E-02
Lratd2	0.961	3.79E-03	**Gatad2a**	-0.570	5.11E-03
Mlycd	0.960	2.47E-03	**Adamts10**	-0.570	1.86E-02
Il3ra	0.960	3.88E-02	**Cnot1**	-0.570	1.81E-02
Stard10	0.959	4.73E-03	**Traf7**	-0.570	7.82E-03
Nkx3-2	0.959	1.67E-02	**Zfpm2**	-0.570	2.15E-02
Cxcl14	0.958	1.93E-05	**Zw10**	-0.570	3.07E-02
Ski	0.957	3.72E-07	**Mrps26**	-0.569	2.61E-02
Tcaim	0.957	1.25E-03	**Txlna**	-0.569	9.59E-03
Cacnb1	0.956	1.95E-03	**Nova2**	-0.569	8.49E-03
Ypel5	0.955	4.03E-04	**Acsl4**	-0.568	3.13E-02
Arsb	0.954	1.44E-05	**Ethe1**	-0.568	3.72E-02
Csf2ra	0.953	4.73E-03	**Apc**	-0.568	3.00E-02
Sesn1	0.953	2.26E-04	**Iah1**	-0.568	2.37E-02
Tmem176a	0.950	6.04E-03	**Snrnp70**	-0.568	1.58E-02
Ago4	0.949	1.06E-02	**Rpl23a**	-0.567	2.75E-02
Tpm1	0.949	3.50E-02	**Eef1a1**	-0.567	1.35E-02
Stk36	0.949	8.75E-03	**Cdc123**	-0.567	6.37E-03

Genes (UP)	log2FoldChange	padj	Genes (Down)	log2FoldChange	padj
Tmem50b	0.949	4.89E-05	**Cbx3**	-0.567	1.27E-02
Degs1	0.948	8.52E-07	**Slx1b**	-0.566	3.42E-02
Stoml1	0.948	4.37E-03	**Flrt3**	-0.566	1.44E-02
Slc6a9	0.947	7.95E-06	**Ubn1**	-0.566	1.55E-02
Jup	0.947	3.72E-05	**Rhoq**	-0.565	9.85E-03
Fbxo25	0.947	7.99E-05	**Zfp518b**	-0.565	4.24E-02
Tmod2	0.946	3.15E-04	**Rfc1**	-0.564	2.26E-02
Furin	0.946	8.03E-06	**Thrap3**	-0.563	1.51E-02
Mcub	0.946	2.10E-02	**Tomm20**	-0.563	2.24E-02
Dixdc1	0.945	3.40E-03	**Haus3**	-0.563	3.77E-02
P3h4	0.945	8.53E-05	**Nono**	-0.563	1.28E-02
Mfhas1	0.945	2.46E-03	**Patz1**	-0.563	1.45E-02
Foxc1	0.945	6.83E-03	**Nfx1**	-0.562	8.83E-03
Nmnat2	0.944	3.62E-02	**Ecd**	-0.562	6.48E-03
Elf1	0.943	1.50E-05	**Gm42047**	-0.562	2.23E-02
Tnfsf12	0.943	7.78E-04	**Tbp**	-0.562	3.40E-02
Ephx1	0.941	5.91E-06	**Elovl6**	-0.562	8.16E-03
Parp11	0.940	9.27E-04	**B4galnt4**	-0.562	3.58E-02
P3h3	0.940	2.43E-04	**Ccdc82**	-0.561	2.98E-02
Enox1	0.940	3.33E-02	**Cinp**	-0.561	2.10E-02
Ciart	0.939	2.17E-03	**Dvl2**	-0.561	1.63E-02
Pmm1	0.938	1.06E-02	**Ddx1**	-0.561	1.77E-02
Cntn3	0.938	2.19E-03	**Ewsr1**	-0.561	1.02E-02
Ccdc159	0.937	9.26E-03	**Acat1**	-0.561	4.82E-02
Castor1	0.937	4.70E-02	**Lrch2**	-0.560	1.40E-02
Mbnl2	0.936	3.75E-07	**Zfp719**	-0.560	2.13E-02
Tmem241	0.936	6.23E-03	**Mrpl47**	-0.560	3.02E-02
Vwa8	0.935	1.54E-02	**Hdgfl3**	-0.560	2.02E-02
Ube2h	0.934	3.90E-04	**Rps24**	-0.560	1.80E-02
Stim1	0.934	1.19E-03	**Zbtb2**	-0.559	3.48E-02
Triqk	0.934	1.97E-02	**Tent4b**	-0.558	2.24E-02
Frrs1l	0.934	1.47E-02	**Med1**	-0.558	1.41E-02
Cast	0.932	4.42E-03	**Bcas2**	-0.558	8.58E-03
Gnpda2	0.932	4.42E-03	**Slain2**	-0.558	9.14E-03
Azin1	0.931	5.08E-07	**Mrpl21**	-0.558	4.22E-02
Ghdc	0.931	3.49E-05	**1700037H04Rik**	-0.557	7.08E-03
Eml3	0.930	6.96E-04	**Midn**	-0.557	9.85E-03
Ginm1	0.929	9.41E-06	**Mtpap**	-0.557	3.57E-02
Galc	0.929	1.83E-03	**Rbm17**	-0.557	2.51E-02
Fnta	0.929	1.27E-04	**Polr2b**	-0.556	1.62E-02
Ophn1	0.927	3.22E-03	**Aqr**	-0.555	3.43E-02
Fosl2	0.927	2.82E-02	**Gphn**	-0.555	4.60E-02
Sema6a	0.927	1.63E-03	**Aars2**	-0.555	1.71E-02

Genes (UP)	log2FoldChange	padj	Genes (Down)	log2FoldChange	padj
Creg1	0.926	7.97E-05	**Ino80b**	-0.555	4.45E-02
Rerg	0.926	1.58E-03	**Nutf2**	-0.555	2.03E-02
Rab30	0.926	5.29E-04	**Chic2**	-0.555	1.54E-02
Tceal8	0.926	7.12E-03	**Ercc2**	-0.554	3.25E-02
Fgl2	0.925	3.42E-02	**Stag1**	-0.554	2.32E-02
Zfp469	0.924	2.33E-02	**Eef1d**	-0.553	4.80E-02
Clstn2	0.924	1.97E-03	**Rwdd4a**	-0.553	1.18E-02
Arhgap24	0.924	1.57E-02	**Eif3d**	-0.553	1.40E-02
Tsc22d1	0.924	7.99E-04	**Unk**	-0.553	1.11E-02
Kif1c	0.924	1.06E-06	**Pcnt**	-0.552	4.86E-02
Isoc2a	0.923	1.17E-03	**Mrpl44**	-0.552	2.20E-02
Dab2	0.921	2.69E-03	**Xpo1**	-0.551	4.41E-02
Pacsin3	0.921	2.54E-03	**Ftsj1**	-0.551	2.34E-02
Dlg5	0.921	1.03E-05	**Ints4**	-0.551	1.52E-02
Tmem175	0.919	5.94E-03	**Wdr83os**	-0.550	1.40E-02
Tspan3	0.919	1.13E-03	**Ppp1r7**	-0.550	9.36E-03
Arrdc1	0.918	2.77E-02	**Safb2**	-0.550	8.74E-03
Ugp2	0.918	4.46E-04	**Mrpl23**	-0.549	2.02E-02
St5	0.918	9.41E-03	**Smug1**	-0.549	3.57E-02
Rab4b	0.917	1.32E-04	**S100pbp**	-0.549	1.88E-02
App	0.917	2.30E-05	**Ppp4c**	-0.548	2.80E-02
Nmrk1	0.916	3.66E-02	**Bub3**	-0.547	8.77E-03
Slc22a23	0.916	1.26E-03	**Cisd2**	-0.547	1.77E-02
Gstm6	0.914	2.51E-02	**U2af2**	-0.547	1.95E-02
Meak7	0.914	1.92E-02	**Stmn1**	-0.547	9.23E-03
Aamdc	0.914	1.11E-02	**Cpsf1**	-0.547	1.05E-02
Creld1	0.913	3.54E-04	**Tubgcp3**	-0.547	9.86E-03
Smim8	0.913	8.81E-03	**Tomm5**	-0.547	4.60E-02
Ganc	0.911	9.23E-03	**Guf1**	-0.547	2.31E-02
Reep1	0.911	7.67E-04	**Pfdn2**	-0.546	2.47E-02
Zbtb7b	0.910	3.98E-05	**Nup35**	-0.546	3.25E-02
Oxsm	0.909	2.00E-02	**Cdc23**	-0.546	2.65E-02
Sri	0.908	9.17E-06	**Mlst8**	-0.545	2.07E-02
Pigv	0.907	1.02E-02	**Mrpl2**	-0.545	3.23E-02
Zkscan14	0.906	4.26E-02	**Ctdspl2**	-0.545	4.31E-02
Efnb1	0.906	8.93E-04	**Xrcc6**	-0.545	2.31E-02
Asah2	0.905	1.38E-02	**Kmt5c**	-0.545	2.26E-02
Cd151	0.904	6.42E-05	**Jmjd1c**	-0.545	3.98E-02
Notch1	0.903	9.20E-07	**Casc3**	-0.545	7.26E-03
Ndrg3	0.903	1.74E-04	**Rpl13**	-0.544	2.52E-02
Slc16a7	0.903	2.83E-02	**Cherp**	-0.544	1.77E-02
Arsk	0.902	9.38E-04	**Zfp668**	-0.543	2.70E-02
Naga	0.901	6.90E-04	**Mrpl11**	-0.543	1.65E-02

Genes (UP)	log2FoldChange	padj	Genes (Down)	log2FoldChange	padj
Ptprf	0.900	2.12E-04	**Hacd1**	-0.543	2.49E-02
Plpp6	0.900	3.38E-02	**Gga3**	-0.543	3.24E-02
Numbl	0.900	3.96E-03	**Cfap20**	-0.542	2.38E-02
Gm14325	0.898	2.98E-03	**Hint1**	-0.542	4.94E-02
Acy3	0.898	3.79E-02	**Polrmt**	-0.542	9.79E-03
Gnal	0.898	3.63E-02	**Ankhd1**	-0.541	3.06E-02
Crot	0.896	1.62E-05	**Dnaja1**	-0.540	4.48E-03
Pcdhb22	0.896	3.70E-02	**Rpl19**	-0.540	4.50E-02
Trnp1	0.895	2.14E-02	**Zfp710**	-0.540	1.57E-02
Apbb1	0.895	4.15E-05	**Rpsa**	-0.540	3.32E-02
Etfrf1	0.895	1.22E-02	**Csrnp2**	-0.539	2.78E-02
Pttg1ip	0.895	8.56E-05	**Arglu1**	-0.538	6.17E-03
Adam15	0.894	4.10E-06	**Mast2**	-0.538	3.70E-02
Rcn2	0.894	1.10E-02	**Mafg**	-0.537	1.63E-02
Daam1	0.892	1.48E-03	**Raly**	-0.537	2.00E-02
Gxylt2	0.890	3.82E-02	**Prmt6**	-0.537	3.57E-02
Decr2	0.888	7.50E-04	**Ncoa5**	-0.537	7.42E-03
Dcaf11	0.888	1.33E-03	**Rad1**	-0.536	4.63E-02
Rhob	0.888	1.22E-04	**Eif4enif1**	-0.536	1.88E-02
Nfat5	0.888	3.94E-03	**Zmym2**	-0.536	1.71E-02
Ankrd50	0.888	5.99E-05	**Abcf2**	-0.536	2.23E-02
St3gal6	0.887	8.07E-04	**Timm23**	-0.536	3.46E-02
Rrbp1	0.886	1.25E-03	**Tmem183a**	-0.535	2.49E-02
Metrnl	0.884	1.51E-02	**Polr2m**	-0.534	8.05E-03
Tmem218	0.882	2.71E-02	**Mrps34**	-0.534	3.35E-02
Ece1	0.882	4.45E-04	**Rnf2**	-0.533	2.13E-02
Dbndd2	0.882	2.78E-03	**Rps9**	-0.533	4.31E-02
Foxf1	0.881	3.03E-02	**Ppp1cc**	-0.533	1.52E-02
Ksr1	0.880	1.74E-03	**Ppm1m**	-0.533	1.90E-02
Plxnb1	0.880	1.53E-04	**Parl**	-0.532	1.73E-02
Clip4	0.880	1.41E-02	**Tubgcp6**	-0.532	1.65E-02
Dhrs7	0.880	1.48E-02	**Mlx**	-0.531	2.11E-02
Flot2	0.880	2.82E-02	**Tcf3**	-0.531	7.75E-03
Aplp1	0.880	2.11E-02	**Elp2**	-0.530	2.03E-02
Ppp1r13b	0.879	1.40E-02	**Ubfd1**	-0.530	1.20E-02
Anxa11	0.878	4.57E-02	**Nsg1**	-0.530	1.79E-02
Fech	0.878	2.65E-04	**Eif3m**	-0.530	4.11E-02
Sash1	0.877	3.71E-03	**Mrpl18**	-0.529	2.53E-02
Txndc16	0.877	1.69E-04	**Rbpj**	-0.529	4.99E-02
Ostf1	0.876	1.32E-05	**Wsb2**	-0.529	1.36E-02
Rps6ka4	0.876	1.43E-03	**Cbx1**	-0.528	8.82E-03
Pip4k2c	0.876	7.38E-05	**Mtss1**	-0.528	4.61E-02
Arid5b	0.873	3.27E-05	**Abi2**	-0.527	4.49E-02

Genes (UP)	log2FoldChange	padj	Genes (Down)	log2FoldChange	padj
Taf13	0.871	1.79E-05	**Osbpl10**	-0.526	4.21E-02
Mlc1	0.871	3.68E-02	**Cxxc1**	-0.525	2.46E-02
Nol3	0.871	1.89E-02	**Tent2**	-0.524	3.36E-02
Mocs1	0.871	3.83E-03	**Pan2**	-0.524	2.74E-02
Shisal1	0.871	2.21E-02	**Polr3f**	-0.524	3.79E-02
Dmac2l	0.870	5.04E-03	**Brd3**	-0.524	2.38E-02
Apobec1	0.870	1.87E-02	**Brpf1**	-0.523	4.41E-02
Tfeb	0.869	1.30E-03	**Rap1a**	-0.523	1.27E-02
Chrnb2	0.869	4.10E-02	**Mrpl15**	-0.523	1.87E-02
Ppt1	0.869	3.45E-05	**Ddx23**	-0.522	1.84E-02
Hdhd2	0.868	9.40E-05	**Lcorl**	-0.522	3.26E-02
Cdh2	0.868	6.91E-03	**Dcun1d5**	-0.522	4.43E-02
Slc39a13	0.868	2.22E-04	**Galnt7**	-0.521	1.71E-02
Tmem246	0.867	1.27E-02	**Pard6g**	-0.521	4.66E-02
Tmem8b	0.867	4.81E-03	**Slc39a14**	-0.521	3.37E-02
Mfsd13a	0.866	2.44E-02	**Ogg1**	-0.520	4.75E-02
Pik3c2a	0.866	2.71E-04	**Pmpca**	-0.520	1.00E-02
Bcar1	0.865	2.54E-04	**Smarce1**	-0.520	9.76E-03
Mtmr10	0.864	1.20E-04	**Mllt1**	-0.520	1.86E-02
Rnf181	0.864	3.66E-03	**Lonrf2**	-0.519	4.41E-02
Cadm1	0.864	3.20E-04	**Mrpl34**	-0.519	1.44E-02
9330182L06Rik	0.863	8.24E-05	**Mrpl35**	-0.519	4.64E-02
Anxa5	0.863	3.76E-04	**Xrcc5**	-0.519	4.35E-02
Ttc28	0.863	3.87E-05	**Cstf2**	-0.519	8.74E-03
Pdzrn3	0.863	1.67E-02	**Pgap1**	-0.518	4.42E-02
Cd81	0.863	3.32E-04	**Pitpnb**	-0.518	4.21E-02
Nek6	0.862	1.08E-02	**Baz1b**	-0.518	4.19E-02
Rnf215	0.862	3.04E-04	**Rps15**	-0.517	1.20E-02
Acvr1	0.860	2.60E-03	**Srrm2**	-0.517	3.11E-02
Tle3	0.860	1.63E-04	**Zranb2**	-0.516	3.20E-02
Slc44a2	0.860	4.46E-06	**Tial1**	-0.516	1.29E-02
Pank1	0.859	2.46E-04	**Papola**	-0.516	2.21E-02
Sgk3	0.857	2.75E-02	**Pkp4**	-0.515	1.66E-02
Ostm1	0.857	8.28E-06	**Rpl7**	-0.515	2.65E-02
Fuom	0.856	2.17E-02	**Mpzl1**	-0.515	4.47E-02
Abca2	0.856	8.36E-05	**Nudt21**	-0.514	2.61E-02
Atf5	0.856	3.01E-02	**Lrrc47**	-0.514	1.38E-02
Glrb	0.853	4.25E-03	**Ints12**	-0.513	2.47E-02
Dhrs11	0.853	4.05E-02	**Usp3**	-0.513	3.28E-02
Slitrk2	0.852	1.57E-02	**Apaf1**	-0.512	2.52E-02
Sptbn1	0.852	6.47E-03	**Agap3**	-0.512	1.64E-02
Slc2a6	0.852	1.32E-02	**Pdcd7**	-0.511	3.79E-02
Galnt4	0.852	5.32E-04	**Brpf3**	-0.511	2.97E-02

Genes (UP)	log2FoldChange	padj	Genes (Down)	log2FoldChange	padj
Shank3	0.852	7.27E-04	**Samd1**	-0.511	2.58E-02
Them4	0.851	3.20E-02	**Hsph1**	-0.510	2.29E-02
Msx1	0.850	1.95E-02	**Atl2**	-0.509	4.61E-02
Pigh	0.850	1.35E-02	**Rpl29**	-0.509	2.95E-02
Slc4a3	0.850	5.16E-03	**Ddx47**	-0.509	2.89E-02
Krcc1	0.849	2.22E-04	**Ltbp1**	-0.509	1.76E-02
Srr	0.849	9.35E-03	**Cactin**	-0.508	3.69E-02
Rab36	0.849	6.42E-03	**Ubtf**	-0.508	1.05E-02
Ppp1r3f	0.849	1.80E-02	**Ranbp3**	-0.508	2.69E-02
Tnip1	0.848	3.02E-04	**Odf2**	-0.508	4.37E-02
Mgat3	0.848	1.28E-03	**Srp68**	-0.507	2.84E-02
Cdipt	0.847	9.27E-05	**Capn15**	-0.507	2.64E-02
Tpk1	0.847	4.50E-02	**Gtf3c4**	-0.506	1.95E-02
Cdc42bpg	0.847	4.53E-04	**Clns1a**	-0.506	2.49E-02
Tbc1d9b	0.846	3.83E-03	**Fam98a**	-0.506	3.10E-02
Tvp23a	0.844	1.43E-02	**Cdc37**	-0.505	3.46E-02
Dclk1	0.843	1.52E-03	**Rbm22**	-0.504	2.35E-02
Tom1	0.842	3.04E-03	**Pafah1b2**	-0.504	3.00E-02
Lifr	0.841	1.75E-04	**Knop1**	-0.504	1.74E-02
Lamc1	0.841	2.30E-06	**Paxbp1**	-0.504	1.95E-02
Aldh2	0.841	6.38E-04	**Ehmt1**	-0.504	2.08E-02
Rnf32	0.840	4.91E-02	**Ccnt1**	-0.503	3.90E-02
Fzd8	0.839	5.69E-03	**Neurl4**	-0.503	1.49E-02
Glrx	0.839	2.99E-03	**Prpf4b**	-0.503	1.67E-02
Mpv17l	0.836	3.35E-03	**Rnf168**	-0.503	2.81E-02
Bdh2	0.836	3.59E-03	**Timm21**	-0.503	4.30E-02
Pfkp	0.836	3.26E-02	**Elp3**	-0.502	1.82E-02
Clip3	0.836	2.57E-05	**Fam76b**	-0.501	2.85E-02
Paxx	0.835	1.47E-02	**Txnl1**	-0.500	4.75E-02
Scp2	0.834	1.46E-03	**Eif5**	-0.500	3.87E-02
Rsu1	0.834	1.62E-04	**Polr2a**	-0.500	4.36E-02
Rbms1	0.832	2.16E-02	**Cfdp1**	-0.500	2.01E-02
Ccdc157	0.832	8.04E-03	**Larp7**	-0.500	2.84E-02
2610306M01Rik	0.832	1.53E-02	**Pum2**	-0.499	3.04E-02
Myd88	0.832	3.70E-02	**Trir**	-0.499	2.86E-02
Phlpp1	0.831	7.97E-04	**Adk**	-0.499	2.21E-02
Aldh3a2	0.830	5.51E-05	**Nop53**	-0.499	1.34E-02
Abhd12	0.829	1.01E-02	**Rpp25l**	-0.499	4.63E-02
Fam174a	0.829	5.55E-04	**Cyb5r4**	-0.499	3.00E-02
Plcd4	0.829	9.13E-03	**Bri3bp**	-0.498	1.63E-02
Wfs1	0.828	5.81E-05	**Qsox2**	-0.497	3.41E-02
Pcdhb14	0.828	3.00E-02	**Usp45**	-0.497	2.46E-02
Phldb2	0.827	1.88E-04	**Cdc16**	-0.496	1.95E-02

Genes (UP)	log2FoldChange	padj	Genes (Down)	log2FoldChange	padj
Lacc1	0.826	2.24E-03	**Ptbp3**	-0.495	3.55E-02
Ngly1	0.826	2.04E-03	**Fkbp3**	-0.495	4.56E-02
Trim56	0.826	7.21E-04	**Sltm**	-0.494	4.65E-02
Fzd7	0.826	4.70E-03	**Tufm**	-0.493	1.69E-02
Mt1	0.826	2.74E-02	**Rpl22**	-0.493	2.73E-02
Kif1bp	0.825	4.66E-04	**Wipf1**	-0.493	4.17E-02
Casp8	0.825	4.81E-02	**Hnrnpl**	-0.492	1.98E-02
Gna13	0.825	2.63E-04	**Eny2**	-0.492	4.22E-02
Ctnnbip1	0.824	1.25E-02	**Pbrm1**	-0.492	3.72E-02
Cpq	0.823	6.75E-03	**Nom1**	-0.490	4.77E-02
Cacnb3	0.823	8.90E-03	**Ccm2**	-0.490	3.00E-02
Slc35a5	0.823	4.02E-03	**Ccnh**	-0.489	3.39E-02
Lysmd1	0.822	2.53E-02	**Prelid1**	-0.488	3.47E-02
Rab33b	0.822	1.87E-03	**Ppig**	-0.488	4.70E-02
Mib2	0.822	6.50E-04	**Plaa**	-0.486	4.34E-02
Tspyl4	0.821	3.81E-03	**Psmc5**	-0.486	3.58E-02
Smox	0.821	2.44E-02	**Rasa1**	-0.486	4.48E-02
Naglu	0.821	1.11E-02	**Timm44**	-0.486	3.65E-02
Ids	0.821	2.51E-04	**Aprt**	-0.486	4.02E-02
Garnl3	0.820	7.84E-03	**Psmb6**	-0.485	3.81E-02
Pnpla8	0.820	2.50E-02	**Clk2**	-0.485	2.54E-02
Dtx3	0.820	8.13E-04	**Trmt2a**	-0.485	4.31E-02
Atp8a1	0.819	2.38E-02	**Pdcd5**	-0.484	4.97E-02
Zer1	0.819	1.33E-03	**Cdyl**	-0.484	3.20E-02
Jazf1	0.819	1.18E-02	**Ptpn1**	-0.484	1.61E-02
Shisa5	0.819	2.27E-03	**Uimc1**	-0.483	4.62E-02
Lrrc27	0.818	4.22E-02	**Stk24**	-0.483	2.76E-02
Trappc2	0.818	3.08E-03	**Socs4**	-0.483	2.62E-02
Tango2	0.818	4.53E-03	**Rbbp7**	-0.483	2.81E-02
1810037I17Rik	0.818	5.45E-05	**Ints5**	-0.482	4.78E-02
Pnpla2	0.818	4.92E-03	**Gtf2a2**	-0.481	3.20E-02
Snx13	0.817	1.17E-02	**Nsmce1**	-0.481	4.31E-02
Cisd3	0.817	3.74E-02	**Nt5c3b**	-0.481	3.20E-02
Aldh1l2	0.815	1.23E-03	**Eya3**	-0.481	3.20E-02
Fam49a	0.815	3.37E-02	**E4f1**	-0.479	4.98E-02
Shank2	0.813	1.36E-02	**Ddx5**	-0.479	1.54E-02
Manba	0.813	2.46E-04	**Gfm2**	-0.478	4.12E-02
Tmem250-ps	0.813	2.20E-03	**Tmem70**	-0.478	3.01E-02
Emilin1	0.812	6.16E-05	**Ccnl1**	-0.477	4.13E-02
Wwtr1	0.811	1.12E-03	**Drg1**	-0.477	4.31E-02
Ikbkg	0.811	9.68E-05	**Rnf20**	-0.476	2.08E-02
Fbxo9	0.811	3.50E-04	**Zwint**	-0.476	4.33E-02
Hykk	0.810	1.05E-02	**Mtdh**	-0.475	3.50E-02

Genes (UP)	log2FoldChange	padj	Genes (Down)	log2FoldChange	padj
Mafb	0.809	5.04E-03	**Dpy19l1**	-0.475	2.59E-02
Erlec1	0.808	1.86E-03	**Kif2a**	-0.474	4.47E-02
Abhd5	0.808	1.68E-03	**Ppp2r2d**	-0.473	2.57E-02
Dock4	0.807	4.12E-03	**Cpsf7**	-0.473	3.52E-02
B4gat1	0.807	1.55E-04	**Sarnp**	-0.473	4.13E-02
Kat2b	0.806	2.05E-03	**Psmd12**	-0.472	4.42E-02
B230217C12Rik	0.805	6.17E-03	**Eif3i**	-0.472	2.38E-02
Sulf2	0.805	4.77E-04	**Cox10**	-0.471	4.35E-02
Pgpep1	0.805	4.11E-03	**Brd4**	-0.471	4.18E-02
Depdc7	0.804	2.37E-02	**Dhx8**	-0.471	4.12E-02
Rnf13	0.804	8.82E-04	**Bmi1**	-0.470	2.09E-02
Lpl	0.804	2.85E-03	**Nt5c**	-0.470	4.13E-02
Arhgap44	0.803	1.71E-02	**Hmgxb3**	-0.470	4.43E-02
Scamp1	0.803	1.00E-02	**Lima1**	-0.470	4.13E-02
Itgb8	0.803	4.46E-04	**Rbbp4**	-0.469	1.73E-02
Asah1	0.802	4.72E-05	**Rell1**	-0.468	4.12E-02
1500009L16Rik	0.802	1.13E-02	**Rcor1**	-0.468	3.29E-02
Tnfrsf21	0.801	3.25E-02	**Ddx19a**	-0.468	2.70E-02
Utrn	0.800	9.95E-03	**Ipmk**	-0.468	3.59E-02
Inpp1	0.800	4.95E-03	**Hif1an**	-0.467	2.63E-02
Slc39a11	0.800	1.47E-03	**Gspt1**	-0.467	4.70E-02
Zfyve1	0.800	2.50E-03	**Vbp1**	-0.467	3.82E-02
Cpped1	0.800	4.75E-03	**Tomm22**	-0.467	3.12E-02
Yipf4	0.799	7.54E-04	**Ube2k**	-0.466	3.66E-02
Gpr45	0.799	3.76E-02	**Rbm15b**	-0.466	3.23E-02
Rfx2	0.799	1.76E-02	**Eif2b5**	-0.466	3.39E-02
Vamp1	0.798	2.52E-02	**Mrpl17**	-0.465	3.75E-02
Acot1	0.797	6.81E-03	**Phf13**	-0.465	4.54E-02
Paqr4	0.797	1.78E-02	**Scaf4**	-0.465	4.72E-02
Cttnbp2	0.797	3.13E-02	**Phb**	-0.464	3.69E-02
Mfn2	0.797	5.73E-04	**Cetn2**	-0.464	3.26E-02
Ghitm	0.796	7.97E-05	**Mrps18a**	-0.464	4.45E-02
Slc39a1	0.796	9.97E-05	**Ube2e3**	-0.462	3.37E-02
Ctbs	0.795	1.02E-02	**Sfswap**	-0.462	2.52E-02
Ralgps1	0.795	2.28E-02	**R3hcc1**	-0.462	3.62E-02
Fahd1	0.794	1.25E-02	**Lin7c**	-0.460	4.90E-02
Tmcc3	0.794	7.35E-04	**Ppp2r2a**	-0.460	2.21E-02
Hspa1b	0.793	2.79E-02	**Ciao2a**	-0.460	4.21E-02
Jag1	0.793	4.78E-02	**Mrpl28**	-0.459	4.08E-02
Cald1	0.792	4.99E-04	**Ppp1r15b**	-0.459	4.26E-02
Fzd1	0.791	2.41E-02	**Eif3l**	-0.459	4.75E-02
Atrn	0.791	1.75E-02	**Map3k11**	-0.459	4.42E-02
Rbms3	0.791	1.19E-03	**Sde2**	-0.458	3.83E-02

Genes (UP)	log2FoldChange	padj	Genes (Down)	log2FoldChange	padj
Stradb	0.791	3.51E-03	**Cdk2ap1**	-0.457	2.47E-02
Ndst1	0.791	2.73E-05	**Hexim1**	-0.457	2.25E-02
C1qtnf6	0.791	2.19E-03	**Clcn6**	-0.455	3.46E-02
3830406C13Rik	0.791	1.51E-03	**Puf60**	-0.455	2.58E-02
Cd302	0.790	1.57E-03	**Tpst1**	-0.454	4.46E-02
Fam102a	0.789	8.47E-03	**Rbm15**	-0.454	4.50E-02
Lamp2	0.789	2.40E-04	**Hnrnpk**	-0.452	1.86E-02
Car2	0.788	2.68E-02	**Sephs1**	-0.452	4.29E-02
Ap5s1	0.788	3.74E-03	**Phrf1**	-0.452	3.42E-02
Tmem62	0.788	1.04E-03	**Rhot2**	-0.451	3.79E-02
Mapkapk3	0.788	5.12E-03	**Eif3k**	-0.450	4.98E-02
Aard	0.787	4.46E-02	**Sumo2**	-0.448	4.43E-02
Rubcn	0.787	7.37E-05	**Zcchc14**	-0.448	4.12E-02
Fbxo36	0.787	4.26E-02	**Khdc4**	-0.447	4.21E-02
Castor2	0.786	2.01E-03	**Stat5b**	-0.447	4.58E-02
Lman2l	0.785	2.61E-04	**Smarcad1**	-0.446	4.53E-02
Laptm4a	0.784	5.42E-03	**Eif4h**	-0.445	4.44E-02
Lrrc4c	0.784	4.95E-02	**Laptm4b**	-0.445	3.38E-02
Kcnk13	0.783	1.61E-03	**Sf3b2**	-0.444	2.28E-02
Tfpi	0.783	4.46E-02	**Aebp2**	-0.444	3.30E-02
Ggcx	0.783	1.72E-03	**Dohh**	-0.443	4.35E-02
Atg9a	0.782	8.57E-04	**Maz**	-0.443	2.57E-02
Sdc3	0.782	2.85E-03	**Vangl2**	-0.443	4.12E-02
Sdc2	0.782	4.08E-03	**Acly**	-0.442	2.36E-02
Psme2	0.781	2.85E-02	**Phf2**	-0.441	4.24E-02
Sirt2	0.780	6.78E-03	**Sp1**	-0.440	4.35E-02
Bcl2l1	0.779	3.22E-03	**Dhx30**	-0.440	2.68E-02
Nectin1	0.779	7.82E-03	**Clasp1**	-0.439	3.78E-02
Adam10	0.779	8.31E-05	**Glyr1**	-0.437	3.64E-02
Tmem117	0.778	2.21E-02	**Tsn**	-0.435	3.14E-02
Pcyox1	0.777	2.63E-05	**Ndufab1**	-0.430	3.70E-02
Atp6v0e	0.777	1.38E-02	**Dcakd**	-0.428	4.76E-02
Lrpap1	0.776	1.78E-04	**Slk**	-0.428	4.58E-02
Dnajc3	0.776	1.39E-04	**Psma5**	-0.427	3.52E-02
P4htm	0.776	2.19E-02	**Aak1**	-0.427	3.97E-02
Fam171b	0.775	2.70E-03	**Khdrbs1**	-0.424	3.82E-02
Rab4a	0.774	4.04E-03	**Otub1**	-0.423	3.76E-02
Dysf	0.773	4.26E-02	**Spcs3**	-0.421	4.28E-02
Gys1	0.773	1.51E-03	**Zc3h4**	-0.421	4.18E-02
Os9	0.772	4.04E-04	**Kdm1a**	-0.416	3.90E-02
Tmbim6	0.771	1.72E-04	**Snrpa**	-0.416	4.11E-02
Fam168a	0.771	1.27E-03	**Cops7a**	-0.415	4.28E-02
Gnai2	0.771	2.56E-04	**1110004F10Rik**	-0.414	4.59E-02

Genes (UP)	log2FoldChange	padj	Genes (Down)	log2FoldChange	padj
Neto2	0.771	5.51E-05	**Pip4k2b**	-0.412	4.65E-02
Osbpl5	0.771	3.83E-03			
Cib1	0.770	1.65E-03			
Pxk	0.770	3.04E-03			
Yjefn3	0.769	4.58E-02			
Mblac2	0.769	4.60E-03			
Kif1a	0.768	1.17E-03			
Nim1k	0.768	2.52E-03			
Cds2	0.768	5.64E-03			
Adgrl1	0.767	5.55E-03			
Cux1	0.767	1.86E-04			
Kcnb1	0.766	5.76E-03			
Prr7	0.766	5.15E-03			
Gm12258	0.764	4.56E-02			
Itgb1	0.764	7.37E-05			
Trappc9	0.764	9.70E-04			
Unc45a	0.763	2.43E-03			
Map2k1	0.763	6.87E-04			
Rusc1	0.763	2.98E-02			
Efr3b	0.762	3.76E-02			
Stard3nl	0.762	2.81E-04			
Nceh1	0.761	6.64E-05			
Fer1l5	0.761	1.81E-02			
Decr1	0.760	8.96E-03			
Psap	0.760	5.90E-04			
Pknox2	0.760	1.25E-02			
Celsr2	0.760	1.49E-04			
Porcn	0.759	3.00E-02			
Rabac1	0.759	9.76E-04			
Galnt14	0.758	3.05E-02			
Hdac9	0.758	2.96E-02			
Usp11	0.758	2.68E-02			
Acot9	0.756	4.08E-02			
Acot2	0.755	6.89E-03			
Tmem245	0.755	1.32E-04			
Fam114a1	0.755	3.80E-02			
Inpp5k	0.755	4.75E-02			
Mettl7a1	0.755	8.16E-03			
Nckap5	0.754	1.16E-02			
Dnajc4	0.754	3.26E-02			
Lpcat3	0.753	1.66E-03			
Igsf8	0.752	2.42E-03			
Firre	0.751	6.89E-04			

Genes (UP)	log2FoldChange	padj	Genes (Down)	log2FoldChange	padj
Pcmtd1	0.751	2.57E-02			
Tulp4	0.751	6.63E-04			
Adgrb1	0.750	3.01E-02			
Adam12	0.748	4.59E-03			
Arap1	0.748	8.17E-03			
Tmem143	0.747	2.08E-02			
Tpi1	0.746	1.57E-03			
Borcs6	0.746	7.99E-03			
Habp4	0.746	3.05E-03			
Amigo3	0.746	4.42E-02			
1110012L19Rik	0.744	6.73E-03			
Cry2	0.744	8.64E-03			
Oaz2	0.744	1.63E-03			
Txndc5	0.743	8.93E-04			
Slco3a1	0.743	3.85E-03			
Mtm1	0.742	1.44E-02			
Wdr6	0.741	3.06E-03			
Arhgap23	0.741	1.37E-03			
Plcd1	0.741	6.59E-03			
Yipf1	0.739	1.86E-03			
Kifc3	0.738	1.39E-02			
Dand5	0.738	4.86E-02			
Adgrl3	0.738	3.53E-04			
Slc12a9	0.738	2.99E-03			
Reep6	0.738	5.03E-03			
Mkrn1	0.737	4.91E-02			
Rtl8a	0.737	6.76E-03			
Mpst	0.736	8.19E-03			
Gnb5	0.736	5.81E-03			
Gabarap	0.735	8.50E-04			
Nxn	0.735	1.40E-02			
Tmem38b	0.734	1.20E-02			
Nrp2	0.734	1.07E-02			
Slc29a3	0.734	1.88E-03			
Sema4b	0.734	1.80E-03			
Tbc1d2b	0.733	1.05E-03			
Sdf2	0.733	1.58E-03			
Pld3	0.733	2.39E-02			
Tnks1bp1	0.732	1.47E-02			
Mta3	0.731	1.69E-03			
Arhgef10l	0.731	1.47E-03			
Ak3	0.731	8.99E-03			
Dpp8	0.730	5.77E-03			

Genes (UP)	log2FoldChange	padj	Genes (Down)	log2FoldChange	padj
Per1	0.730	2.59E-02			
Hspa2	0.730	9.78E-03			
Naa80	0.729	7.57E-03			
Rnf103	0.729	1.47E-02			
Fam3a	0.728	2.96E-03			
Nxt2	0.728	6.53E-04			
Pak3	0.728	2.23E-02			
St6galnac6	0.727	1.02E-02			
Scamp5	0.727	1.87E-03			
Gca	0.726	1.46E-02			
Ifit2	0.725	2.99E-03			
Smim20	0.725	1.48E-02			
Mpp5	0.724	2.16E-04			
Serinc1	0.724	1.46E-03			
Tpp1	0.724	7.38E-03			
Hs6st1	0.721	3.79E-02			
Klhl28	0.721	7.31E-03			
Etfdh	0.721	2.43E-02			
Nr3c1	0.721	1.77E-02			
Nr1d2	0.721	1.53E-02			
Hist1h2bc	0.721	1.86E-02			
Dact3	0.720	4.75E-03			
Eef2k	0.720	2.28E-03			
Zfp641	0.720	4.11E-02			
Ift122	0.719	6.47E-04			
Ankrd12	0.718	1.01E-02			
Mafk	0.718	2.39E-02			
Ccndbp1	0.717	4.21E-03			
Dnajb2	0.717	1.30E-02			
Pgm1	0.717	1.55E-03			
Evi5l	0.716	1.73E-02			
Pnrc1	0.716	3.71E-02			
Mief2	0.716	5.40E-03			
Ctnnd2	0.714	2.44E-02			
Nfe2l1	0.714	2.21E-04			
Kidins220	0.713	1.01E-02			
Fuca1	0.713	7.47E-04			
Acaa2	0.711	1.47E-02			
Micu2	0.710	9.38E-04			
Arl2	0.710	8.86E-03			
Rras	0.709	2.24E-03			
Nfkbiz	0.709	1.80E-02			
Rfx5	0.709	2.63E-02			

Genes (UP)	log2FoldChange	padj	Genes (Down)	log2FoldChange	padj
Ankra2	0.709	8.77E-03			
Snx32	0.707	4.47E-02			
Sobp	0.707	8.70E-03			
Wdr81	0.707	9.25E-03			
Nbdy	0.707	5.28E-03			
E130114P18Rik	0.706	6.04E-03			
Sft2d2	0.705	1.06E-03			
Gns	0.705	6.25E-04			
Smim13	0.705	2.21E-02			
Pafah2	0.704	2.24E-03			
Bicdl1	0.704	3.66E-02			
Acp2	0.703	2.19E-03			
Comt	0.703	5.59E-03			
Irak4	0.703	2.91E-02			
Tsc22d4	0.702	2.18E-03			
Stx2	0.702	2.85E-03			
Mboat2	0.702	3.37E-02			
Map1lc3b	0.702	2.52E-02			
Pgap2	0.702	2.31E-02			
2810402E24Rik	0.702	2.73E-02			
Fgd6	0.700	2.42E-02			
Vamp4	0.700	1.79E-02			
Samd14	0.699	5.90E-03			
Ppip5k1	0.698	2.89E-02			
Osbpl9	0.698	1.90E-03			
1810058I24Rik	0.698	9.22E-03			
Smarca1	0.698	4.45E-02			
Pfkfb2	0.698	9.26E-03			
Spire1	0.697	2.80E-03			
Gba	0.696	5.20E-04			
Pigyl	0.695	2.63E-02			
Rftn2	0.695	6.80E-03			
Lrrc8d	0.694	5.90E-03			
Dcaf6	0.694	1.26E-03			
Plcb4	0.694	6.84E-03			
Scd2	0.693	7.00E-03			
Tmem184c	0.693	6.81E-03			
Me1	0.693	1.02E-03			
Fkbp7	0.692	2.39E-02			
Zhx2	0.690	1.72E-03			
Ywhah	0.690	4.86E-02			
Tab2	0.690	1.33E-02			
Gnaq	0.689	4.25E-03			

Genes (UP)	log2FoldChange	padj	Genes (Down)	log2FoldChange	padj
Gucy1b1	0.688	2.70E-03			
Osbpl2	0.688	2.55E-03			
Rab5b	0.688	4.68E-03			
S100a10	0.687	1.47E-02			
Nat2	0.686	4.48E-02			
Lypd6	0.686	4.86E-02			
Fkbp15	0.686	2.94E-03			
Abca3	0.684	2.35E-02			
Mtmr6	0.684	2.25E-02			
Slc41a1	0.684	3.57E-03			
Negr1	0.684	1.12E-02			
Nlgn2	0.684	8.19E-04			
Per2	0.684	2.27E-02			
Ddr2	0.683	8.98E-04			
Arpin	0.682	3.01E-02			
Arrdc3	0.682	3.66E-02			
Prrx1	0.682	3.73E-03			
Klhl26	0.681	2.54E-02			
Atp6ap1	0.681	3.55E-04			
Tecpr1	0.679	6.89E-03			
Kank2	0.679	4.18E-02			
Tbc1d12	0.677	1.65E-02			
Acadm	0.677	1.93E-03			
Tmlhe	0.676	4.17E-02			
Mfsd6	0.676	3.07E-02			
Cachd1	0.676	6.08E-04			
Dnajc18	0.675	1.89E-02			
Dock9	0.675	9.87E-03			
Sel1l	0.675	6.48E-04			
Hist2h2be	0.675	2.97E-02			
Kifap3	0.674	1.47E-03			
Rab2b	0.674	3.40E-02			
Ifitm2	0.674	3.89E-03			
Wdr19	0.673	8.25E-03			
Ext2	0.673	1.05E-03			
Jmy	0.673	2.25E-02			
Mocs2	0.671	1.57E-03			
Gabarapl1	0.671	2.28E-02			
Reep5	0.670	6.29E-04			
Tmx4	0.670	8.02E-03			
Tmub2	0.669	1.74E-02			
Snx14	0.669	2.57E-02			
Slc25a20	0.669	1.33E-02			

Genes (UP)	log2FoldChange	padj	Genes (Down)	log2FoldChange	padj
9530068E07Rik	0.669	3.36E-04			
Esyt1	0.668	4.02E-02			
Palm	0.668	3.80E-03			
Bend6	0.667	4.12E-02			
Rtl8b	0.666	2.82E-02			
Coro7	0.666	2.36E-02			
Tbc1d10a	0.666	6.01E-03			
Fryl	0.666	1.01E-02			
Camta2	0.666	1.32E-02			
Cnnm2	0.666	1.16E-02			
A830082K12Rik	0.665	1.77E-02			
Apip	0.663	9.72E-03			
Pex7	0.662	1.45E-02			
Wwp2	0.662	9.95E-03			
Erlin2	0.661	3.25E-03			
Atp6v1f	0.661	1.65E-03			
Mgrn1	0.661	6.26E-03			
Arl6ip5	0.660	5.83E-03			
Edem2	0.660	2.35E-02			
Hexa	0.659	5.08E-03			
Mpv17l2	0.659	1.88E-02			
Dip2a	0.659	3.59E-03			
Lxn	0.659	1.79E-02			
Dpy19l3	0.659	2.29E-02			
Glmp	0.658	1.71E-02			
Bace1	0.658	1.94E-03			
Ptgr1	0.658	5.91E-03			
Psme1	0.657	1.77E-02			
Retsat	0.656	3.26E-02			
Jakmip2	0.656	4.30E-03			
Gli3	0.655	1.71E-03			
Cyb5b	0.655	5.57E-03			
Hmox1	0.654	1.97E-02			
Sox8	0.654	5.80E-04			
Rap2a	0.654	3.47E-03			
Pag1	0.653	1.23E-03			
Casc4	0.652	2.73E-03			
Lmbrd1	0.652	2.19E-02			
Ano10	0.652	1.54E-03			
Atraid	0.652	5.81E-03			
Trim2	0.652	5.40E-03			
Ubac1	0.651	3.90E-02			
Arfip1	0.651	3.87E-02			

Genes (UP)	log2FoldChange	padj	Genes (Down)	log2FoldChange	padj
Erbb2	0.650	5.93E-03			
Chmp2b	0.650	1.81E-03			
Arel1	0.649	6.01E-03			
Bhlhe40	0.649	1.93E-02			
Scaper	0.649	2.97E-02			
Add1	0.649	7.95E-03			
Tob1	0.649	2.99E-03			
Carmil3	0.648	4.26E-02			
Pex6	0.648	1.53E-02			
Magi3	0.647	3.48E-03			
Tmem19	0.646	1.21E-02			
Ctnna1	0.645	4.73E-04			
Elovl1	0.644	6.63E-03			
Nr2f1	0.643	1.88E-02			
Bcl9l	0.643	2.04E-02			
Eci2	0.643	4.20E-02			
Wnk1	0.643	2.09E-02			
Pnpla6	0.643	1.41E-02			
Ipo13	0.642	2.24E-03			
Atp6v0e2	0.642	5.32E-03			
Dtnb	0.642	3.80E-03			
Agbl5	0.642	3.77E-02			
Megf8	0.639	3.13E-03			
Bag3	0.638	3.36E-03			
Snap29	0.637	2.15E-02			
Mpv17	0.636	1.05E-02			
Galnt1	0.636	4.12E-03			
Hipk3	0.635	1.74E-02			
Serpine2	0.635	6.96E-04			
Ssbp2	0.635	7.96E-03			
Magee1	0.635	1.11E-02			
Ifngr1	0.634	2.67E-03			
Tmem127	0.634	4.03E-03			
Gng12	0.634	6.84E-03			
Pacs2	0.634	3.35E-02			
Hk1	0.634	7.46E-03			
Gm42517	0.633	3.52E-02			
Tmem50a	0.632	4.41E-03			
Hivep1	0.632	2.40E-02			
Chst12	0.632	1.13E-02			
Pde4dip	0.631	1.18E-02			
Fam124a	0.630	3.14E-02			
Zcchc24	0.630	8.80E-04			

Genes (UP)	log2FoldChange	padj	Genes (Down)	log2FoldChange	padj
Hsd17b7	0.630	1.29E-03			
Bsdc1	0.630	3.49E-02			
Wdr1	0.628	2.55E-03			
Lactb	0.627	4.05E-02			
Tm2d2	0.626	9.18E-03			
Dsel	0.626	3.83E-02			
Hlcs	0.625	3.99E-02			
Extl3	0.625	1.15E-02			
Cpt2	0.625	3.08E-02			
Chp1	0.623	7.70E-03			
Stambp	0.623	3.29E-02			
Slc2a10	0.622	1.94E-02			
Clcn3	0.622	2.65E-02			
Eps15	0.622	2.68E-03			
Slc35e4	0.622	1.86E-02			
Cc2d1a	0.621	7.61E-03			
Abcd3	0.621	1.04E-02			
Sqstm1	0.621	7.85E-03			
Apeh	0.620	5.22E-03			
Otud1	0.620	3.42E-02			
Fam53b	0.620	3.39E-02			
Kctd1	0.619	2.84E-02			
Ier5	0.619	2.43E-03			
Tgoln1	0.618	5.82E-03			
Vps41	0.617	1.22E-02			
Myo9a	0.617	2.27E-02			
Secisbp2l	0.616	9.66E-03			
AU040320	0.615	6.95E-03			
Tmem59	0.615	3.89E-03			
Flot1	0.614	2.02E-03			
Sipa1l2	0.614	1.55E-02			
Ndufa1	0.614	1.36E-02			
Tpra1	0.614	4.42E-02			
Pts	0.613	3.92E-02			
Glt8d1	0.613	6.01E-03			
Capns1	0.613	2.04E-03			
Trafd1	0.612	1.07E-02			
Afap1	0.611	2.80E-02			
Prmt2	0.611	1.65E-02			
Ptch1	0.610	2.77E-03			
Sema4g	0.610	2.00E-02			
Afdn	0.610	6.84E-03			
Plgrkt	0.609	2.16E-02			

Genes (UP)	log2FoldChange	padj	Genes (Down)	log2FoldChange	padj
Gm14326	0.608	4.19E-02			
Cmtm6	0.606	3.57E-02			
Vps37a	0.606	2.49E-03			
Samd8	0.604	1.52E-02			
Tmem104	0.604	1.54E-02			
Megf9	0.604	4.04E-02			
Phkb	0.603	3.35E-02			
Zbtb38	0.601	4.86E-02			
Smarcd3	0.600	1.03E-02			
Ggt7	0.600	3.21E-02			
Hsbp1	0.600	5.63E-03			
Ctsa	0.599	3.59E-02			
Tpst2	0.599	6.49E-03			
Mir22hg	0.599	3.76E-02			
Elovl5	0.598	1.48E-03			
Dlg1	0.598	8.59E-03			
Ccser2	0.597	4.53E-02			
Zdhhc15	0.597	3.36E-02			
Cflar	0.597	8.80E-03			
Kif1b	0.596	1.15E-02			
Tbcel	0.594	3.55E-02			
Kctd11	0.593	3.50E-02			
Meis3	0.592	3.10E-02			
Klc4	0.592	4.60E-02			
Ubc	0.592	1.75E-02			
Ccdc92	0.592	2.57E-02			
Mttp	0.588	1.92E-02			
Lbh	0.587	8.05E-03			
Cyb561d2	0.587	3.29E-02			
Jam2	0.586	3.35E-02			
Elmo2	0.586	2.85E-03			
Snn	0.585	2.59E-02			
Mprip	0.585	3.35E-03			
Scarb2	0.584	2.48E-02			
Clstn1	0.582	9.42E-03			
Slc35f5	0.582	1.06E-02			
Amfr	0.581	1.85E-03			
Cask	0.581	9.34E-03			
Hps5	0.581	1.54E-02			
Add3	0.580	3.46E-02			
Flad1	0.579	1.93E-02			
Herpud2	0.578	8.07E-03			
Chid1	0.578	1.42E-02			

Genes (UP)	log2FoldChange	padj	Genes (Down)	log2FoldChange	padj
Rcan3	0.577	1.02E-02			
Mink1	0.576	4.90E-02			
Cyfip1	0.576	1.04E-02			
Rnh1	0.576	2.00E-02			
Slc26a6	0.576	3.56E-02			
Cacna2d1	0.574	1.55E-02			
Kctd7	0.574	3.59E-02			
Fth1	0.573	2.82E-02			
Rhobtb3	0.573	3.83E-03			
Gdi1	0.573	1.51E-02			
Ctps2	0.573	3.08E-02			
Xpr1	0.573	4.18E-02			
Efr3a	0.572	2.21E-02			
Sox2	0.569	1.01E-02			
Tax1bp3	0.569	4.63E-02			
Fam219a	0.569	1.25E-02			
Gaa	0.569	1.65E-02			
Mfsd12	0.567	3.52E-02			
Rab5a	0.567	2.57E-02			
Maoa	0.566	2.68E-02			
Gpr137	0.566	3.83E-02			
Rnf170	0.565	2.40E-02			
Fads2	0.565	2.60E-02			
Nub1	0.564	1.92E-02			
Ptprg	0.564	3.22E-03			
Atp6v0a2	0.562	7.32E-03			
Snx19	0.561	1.03E-02			
BC004004	0.561	1.10E-02			
Serinc3	0.560	4.55E-03			
Rrm2b	0.559	1.72E-02			
Wdr59	0.559	1.43E-02			
Galk2	0.558	1.54E-02			
Trmt2b	0.558	4.07E-02			
Ap1b1	0.557	4.69E-03			
B4galt4	0.557	2.51E-02			
Chmp5	0.556	1.12E-02			
Bmp2k	0.556	4.20E-02			
Enah	0.555	2.82E-02			
Amn1	0.555	4.69E-02			
Fcho2	0.555	2.70E-02			
Rilpl2	0.554	3.19E-02			
Nsmf	0.554	2.25E-02			
Bfar	0.553	3.51E-02			

Genes (UP)	log2FoldChange	padj	Genes (Down)	log2FoldChange	padj
Slc35a2	0.551	2.95E-02			
Zfyve21	0.551	4.11E-02			
Ankib1	0.551	1.02E-02			
Srd5a3	0.551	3.92E-02			
Fbxo10	0.550	2.65E-02			
Galnt2	0.550	3.35E-02			
Bloc1s3	0.550	3.12E-02			
Ift57	0.550	3.08E-02			
Abhd8	0.548	4.41E-03			
Syap1	0.548	2.83E-02			
Kif3b	0.548	1.08E-02			
Rnf166	0.547	4.08E-02			
Fam45a	0.545	2.46E-02			
Cacna1a	0.544	1.59E-02			
Apmap	0.543	2.47E-02			
Etfb	0.542	2.21E-02			
Micu1	0.542	2.89E-02			
Nptn	0.541	5.92E-03			
Btg1	0.541	4.62E-02			
Ncstn	0.540	7.56E-03			
Dclk2	0.539	2.60E-02			
Dnajb4	0.538	1.70E-02			
Atg4a	0.538	3.07E-02			
Sumf1	0.538	8.77E-03			
Mtpn	0.537	7.15E-03			
Rab21	0.537	8.24E-03			
Man2b1	0.537	1.64E-02			
Emc3	0.537	2.50E-02			
Cyb5a	0.536	2.66E-02			
Ppic	0.535	1.07E-02			
Gyg	0.535	9.92E-03			
Mid2	0.535	1.72E-02			
Cnn3	0.535	3.08E-02			
Impact	0.534	2.39E-02			
Atg12	0.530	2.69E-02			
Tnfrsf1a	0.530	1.64E-02			
Aff1	0.529	1.68E-02			
Arhgef17	0.529	9.29E-03			
Abcc10	0.529	4.87E-02			
Rnf24	0.528	4.09E-02			
Rab39b	0.526	4.92E-02			
Asap1	0.526	1.03E-02			
Slc25a23	0.525	1.77E-02			

Genes (UP)	log2FoldChange	padj	Genes (Down)	log2FoldChange	padj
Ptdss2	0.525	1.63E-02			
Insig1	0.525	3.51E-02			
Dhrs4	0.524	4.16E-02			
Msrb1	0.524	4.16E-02			
Rassf8	0.524	1.71E-02			
Ttc8	0.523	4.68E-02			
Ndufv3	0.523	4.40E-02			
Vps26c	0.522	3.57E-02			
Aldh7a1	0.521	2.92E-02			
Cog7	0.521	3.18E-02			
Renbp	0.521	4.94E-02			
Kdsr	0.521	2.91E-02			
Abi1	0.521	4.17E-02			
Fmnl2	0.520	1.15E-02			
Mad2l2	0.518	4.87E-02			
Paip2b	0.518	1.06E-02			
Pfn2	0.518	3.24E-02			
Pex2	0.517	1.79E-02			
Hexb	0.517	3.40E-02			
Ccdc91	0.516	3.71E-02			
Zkscan5	0.514	4.17E-02			
Dusp3	0.514	4.91E-02			
Tmem9	0.514	3.07E-02			
Sh3bgrl3	0.513	3.59E-02			
Zfand3	0.512	1.18E-02			
Vhl	0.511	4.94E-02			
Arhgap5	0.511	1.82E-02			
Wdr47	0.510	3.26E-02			
Rab10	0.510	4.83E-02			
Fndc3b	0.510	1.19E-02			
Tm7sf2	0.509	2.45E-02			
Mbd1	0.508	3.51E-02			
Foxg1	0.508	1.55E-02			
Slc23a2	0.507	4.56E-02			
Aph1b	0.507	2.11E-02			
Itsn1	0.507	2.29E-02			
Bcap31	0.506	1.73E-02			
Hmgn3	0.505	4.35E-02			
Axin2	0.505	3.77E-02			
Mapkap1	0.503	1.81E-02			
Tmem167b	0.502	2.41E-02			
Qk	0.502	3.82E-02			
Pgrmc1	0.501	2.65E-02			

Genes (UP)	log2FoldChange	padj	Genes (Down)	log2FoldChange	padj
Sccpdh	0.501	2.85E-02			
Tram2	0.501	4.07E-02			
Tln1	0.500	1.47E-02			
Tmem135	0.500	4.17E-02			
Prkacb	0.500	2.29E-02			
Insig2	0.499	3.74E-02			
St3gal2	0.499	2.44E-02			
Rab9	0.498	3.76E-02			
Arl8a	0.497	3.90E-02			
Clptm1	0.495	1.54E-02			
Snx3	0.494	1.32E-02			
Ubl7	0.494	4.02E-02			
Brat1	0.493	3.39E-02			
Acot13	0.493	4.30E-02			
Wipi2	0.492	1.49E-02			
Slc4a2	0.492	3.88E-02			
Fbh1	0.488	2.54E-02			
Taok3	0.487	4.05E-02			
Chpf	0.486	4.87E-02			
Stx7	0.485	2.51E-02			
Epm2aip1	0.485	2.51E-02			
Gde1	0.482	2.37E-02			
Inpp4a	0.482	4.90E-02			
Dnm2	0.480	2.68E-02			
Nicn1	0.480	4.93E-02			
Dennd4a	0.480	3.87E-02			
Mvb12b	0.479	2.05E-02			
Capn2	0.478	2.58E-02			
Acaa1a	0.478	4.70E-02			
Acss2	0.478	3.13E-02			
Mindy1	0.477	4.42E-02			
Plxnb2	0.475	3.06E-02			
Sec62	0.473	3.20E-02			
Lonp2	0.467	2.33E-02			
Ptgfrn	0.467	2.21E-02			
Pdk3	0.464	3.66E-02			
Cap1	0.464	1.96E-02			
Twsg1	0.464	3.43E-02			
Rit1	0.462	3.56E-02			
Tenm3	0.461	4.68E-02			
Usp20	0.459	3.42E-02			
Hs2st1	0.459	3.23E-02			
Ppm1f	0.458	2.91E-02			

Genes (UP)	log2FoldChange	padj	Genes (Down)	log2FoldChange	padj
Rdh11	0.458	3.51E-02			
Cpe	0.453	1.99E-02			
Slc38a10	0.453	3.01E-02			
AC149090.1	0.451	3.08E-02			
Uggt1	0.448	3.86E-02			
Rasa3	0.447	4.37E-02			
Rtn3	0.437	3.20E-02			
Glb1	0.436	4.39E-02			
Mpp1	0.434	3.59E-02			
Cant1	0.432	4.93E-02			
Trak1	0.428	3.93E-02			
Gosr2	0.427	4.72E-02			
Atl3	0.424	3.80E-02			
Anapc16	0.424	4.75E-02			
Pfkl	0.418	3.58E-02			
Cic	0.413	3.86E-02			
Ankrd13c	0.411	4.45E-02			
Snx27	0.409	3.80E-02			

8.2 Significantly Altered Pathways induced by BMP4/FGF-treatment

PATHWAY	padj	NES	leadingEdge Genes
HALLMARK_EPITHELIAL_MESENCHYMAL_TRANSITION	7.75E-23	2.64	Acta2 Sntb1 Slit3 Lrp1 Col6a2 Itgb3 Col1a1 Scg2 Pdgfrb Vcam1 Fmod Gadd45b Ptx3 Fstl1 Slc6a8 Ecm1 Fgf2 Ccn2 Cdh11 Tgm2 Igfbp3 Oxtr Itgb5 Col1a2 Bgn Postn Htra1 Thy1 Dpysl3 Col11a1 Igfbp2 Serpinh1 Itgav Lox Sgcb Pmp22 Eln Fbln5 Col5a1 Sparc Lamc2 Plod1 Mgp Col4a2 Mfap5 Id2 Myl9 Crlf1 Loxl1 Mmp14 Notch2 Lamc1 Sfrp1 Timp3 Col5a3 Snai2 Tpm2 Col4a1 Nid2 Col6a3 Itgb1 Fas Qsox1 Rhob Wnt5a Tgfb1 Cadm1 Cald1 Serpine2 Fuca1 Efemp2 Itga2 Pmepa1 Lama2 Ccn1 Dab2 Prrx1 Col5a2 Adam12 Col12a1 Fzd8 Fn1 Cdh2 Tnfaip3 Magee1 Slit2 Lama3 Sat1 Sdc4 Emp3 Vegfc Rgs4 Msx1 Aplp1 Col16a1 Foxc2 Pfn2 Tpm1 Tnfrsf11b Mylk Col8a2 Fstl3 Glipr1 Col7a1 Eno2 Fermt2 Gadd45a Pthlh Comp Edil3 Cd44 P3h1 Calu Mmp2 Flna Vegfa Sgcg
HALLMARK_MYOGENESIS	5.86E-19	2.49	Casq1 Agrn Col6a2 Col1a1 Cryab Fhl1 Gadd45b Igfbp7 Slc6a8 Ak1 Sorbs1 Fgf2 Mras Sphk1 Eno3 Ablim1 Myl6b Igfbp3 Prnp Clu Sspn Itgb5 Mef2c Hspb8 Gpx3 Myl4 Rb1 Gnao1 Sparc Speg Col4a2 Cd36 Notch1 Agl Nav2 Hrc Sod3 Cav3 Mapre3 Myh8 Sgca Tpm2 App Col6a3 Pfkm Hbegf Ctf1 Itgb1 Fkbp1b Ldb3 Tgfb1 Atp6ap1 Fxyd1 Gsn Casq2 Reep1 Wwtr1 Psen2 Lama2 Ache Ppp1r3c Adam12 Ncam1 Sirt2 Nos1 Pcx Hspb2 Pde4dip Pygm Dmpk Kifc3 Cox6a2 Gaa Nqo1 Bhlhe40 Igf1 Chrnb1 Plxnb2 Cnn3 Aplnr Rit1 Mylk Myh3 Col15a1 Pdlim7 Tnnt3 Large1 Adcy9 Myog
HALLMARK_INTERFERON_ALPHA_RESPONSE	1.04E-10	2.33	Ifit3 Txnip Samd9l Lgals3bp Parp14 Ifi44 Irf7 Csf1 Ifi35 Ifi27 C1s1 Parp9 Cd47 Ddx60 Parp12 Cmpk2 Tap1 Rtp4 Gmpr Elf1 Trim12c Eif2ak2 Rsad2 Irf9 Uba7 Usp18 Ifih1 Isg20 Trim25 Ifit2 Casp1 Ifitm2 Isg15 B2m Psmb8 Trafd1 Stat2 Herc6 Helz2 Psme1 Ifitm1 Nub1 Psmb9 Trim21 Psme2 Casp8 Ube2l6 Il4ra Cxcl10
HALLMARK_INTERFERON_GAMMA_RESPONSE	1.04E-10	2.19	Tapbp Vcam1 Ifit3 Txnip Samd9l Lgals3bp Parp14 Sspn Xaf1 Ifi44 Znfx1 Irf7 Psmb10 Ifi35 Ifi27 Lats2 C1s1 Stat1 Zbp1 Ddx60 Parp12 Cmpk2 Tap1 Mvp Vamp5 Sri Rtp4 Arid5b Cfh Fas Serping1 Eif2ak2 Rsad2 Irf9 Oas2 Vamp8 Rnf213 Usp18 H2-DMa Ifih1 Isg20 Trim25 Ifit2 Casp1 Cd274 Nod1 Ifitm2 Isg15 B2m Psmb8 Socs1 Tnfaip3 Casp4 Trafd1 Stat2 Herc6 Helz2 Psme1 Psmb9 Trim21 Irf5 Psme2 Pfkp Fgl2 Myd88 Btg1 Casp8 Pla2g4a Ube2l6 Gch1 Il4ra Cxcl10

PATHWAY	padj	NES	leadingEdge Genes
			Tnfsf10 Ciita H2-Aa Epsti1 Bpgm Nfkbia Jak2 Sppl2a Oasl1 Ifi44l Trim26 Dhx58
HALLMARK_HYPOXIA	1.04E-10	2.15	Ncan Cav1 Aldoc Gpc4 Prkca Ccn2 Tgm2 Eno3 Cp Anxa2 Igfbp3 Foxo3 F3 Bgn Slc6a6 Ackr3 Gcnt2 Lox Col5a1 Cavin3 S100a4 Fbp1 Prdx5 Ampd3 Ilvbl Ppargc1a Ndst1 Bcan Pdk1 P4ha1 Dpysl4 Nagk Rora Ids Stbd1 Ugp2 Gys1 Pgm1 Tpi1 Ccn1 Isg20 Tgfb3 Sdc3 Glrx Kif5a Sdc2 Ppp1r3c Pdgfb Hexa Angptl4 Ndrg1 Tpst2 Hk1 Tnfaip3 Pygm Cited2 Sdc4 Tes Gaa Nr3c1 Lxn Bhlhe40 Hmox1 Mt1 Fosl2 Plac8 Pfkp Pfkl Pdk3 Hs3st1 Pnrc1 Btg1 Gpc3 Vhl Efna3 Eno2 Map3k1 Large1
HALLMARK_UV_RESPONSE_DN	6.59E-09	2.13	Smad7 Cav1 Itgb3 Col1a1 Id1 Pdgfrb Prkca Atp2b4 Igfbp5 Anxa2 Nrp1 Sipa1l1 Col1a2 F3 Dbp Atxn1 Plpp3 Col11a1 Met Pmp22 Fbln5 Pdlim5 Pparg Gcnt1 Prkce Anxa4 Notch2 Lamc1 Sri Snai2 Lpar1 Bmpr1a Ddah1 Ccn1 Ptprm Dab2 Kit Sdc2 Mgll Col5a2 Dmac2l Erbb2 Plcb4 Dlg1 Slc22a18 Cited2 Nr1d2 Cacna1a Atrn Nr3c1 Bhlhe40 Rgs4 Mt1 Add3 Insig1
HALLMARK_COAGULATION	1.42E-07	2.07	Lrp1 Itgb3 Hmgcs2 Lgmn Clu Ctso F3 Htra1 Mmp11 Adam9 Sparc C3 C1s1 S100a13 P2ry1 Ctsl Mmp14 Cd9 Ctsb Timp3 Furin Cfh Serping1 Csrp1 Lamp2 A2m Ctsh Gsn Prss23 Itga2 Acox2 S100a1 Anxa1 Wdr1 Pdgfb Fn1 Cpq Sirt2 Gng12 Capn5 C2 Capn2 Usp11 Klkb1 Pef1 Dusp14 Comp Tmprss6 Fga Mmp2 Klf7 F8 Dct Cfi
HALLMARK_XENOBIOTIC_METABOLISM	1.79E-08	2.02	Atoh8 Ndrg2 Dhrs1 Cyp4f14 Slc6a6 Psmb10 Pdk4 Gcnt2 Apoe Esr1 Pdlim5 Tgfb2 Fbp1 Cd36 Pink1 Xdh Id2 Fmo1 Ephx1 Npc1 Acox1 Crot Hsd11b1 Entpd5 Lcat Jup Fas Hacl1 Cdo1 Tmbim6 Bcar1 Aldh2 Ninj1 Acox2 Aox1 Elovl5 Acp2 Slc12a4 Fah Bphl Acox3 Ech1 Comt Ptgr1 Aqp9 Pcx Papss2 Pmm1 Dhrs7 Tnfrsf1a Nqo1 Hmox1 Gabarapl1 Gstm4 Etfdh Enpep Smox Igf1 Pgrmc1 Cyb5a Car2 Maoa Retsat Cda Pts Vnn1 Tmem176b Upb1 Mpp2 Gch1 Abcc3 Abcc2 Slc46a3 Ap4b1 Ptges Abcd2 Cyfip2
HALLMARK_ADIPOGENESIS	4.99E-08	1.99	Angpt1 Sorbs1 Sspn Hspb8 Stom Gpx3 Phyh Apoe Gpx4 Agpat3 Sncg C3 Tst Pparg Omd Cd36 Bcl6 Cmbl Acox1 Col4a1 Cd151 Mgst3 Ghitm Lifr Sqor Dnajb9 Reep5 Aldh2 Pdcd4 Me1 Ephx2 Fabp4 Scp2 Pgm1 Cd302 Cidea Lpcat3 Acadm Gpd2 Ifngr1 Lpl Tob1 Fah Stat5a Mgll Enpp2 Ech1 Reep6 Angptl4 Sult1a1 Decr1 Acaa2 Dhrs7 Abca1 Ubc Etfb Itsn1 Cpt2 Rtn3 Retsat Pfkl Pim3 Esyt1 Mylk
HALLMARK_APOPTOSIS	2.40E-07	1.98	Pea15a Smad7 Cav1 Pdgfrb Nedd9 Gadd45b Timp2 Txnip Clu Bgn Emp1 Gpx3 Gstm2 Ccnd2 Hspb1 Gpx4 Tgfb2 Cyld Tap1 Timp3 Dap App Ppt1 Plppr4 Fas Rhob Dnajc3 Lef1 Bmf Gsn Pdcd4 Il18 Psen2

PATHWAY	padj	NES	leadingEdge Genes
			Tspo Ank Anxa1 Isg20 Ifngr1 Bcl2l1 Casp1 Erbb2 Sqstm1 Add1 Cflar Rnasel Casp4 Lmna Sat1 Bcap31 Hmox1 Hgf
HALLMARK_INFLAMMATORY_RESPONSE	2.02E-07	1.98	Slc1a2 Tapbp Axl Slc7a2 Itgb3 Edn1 Pcdh7 Rgs16 Sphk1 F3 Irf7 Sema4d Csf1 Met Slc4a4 Fzd5 Cx3cl1 Tlr2 Mmp14 Sri Rtp4 Lpar1 Hbegf Pdpn Eif2ak2 Ahr Itgb8 Irak2 Il18 Ndp Cd82 Scn1b Aqp9 Ccl20 Tacr1 Kif1b Abca1 Emp3 Ifitm1 Osmr Aplnr Stab1 Abi1 Ptpre Gpc3 Gabbr1 Mxd1 Tlr1 Gch1 Il4ra Cxcl10 Tnfsf10 Tlr3 Slc31a2 Chst2
HALLMARK_TGF_BETA_SIGNALING	7.91E-05	1.97	Nog Smad7 Smad6 Ltbp2 Id1 Id3 Ski Id2 Furin Bmpr2 Fnta Bmpr1a Tgfb1 Rab31 Wwtr1 Pmepa1 Acvr1 Sptbn1 Eng
HALLMARK_KRAS_SIGNALING_DN	3.24E-06	1.90	Col2a1 Edn1 Dlk2 Grid2 Copz2 Igfbp2 Pdk2 Clstn3 Ptprj Tcf7l1 Tgfb2 Idua Cpeb3 Coq8a Thrb Slc38a3 Tlx1 Celsr2 P2rx6 Rsad2 Gdnf Nr4a2 Kcnn1 Kcnd1 Efhd1 Itih3 Sncb Adra2c Hc Slc29a3 Klhdc8a Slc12a3 Dtnb Nos1 Zc2hc1c Slc25a23 Snn Slc16a7 Fggy Mfsd6 Fgfr3 Edar Stag3 Prkn Arpp21 Camk1d
HALLMARK_HEDGEHOG_SIGNALING	8.72E-04	1.87	Nrcam Scg2 Nrp1 Unc5c Thy1 Celsr1 Shh Tle3 Cdk6 Ache Ptch1 Ophn1 Nrp2 L1cam
HALLMARK_BILE_ACID_METABOLISM	7.50E-05	1.86	Cyp46a1 Abca9 Phyh Atxn1 Aldh1a1 Cyp7b1 Prdx5 Abcd1 Hsd3b7 Npc1 Crot Pfkm Abca2 Hacl1 Efhc1 Optn Pex11a Ephx2 Scp2 Mlycd Aqp9 Abcd3 Slc22a18 Pex7 Abca1 Pex6 Dio2 Hsd17b11 Lonp2 Abca3 Pnpla8 Fads2 Abca5 Retsat Slc23a2 Pex11g Paox Ttr Acsl1 Abcd2 Abca6 Nr3c2 Pex13 Nudt12 Hsd17b4 Abcg4 Cat Bbox1 Ar Cyp39a1 Aldh9a1
HALLMARK_APICAL_JUNCTION	5.60E-06	1.84	Itga3 Vcam1 Cnn2 Nrxn2 Cdh11 Thy1 Epb41l2 Adam23 Thbs3 Adam9 Lamc2 Cadm2 Cx3cl1 Arhgef6 Speg Parva Nfasc Myl9 Adra1b Adam15 Cldn19 Sgce B4galt1 Jup Itgb1 Ikbkg Rsu1 Actn1 Gnai2 Ctnna1 Cadm3 Nlgn2 Itga2 Dmp1 Cdsn Tspan4 Rras Sdc3 Cd274 Cldn9 Layn Tmem8b Col17a1 Nectin1 Dlg1 Negr1 Slit2 Lama3 Itga10 Icam5 Cap1 Col16a1 Insig1 Tnfrsf11b Traf1 Ywhah Alox8 Cdh15 Pcdh1 Pik3r3 Hadh Mmp2 Flnc Itgb4 Irs1
HALLMARK_KRAS_SIGNALING_UP	7.83E-06	1.83	Sema3b Rgs16 Igf2 Igfbp3 Nrp1 Ephb2 Emp1 Gucy1a1 Ccnd2 Mmp11 Tmem158 Kif5c Reln Id2 Vwa5a Pcp4 Tspan7 Crot Hsd11b1 Jup Hbegf Cfh Mtmr10 Pcsk1n Evi5 Klf4 Fuca1 Tmem100 Spon1 Itga2 Gprc5b Ank Cidea Atg10 Glrx Epb41l3 Prrx1 Gpnmb Csf2ra Mafb Angptl4 Tmem176a Scn1b Eng Psmb8 Tnfaip3 Ccl20 Scg5 Ngf Cpe Car2 Hdac9 Dock2 Fgf9 Traf1 Tfpi Ccser2 Tmem176b Fbxo4 Map3k1 Adgra2 Adam17 Cxcl10 Gng11
HALLMARK_COMPLEMENT	1.20E-05	1.81	Lrp1 Ctsd Timp2 Lgmn Cp Clu Ctso F3 Irf7 Mt3 Adam9 C3 C1s1 S100a13 Col4a2 Spock2 Lipa Cd36 Ctsl Mmp14 Ctsb Cfh

PATHWAY	padj	NES	leadingEdge Genes
			Serping1 Csrp1 Lamp2 Gnai2 Anxa5 Ctsh Pdp1 Me1 Prkcd Gpd2 Casp1 Dock4 Pdgfb Notch4 Fn1 Cpq Dock9 Tnfaip3 Casp4 Gca Psmb9 Gata3 C2 Car2 Klkb1 Hspa1a Cda Msrb1 Pla2g4a Pclo Atox1 Usp8 Tmprss6 Prcp
HALLMARK_ANGIOGENESIS	3.15E-03	1.79	Fstl1 Nrp1 Postn Ccnd2 Itgav S100a4 App Lrpap1 Apoh Lpl Fgfr1 Col5a2 Pdgfa Slco2a1 Msx1 Tnfrsf21 Jag1
HALLMARK_CHOLESTEROL_HOMEOSTASIS	1.26E-03	1.75	Sema3b Aldoc Fabp5 Gpx8 Lgmn Clu S100a11 Pparg Cd9 Cpeb2 Abca2 Anxa5 Hsd17b7 Lpl Ech1 Tm7sf2 Fads2 Atf5 Acss2 Pdk3 Pnrc1 Jag1
HALLMARK_APICAL_SURFACE	1.76E-03	1.75	Mdga1 Scube1 Thy1 Hspb1 Cx3cl1 Mal App B4galt1 Adam10 Rtn4rl1 Slc22a12 Sulf2 Tmem8b Gata3 Atp6v0a4 Flot2 Slc2a4 Afap1l2 Pkhd1 Efna5
HALLMARK_IL2_STAT5_SIGNALING	4.36E-05	1.75	Hopx Col6a1 Gadd45b Pth1r Ecm1 Plpp1 Ahnak Rgs16 Tgm2 Eno3 Ikzf2 Nrp1 Prnp Emp1 Serpinb6a Ccnd2 Csf1 Itgav Gpx4 Anxa4 Furin Plec Ckap4 P4ha1 Bmpr2 Rhob Syt11 Rora Ttc39b Cd81 Ahr S100a1 Lrig1 Icos Ifngr1 Gucy1b1 Ptch1 Fah Bcl2l1 Coch Ndrg1 Socs1 Cyfip1 Socs2 Nfkbiz Bhlhe40 Rnh1 Aplp1 Gabarapl1 Snx14 Car2 Tnfrsf21 Ikzf4 Fgl2 Twsg1 Traf1 Il3ra Mxd1 Il4ra Cxcl10 Tnfsf10 Enpp1 Cd44 Muc1
HALLMARK_ESTROGEN_RESPONSE_LATE	1.09E-04	1.71	Ass1 Cav1 Slc24a3 Sema3b Fabp5 Emp2 Atp2b4 Hmgcs2 Cyp26b1 Hspb8 Il6st Chst8 Itpk1 Slc26a2 Lamc2 Tst Id2 Dynlt3 Myof Pcp4 Cd9 Dlg5 Cxcl14 Cacna2d2 Hr Aldh3a2 Wfs1 Celsr2 Plxnb1 Rab31 Prss23 Slc2a8 Klf4 Pdcd4 Acox2 Elovl5 Mocs2 Amfr Chpt1 Isg20 Tob1 Foxc1 Papss2 Slc22a5 Plaat3 Frk Aff1 Cpe Etfb Abca3 Sfn Car2 Trim29 Add3 Fgfr3 Cox6c Ret Large1 Pdlim3 Cd44 Scnn1a Ptges Prkar2b Ptger3 Llgl2 Jak2 Il17rb Flnb
HALLMARK_IL6_JAK_STAT3_SIGNALING	1.76E-03	1.68	Itgb3 Pdgfc Il6st Csf1 Stat1 Tlr2 Cd36 Cd9 Acvrl1 Fas Irf9 Tgfb1 A2m Il13ra1 Ifngr1 Csf2ra Socs1 Stat2 Tnfrsf1a Hmox1 Osmr Tnfrsf21 Myd88 Il3ra Il4ra Cxcl10 Cd44 Il17rb Cntfr Il2rg
HALLMARK_P53_PATHWAY	1.74E-04	1.64	Ctsd Ak1 Rgs16 Txnip Sphk1 Foxo3 Stom Ccnd2 Gm2a Rb1 S100a4 Notch1 Vwa5a Tap1 Cebpa Abat Ephx1 Abhd4 Tcn2 App Coq8a Hbegf Vdr Fas Mxd4 Ctsf Sesn1 Ccng1 Tgfb1 Cd81 Klf4 Fuca1 Ninj1 Tsc22d1 Vamp8 Cdkn2b Serpinb5 Ier5 Tob1 Casp1 Cd82 Pdgfa Mapkapk3 Ndrg1 Ankra2 Socs1 Pmm1 Trafd1 Phlda3 Trp63 Sat1 S100a10 Prmt2 Hmox1 Sfn Plxnb2 Retsat Ptpre Btg1 Tax1bp3 Slc3a2 Mxd1 Alox8 Tgfa Gadd45a
HALLMARK_FATTY_ACID_METABOLISM	9.60E-04	1.64	Hmgcs2 Eno3 Aldh1a1 Cd36 Cpt1a Fmo1 Glul Ephx1 Acox1 Aldh3a2 Hsdl2 Trp53inp2 Me1 Hsd17b7 Serinc1 Elovl5 Cidea Acadm Gpd2 Mlycd Prdx6 Bphl Mgll Ech1 Reep6 Acot2 Decr1 Slc22a5 S100a10 Acaa2

PATHWAY	padj	NES	leadingEdge Genes
			Psme1 Ehhadh Hsd17b11 Gabarapl1 Etfdh Car2 Maoa Cpt2 Retsat Rdh11 Pts Eci2 Acaa1a Vnn1 Ywhah Eno2 Uros Ube2l6 Acadvl Mcee G0s2 Rap1gds1 Mdh1 Acsl1 Hadh D2hgdh Pcbd1 Acot8 Hsd17b4 Crat Aco2 Ppara Acss1 Gcdh Hadhb Hmgcs1 Hibch Aldh9a1 Ugdh Pdha1 Tdo2
HALLMARK_HEME_METABOLISM	2.43E-03	1.54	Endod1 Bcam Slc6a8 Igsf3 Foxo3 Aldh6a1 Myl4 Sidt2 C3 Lrp10 Abcg2 Dmtn Ctsb Slc6a9 Tmem9b Mgst3 Optn Pdzk1ip1 Nfe2l1 Lamp2 Fech Snca Fbxo9 Ypel5 Aldh1l1 Dcaf11 Ezh1 Daam1 Kat2b Mfhas1 Cast Tns1 Add1 Pcx Nr3c1 Gde1 Smox Clcn3 Car2 Atg4a Mboat2 Mpp1 Ubac1 Ccdc28a Bmp2k Mkrn1 Uros Adipor1 Fn3k Htatip2 Arhgef12 Bpgm Nek7 Ncoa4 Bnip3l Slc22a4 Rap1gap Ppox Hagh Selenbp1 Cat Ppp2r5b Tspo2 Cir1 Mxi1
HALLMARK_ESTROGEN_RESPONSE_EARLY	1.88E-03	1.53	Slc24a3 Sema3b Endod1 Slc7a2 Tgm2 Adcy1 Ablim1 Cyp26b1 Hspb8 Il6st Itpk1 Celsr1 Slc26a2 Retreg1 Sybu Dynlt3 Nav2 Myof Abat Kazn Elf1 B4galt1 Hr Wfs1 Celsr2 Zfp185 Rab31 Pex11a Prss23 Klf4 Reep1 Lrig1 Elovl5 Amfr Chpt1 Tob1 Rhobtb3 Foxc1 Papss2 Slc22a5 Plaat3 Frk Aff1 Bhlhe40 Abca3 Sfn Add3 Mindy1 Cant1 Rhod Med13l Ret Adcy9 Pdlim3 Cd44 Muc1 Wwc1 Scnn1a Ptges
HALLMARK_PEROXISOME	5.97E-03	1.50	Atxn1 Aldh1a1 Sema3c Prdx5 Abcd1 Hsd3b7 Mvp Acox1 Crabp1 Cadm1 Pex11a Ephx2 Tspo Scp2 Elovl5 Mlycd Abcb9 Ech1 Abcd3 Pex6 Pex2 Ehhadh Hsd17b11 Lonp2 Retsat Rdh11 Eci2 Slc23a2 Acaa1a Ywhah Pex5 Ttr Acsl1 Abcd2 Pex13 Bcl10 Acot8 Abcc8 Hsd17b4 Crat Abcb1a Fis1 Cat Abcb4
HALLMARK_TNFA_SIGNALING_VIA_NFKB	1.78E-02	1.38	Edn1 Gadd45b Ptx3 Sphk1 Spsb1 F3 Il6st Ackr3 Plpp3 Csf1 Pdlim5 Tlr2 Serpinb8 Id2 Tap1 Bcl6 B4galt1 Cebpd Hbegf Rhob Tnip1 Nr4a2 Klf4 Ninj1 Tsc22d1 Il18 Pmepa1 Ccn1 Ifih1 Ier5 Ifit2 Nfat5 Stat5a Sqstm1 Cflar Tnfaip3 Ccl20 Slc2a6 Sat1 Sdc4 Abca1 Dnajb4 Bhlhe40 Per1 Snn Fosl2 Pnrc1 Traf1 Ptpre Btg1 Jag1 Mxd1 Rcan1 Gadd45a Gch1 Cxcl10 G0s2 Cd44
HALLMARK_ALLOGRAFT_REJECTION	4.24E-02	1.36	Tapbp Irf7 Psmb10 Thy1 Ccnd2 Csf1 Stat1 Tgfb2 Gcnt1 Tlr2 Cd47 Degs1 Tap1 Tap2 Apbb1 Fas Tgfb1 Il18 Cd247 H2-DMa Ache Ifngr1 Galnt1 B2m Tlr6 Socs1 C2 Hdac9 Stab1 Abi1 Srgn Fcgr2b Tlr1 Il4ra Tlr3
HALLMARK_SPERMATOGENESIS	1.88E-03	-1.58	Gad1 Dcc Ncaph Rfc4 Ttk Tle4 Ddx25 Psmg1 Kif2c Ezh2 Topbp1 Dbf4 Slc12a2 Coil Bub1 Aurka Ccnb2 Nek2 Cdk1 Tsn Mast2 Sirt1 Il12rb2 Parp2 Gpr182 Csnk2a2 Hspa1l Mllt10 Vdac3 Mlf1 Cftr Strbp Tssk2 Pias2 Clpb Phf7 Arl4a Spata6 Oaz3 Pebp1
HALLMARK_MTORC1_SIGNALING	1.20E-05	-1.74	Ung Cdc25a Stc1 Ccnf Mcm2 Gga2 Mcm4 Txnrd1 Slc7a11 Psme3 Rrm2 Dhfr Psmg1 Nup205 Tfrc Hspd1 Hk2 Polr3g Uchl5 Ppa1

PATHWAY	padj	NES	leadingEdge Genes
			Tubg1 Ssr1 Lta4h Gsr Hmbs Tomm40 Etf1 Btg2 Plk1 Tmem97 Hspe1 Shmt2 Bcat1 Eef1e1 Nufip1 Elovl6 Rrp9 Mthfd2 Bub1 Aurka Nfil3 Cth Slc1a5 Cct6a Abcf2 Acly Gmps Pdap1 Srd5a1 Pitpnb Hprt Psmd12 Stip1 Psmc6 Psma3 Idi1 Cdkn1a Nfkbib Ifrd1 Cacybp Hspa9 Eif2s2 Psmb5 Mthfd2l Hspa4 Psmc4 Pno1 Psmd14 Ppia Tcea1 Ifi30 Ube2d3 Coro1a
HALLMARK_MITOTIC_SPINDLE	1.07E-05	-1.74	Lmnb1 Bin1 Kif11 Espl1 Fbxo5 Incenp Birc5 Brca2 Ttk Net1 Kif15 Kif22 Kif2c Epb41 Nin Cenpf Pif1 Top2a Cenpe Cntrl Nusap1 Smc3 Lrpprc Arhgap29 Plk1 Ssh2 Sass6 Bub1 Aurka Tubgcp3 Smc1a Trio Dlgap5 Ccnb2 Kif20b Nek2 Smc4 Tubgcp6 Cdk1 Cep57 Sac3d1 Cntrob Rfc1 Arhgap10 Arap3 Ndc80 Apc Kntc1 Clasp1 Rhot2 Map3k11 Tpx2 Rasa1 Kif4 Cenpj Pcnt Pxn Cep192 Prc1 Cep72 Kif23 Ppp4r2 Rapgef6 Alms1 Racgap1 Cep131 Ect2 Arhgef2 Cdc42ep1 Cyth2 Tubgcp5 Wasf1 Map1s
HALLMARK_UNFOLDED_PROTEIN_RESPONSE	1.07E-05	-1.94	Dkc1 Nolc1 Nhp2 Cnot6 Sdad1 Eif4a1 Exosc1 Nfya Lsm4 Npm1 Nop56 Exosc2 Banf1 Zbtb17 Eif4a3 Imp3 Ssr1 Nfyb Eif4e Khsrp Rrp9 Fus Exosc10 Mthfd2 Eif2s1 Iars Mtrex Cks1b Cxxc1 Exosc9 Ddx10 Dcp1a Atf4 Eif4g1 Hspa9 Tars Rps14 Nop14 Dcp2 Eef2 Aldh18a1
HALLMARK_DNA_REPAIR	6.59E-09	-2.13	Nme4 Pold1 Pola2 Pold3 Lig1 Ercc8 Umps Rfc4 Alyref Prim1 Pom121 Pcna Dut Aaas Rpa2 Nme1 Sf3a3 Impdh2 Rnmt Rfc2 Pola1 Snapc4 Dgcr8 Rad51 Ercc1 Srsf6 Polr2f Polr1c Nfx1 Itpa Taf1c Rfc5 Polr2h Polr2e Tyms Rev3l Sac3d1 Polr2c Fen1 Rae1 Clp1 Nudt21 Ssrp1 Gtf2a2 Ercc2 Cetn2 Aprt Nt5c Hprt Zwint Polr2a Nelfcd Nelfe Polr3c Pde4b Upf3b Tarbp2 Gtf3c5 Polr2d Nt5c3 Mrpl40 Cstf3 Adrm1 Rbx1 Taf6 Polr2i Mpg Cox17 Rpa3 Polr2g Polr2k Polh Rad52 Guk1 Smad5 Gtf2f1 Taf10
HALLMARK_MYC_TARGETS_V2	9.48E-25	-3.26	Myc Ung Dctpp1 Mcm5 Srm Nolc1 Cdk4 Tbrg4 Dusp2 Ppan Pus1 Mcm4 Grwd1 Bysl Mrto4 Tcof1 Ddx18 Mybbp1a Pa2g4 Gnl3 Npm1 Nop56 Noc4l Pprc1 Pes1 Nop2 Rcl1 Plk4 Hspd1 Wdr43 Nop16 Hk2 Rrp12 Nip7 Slc29a2 Farsa Wdr74 Utp20 Plk1 Tmem97 Hspe1 Mphosph10 Ndufaf4 Prmt3 Rrp9 Cbx3 Ipo4 Aimp2 Phb Las1l
HALLMARK_G2M_CHECKPOINT	2.28E-43	-3.44	Lmnb1 E2f2 Myc Nasp Cdc25a Mcm3 Cdc7 Pola2 Kif11 Mcm5 Cdc6 Ccnf Mtf2 Dkc1 Tmpo Nolc1 Cdk4 Hnrnpd Lbr Espl1 Exo1 Rad54l Hira Smarcc1 Mcm2 Fbxo5 Hmgb3 Incenp Birc5 Chek1 Mcm6 Brca2 Mybl2 Ttk Srsf2 Pole Tfdp1 Smc2 G3bp1 Kif15 Suv39h1 Snrpd1 Sfpq Aurkb Kif22 Mad2l1 E2f4 Rpa2 Prmt5 Kif2c Polq Ctcf Cenpf Knl1 Ezh2 Srsf1 Cdc45 Rbl1 Stil Plk4 Cenpa Top2a Tra2b Pbk Ube2c Cenpe Casp8ap2 E2f3 Ccna2 Chaf1a Nup50 Dtymk Cks2

PATHWAY	padj	NES	leadingEdge Genes
			Dbf4 Srsf10 Ncl Jpt1 Hnrnpu Mki67 Nusap1 Nsd2 Prim2 Hmmr Plk1 Slc12a2 Ilf3 Orc6 Top1 Syncrip Tacc3 Bub3 Cbx1 Stmn1 Bub1 Aurka Troap Ewsr1 Smc1a Ccnb2 Traip Kif20b Nek2 Smc4 Gins2 Prpf4b Cdk1 Slc7a1 Ube2s Cks1b Stag1 Kmt5a Ndc80 Bard1 Ccnt1 Cdc20 Kpnb1 Odf2 Xpo1 Tpx2 Kif4 Gspt1 Prc1 Upf1 Kif23 Dr1 Ythdc1 Racgap1 Mapk14 Hmga1b Nup98 Orc5 Arid4a Smad3 Rad21 Uck2
HALLMARK_MYC_TARGETS_V1	2.50E-49	-3.67	Hnrnpa3 Myc Cad Mcm5 Srm Lsm2 Srsf7 Nolc1 Cdk4 Hnrnpd Mcm7 C1qbp Smarcc1 Mcm2 Nhp2 Mcm4 Srsf3 Dek Mcm6 Rfc4 Ywhaq Srsf2 Eif4a1 Fbl Tfdp1 Pold2 Rsl1d1 Pcna G3bp1 Ncbp1 Ruvbl2 Usp1 Dut Snrpd1 Ddx18 Pa2g4 Mad2l1 Tomm70a Tardbp Gnl3 Npm1 Ddx21 Nop56 Cnbp Apex1 Ran Rnps1 Mrps18b Sf3a1 Nme1 Srsf1 Cdc45 Trim28 Serbp1 Cct5 Ranbp1 Snrpg Cdk2 Pwp1 Hspd1 Impdh2 Tra2b Nop16 Hnrnpa1 Uba2 Dhx15 Hnrnpa2b1 Tcp1 Ccna2 Phb2 Snrpb2 Rrm1 Snrpa1 Abce1 Eif3b Kars Ilf2 Hnrnpu Rps5 Orc2 Ppm1g Hdac2 Pcbp1 Sf3b3 Eif4e Etf1 Cct3 Hspe1 Rpl18 Syncrip Cct2 Rrp9 Prpf31 Cstf2 Bub3 Rps6 Ssb Eif2s1 Erh Snrpd3 Snrpd2 Exosc7 Cbx3 Rpl6 Rack1 Eif3d Rpl14 Iars Pabpc4 Tyms Tufm Cct7 Mrpl23 Aimp2 Xrcc6 Cct4 Clns1a Rpl22 Rps10 Ssbp1 Nap1l1 Phb Ndufab1 Vbp1 Rps3 Snrpa Cdc20 Hprt Kpnb1 Xpo1 Eif4h Rps2 Gspt1 Acp1 Hnrnpc Psma7 Pabpc1 Srpk1 Psmc6 Hsp90ab1 Eef1b2 Ifrd1 Eif3j1 Psma1 Psma6 Rplp0 Cyc1 Eif2s2 Mrpl9 Psmc4 Psmd3 Psma2 Got2 Psmd14 Ppia
HALLMARK_E2F_TARGETS	2.50E-49	-3.81	Lmnb1 Shmt1 Hmgb2 Myc Nasp Ung Wdr90 Cdc25a Mcm3 Lyar Dctpp1 Gins1 Dnmt1 Pold1 Pola2 Pold3 Lig1 Mcm5 Tmpo Nolc1 Cdk4 Hnrnpd Timeless Lbr Espl1 Mcm7 Tbrg4 Ccp110 E2f8 Mcm2 Hmgb3 Birc5 Chek1 Mcm4 Rnaseh2a Dek Mcm6 Hells Rad51ap1 Brca2 Mybl2 Srsf2 Pole Slbp Pold2 Pcna Bub1b Usp1 Nup107 Suv39h1 Dut Tipin Pa2g4 Aurkb Kif22 Mad2l1 Melk Rad51c Rrm2 Rpa2 Tubb5 Nop56 Atad2 Kif2c Lsm8 Ctcf Exosc8 Nup205 Ran Ezh2 Nup153 Nme1 Srsf1 Depdc1a Mms22l Ranbp1 Msh2 Trip13 Ak2 Plk4 Tfrc Top2a Prps1 Brca1 Rfc2 Nbn Tra2b Pnn Dck Tk1 Cenpe Spc25 Cdca8 Eed Kif18b Mxd3 Spc24 Ppp1r8 Cenpm Cse1l Tubg1 Cit Cks2 Anp32e Cdca3 Dscc1 Jpt1 Mki67 Cnot9 Orc2 Phf5a Smc3 Ncapd2 Snrpb Psmc3ip Prim2 Hmmr Plk1 Ilf3 Orc6 Ipo7 Syncrip Tacc3 Donson Luc7l3 Mthfd2 Stmn1 Aurka Smc1a Eif2s1 Dlgap5 Ccnb2 Smc6 Smc4 Ing3 Cdk1 Pms2 Gins3 Rfc1 Xrcc6 Ube2s Cks1b Stag1 Nudt21 Pan2 Rbbp7 Ssrp1 Zw10 Asf1b Bard1 Nap1l1 Cdc20 Xpo1 Kif4

PATHWAY	padj	NES	leadingEdge Genes
			Rad1 Gspt1 Dclre1b Ccne1 Ube2t Cdkn1a Psip1 Mlh1 Racgap1 Hmga1b Gins4

8.3 Differentially Expressed Genes in the Proliferating tumour cells 24 hrs post-radiation

Genes (UP)	log2FoldChange	padj	Genes (Down)	log2FoldChange	padj
Gna14	2.59	2.85E-03	Has1	-3.62	1.81E-12
Vgll2	1.70	4.39E-03	Kcnq1ot1	-2.56	1.32E-04
Ifi209	1.70	4.95E-02	Malat1	-2.49	2.45E-05
Prrt4	1.59	1.81E-02	Neb	-2.40	2.96E-05
Fhl2	1.58	2.41E-03	Gm47076	-2.33	1.35E-04
Gm19541	1.57	9.82E-06	Gm8251	-2.11	9.08E-04
Hs3st1	1.53	3.64E-03	F730035M05Rik	-2.10	1.89E-03
Chrna5	1.53	2.89E-02	Zbtb20	-2.07	3.06E-08
Baalc	1.49	6.95E-03	Slc16a4	-1.99	1.98E-07
Kcp	1.48	4.83E-02	4933433G19Rik	-1.96	1.92E-04
Gm30074	1.42	3.50E-02	Gm42664	-1.95	2.16E-07
Ccn2	1.41	1.99E-09	Syne2	-1.91	2.14E-106
Cdk5r2	1.40	3.65E-02	Gm20342	-1.84	2.25E-05
Kcng4	1.33	4.46E-02	Dnah17	-1.82	3.35E-06
Pdgfb	1.29	1.66E-04	Gm29361	-1.79	3.76E-03
Nrip3	1.29	1.22E-02	Fat3	-1.76	1.97E-42
Gm38414	1.23	1.47E-02	Gm42463	-1.73	3.55E-03
Ifit1	1.22	1.15E-02	Gm15893	-1.67	3.52E-02
Tinagl1	1.22	8.20E-03	Pram1	-1.65	3.03E-02
Atoh8	1.22	2.65E-02	Hmcn1	-1.63	1.36E-15
Slc9a2	1.21	4.90E-02	Itgae	-1.60	6.97E-03
Hist2h3c1	1.16	2.18E-03	B230334C09Rik	-1.58	4.22E-25
Pdzd3	1.15	3.12E-02	Dst	-1.58	########
Ass1	1.12	1.34E-03	Xist	-1.57	########
Igfbp7	1.09	3.56E-02	1700109H08Rik	-1.57	2.39E-04
Hkdc1	1.08	8.08E-03	Gm14257	-1.55	2.11E-02
Crh	1.07	2.67E-02	Gm48747	-1.54	1.22E-03
Ceacam1	1.06	5.07E-03	Wnt2b	-1.53	3.10E-02
Tnfrsf25	1.05	4.10E-02	Lca5l	-1.47	4.60E-02
Dnajb3	1.04	4.76E-02	Herc1	-1.45	5.98E-84
Hspb1	1.03	9.76E-03	Macf1	-1.45	1.54E-93
Dact2	1.03	1.73E-03	Fat4	-1.42	1.11E-20
Areg	1.02	2.21E-03	4932438A13Rik	-1.42	8.80E-46
Gm49774	1.02	2.32E-02	Mdn1	-1.41	1.77E-49
Serpinb5	1.02	5.74E-03	Gm43660	-1.41	5.06E-03
Ccl7	1.02	3.63E-04	Kmt2d	-1.40	1.40E-53
Klrg2	0.99	2.79E-02	Ubr4	-1.40	########
Car3	0.99	1.47E-07	1700109K24Rik	-1.39	4.54E-02
Stbd1	0.99	2.53E-02	Kmt2a	-1.39	3.59E-81
Coch	0.98	5.18E-07	A230057D06Rik	-1.37	1.14E-03

Genes (UP)	log2FoldChange	padj	Genes (Down)	log2FoldChange	padj
Dkk2	0.97	4.00E-02	Kmt2c	-1.36	1.07E-59
Ina	0.97	1.48E-03	Naaladl2	-1.36	8.08E-03
Tes	0.96	5.22E-05	mt-Nd3	-1.36	7.17E-07
Ccl2	0.95	4.14E-12	Gm28229	-1.36	1.22E-02
Nr1h3	0.94	2.70E-02	Erbb4	-1.33	4.14E-18
Fbxl8	0.93	6.09E-03	Zc3h6	-1.33	1.95E-05
Nrtn	0.93	4.43E-02	Far2	-1.32	2.11E-02
Emb	0.92	1.22E-02	Ttn	-1.32	4.04E-03
Shisa8	0.92	5.49E-03	Hipk4	-1.32	4.70E-02
E330020D12Rik	0.91	3.82E-02	Zbtb37	-1.32	1.17E-19
Tspan8	0.89	2.15E-03	Mycbp2	-1.31	8.88E-68
Stmn4	0.87	3.84E-03	Gm38190	-1.30	2.71E-02
Fam155a	0.86	1.93E-02	Fam228b	-1.29	1.94E-02
Gch1	0.86	1.57E-04	Birc6	-1.28	3.08E-79
Eef1a2	0.84	2.18E-02	Fat1	-1.27	########
Apobec3	0.83	3.22E-02	Mki67	-1.27	2.82E-08
Barx1	0.82	8.80E-03	Gm38394	-1.26	1.61E-05
Tnfrsf23	0.81	2.38E-03	Lrp2	-1.26	1.41E-11
Chac1	0.80	8.55E-04	Huwe1	-1.25	########
Nefl	0.79	6.67E-09	Mpeg1	-1.25	1.33E-02
Capg	0.79	1.23E-02	Lrp1	-1.24	########
Nfil3	0.79	2.31E-06	Zfhx3	-1.24	4.79E-11
Vgf	0.79	4.63E-14	Pcdhgc5	-1.22	5.67E-03
Smagp	0.78	4.49E-02	Nf1	-1.21	1.44E-42
Csf2ra	0.78	4.10E-02	Herc2	-1.20	5.29E-56
Galt	0.74	2.15E-02	Dgkh	-1.20	1.94E-25
Ccdc184	0.73	2.85E-04	Hipk2	-1.20	4.16E-29
Gsx1	0.73	2.09E-03	Rnf213	-1.19	3.63E-25
Htra3	0.73	1.18E-02	Dync2h1	-1.19	3.68E-23
Il34	0.73	6.04E-04	Wdfy3	-1.19	3.49E-82
Gbp2	0.72	1.03E-04	Dync1h1	-1.18	3.87E-95
Msl3l2	0.72	1.39E-02	Gm26724	-1.17	2.72E-02
Plcg2	0.71	3.02E-06	Smg1	-1.16	5.13E-60
Filip1l	0.71	1.10E-03	8030451A03Rik	-1.15	2.40E-02
Tmem179	0.70	4.90E-03	Vmn2r1	-1.14	3.62E-02
Pdlim1	0.70	2.38E-07	Ccdc78	-1.13	2.40E-04
Tph2	0.70	3.41E-02	Clcn1	-1.12	4.43E-02
Gstm2	0.69	1.49E-02	Vps13b	-1.12	1.20E-22
Glipr2	0.69	3.81E-07	Akap9	-1.12	4.80E-47
Trim47	0.69	8.31E-03	Gm16185	-1.12	2.78E-03

Genes (UP)	log2FoldChange	padj	Genes (Down)	log2FoldChange	padj
Dok5	0.69	2.80E-03	Cep350	-1.12	4.32E-30
Dhrs3	0.69	6.76E-03	Onecut2	-1.11	6.26E-06
Xbp1	0.69	9.91E-14	Vps13d	-1.11	4.02E-30
Sema3e	0.69	2.32E-03	Lpp	-1.11	6.44E-22
Cgref1	0.68	4.12E-02	Prkdc	-1.11	2.56E-17
Calhm5	0.68	2.86E-02	Vps13c	-1.10	1.05E-21
Rarres1	0.68	2.24E-02	Gm50322	-1.09	1.54E-04
Emcn	0.67	3.80E-02	Nbeal1	-1.09	7.48E-15
Banp	0.67	2.38E-07	Lrrc29	-1.08	4.55E-02
Pex5l	0.67	1.22E-04	Cenpf	-1.08	5.13E-29
Smpd3	0.67	3.40E-05	Pclo	-1.07	4.26E-04
Amigo2	0.67	5.45E-03	Sacs	-1.07	2.32E-32
Osbp2	0.67	3.53E-03	A830082N09Rik	-1.07	7.52E-03
1600014C10Rik	0.66	8.80E-03	Tnrc6b	-1.07	2.08E-37
Sqor	0.66	7.86E-03	Ino80d	-1.06	4.67E-20
Lamc2	0.66	2.82E-02	Atm	-1.06	9.16E-32
Cxcl14	0.66	3.70E-05	Airn	-1.05	9.24E-03
Adra1b	0.65	3.10E-02	Lcor	-1.05	9.51E-10
Fam117a	0.65	2.23E-02	Nav1	-1.04	1.31E-54
Rgs2	0.65	5.20E-03	Gm1976	-1.04	9.16E-05
Camkk1	0.65	4.42E-03	Zfp704	-1.04	5.75E-33
Tubb4a	0.65	5.85E-05	Cd46	-1.04	3.24E-02
Trnp1	0.65	4.78E-02	Hspg2	-1.03	3.52E-60
Anxa1	0.65	9.05E-04	Fmn1	-1.03	3.24E-02
Ly6e	0.64	2.36E-04	Zfhx2	-1.03	2.40E-02
Gm13889	0.64	4.39E-10	Fras1	-1.03	1.99E-19
Fetub	0.63	2.00E-02	Col12a1	-1.01	3.80E-14
Hebp2	0.63	3.81E-02	Stard9	-1.01	1.18E-16
Cntnap4	0.62	2.71E-02	Msh5	-1.01	4.98E-02
Plp2	0.62	4.07E-02	D130040H23Rik	-1.00	1.97E-02
Hspa1b	0.62	3.75E-03	Brca2	-1.00	4.70E-19
Zcchc12	0.62	6.00E-10	Sbsn	-1.00	2.99E-02
Cxcl10	0.62	3.30E-03	BC005561	-1.00	1.50E-06
Bmerb1	0.62	1.03E-04	Rev3l	-1.00	2.52E-51
Rab26	0.61	1.37E-03	Gm43031	-1.00	3.05E-07
Lcmt2	0.61	6.65E-04	Hectd4	-0.99	7.12E-28
Spp1	0.61	7.79E-17	Frem2	-0.99	3.48E-03
Cavin2	0.61	3.71E-05	Tet1	-0.98	1.88E-16
Ube2ql1	0.60	1.15E-10	Ubn2	-0.98	2.40E-18

Genes (UP)	log2FoldChange	padj	Genes (Down)	log2FoldChange	padj
Prmt2	0.60	3.61E-12	Synm	-0.98	4.29E-02
Lpin3	0.60	1.28E-02	Med12l	-0.98	1.55E-14
Afg1l	0.59	1.26E-02	Ncam2	-0.97	3.43E-05
Cryab	0.59	1.05E-03	Gm50012	-0.97	3.27E-02
Cst6	0.59	5.83E-03	Bmpr2	-0.97	3.73E-36
Gbp3	0.59	7.76E-06	Gm49602	-0.97	3.63E-03
Rrad	0.58	4.79E-03	Gm9821	-0.96	2.92E-02
Fbxl15	0.58	5.99E-03	Itpr2	-0.96	1.86E-26
Gm43566	0.58	4.44E-02	Prrc2c	-0.96	3.15E-56
Btbd17	0.58	1.43E-11	Syne1	-0.95	5.33E-21
Pcyox1l	0.58	7.76E-06	Usf3	-0.95	5.50E-24
Kcnk13	0.58	3.26E-04	Ntrk3	-0.95	7.94E-17
Afap1l1	0.58	1.24E-03	Il20rb	-0.94	9.07E-03
Lxn	0.58	2.54E-08	Gucy1a2	-0.94	1.46E-03
Fam131a	0.57	5.18E-04	Tmem245	-0.94	5.95E-31
Plaur	0.57	7.63E-03	Gm21781	-0.93	1.46E-04
Gpnmb	0.57	2.20E-02	Pkd1	-0.93	4.23E-56
Epha2	0.57	5.42E-05	Chd7	-0.93	3.60E-34
Aig1	0.57	6.10E-07	Gm41442	-0.92	5.61E-04
Uchl1	0.57	2.92E-15	Tet2	-0.92	2.37E-22
Slco3a1	0.56	1.45E-07	Fbn1	-0.92	5.81E-43
Sema3f	0.56	1.10E-02	Nfat5	-0.91	1.28E-34
Mcub	0.56	1.78E-02	Lyst	-0.91	1.13E-10
Mrps6	0.55	1.68E-10	Fryl	-0.91	2.85E-36
Sesn2	0.55	1.57E-06	Nav2	-0.90	5.77E-43
Rai2	0.55	2.49E-02	Srcap	-0.90	9.16E-32
Tradd	0.55	1.11E-02	Acvr2b	-0.90	1.15E-03
Gm42372	0.55	1.19E-03	Fbn2	-0.90	4.43E-52
S100a6	0.55	4.85E-04	Phip	-0.90	1.85E-25
Nupr1	0.54	1.77E-03	Gm12940	-0.90	1.80E-04
Emp3	0.54	7.35E-03	Myo9a	-0.90	4.96E-20
Liph	0.54	5.01E-03	Pou2f1	-0.89	3.30E-11
Akr1b8	0.54	7.92E-03	Spaca6	-0.89	2.04E-05
Hs1bp3	0.54	3.54E-03	Trrap	-0.88	2.70E-46
Trmt1l	0.54	1.54E-05	Ago3	-0.88	1.87E-10
Ptprn	0.54	3.18E-04	Ash1l	-0.88	1.01E-34
Sel1l3	0.54	1.72E-03	Zc3h11a	-0.88	5.65E-04
Ctsf	0.53	3.13E-03	Apc	-0.88	3.11E-47
Eya2	0.53	1.42E-02	Mga	-0.88	4.77E-25
Tmod1	0.53	2.24E-02	Ep400	-0.87	4.09E-43
Pex26	0.53	3.63E-02	Cbl	-0.87	5.72E-43
Dusp5	0.53	1.99E-02	Usp34	-0.87	4.19E-39

Genes (UP)	log2FoldChange	padj	Genes (Down)	log2FoldChange	padj
Dlgap3	0.53	3.48E-02	Ccdc73	-0.87	1.87E-02
Akr1b10	0.53	1.58E-04	Igip	-0.87	1.78E-05
Plin2	0.53	3.39E-06	Braf	-0.87	7.41E-12
Dedd2	0.52	2.15E-02	Lrba	-0.87	5.52E-12
Pdrg1	0.52	7.35E-05	Alms1	-0.87	4.04E-12
Srpx2	0.52	4.29E-02	Ptpn4	-0.86	4.44E-19
Lix1	0.52	1.42E-03	Fbxo48	-0.86	9.59E-03
Cnn2	0.52	2.06E-09	Csmd2	-0.85	5.11E-21
Pold4	0.52	4.38E-03	Ago2	-0.85	2.31E-39
Ankrd9	0.52	1.21E-02	Thbd	-0.85	4.84E-02
Lmo2	0.52	3.87E-02	Akap13	-0.85	1.81E-30
Gpc4	0.52	2.88E-05	mt-Nd5	-0.85	5.18E-46
Mdfi	0.51	1.42E-02	Fut9	-0.84	1.05E-09
Lgr6	0.51	2.47E-02	Nktr	-0.84	1.08E-19
Crip2	0.51	1.31E-06	Traf3ip2	-0.84	1.28E-02
Zfp467	0.51	6.85E-04	Map1b	-0.84	2.82E-36
Fam174b	0.51	1.44E-03	Mir100hg	-0.84	6.30E-09
Hmox1	0.51	2.38E-05	Xrn1	-0.83	1.15E-21
Pou3f1	0.51	1.44E-06	Celsr2	-0.83	6.79E-31
Cib2	0.51	5.06E-03	Htt	-0.83	2.49E-32
Tm4sf1	0.51	1.32E-09	B930095G15Rik	-0.83	5.28E-03
Vwc2	0.50	9.82E-03	Rora	-0.83	4.07E-06
Fbxo25	0.50	2.65E-03	Usp24	-0.83	1.83E-33
Gpx1	0.50	3.42E-11	Usp9x	-0.83	1.65E-34
Arc	0.50	1.53E-03	Golgb1	-0.82	3.07E-22
Renbp	0.50	4.04E-05	Ptar1	-0.82	4.74E-25
Ccdc92	0.50	2.43E-03	Cep250	-0.81	1.56E-18
Efna2	0.50	1.57E-02	Setx	-0.81	2.47E-23
Herpud1	0.50	1.11E-04	Aspm	-0.81	6.79E-18
Atf5	0.50	4.67E-08	Myo5b	-0.81	4.02E-02
Eef1akmt4	0.49	3.27E-02	Spen	-0.81	1.17E-22
Pxdc1	0.49	4.14E-05	Vps13a	-0.81	3.65E-15
Creg1	0.49	2.03E-03	Nsd1	-0.80	6.46E-22
Car2	0.49	2.20E-04	Cfap54	-0.80	4.09E-02
Sdf2l1	0.49	5.05E-04	Mmp16	-0.79	2.56E-02
Uros	0.49	2.79E-02	Diaph2	-0.79	1.09E-09
Dalrd3	0.49	2.26E-03	Igsf9b	-0.79	2.78E-18
Lin37	0.49	9.85E-03	Pcdhb21	-0.78	6.44E-03
Errfi1	0.49	2.01E-04	Ccdc15	-0.78	3.12E-03
Trim46	0.49	1.03E-03	Zc3h12c	-0.77	9.16E-08
Gnaz	0.48	2.32E-03	Nfia	-0.76	2.87E-03

Genes (UP)	log2FoldChange	padj	Genes (Down)	log2FoldChange	padj
Prkar1b	0.48	1.25E-02	**Cnot6l**	-0.76	1.62E-15
Cebpb	0.48	3.00E-03	**B9d1**	-0.76	1.94E-03
Taf1c	0.48	5.86E-03	**Trip11**	-0.76	6.52E-15
Cebpd	0.48	6.01E-03	**Atrx**	-0.76	2.61E-24
Coq4	0.48	4.79E-02	**Slc1a2**	-0.76	1.21E-04
Trib3	0.48	2.51E-02	**Bod1l**	-0.76	8.90E-22
Crispld2	0.48	1.46E-06	**Hook3**	-0.75	5.61E-15
Slc25a38	0.48	5.92E-03	**Lnpep**	-0.75	2.92E-24
Adgre5	0.47	2.13E-05	**Chd6**	-0.75	3.01E-20
Il10rb	0.47	3.17E-02	**Qser1**	-0.75	3.53E-21
Clu	0.47	9.80E-04	**Soga1**	-0.75	1.32E-03
Relb	0.47	1.43E-02	**Nipbl**	-0.75	3.79E-26
Trim16	0.47	4.71E-04	**Gm38393**	-0.75	1.40E-02
Rhpn1	0.47	3.02E-02	**Asxl2**	-0.75	3.99E-16
Cebpa	0.47	7.34E-03	**Insr**	-0.74	1.83E-15
Vax2	0.47	3.01E-02	**Ubr5**	-0.74	1.82E-33
Ogfod2	0.47	1.56E-02	**Zfp292**	-0.74	8.06E-10
Rnf182	0.47	8.20E-03	**Gramd1c**	-0.74	2.91E-02
Pepd	0.47	1.45E-04	**Nhsl2**	-0.74	1.08E-10
Galnt18	0.47	6.47E-04	**Med13**	-0.74	8.40E-16
Tst	0.47	3.40E-03	**Pcdhb19**	-0.74	7.02E-04
Galm	0.47	1.10E-02	**Phc3**	-0.74	1.33E-17
Sgk1	0.47	2.92E-10	**Cplane1**	-0.74	2.21E-09
Tmem108	0.46	1.17E-02	**Fzd3**	-0.73	1.22E-27
Ubtd1	0.46	1.75E-04	**Taok1**	-0.73	8.48E-25
Anxa3	0.46	2.89E-06	**Nfib**	-0.73	2.46E-23
Oaf	0.46	2.78E-02	**Mecp2**	-0.73	2.54E-17
Htra1	0.46	6.32E-07	**Tanc2**	-0.72	9.46E-11
Hsph1	0.46	1.84E-13	**Irs1**	-0.72	3.30E-08
Rbm45	0.46	1.11E-04	**Ttc28**	-0.72	1.43E-18
Mypop	0.46	6.21E-03	**Tmem265**	-0.72	1.51E-03
Dpp7	0.46	3.82E-02	**Zc3h12b**	-0.72	3.21E-05
Camkv	0.46	8.97E-03	**Setbp1**	-0.72	3.42E-09
Itga3	0.46	1.77E-03	**Crebbp**	-0.72	2.65E-15
Pdlim7	0.46	5.11E-04	**Adgrv1**	-0.72	2.70E-04
Gmppb	0.45	1.35E-02	**Fam199x**	-0.72	3.42E-12
Dner	0.45	1.34E-05	**Zfp469**	-0.71	9.79E-10
Rpusd1	0.45	2.41E-02	**Nin**	-0.71	3.66E-19
Fbln1	0.45	6.75E-12	**Dock3**	-0.71	7.70E-13
Efnb2	0.45	3.52E-04	**Zgrf1**	-0.71	3.02E-09
Tesc	0.45	3.12E-02	**Srrm2**	-0.71	1.38E-23

Genes (UP)	log2FoldChange	padj	Genes (Down)	log2FoldChange	padj
E030030I06Rik	0.45	2.92E-03	Akap6	-0.71	7.02E-04
Angptl2	0.45	1.42E-02	Yod1	-0.71	2.32E-04
Ftl1	0.45	2.45E-02	Gpc6	-0.71	2.83E-06
Dapk3	0.45	1.64E-06	Scn8a	-0.71	1.32E-06
Mns1	0.45	3.09E-03	Nbea	-0.70	8.92E-18
Gstt1	0.45	4.14E-02	D930016D06Rik	-0.70	1.97E-04
D6Wsu163e	0.45	1.09E-02	Mbd5	-0.70	8.75E-08
Pou4f1	0.45	1.67E-02	Dmxl1	-0.70	1.60E-15
Fam72a	0.44	2.42E-02	Cacna1c	-0.70	1.19E-09
Actn1	0.44	2.04E-06	Ildr2	-0.70	1.30E-06
Celf4	0.44	6.44E-03	Myo5a	-0.70	4.01E-24
Ptgr1	0.44	4.49E-03	Ttbk2	-0.70	7.04E-08
Fblim1	0.44	6.97E-03	Ahnak	-0.70	6.09E-03
Kif26a	0.44	4.24E-02	E130308A19Rik	-0.70	5.74E-05
Ddit4l	0.44	3.16E-02	Gan	-0.69	1.36E-11
Grm4	0.44	8.76E-03	Tet3	-0.69	5.11E-18
Josd2	0.44	8.76E-05	Rc3h1	-0.69	1.70E-08
Anxa2	0.44	2.61E-08	Mfsd4a	-0.69	5.65E-05
S100a4	0.44	4.96E-02	Arhgap32	-0.69	2.38E-20
Pcp4l1	0.44	4.13E-02	Wnk1	-0.68	1.49E-34
Cdkn2b	0.44	2.74E-03	Atxn1	-0.68	3.21E-02
Cd248	0.44	1.98E-02	Ppp1r9a	-0.68	6.25E-14
Snap47	0.44	4.02E-07	Scai	-0.68	2.16E-06
Clcf1	0.44	4.18E-03	mt-Nd6	-0.68	3.81E-02
Adcy8	0.43	1.20E-02	Bptf	-0.68	7.51E-22
Tnip1	0.43	8.64E-03	Pcdh15	-0.68	6.58E-08
Pnrc1	0.43	5.64E-04	Tenm3	-0.67	8.25E-20
Dxo	0.43	1.24E-02	Knl1	-0.66	1.43E-07
Naaa	0.43	4.40E-02	Zfp462	-0.66	1.14E-15
Calr	0.43	1.49E-14	Rsf1	-0.66	6.80E-16
Sox7	0.43	3.69E-03	Zfp871	-0.66	6.25E-14
Olfm1	0.43	1.15E-05	Ptprz1	-0.66	6.63E-33
Ier3	0.43	2.92E-07	Prune2	-0.66	6.66E-05
Atcay	0.43	1.02E-02	Hivep3	-0.65	3.19E-06
Hspa5	0.43	2.26E-12	Eml5	-0.65	6.99E-06
Galk2	0.43	2.09E-03	Pdpr	-0.65	1.17E-06
Serpinh1	0.43	2.38E-03	Arid1a	-0.65	1.86E-27
Them6	0.43	6.59E-03	Fsd1l	-0.65	1.40E-03
Copz2	0.43	3.14E-02	Aff4	-0.65	1.44E-27

Genes (UP)	log2FoldChange	padj	Genes (Down)	log2FoldChange	padj
Rab3d	0.43	1.88E-02	Fign	-0.65	1.67E-03
Snrnp25	0.43	1.35E-04	Klf11	-0.65	8.67E-04
Anxa7	0.43	1.43E-02	Dicer1	-0.65	8.37E-17
Zfp428	0.43	1.12E-03	Zfp652	-0.65	1.58E-11
Exog	0.42	2.71E-03	Brwd3	-0.65	1.92E-11
Gpx3	0.42	1.92E-02	Tmem170b	-0.65	9.14E-12
Uap1l1	0.42	6.24E-03	Ncor2	-0.65	3.76E-29
Tubb3	0.42	7.93E-08	Raph1	-0.65	8.95E-06
Sirt7	0.42	4.19E-03	Map3k2	-0.65	2.33E-07
Lactb	0.42	1.70E-02	Dennd5b	-0.64	7.52E-08
Lmcd1	0.42	3.78E-03	Trps1	-0.64	9.91E-14
Mrpl21	0.42	4.00E-03	Lrrc58	-0.64	1.31E-17
Pcsk1n	0.42	1.10E-08	Per3	-0.64	2.43E-03
H2afj	0.42	2.14E-06	Peak1	-0.64	2.73E-16
Syt4	0.42	1.33E-03	Rnf165	-0.64	1.01E-04
Pgbd5	0.42	3.88E-03	Chd2	-0.64	1.03E-12
Cog4	0.42	2.34E-07	Rabgap1l	-0.64	2.83E-07
Ctsz	0.42	2.32E-02	Fry	-0.64	2.48E-03
Aldh1a3	0.42	4.61E-05	Lcorl	-0.64	1.79E-08
Cited2	0.41	1.37E-05	Piezo2	-0.64	2.45E-05
Pdlim4	0.41	6.80E-05	N4bp2	-0.64	9.46E-10
Sf3b5	0.41	2.08E-05	Pbrm1	-0.63	3.73E-14
Il33	0.41	2.83E-02	Klhl11	-0.63	2.80E-05
Pdgfa	0.41	3.72E-03	Pikfyve	-0.63	3.44E-12
Cdk2ap2	0.41	2.46E-03	D630045J12 Rik	-0.63	4.86E-09
Igsf21	0.41	3.22E-04	Zdhhc21	-0.63	3.08E-12
Pdia4	0.41	1.88E-09	Wnk3	-0.63	8.98E-08
Gmpr	0.41	4.85E-02	Spin4	-0.63	1.95E-02
Meis3	0.41	2.20E-02	Trio	-0.63	5.88E-21
Gm47283	0.41	5.71E-03	Dchs1	-0.63	5.30E-25
Rps12	0.41	4.00E-02	Zmiz1	-0.63	3.24E-31
Cxcr4	0.41	7.19E-04	Thsd7a	-0.63	4.34E-09
Ercc1	0.41	1.74E-03	Dcp2	-0.63	8.37E-17
1110008P1 4Rik	0.41	1.19E-02	Sbf2	-0.63	9.64E-19
Mrpl49	0.41	8.71E-04	Cep290	-0.62	2.34E-04
Selenom	0.41	7.91E-04	Uvssa	-0.62	1.01E-05
Zfat	0.40	4.31E-02	Hlf	-0.62	3.68E-05
Qpct	0.40	1.76E-03	Ccdc88a	-0.62	7.91E-16
Prr7	0.40	3.08E-02	Mast4	-0.62	1.02E-10
Rtn4rl1	0.40	1.83E-02	Lats1	-0.62	4.93E-13

Genes (UP)	log2FoldChange	padj	Genes (Down)	log2FoldChange	padj
Fbxo32	0.40	1.57E-02	**Pcnt**	-0.62	1.32E-09
Neu1	0.40	5.97E-05	**Setd2**	-0.62	4.77E-18
Ndp	0.40	1.39E-02	**Grm5**	-0.62	2.23E-12
Tm2d3	0.40	1.19E-02	**Nrxn1**	-0.62	3.51E-14
Gadd45g	0.40	1.12E-07	**Mir9-3hg**	-0.61	5.00E-03
Rbpms2	0.40	1.99E-04	**Ep300**	-0.61	5.49E-20
Mrps12	0.40	9.86E-04	**Bach2**	-0.61	1.48E-06
Rsrp1	0.40	1.56E-04	**Utrn**	-0.61	1.89E-18
Serpini1	0.40	3.41E-02	**Pcdhac2**	-0.61	3.67E-02
Phospho2	0.40	1.01E-02	**Setd1b**	-0.61	1.12E-09
Map1lc3a	0.40	7.35E-05	**Ro60**	-0.61	4.67E-11
Tusc2	0.40	4.42E-02	**Nr2c2**	-0.61	1.70E-08
Ncbp2	0.40	5.78E-05	**Rif1**	-0.61	1.74E-13
Stn1	0.40	2.83E-02	**Maml2**	-0.61	2.92E-11
Slc25a10	0.40	3.38E-04	**Pcm1**	-0.61	1.71E-15
Hic1	0.40	3.17E-03	**Dcc**	-0.60	8.11E-07
Grb14	0.40	1.37E-04	**Ubxn7**	-0.60	2.33E-08
Creld2	0.40	2.23E-04	**Tead1**	-0.60	1.46E-25
Junb	0.39	3.78E-03	**Lama1**	-0.60	6.02E-04
Acot7	0.39	9.00E-05	**Arid2**	-0.60	1.50E-20
Hist1h2bc	0.39	3.79E-04	**Amer1**	-0.60	5.12E-08
Scand1	0.39	1.08E-02	**Lama5**	-0.60	1.77E-13
Uck1	0.39	1.35E-04	**Ranbp2**	-0.60	1.87E-19
Myo1e	0.39	7.50E-03	**Sptbn2**	-0.60	1.10E-05
P3h1	0.39	1.24E-04	**Baz2b**	-0.60	5.36E-09
Txnl4a	0.39	5.10E-03	**Carf**	-0.60	4.29E-03
Fkbp10	0.39	2.34E-04	**Atad5**	-0.60	2.02E-08
Atg101	0.39	3.63E-03	**Kat6a**	-0.59	6.38E-17
S100a10	0.39	5.86E-04	**Cdk5rap2**	-0.59	3.99E-17
Ppp1r3c	0.39	2.52E-02	**Hectd1**	-0.59	3.41E-20
Ninj1	0.39	2.65E-03	**Bahcc1**	-0.59	7.70E-17
Clta	0.39	2.54E-08	**Ubr3**	-0.59	4.60E-20
Taf10	0.39	4.99E-05	**Cep97**	-0.59	8.87E-05
Ndrg4	0.39	2.07E-04	**Stox2**	-0.59	5.59E-18
Eef1akmt1	0.39	9.96E-03	**Rictor**	-0.59	2.33E-07
Orai1	0.39	2.63E-03	**Dmxl2**	-0.59	6.12E-06
Tmem50b	0.38	4.40E-04	**Ralgapa1**	-0.58	3.61E-12
Inf2	0.38	2.26E-02	**Kif24**	-0.58	2.63E-04
Stambpl1	0.38	9.42E-06	**Kmt2e**	-0.58	8.60E-16
Pla2g6	0.38	7.78E-04	**Ticrr**	-0.58	2.31E-08
Med11	0.38	3.56E-02	**Zfp827**	-0.58	2.52E-07
Selenos	0.38	7.33E-05	**Igf1r**	-0.58	9.50E-15

Genes (UP)	log2FoldChange	padj	Genes (Down)	log2FoldChange	padj
Rras2	0.38	1.11E-02	Chd9	-0.58	6.68E-09
D030056L22Rik	0.38	1.30E-03	Ankrd11	-0.58	2.90E-20
Pfkp	0.38	6.61E-04	Gm42047	-0.58	8.75E-27
Anxa5	0.38	5.65E-10	Vamp1	-0.58	2.51E-02
Hpcal1	0.38	1.35E-03	Hdx	-0.58	1.33E-02
Ctsl	0.38	2.38E-07	Tnrc18	-0.58	3.17E-17
Cbr3	0.38	1.59E-02	Helz	-0.57	4.47E-11
Cib1	0.38	6.24E-03	Kcnn3	-0.57	1.33E-05
Glmp	0.37	1.61E-05	Dennd4a	-0.57	2.85E-09
Cacnb3	0.37	9.11E-04	Rai1	-0.57	5.86E-14
Crtap	0.37	3.00E-04	Szt2	-0.57	1.96E-06
Hapln4	0.37	9.31E-04	Gm17066	-0.57	4.30E-02
Sh3bgrl3	0.37	2.43E-02	Pcdh7	-0.57	3.98E-08
Lcmt1	0.37	4.42E-03	Med13l	-0.57	2.46E-12
Tmem208	0.37	1.63E-02	Cep85l	-0.57	1.15E-04
Slc25a19	0.37	9.79E-03	Hivep1	-0.57	8.50E-10
Dynll1	0.37	1.01E-08	Slc6a11	-0.57	2.58E-07
Cybc1	0.37	1.93E-02	Rorb	-0.56	1.70E-08
Rita1	0.37	4.76E-02	Zkscan8	-0.56	7.84E-06
Cd3eap	0.37	5.23E-03	Slc25a27	-0.56	9.31E-03
Rcan2	0.37	3.79E-04	Cpeb4	-0.56	2.80E-12
Gpn2	0.37	2.50E-02	Akap11	-0.56	8.51E-18
Nr2f6	0.37	4.41E-03	Trim71	-0.56	8.64E-03
Med31	0.37	3.41E-02	Itgb8	-0.56	4.99E-09
L3hypdh	0.37	1.60E-02	Atr	-0.56	4.23E-06
Msrb1	0.37	5.67E-03	Erbin	-0.56	6.95E-20
Gcdh	0.37	1.86E-02	Notch2	-0.56	1.10E-10
Sertad1	0.37	4.92E-02	Snhg14	-0.56	1.42E-02
Tmem160	0.37	1.11E-03	Elk4	-0.56	3.32E-05
Asns	0.37	5.86E-05	Igsf10	-0.56	2.84E-04
Nrn1	0.37	2.51E-04	Hcfc1	-0.56	1.85E-24
Akr1b3	0.36	1.24E-07	Nav3	-0.56	2.53E-12
Tmem230	0.36	1.95E-02	Ralgapa2	-0.56	3.53E-07
Mrpl34	0.36	7.65E-05	Hivep2	-0.55	3.23E-07
Aga	0.36	1.72E-02	Chd8	-0.55	6.13E-13
Mfsd12	0.36	2.10E-02	Pde3a	-0.55	3.28E-05
Rcan1	0.36	1.24E-02	Rbm41	-0.55	3.35E-04
Rgs19	0.36	3.24E-02	Rcor3	-0.55	4.00E-03
Nucb1	0.36	1.50E-07	Trim56	-0.55	3.35E-07
Acot9	0.36	2.67E-02	Ssh2	-0.55	2.42E-08
Atp6v0b	0.36	2.18E-04	Xrcc3	-0.55	3.31E-03

Genes (UP)	log2FoldChange	padj	Genes (Down)	log2FoldChange	padj
Hist1h4i	0.36	9.72E-03	Celsr1	-0.55	1.71E-02
Shb	0.36	2.40E-02	Armcx4	-0.55	1.41E-18
Pter	0.36	4.67E-04	Zfp26	-0.55	6.76E-06
Chordc1	0.36	3.14E-04	Arhgef12	-0.55	3.07E-16
Pgd	0.36	9.52E-07	Mdm4	-0.55	9.41E-10
Rcn3	0.36	2.60E-02	Map3k1	-0.55	4.05E-08
Slc18b1	0.36	9.56E-03	mt-Co1	-0.54	4.06E-16
Igfbp2	0.36	1.58E-07	Sdk2	-0.54	1.94E-08
Gm10076	0.36	5.15E-05	Brwd1	-0.54	2.73E-08
Olfml2b	0.36	4.94E-04	Zfp398	-0.54	9.63E-04
Fsd1	0.36	2.38E-02	Rfx3	-0.54	6.74E-06
Rai14	0.36	1.49E-02	Setd5	-0.54	4.21E-18
Dap	0.36	1.56E-04	Dok6	-0.54	1.51E-03
Pde1b	0.36	8.23E-03	Prkaa2	-0.54	2.62E-03
Fhl3	0.36	2.30E-02	Sptbn1	-0.54	4.01E-20
Mkrn1	0.36	1.31E-02	Lrp6	-0.54	6.09E-10
Ldah	0.36	7.36E-03	Eif4g3	-0.54	1.53E-15
Ddt	0.36	7.08E-03	Phactr2	-0.54	1.55E-04
Prelp	0.36	3.53E-02	Creb5	-0.54	6.92E-10
Atp6v0c	0.36	4.66E-06	Bicd1	-0.54	6.44E-03
Cotl1	0.36	8.35E-09	Plce1	-0.54	7.65E-08
Npnt	0.36	2.28E-03	Tpr	-0.54	5.60E-19
Kti12	0.36	2.13E-02	Pcnx	-0.54	9.35E-14
Apeh	0.36	1.98E-03	Mrtfb	-0.54	2.42E-08
Tufm	0.35	4.68E-07	Arhgap21	-0.54	6.66E-16
Lhpp	0.35	1.79E-02	Tnks	-0.53	1.93E-17
Baiap2	0.35	3.09E-03	Cecr2	-0.53	3.78E-04
Nfkbib	0.35	1.78E-02	Gm3764	-0.53	1.07E-09
Gstp1	0.35	5.08E-05	Crybg3	-0.53	9.46E-05
Map1lc3b	0.35	7.33E-06	Mib1	-0.53	5.04E-13
Itgb5	0.35	3.47E-03	Jmjd1c	-0.53	5.97E-13
Efhd2	0.35	3.80E-03	Acaca	-0.53	2.16E-12
Gpaa1	0.35	1.25E-02	Mtor	-0.53	5.17E-12
Nfkbia	0.35	1.45E-03	Brsk2	-0.53	2.41E-02
Atp5g1	0.35	2.24E-05	Fnip2	-0.53	1.43E-09
Sox3	0.35	2.38E-06	Gm37494	-0.53	1.61E-05
Syvn1	0.35	3.13E-03	Tbl1xr1	-0.53	3.85E-10
Vat1l	0.35	3.56E-02	Nrip1	-0.53	9.11E-04
Ankrd54	0.35	1.20E-02	Ankrd52	-0.52	2.70E-17
Tspyl4	0.35	8.66E-03	Eya4	-0.52	2.87E-02
Gm43549	0.35	3.03E-02	Gli3	-0.52	9.19E-05
Ctsa	0.35	1.73E-03	Spg11	-0.52	1.62E-07

Genes (UP)	log2FoldChange	padj	Genes (Down)	log2FoldChange	padj
Ier5	0.35	2.16E-02	Mbtps2	-0.52	1.41E-06
Ttll1	0.35	4.27E-03	Samd8	-0.52	9.46E-11
Apba3	0.35	4.41E-03	Tmod2	-0.52	2.91E-12
Prr13	0.34	4.49E-03	Vcan	-0.52	1.84E-13
Dnajb11	0.34	2.13E-05	Uggt2	-0.52	1.48E-03
Ppa1	0.34	7.87E-06	Slc6a1	-0.52	9.57E-09
CAAA01118383.1	0.34	2.17E-02	Kdm5a	-0.52	1.67E-10
Rbm38	0.34	2.86E-02	Tenm4	-0.51	4.55E-02
Tbc1d10a	0.34	1.82E-03	Thoc2	-0.51	1.39E-11
Tada3	0.34	1.36E-02	Atp11c	-0.51	1.69E-06
Upp1	0.34	3.45E-02	Arhgap11a	-0.51	6.80E-08
Fads3	0.34	4.89E-03	Tasor2	-0.51	2.16E-08
Snrpa	0.34	9.03E-06	Cux1	-0.51	5.55E-09
Ormdl1	0.34	2.10E-02	Pggt1b	-0.51	9.64E-07
Spns1	0.34	1.61E-03	Tasor	-0.51	2.67E-04
Psph	0.34	8.85E-04	Hipk1	-0.51	3.24E-15
Pdia3	0.34	1.00E-08	Baz2a	-0.51	1.02E-15
Arpc3	0.34	8.04E-06	Son	-0.51	5.11E-18
Grina	0.34	8.73E-06	Usp54	-0.51	2.40E-04
Shisa5	0.34	4.73E-04	Prox1	-0.51	5.86E-07
Cnppd1	0.34	1.93E-02	Tnrc6c	-0.51	1.62E-12
Ehd2	0.34	6.51E-06	Ppp2r3a	-0.51	3.79E-07
Slc35f6	0.34	9.52E-03	Golga4	-0.51	5.68E-10
Lamtor5	0.34	8.64E-03	Stil	-0.51	4.98E-05
Fam133b	0.34	9.76E-03	Rlim	-0.51	3.53E-09
Rbm42	0.34	2.13E-05	Dock4	-0.51	3.18E-05
Rps26	0.34	1.81E-06	Pygl	-0.51	1.27E-03
Ubl7	0.34	5.38E-03	Cpd	-0.51	2.02E-13
Ehd4	0.34	1.99E-02	Kif1b	-0.51	1.77E-19
Chst12	0.34	3.96E-02	Ncoa6	-0.51	7.31E-10
Tomm6	0.33	2.05E-03	Abca1	-0.51	1.30E-05
Cd24a	0.33	1.16E-07	Pcdh11x	-0.51	9.53E-03
Pdia6	0.33	5.68E-07	Rad54l2	-0.51	1.29E-09
Eps8	0.33	2.33E-03	Ncapg2	-0.50	5.49E-08
Scrn1	0.33	1.09E-04	Faxc	-0.50	7.00E-06
Bin1	0.33	1.84E-05	Nckap5	-0.50	2.85E-03
Adm	0.33	1.79E-02	Gse1	-0.50	2.31E-08
P4ha1	0.33	3.71E-05	Negr1	-0.50	3.08E-02
1110059E24Rik	0.33	4.70E-03	Cep295	-0.50	6.41E-06
Dok7	0.33	4.39E-02	Chl1	-0.50	1.44E-05

Genes (UP)	log2FoldChange	padj	Genes (Down)	log2FoldChange	padj
Hbegf	0.33	4.72E-05	Phykpl	-0.50	1.06E-03
Nubp2	0.33	7.69E-03	Kdm7a	-0.50	2.80E-05
Tmem158	0.33	2.01E-04	Pank3	-0.50	6.08E-16
Mettl21a	0.33	3.41E-02	Otud4	-0.50	7.82E-10
Tmeff2	0.33	3.72E-02	Purb	-0.50	2.78E-17
Sparc	0.33	7.92E-10	Hectd2	-0.50	2.74E-06
Twf2	0.33	1.18E-02	Bdp1	-0.50	3.35E-06
Brms1	0.33	3.11E-02	Usp49	-0.50	5.78E-06
Mmp17	0.33	5.33E-03	AU020206	-0.50	4.26E-05
Rab5if	0.33	8.43E-04	Notch1	-0.50	1.50E-16
Rplp1	0.33	1.94E-07	Slco5a1	-0.50	6.60E-03
Zfp622	0.33	3.78E-03	Ofd1	-0.50	2.60E-03
Arntl	0.33	1.33E-02	Cep192	-0.50	2.41E-08
Wdr18	0.33	1.46E-03	Pole	-0.50	3.78E-10
Pcx	0.33	6.33E-03	Eea1	-0.49	1.71E-07
Fam114a1	0.33	8.76E-03	Fyco1	-0.49	3.44E-03
Gm1673	0.33	1.70E-02	Nlgn1	-0.49	1.41E-03
Tex264	0.33	4.39E-02	Polr2a	-0.49	1.93E-17
Fth1	0.33	1.58E-07	Zfp369	-0.49	3.32E-03
Tcn2	0.33	1.67E-03	Ubr1	-0.49	7.20E-07
Mcfd2	0.33	5.53E-04	Pcdh17	-0.49	5.53E-04
Vat1	0.33	6.74E-06	Ptprd	-0.49	3.12E-02
Dhrs7b	0.32	5.19E-03	Tcp11l1	-0.49	7.99E-04
Pam	0.32	6.69E-06	Itga4	-0.49	4.64E-11
Cbr1	0.32	1.48E-02	Qk	-0.49	5.17E-13
Rnasek	0.32	1.14E-03	Abl2	-0.49	9.02E-11
Pld3	0.32	1.91E-04	Pms1	-0.49	4.05E-02
Atp6v0d1	0.32	5.70E-05	Prrc2b	-0.49	2.34E-16
Trafd1	0.32	1.17E-02	Nova1	-0.49	4.45E-09
Manf	0.32	1.61E-04	Adgrl3	-0.49	3.98E-06
Rnd3	0.32	2.77E-03	Ncor1	-0.48	1.93E-15
Nfkb2	0.32	1.76E-02	Zkscan1	-0.48	6.31E-07
2410004B18Rik	0.32	9.58E-03	Cdc42bpa	-0.48	1.48E-08
Cdkn2a	0.32	1.08E-04	Atad2b	-0.48	4.57E-06
P3h2	0.32	3.24E-02	Pik3c2b	-0.48	2.04E-02
Ddx41	0.32	2.43E-03	Ankhd1	-0.48	1.12E-09
Cap2	0.32	2.42E-03	Polq	-0.48	6.74E-04
Pde2a	0.32	2.14E-03	Dnhd1	-0.48	1.97E-02
Tmc6	0.32	2.70E-02	Aak1	-0.48	1.16E-17
Sumf2	0.32	2.70E-02	Rbm33	-0.48	1.79E-10
Ppic	0.32	2.37E-04	Sox6	-0.48	6.25E-13

Genes (UP)	log2FoldChange	padj	Genes (Down)	log2FoldChange	padj
Fkbp14	0.32	3.46E-03	Myh10	-0.48	9.85E-17
Taf6l	0.32	2.91E-02	mt-Cytb	-0.48	7.09E-11
Mif	0.32	6.47E-04	Vash1	-0.48	8.44E-12
Syn1	0.32	1.04E-02	Slc4a4	-0.48	3.30E-09
Cystm1	0.32	1.46E-02	Arfgef2	-0.48	6.80E-08
Laptm4b	0.32	6.99E-07	Utp20	-0.47	4.42E-09
Tpm1	0.32	9.44E-08	Sp1	-0.47	2.22E-09
Nefm	0.32	2.10E-04	Gatad2b	-0.47	5.32E-09
Grn	0.32	5.65E-05	Usp31	-0.47	9.06E-08
Cavin1	0.32	4.62E-07	Xpo4	-0.47	1.02E-07
Prelid1	0.32	1.14E-05	Arap2	-0.47	1.28E-11
Lgmn	0.32	2.56E-03	Pcmtd1	-0.47	4.95E-06
Rhou	0.32	6.94E-04	Med1	-0.47	1.72E-07
Eno1	0.32	8.09E-06	Dennd4c	-0.47	9.82E-06
Spr	0.32	7.46E-04	Amer2	-0.47	7.96E-04
Ptges2	0.32	3.14E-02	Hmbox1	-0.47	2.60E-08
Mfsd11	0.32	3.45E-02	Adgrl1	-0.47	2.97E-12
Dtx2	0.32	2.84E-02	Thada	-0.47	5.86E-05
Sgsm3	0.32	3.72E-03	mt-Nd4	-0.47	5.73E-14
Dus3l	0.32	4.92E-03	Dip2b	-0.47	8.71E-11
Spg21	0.32	5.99E-03	Zbtb41	-0.47	4.75E-07
Ccnd3	0.31	1.89E-04	Rasal2	-0.47	2.16E-07
Id3	0.31	1.91E-05	Zxdb	-0.47	3.86E-02
Chchd2	0.31	1.34E-05	Kif13a	-0.47	1.63E-09
Rpl6	0.31	1.33E-05	Adam22	-0.47	7.66E-04
Rnpep	0.31	1.81E-03	Sp4	-0.47	7.54E-03
Aldoa	0.31	5.18E-07	Cenpe	-0.47	2.37E-07
Gle1	0.31	1.17E-03	Kif21b	-0.46	5.88E-13
Psmg3	0.31	4.55E-02	Zfp280c	-0.46	6.04E-05
Rrp8	0.31	3.75E-03	Dleu2	-0.46	3.06E-02
6430548M08Rik	0.31	2.60E-02	Dido1	-0.46	3.55E-10
Jup	0.31	4.71E-03	Foxn3	-0.46	2.73E-05
C1ql3	0.31	1.13E-02	Tnpo1	-0.46	5.20E-13
Mthfd2	0.31	3.12E-04	Sema5a	-0.46	1.07E-04
Abhd17a	0.31	5.41E-04	Cit	-0.46	3.17E-06
Creld1	0.31	1.63E-03	Pygo1	-0.46	1.51E-03
Slc25a29	0.31	2.99E-02	Afdn	-0.46	1.45E-11
Zfp703	0.31	1.89E-03	Shc3	-0.46	8.60E-07
Elob	0.31	8.46E-04	Rc3h2	-0.46	1.69E-06
S1pr2	0.31	6.70E-03	Slc4a7	-0.46	2.34E-09
Ostf1	0.31	1.46E-02	Rfx7	-0.46	2.31E-08

Genes (UP)	log2FoldChange	padj	Genes (Down)	log2FoldChange	padj
Rgs16	0.31	3.69E-03	Mphosph9	-0.46	1.18E-04
Impdh1	0.31	1.54E-02	Asxl1	-0.46	5.75E-08
Ehd3	0.31	6.51E-03	Gsk3b	-0.46	2.11E-12
Atp6v1f	0.31	3.76E-03	Epg5	-0.46	6.92E-04
Tmem120a	0.31	1.20E-02	Cbx5	-0.46	7.05E-10
Lhfpl2	0.31	5.20E-03	Sh3pxd2a	-0.46	1.13E-10
Ppm1m	0.31	1.39E-02	Tulp4	-0.46	3.02E-11
Atp1b1	0.31	6.17E-03	Chst3	-0.45	4.29E-06
2310022A10Rik	0.31	4.33E-02	Bend3	-0.45	6.63E-04
Eif4ebp1	0.31	1.18E-02	Cntrl	-0.45	1.33E-04
Pex6	0.31	1.74E-03	Ahctf1	-0.45	3.85E-07
Pgp	0.31	5.35E-04	Cspp1	-0.45	1.04E-03
Ccnjl	0.31	1.79E-02	Ncoa2	-0.45	3.51E-08
Hras	0.31	7.99E-04	Dyrk2	-0.45	3.25E-04
Gba	0.31	1.32E-03	Lifr	-0.45	5.66E-04
Slc35a2	0.31	5.65E-03	Egfr	-0.45	3.51E-10
Hspa8	0.31	1.20E-07	Ankrd17	-0.45	5.76E-13
Rpl29	0.31	9.20E-05	Lrrc8b	-0.45	1.11E-09
Shmt2	0.31	4.14E-04	Tln2	-0.45	1.20E-04
Galnt17	0.30	1.92E-02	Ctdspl2	-0.45	7.24E-04
Lipa	0.30	3.24E-03	Psd3	-0.45	1.35E-08
Capn10	0.30	2.30E-02	Dtl	-0.45	1.56E-05
Sqstm1	0.30	7.44E-06	Mmd2	-0.45	3.11E-02
Matn2	0.30	4.44E-04	Map1a	-0.45	9.81E-08
Pcbp3	0.30	1.17E-02	Lrig2	-0.44	2.89E-03
Pycrl	0.30	7.63E-03	Lpin1	-0.44	4.04E-10
Tpgs1	0.30	1.97E-02	Zc3h13	-0.44	2.83E-06
Nxn	0.30	2.03E-03	Pdgfra	-0.44	1.72E-05
Rtf2	0.30	6.92E-03	Zfc3h1	-0.44	1.72E-06
Atp6v0e	0.30	2.17E-03	Plxna1	-0.44	4.12E-11
Hoxa5	0.30	9.34E-03	Zzef1	-0.44	1.94E-07
Noa1	0.30	4.14E-03	Ddx3x	-0.44	4.93E-13
Slc39a3	0.30	6.20E-03	Slk	-0.44	1.83E-08
Rplp2	0.30	2.33E-05	Wwp1	-0.44	4.02E-05
Urod	0.30	4.67E-02	Pde4d	-0.44	2.67E-02
Ccdc102a	0.30	1.83E-02	Cirbp	-0.44	1.46E-04
Phb	0.30	1.37E-05	Plxnb1	-0.44	3.46E-07
Tmbim4	0.30	1.66E-02	Bicra	-0.44	2.12E-04
Aldh2	0.30	4.13E-04	Ckap5	-0.44	1.25E-09
S1pr1	0.30	2.12E-03	Phf20l1	-0.44	1.64E-06
Yif1a	0.30	1.43E-02	Trim66	-0.44	4.39E-02

Genes (UP)	log2FoldChange	padj	Genes (Down)	log2FoldChange	padj
Pnpla2	0.30	1.41E-02	Appl1	-0.44	7.45E-06
Fbxo9	0.30	1.47E-02	Fn1	-0.44	6.62E-08
Rnaseh2c	0.30	1.52E-03	Uprt	-0.44	6.47E-03
2510039O18Rik	0.30	2.20E-03	Arhgap33	-0.44	3.85E-05
Rpl26	0.30	8.16E-04	Tab3	-0.44	1.69E-03
Rmc1	0.30	4.86E-02	Pds5b	-0.44	2.16E-08
Rps10	0.30	2.54E-04	Cspg4	-0.44	2.51E-05
Hexb	0.30	4.86E-02	Ttyh1	-0.44	9.69E-04
Ift20	0.30	2.13E-02	Cttnbp2	-0.44	2.32E-02
Phgdh	0.30	1.42E-05	Srgap1	-0.43	2.61E-03
Rps15a	0.30	2.63E-04	Klf12	-0.43	8.82E-06
Scamp3	0.30	3.55E-03	Zfp318	-0.43	8.48E-05
Bcap31	0.30	5.86E-05	Pcif1	-0.43	4.16E-06
Smarcd2	0.30	8.11E-03	Eif2ak2	-0.43	8.90E-05
Ube2f	0.30	9.12E-03	Casp8ap2	-0.43	2.43E-04
Arl4c	0.30	3.08E-03	Pik3c2a	-0.43	2.41E-06
Nt5dc2	0.30	1.65E-05	Mpdz	-0.43	2.57E-06
Zfyve27	0.30	2.48E-02	E130307A14Rik	-0.43	2.84E-02
Cd151	0.30	1.08E-04	Lsamp	-0.43	2.22E-03
Map6	0.30	2.24E-02	Tgfbr1	-0.43	1.53E-04
Vps18	0.30	2.29E-02	Sec16a	-0.43	3.26E-08
Ctsd	0.29	1.52E-05	Pard3b	-0.43	2.04E-02
Hspa2	0.29	4.44E-02	Klf7	-0.43	4.47E-05
Cacng5	0.29	4.20E-02	Ncoa1	-0.43	1.43E-06
Pdpn	0.29	3.05E-02	Cntln	-0.43	4.71E-03
Bcat1	0.29	4.51E-03	Ptprg	-0.43	1.10E-08
Igfbp3	0.29	7.34E-06	Pcdh19	-0.43	1.10E-03
Zpr1	0.29	1.96E-02	Plagl2	-0.43	5.65E-03
Cog8	0.29	2.20E-02	Dgke	-0.42	8.97E-03
Rps18	0.29	1.06E-04	AW554918	-0.42	2.86E-02
Slc15a4	0.29	3.21E-02	Zbtb10	-0.42	2.14E-04
Stk16	0.29	8.38E-03	Rgs7bp	-0.42	2.11E-05
Emp2	0.29	1.16E-03	Arhgap5	-0.42	1.58E-05
Lamp1	0.29	3.00E-05	Ccdc82	-0.42	3.37E-03
Smg8	0.29	1.69E-02	Nhs	-0.42	3.72E-02
Yipf3	0.29	4.33E-03	Hdac4	-0.42	1.40E-05
Sharpin	0.29	4.31E-02	9930021J03Rik	-0.42	2.67E-05
Hax1	0.29	2.76E-03	Smad5	-0.42	2.97E-09
Nptx1	0.29	6.01E-03	Peg10	-0.42	6.05E-15

Genes (UP)	log2FoldChange	padj	Genes (Down)	log2FoldChange	padj
Akirin2	0.29	2.82E-03	Zfp267	-0.42	4.02E-04
Taf12	0.29	4.87E-02	Ddr2	-0.42	5.01E-10
Noc4l	0.29	1.39E-02	Usp37	-0.42	9.95E-06
P4hb	0.29	1.38E-06	Zfp536	-0.42	1.85E-02
Saraf	0.29	1.18E-04	Cpsf6	-0.42	1.24E-09
Rnf181	0.29	6.00E-03	Prr14l	-0.42	6.29E-07
Chst7	0.29	6.92E-04	Nexmif	-0.42	1.75E-04
Plod3	0.29	6.71E-05	Mob1b	-0.42	5.05E-07
Eif1b	0.29	4.97E-03	Zfp236	-0.42	2.03E-05
Ttc4	0.29	4.05E-02	Ube3a	-0.42	4.05E-08
Wdr1	0.29	1.69E-05	C530008M17Rik	-0.42	4.44E-09
Psat1	0.29	3.63E-04	Bcor	-0.42	3.56E-06
Eif3k	0.29	3.63E-04	Hipk3	-0.42	2.43E-05
Npdc1	0.29	3.16E-03	Mysm1	-0.41	1.04E-03
Ube2c	0.29	3.93E-03	Xiap	-0.41	4.22E-08
Bud31	0.29	6.26E-03	Mbnl1	-0.41	1.14E-06
Csrp1	0.29	1.42E-03	Ylpm1	-0.41	4.75E-08
Mrpl4	0.29	1.04E-02	Sec24a	-0.41	1.04E-05
Ciao2b	0.29	1.93E-02	Ddx6	-0.41	4.68E-07
Arpc1b	0.28	1.58E-05	Jade1	-0.41	1.40E-05
Sgta	0.28	7.73E-04	Zc3hav1l	-0.41	2.08E-02
Vmp1	0.28	1.71E-04	Kmt2b	-0.41	4.55E-08
Vim	0.28	1.36E-08	Spopl	-0.41	1.48E-02
Atf4	0.28	6.61E-04	Rbm25	-0.41	3.54E-09
Slc25a3	0.28	2.23E-05	Cnot1	-0.41	6.41E-12
Atg4d	0.28	3.36E-02	Ythdc2	-0.41	3.87E-03
Tuba1c	0.28	3.11E-02	Taf1	-0.41	3.46E-07
Aurka	0.28	1.28E-02	G2e3	-0.41	2.49E-04
Hes6	0.28	9.69E-03	Itga1	-0.41	6.60E-03
Dnaja3	0.28	4.00E-03	Plec	-0.41	1.64E-08
Rnf19b	0.28	1.66E-02	Klf15	-0.41	1.70E-02
Slc27a4	0.28	8.86E-03	Naa16	-0.41	4.80E-03
Ints12	0.28	4.98E-02	Rprd2	-0.41	8.55E-05
Coro1b	0.28	3.36E-03	Phlpp2	-0.41	6.40E-04
Glrx5	0.28	3.74E-04	Clasp1	-0.41	9.78E-08
Ppt2	0.28	2.23E-03	Gli2	-0.41	1.82E-02
Lman2l	0.28	4.54E-02	Notch3	-0.41	1.02E-07
Tmem35a	0.28	3.68E-04	Sos1	-0.41	3.05E-07
Gtf2h3	0.28	2.28E-02	Slc30a1	-0.41	4.78E-03
Edf1	0.28	1.06E-03	Zfp945	-0.41	1.12E-02
Sac3d1	0.28	4.77E-02	Sorbs1	-0.40	1.23E-02

Genes (UP)	log2FoldChange	padj	Genes (Down)	log2FoldChange	padj
Adrb1	0.28	2.19E-02	Utp14b	-0.40	1.71E-06
Ube2e2	0.28	9.59E-03	Npas3	-0.40	1.28E-06
Bsg	0.28	5.98E-06	Slc7a2	-0.40	3.82E-02
Dhrs1	0.28	1.47E-02	Prpf8	-0.40	4.20E-14
Ifi27	0.28	1.88E-02	Abca5	-0.40	3.28E-02
Trp53i11	0.28	1.42E-03	Dnajb14	-0.40	8.79E-05
Cln5	0.28	9.23E-03	Bard1	-0.40	4.93E-03
Sipa1	0.28	8.89E-03	Rbbp6	-0.40	1.25E-07
Eef1g	0.28	9.72E-07	Slfn9	-0.40	3.21E-04
Smox	0.28	2.82E-02	Slc9a8	-0.40	3.88E-03
Tmem70	0.28	4.54E-03	D5Ertd579e	-0.40	1.98E-07
Atox1	0.28	7.50E-03	Kcnb1	-0.40	2.73E-02
Rabif	0.28	2.79E-02	Gas2l3	-0.40	6.65E-04
Mlx	0.28	2.12E-02	Sema6a	-0.40	2.52E-06
Eif3f	0.28	3.74E-06	Zfp142	-0.40	1.74E-03
Unc45a	0.28	1.24E-02	Cdk19	-0.40	4.71E-06
Gemin7	0.28	2.15E-02	Xylt1	-0.40	2.08E-09
Ndel1	0.28	6.20E-03	Chd4	-0.40	3.08E-12
Tmem126a	0.28	2.87E-02	Atf7	-0.40	6.03E-06
Fnta	0.28	6.09E-03	Hnrnpd	-0.40	6.08E-06
Agpat4	0.28	1.04E-02	Igf2r	-0.40	1.46E-07
BC005624	0.28	4.06E-02	Ddx46	-0.40	6.39E-09
Lgals1	0.28	1.53E-07	Rock1	-0.40	1.84E-06
Thoc5	0.28	9.80E-03	Otud7b	-0.40	1.33E-07
Man2b1	0.28	7.92E-03	Ppp1r12b	-0.40	2.70E-04
Pck2	0.28	5.65E-03	Zfp280d	-0.40	3.65E-03
Atp6v1c1	0.28	5.55E-03	Rnf169	-0.40	1.52E-03
Dcun1d2	0.28	3.37E-02	Zfp445	-0.40	1.31E-06
Inpp5a	0.28	1.46E-02	Cdk12	-0.40	7.32E-05
Ssr2	0.28	4.21E-05	Sbno1	-0.40	2.98E-07
Hsbp1	0.27	1.14E-04	Ndst1	-0.39	3.91E-10
Pus1	0.27	4.18E-02	Pgap1	-0.39	8.63E-06
Rela	0.27	7.42E-03	Zfyve26	-0.39	9.40E-04
Nup35	0.27	2.24E-02	Rsbn1	-0.39	5.61E-03
Cdk5	0.27	1.25E-02	Atp7a	-0.39	5.55E-03
Hsd17b10	0.27	3.31E-03	Cep170	-0.39	8.01E-09
Atp5l	0.27	2.24E-02	Adgrb3	-0.39	1.31E-03
BC031181	0.27	7.21E-03	Zfp106	-0.39	1.08E-08
Dbn1	0.27	2.69E-03	Ttll4	-0.39	1.24E-06
Acd	0.27	2.29E-02	9330182L06Rik	-0.39	1.36E-02
Myl12b	0.27	9.77E-04	Creb1	-0.39	1.50E-04

Genes (UP)	log2FoldChange	padj	Genes (Down)	log2FoldChange	padj
Ppp2r5b	0.27	2.47E-03	Nsd2	-0.39	3.78E-09
Thap11	0.27	9.03E-03	Synj1	-0.39	1.47E-03
Fau	0.27	1.58E-05	Kcnd3	-0.39	6.61E-10
Gapdh	0.27	1.40E-04	Abi2	-0.39	9.47E-08
Egln3	0.27	4.47E-02	Znrf3	-0.39	2.80E-04
Gas2l1	0.27	9.54E-03	Grk3	-0.39	2.65E-04
Atp5o	0.27	2.64E-04	Kif14	-0.39	5.38E-03
Mrpl38	0.27	5.82E-03	Arhgef11	-0.39	1.09E-08
Tmem59	0.27	1.91E-04	Atxn1l	-0.39	8.22E-06
Snf8	0.27	9.76E-03	Ankrd12	-0.39	5.86E-03
Ehd1	0.27	8.25E-04	Pcf11	-0.39	1.61E-03
Mmadhc	0.27	3.09E-03	Clock	-0.39	1.52E-05
Rpl18a	0.27	7.95E-05	Arfgef1	-0.39	5.05E-05
Pofut2	0.27	7.20E-04	Arid4b	-0.39	5.66E-04
Rpl28	0.27	7.67E-06	Atp13a3	-0.39	6.01E-08
Eif3h	0.27	1.97E-05	Herc3	-0.39	1.29E-02
Ap2s1	0.27	6.26E-04	Lmbrd2	-0.39	8.22E-06
Rab3a	0.27	2.33E-02	Kif15	-0.39	2.99E-04
Puf60	0.27	2.45E-04	Plxna2	-0.39	2.36E-06
Samd1	0.27	3.12E-02	Flnb	-0.39	1.26E-10
Mpv17l2	0.27	2.84E-02	Zfp609	-0.38	4.04E-07
Lratd1	0.27	2.88E-03	Stxbp5	-0.38	4.27E-04
Pgls	0.27	6.35E-03	Uhrf1bp1l	-0.38	2.29E-06
Rnf114	0.27	2.39E-02	Heca	-0.38	2.17E-03
Aldh7a1	0.27	6.21E-03	Piezo1	-0.38	1.91E-04
Mrps26	0.27	1.92E-02	Ppm1l	-0.38	2.17E-07
Bag1	0.27	1.23E-03	Zfp329	-0.38	2.10E-02
Pnp	0.27	1.48E-02	Zfp367	-0.38	3.77E-03
Anxa6	0.27	5.94E-06	Mbtd1	-0.38	7.36E-05
Ppib	0.27	5.19E-03	Lrrc7	-0.38	4.79E-02
Scly	0.27	4.43E-02	Gria2	-0.38	5.63E-03
Vps26c	0.27	3.93E-02	Megf8	-0.38	2.56E-07
Amph	0.27	3.03E-02	Chd1	-0.38	5.01E-07
Prkcsh	0.27	1.00E-04	Itgav	-0.38	1.15E-08
Commd4	0.27	4.77E-02	Rbm26	-0.38	3.79E-06
Mdh1	0.27	2.51E-04	Pbx1	-0.38	1.30E-06
Rpl10	0.27	9.82E-06	Atp1a2	-0.38	4.86E-02
Lrp10	0.26	1.12E-03	Anapc1	-0.38	1.85E-09
Hmga2	0.26	1.81E-03	Tnik	-0.38	2.77E-10
Gstm7	0.26	3.04E-02	Astn1	-0.38	5.14E-07
Smtn	0.26	2.46E-03	Cmtm4	-0.38	3.61E-07
Snrpc	0.26	1.28E-03	Med12	-0.38	6.13E-07

Genes (UP)	log2FoldChange	padj	Genes (Down)	log2FoldChange	padj
Mllt11	0.26	7.45E-03	Mtf2	-0.38	9.50E-03
Taf13	0.26	2.59E-02	Nova2	-0.38	2.52E-04
Mmab	0.26	2.57E-02	Cltc	-0.38	3.08E-12
Stard3	0.26	6.46E-03	Iws1	-0.38	9.88E-06
Csnk2b	0.26	9.40E-04	Arnt2	-0.37	4.27E-07
Cbx4	0.26	3.31E-02	E330009J07 Rik	-0.37	1.90E-02
Lmna	0.26	1.44E-02	Lrrcc1	-0.37	2.60E-02
Kif1bp	0.26	1.50E-02	Kat6b	-0.37	1.37E-03
Eif4a2	0.26	4.27E-04	Trpm7	-0.37	1.00E-05
Cetn2	0.26	1.40E-03	Zfp451	-0.37	1.40E-04
Ubb	0.26	7.63E-05	Ern1	-0.37	1.98E-02
Rps13	0.26	1.04E-03	Sestd1	-0.37	9.73E-05
Aar2	0.26	3.33E-02	Zbtb38	-0.37	5.92E-03
Selenop	0.26	4.18E-03	Slc26a2	-0.37	9.19E-03
Mob3a	0.26	3.41E-02	Rbl1	-0.37	1.41E-03
Mxi1	0.26	2.24E-02	Camsap2	-0.37	3.15E-06
Sh3glb2	0.26	2.07E-02	Zhx3	-0.37	1.43E-04
Plod1	0.26	5.96E-03	5730455P1 6Rik	-0.37	2.05E-03
Armc10	0.26	2.70E-02	Smchd1	-0.37	1.14E-06
Fam114a2	0.26	1.54E-02	Rreb1	-0.37	3.98E-03
Bcar1	0.26	1.20E-02	Impad1	-0.37	3.40E-08
Capns1	0.26	3.92E-05	Clip1	-0.37	9.29E-04
Actg1	0.26	1.09E-04	Grik3	-0.37	8.88E-03
Mrpl22	0.26	3.67E-02	Rps6ka3	-0.37	1.41E-07
Dusp1	0.26	2.19E-02	Hdgfl3	-0.37	1.08E-03
Ugp2	0.26	1.04E-03	Zyg11b	-0.37	2.51E-05
Limk1	0.26	1.49E-02	Rasa2	-0.37	7.83E-04
Fam107b	0.26	6.91E-03	Dhx9	-0.37	3.36E-10
Hgs	0.26	1.66E-02	Nup210	-0.37	9.77E-07
Polr1d	0.26	2.69E-03	Btbd7	-0.37	7.47E-06
Snrpd2	0.26	1.19E-03	Bach1	-0.36	5.65E-03
Ap2m1	0.26	1.32E-04	Nsd3	-0.36	3.98E-05
Jpt1	0.26	5.39E-04	Zfyve9	-0.36	2.91E-03
Fam104a	0.26	1.97E-02	Spata13	-0.36	1.61E-06
Dcakd	0.26	2.77E-03	Mef2c	-0.36	3.11E-02
Ttc5	0.26	3.65E-02	Zcchc7	-0.36	4.67E-02
Cc2d1a	0.26	4.31E-02	Ltn1	-0.36	1.23E-05
Ppil2	0.26	3.71E-02	Tnrc6a	-0.36	1.78E-07
Btg1	0.26	2.79E-03	Neto1	-0.36	2.29E-02
Cstb	0.26	2.53E-02	Ptch1	-0.36	1.59E-05

Genes (UP)	log2FoldChange	padj	Genes (Down)	log2FoldChange	padj
Nans	0.26	1.24E-02	Ino80	-0.36	7.61E-04
Cbs	0.26	1.01E-02	Fasn	-0.36	9.79E-10
Farsa	0.26	1.76E-03	Haus6	-0.36	1.98E-04
Dctn3	0.26	3.31E-02	Pds5a	-0.36	3.59E-08
Cox7a2	0.26	9.07E-03	Zcchc14	-0.36	1.24E-07
Cd9	0.26	5.53E-04	Phlpp1	-0.36	4.24E-08
Atf6b	0.26	5.95E-04	Rock2	-0.36	2.05E-06
Dohh	0.26	1.17E-02	Dop1a	-0.36	7.37E-03
Tmem14c	0.26	4.46E-03	Fam76b	-0.36	3.17E-03
Lrrc42	0.26	2.17E-02	Kntc1	-0.36	9.00E-05
Prkag2	0.26	3.24E-02	Wdr7	-0.36	1.46E-04
Acsl5	0.25	2.45E-02	Zmat3	-0.36	2.14E-05
Myl12a	0.25	3.15E-05	Bbx	-0.36	1.84E-04
Ngdn	0.25	4.08E-02	Clasp2	-0.36	1.56E-06
Rab3b	0.25	3.73E-04	Senp1	-0.36	1.14E-04
Hexa	0.25	5.77E-03	Zeb2	-0.36	4.97E-06
Mrps21	0.25	2.56E-02	Akt3	-0.36	1.36E-03
Bnip3l	0.25	3.18E-03	Abca2	-0.36	3.42E-05
Serp1	0.25	6.00E-05	Trip12	-0.36	3.75E-09
Bud23	0.25	3.53E-02	Gon4l	-0.36	5.39E-06
Eef1b2	0.25	9.26E-05	Mtr	-0.36	6.43E-04
Pdxp	0.25	1.42E-02	Thrap3	-0.36	1.90E-07
Usp20	0.25	4.13E-02	Zfp148	-0.36	1.67E-04
Tnfrsf12a	0.25	3.65E-02	Larp1	-0.36	4.03E-08
Cpne2	0.25	3.87E-02	Peg3	-0.36	7.01E-07
E130309D02Rik	0.25	1.50E-02	Manea	-0.36	1.83E-03
Lyn	0.25	1.39E-02	Bicral	-0.36	1.85E-02
Rps24	0.25	9.42E-05	Cmip	-0.35	2.21E-04
Pfdn5	0.25	8.35E-03	Prr12	-0.35	8.93E-06
Rps5	0.25	1.05E-04	Zfp74	-0.35	4.16E-02
Cope	0.25	2.47E-03	Prdm10	-0.35	2.76E-02
Esd	0.25	1.46E-03	Zeb1	-0.35	3.62E-08
Plpbp	0.25	3.89E-02	Traf6	-0.35	2.01E-03
Fhl1	0.25	4.39E-03	Msi2	-0.35	4.24E-06
Dnajb1	0.25	3.18E-02	Agap1	-0.35	1.58E-08
Utp4	0.25	1.16E-02	Alg10b	-0.35	7.03E-08
Rplp0	0.25	6.99E-06	Tmc3	-0.35	1.97E-02
Chn1	0.25	5.71E-03	Stag1	-0.35	2.30E-04
Serf2	0.25	1.43E-03	Rbms3	-0.35	3.09E-03
Rnf14	0.25	2.99E-03	Cdk2ap1	-0.35	1.79E-04
Ak3	0.25	2.50E-02	Clspn	-0.35	2.18E-04

Genes (UP)	log2FoldChange	padj	Genes (Down)	log2FoldChange	padj
Atp6v1d	0.25	9.37E-03	Zfp266	-0.35	5.23E-04
Psme1	0.25	4.02E-02	Homer1	-0.35	3.69E-03
Trf	0.25	3.26E-03	Pik3r1	-0.35	6.59E-08
Bcl2l1	0.25	2.17E-02	Btaf1	-0.35	1.05E-04
Rpl8	0.25	1.04E-05	Zfx	-0.35	7.42E-05
Arf5	0.25	1.69E-03	Stag2	-0.35	1.01E-06
Slc1a4	0.25	1.46E-02	Sspn	-0.35	1.43E-02
Tmed3	0.25	1.72E-02	Rere	-0.35	4.50E-06
Gcsh	0.25	6.18E-03	Atad2	-0.35	2.82E-06
Slc37a3	0.25	2.53E-02	Klf13	-0.35	3.41E-05
Tars	0.25	2.09E-03	Atp8a1	-0.35	2.74E-03
Praf2	0.25	1.31E-02	Elmsan1	-0.35	3.64E-03
Snx6	0.25	4.67E-03	Slc12a6	-0.35	5.42E-03
Timp2	0.25	2.21E-03	Rapgef6	-0.35	1.32E-03
Sap30	0.25	3.71E-02	Slc5a3	-0.35	8.01E-09
Higd1a	0.25	2.67E-02	Phf20	-0.35	9.33E-05
Atp5j2	0.25	1.53E-03	Trim33	-0.35	1.49E-05
Uqcr10	0.25	5.49E-03	Fam120c	-0.35	6.39E-03
Coa3	0.25	3.17E-02	Eif5a2	-0.35	5.25E-03
Polr1c	0.25	2.47E-02	Nbas	-0.35	2.48E-04
Rpl7	0.25	4.32E-05	Mgat5	-0.35	1.48E-04
Vcam1	0.25	4.13E-02	Osbpl8	-0.35	8.60E-06
Micos13	0.25	4.29E-02	Emsy	-0.35	9.40E-04
Otud6b	0.25	3.95E-02	Tcf4	-0.34	1.15E-08
Alas1	0.25	4.84E-02	Rest	-0.34	2.01E-04
Fzd1	0.25	1.39E-02	Dnajc13	-0.34	9.25E-07
Smpd1	0.24	1.18E-02	Dyrk1a	-0.34	4.15E-05
Slc35b1	0.24	1.04E-02	Prrc2a	-0.34	1.07E-09
Dusp3	0.24	2.84E-02	Abcb7	-0.34	2.06E-03
Rnf187	0.24	3.34E-04	Mical3	-0.34	1.30E-03
Sympk	0.24	6.25E-04	Ric1	-0.34	7.66E-04
Pfdn1	0.24	6.65E-03	Ssh1	-0.34	1.40E-02
Sms	0.24	9.99E-05	Il17rd	-0.34	1.85E-02
Nck2	0.24	2.07E-02	Spag9	-0.34	1.38E-08
Gde1	0.24	8.65E-03	Sesn3	-0.34	6.42E-06
Rpsa	0.24	2.88E-05	Ncan	-0.34	1.42E-08
Txndc15	0.24	1.32E-02	Mar-06	-0.34	1.14E-06
Gabarapl2	0.24	4.27E-02	Cdc73	-0.34	9.08E-04
Ghitm	0.24	2.96E-04	Kdm3b	-0.34	6.18E-06
Selenoh	0.24	1.67E-02	Luc7l2	-0.34	6.50E-05
Pdzd11	0.24	4.25E-02	Zfp507	-0.34	7.73E-04
Pak1ip1	0.24	1.18E-02	Mdc1	-0.34	7.67E-06

Genes (UP)	log2FoldChange	padj	Genes (Down)	log2FoldChange	padj
Spty2d1	0.24	9.91E-03	**Arid1b**	-0.34	3.64E-05
Coro2b	0.24	1.46E-02	**Lrp8**	-0.34	3.94E-06
Uqcrh	0.24	4.27E-03	**Mindy2**	-0.34	4.50E-06
Tbc1d13	0.24	3.25E-02	**Cdh6**	-0.34	2.94E-04
Por	0.24	4.46E-04	**Tmtc2**	-0.34	1.58E-03
Igfbp4	0.24	2.18E-04	**Bhlhe40**	-0.34	8.84E-06
Vps52	0.24	6.42E-03	**Dnmt3a**	-0.34	9.59E-06
Grwd1	0.24	3.49E-02	**Numa1**	-0.34	1.05E-05
Rpl27a	0.24	2.94E-03	**Larp4**	-0.33	1.04E-05
Aplp1	0.24	1.08E-02	**Aff1**	-0.33	3.90E-04
Rassf3	0.24	7.99E-04	**C1galt1**	-0.33	4.80E-03
Rnf41	0.24	1.49E-02	**Wdr76**	-0.33	1.64E-02
Hyou1	0.24	7.24E-04	**Ecpas**	-0.33	2.16E-05
Chpf	0.24	7.17E-03	**Dock1**	-0.33	4.03E-07
Tomm34	0.24	4.07E-02	**Cad**	-0.33	3.26E-07
Rpl13	0.24	1.19E-04	**Dscam**	-0.33	5.02E-03
Ppp1r2	0.24	6.40E-04	**Rlf**	-0.33	2.08E-02
Tfip11	0.24	4.41E-02	**Lss**	-0.33	8.13E-09
Atp6ap1	0.24	3.50E-04	**Atl3**	-0.33	1.33E-04
Thop1	0.24	4.83E-03	**Blm**	-0.33	2.95E-03
Tm2d2	0.24	3.73E-02	**C2cd3**	-0.33	1.09E-04
Emc4	0.24	4.86E-02	**Dock11**	-0.33	3.46E-03
Nsg1	0.24	3.11E-02	**Tcerg1**	-0.33	4.64E-06
Rexo2	0.24	1.25E-02	**Svil**	-0.33	5.00E-03
Bex3	0.24	2.82E-03	**Satb1**	-0.33	1.53E-05
Dstn	0.24	6.14E-04	**Srgap2**	-0.33	1.26E-06
Pigs	0.24	5.89E-03	**Zfp606**	-0.33	2.03E-02
Tulp3	0.24	1.52E-03	**Igsf3**	-0.33	3.95E-04
Adamts7	0.24	3.12E-02	**Slc36a4**	-0.33	2.95E-03
Nifk	0.24	1.98E-02	**Safb2**	-0.33	1.15E-03
Ybx1	0.24	3.98E-05	**Sash1**	-0.33	1.38E-04
Uqcrc1	0.24	1.01E-03	**Ank2**	-0.33	4.82E-07
Tmem214	0.24	2.21E-02	**Phf3**	-0.33	2.45E-05
Tbcb	0.24	1.57E-02	**Myo6**	-0.33	2.63E-06
Ap1b1	0.24	1.10E-02	**Dock7**	-0.33	3.33E-07
Pex13	0.24	4.22E-02	**Tcf20**	-0.33	1.84E-04
Gap43	0.24	9.30E-05	**Prpf39**	-0.33	6.18E-03
Zfyve1	0.24	4.14E-02	**Fam193a**	-0.33	1.13E-03
Atp6v1e1	0.24	3.37E-03	**Scaf11**	-0.33	5.19E-06
Arl6ip5	0.24	3.70E-02	**Robo1**	-0.33	2.41E-03
Stip1	0.24	1.43E-04	**Alkbh8**	-0.32	1.28E-02
Asna1	0.24	3.43E-03	**Bclaf1**	-0.32	5.62E-07

Genes (UP)	log2FoldChange	padj	Genes (Down)	log2FoldChange	padj
Sf3b4	0.24	4.66E-03	Klhdc10	-0.32	1.10E-04
Carhsp1	0.24	1.49E-02	Frs2	-0.32	1.37E-03
Polr2g	0.24	2.95E-02	Per1	-0.32	1.29E-03
Rack1	0.24	1.53E-04	Rps6kb1	-0.32	2.39E-03
Cyb5r4	0.24	3.41E-02	Pola1	-0.32	2.11E-04
Calm1	0.23	4.32E-05	Ralgapb	-0.32	1.07E-04
Ccnyl1	0.23	1.13E-02	Pask	-0.32	3.72E-02
Wsb2	0.23	4.34E-03	Nes	-0.32	8.01E-07
Abcg2	0.23	9.32E-03	Vcpip1	-0.32	1.02E-03
Fkbp1a	0.23	9.72E-05	Sema6d	-0.32	5.24E-07
Cars	0.23	1.63E-02	Agrn	-0.32	8.56E-07
Frmd8	0.23	2.31E-03	Klhl24	-0.32	1.15E-03
1810058I24 Rik	0.23	3.11E-02	Cdkl5	-0.32	3.61E-02
Rps9	0.23	1.15E-04	Dclk2	-0.32	1.33E-04
Qars	0.23	1.45E-02	Adar	-0.32	1.20E-03
Pias4	0.23	3.74E-02	Shprh	-0.32	5.68E-04
Sema4b	0.23	2.77E-02	Zmym4	-0.32	6.47E-04
Gsn	0.23	1.28E-02	Sh3pxd2b	-0.32	7.03E-08
Rpl10a	0.23	4.30E-03	Sfmbt1	-0.32	2.67E-02
Plk2	0.23	3.65E-04	Kif13b	-0.32	7.92E-03
Epop	0.23	4.86E-02	Rbm15	-0.32	4.42E-03
Tmed9	0.23	4.90E-03	Resf1	-0.32	3.36E-02
Sap30bp	0.23	1.93E-02	Nphp3	-0.32	4.80E-02
Sat1	0.23	3.67E-02	Lrch2	-0.32	3.43E-03
Cdc34	0.23	2.08E-02	Atxn7	-0.32	1.63E-02
Cldn12	0.23	3.99E-02	Arhgap35	-0.32	1.27E-05
Bop1	0.23	4.58E-03	Tef	-0.32	1.11E-02
Mfsd5	0.23	4.39E-02	Amotl1	-0.32	7.66E-07
Srprb	0.23	5.16E-03	Man2a1	-0.31	3.91E-03
Ncln	0.23	9.76E-03	Gpr161	-0.31	7.25E-03
H13	0.23	7.69E-03	Ireb2	-0.31	2.20E-04
Mknk2	0.23	1.40E-03	Fancm	-0.31	1.18E-02
Slc3a2	0.23	2.03E-03	Cnot6	-0.31	6.29E-05
Bri3	0.23	2.31E-02	Baz1b	-0.31	2.82E-06
Actn4	0.23	1.15E-03	Phka2	-0.31	3.39E-02
Ric8a	0.23	4.86E-02	Glg1	-0.31	6.50E-08
Ube2a	0.23	1.27E-02	Brip1	-0.31	4.02E-02
Irf2bp1	0.23	2.14E-02	Nhlrc2	-0.31	3.69E-04
Kdelr2	0.23	1.15E-03	Foxn2	-0.31	7.76E-03
Ndufs7	0.23	3.63E-02	Top2b	-0.31	1.47E-06
Slc9a3r1	0.23	1.57E-02	Ascc3	-0.31	2.33E-03

Genes (UP)	log2FoldChange	padj	Genes (Down)	log2FoldChange	padj
Pygo2	0.23	7.36E-03	Fam210a	-0.31	1.14E-02
Prdx1	0.23	2.70E-04	Syt6	-0.31	2.79E-03
Vps29	0.23	2.71E-02	Zfp629	-0.31	2.11E-03
Srf	0.23	3.93E-02	Dek	-0.31	3.34E-04
Tjap1	0.23	4.31E-02	Trak1	-0.31	4.61E-05
Rps16	0.23	2.17E-04	Heatr5b	-0.31	6.43E-04
Wars	0.23	4.26E-03	Mis18bp1	-0.31	1.23E-02
Uqcrq	0.23	1.49E-03	E2f7	-0.31	1.28E-02
Rsl24d1	0.23	1.40E-02	Brd4	-0.31	2.38E-06
Pabpc1	0.23	5.42E-05	Tns1	-0.31	5.96E-03
Tmem173	0.23	8.65E-03	Rapgef2	-0.31	2.71E-06
Rps7	0.23	6.15E-03	Zswim6	-0.31	9.46E-04
Ndufa10	0.23	5.27E-03	Fmnl2	-0.31	8.93E-05
Rpl34	0.23	2.78E-03	Myo16	-0.31	3.80E-04
Vps26a	0.23	1.08E-02	Eif3a	-0.31	8.72E-07
Med22	0.23	2.85E-02	Gpatch2	-0.31	3.40E-02
Akirin1	0.23	2.13E-02	Ercc6	-0.31	1.36E-02
Mrpl28	0.22	1.01E-02	Megf9	-0.31	1.98E-03
Drg2	0.22	1.55E-02	Stard4	-0.31	4.07E-06
Cox4i1	0.22	6.51E-04	Top2a	-0.31	1.29E-03
Ubfd1	0.22	1.63E-02	Gabbr1	-0.31	4.93E-03
B2m	0.22	8.65E-03	Igfbp5	-0.31	2.42E-06
Med17	0.22	3.64E-02	Tecpr2	-0.31	1.30E-02
Gps1	0.22	3.53E-03	Atp2b4	-0.31	9.59E-03
Rpl14	0.22	3.07E-04	Lmtk2	-0.31	2.12E-03
Fam234a	0.22	2.70E-02	Lrp4	-0.31	1.58E-03
Napa	0.22	6.39E-03	Npat	-0.31	4.68E-03
Surf4	0.22	1.85E-03	Itpr1	-0.31	1.60E-03
Prpf3	0.22	2.24E-02	Jmy	-0.31	6.64E-03
Micu1	0.22	2.72E-02	Focad	-0.31	1.40E-02
Olfml3	0.22	6.09E-03	Gpcpd1	-0.31	1.85E-02
Pebp1	0.22	1.20E-04	Nudcd3	-0.31	1.69E-03
Rpl24	0.22	2.52E-03	Vps37a	-0.31	1.04E-03
Mrpl17	0.22	1.22E-02	Ddi2	-0.30	5.14E-03
Rpl36	0.22	3.91E-03	Kdm6a	-0.30	1.29E-03
Jmjd6	0.22	2.58E-02	Slc25a36	-0.30	2.38E-03
Tmem165	0.22	1.08E-02	Tmem131	-0.30	4.33E-05
Slc4a2	0.22	4.17E-02	Shank3	-0.30	2.46E-02
Ndufs8	0.22	1.47E-02	Clip4	-0.30	3.24E-02
Pqbp1	0.22	3.58E-02	Lhfpl4	-0.30	9.16E-03
Adsl	0.22	1.28E-02	Nr1d2	-0.30	1.28E-02
Spcs1	0.22	2.71E-02	Secisbp2l	-0.30	8.75E-05

Genes (UP)	log2FoldChange	padj	Genes (Down)	log2FoldChange	padj
Eif3l	0.22	4.71E-03	Kcnj10	-0.30	1.84E-03
Glrx3	0.22	2.09E-03	Rsbn1l	-0.30	1.62E-02
Cox6a1	0.22	1.01E-03	Smc1a	-0.30	3.41E-05
Aprt	0.22	3.42E-02	Naa50	-0.30	1.38E-05
Nme2	0.22	3.63E-04	Ptbp3	-0.30	6.47E-04
Map2k2	0.22	1.26E-02	Cacna1h	-0.30	3.39E-04
Skp1a	0.22	5.65E-04	Nup98	-0.30	8.75E-05
Sord	0.22	2.84E-02	Cd2ap	-0.30	9.59E-04
G6pdx	0.22	3.94E-03	Chml	-0.30	2.80E-02
Xrcc1	0.22	3.03E-02	Oga	-0.30	9.31E-05
Dad1	0.22	1.54E-02	Kdm6b	-0.30	7.91E-05
Atp5d	0.22	3.64E-03	Gtf2a1	-0.30	3.80E-03
Cnp	0.22	2.83E-02	Erc1	-0.30	1.90E-02
Npc2	0.22	1.28E-03	Dennd1b	-0.30	4.20E-02
Mxd4	0.22	2.24E-02	Ptpn14	-0.30	1.46E-02
Mfge8	0.22	3.64E-03	Sos2	-0.30	6.33E-03
Bag3	0.22	4.95E-02	Ago1	-0.30	5.15E-05
Tmco3	0.21	3.14E-02	Strn	-0.30	1.28E-03
Lbh	0.21	3.80E-03	Ankrd26	-0.30	1.52E-02
Prdx2	0.21	6.59E-04	Cep135	-0.30	3.94E-02
Grpel1	0.21	4.13E-02	Rb1	-0.30	6.66E-03
Hnrnpc	0.21	1.42E-03	Agl	-0.30	8.58E-04
Tecr	0.21	6.28E-04	Kif1a	-0.30	1.69E-06
Pmpcb	0.21	9.17E-03	Pum2	-0.30	2.66E-05
Sec22b	0.21	1.17E-02	Robo2	-0.30	2.03E-02
Sec13	0.21	4.88E-03	Wapl	-0.29	3.14E-04
Clpb	0.21	3.07E-02	Gpatch8	-0.29	4.77E-04
Rps20	0.21	3.00E-02	Rev1	-0.29	4.76E-02
Derl1	0.21	1.47E-02	Phka1	-0.29	3.47E-03
Hint1	0.21	9.66E-03	Fcho2	-0.29	8.80E-03
Psmb4	0.21	8.32E-04	Prkce	-0.29	2.17E-02
Tmco1	0.21	4.68E-02	Mms22l	-0.29	1.93E-02
Cox14	0.21	4.46E-02	Cblb	-0.29	4.91E-02
Gnas	0.21	8.31E-03	Rgs12	-0.29	6.71E-03
Gng5	0.21	1.76E-02	Neurl1b	-0.29	9.04E-03
Cap1	0.21	3.13E-03	Hnrnpdl	-0.29	1.17E-05
Cdipt	0.21	2.67E-02	Ibtk	-0.29	1.05E-03
Lap3	0.21	4.84E-03	Mef2a	-0.29	1.13E-03
Hey1	0.21	1.74E-02	Dzip3	-0.29	6.39E-03
Cpe	0.21	5.54E-03	Pkd2	-0.29	3.48E-04
Fzr1	0.21	2.86E-02	Pura	-0.29	1.01E-02
Dynlrb1	0.21	1.52E-02	Enah	-0.29	1.07E-04

Genes (UP)	log2FoldChange	padj	Genes (Down)	log2FoldChange	padj
Tbrg1	0.21	2.57E-02	Tut7	-0.29	2.33E-03
Akt1s1	0.21	2.60E-02	Pag1	-0.29	1.95E-02
Ddx18	0.21	4.36E-02	Mier1	-0.29	1.36E-02
Maea	0.21	5.55E-03	Fmn2	-0.29	2.57E-02
Cuta	0.21	4.81E-02	Pitpnm2	-0.29	2.92E-02
Fkbp8	0.21	2.95E-03	Lnpk	-0.29	1.85E-02
Cers5	0.21	2.24E-02	Pan3	-0.29	1.32E-02
Abhd8	0.21	2.26E-02	Snrnp200	-0.29	9.28E-07
Ap1s1	0.21	6.72E-03	Sox11	-0.29	5.53E-04
Ifitm2	0.21	9.96E-03	Flna	-0.29	7.98E-08
Serpine2	0.21	3.78E-03	Cul5	-0.29	1.74E-03
Mfsd1	0.21	8.08E-03	Uhrf1bp1	-0.29	4.76E-03
Cox6b1	0.21	5.00E-03	Iqgap3	-0.29	6.14E-03
Trap1	0.21	4.09E-02	1500004A13Rik	-0.29	1.67E-02
Epn1	0.21	5.42E-03	Wdhd1	-0.29	5.09E-03
Copz1	0.21	4.58E-03	Mettl4	-0.29	3.89E-02
Pfn1	0.21	5.65E-04	Pde7b	-0.29	2.31E-02
Cdc42ep1	0.21	4.48E-03	Sipa1l3	-0.29	8.02E-04
Itm2c	0.21	1.66E-03	Tmed8	-0.29	1.33E-02
Cd81	0.21	3.13E-03	Dennd4b	-0.29	4.39E-02
Pgam1	0.21	1.90E-02	Smc3	-0.29	4.01E-05
Eif3i	0.21	5.96E-03	Zfp644	-0.29	1.42E-02
Ywhah	0.21	1.94E-03	Pdzd8	-0.29	1.49E-03
Trim27	0.21	2.75E-02	Atg2b	-0.29	9.48E-03
Gaa	0.21	3.35E-03	Haghl	-0.29	2.40E-02
Peg13	0.21	2.58E-02	Iqgap2	-0.29	1.62E-03
Dnm2	0.21	1.13E-02	Kif20b	-0.29	1.92E-02
Srpr	0.21	1.06E-02	Ppp1r12a	-0.29	6.91E-05
Ahsa1	0.21	2.19E-02	AW549877	-0.29	3.21E-03
Gatad1	0.21	8.29E-03	Atrn	-0.29	1.17E-03
Cnih1	0.21	1.27E-02	Cdk13	-0.29	1.37E-03
Bex2	0.21	1.24E-02	Prpf40a	-0.29	2.66E-04
Psmd8	0.20	6.60E-03	Glis3	-0.28	4.27E-03
Tspan5	0.20	4.26E-02	Tfdp2	-0.28	8.79E-03
Ppp5c	0.20	9.92E-03	Clcn6	-0.28	8.90E-04
Tmsb10	0.20	1.68E-03	Etv1	-0.28	1.21E-04
Ckb	0.20	1.10E-03	Sox5	-0.28	3.72E-02
Cactin	0.20	4.45E-02	Gcn1	-0.28	1.06E-05
Irf2bp2	0.20	2.83E-02	Fmr1	-0.28	3.68E-04
Josd1	0.20	3.39E-02	Rsrc1	-0.28	1.48E-02
Ctsb	0.20	1.03E-03	Reln	-0.28	2.01E-02

Genes (UP)	log2FoldChange	padj	Genes (Down)	log2FoldChange	padj
Eef1a1	0.20	2.98E-04	Pan2	-0.28	4.76E-03
Ctdnep1	0.20	2.62E-02	Rgma	-0.28	2.80E-02
Taldo1	0.20	4.71E-03	Fbxl18	-0.28	1.27E-02
Pgrmc1	0.20	7.60E-03	Man1a2	-0.28	9.18E-05
Cerk	0.20	2.03E-02	Fnip1	-0.28	1.57E-02
Ndufa7	0.20	4.02E-02	Mdga2	-0.28	2.40E-02
Efemp2	0.20	4.71E-02	Suco	-0.28	3.18E-03
Aimp1	0.20	4.63E-02	Zfp638	-0.28	2.88E-03
Sh3kbp1	0.20	1.67E-02	Magi2	-0.28	5.00E-03
Gstm1	0.20	2.67E-02	Zcchc24	-0.28	1.63E-05
Myl6	0.20	1.11E-02	Phkb	-0.28	5.99E-03
Psma7	0.20	7.44E-03	Cacna2d1	-0.28	2.65E-02
Idh3b	0.20	1.29E-02	Xpr1	-0.28	3.54E-03
Ndufa9	0.20	2.39E-02	Ltbp4	-0.28	3.26E-03
Abcf2	0.20	1.78E-02	Srek1	-0.28	5.13E-03
Atp6v1h	0.20	2.01E-02	Supt16	-0.28	2.53E-03
Timm50	0.20	2.57E-02	Tlk1	-0.28	2.19E-03
Copg1	0.20	1.10E-02	Rbm3	-0.28	5.80E-06
Rpl9	0.20	6.20E-04	Amot	-0.28	1.38E-03
Ywhaq	0.20	1.62E-03	Zfp646	-0.28	2.67E-03
Shc1	0.20	4.77E-02	Slc35a3	-0.28	1.63E-02
Sec14l1	0.20	9.91E-03	Togaram1	-0.28	3.96E-02
H2-K1	0.20	4.02E-02	Gxylt1	-0.28	3.21E-03
Rps11	0.20	3.45E-03	Slc6a6	-0.28	2.48E-05
Degs1	0.20	3.22E-02	Suz12	-0.28	2.79E-04
Eef1d	0.20	1.39E-02	Arhgap26	-0.28	3.78E-03
Ppp1r37	0.20	3.43E-02	Cabin1	-0.28	5.47E-04
Ostc	0.20	1.24E-02	Micall1	-0.28	4.46E-02
Ldhb	0.20	2.16E-02	Zfp512b	-0.28	1.09E-02
Lzts2	0.20	3.49E-02	Rad50	-0.28	3.47E-02
Gabarap	0.20	1.38E-02	Slc9a1	-0.27	4.76E-02
Anapc5	0.20	9.46E-04	Zfp516	-0.27	7.56E-03
Sars	0.20	3.51E-03	Ubr2	-0.27	1.40E-04
Scpep1	0.20	8.97E-03	Tug1	-0.27	4.04E-04
Dhx40	0.20	3.46E-02	Far1	-0.27	2.91E-03
Tle5	0.20	1.05E-03	Rnf144a	-0.27	3.22E-02
Atic	0.20	1.39E-02	Mtx3	-0.27	3.19E-02
Ywhab	0.20	3.15E-03	Syncrip	-0.27	3.90E-04
Gars	0.20	5.04E-03	Anp32e	-0.27	6.47E-04
Reep5	0.20	2.09E-02	Dnmt1	-0.27	3.44E-06
Bmp1	0.20	5.86E-03	Vps54	-0.27	7.65E-03
Ndufab1	0.20	1.57E-02	Gnaq	-0.27	3.85E-04

Genes (UP)	log2FoldChange	padj	Genes (Down)	log2FoldChange	padj
Fam53c	0.20	4.29E-02	Espl1	-0.27	4.85E-03
Sdhd	0.20	2.16E-02	Kcnip1	-0.27	4.99E-02
Ptms	0.20	5.53E-04	Ptpn13	-0.27	2.51E-03
H3f3a	0.20	1.17E-03	Map2	-0.27	3.10E-04
Hdac1	0.20	1.30E-02	Sec22c	-0.27	2.33E-02
Rpl22	0.20	1.10E-02	Nup214	-0.27	5.61E-03
Nme1	0.20	5.93E-03	Chpf2	-0.27	1.32E-02
Suclg1	0.20	2.79E-02	Kidins220	-0.27	3.19E-04
Rpl17	0.20	4.11E-03	Fam160b1	-0.27	6.28E-03
Nop2	0.20	1.91E-02	Nup160	-0.27	1.48E-02
Ttyh2	0.20	1.98E-02	Oip5os1	-0.27	1.37E-03
Psmb5	0.20	1.19E-02	Slc12a2	-0.27	1.39E-03
Hmg20b	0.19	3.90E-02	Ccdc6	-0.27	1.26E-03
Sh3gl1	0.19	2.83E-02	Fancd2	-0.27	4.35E-02
Farsb	0.19	3.72E-02	Yes1	-0.27	1.84E-02
Ptcd3	0.19	3.87E-02	Kif2a	-0.27	2.25E-03
Actb	0.19	3.48E-04	Ncl	-0.26	5.15E-05
Ndufb5	0.19	4.38E-02	Galnt11	-0.26	4.00E-02
Rnf10	0.19	9.96E-03	Dip2a	-0.26	1.23E-03
Mcl1	0.19	5.92E-03	Bcl9	-0.26	1.40E-02
Zyx	0.19	4.69E-02	Zzz3	-0.26	1.76E-03
Ppia	0.19	1.05E-03	Acsl4	-0.26	2.58E-04
Myc	0.19	3.60E-02	Dip2c	-0.26	6.39E-04
Txn1	0.19	8.23E-03	Inka2	-0.26	2.21E-04
Prdx3	0.19	3.79E-02	Usp7	-0.26	3.90E-04
Fscn1	0.19	6.04E-03	Pde7a	-0.26	3.42E-03
Rhob	0.19	2.24E-02	Dpp8	-0.26	4.41E-03
Psmb6	0.19	1.24E-02	Tbc1d16	-0.26	1.73E-02
Psmb3	0.19	1.65E-02	Heatr5a	-0.26	2.55E-03
Qdpr	0.19	3.27E-02	Fnbp1l	-0.26	1.29E-03
Aldh18a1	0.19	2.32E-02	Zfp91	-0.26	5.76E-04
Rps3	0.19	6.44E-04	Smc5	-0.26	8.08E-03
Rpl37a	0.19	1.43E-02	Epb41	-0.26	7.26E-03
Ipo4	0.19	1.70E-02	Ice1	-0.26	3.55E-03
Rpl19	0.19	1.02E-03	Tia1	-0.26	2.22E-02
Agpat1	0.19	2.90E-02	Usp45	-0.26	3.94E-02
Mdh2	0.19	9.12E-03	Apc2	-0.26	1.47E-02
Srm	0.19	2.16E-02	Heg1	-0.26	9.23E-03
Acsbg1	0.19	1.05E-02	Smc6	-0.26	6.23E-03
Clns1a	0.19	3.15E-02	Skil	-0.26	4.91E-02
Rars	0.19	1.87E-02	E2f3	-0.26	7.30E-03
Pgk1	0.19	1.94E-03	Larp4b	-0.26	1.86E-03

Genes (UP)	log2FoldChange	padj	Genes (Down)	log2FoldChange	padj
Tuba1a	0.19	1.95E-03	Rapgef1	-0.26	2.25E-04
Oaz2	0.19	2.18E-02	Socs4	-0.26	1.90E-02
Rab5c	0.19	1.30E-02	Fus	-0.26	1.38E-05
4933434E20 Rik	0.19	4.71E-02	Rhobtb3	-0.26	2.43E-03
Rab1b	0.19	9.67E-03	Rnf141	-0.26	2.58E-02
Emc3	0.19	4.38E-02	Pnisr	-0.25	1.83E-02
Rps2	0.19	5.27E-03	Yipf6	-0.25	1.11E-02
Rpl31	0.19	3.74E-03	Man2a2	-0.25	1.05E-03
Vasp	0.19	1.71E-02	Naa15	-0.25	9.46E-04
Timm23	0.19	4.63E-02	Fam168a	-0.25	1.04E-03
Pkm	0.19	1.52E-03	Nmt2	-0.25	4.54E-02
Alg2	0.19	4.62E-02	Dclk1	-0.25	2.35E-03
Tsc22d1	0.19	8.43E-03	Dot1l	-0.25	6.74E-04
Timm13	0.19	3.73E-02	Usp32	-0.25	4.62E-03
Dusp6	0.19	3.76E-03	U2surp	-0.25	1.97E-03
Gipc1	0.19	3.44E-02	Ocrl	-0.25	1.57E-02
Btf3	0.19	6.60E-03	Ptprs	-0.25	1.58E-05
Garem2	0.19	4.79E-02	Adamts1	-0.25	4.07E-03
Pik3r3	0.19	1.06E-02	Magi3	-0.25	1.46E-02
Yars	0.19	2.45E-02	Dhfr	-0.25	3.03E-02
Rhoc	0.18	1.29E-02	Hsd17b7	-0.25	1.97E-03
Kat2a	0.18	3.25E-02	Dock10	-0.25	2.85E-03
Rpl11	0.18	2.85E-03	Ick	-0.25	1.38E-02
Rps3a1	0.18	2.11E-03	Cflar	-0.25	3.14E-02
Maged2	0.18	2.05E-02	Fanca	-0.25	4.96E-02
Rps25	0.18	3.89E-03	Mid2	-0.25	1.29E-02
Tceal9	0.18	1.49E-02	Usp1	-0.25	1.34E-02
Psmd6	0.18	2.23E-02	Mef2d	-0.25	1.78E-03
Rpl12	0.18	5.42E-03	Ddx42	-0.25	2.66E-03
Prdx6	0.18	3.66E-02	Pou6f1	-0.25	9.74E-03
Psmc5	0.18	2.03E-02	Fndc1	-0.25	4.99E-02
Mest	0.18	6.44E-03	Bmpr1a	-0.25	7.05E-04
Lfng	0.18	4.79E-02	Ccp110	-0.25	2.91E-02
Pttg1ip	0.18	2.69E-02	Ids	-0.25	1.60E-03
Odc1	0.18	2.63E-02	Samd4	-0.25	1.87E-02
Hmga1	0.18	3.29E-02	Lin7c	-0.25	1.02E-02
Aplp2	0.18	3.13E-03	Nfix	-0.25	3.45E-03
Itm2b	0.18	9.82E-03	Dennd1a	-0.25	4.67E-02
Rps4x	0.18	1.28E-03	Tsc22d2	-0.25	4.51E-03
Plat	0.18	8.77E-03	Tln1	-0.25	2.12E-04
Gorasp2	0.18	1.40E-02	Hnrnpul1	-0.25	1.22E-04

Genes (UP)	log2FoldChange	padj	Genes (Down)	log2FoldChange	padj
Pin1	0.18	3.52E-02	Usp48	-0.25	5.34E-03
Rps27a	0.18	6.95E-03	Adam12	-0.25	2.84E-03
Ppme1	0.18	3.79E-02	Myo9b	-0.25	1.90E-03
Arf4	0.18	1.09E-02	Fnbp4	-0.25	1.27E-02
Mapk8ip1	0.18	3.21E-02	Lrrk2	-0.25	2.23E-02
Tpt1	0.18	1.46E-03	St8sia1	-0.25	9.33E-04
Drg1	0.18	4.64E-02	Marf1	-0.25	2.13E-02
Ociad1	0.18	2.36E-02	Phf14	-0.25	2.18E-02
Eif3c	0.18	4.49E-03	Atp2b1	-0.25	4.03E-04
Sec31a	0.18	1.34E-02	Kpna1	-0.24	1.15E-02
Ergic3	0.18	4.41E-02	Msh6	-0.24	2.47E-03
Ldha	0.18	1.97E-03	Nek9	-0.24	3.13E-03
Arpc1a	0.18	2.70E-02	Nup155	-0.24	6.10E-03
Emc10	0.18	2.04E-02	Nasp	-0.24	1.09E-03
Os9	0.18	4.80E-02	Cdh4	-0.24	8.65E-03
Impa1	0.18	4.97E-02	Scaf4	-0.24	1.72E-02
Rps8	0.18	3.33E-03	Rbm27	-0.24	2.11E-02
Ckap4	0.18	2.48E-02	Peli2	-0.24	3.57E-02
Irf2bpl	0.18	1.29E-02	Eml4	-0.24	3.77E-03
Klhdc3	0.18	3.47E-02	Wasf3	-0.24	9.58E-03
Zfp706	0.18	1.36E-02	Pafah1b1	-0.24	1.72E-03
Ddost	0.18	2.15E-02	Adcyap1r1	-0.24	7.15E-03
Rtn1	0.18	5.88E-03	2610507B11Rik	-0.24	2.01E-04
Dctn1	0.18	3.52E-02	Lig3	-0.24	1.30E-02
Snx3	0.18	1.40E-02	Fbxo11	-0.24	2.16E-03
Capzb	0.18	2.29E-02	Ccdc50	-0.24	1.45E-03
Snu13	0.18	2.91E-02	Hnrnpr	-0.24	2.56E-03
Arf6	0.18	4.26E-02	Chd3	-0.24	4.41E-03
Atp6v0e2	0.17	2.84E-02	Epm2aip1	-0.24	2.68E-02
Rtn4	0.17	4.27E-03	Srgap3	-0.24	7.82E-03
Sin3b	0.17	1.66E-02	Dis3	-0.24	8.23E-03
Chmp1a	0.17	4.98E-02	Ptprf	-0.24	1.52E-04
Slc35b2	0.17	4.49E-02	Sptan1	-0.24	4.99E-05
Rpn1	0.17	1.48E-02	Atrnl1	-0.24	2.95E-03
Mtch1	0.17	7.92E-03	Zranb1	-0.24	1.29E-02
Pomp	0.17	3.55E-02	Msl2	-0.24	2.39E-02
Lman2	0.17	2.41E-02	Cdc27	-0.24	1.08E-02
Arl6ip1	0.17	3.34E-02	Prkcb	-0.24	6.10E-03
Rpl23a	0.17	4.78E-02	Srrm1	-0.24	2.05E-03
Dnaja1	0.17	2.87E-02	Dvl3	-0.24	4.52E-03
Rpl21	0.17	6.20E-03	Celf2	-0.24	6.67E-03

Genes (UP)	log2FoldChange	padj	Genes (Down)	log2FoldChange	padj
Lypla2	0.17	2.75E-02	Vkorc1l1	-0.24	1.09E-02
Ldb1	0.17	4.10E-02	Hnrnpa3	-0.24	1.40E-03
Clptm1	0.17	2.23E-02	Ankrd28	-0.24	4.35E-03
Psmc4	0.17	4.02E-02	Mon2	-0.24	2.47E-03
Hsp90b1	0.17	3.96E-02	Nufip2	-0.24	2.37E-02
Rpl18	0.17	5.66E-03	Hells	-0.23	1.49E-02
Nedd8	0.17	4.46E-02	Cspg5	-0.23	1.14E-02
Rpn2	0.17	1.19E-02	Traf3	-0.23	5.38E-03
Atp6v1b2	0.17	2.45E-02	Esyt2	-0.23	2.36E-02
Raly	0.17	1.81E-02	Rrbp1	-0.23	3.16E-04
Tsen34	0.17	3.52E-02	Nfrkb	-0.23	3.53E-02
Sec61a1	0.17	1.45E-02	Arhgap31	-0.23	1.53E-03
Ints3	0.17	3.71E-02	Tut4	-0.23	3.41E-02
Psap	0.17	4.79E-03	Prkd3	-0.23	3.35E-03
Nars	0.17	1.85E-02	Mllt6	-0.23	1.98E-02
Cyc1	0.17	2.01E-02	Usp47	-0.23	5.43E-04
M6pr	0.17	4.86E-02	Evi5	-0.23	7.35E-03
Cdc37	0.17	2.57E-02	Myef2	-0.23	4.38E-03
Bub3	0.17	3.94E-02	Klf10	-0.23	1.69E-02
Sod1	0.17	3.11E-02	Rfx4	-0.23	1.25E-02
Atp5h	0.17	3.32E-02	Cask	-0.23	2.27E-03
Mtap	0.17	4.60E-02	4931406P16Rik	-0.23	2.85E-02
Prpf19	0.16	3.24E-02	Neo1	-0.23	3.13E-03
Col18a1	0.16	4.63E-02	Ppp6r2	-0.23	4.52E-02
Mlf2	0.16	7.47E-03	Polr1a	-0.23	4.95E-03
Sdcbp	0.16	2.24E-02	Oxr1	-0.23	8.99E-04
Eif5a	0.16	4.65E-03	Tjp1	-0.23	4.76E-04
Tspan3	0.16	1.78E-02	Jarid2	-0.23	4.00E-02
Eif1	0.16	1.78E-02	Zfp354c	-0.23	3.93E-02
Cops6	0.16	3.68E-02	Kif11	-0.23	3.81E-02
Atp5g3	0.16	1.54E-02	Slmap	-0.23	3.67E-03
Aars	0.16	3.31E-02	Ppp2r5e	-0.23	1.90E-02
Colgalt1	0.16	4.56E-02	Ctif	-0.23	3.72E-02
Psma1	0.16	4.88E-02	Pogz	-0.23	1.55E-02
Sar1a	0.16	2.73E-02	Zfp334	-0.23	4.51E-02
Psmd4	0.16	4.17E-02	Nr3c1	-0.23	3.15E-02
Aldoc	0.16	3.52E-02	Ktn1	-0.23	4.50E-03
Marcksl1	0.16	1.72E-02	Lbr	-0.23	2.83E-02
Tmed2	0.16	3.97E-02	Plxnb2	-0.23	4.04E-04
Hsp90aa1	0.16	1.32E-02	Brd8	-0.23	1.08E-02
Dhcr7	0.16	1.13E-02	Adam19	-0.23	1.17E-03

Genes (UP)	log2FoldChange	padj	Genes (Down)	log2FoldChange	padj
Tpi1	0.16	2.56E-02	Tnc	-0.23	1.09E-04
Rpl41	0.16	2.94E-02	Ipo8	-0.23	2.16E-02
Slc25a4	0.16	9.01E-03	Gab2	-0.23	2.76E-02
Kars	0.16	2.30E-02	Psme4	-0.23	1.44E-03
Ppp1ca	0.16	2.76E-02	Pigm	-0.23	2.00E-02
Psmb1	0.16	3.81E-02	Rnf38	-0.23	2.05E-02
Sox9	0.16	4.23E-02	Stk38l	-0.23	1.52E-02
Psmc2	0.15	4.44E-02	Xpo1	-0.22	3.42E-03
Vdac1	0.15	1.56E-02	Ppig	-0.22	2.32E-02
Rpl32	0.15	1.52E-02	Hip1	-0.22	5.40E-05
Wls	0.15	4.87E-02	Arhgef17	-0.22	7.63E-03
Atp5f1	0.15	2.38E-02	Zc3h4	-0.22	5.09E-03
Slc16a2	0.15	4.05E-02	Dusp11	-0.22	1.96E-03
Laptm4a	0.15	4.99E-02	2900097C17Rik	-0.22	2.43E-03
Naca	0.15	1.69E-02	Scd1	-0.22	8.93E-05
Cfl1	0.15	1.91E-02	Neto2	-0.22	9.12E-04
Rhoa	0.15	2.29E-02	Hmgb2	-0.22	4.02E-02
Slc25a39	0.15	4.21E-02	Il6st	-0.22	1.09E-02
Hsd17b12	0.15	3.42E-02	Brd1	-0.22	8.36E-03
Cct4	0.15	4.58E-02	Atf7ip	-0.22	6.60E-03
Rpl7a	0.15	1.48E-02	Pdcd11	-0.22	1.24E-02
Rpl13a	0.15	1.04E-02	Ccser2	-0.22	4.80E-03
Selenof	0.15	2.90E-02	Tacc1	-0.22	1.27E-02
Vdac2	0.15	3.36E-02	Uhmk1	-0.22	9.69E-03
Pcbp1	0.15	3.08E-02	Etnk1	-0.22	8.54E-03
Arpc2	0.14	4.44E-02	Gtf3c4	-0.22	2.17E-02
Uba1	0.14	2.13E-02	Wdr26	-0.22	4.16E-04
Tmbim6	0.14	2.48E-02	Map3k4	-0.22	2.02E-02
Rpl4	0.14	2.80E-02	Washc4	-0.22	3.49E-02
Atxn10	0.14	4.38E-02	Gfpt1	-0.22	8.97E-03
Akr1a1	0.14	4.56E-02	Dlg5	-0.22	1.21E-02
Gnai2	0.14	2.68E-02	Mkln1	-0.22	3.34E-02
Fdps	0.14	2.39E-02	Rfc1	-0.22	7.56E-03
Lrrc59	0.14	3.63E-02	Nup153	-0.22	5.45E-03
Cnn3	0.13	4.22E-02	Smarca5	-0.22	3.54E-03
Cct3	0.13	3.94E-02	Trp53bp1	-0.22	3.99E-02
Rpl27	0.13	4.20E-02	Sorcs1	-0.22	1.07E-02
H2afz	0.13	4.92E-02	Slf2	-0.22	5.28E-03
Rpl5	0.13	4.37E-02	Ccnt1	-0.22	2.68E-02
Msn	0.13	3.55E-02	Sec63	-0.22	2.51E-03
Eef2	0.13	4.00E-02	Rad21	-0.22	4.86E-03

Genes (UP)	log2FoldChange	padj	Genes (Down)	log2FoldChange	padj
			Ppp6r3	-0.22	3.18E-03
			Smc2	-0.22	2.87E-02
			Ppp3cb	-0.21	3.62E-02
			Camsap1	-0.21	2.49E-02
			Pik3ca	-0.21	9.17E-03
			Usp6nl	-0.21	3.54E-02
			Htatsf1	-0.21	3.80E-02
			Elovl6	-0.21	2.99E-03
			Exoc5	-0.21	1.43E-02
			Phf2	-0.21	6.70E-03
			Gigyf2	-0.21	2.78E-02
			Zbtb18	-0.21	9.72E-03
			R3hdm2	-0.21	2.33E-02
			Tbl1x	-0.21	4.19E-03
			Rmnd5a	-0.21	1.57E-02
			Jak2	-0.21	4.29E-02
			Syt11	-0.21	6.92E-04
			Gapvd1	-0.21	1.82E-02
			Pcdh9	-0.21	3.88E-02
			Ctdsp2	-0.21	3.37E-03
			Synrg	-0.21	3.87E-02
			Abcd3	-0.21	2.47E-03
			Cpne3	-0.21	4.09E-02
			Cdc42bpb	-0.21	5.02E-03
			Nhsl1	-0.21	7.62E-03
			Gpm6a	-0.21	2.04E-02
			R3hdm1	-0.21	1.79E-02
			Hnrnpul2	-0.21	4.66E-03
			Nvl	-0.21	3.43E-02
			Acap2	-0.21	2.24E-02
			Fam120a	-0.20	7.36E-04
			Klf3	-0.20	1.08E-02
			Xpo7	-0.20	1.24E-02
			Mark1	-0.20	4.66E-02
			Acss2	-0.20	8.39E-03
			Tmpo	-0.20	6.67E-03
			Hmgcr	-0.20	5.48E-04
			Pou3f3	-0.20	3.24E-03
			Zdhhc20	-0.20	1.49E-02
			Ctnnd2	-0.20	5.99E-03
			Pcnx3	-0.20	3.70E-02
			Mapk8ip3	-0.20	1.25E-02

Genes (UP)	log2FoldChange	padj	Genes (Down)	log2FoldChange	padj
			Mmp15	-0.20	1.55E-03
			Sall3	-0.20	9.40E-03
			Kdm5c	-0.20	4.43E-03
			Cds2	-0.20	2.23E-02
			Ctcf	-0.20	2.47E-02
			Ythdf3	-0.20	4.08E-02
			Setd1a	-0.20	1.77E-02
			Srsf5	-0.20	1.70E-02
			Adamts9	-0.20	2.27E-02
			Gng12	-0.20	9.58E-03
			Brpf1	-0.20	4.87E-02
			Pum1	-0.20	2.18E-02
			Smad2	-0.20	4.86E-02
			Appbp2	-0.20	1.92E-02
			Matr3	-0.20	9.94E-03
			Wiz	-0.20	2.13E-02
			Trak2	-0.20	2.24E-02
			Csnk2a1	-0.19	1.85E-02
			Ipmk	-0.19	3.35E-02
			Smad4	-0.19	3.86E-02
			Sin3a	-0.19	3.36E-02
			Sf3b1	-0.19	2.30E-03
			Mtss2	-0.19	2.12E-03
			Limch1	-0.19	4.73E-02
			Adgrl2	-0.19	7.69E-03
			Zfp24	-0.19	3.93E-02
			Plcg1	-0.19	2.02E-02
			Med14	-0.19	1.76E-02
			Slc16a1	-0.19	2.17E-02
			Nlgn2	-0.19	2.00E-02
			Smg7	-0.19	2.43E-02
			Ahcyl1	-0.19	3.37E-03
			Myo18a	-0.19	1.11E-02
			Pfas	-0.19	3.08E-02
			Ankfy1	-0.19	2.28E-02
			Adnp	-0.19	9.56E-03
			Abhd2	-0.19	1.39E-02
			Mvb12b	-0.19	3.47E-02
			Abl1	-0.19	3.79E-02
			Gpm6b	-0.19	1.66E-03
			Kif5b	-0.19	1.05E-02
			Camkk2	-0.19	1.34E-02

Genes (UP)	log2FoldChange	padj	Genes (Down)	log2FoldChange	padj
			Pcgf3	-0.19	2.15E-02
			Lig1	-0.19	4.46E-02
			Lamc1	-0.18	4.25E-02
			Snx27	-0.18	1.75E-02
			Spry1	-0.18	2.42E-02
			Frmd4a	-0.18	3.68E-02
			Camk2b	-0.18	4.25E-02
			Uck2	-0.18	3.03E-02
			Stat3	-0.18	6.93E-03
			Rptor	-0.18	3.01E-02
			Slc38a1	-0.18	2.83E-02
			Asap1	-0.18	3.98E-02
			Clcn3	-0.18	3.88E-02
			Itga6	-0.18	1.26E-02
			Pak2	-0.18	2.23E-02
			Bcl2l13	-0.18	4.18E-02
			Fndc3b	-0.18	1.80E-02
			Mtdh	-0.18	2.33E-02
			Ankib1	-0.18	4.37E-02
			Dennd5a	-0.18	4.27E-03
			Nup205	-0.18	4.87E-02
			Gbf1	-0.17	3.72E-02
			Casc4	-0.17	4.34E-02
			Tm9sf3	-0.17	1.66E-02
			Ccnd2	-0.17	8.97E-03
			Tnks2	-0.17	1.20E-02
			Ncam1	-0.17	4.22E-02
			Farp1	-0.17	3.96E-02
			Smarcc1	-0.17	1.13E-02
			Mast2	-0.17	3.49E-02
			Ube4b	-0.17	3.48E-02
			Myo10	-0.17	2.80E-02
			Nacc1	-0.17	1.85E-02
			Actr2	-0.16	2.62E-02
			Eif4ebp2	-0.16	1.50E-02
			Dag1	-0.16	2.07E-02
			Gna13	-0.16	3.00E-02
			Tcaf1	-0.16	3.41E-02
			Ednrb	-0.16	4.45E-02
			Epn2	-0.16	1.19E-02
			Zc3h7b	-0.16	2.70E-02
			Fubp1	-0.16	4.91E-02

Genes (UP)	log2FoldChange	padj	Genes (Down)	log2FoldChange	padj
			Pom121	-0.16	4.54E-02
			Ipo5	-0.16	2.23E-02
			Cand1	-0.16	1.95E-02
			Smarca4	-0.16	1.51E-02
			Ttc3	-0.16	3.20E-02
			Tanc1	-0.16	3.94E-02
			Gtf3c2	-0.16	4.96E-02
			Nedd4	-0.16	1.23E-02
			Ptpn11	-0.16	2.37E-02
			Dcaf7	-0.15	3.81E-02
			Ano6	-0.15	2.69E-02
			Ipo7	-0.15	4.76E-02
			Hnrnpu	-0.15	1.24E-02
			Rrm2	-0.15	4.76E-02
			Tardbp	-0.15	4.44E-02
			Hnrnpa1	-0.15	1.98E-02
			Hnrnph1	-0.15	4.40E-02
			Gtf3c1	-0.14	4.17E-02
			Ide	-0.14	3.81E-02
			Hmgcs1	-0.14	2.96E-02
			Adgrg1	-0.14	4.70E-02
			Ewsr1	-0.14	3.71E-02
			Srebf2	-0.14	3.26E-02

8.4 Differentially Expressed Genes in the BMP4/FGF-treated tumour cells 24 hrs post-irradiation

Genes (Up)	log2FoldChange	padj	Genes (Down)	log2FoldChange	padj
Clec18a	1.20	2.83E-02	Myt1	-1.85	1.58E-07
Hic1	1.14	2.48E-03	Pcdh15	-1.56	1.96E-02
Fhl2	1.04	4.17E-02	Syne2	-1.54	5.35E-03
Coch	1.02	1.18E-02	Zbtb20	-1.45	2.60E-03
Apol9b	0.96	1.49E-02	Fat3	-1.44	4.29E-02
Pik3cd	0.87	4.15E-02	Phactr3	-1.39	4.95E-02
Dhrs3	0.84	3.99E-02	Dst	-1.35	6.90E-03
Dusp5	0.83	1.42E-02	Fat4	-1.32	3.01E-18
Xaf1	0.82	1.41E-03	Pcdhga9	-1.31	3.88E-02
Gja5	0.77	1.77E-03	Macf1	-1.28	3.41E-03
Klf5	0.76	9.62E-03	Hmcn1	-1.24	7.97E-03
Diras2	0.74	1.23E-11	mt-Nd3	-1.20	3.90E-05
Gm26917	0.70	1.92E-13	Fry	-1.19	1.95E-15
Islr2	0.69	3.90E-03	Lrp1	-1.18	9.55E-05
Apol9a	0.69	2.47E-02	Sox10	-1.17	1.82E-03
Casq1	0.68	1.60E-03	Ubr4	-1.14	2.08E-04
Serpinf1	0.67	1.23E-09	Frem2	-1.14	1.96E-10
Spp1	0.67	7.92E-06	Kmt2c	-1.12	1.12E-02
Rarb	0.67	5.76E-03	Slc6a11	-1.11	7.02E-03
Gsx1	0.67	4.69E-02	Pclo	-1.10	1.63E-04
Ifi35	0.65	3.40E-02	Erbb4	-1.09	4.35E-10
Cebpa	0.65	1.22E-09	4932438A13Rik	-1.07	1.09E-02
Bambi	0.64	4.71E-03	Xist	-1.06	3.29E-02
Pdgfb	0.64	5.36E-03	Kmt2a	-1.05	6.83E-03
Ogn	0.64	4.83E-02	Fat1	-1.03	2.64E-02
Tbx2	0.64	2.50E-07	Rtl9	-1.02	3.02E-02
Gpc3	0.64	3.06E-02	Tenm2	-1.02	3.83E-02
Eef1a2	0.64	1.13E-07	Vps13d	-1.02	1.32E-02
Rai14	0.63	3.28E-05	Kmt2d	-1.02	1.30E-02
Ecm1	0.63	2.72E-06	Herc1	-1.01	2.14E-02
Gm42372	0.63	3.18E-02	Syne1	-1.01	4.07E-02
Anxa3	0.63	9.80E-06	Herc2	-1.00	1.30E-02
Ndrg1	0.63	2.72E-03	mt-Co3	-1.00	1.67E-03
Ifi44	0.62	1.14E-02	Dync2h1	-0.99	4.88E-09
Atoh8	0.62	2.42E-08	Dll3	-0.98	2.81E-05
Scube3	0.61	1.23E-08	Tmem132b	-0.97	7.13E-03

Genes (Up)	log2FoldChange	padj	Genes (Down)	log2FoldChange	padj
Depdc7	0.61	3.34E-02	Gm43031	-0.97	1.38E-04
Mylip	0.61	3.06E-02	Dync1h1	-0.97	3.66E-03
C1qtnf1	0.61	1.28E-03	Huwe1	-0.97	8.25E-03
Fosl2	0.61	1.09E-04	Wdfy3	-0.94	4.53E-03
Col6a2	0.61	5.49E-09	Vps13b	-0.93	2.42E-08
S100a4	0.60	1.80E-05	Mycbp2	-0.93	3.47E-11
Epha2	0.60	1.16E-02	Sacs	-0.92	1.23E-08
Maff	0.59	1.90E-03	Birc6	-0.91	1.27E-02
Abcc12	0.59	3.66E-04	Hectd4	-0.91	3.11E-12
Ptprn	0.57	5.67E-03	Efhc1	-0.90	3.00E-05
Ube2l6	0.57	1.77E-02	Grin2b	-0.89	4.99E-02
Sox7	0.56	1.07E-02	Ptprz1	-0.88	1.02E-16
Bgn	0.56	1.22E-09	Tmem178b	-0.87	1.02E-02
Col11a2	0.56	4.40E-03	Lrp1b	-0.87	4.40E-02
Fmod	0.56	3.05E-06	Akap9	-0.87	1.63E-08
Nucb2	0.55	4.07E-02	Kcna2	-0.86	1.55E-05
Ass1	0.55	6.94E-05	Igip	-0.85	2.94E-06
Srpx2	0.54	4.43E-02	Rev3l	-0.85	6.60E-14
Oasl2	0.54	1.76E-03	Nrarp	-0.84	9.36E-04
Smad6	0.54	1.49E-03	Prune2	-0.84	1.46E-06
Clcf1	0.54	1.30E-02	Zfp704	-0.83	2.77E-11
Spry4	0.53	1.92E-05	Fras1	-0.83	4.79E-06
Lamc2	0.53	1.01E-02	Lpp	-0.83	1.10E-07
Anxa1	0.53	1.97E-02	Mc5r	-0.83	2.28E-02
S100a6	0.53	2.00E-05	Prkdc	-0.82	8.70E-06
Dusp6	0.53	2.32E-08	Nrxn3	-0.82	1.71E-02
Bst2	0.53	2.34E-04	Igsf9b	-0.82	1.67E-08
Irf7	0.52	2.85E-02	Svep1	-0.82	3.78E-04
Ccn2	0.52	2.40E-03	Chd7	-0.81	2.54E-11
Samd9l	0.52	7.70E-04	Zfhx3	-0.81	7.47E-04
Angptl2	0.52	4.97E-02	Mki67	-0.80	1.48E-02
Tmem39a	0.51	3.99E-02	Cfap54	-0.80	4.00E-02
Tspo	0.51	1.33E-02	Vps13c	-0.79	4.76E-06
Smad7	0.51	4.74E-03	Lrp2	-0.78	6.85E-05
Lmcd1	0.49	1.37E-02	Stard9	-0.78	8.68E-05
Jag1	0.48	1.30E-04	Scn8a	-0.77	1.41E-04
Adrb1	0.48	2.69E-03	Nf1	-0.77	1.83E-12
Npnt	0.48	6.70E-04	mt-Nd6	-0.77	2.95E-02
Fbln5	0.48	1.07E-03	Mir9-3hg	-0.76	3.61E-04
Lurap1l	0.48	3.01E-02	Tanc2	-0.75	1.02E-07
Nog	0.48	2.24E-03	Lyst	-0.75	3.35E-04
Cnn2	0.48	3.00E-05	Dll1	-0.75	1.55E-05
Mest	0.48	7.92E-06	Brca2	-0.75	4.76E-05

Genes (Up)	log2FoldChange	padj	Genes (Down)	log2FoldChange	padj
Igfbp3	0.47	3.58E-09	Itpr2	-0.75	4.88E-09
Zfp57	0.47	1.64E-02	Adgrv1	-0.75	1.26E-03
Sema3f	0.47	1.61E-02	Ep400	-0.75	9.29E-11
S100a11	0.47	1.18E-03	Fbn1	-0.73	4.23E-08
Foxo6	0.47	3.38E-02	Cspg4	-0.73	1.14E-09
Adamts14	0.46	3.41E-03	Utrn	-0.73	5.33E-08
Slc25a22	0.46	2.74E-02	St6gal2	-0.72	3.51E-02
Pou3f1	0.46	4.24E-02	Dgkh	-0.72	2.16E-03
Mcam	0.45	1.70E-03	Tet1	-0.72	4.76E-05
Efnb2	0.45	1.45E-04	Mgat5b	-0.72	4.21E-02
Rsrp1	0.45	4.08E-05	Slc6a1	-0.72	3.72E-02
Prss23	0.45	2.66E-04	Cep350	-0.71	3.03E-07
Map11	0.45	2.39E-02	Gabbr2	-0.71	1.15E-03
Loxl2	0.44	4.12E-02	B930095G15Rik	-0.71	3.97E-03
Rybp	0.44	9.19E-03	mt-Nd5	-0.70	3.95E-08
Ccn1	0.43	5.01E-03	Ash1l	-0.70	3.61E-08
Tnfrsf12a	0.43	7.02E-03	Reln	-0.69	2.74E-07
Calr	0.43	1.83E-04	Tnrc6b	-0.69	2.42E-08
Prkar2b	0.42	4.78E-04	Abca1	-0.69	3.91E-07
Tgm2	0.42	9.99E-03	Ubn2	-0.69	1.78E-05
Emp1	0.42	1.89E-04	Sv2c	-0.68	3.34E-02
Podxl	0.42	1.18E-03	Il17rd	-0.68	1.88E-05
Col8a1	0.41	3.98E-03	Ino80d	-0.68	6.70E-04
Col6a1	0.41	7.97E-05	Akap13	-0.67	5.08E-07
S100a10	0.41	3.64E-03	Trrap	-0.67	2.79E-06
Gpx3	0.41	3.64E-02	Fryl	-0.66	3.39E-06
Unc5b	0.41	1.53E-03	Csmd2	-0.65	1.40E-05
Gask1b	0.41	4.40E-03	Pdgfra	-0.65	2.86E-06
Prelp	0.40	6.12E-03	Slc4a4	-0.65	6.79E-13
Rgs2	0.40	2.77E-02	Lhfpl3	-0.65	2.23E-05
St3gal6	0.40	3.50E-02	Prrc2c	-0.65	9.54E-07
Trim46	0.40	5.06E-03	Dcc	-0.65	1.92E-02
Ier3	0.39	3.64E-02	Inhbb	-0.65	5.27E-03
Disp3	0.39	7.94E-03	Pkd1	-0.65	1.41E-06
Fzd1	0.39	3.68E-05	Mga	-0.64	5.27E-05
Dusp4	0.38	2.24E-02	Zbtb37	-0.64	3.67E-03
Hsph1	0.38	1.07E-04	Hmgcs2	-0.64	2.89E-02
Tcirg1	0.38	3.57E-03	Tenm4	-0.64	3.08E-02
Igfbp2	0.38	1.33E-05	Fzd3	-0.64	2.44E-10
Dpp7	0.38	4.00E-02	Celsr2	-0.63	6.54E-08
Stambpl1	0.38	1.86E-02	2810459M11Rik	-0.63	4.24E-02
Pdlim7	0.37	8.78E-03	Slc1a2	-0.63	2.34E-12
Mn1	0.37	1.97E-03	Rora	-0.63	1.30E-05

Genes (Up)	log2FoldChange	padj	Genes (Down)	log2FoldChange	padj
Arntl	0.37	2.51E-02	Lmo3	-0.63	7.00E-03
Hbegf	0.37	2.70E-03	Apc	-0.63	5.33E-08
Dynll1	0.37	2.70E-03	Usf3	-0.63	2.22E-04
Lgals3bp	0.37	7.48E-03	Smoc1	-0.63	7.56E-05
Ifitm3	0.37	2.31E-03	Cplane1	-0.62	4.41E-06
Tjap1	0.36	5.23E-03	Dmxl2	-0.62	3.41E-04
Slc39a13	0.36	1.68E-02	Fndc1	-0.62	7.22E-05
Ttc9c	0.36	6.12E-03	Lifr	-0.62	9.18E-08
Pdgfa	0.36	2.91E-02	Cbl	-0.62	3.83E-06
P4ha1	0.36	8.90E-04	Lama1	-0.62	4.04E-02
Efnb1	0.35	2.30E-03	Vcan	-0.61	4.18E-09
Anxa2	0.35	8.85E-04	B3gat2	-0.61	1.90E-02
Lgals9	0.35	3.75E-02	Pou2f1	-0.61	2.58E-03
Col1a1	0.35	2.80E-03	Htt	-0.61	1.76E-04
Dap	0.35	4.90E-03	Med12l	-0.61	2.87E-03
Tpm1	0.35	4.64E-03	Usp34	-0.61	7.42E-06
Ccnd1	0.35	8.14E-04	Cacna2d2	-0.60	2.47E-02
Rassf3	0.34	1.49E-02	Zfhx2	-0.60	3.21E-02
Banp	0.34	3.89E-02	Helz	-0.59	3.45E-06
Uchl1	0.34	3.35E-03	Nrxn1	-0.59	1.08E-06
Hs6st2	0.34	4.32E-02	Lrba	-0.59	3.28E-04
Irf9	0.34	1.91E-02	Usp24	-0.59	7.44E-07
Hyou1	0.33	4.40E-03	Igsf10	-0.59	3.41E-04
Matn2	0.33	6.51E-03	Cecr2	-0.59	4.59E-03
Ehd2	0.33	2.85E-02	Nin	-0.58	2.81E-05
Xbp1	0.33	1.86E-02	Ptpn4	-0.58	1.27E-05
Pxdc1	0.33	2.65E-02	D630045J12Rik	-0.58	6.79E-08
Pdia3	0.33	3.60E-03	Kcnn3	-0.58	1.07E-04
Pfkfb3	0.33	8.26E-03	Cdk6	-0.58	5.84E-05
Spry1	0.33	4.54E-03	Nav1	-0.58	1.19E-05
Ppid	0.33	5.04E-03	Ntrk3	-0.57	8.70E-06
Trmt1l	0.33	4.80E-02	Ptpre	-0.57	3.55E-02
Pdia6	0.33	9.27E-03	Ttbk2	-0.57	4.62E-03
Gm10076	0.32	6.81E-03	Ncor2	-0.57	5.49E-09
Ier5l	0.32	1.72E-02	Gjc1	-0.57	2.31E-02
Uhrf2	0.32	1.54E-02	Dchs1	-0.56	9.69E-09
Actn1	0.32	3.99E-03	Cirbp	-0.56	2.83E-06
Prpsap1	0.32	5.99E-03	Zzef1	-0.55	1.13E-03
Ube2c	0.32	1.36E-02	Kcnc1	-0.55	2.09E-02
Trib1	0.32	4.65E-02	Ago3	-0.55	4.73E-04
Fkbp14	0.31	3.06E-02	Fasn	-0.55	1.13E-07
Khdc4	0.31	9.27E-03	Map1a	-0.55	2.79E-07
Hsf1	0.31	4.12E-02	Pcdhgb1	-0.55	2.77E-02

Genes (Up)	log2FoldChange	padj	Genes (Down)	log2FoldChange	padj
P3h1	0.31	1.71E-02	Zfp462	-0.55	9.96E-06
Lipa	0.31	5.95E-03	Ptgds	-0.54	4.92E-02
Atf5	0.31	5.37E-03	Atp8a1	-0.54	3.00E-07
Nrp1	0.31	2.81E-02	Taok1	-0.54	4.16E-06
Nuak1	0.31	3.47E-02	Cntn1	-0.54	5.33E-08
Kpna4	0.31	5.22E-03	Ednrb	-0.54	3.55E-04
Fkbp10	0.31	5.41E-03	Cenpf	-0.54	4.04E-04
Col5a3	0.31	2.89E-02	Zfp652	-0.54	3.00E-07
Cog4	0.31	1.32E-02	Xrn1	-0.54	9.71E-04
Hsp90b1	0.31	3.16E-03	Pcdh19	-0.54	3.94E-03
Kif20a	0.31	4.83E-02	Egfr	-0.54	5.44E-05
Lgals1	0.30	7.47E-03	Sorl1	-0.54	5.60E-04
Pxk	0.30	3.84E-02	Btg2	-0.53	4.16E-06
Rgs8	0.30	1.86E-02	Tuba4a	-0.52	1.39E-02
Ldha	0.30	3.45E-03	Rab11fip4	-0.52	2.34E-02
Tceal9	0.30	2.14E-02	Xylt1	-0.52	7.00E-07
Cavin1	0.29	4.14E-02	Ntm	-0.52	7.89E-03
Myl12a	0.29	1.65E-02	Trps1	-0.52	3.11E-05
Anxa6	0.29	2.80E-03	Nrip1	-0.52	3.78E-03
Tle3	0.29	1.62E-02	Nfia	-0.52	2.90E-06
Hspa5	0.29	1.32E-02	Setx	-0.52	1.59E-04
Pdia4	0.29	2.68E-02	Astn1	-0.52	1.49E-06
Parp3	0.28	3.09E-02	Lsamp	-0.51	1.19E-05
Cebpg	0.28	3.68E-02	Nbea	-0.51	6.95E-04
Colgalt1	0.28	1.49E-02	Prkcq	-0.51	8.36E-03
P4hb	0.28	6.12E-03	Ago2	-0.51	2.44E-04
Slc35f1	0.28	1.51E-02	Cyp26b1	-0.51	2.80E-02
Tulp3	0.28	1.28E-02	Rorb	-0.51	1.97E-03
Prc1	0.28	1.90E-02	Ppp1r16b	-0.51	3.00E-02
Id1	0.28	3.34E-02	Srcap	-0.51	5.19E-05
Myl6	0.28	2.56E-02	Nsd1	-0.50	1.45E-04
Ephb2	0.27	3.61E-02	Abhd3	-0.50	1.28E-02
Ccnd2	0.27	2.43E-03	Pdpr	-0.50	2.61E-03
Golm1	0.27	1.70E-02	Dpyd	-0.50	1.19E-02
Ctps	0.27	3.83E-02	Ncam2	-0.50	2.83E-02
Anxa5	0.27	1.68E-02	Ttc28	-0.50	6.35E-04
Srsf7	0.27	2.97E-02	Braf	-0.50	3.31E-03
Tmsb10	0.27	3.45E-02	Anks1b	-0.50	2.58E-03
Plk2	0.27	4.59E-02	1500009C09Rik	-0.50	4.82E-03
Sparc	0.27	8.01E-03	Bmpr2	-0.50	1.25E-04
Mrps6	0.27	3.89E-02	Notch2	-0.50	7.92E-04
Eif4a2	0.26	1.64E-02	Tmem229a	-0.50	6.70E-04
Cxxc5	0.26	4.33E-02	Maml2	-0.50	1.19E-04

Genes (Up)	log2FoldChange	padj	Genes (Down)	log2FoldChange	padj
Kpna2	0.26	1.32E-02	Med13	-0.50	2.60E-04
Nucb1	0.26	1.45E-02	Ptar1	-0.50	1.45E-04
Ccnb1	0.26	2.89E-02	Myo5a	-0.49	3.92E-06
Atp6v0b	0.26	4.43E-02	Grm5	-0.49	7.55E-03
Stip1	0.26	2.14E-02	Plxnc1	-0.49	8.32E-04
Jup	0.26	3.32E-02	Rnf144a	-0.49	1.83E-04
Nomo1	0.26	2.83E-02	N4bp2	-0.49	7.14E-03
Htra1	0.26	2.63E-02	Klf12	-0.48	3.99E-03
B2m	0.25	4.30E-02	Nbeal1	-0.48	9.95E-03
Fstl1	0.25	1.77E-02	Kcnd2	-0.48	7.13E-03
Swi5	0.25	3.68E-02	Hook3	-0.48	1.09E-03
Cryab	0.25	4.07E-02	Mycl	-0.48	7.47E-03
Tars	0.25	3.61E-02	Dip2b	-0.48	1.17E-05
Jun	0.25	4.05E-02	Ubr5	-0.48	2.03E-04
Ctsd	0.24	1.27E-02	Mecp2	-0.48	5.73E-05
Ociad1	0.24	3.09E-02	Homer2	-0.48	1.92E-02
Gpx4	0.24	1.82E-02	Sema5a	-0.48	2.83E-03
Sympk	0.24	2.92E-02	Sox6	-0.48	3.91E-07
Atp1a1	0.24	1.65E-02	Alms1	-0.48	1.56E-02
Calu	0.24	2.53E-02	Phc3	-0.48	3.55E-04
Rps12	0.24	4.88E-02	Golgb1	-0.48	6.84E-03
Ckap4	0.24	3.67E-02	Diaph2	-0.48	7.47E-03
Msn	0.23	4.29E-02	Pcdhga1	-0.47	2.99E-02
Hnrnpc	0.23	4.20E-02	Ep300	-0.47	3.17E-04
Itgb1	0.23	3.09E-02	Ttyh1	-0.47	1.31E-05
			Akap6	-0.47	1.62E-02
			Sesn3	-0.47	1.73E-05
			Sdk2	-0.47	6.92E-03
			Atp1a2	-0.47	1.28E-04
			Ptprd	-0.47	9.71E-04
			Zmiz1	-0.47	3.13E-06
			Vps13a	-0.46	2.42E-02
			Myo9a	-0.46	9.09E-04
			Zfp871	-0.46	1.17E-03
			Dlgap1	-0.46	1.56E-03
			Arap2	-0.46	1.55E-03
			Tet2	-0.46	8.30E-03
			Shisa7	-0.46	3.01E-02
			Atrx	-0.46	3.76E-04
			Arhgap32	-0.46	3.17E-04
			Plce1	-0.46	1.16E-04
			Acaca	-0.45	5.60E-04
			Ncoa6	-0.45	1.58E-03

Genes (Up)	log2FoldChange	padj	Genes (Down)	log2FoldChange	padj
			Sash1	-0.45	1.72E-05
			E130307A14Rik	-0.45	1.25E-02
			Notch3	-0.45	4.38E-05
			Dock3	-0.45	1.87E-02
			Arid1a	-0.45	2.37E-04
			Rcor2	-0.45	2.66E-02
			Wnk1	-0.45	1.94E-04
			Ylpm1	-0.45	7.94E-04
			H1f0	-0.45	1.66E-04
			Fut9	-0.45	2.46E-03
			Atxn1	-0.45	1.97E-02
			Rgma	-0.45	2.46E-05
			Plxnb3	-0.45	2.42E-02
			Thsd7a	-0.45	3.02E-03
			Ncoa1	-0.45	1.73E-04
			Lypd1	-0.45	1.33E-02
			Apoe	-0.44	1.78E-03
			Kif1b	-0.44	1.35E-04
			Bod1l	-0.44	7.47E-03
			Zhx3	-0.44	4.35E-05
			Amer2	-0.44	3.98E-03
			Polr2a	-0.44	5.21E-06
			Cadm2	-0.44	1.82E-03
			Trio	-0.44	7.91E-04
			Megf11	-0.44	6.47E-03
			Fam199x	-0.44	4.06E-03
			Srgap1	-0.44	1.49E-02
			Trip11	-0.44	7.72E-03
			Zc3h12b	-0.44	3.78E-02
			Qser1	-0.44	5.37E-03
			Mast4	-0.44	3.09E-02
			Serinc5	-0.43	4.77E-03
			Rsf1	-0.43	3.94E-03
			Nova1	-0.43	1.77E-04
			Insr	-0.43	1.37E-02
			Tet3	-0.43	1.22E-03
			Itgb8	-0.43	6.85E-05
			Sned1	-0.43	4.21E-02
			Acss1	-0.43	1.18E-03
			Gpr179	-0.43	2.04E-02
			Rabgap1l	-0.43	2.65E-03
			Ppp1r9a	-0.42	2.64E-02
			Bach2	-0.42	3.00E-02

Genes (Up)	log2FoldChange	padj	Genes (Down)	log2FoldChange	padj
			Lss	-0.42	1.69E-04
			Tbc1d23	-0.42	4.07E-02
			Ralgapa2	-0.42	5.27E-03
			Sbf2	-0.42	1.71E-04
			Fmn2	-0.42	1.40E-04
			Chd6	-0.42	4.06E-03
			Setd2	-0.42	1.03E-03
			Abhd2	-0.42	3.95E-04
			Glul	-0.42	3.70E-05
			Nup210	-0.42	2.60E-03
			Bptf	-0.42	8.14E-04
			Lnpep	-0.42	1.22E-02
			Dicer1	-0.42	3.21E-03
			Mmd2	-0.42	3.41E-03
			Spen	-0.42	1.13E-02
			Myo10	-0.41	4.35E-05
			Elk4	-0.41	4.89E-03
			Tnik	-0.41	1.88E-03
			Adgrl3	-0.41	4.80E-04
			Pcdh17	-0.41	2.90E-03
			Mrtfb	-0.41	1.15E-02
			Aspm	-0.41	6.88E-03
			Dok6	-0.41	1.87E-02
			Srrm2	-0.41	2.88E-03
			Sep-03	-0.41	5.60E-03
			Phka1	-0.41	4.85E-05
			Pcnx	-0.41	8.45E-04
			Slc38a1	-0.40	1.40E-05
			Mbd5	-0.40	3.06E-02
			Kcnd3	-0.40	5.78E-03
			Dennd4a	-0.40	2.69E-03
			Kcnj10	-0.40	1.00E-04
			Robo1	-0.40	1.97E-03
			Crebbp	-0.40	3.88E-03
			Rfx4	-0.40	6.75E-03
			Lrrc4c	-0.40	2.26E-02
			Robo2	-0.40	4.22E-04
			Rfx3	-0.40	8.06E-03
			Pbrm1	-0.40	2.56E-03
			4930402H24Rik	-0.39	1.46E-04
			Chd2	-0.39	1.08E-02
			Ppp1r3c	-0.39	7.26E-03
			Nfasc	-0.39	2.16E-03

Genes (Up)	log2FoldChange	padj	Genes (Down)	log2FoldChange	padj
			Nav3	-0.39	1.31E-02
			Hectd1	-0.39	1.28E-03
			Brwd1	-0.39	1.62E-02
			Nfib	-0.39	7.75E-05
			Arid2	-0.39	2.69E-03
			Szt2	-0.39	3.96E-02
			Nlgn3	-0.39	4.97E-02
			Sncaip	-0.39	4.33E-02
			Pcdh10	-0.39	5.04E-03
			Txnip	-0.39	4.54E-03
			Tmem170b	-0.39	6.60E-03
			Psd3	-0.38	3.74E-02
			Hcfc1	-0.38	2.44E-03
			Zfp292	-0.38	1.87E-02
			Zkscan1	-0.38	2.75E-03
			Clcn6	-0.38	1.24E-03
			Plpp3	-0.38	9.09E-04
			Adgrb3	-0.38	9.36E-04
			Dock9	-0.38	1.87E-02
			Alcam	-0.38	3.73E-02
			Zdhhc21	-0.38	4.08E-02
			Mib1	-0.38	5.01E-03
			Peg3	-0.38	1.22E-02
			Cpeb4	-0.38	6.46E-03
			Pikfyve	-0.38	2.26E-02
			Zfp827	-0.38	1.56E-02
			Apba2	-0.38	1.25E-02
			Wdr7	-0.38	3.82E-03
			Dmxl1	-0.38	4.60E-02
			Zfp41	-0.37	2.75E-03
			Slc27a1	-0.37	8.08E-03
			Fam120c	-0.37	4.87E-03
			Chd8	-0.37	2.76E-03
			Sptbn1	-0.37	9.38E-04
			Pik3r1	-0.37	6.82E-04
			Jmjd1c	-0.37	2.30E-03
			Akap11	-0.37	1.90E-03
			Kalrn	-0.37	4.72E-02
			Ppp2r3a	-0.37	1.22E-03
			Rictor	-0.37	4.82E-02
			Jmy	-0.37	3.08E-03
			Asrgl1	-0.37	1.11E-03
			Gpam	-0.37	4.78E-04

Genes (Up)	log2FoldChange	padj	Genes (Down)	log2FoldChange	padj
			Peli2	-0.37	1.45E-03
			Cep250	-0.36	4.57E-02
			Sec14l2	-0.36	4.65E-02
			Tnks	-0.36	1.05E-03
			Tacc2	-0.36	2.70E-03
			Adora1	-0.36	3.88E-02
			Kif13a	-0.36	1.23E-03
			AU020206	-0.36	3.37E-02
			Arhgef12	-0.36	8.42E-03
			Slc7a2	-0.36	3.52E-03
			Per1	-0.36	1.71E-02
			Unc5c	-0.36	4.77E-02
			Adgrg1	-0.36	2.88E-02
			Vwa8	-0.36	2.27E-03
			C530008M17Rik	-0.36	1.72E-02
			Kdm5a	-0.35	1.69E-02
			B3gat1	-0.35	1.09E-02
			Spata13	-0.35	1.03E-03
			Ralgapa1	-0.35	2.64E-02
			Magi2	-0.35	4.82E-03
			Nipbl	-0.35	3.89E-02
			Hlf	-0.35	3.05E-02
			Aldh5a1	-0.35	2.08E-02
			Gan	-0.35	4.72E-02
			Gpcpd1	-0.35	5.14E-03
			Tpr	-0.35	7.29E-03
			Cpeb2	-0.35	1.12E-02
			Samd8	-0.35	2.23E-03
			Ccdc88a	-0.35	1.99E-03
			Arhgap21	-0.35	4.54E-03
			Rc3h1	-0.35	3.06E-02
			Ankrd17	-0.35	3.17E-03
			Aff4	-0.35	7.26E-03
			Sdk1	-0.35	1.64E-02
			Ro60	-0.34	1.95E-02
			Hmbox1	-0.34	2.03E-02
			Papln	-0.34	3.74E-02
			Paqr8	-0.34	9.09E-04
			Shank3	-0.34	3.21E-02
			Cst3	-0.34	1.16E-03
			Efr3b	-0.34	2.58E-02
			Mtor	-0.34	7.47E-03
			Aldoc	-0.34	1.46E-02

Genes (Up)	log2FoldChange	padj	Genes (Down)	log2FoldChange	padj
			Wnk2	-0.34	2.32E-02
			Insig1	-0.34	5.84E-05
			Dnmt3a	-0.34	5.84E-03
			Clasp2	-0.34	5.34E-03
			Traf4	-0.34	2.73E-02
			Phlpp1	-0.34	3.34E-04
			Ankrd11	-0.33	3.96E-03
			Lrrc58	-0.33	2.11E-03
			Tlcd1	-0.33	9.04E-03
			Klf7	-0.33	1.14E-02
			Ppm1l	-0.33	4.75E-03
			Fchsd2	-0.33	9.19E-03
			Ank2	-0.33	2.86E-02
			Slc22a17	-0.33	3.90E-02
			Mbtd1	-0.33	2.51E-02
			Wscd1	-0.33	2.44E-02
			Polr3k	-0.33	3.64E-02
			Baz2a	-0.33	4.07E-02
			Ralgps1	-0.33	1.63E-02
			Lpin1	-0.33	3.61E-02
			Erbin	-0.33	5.23E-03
			Fcho2	-0.33	1.52E-02
			Sfxn5	-0.33	2.36E-03
			Dnajb14	-0.32	3.29E-02
			Pcdh7	-0.32	1.13E-02
			Adgrl1	-0.32	2.03E-03
			Pygo1	-0.32	3.80E-02
			Prpf8	-0.32	1.39E-02
			Hmgcs1	-0.32	2.31E-04
			Tulp4	-0.32	2.22E-02
			Pag1	-0.32	2.64E-02
			Pde1c	-0.32	3.28E-02
			Gabbr1	-0.32	1.12E-02
			Rassf2	-0.32	2.89E-02
			Acsl6	-0.31	1.55E-02
			2610507B11Rik	-0.31	5.55E-03
			Lhfpl4	-0.31	3.01E-02
			Sparcl1	-0.31	4.85E-03
			Slc20a2	-0.31	3.50E-02
			Tmod2	-0.31	8.12E-03
			Mgat3	-0.31	1.55E-02
			Npas3	-0.31	8.19E-03
			Hmgcr	-0.31	1.66E-02

Genes (Up)	log2FoldChange	padj	Genes (Down)	log2FoldChange	padj
			Abat	-0.31	2.24E-03
			Cad	-0.30	2.32E-02
			Mapk4	-0.30	4.33E-02
			Smox	-0.30	1.97E-02
			Lats1	-0.30	2.69E-02
			Chd4	-0.30	1.12E-02
			Hipk1	-0.30	8.25E-03
			Gsk3b	-0.30	6.41E-03
			Aldh6a1	-0.30	3.45E-02
			Ubr3	-0.30	4.11E-02
			Cltc	-0.30	1.30E-02
			Wnt7b	-0.30	3.61E-02
			Foxn3	-0.30	4.24E-02
			Syt11	-0.29	1.07E-02
			Zfp106	-0.29	1.30E-02
			Stox2	-0.29	3.77E-02
			Atrn	-0.29	7.13E-03
			Anapc1	-0.29	3.82E-02
			Ndrg2	-0.29	1.21E-02
			Arfgef2	-0.29	2.69E-02
			Cpd	-0.29	3.50E-02
			Nsdhl	-0.29	2.23E-02
			Mt1	-0.29	6.09E-03
			Lrp4	-0.29	3.35E-02
			Ctnnd2	-0.29	1.11E-02
			Gatad2b	-0.29	1.92E-02
			Shisa9	-0.29	2.95E-02
			Dock1	-0.29	2.09E-02
			Gfap	-0.29	4.83E-02
			Klf13	-0.29	1.32E-02
			Ncald	-0.29	1.72E-02
			Sp1	-0.29	2.64E-02
			Plxnb1	-0.28	1.83E-02
			Rere	-0.28	2.14E-02
			Atp1b2	-0.28	4.59E-02
			Myh10	-0.28	3.61E-02
			Dlg5	-0.28	1.64E-02
			Myo16	-0.28	3.64E-02
			Myo6	-0.28	1.39E-02
			Tjp2	-0.28	1.62E-02
			Mboat2	-0.28	1.41E-02
			Ptch1	-0.28	3.25E-02
			Sema6a	-0.28	4.59E-02

Genes (Up)	log2FoldChange	padj	Genes (Down)	log2FoldChange	padj
			Kif21b	-0.28	3.63E-02
			Kmt2e	-0.27	4.88E-02
			Setd5	-0.27	3.61E-02
			Fam234b	-0.27	2.37E-02
			Abca2	-0.27	4.21E-02
			Xpr1	-0.27	4.17E-02
			Prrc2b	-0.27	5.00E-02
			Snn	-0.27	2.20E-02
			Tjp1	-0.27	4.04E-02
			Epb41	-0.27	4.17E-02
			Zeb1	-0.27	1.61E-02
			Vangl2	-0.27	2.62E-02
			Trip12	-0.27	4.67E-02
			Tead1	-0.26	4.43E-02
			Acss2	-0.26	1.60E-02
			Ddx3x	-0.26	1.27E-02
			Il6st	-0.26	1.37E-02
			Cdk5rap2	-0.26	4.80E-02
			Afdn	-0.25	4.99E-02
				-0.25	2.77E-02
			Epas1	-0.25	2.76E-02
			Cds2	-0.25	4.21E-02
			Agap1	-0.25	3.72E-02
			Trak1	-0.25	3.61E-02
			Qk	-0.24	1.92E-02
			Atrnl1	-0.24	4.24E-02
			Tbl1xr1	-0.24	4.83E-02
			Scd1	-0.24	1.62E-02
			Ece1	-0.24	4.23E-02
			Cbx5	-0.24	4.83E-02
			Glud1	-0.23	4.04E-02
			Zcchc24	-0.22	4.67E-02
			Scd2	-0.21	4.04E-02

Reference List

Abuetabh, Y., Wu, H. H., Chai, C., Al Yousef, H., Persad, S., Sergi, C. M., & Leng, R. (2022). DNA damage response revisited: The p53 family and its regulators provide endless cancer therapy opportunities. *Experimental & Molecular Medicine*, *54*(10), 1658–1669. https://doi.org/10.1038/s12276-022-00863-4

Agarwala, S. S., & Kirkwood, J. M. (2000). Temozolomide, a Novel Alkylating Agent with Activity in the Central Nervous System, May Improve the Treatment of Advanced Metastatic Melanoma. *The Oncologist*, *5*(2), 144–151. https://doi.org/10.1634/theoncologist.5-2-144

Aguirre-Ghiso, J. A. (2007). Models, mechanisms and clinical evidence for cancer dormancy. *Nature Reviews. Cancer*, *7*(11), 834–846. https://doi.org/10.1038/nrc2256

Ali, M. Y., Oliva, C. R., Noman, A. S. M., Allen, B. G., Goswami, P. C., Zakharia, Y., Monga, V., Spitz, D. R., Buatti, J. M., & Griguer, C. E. (2020). Radioresistance in Glioblastoma and the Development of Radiosensitizers. *Cancers*, *12*(9), 2511. https://doi.org/10.3390/cancers12092511

Al-Sammarraie, N., & Ray, S. K. (2021). Bone morphogenic protein signaling in spinal cord injury. *Neuroimmunology and Neuroinflammation*, *8*, 53–63. https://doi.org/10.20517/2347-8659.2020.34

Alsop, K., Fereday, S., Meldrum, C., deFazio, A., Emmanuel, C., George, J., Dobrovic, A., Birrer, M. J., Webb, P. M., Stewart, C., Friedlander, M., Fox, S., Bowtell, D., & Mitchell, G.

(2012). BRCA Mutation Frequency and Patterns of Treatment Response in BRCA Mutation–Positive Women With Ovarian Cancer: A Report From the Australian Ovarian Cancer Study Group. *Journal of Clinical Oncology*, *30*(21), 2654–2663. https://doi.org/10.1200/JCO.2011.39.8545

Amarandi, R.-M., Ibanescu, A., Carasevici, E., Marin, L., & Dragoi, B. (2022). Liposomal-Based Formulations: A Path from Basic Research to Temozolomide Delivery Inside Glioblastoma Tissue. *Pharmaceutics*, *14*(2), Article 2. https://doi.org/10.3390/pharmaceutics14020308

Anthony, T. E., Klein, C., Fishell, G., & Heintz, N. (2004). Radial glia serve as neuronal progenitors in all regions of the central nervous system. *Neuron*, *41*(6), 881–890. https://doi.org/10.1016/s0896-6273(04)00140-0

Armstrong, N., Ryder, S., Forbes, C., Ross, J., & Quek, R. G. (2019). A systematic review of the international prevalence of BRCA mutation in breast cancer. *Clinical Epidemiology*, *11*, 543–561. https://doi.org/10.2147/CLEP.S206949

Arrieta, V. A., Dmello, C., McGrail, D. J., Brat, D. J., Lee-Chang, C., Heimberger, A. B., Chand, D., Stupp, R., & Sonabend, A. M. (2023). Immune checkpoint blockade in glioblastoma: From tumor heterogeneity to personalized treatment. *The Journal of Clinical Investigation*, *133*(2). https://doi.org/10.1172/JCI163447

Arun, B., Couch, F. J., Abraham, J., Tung, N., & Fasching, P. A. (2024). BRCA-mutated breast cancer: The unmet need, challenges and therapeutic benefits of genetic testing. *British Journal of Cancer*, *131*(9), 1400–1414. https://doi.org/10.1038/s41416-024-02827-z

Balasubramanian, B., Pogozelski, W. K., & Tullius, T. D. (1998). DNA strand breaking by the hydroxyl radical is governed by the accessible surface areas of the hydrogen atoms of

the DNA backbone. *Proceedings of the National Academy of Sciences of the United States of America*, *95*(17), 9738–9743. https://doi.org/10.1073/pnas.95.17.9738

Banin, S., Moyal, L., Shieh, S., Taya, Y., Anderson, C. W., Chessa, L., Smorodinsky, N. I., Prives, C., Reiss, Y., Shiloh, Y., & Ziv, Y. (1998). Enhanced phosphorylation of p53 by ATM in response to DNA damage. *Science (New York, N.Y.)*, *281*(5383), 1674–1677. https://doi.org/10.1126/science.281.5383.1674

Bankhead, P., Loughrey, M. B., Fernández, J. A., Dombrowski, Y., McArt, D. G., Dunne, P. D., McQuaid, S., Gray, R. T., Murray, L. J., Coleman, H. G., James, J. A., Salto-Tellez, M., & Hamilton, P. W. (2017). QuPath: Open source software for digital pathology image analysis. *Scientific Reports*, *7*(1), 16878. https://doi.org/10.1038/s41598-017-17204-5

Bao, S., Wu, Q., McLendon, R. E., Hao, Y., Shi, Q., Hjelmeland, A. B., Dewhirst, M. W., Bigner, D. D., & Rich, J. N. (2006). Glioma stem cells promote radioresistance by preferential activation of the DNA damage response. *Nature*, *444*(7120), 756–760. https://doi.org/10.1038/nature05236

Barbarese, E., & Barry, C. (1989). Radiation sensitivity of glial cells in primary culture. *Journal of the Neurological Sciences*, *91*(1–2), 97–107. https://doi.org/10.1016/0022-510x(89)90079-8

Bardaweel, S. K., Gul, M., Alzweiri, M., Ishaqat, A., ALSalamat, H. A., & Bashatwah, R. M. (2018). Reactive Oxygen Species: The Dual Role in Physiological and Pathological Conditions of the Human Body. *The Eurasian Journal of Medicine*, *50*(3), 193–201. https://doi.org/10.5152/eurasianjmed.2018.17397

Baskar, R., Lee, K. A., Yeo, R., & Yeoh, K.-W. (2012). Cancer and Radiation Therapy: Current Advances and Future Directions. *International Journal of Medical Sciences*, *9*(3), 193–199. https://doi.org/10.7150/ijms.3635

Bhat, K. P. L., Balasubramaniyan, V., Vaillant, B., Ezhilarasan, R., Hummelink, K., Hollingsworth, F., Wani, K., Heathcock, L., James, J. D., Goodman, L. D., Conroy, S., Long, L., Lelic, N., Wang, S., Gumin, J., Raj, D., Kodama, Y., Raghunathan, A., Olar, A., … Aldape, K. (2013). Mesenchymal Differentiation Mediated by NF-κB Promotes Radiation Resistance in Glioblastoma. *Cancer Cell*, *24*(3), 10.1016/j.ccr.2013.08.001. https://doi.org/10.1016/j.ccr.2013.08.001

Blackford, A. N., & Jackson, S. P. (2017). ATM, ATR, and DNA-PK: The Trinity at the Heart of the DNA Damage Response. *Molecular Cell*, *66*(6), 801–817. https://doi.org/10.1016/j.molcel.2017.05.015

Blomfield, I. M., Rocamonde, B., Masdeu, M. del M., Mulugeta, E., Vaga, S., van den Berg, D. L., Huillard, E., Guillemot, F., & Urbán, N. (2019). Id4 promotes the elimination of the pro-activation factor Ascl1 to maintain quiescence of adult hippocampal stem cells. *eLife*, *8*, e48561. https://doi.org/10.7554/eLife.48561

Bond, A. M., Bhalala, O. G., & Kessler, J. A. (2012). The Dynamic Role of Bone Morphogenetic Proteins in Neural Stem Cell Fate and Maturation. *Developmental Neurobiology*, *72*(7), 1068–1084. https://doi.org/10.1002/dneu.22022

Bonnet, D., & Dick, J. E. (1997). Human acute myeloid leukemia is organized as a hierarchy that originates from a primitive hematopoietic cell. *Nature Medicine*, *3*(7), 730–737. https://doi.org/10.1038/nm0797-730

Bothmer, A., Robbiani, D. F., Feldhahn, N., Gazumyan, A., Nussenzweig, A., & Nussenzweig, M. C. (2010). 53BP1 regulates DNA resection and the choice between classical and alternative end joining during class switch recombination. *The Journal of Experimental Medicine*, *207*(4), 855–865. https://doi.org/10.1084/jem.20100244

Boustani, J., Grapin, M., Laurent, P.-A., Apetoh, L., & Mirjolet, C. (2019). The 6th R of Radiobiology: Reactivation of Anti-Tumor Immune Response. *Cancers*, *11*(6), 860. https://doi.org/10.3390/cancers11060860

Bouwman, P., Aly, A., Escandell, J. M., Pieterse, M., Bartkova, J., van der Gulden, H., Hiddingh, S., Thanasoula, M., Kulkarni, A., Yang, Q., Haffty, B. G., Tommiska, J., Blomqvist, C., Drapkin, R., Adams, D. J., Nevanlinna, H., Bartek, J., Tarsounas, M., Ganesan, S., & Jonkers, J. (2010). 53BP1 loss rescues BRCA1 deficiency and is associated with triple-negative and BRCA-mutated breast cancers. *Nature Structural & Molecular Biology*, *17*(6), 688–695. https://doi.org/10.1038/nsmb.1831

Bowers, D. C., Nathan, P. C., Constine, L., Woodman, C., Bhatia, S., Keller, K., & Bashore, L. (2013). Subsequent neoplasms of the CNS among survivors of childhood cancer: A systematic review. *The Lancet. Oncology*, *14*(8), e321-328. https://doi.org/10.1016/S1470-2045(13)70107-4

Braicu, C., Buse, M., Busuioc, C., Drula, R., Gulei, D., Raduly, L., Rusu, A., Irimie, A., Atanasov, A. G., Slaby, O., Ionescu, C., & Berindan-Neagoe, I. (2019). A Comprehensive Review on MAPK: A Promising Therapeutic Target in Cancer. *Cancers*, *11*(10), Article 10. https://doi.org/10.3390/cancers11101618

Briere, T. M., McAleer, M. F., Levy, L. B., & Yang, J. N. (2017). Sparing of normal tissues with volumetric arc radiation therapy for glioblastoma: Single institution clinical experience.

Radiation Oncology (London, England), *12*(1), 79. https://doi.org/10.1186/s13014-017-0810-3

Brown, N. F., McBain, C., Brazil, L., Peoples, S., Jefferies, S., Harris, F., Plaha, P., Vinayan, A., Brooks, C., Hussain, S., Dutton, S. J., Ng, S., Levy, S., & Coutts, T. (2023). A randomised phase II multicentre study of ipilimumab with temozolomide vs temozolomide alone after surgery and chemoradiotherapy in patients with recently diagnosed glioblastoma: Ipi-Glio. *Journal of Clinical Oncology*. https://doi.org/10.1200/JCO.2023.41.17_suppl.LBA2023

Buisson, R., Boisvert, J. L., Benes, C. H., & Zou, L. (2015). Distinct but Concerted Roles of ATR, DNA-PK, and Chk1 in Countering Replication Stress during S Phase. *Molecular Cell*, *59*(6), 1011–1024. https://doi.org/10.1016/j.molcel.2015.07.029

Bunting, S. F., Callén, E., Wong, N., Chen, H.-T., Polato, F., Gunn, A., Bothmer, A., Feldhahn, N., Fernandez-Capetillo, O., Cao, L., Xu, X., Deng, C.-X., Finkel, T., Nussenzweig, M., Stark, J. M., & Nussenzweig, A. (2010). 53BP1 inhibits homologous recombination in Brca1-deficient cells by blocking resection of DNA breaks. *Cell*, *141*(2), 243–254. https://doi.org/10.1016/j.cell.2010.03.012

Burma, S., Chen, B. P., Murphy, M., Kurimasa, A., & Chen, D. J. (2001). ATM phosphorylates histone H2AX in response to DNA double-strand breaks. *The Journal of Biological Chemistry*, *276*(45), 42462–42467. https://doi.org/10.1074/jbc.C100466200

Burris, H. A., Berlin, J., Arkenau, T., Cote, G. M., Lolkema, M. P., Ferrer-Playan, J., Kalapur, A., Bolleddula, J., Locatelli, G., Goddemeier, T., Gounaris, I., & de Bono, J. (2024). A phase I study of ATR inhibitor gartisertib (M4344) as a single agent and in combination with

carboplatin in patients with advanced solid tumours. *British Journal of Cancer*, *130*(7), 1131–1140. https://doi.org/10.1038/s41416-023-02436-2

Butturini, E., Carcereri de Prati, A., Boriero, D., & Mariotto, S. (2019). Tumor Dormancy and Interplay with Hypoxic Tumor Microenvironment. *International Journal of Molecular Sciences*, *20*(17), 4305. https://doi.org/10.3390/ijms20174305

Campos, B., Gal, Z., Baader, A., Schneider, T., Sliwinski, C., Gassel, K., Bageritz, J., Grabe, N., von Deimling, A., Beckhove, P., Mogler, C., Goidts, V., Unterberg, A., Eckstein, V., & Herold-Mende, C. (2014). Aberrant self-renewal and quiescence contribute to the aggressiveness of glioblastoma. *The Journal of Pathology*, *234*(1), 23–33. https://doi.org/10.1002/path.4366

Cancer Genome Atlas Research Network. (2008). Comprehensive genomic characterization defines human glioblastoma genes and core pathways. *Nature*, *455*(7216), 1061–1068. https://doi.org/10.1038/nature07385

Cantoni, O., Guidarelli, A., Sestili, P., Giacomoni, P. U., & Cattabeni, F. (1994). L-histidine-mediated enhancement of hydrogen peroxide-induced cytotoxicity: Relationships between DNA single/double strand breakage and cell killing. *Pharmacological Research*, *29*(2), 169–178. https://doi.org/10.1016/1043-6618(94)80041-3

Cao, F., Hata, R., Zhu, P., Nakashiro, K., & Sakanaka, M. (2010). Conditional deletion of Stat3 promotes neurogenesis and inhibits astrogliogenesis in neural stem cells. *Biochemical and Biophysical Research Communications*, *394*(3), 843–847. https://doi.org/10.1016/j.bbrc.2010.03.092

Caraci, F., Gulisano, W., Guida, C. A., Impellizzeri, A. A. R., Drago, F., Puzzo, D., & Palmeri, A. (2015). A key role for TGF-β1 in hippocampal synaptic plasticity and memory. *Scientific Reports*, *5*(1), 11252. https://doi.org/10.1038/srep11252

Carén, H., H, B., S, G., E, J., Te, B., A, F., G, W., Ae, T., P, B., S, B., & Sm, P. (2015). Glioblastoma Stem Cells Respond to Differentiation Cues but Fail to Undergo Commitment and Terminal Cell-Cycle Arrest. *Stem Cell Reports*, *5*(5). https://doi.org/10.1016/j.stemcr.2015.09.014

Carlsson, S. K., Brothers, S. P., & Wahlestedt, C. (2014). Emerging treatment strategies for glioblastoma multiforme. *EMBO Molecular Medicine*, *6*(11), 1359–1370. https://doi.org/10.15252/emmm.201302627

Carvajal Ibañez, D., Skabkin, M., Hooli, J., Cerrizuela, S., Göpferich, M., Jolly, A., Volk, K., Zumwinkel, M., Bertolini, M., Figlia, G., Höfer, T., Kramer, G., Anders, S., Teleman, A. A., Marciniak-Czochra, A., & Martin-Villalba, A. (2023). Interferon regulates neural stem cell function at all ages by orchestrating mTOR and cell cycle. *EMBO Molecular Medicine*, *15*(4), e16434. https://doi.org/10.15252/emmm.202216434

Ceccaldi, R., Liu, J. C., Amunugama, R., Hajdu, I., Primack, B., Petalcorin, M. I. R., O'Connor, K. W., Konstantinopoulos, P. A., Elledge, S. J., Boulton, S. J., Yusufzai, T., & D'Andrea, A. D. (2015). Homologous-recombination-deficient tumours are dependent on Polθ-mediated repair. *Nature*, *518*(7538), 258–262. https://doi.org/10.1038/nature14184

Cejka, P., & Symington, L. S. (2021). DNA End Resection: Mechanism and Control. *Annual Review of Genetics*, *55*(Volume 55, 2021), 285–307. https://doi.org/10.1146/annurev-genet-071719-020312

Chahal, M., Thiessen, B., & Mariano, C. (2022). Treatment of Older Adult Patients with Glioblastoma: Moving towards the Inclusion of a Comprehensive Geriatric Assessment for Guiding Management. *Current Oncology*, *29*(1), 360–376. https://doi.org/10.3390/curroncol29010032

Chan, T. A., Hermeking, H., Lengauer, C., Kinzler, K. W., & Vogelstein, B. (1999). 14-3-3Sigma is required to prevent mitotic catastrophe after DNA damage. *Nature*, *401*(6753), 616–620. https://doi.org/10.1038/44188

Chandrasekaran, V., Lea, C., Sosa, J. C., Higgins, D., & Lein, P. J. (2015). Reactive oxygen species are involved in BMP-induced dendritic growth in cultured rat sympathetic neurons. *Molecular and Cellular Neurosciences*, *67*, 116–125. https://doi.org/10.1016/j.mcn.2015.06.007

Chatterjee, S., & Starrett, G. J. (2024). Microhomology-mediated repair machinery and its relationship with HPV-mediated oncogenesis. *Journal of Medical Virology*, *96*(5), e29674. https://doi.org/10.1002/jmv.29674

Chen, B. P. C., Uematsu, N., Kobayashi, J., Lerenthal, Y., Krempler, A., Yajima, H., Löbrich, M., Shiloh, Y., & Chen, D. J. (2007). Ataxia telangiectasia mutated (ATM) is essential for DNA-PKcs phosphorylations at the Thr-2609 cluster upon DNA double strand break. *The Journal of Biological Chemistry*, *282*(9), 6582–6587. https://doi.org/10.1074/jbc.M611605200

Chen, J., Li, Y., Yu, T.-S., McKay, R. M., Burns, D. K., Kernie, S. G., & Parada, L. F. (2012). A restricted cell population propagates glioblastoma growth following chemotherapy. *Nature*, *488*(7412), 522–526. https://doi.org/10.1038/nature11287

Cheng, Q., Barboule, N., Frit, P., Gomez, D., Bombarde, O., Couderc, B., Ren, G.-S., Salles, B., & Calsou, P. (2011). Ku counteracts mobilization of PARP1 and MRN in chromatin damaged with DNA double-strand breaks. *Nucleic Acids Research*, *39*(22), 9605–9619. https://doi.org/10.1093/nar/gkr656

Chinot, O. L., Wick, W., Mason, W., Henriksson, R., Saran, F., Nishikawa, R., Carpentier, A. F., Hoang-Xuan, K., Kavan, P., Cernea, D., Brandes, A. A., Hilton, M., Abrey, L., & Cloughesy, T. (2014). Bevacizumab plus Radiotherapy–Temozolomide for Newly Diagnosed Glioblastoma. *New England Journal of Medicine*, *370*(8), 709–722. https://doi.org/10.1056/NEJMoa1308345

Choi, M., Kipps, T., & Kurzrock, R. (2016). ATM Mutations in Cancer: Therapeutic Implications. *Molecular Cancer Therapeutics*, *15*(8), 1781–1791. https://doi.org/10.1158/1535-7163.MCT-15-0945

Choi, S., Yu, J., Park, A., Dubon, M. J., Do, J., Kim, Y., Nam, D., Noh, J., & Park, K.-S. (2019). BMP-4 enhances epithelial mesenchymal transition and cancer stem cell properties of breast cancer cells via Notch signaling. *Scientific Reports*, *9*(1), 11724. https://doi.org/10.1038/s41598-019-48190-5

Ciccia, A., & Elledge, S. J. (2010). The DNA Damage Response: Making it safe to play with knives. *Molecular Cell*, *40*(2), 179–204. https://doi.org/10.1016/j.molcel.2010.09.019

Clements, M., Simpson Ragdale, H., Garcia-Diaz, C., & Parrinello, S. (2024). Generation of immunocompetent somatic glioblastoma mouse models through in situ transformation of subventricular zone neural stem cells. *STAR Protocols*, *5*(1), 102928. https://doi.org/10.1016/j.xpro.2024.102928

Cole, A. E., Murray, S. S., & Xiao, J. (2016). Bone Morphogenetic Protein 4 Signalling in Neural Stem and Progenitor Cells during Development and after Injury. *Stem Cells International*, *2016*, e9260592. https://doi.org/10.1155/2016/9260592

Coller, H. A., Sang, L., & Roberts, J. M. (2006). A New Description of Cellular Quiescence. *PLOS Biology*, *4*(3), e83. https://doi.org/10.1371/journal.pbio.0040083

Couturier, C. P., Ayyadhury, S., Le, P. U., Nadaf, J., Monlong, J., Riva, G., Allache, R., Baig, S., Yan, X., Bourgey, M., Lee, C., Wang, Y. C. D., Wee Yong, V., Guiot, M.-C., Najafabadi, H., Misic, B., Antel, J., Bourque, G., Ragoussis, J., & Petrecca, K. (2020). Single-cell RNA-seq reveals that glioblastoma recapitulates a normal neurodevelopmental hierarchy. *Nature Communications*, *11*(1), Article 1. https://doi.org/10.1038/s41467-020-17186-5

Dahm-Daphi, J., Sass, C., & Alberti, W. (2000). Comparison of biological effects of DNA damage induced by ionizing radiation and hydrogen peroxide in CHO cells. *International Journal of Radiation Biology*, *76*(1), 67–75. https://doi.org/10.1080/095530000139023

Daneman, R., & Prat, A. (2015). The Blood–Brain Barrier. *Cold Spring Harbor Perspectives in Biology*, *7*(1), a020412. https://doi.org/10.1101/cshperspect.a020412

Darmanis, S., Sloan, S. A., Croote, D., Mignardi, M., Chernikova, S., Samghababi, P., Zhang, Y., Neff, N., Kowarsky, M., Caneda, C., Li, G., Chang, S. D., Connolly, I. D., Li, Y., Barres, B. A., Gephart, M. H., & Quake, S. R. (2017). Single-Cell RNA-Seq Analysis of Infiltrating Neoplastic Cells at the Migrating Front of Human Glioblastoma. *Cell Reports*, *21*(5), 1399–1410. https://doi.org/10.1016/j.celrep.2017.10.030

Deleyrolle, L. P., Harding, A., Cato, K., Siebzehnrubl, F. A., Rahman, M., Azari, H., Olson, S., Gabrielli, B., Osborne, G., Vescovi, A., & Reynolds, B. A. (2011). Evidence for label-

retaining tumour-initiating cells in human glioblastoma. *Brain: A Journal of Neurology*, *134*(Pt 5), 1331–1343. https://doi.org/10.1093/brain/awr081

Derby, S., Jackson, M. R., Williams, K., Stobo, J., Kelly, C., Sweeting, L., Shad, S., Herbert, C., Short, S. C., Williamson, A., James, A., Nowicki, S., Bulbeck, H., & Chalmers, A. J. (2024). Concurrent Olaparib and Radiation Therapy in Older Patients With Newly Diagnosed Glioblastoma: The Phase 1 Dose-Escalation PARADIGM Trial. *International Journal of Radiation Oncology, Biology, Physics*, *118*(5), 1371–1378. https://doi.org/10.1016/j.ijrobp.2024.01.011

Derynck, R., Turley, S. J., & Akhurst, R. J. (2021). TGFβ biology in cancer progression and immunotherapy. *Nature Reviews Clinical Oncology*, *18*(1), 9–34. https://doi.org/10.1038/s41571-020-0403-1

Dick, J. E. (2005). Acute myeloid leukemia stem cells. *Annals of the New York Academy of Sciences*, *1044*, 1–5. https://doi.org/10.1196/annals.1349.001

Ding, L., Cao, J., Lin, W., Chen, H., Xiong, X., Ao, H., Yu, M., Lin, J., & Cui, Q. (2020). The Roles of Cyclin-Dependent Kinases in Cell-Cycle Progression and Therapeutic Strategies in Human Breast Cancer. *International Journal of Molecular Sciences*, *21*(6), 1960. https://doi.org/10.3390/ijms21061960

Dobbs, T. A., Tainer, J. A., & Lees-Miller, S. P. (2010). A structural model for regulation of NHEJ by DNA-PKcs autophosphorylation. *DNA Repair*, *9*(12), 1307–1314. https://doi.org/10.1016/j.dnarep.2010.09.019

Dobolyi, A., Vincze, C., Pál, G., & Lovas, G. (2012). The Neuroprotective Functions of Transforming Growth Factor Beta Proteins. *International Journal of Molecular Sciences*, *13*(7), 8219–8258. https://doi.org/10.3390/ijms13078219

Du, Z., Cai, C., Sims, M., Boop, F. A., Davidoff, A. M., & Pfeffer, L. M. (2017). The effects of type I interferon on glioblastoma cancer stem cells. *Biochemical and Biophysical Research Communications*, *491*(2), 343–348. https://doi.org/10.1016/j.bbrc.2017.07.098

Durgin, J. S., Henderson, F., Nasrallah, M. P., Mohan, S., Wang, S., Lacey, S. F., Melenhorst, J. J., Desai, A. S., Lee, J. Y. K., Maus, M. V., June, C. H., Brem, S., O'Connor, R. S., Binder, Z., & O'Rourke, D. M. (2021). Case Report: Prolonged Survival Following EGFRvIII CAR T Cell Treatment for Recurrent Glioblastoma. *Frontiers in Oncology*, *11*, 669071. https://doi.org/10.3389/fonc.2021.669071

Eixarch, H., Calvo-Barreiro, L., Costa, C., Reverter-Vives, G., Castillo, M., Gil, V., Del Río, J. A., Montalban, X., & Espejo, C. (2020). Inhibition of the BMP Signaling Pathway Ameliorated Established Clinical Symptoms of Experimental Autoimmune Encephalomyelitis. *Neurotherapeutics*, *17*(4), 1988–2003. https://doi.org/10.1007/s13311-020-00885-8

El Touny, L. H., Vieira, A., Mendoza, A., Khanna, C., Hoenerhoff, M. J., & Green, J. E. (2014). Combined SFK/MEK inhibition prevents metastatic outgrowth of dormant tumor cells. *The Journal of Clinical Investigation*, *124*(1), 156–168. https://doi.org/10.1172/JCI70259

Escribano-Díaz, C., Orthwein, A., Fradet-Turcotte, A., Xing, M., Young, J. T. F., Tkáč, J., Cook, M. A., Rosebrock, A. P., Munro, M., Canny, M. D., Xu, D., & Durocher, D. (2013). A cell cycle-dependent regulatory circuit composed of 53BP1-RIF1 and BRCA1-CtIP controls DNA repair pathway choice. *Molecular Cell*, *49*(5), 872–883. https://doi.org/10.1016/j.molcel.2013.01.001

Essers, M. A. G., & Trumpp, A. (2010). Targeting leukemic stem cells by breaking their dormancy. *Molecular Oncology*, *4*(5), 443–450. https://doi.org/10.1016/j.molonc.2010.06.001

Evert, B. A., Salmon, T. B., Song, B., Jingjing, L., Siede, W., & Doetsch, P. W. (2004). Spontaneous DNA damage in Saccharomyces cerevisiae elicits phenotypic properties similar to cancer cells. *The Journal of Biological Chemistry*, *279*(21), 22585–22594. https://doi.org/10.1074/jbc.M400468200

Feldkamp, M. M., Lala, P., Lau, N., Roncari, L., & Guha, A. (1999). Expression of activated epidermal growth factor receptors, Ras-guanosine triphosphate, and mitogen-activated protein kinase in human glioblastoma multiforme specimens. *Neurosurgery*, *45*(6), 1442–1453. https://doi.org/10.1097/00006123-199912000-00034

Field, K. M., Jordan, J. T., Wen, P. Y., Rosenthal, M. A., & Reardon, D. A. (2015). Bevacizumab and glioblastoma: Scientific review, newly reported updates, and ongoing controversies. *Cancer*, *121*(7), 997–1007. https://doi.org/10.1002/cncr.28935

Field, K. M., King, M. T., Simes, J., Espinoza, D., Barnes, E. H., Sawkins, K., Rosenthal, M. A., Cher, L., Hovey, E., Wheeler, H., & Nowak, A. K. (2017). Health-related quality of life outcomes from CABARET: A randomized phase 2 trial of carboplatin and bevacizumab in recurrent glioblastoma. *Journal of Neuro-Oncology*, *133*(3), 623–631. https://doi.org/10.1007/s11060-017-2479-8

Foster, E. R., & Downs, J. A. (2005). Histone H2A phosphorylation in DNA double-strand break repair. *The FEBS Journal*, *272*(13), 3231–3240. https://doi.org/10.1111/j.1742-4658.2005.04741.x

French, H. M., Reid, M., Mamontov, P., Simmons, R. A., & Grinspan, J. B. (2009). Oxidative Stress Disrupts Oligodendrocyte Maturation. *Journal of Neuroscience Research*, *87*(14), 3076–3087. https://doi.org/10.1002/jnr.22139

Fu, M., Zhou, Z., Huang, X., Chen, Z., Zhang, L., Zhang, J., Hua, W., & Mao, Y. (2023). Use of Bevacizumab in recurrent glioblastoma: A scoping review and evidence map. *BMC Cancer*, *23*(1), 544. https://doi.org/10.1186/s12885-023-11043-6

Fugger, K., & West, S. C. (2016). Keeping homologous recombination in check. *Cell Research*, *26*(4), 397–398. https://doi.org/10.1038/cr.2016.25

Fukuda, S., Abematsu, M., Mori, H., Yanagisawa, M., Kagawa, T., Nakashima, K., Yoshimura, A., & Taga, T. (2007). Potentiation of Astrogliogenesis by STAT3-Mediated Activation of Bone Morphogenetic Protein-Smad Signaling in Neural Stem Cells. *Molecular and Cellular Biology*, *27*(13), 4931–4937. https://doi.org/10.1128/MCB.02435-06

Gaillard, H., García-Muse, T., & Aguilera, A. (2015). Replication stress and cancer. *Nature Reviews. Cancer*, *15*(5), 276–289. https://doi.org/10.1038/nrc3916

Gao, H., Chakraborty, G., Lee-Lim, A. P., Mo, Q., Decker, M., Vonica, A., Shen, R., Brogi, E., Brivanlou, A. H., & Giancotti, F. G. (2012). The BMP Inhibitor Coco Reactivates Breast Cancer Cells at Lung Metastatic sites. *Cell*, *150*(4), 764–779. https://doi.org/10.1016/j.cell.2012.06.035

Garcia, V., Phelps, S. E. L., Gray, S., & Neale, M. J. (2011). Bidirectional resection of DNA double-strand breaks by Mre11 and Exo1. *Nature*, *479*(7372), 241–244. https://doi.org/10.1038/nature10515

Garcia-Diaz, C., Pöysti, A., Mereu, E., Clements, M. P., Brooks, L. J., Galvez-Cancino, F., Castillo, S. P., Tang, W., Beattie, G., Courtot, L., Ruiz, S., Roncaroli, F., Yuan, Y.,

Marguerat, S., Quezada, S. A., Heyn, H., & Parrinello, S. (2023). Glioblastoma cell fate is differentially regulated by the microenvironments of the tumor bulk and infiltrative margin. *Cell Reports*, *42*(5), 112472. https://doi.org/10.1016/j.celrep.2023.112472

García-León, J. A., Kumar, M., Boon, R., Chau, D., One, J., Wolfs, E., Eggermont, K., Berckmans, P., Gunhanlar, N., de Vrij, F., Lendemeijer, B., Pavie, B., Corthout, N., Kushner, S. A., Dávila, J. C., Lambrichts, I., Hu, W.-S., & Verfaillie, C. M. (2018). SOX10 Single Transcription Factor-Based Fast and Efficient Generation of Oligodendrocytes from Human Pluripotent Stem Cells. *Stem Cell Reports*, *10*(2), 655–672. https://doi.org/10.1016/j.stemcr.2017.12.014

Garrison, J. I., Berens, M. E., Shapiro, J. R., Treasurywala, S., & Floyd-Smith, G. (1996). Interferon-β inhibits proliferation and progression through S phase of the cell cycle in five glioma cell lines. *Journal of Neuro-Oncology*, *30*(3), 213–223. https://doi.org/10.1007/BF00177272

Gauss, G. H., & Lieber, M. R. (1996). Mechanistic constraints on diversity in human V(D)J recombination. *Molecular and Cellular Biology*, *16*(1), 258–269. https://doi.org/10.1128/MCB.16.1.258

Gilbert, M. R., Dignam, J., Won, M., Blumenthal, D. T., Vogelbaum, M. A., Aldape, K. D., Colman, H., Chakravarti, A., Jeraj, R., Armstrong, T. S., Wefel, J. S., Brown, P. D., Jaeckle, K. A., Schiff, D., Atkins, J. N., Brachman, D., Werner-Wasik, M., Komaki, R., Sulman, E. P., & Mehta, M. P. (2013). RTOG 0825: Phase III double-blind placebo-controlled trial evaluating bevacizumab (Bev) in patients (Pts) with newly diagnosed glioblastoma (GBM). *Journal of Clinical Oncology*, *31*(18_suppl), 1–1. https://doi.org/10.1200/jco.2013.31.18_suppl.1

Gill, S., Thomas, J., Fox, C., Kron, T., Rolfo, A., Leahy, M., Chander, S., Williams, S., Tai, K. H., Duchesne, G. M., & Foroudi, F. (2011). Acute toxicity in prostate cancer patients treated with and without image-guided radiotherapy. *Radiation Oncology (London, England)*, *6*, 145. https://doi.org/10.1186/1748-717X-6-145

Gnügge, R., & Symington, L. S. (2021). DNA end resection during homologous recombination. *Current Opinion in Genetics & Development*, *71*, 99–105. https://doi.org/10.1016/j.gde.2021.07.004

Goff, S. L., Morgan, R. A., Yang, J. C., Sherry, R. M., Robbins, P. F., Restifo, N. P., Feldman, S. A., Lu, Y.-C., Lu, L., Zheng, Z., Xi, L., Epstein, M., McIntyre, L. S., Malekzadeh, P., Raffeld, M., Fine, H. A., & Rosenberg, S. A. (2019). Pilot Trial of Adoptive Transfer of Chimeric Antigen Receptor-transduced T Cells Targeting EGFRvIII in Patients With Glioblastoma. *Journal of Immunotherapy (Hagerstown, Md.: 1997)*, *42*(4), 126–135. https://doi.org/10.1097/CJI.0000000000000260

Gomes, W. A., Mehler, M. F., & Kessler, J. A. (2003). Transgenic overexpression of BMP4 increases astroglial and decreases oligodendroglial lineage commitment. *Developmental Biology*, *255*(1), 164–177. https://doi.org/10.1016/s0012-1606(02)00037-4

Gomez-Puerto, M. C., Iyengar, P. V., García de Vinuesa, A., ten Dijke, P., & Sanchez-Duffhues, G. (2019). Bone morphogenetic protein receptor signal transduction in human disease. *The Journal of Pathology*, *247*(1), 9–20. https://doi.org/10.1002/path.5170

Goodarzi, A. A., Yu, Y., Riballo, E., Douglas, P., Walker, S. A., Ye, R., Härer, C., Marchetti, C., Morrice, N., Jeggo, P. A., & Lees-Miller, S. P. (2006). DNA-PK autophosphorylation

facilitates Artemis endonuclease activity. *The EMBO Journal*, *25*(16), 3880–3889. https://doi.org/10.1038/sj.emboj.7601255

Gottlieb, T. M., & Jackson, S. P. (1993). The DNA-dependent protein kinase: Requirement for DNA ends and association with Ku antigen. *Cell*, *72*(1), 131–142. https://doi.org/10.1016/0092-8674(93)90057-w

Grande, D., Rajendra, E., Mason, B., Galbiati, A., Boulton, S. J., Smith, G. C. M., & Robinson, H. M. R. (2024). Assessment of DNA Double Strand Break Repair Activity Using High-throughput and Quantitative Luminescence-based Reporter Assays. *Journal of Visualized Experiments: JoVE*, *208*. https://doi.org/10.3791/66969

Groelly, F. J., Fawkes, M., Dagg, R. A., Blackford, A. N., & Tarsounas, M. (2023). Targeting DNA damage response pathways in cancer. *Nature Reviews Cancer*, *23*(2), 78–94. https://doi.org/10.1038/s41568-022-00535-5

Gzell, C., Back, M., Wheeler, H., Bailey, D., & Foote, M. (2017). Radiotherapy in Glioblastoma: The Past, the Present and the Future. *Clinical Oncology*, *29*(1), 15–25. https://doi.org/10.1016/j.clon.2016.09.015

Hadfield, G. (1954). The Dormant Cancer Cell. *British Medical Journal*, *2*(4888), 607-610.1.

Halliday, J., Helmy, K., Pattwell, S. S., Pitter, K. L., LaPlant, Q., Ozawa, T., & Holland, E. C. (2014). In vivo radiation response of proneural glioma characterized by protective p53 transcriptional program and proneural-mesenchymal shift. *Proceedings of the National Academy of Sciences of the United States of America*, *111*(14), 5248–5253. https://doi.org/10.1073/pnas.1321014111

Han, X.-X., Cai, C., Yu, L.-M., Wang, M., Yang, W., Hu, D.-Y., Ren, J., Zhu, L.-Y., Deng, J.-J., Chen, Q.-Q., He, H., & Gao, Z. (2022). Glioma stem cells and neural stem cells respond

differently to BMP4 signaling. *Cell Regeneration*, *11*, 36. https://doi.org/10.1186/s13619-022-00136-5

Han, X.-X., Jin, S., Yu, L.-M., Wang, M., Hu, X.-Y., Hu, D.-Y., Ren, J., Zhang, M.-H., Huang, W., Deng, J.-J., Chen, Q.-Q., Gao, Z., He, H., & Cai, C. (2022). Interferon-beta inhibits human glioma stem cell growth by modulating immune response and cell cycle related signaling pathways. *Cell Regeneration*, *11*(1), 23. https://doi.org/10.1186/s13619-022-00123-w

Hanif, F., Muzaffar, K., Perveen, K., Malhi, S. M., & Simjee, S. U. (2017). Glioblastoma Multiforme: A Review of its Epidemiology and Pathogenesis through Clinical Presentation and Treatment. *Asian Pacific Journal of Cancer Prevention : APJCP*, *18*(1), 3–9. https://doi.org/10.22034/APJCP.2017.18.1.3

Hao, Y., Stuart, T., Kowalski, M. H., Choudhary, S., Hoffman, P., Hartman, A., Srivastava, A., Molla, G., Madad, S., Fernandez-Granda, C., & Satija, R. (2024). Dictionary learning for integrative, multimodal and scalable single-cell analysis. *Nature Biotechnology*, *42*(2), 293–304. https://doi.org/10.1038/s41587-023-01767-y

Happold, C., Roth, P., Silginer, M., Florea, A.-M., Lamszus, K., Frei, K., Deenen, R., Reifenberger, G., & Weller, M. (2014). Interferon-β induces loss of spherogenicity and overcomes therapy resistance of glioblastoma stem cells. *Molecular Cancer Therapeutics*, *13*(4), 948–961. https://doi.org/10.1158/1535-7163.MCT-13-0772

Hartley, J. M., Spanswick, V. J., & Hartley, J. A. (2011). Measurement of DNA damage in individual cells using the Single Cell Gel Electrophoresis (Comet) assay. *Methods in Molecular Biology (Clifton, N.J.)*, *731*, 309–320. https://doi.org/10.1007/978-1-61779-080-5_25

Hau, E., Shen, H., Clark, C., Graham, P. H., Koh, E., & L. McDonald, K. (2016). The evolving roles and controversies of radiotherapy in the treatment of glioblastoma. *Journal of Medical Radiation Sciences*, *63*(2), 114–123. https://doi.org/10.1002/jmrs.149

Heinecke, K., Seher, A., Schmitz, W., Mueller, T. D., Sebald, W., & Nickel, J. (2009). Receptor oligomerization and beyond: A case study in bone morphogenetic proteins. *BMC Biology*, *7*(1), 59. https://doi.org/10.1186/1741-7007-7-59

Hennen, E., Safina, D., Haussmann, U., Wörsdörfer, P., Edenhofer, F., Poetsch, A., & Faissner, A. (2013). A LewisX Glycoprotein Screen Identifies the Low Density Lipoprotein Receptor-related Protein 1 (LRP1) as a Modulator of Oligodendrogenesis in Mice *. *Journal of Biological Chemistry*, *288*(23), 16538–16545. https://doi.org/10.1074/jbc.M112.419812

Henson, E. S., & Gibson, S. B. (2006). Surviving cell death through epidermal growth factor (EGF) signal transduction pathways: Implications for cancer therapy. *Cellular Signalling*, *18*(12), 2089–2097. https://doi.org/10.1016/j.cellsig.2006.05.015

Hersh, D. S., Wadajkar, A. S., Roberts, N., Perez, J. G., Connolly, N. P., Frenkel, V., Winkles, J. A., Woodworth, G. F., & Kim, A. J. (2016). Evolving Drug Delivery Strategies to Overcome the Blood Brain Barrier. *Current Pharmaceutical Design*, *22*(9), 1177–1193.

Heubel, B., & Nohe, A. (2021). The Role of BMP Signaling in Osteoclast Regulation. *Journal of Developmental Biology*, *9*(3), 24. https://doi.org/10.3390/jdb9030024

Higgins, G. S., Harris, A. L., Prevo, R., Helleday, T., McKenna, W. G., & Buffa, F. M. (2010). Overexpression of POLQ Confers a Poor Prognosis in Early Breast Cancer Patients. *Oncotarget*, *1*(3), 175–184.

Hills, S. A., & Diffley, J. F. X. (2014). DNA Replication and Oncogene-Induced Replicative Stress. *Current Biology*, *24*(10), R435–R444. https://doi.org/10.1016/j.cub.2014.04.012

Hoang-Minh, L. B., Siebzehnrubl, F. A., Yang, C., Suzuki-Hatano, S., Dajac, K., Loche, T., Andrews, N., Schmoll Massari, M., Patel, J., Amin, K., Vuong, A., Jimenez-Pascual, A., Kubilis, P., Garrett, T. J., Moneypenny, C., Pacak, C. A., Huang, J., Sayour, E. J., Mitchell, D. A., … Deleyrolle, L. P. (2018). Infiltrative and drug-resistant slow-cycling cells support metabolic heterogeneity in glioblastoma. *The EMBO Journal*, *37*(23), e98772. https://doi.org/10.15252/embj.201798772

Hofstetter, C. P., Burkhardt, J.-K., Shin, B. J., Gürsel, D. B., Mubita, L., Gorrepati, R., Brennan, C., Holland, E. C., & Boockvar, J. A. (2012). Protein Phosphatase 2A Mediates Dormancy of Glioblastoma Multiforme-Derived Tumor Stem-Like Cells during Hypoxia. *PLOS ONE*, *7*(1), e30059. https://doi.org/10.1371/journal.pone.0030059

Hu, L., Xu, J., Wang, X., Feng, L., Zhang, C., Wang, J., & Wang, S. (2021). Bone Morphogenetic Protein 4 Alleviates DSS-Induced Ulcerative Colitis Through Activating Intestinal Stem Cell by Target ID3. *Frontiers in Cell and Developmental Biology*, *9*, 700864. https://doi.org/10.3389/fcell.2021.700864

Huchedé, P., Meyer, S., Berthelot, C., Hamadou, M., Bertrand-Chapel, A., Rakotomalala, A., Manceau, L., Tomine, J., Lespinasse, N., Lewandowski, P., Cordier-Bussat, M., Broutier, L., Dutour, A., Rochet, I., Blay, J.-Y., Degletagne, C., Attignon, V., Montero-Carcaboso, A., Grand, M. L., … Castets, M. (2024). *BMP2 and BMP7 cooperate with H3.3K27M to promote quiescence and invasiveness in pediatric diffuse midline gliomas* (p. 2023.08.09.552628). bioRxiv. https://doi.org/10.1101/2023.08.09.552628

Husain, J., & Juurlink, B. H. (1995). Oligodendroglial precursor cell susceptibility to hypoxia is related to poor ability to cope with reactive oxygen species. *Brain Research*, *698*(1–2), 86–94. https://doi.org/10.1016/0006-8993(95)00832-b

Iser, I. C., Lenz, G., & Wink, M. R. (2019). EMT-like process in glioblastomas and reactive astrocytes. *Neurochemistry International*, *122*, 139–143. https://doi.org/10.1016/j.neuint.2018.11.016

Iser, I. C., Pereira, M. B., Lenz, G., & Wink, M. R. (2017). The Epithelial-to-Mesenchymal Transition-Like Process in Glioblastoma: An Updated Systematic Review and In Silico Investigation. *Medicinal Research Reviews*, *37*(2), 271–313. https://doi.org/10.1002/med.21408

Iwadate, Y. (2016). Epithelial-mesenchymal transition in glioblastoma progression. *Oncology Letters*, *11*(3), 1615–1620. https://doi.org/10.3892/ol.2016.4113

Iyer, A., Hamers, A. A. J., & Pillai, A. B. (2022). CyTOF® for the Masses. *Frontiers in Immunology*, *13*, 815828. https://doi.org/10.3389/fimmu.2022.815828

Jackson, S. P., & Bartek, J. (2009). The DNA-damage response in human biology and disease. *Nature*, *461*(7267), 1071–1078. https://doi.org/10.1038/nature08467

Jang, M., Kim, S. S., & Lee, J. (2013). Cancer cell metabolism: Implications for therapeutic targets. *Experimental & Molecular Medicine*, *45*(10), e45–e45. https://doi.org/10.1038/emm.2013.85

Javed, S. R., Lord, S., El Badri, S., Harman, R., Holmes, J., Kamzi, F., Maughan, T., McIntosh, D., Mukherjee, S., Ooms, A., Radhakrishna, G., Shaw, P., & Hawkins, M. A. (2024). CHARIOT: A phase I study of berzosertib with chemoradiotherapy in oesophageal and

other solid cancers using time to event continual reassessment method. *British Journal of Cancer*, *130*(3), 467–475. https://doi.org/10.1038/s41416-023-02542-1

Jensen, G. S., Leon-Palmer, N. E., & Townsend, K. L. (2021). Bone morphogenetic proteins (BMPs) in the central regulation of energy balance and adult neural plasticity. *Metabolism*, *123*, 154837. https://doi.org/10.1016/j.metabol.2021.154837

Ji, T., Takabayashi, H., Mao, M., Han, X., Xue, X., Brazil, J., Eaton, K., Shah, Y., & Todisco, A. (2016). Regulation and function of Bone Morphogenetic Protein signaling in colonic injury and inflammation. *American Journal of Physiology. Gastrointestinal and Liver Physiology*, *312*, ajpgi.00169.2016. https://doi.org/10.1152/ajpgi.00169.2016

Jorgovanovic, D., Song, M., Wang, L., & Zhang, Y. (2020). Roles of IFN-γ in tumor progression and regression: A review. *Biomarker Research*, *8*(1), 49. https://doi.org/10.1186/s40364-020-00228-x

Jurkovicova, D., Neophytou, C. M., Gašparović, A. Č., & Gonçalves, A. C. (2022). DNA Damage Response in Cancer Therapy and Resistance: Challenges and Opportunities. *International Journal of Molecular Sciences*, *23*(23), 14672. https://doi.org/10.3390/ijms232314672

Kalinina, E. V., Chernov, N. N., & Novichkova, M. D. (2014). Role of glutathione, glutathione transferase, and glutaredoxin in regulation of redox-dependent processes. *Biochemistry. Biokhimiia*, *79*(13), 1562–1583. https://doi.org/10.1134/S0006297914130082

Kang, M. A., So, E.-Y., Simons, A. L., Spitz, D. R., & Ouchi, T. (2012). DNA damage induces reactive oxygen species generation through the H2AX-Nox1/Rac1 pathway. *Cell Death & Disease*, *3*(1), e249. https://doi.org/10.1038/cddis.2011.134

Karanam, K., Kafri, R., Loewer, A., & Lahav, G. (2012). Quantitative live cell imaging reveals a gradual shift between DNA repair mechanisms and a maximal use of HR in mid-S phase. *Molecular Cell*, *47*(2), 320–329. https://doi.org/10.1016/j.molcel.2012.05.052

Kestens, C., Siersema, P. D., Offerhaus, G. J. A., & Baal, J. W. P. M. van. (2016). BMP4 Signaling Is Able to Induce an Epithelial-Mesenchymal Transition-Like Phenotype in Barrett's Esophagus and Esophageal Adenocarcinoma through Induction of SNAIL2. *PLOS ONE*, *11*(5), e0155754. https://doi.org/10.1371/journal.pone.0155754

Khakipoor, S., Ophoven, C., Schrödl-Häußel, M., Feuerstein, M., Heimrich, B., Deitmer, J. W., & Roussa, E. (2017). TGF-β signaling directly regulates transcription and functional expression of the electrogenic sodium bicarbonate cotransporter 1, NBCe1 (SLC4A4), via Smad4 in mouse astrocytes. *Glia*, *65*(8), 1361–1375. https://doi.org/10.1002/glia.23168

Khodr, V., Machillot, P., Migliorini, E., Reiser, J.-B., & Picart, C. (2020). *High throughput measurements of BMP/BMP receptors interactions using bio-layer interferometry* (p. 2020.10.20.348060). bioRxiv. https://doi.org/10.1101/2020.10.20.348060

Kim, M. M., Umemura, Y., & Leung, D. (2018). Bevacizumab and Glioblastoma: Past, Present, and Future Directions. *The Cancer Journal*, *24*(4), 180. https://doi.org/10.1097/PPO.0000000000000326

Kim, S. T., Smith, S. A., Mortimer, P., Loembé, A.-B., Cho, H., Kim, K.-M., Smith, C., Willis, S., Irurzun-Arana, I., Berges, A., Hong, J. Y., Park, S. H., Park, J. O., Park, Y. S., Lim, H. Y., Kang, W. K., Kozarewa, I., Pierce, A. J., Dean, E., & Lee, J. (2021). Phase I Study of Ceralasertib (AZD6738), a Novel DNA Damage Repair Agent, in Combination with

Weekly Paclitaxel in Refractory Cancer. *Clinical Cancer Research*, *27*(17), 4700–4709. https://doi.org/10.1158/1078-0432.CCR-21-0251

Kominsky, S., Johnson, H. M., Bryan, G., Tanabe, T., Hobeika, A. C., Subramaniam, P. S., & Torres, B. (1998). IFNγ inhibition of cell growth in glioblastomas correlates with increased levels of the cyclin dependent kinase inhibitor p21WAF1/CIP1. *Oncogene*, *17*(23), 2973–2979. https://doi.org/10.1038/sj.onc.1202217

Korsunsky, I., Millard, N., Fan, J., Slowikowski, K., Zhang, F., Wei, K., Baglaenko, Y., Brenner, M., Loh, P., & Raychaudhuri, S. (2019). Fast, sensitive, and accurate integration of single cell data with Harmony. *Nature Methods*, *16*(12), 1289–1296. https://doi.org/10.1038/s41592-019-0619-0

Kriegstein, A., & Alvarez-Buylla, A. (2009). The Glial Nature of Embryonic and Adult Neural Stem Cells. *Annual Review of Neuroscience*, *32*, 149–184. https://doi.org/10.1146/annurev.neuro.051508.135600

Kuchenbaecker, K. B., Hopper, J. L., Barnes, D. R., Phillips, K.-A., Mooij, T. M., Roos-Blom, M.-J., Jervis, S., van Leeuwen, F. E., Milne, R. L., Andrieu, N., Goldgar, D. E., Terry, M. B., Rookus, M. A., Easton, D. F., Antoniou, A. C., & and the BRCA1 and BRCA2 Cohort Consortium. (2017). Risks of Breast, Ovarian, and Contralateral Breast Cancer for BRCA1 and BRCA2 Mutation Carriers. *JAMA*, *317*(23), 2402–2416. https://doi.org/10.1001/jama.2017.7112

Kuo, L. J., & Yang, L.-X. (2008). Gamma-H2AX - a novel biomarker for DNA double-strand breaks. *In Vivo (Athens, Greece)*, *22*(3), 305–309.

Lacroix, M., Abi-Said, D., Fourney, D. R., Gokaslan, Z. L., Shi, W., DeMonte, F., Lang, F. F., McCutcheon, I. E., Hassenbusch, S. J., Holland, E., Hess, K., Michael, C., Miller, D., &

Sawaya, R. (2001). A multivariate analysis of 416 patients with glioblastoma multiforme: Prognosis, extent of resection, and survival. *Journal of Neurosurgery*, *95*(2), 190–198. https://doi.org/10.3171/jns.2001.95.2.0190

Lan, T., Zhao, Z., Qu, Y., Zhang, M., Wang, H., Zhang, Z., Zhou, W., Fan, X., Yu, C., Zhan, Q., & Song, Y. (2016). Targeting hyperactivated DNA-PKcs by KU0060648 inhibits glioma progression and enhances temozolomide therapy via suppression of AKT signaling. *Oncotarget*, *7*(34), 55555–55571. https://doi.org/10.18632/oncotarget.10864

Lan, X., Jörg, D. J., Cavalli, F. M. G., Richards, L. M., Nguyen, L. V., Vanner, R. J., Guilhamon, P., Lee, L., Kushida, M. M., Pellacani, D., Park, N. I., Coutinho, F. J., Whetstone, H., Selvadurai, H. J., Che, C., Luu, B., Carles, A., Moksa, M., Rastegar, N., … Dirks, P. B. (2017). Fate mapping of human glioblastoma reveals an invariant stem cell hierarchy. *Nature*, *549*(7671), 227–232. https://doi.org/10.1038/nature23666

Lecona, E., & Fernandez-Capetillo, O. (2018). Targeting ATR in cancer. *Nature Reviews Cancer*, *18*(9), 586–595. https://doi.org/10.1038/s41568-018-0034-3

Ledermann, J. A. (2016). PARP inhibitors in ovarian cancer. *Annals of Oncology*, *27*, i40–i44. https://doi.org/10.1093/annonc/mdw094

Lee, M.-N., Tseng, R.-C., Hsu, H.-S., Chen, J.-Y., Tzao, C., Ho, W. L., & Wang, Y.-C. (2007). Epigenetic inactivation of the chromosomal stability control genes BRCA1, BRCA2, and XRCC5 in non-small cell lung cancer. *Clinical Cancer Research: An Official Journal of the American Association for Cancer Research*, *13*(3), 832–838. https://doi.org/10.1158/1078-0432.CCR-05-2694

Lee, R. X., & Tang, F. R. (2022). Radiation-induced neuropathological changes in the oligodendrocyte lineage with relevant clinical manifestations and therapeutic

strategies. *International Journal of Radiation Biology*, *98*(10), 1519–1531. https://doi.org/10.1080/09553002.2022.2055804

Lemée, F., Bergoglio, V., Fernandez-Vidal, A., Machado-Silva, A., Pillaire, M.-J., Bieth, A., Gentil, C., Baker, L., Martin, A.-L., Leduc, C., Lam, E., Magdeleine, E., Filleron, T., Oumouhou, N., Kaina, B., Seki, M., Grimal, F., Lacroix-Triki, M., Thompson, A., … Cazaux, C. (2010). DNA polymerase θ up-regulation is associated with poor survival in breast cancer, perturbs DNA replication, and promotes genetic instability. *Proceedings of the National Academy of Sciences of the United States of America*, *107*(30), 13390–13395. https://doi.org/10.1073/pnas.0910759107

Lim, J. L., van der Pol, S. M. A., Baron, W., McCord, J. M., de Vries, H. E., & van Horssen, J. (2016). Protandim Protects Oligodendrocytes against an Oxidative Insult. *Antioxidants*, *5*(3), 30. https://doi.org/10.3390/antiox5030030

Liu, K., Zheng, M., Lu, R., Du, J., Zhao, Q., Li, Z., Li, Y., & Zhang, S. (2020). The role of CDC25C in cell cycle regulation and clinical cancer therapy: A systematic review. *Cancer Cell International*, *20*(1), 213. https://doi.org/10.1186/s12935-020-01304-w

Lord, C. J., & Ashworth, A. (2012). The DNA damage response and cancer therapy. *Nature*, *481*(7381), 287–294. https://doi.org/10.1038/nature10760

Louis, D. N., Perry, A., Reifenberger, G., von Deimling, A., Figarella-Branger, D., Cavenee, W. K., Ohgaki, H., Wiestler, O. D., Kleihues, P., & Ellison, D. W. (2016). The 2016 World Health Organization Classification of Tumors of the Central Nervous System: A summary. *Acta Neuropathologica*, *131*(6), 803–820. https://doi.org/10.1007/s00401-016-1545-1

Louis, D. N., Perry, A., Wesseling, P., Brat, D. J., Cree, I. A., Figarella-Branger, D., Hawkins, C., Ng, H. K., Pfister, S. M., Reifenberger, G., Soffietti, R., von Deimling, A., & Ellison, D. W.

(2021). The 2021 WHO Classification of Tumors of the Central Nervous System: A summary. *Neuro-Oncology*, *23*(8), 1231–1251. https://doi.org/10.1093/neuonc/noab106

Luksik, A. S., Yazigi, E., Shah, P., & Jackson, C. M. (2023). CAR T Cell Therapy in Glioblastoma: Overcoming Challenges Related to Antigen Expression. *Cancers*, *15*(5), 1414. https://doi.org/10.3390/cancers15051414

Ma, J.-L., Kim, E. M., Haber, J. E., & Lee, S. E. (2003). Yeast Mre11 and Rad1 proteins define a Ku-independent mechanism to repair double-strand breaks lacking overlapping end sequences. *Molecular and Cellular Biology*, *23*(23), 8820–8828. https://doi.org/10.1128/MCB.23.23.8820-8828.2003

Mabie, P. C., Mehler, M. F., Marmur, R., Papavasiliou, A., Song, Q., & Kessler, J. A. (1997). Bone Morphogenetic Proteins Induce Astroglial Differentiation of Oligodendroglial–Astroglial Progenitor Cells. *Journal of Neuroscience*, *17*(11), 4112–4120. https://doi.org/10.1523/JNEUROSCI.17-11-04112.1997

Majd, N. K., Yap, T. A., Koul, D., Balasubramaniyan, V., Li, X., Khan, S., Gandy, K. S., Yung, W. K. A., & de Groot, J. F. (2021). The promise of DNA damage response inhibitors for the treatment of glioblastoma. *Neuro-Oncology Advances*, *3*(1), vdab015. https://doi.org/10.1093/noajnl/vdab015

Mao, Z., Bozzella, M., Seluanov, A., & Gorbunova, V. (2008). DNA repair by nonhomologous end joining and homologous recombination during cell cycle in human cells. *Cell Cycle (Georgetown, Tex.)*, *7*(18), 2902–2906.

Mari, P.-O., Florea, B. I., Persengiev, S. P., Verkaik, N. S., Brüggenwirth, H. T., Modesti, M., Giglia-Mari, G., Bezstarosti, K., Demmers, J. A. A., Luider, T. M., Houtsmuller, A. B., &

van Gent, D. C. (2006). Dynamic assembly of end-joining complexes requires interaction between Ku70/80 and XRCC4. *Proceedings of the National Academy of Sciences of the United States of America*, *103*(49), 18597–18602. https://doi.org/10.1073/pnas.0609061103

Mateos-Gomez, P. A., Gong, F., Nair, N., Miller, K. M., Lazzerini-Denchi, E., & Sfeir, A. (2015). Mammalian polymerase θ promotes alternative NHEJ and suppresses recombination. *Nature*, *518*(7538), 254–257. https://doi.org/10.1038/nature14157

Matsuoka, S., Rotman, G., Ogawa, A., Shiloh, Y., Tamai, K., & Elledge, S. J. (2000). Ataxia telangiectasia-mutated phosphorylates Chk2 in vivo and in vitro. *Proceedings of the National Academy of Sciences of the United States of America*, *97*(19), 10389–10394.

McCracken, D. J., Schupper, A. J., Lakomkin, N., Malcolm, J., Bray, D. P., & Hadjipanayis, C. G. (2022). Turning on the light for brain tumor surgery: A 5-aminolevulinic acid story. *Neuro-Oncology*, *24*(Suppl 6), S52. https://doi.org/10.1093/neuonc/noac191

McKinnon, C., Nandhabalan, M., Murray, S. A., & Plaha, P. (2021). Glioblastoma: Clinical presentation, diagnosis, and management. *BMJ*, *374*, n1560. https://doi.org/10.1136/bmj.n1560

Meimand, S. E., Pour-Rashidi, A., Shahrbabak, M. M., Mohammadi, E., Meimand, F. E., & Rezaei, N. (2022). The Prognostication Potential of *BRCA* Genes Expression in Gliomas: A Genetic Survival Analysis Study. *World Neurosurgery*, *157*, e123–e128. https://doi.org/10.1016/j.wneu.2021.09.107

Migliozzi, S., Oh, Y. T., Hasanain, M., Garofano, L., D'Angelo, F., Najac, R. D., Picca, A., Bielle, F., Di Stefano, A. L., Lerond, J., Sarkaria, J. N., Ceccarelli, M., Sanson, M., Lasorella, A., & Iavarone, A. (2023). Integrative multi-omics networks identify PKCδ and DNA-PK as

master kinases of glioblastoma subtypes and guide targeted cancer therapy. *Nature Cancer*, *4*(2), 181–202. https://doi.org/10.1038/s43018-022-00510-x

Mikawa, S., Wang, C., & Sato, K. (2006). Bone morphogenetic protein-4 expression in the adult rat brain. *The Journal of Comparative Neurology*, *499*(4), 613–625. https://doi.org/10.1002/cne.21125

Miller, K. D., Ostrom, Q. T., Kruchko, C., Patil, N., Tihan, T., Cioffi, G., Fuchs, H. E., Waite, K. A., Jemal, A., Siegel, R. L., & Barnholtz-Sloan, J. S. (2021). Brain and other central nervous system tumor statistics, 2021. *CA: A Cancer Journal for Clinicians*, *71*(5), 381–406. https://doi.org/10.3322/caac.21693

Mira, H., Andreu, Z., Suh, H., Lie, D. C., Jessberger, S., Consiglio, A., San Emeterio, J., Hortigüela, R., Marqués-Torrejón, M. A., Nakashima, K., Colak, D., Götz, M., Fariñas, I., & Gage, F. H. (2010). Signaling through BMPR-IA regulates quiescence and long-term activity of neural stem cells in the adult hippocampus. *Cell Stem Cell*, *7*(1), 78–89. https://doi.org/10.1016/j.stem.2010.04.016

Mitrovic, B., Ignarro, L. J., Montestruque, S., Smoll, A., & Merrill, J. E. (1994). Nitric oxide as a potential pathological mechanism in demyelination: Its differential effects on primary glial cells in vitro. *Neuroscience*, *61*(3), 575–585. https://doi.org/10.1016/0306-4522(94)90435-9

Moen, M. D. (2010). Bevacizumab: In previously treated glioblastoma. *Drugs*, *70*(2), 181–189. https://doi.org/10.2165/11203890-000000000-00000

Morganti, S., Marra, A., De Angelis, C., Toss, A., Licata, L., Giugliano, Federica, Taurelli Salimbeni, B., Berton Giachetti, P. P. M., Esposito, A., Giordano, A., Bianchini, G., Garber, J. E., Curigliano, G., Lynce, F., & Criscitiello, C. (2024). PARP Inhibitors for

Breast Cancer Treatment: A Review. *JAMA Oncology*, *10*(5), 658–670. https://doi.org/10.1001/jamaoncol.2023.7322

Morikawa, M., Derynck, R., & Miyazono, K. (2016). TGF-β and the TGF-β Family: Context-Dependent Roles in Cell and Tissue Physiology. *Cold Spring Harbor Perspectives in Biology*, *8*(5), a021873. https://doi.org/10.1101/cshperspect.a021873

Morita, J., Kano, K., Kato, K., Takita, H., Sakagami, H., Yamamoto, Y., Mihara, E., Ueda, H., Sato, T., Tokuyama, H., Arai, H., Asou, H., Takagi, J., Ishitani, R., Nishimasu, H., Nureki, O., & Aoki, J. (2016). Structure and biological function of ENPP6, a choline-specific glycerophosphodiester-phosphodiesterase. *Scientific Reports*, *6*(1), 20995. https://doi.org/10.1038/srep20995

Nakashima, K., Takizawa, T., Ochiai, W., Yanagisawa, M., Hisatsune, T., Nakafuku, M., Miyazono, K., Kishimoto, T., Kageyama, R., & Taga, T. (2001). BMP2-mediated alteration in the developmental pathway of fetal mouse brain cells from neurogenesis to astrocytogenesis. *Proceedings of the National Academy of Sciences*, *98*(10), 5868–5873. https://doi.org/10.1073/pnas.101109698

Nakashima, K., Yanagisawa, M., Arakawa, H., & Taga, T. (1999). Astrocyte differentiation mediated by LIF in cooperation with BMP2. *FEBS Letters*, *457*(1), 43–46. https://doi.org/10.1016/s0014-5793(99)00997-7

Narod, S. A., & Salmena, L. (2011). BRCA1 and BRCA2 Mutations and Breast Cancer. *Discovery Medicine*, *12*(66), 445–453.

Neftel, C., Laffy, J., Filbin, M. G., Hara, T., Shore, M. E., Rahme, G. J., Richman, A. R., Silverbush, D., Shaw, M. L., Hebert, C. M., Dewitt, J., Gritsch, S., Perez, E. M., Gonzalez Castro, L. N., Lan, X., Druck, N., Rodman, C., Dionne, D., Kaplan, A., … Suvà, M. L.

(2019). An Integrative Model of Cellular States, Plasticity, and Genetics for Glioblastoma. *Cell*, *178*(4), 835-849.e21. https://doi.org/10.1016/j.cell.2019.06.024

Nielsen, J. A., Berndt, J. A., Hudson, L. D., & Armstrong, R. C. (2004). Myelin transcription factor 1 (Myt1) modulates the proliferation and differentiation of oligodendrocyte lineage cells. *Molecular and Cellular Neurosciences*, *25*(1), 111–123. https://doi.org/10.1016/j.mcn.2003.10.001

Niklasson, M., Bergström, T., Jarvius, M., Sundström, A., Nyberg, F., Haglund, C., Larsson, R., Westermark, B., Segerman, B., & Segerman, A. (2019). Mesenchymal transition and increased therapy resistance of glioblastoma cells is related to astrocyte reactivity. *The Journal of Pathology*, *249*(3), 295–307. https://doi.org/10.1002/path.5317

Niklasson, M., Dalmo, E., Segerman, A., Rendo, V., & Westermark, B. (2024). *BMP4 induces a p21-dependent cell state shift in glioblastoma linking mesenchymal transition to senescence* (p. 2024.06.20.599819). bioRxiv. https://doi.org/10.1101/2024.06.20.599819

Obrador, E., Moreno-Murciano, P., Oriol-Caballo, M., López-Blanch, R., Pineda, B., Gutiérrez-Arroyo, J. L., Loras, A., Gonzalez-Bonet, L. G., Martinez-Cadenas, C., Estrela, J. M., & Marqués-Torrejón, M. Á. (2024). Glioblastoma Therapy: Past, Present and Future. *International Journal of Molecular Sciences*, *25*(5). Scopus. https://doi.org/10.3390/ijms25052529

O'Connor, S. A., Feldman, H. M., Arora, S., Hoellerbauer, P., Toledo, C. M., Corrin, P., Carter, L., Kufeld, M., Bolouri, H., Basom, R., Delrow, J., McFaline-Figueroa, J. L., Trapnell, C., Pollard, S. M., Patel, A., Paddison, P. J., & Plaisier, C. L. (2021). Neural G0: A quiescent-

like state found in neuroepithelial-derived cells and glioma. *Molecular Systems Biology*, *17*(6), e9522. https://doi.org/10.15252/msb.20209522

Ojalvo-Sanz, A. C., & López-Mascaraque, L. (2021). Gliogenic Potential of Single Pallial Radial Glial Cells in Lower Cortical Layers. *Cells*, *10*(11), 3237. https://doi.org/10.3390/cells10113237

Omuro, A., Brandes, A. A., Carpentier, A. F., Idbaih, A., Reardon, D. A., Cloughesy, T., Sumrall, A., Baehring, J., van den Bent, M., Bähr, O., Lombardi, G., Mulholland, P., Tabatabai, G., Lassen, U., Sepulveda, J. M., Khasraw, M., Vauleon, E., Muragaki, Y., Di Giacomo, A. M., … Weller, M. (2023). Radiotherapy combined with nivolumab or temozolomide for newly diagnosed glioblastoma with unmethylated MGMT promoter: An international randomized phase III trial. *Neuro-Oncology*, *25*(1), 123–134. https://doi.org/10.1093/neuonc/noac099

Oppenlander, M. E., Wolf, A. B., Snyder, L. A., Bina, R., Wilson, J. R., Coons, S. W., Ashby, L. S., Brachman, D., Nakaji, P., Porter, R. W., Smith, K. A., Spetzler, R. F., & Sanai, N. (2014). An extent of resection threshold for recurrent glioblastoma and its risk for neurological morbidity. *Journal of Neurosurgery*, *120*(4), 846–853. https://doi.org/10.3171/2013.12.JNS13184

O'Rourke, D. M., Nasrallah, M. P., Desai, A., Melenhorst, J. J., Mansfield, K., Morrissette, J. J. D., Martinez-Lage, M., Brem, S., Maloney, E., Shen, A., Isaacs, R., Mohan, S., Plesa, G., Lacey, S. F., Navenot, J.-M., Zheng, Z., Levine, B. L., Okada, H., June, C. H., … Maus, M. V. (2017). A single dose of peripherally infused EGFRvIII-directed CAR T cells mediates antigen loss and induces adaptive resistance in patients with recurrent glioblastoma.

Science Translational Medicine, *9*(399), eaaa0984. https://doi.org/10.1126/scitranslmed.aaa0984

Ortega, M. C., Bribián, A., Peregrín, S., Gil, M. T., Marín, O., & de Castro, F. (2012). Neuregulin-1/ErbB4 signaling controls the migration of oligodendrocyte precursor cells during development. *Experimental Neurology*, *235*(2), 610–620. https://doi.org/10.1016/j.expneurol.2012.03.015

Ostrom, Q. T., Cioffi, G., Waite, K., Kruchko, C., & Barnholtz-Sloan, J. S. (2021). CBTRUS Statistical Report: Primary Brain and Other Central Nervous System Tumors Diagnosed in the United States in 2014-2018. *Neuro-Oncology*, *23*(12 Suppl 2), iii1–iii105. https://doi.org/10.1093/neuonc/noab200

Ou, A., Yung, W. K. A., & Majd, N. (2020). Molecular Mechanisms of Treatment Resistance in Glioblastoma. *International Journal of Molecular Sciences*, *22*(1), 351. https://doi.org/10.3390/ijms22010351

Pan, P. C., & Magge, R. S. (2020). Mechanisms of EGFR Resistance in Glioblastoma. *International Journal of Molecular Sciences*, *21*(22), 8471. https://doi.org/10.3390/ijms21228471

Panieri, E., & Santoro, M. M. (2016). ROS homeostasis and metabolism: A dangerous liason in cancer cells. *Cell Death & Disease*, *7*(6), e2253–e2253. https://doi.org/10.1038/cddis.2016.105

Patel, A. P., Tirosh, I., Trombetta, J. J., Shalek, A. K., Gillespie, S. M., Wakimoto, H., Cahill, D. P., Nahed, B. V., Curry, W. T., Martuza, R. L., Louis, D. N., Rozenblatt-Rosen, O., Suvà, M. L., Regev, A., & Bernstein, B. E. (2014). Single-cell RNA-seq highlights intratumoral

heterogeneity in primary glioblastoma. *Science (New York, N.Y.)*, *344*(6190), 1396–1401. https://doi.org/10.1126/science.1254257

Pei, J., Pan, X., Wei, G., & Hua, Y. (2023). Research progress of glutathione peroxidase family (GPX) in redoxidation. *Frontiers in Pharmacology*, *14*, 1147414. https://doi.org/10.3389/fphar.2023.1147414

Peretto, P., Cummings, D., Modena, C., Behrens, M., Venkatraman, G., Fasolo, A., & Margolis, F. L. (2002). BMP mRNA and protein expression in the developing mouse olfactory system. *The Journal of Comparative Neurology*, *451*(3), 267–278. https://doi.org/10.1002/cne.10343

Phillips, H. S., Kharbanda, S., Chen, R., Forrest, W. F., Soriano, R. H., Wu, T. D., Misra, A., Nigro, J. M., Colman, H., Soroceanu, L., Williams, P. M., Modrusan, Z., Feuerstein, B. G., & Aldape, K. (2006). Molecular subclasses of high-grade glioma predict prognosis, delineate a pattern of disease progression, and resemble stages in neurogenesis. *Cancer Cell*, *9*(3), 157–173. https://doi.org/10.1016/j.ccr.2006.02.019

Platanias, L. C. (2005). Mechanisms of type-I- and type-II-interferon-mediated signalling. *Nature Reviews Immunology*, *5*(5), 375–386. https://doi.org/10.1038/nri1604

Podhorecka, M., Skladanowski, A., & Bozko, P. (2010). H2AX Phosphorylation: Its Role in DNA Damage Response and Cancer Therapy. *Journal of Nucleic Acids*, *2010*, 920161. https://doi.org/10.4061/2010/920161

Pollard, S. M., Yoshikawa, K., Clarke, I. D., Danovi, D., Stricker, S., Russell, R., Bayani, J., Head, R., Lee, M., Bernstein, M., Squire, J. A., Smith, A., & Dirks, P. (2009a). Glioma Stem Cell Lines Expanded in Adherent Culture Have Tumor-Specific Phenotypes and Are Suitable

for Chemical and Genetic Screens. *Cell Stem Cell*, *4*(6), 568–580. https://doi.org/10.1016/j.stem.2009.03.014

Pollard, S. M., Yoshikawa, K., Clarke, I. D., Danovi, D., Stricker, S., Russell, R., Bayani, J., Head, R., Lee, M., Bernstein, M., Squire, J. A., Smith, A., & Dirks, P. (2009b). Glioma Stem Cell Lines Expanded in Adherent Culture Have Tumor-Specific Phenotypes and Are Suitable for Chemical and Genetic Screens. *Cell Stem Cell*, *4*(6), 568–580. https://doi.org/10.1016/j.stem.2009.03.014

Preusser, M., de Ribaupierre, S., Wöhrer, A., Erridge, S. C., Hegi, M., Weller, M., & Stupp, R. (2011). Current concepts and management of glioblastoma. *Annals of Neurology*, *70*(1), 9–21. https://doi.org/10.1002/ana.22425

Rampazzo, E., Dettin, M., Maule, F., Scabello, A., Calvanese, L., D'Auria, G., Falcigno, L., Porcù, E., Zamuner, A., Della Puppa, A., Boso, D., Basso, G., & Persano, L. (2017). A synthetic BMP-2 mimicking peptide induces glioblastoma stem cell differentiation. *Biochimica et Biophysica Acta (BBA) - General Subjects*, *1861*(9), 2282–2292. https://doi.org/10.1016/j.bbagen.2017.07.001

Reimann, M., Lee, S., & Schmitt, C. A. (2024). Cellular senescence: Neither irreversible nor reversible. *Journal of Experimental Medicine*, *221*(4), e20232136. https://doi.org/10.1084/jem.20232136

Reinhardt, H. C., & Yaffe, M. B. (2009). Kinases that control the cell cycle in response to DNA damage: Chk1, Chk2, and MK2. *Current Opinion in Cell Biology*, *21*(2), 245–255. https://doi.org/10.1016/j.ceb.2009.01.018

Rice, T., Lachance, D. H., Molinaro, A. M., Eckel-Passow, J. E., Walsh, K. M., Barnholtz-Sloan, J., Ostrom, Q. T., Francis, S. S., Wiemels, J., Jenkins, R. B., Wiencke, J. K., & Wrensch,

M. R. (2016). Understanding inherited genetic risk of adult glioma – a review. *Neuro-Oncology Practice*, *3*(1), 10–16. https://doi.org/10.1093/nop/npv026

Richards, L. M., Whitley, O. K. N., MacLeod, G., Cavalli, F. M. G., Coutinho, F. J., Jaramillo, J. E., Svergun, N., Riverin, M., Croucher, D. C., Kushida, M., Yu, K., Guilhamon, P., Rastegar, N., Ahmadi, M., Bhatti, J. K., Bozek, D. A., Li, N., Lee, L., Che, C., … Pugh, T. J. (2021). Gradient of Developmental and Injury Response transcriptional states defines functional vulnerabilities underpinning glioblastoma heterogeneity. *Nature Cancer*, *2*(2), 157–173. https://doi.org/10.1038/s43018-020-00154-9

Richichi, C., Brescia, P., Alberizzi, V., Fornasari, L., & Pelicci, G. (2013). Marker-independent Method for Isolating Slow-Dividing Cancer Stem Cells in Human Glioblastoma. *Neoplasia (New York, N.Y.)*, *15*(7), 840–847.

Roche, J. (2018). The Epithelial-to-Mesenchymal Transition in Cancer. *Cancers*, *10*(2), 52. https://doi.org/10.3390/cancers10020052

Rodriguez-Berriguete, G., Ranzani, M., Prevo, R., Puliyadi, R., Machado, N., Bolland, H. R., Millar, V., Ebner, D., Boursier, M., Cerutti, A., Cicconi, A., Galbiati, A., Grande, D., Grinkevich, V., Majithiya, J. B., Piscitello, D., Rajendra, E., Stockley, M. L., Boulton, S. J., … Higgins, G. S. (2023). Small-Molecule Polθ Inhibitors Provide Safe and Effective Tumor Radiosensitization in Preclinical Models. *Clinical Cancer Research*, *29*(8), 1631–1642. https://doi.org/10.1158/1078-0432.CCR-22-2977

Rogakou, E. P., Pilch, D. R., Orr, A. H., Ivanova, V. S., & Bonner, W. M. (1998). DNA double-stranded breaks induce histone H2AX phosphorylation on serine 139. *The Journal of Biological Chemistry*, *273*(10), 5858–5868. https://doi.org/10.1074/jbc.273.10.5858

Rosińska, S., & Gavard, J. (2021). Tumor Vessels Fuel the Fire in Glioblastoma. *International Journal of Molecular Sciences*, *22*(12), 6514. https://doi.org/10.3390/ijms22126514

Rothkamm, K., Krüger, I., Thompson, L. H., & Löbrich, M. (2003). Pathways of DNA double-strand break repair during the mammalian cell cycle. *Molecular and Cellular Biology*, *23*(16), 5706–5715. https://doi.org/10.1128/MCB.23.16.5706-5715.2003

Rowe, L. A., Degtyareva, N., & Doetsch, P. W. (2008). DNA damage-induced reactive oxygen species (ROS) stress response in *Saccharomyces cerevisiae*. *Free Radical Biology and Medicine*, *45*(8), 1167–1177. https://doi.org/10.1016/j.freeradbiomed.2008.07.018

Sachdeva, R., Wu, M., Johnson, K., Kim, H., Celebre, A., Shahzad, U., Graham, M. S., Kessler, J. A., Chuang, J. H., Karamchandani, J., Bredel, M., Verhaak, R., & Das, S. (2019). BMP signaling mediates glioma stem cell quiescence and confers treatment resistance in glioblastoma. *Scientific Reports*, *9*(1), Article 1. https://doi.org/10.1038/s41598-019-51270-1

Saikali, S., Avril, T., Collet, B., Hamlat, A., Bansard, J.-Y., Drenou, B., Guegan, Y., & Quillien, V. (2007). Expression of nine tumour antigens in a series of human glioblastoma multiforme: Interest of EGFRvIII, IL-13Ralpha2, gp100 and TRP-2 for immunotherapy. *Journal of Neuro-Oncology*, *81*(2), 139–148. https://doi.org/10.1007/s11060-006-9220-3

Savary, K., Caglayan, D., Caja, L., Tzavlaki, K., Bin Nayeem, S., Bergström, T., Jiang, Y., Uhrbom, L., Forsberg-Nilsson, K., Westermark, B., Heldin, C.-H., Ferletta, M., & Moustakas, A. (2013). Snail depletes the tumorigenic potential of glioblastoma. *Oncogene*, *32*(47), 5409–5420. https://doi.org/10.1038/onc.2013.67

Sax, K. (1938). Chromosome Aberrations Induced by X-Rays. *Genetics*, *23*(5), 494–516. https://doi.org/10.1093/genetics/23.5.494

Schraufstätter, I., Hyslop, P. A., Jackson, J. H., & Cochrane, C. G. (1988). Oxidant-induced DNA damage of target cells. *The Journal of Clinical Investigation*, *82*(3), 1040–1050. https://doi.org/10.1172/JCI113660

Sedelnikova, O. A., Rogakou, E. P., Panyutin, I. G., & Bonner, W. M. (2002). Quantitative Detection of 125IdU-Induced DNA Double-Strand Breaks with γ-H2AX Antibody. *Radiation Research*, *158*(4), 486–492. https://doi.org/10.1667/0033-7587(2002)158[0486:QDOIID]2.0.CO;2

Sfeir, A., & Symington, L. S. (2015). Microhomology-mediated end joining: A back-up survival mechanism or dedicated pathway? *Trends in Biochemical Sciences*, *40*(11), 701–714. https://doi.org/10.1016/j.tibs.2015.08.006

Shaffer, R., Nichol, A. M., Vollans, E., Fong, M., Nakano, S., Moiseenko, V., Schmuland, M., Ma, R., McKenzie, M., & Otto, K. (2010). A comparison of volumetric modulated arc therapy and conventional intensity-modulated radiotherapy for frontal and temporal high-grade gliomas. *International Journal of Radiation Oncology, Biology, Physics*, *76*(4), 1177–1184. https://doi.org/10.1016/j.ijrobp.2009.03.013

Shang, Z., Yu, L., Lin, Y.-F., Matsunaga, S., Shen, C.-Y., & Chen, B. P. C. (2014). DNA-PKcs activates the Chk2–Brca1 pathway during mitosis to ensure chromosomal stability. *Oncogenesis*, *3*(2), e85–e85. https://doi.org/10.1038/oncsis.2013.49

Sharma, S., Javadekar, S. M., Pandey, M., Srivastava, M., Kumari, R., & Raghavan, S. C. (2015). Homology and enzymatic requirements of microhomology-dependent alternative end joining. *Cell Death & Disease*, *6*(3), e1697. https://doi.org/10.1038/cddis.2015.58

Shaw, R. J., & Cantley, L. C. (2006). Ras, PI(3)K and mTOR signalling controls tumour cell growth. *Nature*, *441*(7092), 424–430. https://doi.org/10.1038/nature04869

Shen, T., & Huang, S. (2012). The role of Cdc25A in the regulation of cell proliferation and apoptosis. *Anti-Cancer Agents in Medicinal Chemistry*, *12*(6), 631–639.

Shen, W., Yu, Q., Pu, Y., & Xing, C. (2022). Upregulation of Long Noncoding RNA MALAT1 in Colorectal Cancer Promotes Radioresistance and Aggressive Malignance. *International Journal of General Medicine*, *15*, 8365–8380. https://doi.org/10.2147/IJGM.S393270

Sherr, C. J., & Weber, J. D. (2000). The ARF/p53 pathway. *Current Opinion in Genetics & Development*, *10*(1), 94–99. https://doi.org/10.1016/S0959-437X(99)00038-6

Shibata, A., & Jeggo, P. A. (2021). ATM's Role in the Repair of DNA Double-Strand Breaks. *Genes*, *12*(9), 1370. https://doi.org/10.3390/genes12091370

Sies, H., Belousov, V. V., Chandel, N. S., Davies, M. J., Jones, D. P., Mann, G. E., Murphy, M. P., Yamamoto, M., & Winterbourn, C. (2022). Defining roles of specific reactive oxygen species (ROS) in cell biology and physiology. *Nature Reviews Molecular Cell Biology*, *23*(7), 499–515. https://doi.org/10.1038/s41580-022-00456-z

Simone, S., Cosola, C., Loverre, A., Cariello, M., Sallustio, F., Rascio, F., Gesualdo, L., Schena, F. P., Grandaliano, G., & Pertosa, G. (2012). BMP-2 induces a profibrotic phenotype in adult renal progenitor cells through Nox4 activation. *American Journal of Physiology. Renal Physiology*, *303*(1), F23-34. https://doi.org/10.1152/ajprenal.00328.2011

Singh, S. K., Clarke, I. D., Hide, T., & Dirks, P. B. (2004). Cancer stem cells in nervous system tumors. *Oncogene*, *23*(43), 7267–7273. https://doi.org/10.1038/sj.onc.1207946

Singleton, B. K., Torres-Arzayus, M. I., Rottinghaus, S. T., Taccioli, G. E., & Jeggo, P. A. (1999). The C terminus of Ku80 activates the DNA-dependent protein kinase catalytic subunit. *Molecular and Cellular Biology*, *19*(5), 3267–3277. https://doi.org/10.1128/MCB.19.5.3267

Sirota, N. P., Zhanataev, A. K., Kuznetsova, E. A., Khizhnyak, E. P., Anisina, E. A., & Durnev, A. D. (2014). Some causes of inter-laboratory variation in the results of comet assay. *Mutation Research. Genetic Toxicology and Environmental Mutagenesis*, *770*, 16–22. https://doi.org/10.1016/j.mrgentox.2014.05.003

Smith, J., Tho, L. M., Xu, N., & Gillespie, D. A. (2010). The ATM-Chk2 and ATR-Chk1 pathways in DNA damage signaling and cancer. *Advances in Cancer Research*, *108*, 73–112. https://doi.org/10.1016/B978-0-12-380888-2.00003-0

Sofroniew, M. V. (2020). Astrocyte Reactivity: Subtypes, States, and Functions in CNS Innate Immunity. *Trends in Immunology*, *41*(9), 758–770. https://doi.org/10.1016/j.it.2020.07.004

Sopik, V., Phelan, C., Cybulski, C., & Narod, S. a. (2015). BRCA1 and BRCA2 mutations and the risk for colorectal cancer. *Clinical Genetics*, *87*(5), 411–418. https://doi.org/10.1111/cge.12497

Sorescu, G. P., Song, H., Tressel, S. L., Hwang, J., Dikalov, S., Smith, D. A., Boyd, N. L., Platt, M. O., Lassègue, B., Griendling, K. K., & Jo, H. (2004). Bone Morphogenic Protein 4 Produced in Endothelial Cells by Oscillatory Shear Stress Induces Monocyte Adhesion by Stimulating Reactive Oxygen Species Production From a Nox1-Based NADPH Oxidase. *Circulation Research*, *95*(8), 773–779. https://doi.org/10.1161/01.RES.0000145728.22878.45

Sosa, M. S., Bragado, P., & Aguirre-Ghiso, J. A. (2014). Mechanisms of disseminated cancer cell dormancy: An awakening field. *Nature Reviews. Cancer*, *14*(9), 611–622. https://doi.org/10.1038/nrc3793

Sottoriva, A., Spiteri, I., Piccirillo, S. G. M., Touloumis, A., Collins, V. P., Marioni, J. C., Curtis, C., Watts, C., & Tavaré, S. (2013). Intratumor heterogeneity in human glioblastoma reflects cancer evolutionary dynamics. *Proceedings of the National Academy of Sciences of the United States of America*, *110*(10), 4009–4014. https://doi.org/10.1073/pnas.1219747110

Soubeyrand, S., Pope, L., De Chasseval, R., Gosselin, D., Dong, F., de Villartay, J.-P., & Haché, R. J. G. (2006). Artemis phosphorylated by DNA-dependent protein kinase associates preferentially with discrete regions of chromatin. *Journal of Molecular Biology*, *358*(5), 1200–1211. https://doi.org/10.1016/j.jmb.2006.02.061

Srinivas, U. S., Tan, B. W. Q., Vellayappan, B. A., & Jeyasekharan, A. D. (2019). ROS and the DNA damage response in cancer. *Redox Biology*, *25*, 101084. https://doi.org/10.1016/j.redox.2018.101084

Stanke, K. M., Wilson, C., & Kidambi, S. (2021). High Expression of Glycolytic Genes in Clinical Glioblastoma Patients Correlates With Lower Survival. *Frontiers in Molecular Biosciences*, *8*. https://doi.org/10.3389/fmolb.2021.752404

Steel, G. G., McMillan, T. J., & Peacock, J. H. (1989). The 5Rs of Radiobiology. *International Journal of Radiation Biology*, *56*(6), 1045–1048. https://doi.org/10.1080/09553008914552491

Stummer, W., Pichlmeier, U., Meinel, T., Wiestler, O. D., Zanella, F., Reulen, H.-J., & ALA-Glioma Study Group. (2006). Fluorescence-guided surgery with 5-aminolevulinic acid

for resection of malignant glioma: A randomised controlled multicentre phase III trial. *The Lancet. Oncology*, *7*(5), 392–401. https://doi.org/10.1016/S1470-2045(06)70665-9

Stupp, R., Hegi, M. E., Mason, W. P., van den Bent, M. J., Taphoorn, M. J., Janzer, R. C., Ludwin, S. K., Allgeier, A., Fisher, B., Belanger, K., Hau, P., Brandes, A. A., Gijtenbeek, J., Marosi, C., Vecht, C. J., Mokhtari, K., Wesseling, P., Villa, S., Eisenhauer, E., … Mirimanoff, R.-O. (2009). Effects of radiotherapy with concomitant and adjuvant temozolomide versus radiotherapy alone on survival in glioblastoma in a randomised phase III study: 5-year analysis of the EORTC-NCIC trial. *The Lancet Oncology*, *10*(5), 459–466. https://doi.org/10.1016/S1470-2045(09)70025-7

Stupp, R., Mason, W. P., van den Bent, M. J., Weller, M., Fisher, B., Taphoorn, M. J. B., Belanger, K., Brandes, A. A., Marosi, C., Bogdahn, U., Curschmann, J., Janzer, R. C., Ludwin, S. K., Gorlia, T., Allgeier, A., Lacombe, D., Cairncross, J. G., Eisenhauer, E., & Mirimanoff, R. O. (2005). Radiotherapy plus Concomitant and Adjuvant Temozolomide for Glioblastoma. *New England Journal of Medicine*, *352*(10), 987–996. https://doi.org/10.1056/NEJMoa043330

Sulman, E. P., Ismaila, N., Armstrong, T. S., Tsien, C., Batchelor, T. T., Cloughesy, T., Galanis, E., Gilbert, M., Gondi, V., Lovely, M., Mehta, M., Mumber, M. P., Sloan, A., & Chang, S. M. (2017). Radiation Therapy for Glioblastoma: American Society of Clinical Oncology Clinical Practice Guideline Endorsement of the American Society for Radiation Oncology Guideline. *Journal of Clinical Oncology: Official Journal of the American Society of Clinical Oncology*, *35*(3), 361–369. https://doi.org/10.1200/JCO.2016.70.7562

Sun, H., Liu, C., Han, F., Lin, X., Cao, L., Liu, C., Ji, Q., Cui, J., Yao, Y., Wang, B., Liao, Y., Nie, H., Zhang, Y., & Li, Y. (2023). The regulation loop of MARVELD1 interacting with PARP1 in DNA damage response maintains genome stability and promotes therapy resistance of cancer cells. *Cell Death & Differentiation*, *30*(4), 922–937. https://doi.org/10.1038/s41418-023-01118-z

Sun, Y., Hu, J., Zhou, L., Pollard, S. M., & Smith, A. (2011). Interplay between FGF2 and BMP controls the self-renewal, dormancy and differentiation of rat neural stem cells. *Journal of Cell Science*, *124*(11), 1867–1877. https://doi.org/10.1242/jcs.085506

Szu, J. I., & Binder, D. K. (2016). The Role of Astrocytic Aquaporin-4 in Synaptic Plasticity and Learning and Memory. *Frontiers in Integrative Neuroscience*, *10*, 8. https://doi.org/10.3389/fnint.2016.00008

Szylberg, M., Sokal, P., Śledzińska, P., Bebyn, M., Krajewski, S., Szylberg, Ł., Szylberg, A., Szylberg, T., Krystkiewicz, K., Birski, M., Harat, M., Włodarski, R., & Furtak, J. (2022). MGMT Promoter Methylation as a Prognostic Factor in Primary Glioblastoma: A Single-Institution Observational Study. *Biomedicines*, *10*(8), 2030. https://doi.org/10.3390/biomedicines10082030

Taal, W., Oosterkamp, H. M., Walenkamp, A. M. E., Dubbink, H. J., Beerepoot, L. V., Hanse, M. C. J., Buter, J., Honkoop, A. H., Boerman, D., de Vos, F. Y. F., Dinjens, W. N. M., Enting, R. H., Taphoorn, M. J. B., van den Berkmortel, F. W. P. J., Jansen, R. L. H., Brandsma, D., Bromberg, J. E. C., van Heuvel, I., Vernhout, R. M., … van den Bent, M. J. (2014). Single-agent bevacizumab or lomustine versus a combination of bevacizumab plus lomustine in patients with recurrent glioblastoma (BELOB trial): A randomised controlled phase 2

trial. *The Lancet. Oncology*, *15*(9), 943–953. https://doi.org/10.1016/S1470-2045(14)70314-6

Tavecchio, M., Munck, J. M., Cano, C., Newell, D. R., & Curtin, N. J. (2012). Further characterisation of the cellular activity of the DNA-PK inhibitor, NU7441, reveals potential cross-talk with homologous recombination. *Cancer Chemotherapy and Pharmacology*, *69*(1), 155–164. https://doi.org/10.1007/s00280-011-1662-4

Tejero, R., Huang, Y., Katsyv, I., Kluge, M., Lin, J.-Y., Tome-Garcia, J., Daviaud, N., Wang, Y., Zhang, B., Tsankova, N. M., Friedel, C. C., Zou, H., & Friedel, R. H. (2019). Gene signatures of quiescent glioblastoma cells reveal mesenchymal shift and interactions with niche microenvironment. *EBioMedicine*, *42*, 252–269. https://doi.org/10.1016/j.ebiom.2019.03.064

Thada, V., & Cortez, D. (2021). ATR activation is regulated by dimerization of ATR activating proteins. *Journal of Biological Chemistry*, *296*. https://doi.org/10.1016/j.jbc.2021.100455

Thorburne, S. K., & Juurlink, B. H. (1996). Low glutathione and high iron govern the susceptibility of oligodendroglial precursors to oxidative stress. *Journal of Neurochemistry*, *67*(3), 1014–1022. https://doi.org/10.1046/j.1471-4159.1996.67031014.x

Thyme, S. B., & Schier, A. F. (2016). Polq-Mediated End Joining Is Essential for Surviving DNA Double-Strand Breaks during Early Zebrafish Development. *Cell Reports*, *15*(4), 707–714. https://doi.org/10.1016/j.celrep.2016.03.072

Timme, C. R., Rath, B. H., O'Neill, J. W., Camphausen, K., & Tofilon, P. J. (2018). The DNA-PK Inhibitor VX-984 Enhances the Radiosensitivity of Glioblastoma Cells Grown In Vitro

and as Orthotopic Xenografts. *Molecular Cancer Therapeutics*, *17*(6), 1207–1216. https://doi.org/10.1158/1535-7163.MCT-17-1267

Uxa, S., Castillo-Binder, P., Kohler, R., Stangner, K., Müller, G. A., & Engeland, K. (2021). Ki-67 gene expression. *Cell Death & Differentiation*, *28*(12), 3357–3370. https://doi.org/10.1038/s41418-021-00823-x

Vakifahmetoglu, H., Olsson, M., & Zhivotovsky, B. (2008). Death through a tragedy: Mitotic catastrophe. *Cell Death & Differentiation*, *15*(7), 1153–1162. https://doi.org/10.1038/cdd.2008.47

Verhaak, R. G. W., Hoadley, K. A., Purdom, E., Wang, V., Qi, Y., Wilkerson, M. D., Miller, C. R., Ding, L., Golub, T., Mesirov, J. P., Alexe, G., Lawrence, M., O'Kelly, M., Tamayo, P., Weir, B. A., Gabrie, S., Winckler, W., Gupta, S., Jakkula, L., … Hayes, D. N. (2010). An integrated genomic analysis identifies clinically relevant subtypes of glioblastoma characterized by abnormalities in PDGFRA, IDH1, EGFR and NF1. *Cancer Cell*, *17*(1), 98. https://doi.org/10.1016/j.ccr.2009.12.020

Vredenburgh, J. J., Desjardins, A., Herndon, J. E., Dowell, J. M., Reardon, D. A., Quinn, J. A., Rich, J. N., Sathornsumetee, S., Gururangan, S., Wagner, M., Bigner, D. D., Friedman, A. H., & Friedman, H. S. (2007). Phase II trial of bevacizumab and irinotecan in recurrent malignant glioma. *Clinical Cancer Research: An Official Journal of the American Association for Cancer Research*, *13*(4), 1253–1259. https://doi.org/10.1158/1078-0432.CCR-06-2309

Wang, G.-F., Niu, X., Liu, H., Dong, Q., Yao, Y., Wang, D., Liu, X., & Cao, C. (2021). C-Abl kinase regulates cell proliferation and ionizing radiation-induced G2/M arrest via

phosphorylation of FHL2. *FEBS Open Bio*, *11*(6), 1731–1738. https://doi.org/10.1002/2211-5463.13177

Wang, H., & Xu, X. (2017). Microhomology-mediated end joining: New players join the team. *Cell & Bioscience*, *7*(1), 6. https://doi.org/10.1186/s13578-017-0136-8

Wang, J., Wakeman, T. P., Lathia, J. D., Hjelmeland, A. B., Wang, X.-F., White, R. R., Rich, J. N., & Sullenger, B. A. (2010). Notch promotes radioresistance of glioma stem cells. *Stem Cells (Dayton, Ohio)*, *28*(1), 17–28. https://doi.org/10.1002/stem.261

Wang, M., Wu, W., Wu, W., Rosidi, B., Zhang, L., Wang, H., & Iliakis, G. (2006). PARP-1 and Ku compete for repair of DNA double strand breaks by distinct NHEJ pathways. *Nucleic Acids Research*, *34*(21), 6170–6182. https://doi.org/10.1093/nar/gkl840

Wang, Q., Hu, B., Hu, X., Kim, H., Squatrito, M., Scarpace, L., deCarvalho, A. C., Lyu, S., Li, P., Li, Y., Barthel, F., Cho, H. J., Lin, Y.-H., Satani, N., Martinez-Ledesma, E., Zheng, S., Chang, E., Sauvé, C.-E. G., Olar, A., … Verhaak, R. G. W. (2017). Tumor Evolution of Glioma-Intrinsic Gene Expression Subtypes Associates with Immunological Changes in the Microenvironment. *Cancer Cell*, *32*(1), 42-56.e6. https://doi.org/10.1016/j.ccell.2017.06.003

Wang, R. N., Green, J., Wang, Z., Deng, Y., Qiao, M., Peabody, M., Zhang, Q., Ye, J., Yan, Z., Denduluri, S., Idowu, O., Li, M., Shen, C., Hu, A., Haydon, R. C., Kang, R., Mok, J., Lee, M. J., Luu, H. L., & Shi, L. L. (2014). Bone Morphogenetic Protein (BMP) signaling in development and human diseases. *Genes & Diseases*, *1*(1), 87–105. https://doi.org/10.1016/j.gendis.2014.07.005

Wang, R., Sun, Y., Li, C., Xue, Y., & Ba, X. (2023). Targeting the DNA Damage Response for Cancer Therapy. *International Journal of Molecular Sciences*, *24*(21), Article 21. https://doi.org/10.3390/ijms242115907

Wang, Y., Xu, H., Liu, T., Huang, M., Butter, P.-P., Li, C., Zhang, L., Kao, G. D., Gong, Y., Maity, A., Koumenis, C., & Fan, Y. (2018). Temporal DNA-PK activation drives genomic instability and therapy resistance in glioma stem cells. *JCI Insight*, *3*(3), e98096. https://doi.org/10.1172/jci.insight.98096

Warters, R. L., Lyons, B. W., Ridinger, D. N., & Dethlefsen, L. A. (1985). DNA damage repair in quiescent murine mammary carcinoma cells in culture. *Biochimica et Biophysica Acta (BBA) - Gene Structure and Expression*, *824*(4), 357–364. https://doi.org/10.1016/0167-4781(85)90043-0

Weber, A. M., & Ryan, A. J. (2015). ATM and ATR as therapeutic targets in cancer. *Pharmacology & Therapeutics*, *149*, 124–138. https://doi.org/10.1016/j.pharmthera.2014.12.001

Willems, P., Claes, K., Baeyens, A., Vandersickel, V., Werbrouck, J., De Ruyck, K., Poppe, B., Van den Broecke, R., Makar, A., Marras, E., Perletti, G., Thierens, H., & Vral, A. (2008). Polymorphisms in nonhomologous end-joining genes associated with breast cancer risk and chromosomal radiosensitivity. *Genes, Chromosomes & Cancer*, *47*(2), 137–148. https://doi.org/10.1002/gcc.20515

Wilson, K. M., & Keng, P. C. (1989). Radiation-induced DNA Damage and Repair in Quiescent and Proliferating Human Tumor Cells in Vitro. *International Journal of Radiation Biology*, *55*(3), 385–395. https://doi.org/10.1080/09553008914550431

Wu, D., Chen, Q., Chen, X., Han, F., Chen, Z., & Wang, Y. (2023). The blood–brain barrier: Structure, regulation, and drug delivery. *Signal Transduction and Targeted Therapy*, *8*(1), 1–27. https://doi.org/10.1038/s41392-023-01481-w

Xie, X. P., Laks, D. R., Sun, D., Ganbold, M., Wang, Z., Pedraza, A. M., Bale, T., Tabar, V., Brennan, C., Zhou, X., & Parada, L. F. (2022). Quiescent human glioblastoma cancer stem cells drive tumor initiation, expansion, and recurrence following chemotherapy. *Developmental Cell*, *57*(1), 32-46.e8. https://doi.org/10.1016/j.devcel.2021.12.007

Ximerakis, M., Lipnick, S. L., Innes, B. T., Simmons, S. K., Adiconis, X., Dionne, D., Mayweather, B. A., Nguyen, L., Niziolek, Z., Ozek, C., Butty, V. L., Isserlin, R., Buchanan, S. M., Levine, S. S., Regev, A., Bader, G. D., Levin, J. Z., & Rubin, L. L. (2019). Single-cell transcriptomic profiling of the aging mouse brain. *Nature Neuroscience*, *22*(10), 1696–1708. https://doi.org/10.1038/s41593-019-0491-3

Xu, X., Zheng, L., Yuan, Q., Zhen, G., Crane, J. L., Zhou, X., & Cao, X. (2018). Transforming growth factor-β in stem cells and tissue homeostasis. *Bone Research*, *6*(1), 1–31. https://doi.org/10.1038/s41413-017-0005-4

Xue, D., Zhou, X., & Qiu, J. (2020). Emerging role of NRF2 in ROS-mediated tumor chemoresistance. *Biomedicine & Pharmacotherapy*, *131*, 110676. https://doi.org/10.1016/j.biopha.2020.110676

Yamaguchi, H., Uchihori, Y., Yasuda, N., Takada, M., & Kitamura, H. (2005). Estimation of yields of OH radicals in water irradiated by ionizing radiation. *Journal of Radiation Research*, *46*(3), 333–341. https://doi.org/10.1269/jrr.46.333

Yang, C., Tian, G., Dajac, M., Doty, A., Wang, S., Lee, J.-H., Rahman, M., Huang, J., Reynolds, B. A., Sarkisian, M. R., Mitchell, D., & Deleyrolle, L. P. (2022). Slow-Cycling Cells in

Glioblastoma: A Specific Population in the Cellular Mosaic of Cancer Stem Cells. *Cancers*, *14*(5), 1126. https://doi.org/10.3390/cancers14051126

Yang, Z., & Wang, K. K. W. (2015). Glial Fibrillary acidic protein: From intermediate filament assembly and gliosis to neurobiomarker. *Trends in Neurosciences*, *38*(6), 364–374. https://doi.org/10.1016/j.tins.2015.04.003

Yao, M., Wang, Y., Zhang, P., Chen, H., Xu, Z., Jiao, J., & Yuan, Z. (2014). BMP2-SMAD Signaling Represses the Proliferation of Embryonic Neural Stem Cells through YAP. *Journal of Neuroscience*, *34*(36), 12039–12048. https://doi.org/10.1523/JNEUROSCI.0486-14.2014

Yeh, A. C., & Ramaswamy, S. (2015). Mechanisms of Cancer Cell Dormancy—Another Hallmark of Cancer? *Cancer Research*, *75*(23), 5014–5022. https://doi.org/10.1158/0008-5472.CAN-15-1370

Yin, A., Zhang, L., Cheng, J., Dong, Y., Liu, B., Han, N., & Zhang, X. (2013). Radiotherapy Plus Concurrent or Sequential Temozolomide for Glioblastoma in the Elderly: A Meta-Analysis. *PLOS ONE*, *8*(9), e74242. https://doi.org/10.1371/journal.pone.0074242

Yokoya, A., Shikazono, N., Fujii, K., Urushibara, A., Akamatsu, K., & Watanabe, R. (2008). DNA damage induced by the direct effect of radiation. *Radiation Physics and Chemistry*, *77*(10), 1280–1285. https://doi.org/10.1016/j.radphyschem.2008.05.021

Yoshikawa, M. H., Rabelo, N. N., Telles, J. P. M., & Figueiredo, E. G. (2023). Modifiable risk factors for glioblastoma: A systematic review and meta-analysis. *Neurosurgical Review*, *46*(1), 143. https://doi.org/10.1007/s10143-023-02051-y

Yuan, J., Levitin, H. M., Frattini, V., Bush, E. C., Boyett, D. M., Samanamud, J., Ceccarelli, M., Dovas, A., Zanazzi, G., Canoll, P., Bruce, J. N., Lasorella, A., Iavarone, A., & Sims, P. A.

(2018). Single-cell transcriptome analysis of lineage diversity in high-grade glioma. *Genome Medicine*, *10*(1), 57. https://doi.org/10.1186/s13073-018-0567-9

Zatreanu, D., Robinson, H. M. R., Alkhatib, O., Boursier, M., Finch, H., Geo, L., Grande, D., Grinkevich, V., Heald, R. A., Langdon, S., Majithiya, J., McWhirter, C., Martin, N. M. B., Moore, S., Neves, J., Rajendra, E., Ranzani, M., Schaedler, T., Stockley, M., … Lord, C. J. (2021). Polθ inhibitors elicit BRCA-gene synthetic lethality and target PARP inhibitor resistance. *Nature Communications*, *12*(1), 3636. https://doi.org/10.1038/s41467-021-23463-8

Zeng, C., Duan, S., Zhao, L., & Jiang, J. (2024). Hsa-miR-92b-3p Targeting FHL2 to Enhance Radiosensitivity of Nasopharyngeal Carcinoma. *Biochemical Genetics*. https://doi.org/10.1007/s10528-024-10741-5

Zhang, C., Wang, Z., Liu, H., Wang, Z., & Jia, W. (2023). Characterization of tumor-associated reactive astrocytes in gliomas by single-cell and bulk tumor sequencing. *Frontiers in Neurology*, *14*. https://doi.org/10.3389/fneur.2023.1193844

Zhang, J., Wang, X., Vikash, V., Ye, Q., Wu, D., Liu, Y., & Dong, W. (2016). ROS and ROS-Mediated Cellular Signaling. *Oxidative Medicine and Cellular Longevity*, *2016*(1), 4350965. https://doi.org/10.1155/2016/4350965

Zhang, J., Zeng, Q., & She, M. (2023). The roles of FHL2 in cancer. *Clinical and Experimental Medicine*, *23*(7), 3113–3124. https://doi.org/10.1007/s10238-023-01076-3

Zhang, X.-P., Liu, F., & Wang, W. (2011). Two-phase dynamics of p53 in the DNA damage response. *Proceedings of the National Academy of Sciences*, *108*(22), 8990–8995. https://doi.org/10.1073/pnas.1100600108

Zhao, H., & Piwnica-Worms, H. (2001). ATR-mediated checkpoint pathways regulate phosphorylation and activation of human Chk1. *Molecular and Cellular Biology*, *21*(13), 4129–4139. https://doi.org/10.1128/MCB.21.13.4129-4139.2001

Zhao, X., Zhang, J., Zhang, W., Dai, R., Xu, J., Li, Z., & Yang, L. (2021). The Relationship Between Circulating Bone Morphogenetic Protein-4 and Inflammation Cytokines in Patients Undergoing Thoracic Surgery: A Prospective Randomized Study. *Journal of Inflammation Research*, *14*, 4069–4077. https://doi.org/10.2147/JIR.S324775

Zhou, J., Gelot, C., Pantelidou, C., Li, A., Yücel, H., Davis, R. E., Färkkilä, A., Kochupurakkal, B., Syed, A., Shapiro, G. I., Tainer, J. A., Blagg, B. S. J., Ceccaldi, R., & D'Andrea, A. D. (2021). A first-in-class polymerase theta inhibitor selectively targets homologous-recombination-deficient tumors. *Nature Cancer*, *2*(6), 598–610. https://doi.org/10.1038/s43018-021-00203-x

Zhou, W., Sun, M., Li, G.-H., Wu, Y.-Z., Wang, Y., Jin, F., Zhang, Y.-Y., Yang, L., & Wang, D.-L. (2013). Activation of the phosphorylation of ATM contributes to radioresistance of glioma stem cells. *Oncology Reports*, *30*(4), 1793–1801. https://doi.org/10.3892/or.2013.2614

Zhou, Y., Liu, L., Tao, S., Yao, Y., Wang, Y., Wei, Q., Shao, A., & Deng, Y. (2021). Parthanatos and its associated components: Promising therapeutic targets for cancer. *Pharmacological Research*, *163*, 105299. https://doi.org/10.1016/j.phrs.2020.105299

Zienert, E., Eke, I., Aust, D., & Cordes, N. (2015). LIM-only protein FHL2 critically determines survival and radioresistance of pancreatic cancer cells. *Cancer Letters*, *364*(1), 17–24. https://doi.org/10.1016/j.canlet.2015.04.019

Zou, L., & Elledge, S. J. (2003). Sensing DNA Damage Through ATRIP Recognition of RPA-ssDNA Complexes. *Science*, *300*(5625), 1542–1548. https://doi.org/10.1126/science.1083430